3D BIOPRINTING IN TISSUE AND ORGAN REGENERATION

Yang Wu
Jerry Fuh
Ibrahim Tarik Ozbolat

3D Bioprinting in Tissue and Organ Regeneration

This page intentionally left blank

3D Bioprinting in Tissue and Organ Regeneration

Yang Wu
School of Mechanical Engineering and Automation,
Harbin Institute of Technology, Shenzhen, China

Jerry Fuh
Department of Mechanical Engineering,
National University of Singapore, Singapore

Ibrahim Tarik Ozbolat
Engineering Science and Mechanics Department,
Department of Biomedical Engineering, and
Department of Neurosurgery, Penn State University,
State College, PA, United States

ELSEVIER

ACADEMIC PRESS
An imprint of Elsevier

Academic Press is an imprint of Elsevier
125 London Wall, London EC2Y 5AS, United Kingdom
525 B Street, Suite 1650, San Diego, CA 92101, United States
50 Hampshire Street, 5th Floor, Cambridge, MA 02139, United States
The Boulevard, Langford Lane, Kidlington, Oxford OX5 1GB, United Kingdom

Notices

Knowledge and best practice in this field are constantly changing. As new research and experience broaden our understanding, changes in research methods, professional practices, or medical treatment may become necessary.

Practitioners and researchers must always rely on their own experience and knowledge in evaluating and using any information, methods, compounds, or experiments described herein. In using such information or methods they should be mindful of their own safety and the safety of others, including parties for whom they have a professional responsibility.

To the fullest extent of the law, neither the Publisher nor the authors, contributors, or editors, assume any liability for any injury and/or damage to persons or property as a matter of products liability, negligence or otherwise, or from any use or operation of any methods, products, instructions, or ideas contained in the material herein.

ISBN: 978-0-12-824291-9

Publisher: Stacy Masucci
Acquisitions Editor: Elizabeth A Brown
Editorial Project Manager: Samantha Allard
Production Project Manager: Selvaraj Raviraj
Cover Designer: Miles Hitchen

Typeset by TNQ Technologies

Contents

Author bios

Dr. Yang Wu is an Assistant Professor in the School of Mechanical Engineering and Automation at Harbin Institute of Technology, Shenzhen, China. Dr. Wu has been carrying out research in the field of 3D bioprinting and regenerative medicine since his PhD study in 2012, particularly in the application area of connective tissue repairs such as cartilage and tendon. Dr. Wu has published more than 30 research and review articles in renowned journals and books in the field, as well as several patents. His research work has been reported by several scientific and technological media. He serves as an editorial board member in some journals in the field of biofabrication and biomedical engineering. He also serves as a reviewer for several renowned journals in his research field.

Dr. Jerry Fuh is a Professor in the Department of Mechanical Engineering at the National University of Singapore (NUS). He has devoted himself to the research of additive manufacturing or 3D printing processes and materials since 1995. He has published over 300 technical papers in design- and manufacturing-related areas. In 2016, he and his colleagues established a 3DP-enabled biomedical hub within the NUS premise across five different faculties, i.e., engineering, science, design, dental, and medicine, to be one of its few kinds to promote transnational works on biomedical and healthcare research under the NAMIC and University Funding.

Dr. Ibrahim T. Ozbolat is a Professor of Engineering Science and Mechanics Department, Biomedical Engineering Department, and Neurosurgery Department and a faculty member of the Huck Institutes of the Life Sciences, Materials Research Institute, and Center for Neural Engineering at Penn State. Dr. Ozbolat's major research is in the areas of bioprinting and tissue engineering. His research has been widely published, received various awards, and has been featured in national and international media and press numerous times. He has delivered over 100 invited talks and keynotes at national and international forums and conferences. His technology spun off two start-up companies and he is an advisory board member for multiple leading companies in bioprinting.

This page intentionally left blank

Preface

Three-dimensional (3D) bioprinting is the utilization of layer-by-layer methods to deposit bioinks such as cells, growth factors, and biomaterials to fabricate biomedical parts that maximally imitate natural tissue/organ characteristics. In the past decade, bioprinting has considerably advanced and a large number of studies have shown attractive outcomes in different applications. The 3D bioprinting market is projected to reach USD 1647.4 million by 2024. This burgeoning technology appears promising for evolving tissue engineering toward functional tissue and organ regeneration, ultimately alleviating organ shortage.

In this regard, the development of a comprehensive book covering the state-of-the-art advance in applications of bioprinting is valuable for academia, the public, and industry. This book is organized into three major parts, and it benefits the readers to understand bioprinting from varied angles. First of all, this book contains a comprehensive discussion, covering the major considerations during the prebioprinting, bioprinting, and postbioprinting stages, which gives the readers an overview to understand the technical process of designing and manufacturing a bioprinted product. Secondly, a major portion of this book covers detailed descriptions of different applications of bioprinting, including skin, cartilage, bone, vascularized tissue, and organs, which helps the bioengineers, manufacturing engineers, and clinicians to understand the biofabrication approaches of the given tissue/organ type, such as the selections of bioink, bioprinter type, and appropriate process. Especially, intraoperative bioprinting is highlighted in a separate chapter, which has been widely considered as one of the important future trends of bioprinting. Lastly, ethical and regulatory concerns about the clinical utilization of bioprinting will also be discussed, which offers the reader a unique insight into the social responsibility of researchers and practitioners in this field. Overall, compared to current books that largely focus on bioprinting techniques, this book is more application-oriented, showing the audience the great value of bioprinting. This book is a great source for senior undergraduate and graduate students who are interested in bioprinting and is recommended to be used as a textbook for bioprinting-related courses. This book could play an instructive role in developing medical products using bioprinting for industry professionals. Researchers in the disciplines of biomedical engineering, mechanical engineering, and medicine can refer to this book for the latest advance in this field.

The book is outlined in 9 chapters namely Introduction, Considerations of Bioprinting, Bioprinting of Cartilage, Bioprinting of Bone, Bioprinting of Skin, Bioprinting of

Vascularized Tissues, Bioprinting of Other Tissues and Organs, Intraoperative Bioprinting, and Ethical and Regulatory Concerns of Bioprinting.

Chapter 1 covers the background introduction about different bioprinting modalities in terms of their principles, setups, pros, cons, etc. Chapter 2 systematically discusses the considerations in the entire bioprinting procedure. Each stage (i.e., prebioprinting, bioprinting, and postbioprinting) can influence others and has a bearing on the performance of fabricated constructs.

In Chapters 3–5, the bioprinting of three major tissue types is discussed, including cartilage, bone, and skin, respectively. For each tissue type, the state-of-the-art research is depicted and different phases such as 3D modeling, biomaterials, bioprinting technologies, and characterizations are described. Chapter 6 presents the latest progress in bioprinting of vascularized and functional tissues to the reader, which is an intermediate stage toward achieving organ-level complexity and effective long-term clinical outcomes. In Chapter 7, applications of bioprinting in the regeneration of other tissues and organs such as cardiac tissue, kidney, liver, nerve tissue, pancreatic tissue, and lung are demonstrated and reviewed together.

Chapter 8 highlights the intraoperative bioprinting techniques, in which the defect is repaired via bioprinting on a live subject in a surgical setting. Current achievements and limitations of intraoperative bioprinting are provided from engineering and clinical points of view. Chapter 9 presents the challenges of bioprinting in terms of ethics, policies, regulations, and social acceptance, summarizing the future chances and social responsibility of researchers and practitioners in the field of bioprinting.

CHAPTER 1

Introduction

1.1 Bioprinting: principle and classification

Three-dimensional (3D) printing has its root in polymer printing, which began with the invention of stereolithography by Hull [1]. Polymer printing gave rise to several branches of 3D printing, including metal printing and bioprinting [2]. In 1988, Klebe used cytoscribing technology for two-dimensional (2D) micropositioning of proteins to create 2D patterns [3]. By the late 1990s, scientists began to develop 2D bioprinting techniques with living cells using such micropositioning techniques, which made complex tissue fabrication possible. A major breakthrough in this regard was seen in 2000 when Thomas Boland modified an inkjet printer to bioprint cells into a Petri dish, giving rise to the first bioprinter [4,5]. Anthony Atala of the Wake Forest Institute for Regenerative Medicine provided the first case of a fully printed organ, with the miniature kidney in 2002 [6]. The concept of tissue spheroids was later discovered in 2008, paving the way for rapid tissue and organ generation by implanting spheroids in scaffolds [7]. In the same year, Objet Geometries Ltd. developed multilateral printing, which further increased the potential developments in bioprinting [8]. In 2009, the first commercial bioprinter was Novogen MMX developed by Organovo [9], and scaffold-free vascular constructs were created [3]. Since then, various bioprinters have been developed to bioprint a wide array of tissues from cartilage and bone to muscle and liver [10−12]. Such advances are targeted toward a common goal, which is to combine cells and biomaterials to fabricate tissue constructs. This allows for the accurate deposition of cells with high resolution and is, therefore, a promising tool for organ-on-a-chip drug screening systems and tissue fabrication for regenerative medicine [11,13−15]. Bioprinting can be combined with computer-aided design/computer-aided manufacturing (CAD/CAM) technologies [16,17], which allows the use of patient-specific images to develop anatomically correct tissues or organs with appropriate volumetric measurements. Thus, wide diversity of knowledge is required in the field of bioprinting, with a variety of concepts pertaining to mechanical design, machine fabrication, and regenerative medicine coming together to find an answer for the current shortage of transplant organs and their side effects.

Bioprinting can be defined as the spatial patterning of living cells and other biologics by stacking and assembling them using a computer-aided layer-by-layer deposition approach for fabrication of living tissue and organ analogs for tissue engineering, regenerative

3D Bioprinting in Tissue and Organ Regeneration. https://doi.org/10.1016/B978-0-12-824291-9.18002-9

medicine, pharmacokinetic, cancer research [18] and other biological studies [19]. With the emergence of bioprinting in medical and pharmaceutical research [20], the substantial evolution in bioprinter designs has also taken place with successful commercialization of several bioprinters [4]. In order to execute bioprinting, three major components are essential, namely a bioink, an appropriate bioprinting process (modality), and a bioprinter (Fig. 1.1). Briefly, according to their working mechanism, bioprinting technologies can be classified into three major modalities including extrusion-based bioprinting (EBB), droplet-based bioprinting (DBB), and laser-based bioprinting (LBB) [19,21], which can be used alone or in combination for tissue fabrication [9].

1.1.1 Extrusion-based bioprinting

Extrusion-based bioprinting (EBB) deposits bioink from a syringe or nozzle-based system onto a build platform based on a CAD design of the structure being printed. Based on the design, the software is able to determine the locations on the build platform where the bioink must be extruded onto, in order to generate the desired 3D structure. The extrusion is performed in the form of cylindrical depositions of the material, using pneumatic, mechanical, or solenoid driven deposition system, as shown in Fig. 1.1 [19]. The

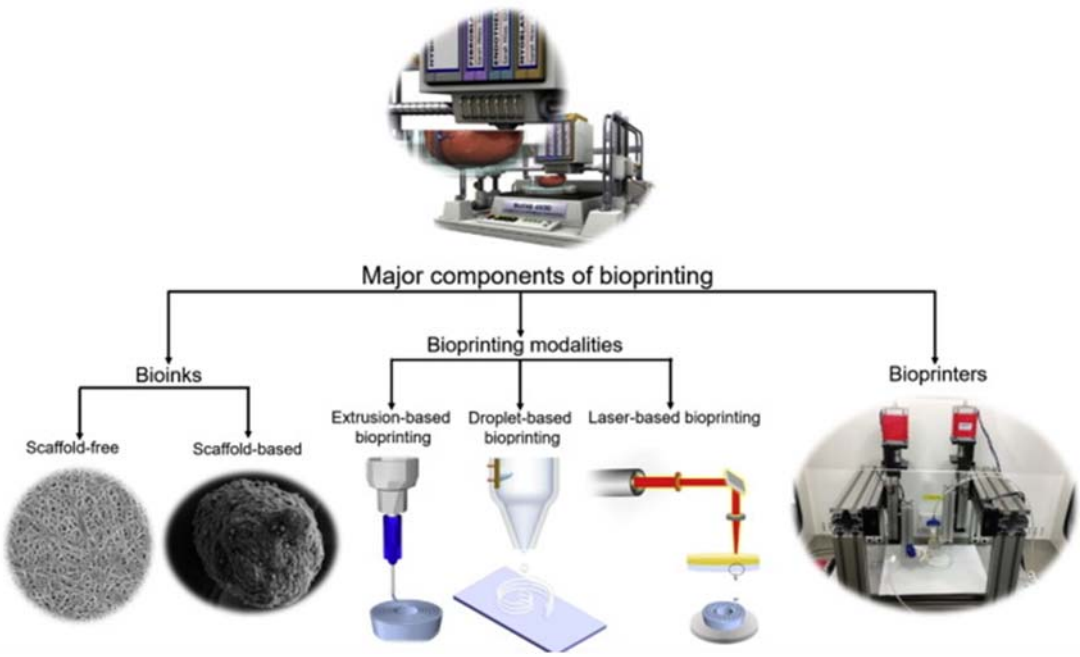

Figure 1.1
A schematic representation of the major components of bioprinting. *Bioprinter concept image: courtesy of Christopher Barnatt.*

deposition system is selected based on the sensitivity of the bioink, with the aim of gradually pushing it down without damaging cells present in the ink. Compared to other processes, it offers greater printing speed, and a large variety of bioinks are able to be used including scaffold-free inks (such as tissue spheroids and strands) or scaffold-based inks (such as hydrogels) [19]. Additionally, it provides better structural integrity due to the continuous deposition of filaments and easily incorporates with CAD software [9]. Postprinting cell viability is usually between 40% and 80% [22,23]. With the optimization of printing parameters such as deposition rate, pressure, and temperature, cell viability can be as high as 97% in the case of materials such as cell-laden gelatin methacrylamide constructs [24]. This technique has been derived from the material extrusion process from conventional additive manufacturing, and research has found EBB to be the most suitable method for the creation of large-scale constructs, primarily due to the aforementioned structural integrity. However, large constructs tend to affect cell viability, as the cells are exposed to dehydration and lack of nutrients during the long printing duration [19]. The technology also has a relatively poor resolution, with 100 μm as the optimal resolution [25,26]. EBB also requires the user to understand the rheology of the biomaterial, as shear stress on the wall of the nozzle tip and other areas of the printer may damage the living cells and alter the fluid properties, depending on its shear thinning capabilities [23].

1.1.2 Droplet-based bioprinting

Droplet-based bioprinting (DBB) manipulates bioink stored in a cartridge to form droplets utilizing gravity, atmospheric pressure, and fluid mechanics, in order to form constructs by controlling fluid properties such as surface tension and viscosity [21]. DBB originates from traditional paper printing, with Klebe's research in 1987 exhibiting the possibility of printing cells for the first time [3]. Four different methods of droplet formation can be utilized for this purpose, including inkjet [5,27], electrohydrodynamic jet [28–30], acoustic-droplet-ejection [31], and microvalve [32]. Among these, inkjet bioprinting has been the most common process, due to its simplistic principle of utilizing fluid mechanics, atmospheric pressure, and gravity to generate droplets [21]. Additionally, DBB offers many advantages from the perspective of biomaterials that can be used in this process, such as alginate, collagen, gelatin, and fibrin, along with providing the conditions needed for each material's cross-linking mechanism and cell viability [9,21,33]. The aforementioned issue of resolution seen in EBB is much more complex in the case of DBB, which is dependent on the process being used [34]. However, DBB has attracted interest in researchers due to its simplicity and low cost, and the possibility of rapid deposition using multiple nozzles [21]. DBB has cell viability of greater than 85% in some cases and good control over deposition rate and bioink volume [5,35]. However, there is a tendency of the orifice to clog easily, and the types of bioinks able to be used are very limited compared to EBB, considering the rheological properties needed for this process [21].

1.1.3 Laser-based bioprinting

Laser-based bioprinting (LBB) utilizes a laser pulse directed via mirrors onto a bioink layer above the substrate. This induces a high-pressure bubble to be formed by the ensuing heat, displacing some of the ink and spurring cell-laden droplets to be deposited on the substrate. This process is repeated several times in a layerwise fashion to fabricate the final construct [36,37]. LBB consists of two types, including processes based on photopolymerization (i.e., stereolithography and its modifications) and processes based on cell transfer (i.e., laser-induced forward transfer) [26]. The processes based on cell transfer use a laser pulse to create a bubble at the interface of a donor layer and ribbon layer which propels the bioink to create a jet [38]. They have high initial cell viability at greater than 95%. However, this tends to decrease with time, and becomes less than extrusion- and droplet-based printing [39]. On the other hand, processes based on photopolymerization use an ultraviolet (UV) laser to cure photo-cross-linkable hydrogels in a vat. Compared to EBB and DBB, LBB is a complex process, requiring complex machinery and extensive process control. The complexity associated with the use of a laser affects cell viability and material properties [40]. In addition, the process also requires the biomaterial to be compatible over several criteria, from fluid mechanics to rapid cross-linking after printing, introducing greater limitation for materials than DBB [37]. However, such complexity offers several benefits. For example, LBB has the highest resolution and precision among all three methods [37]. A unique advantage of LBB is to print multiple materials with good cell density, introducing the possibility of printing multiple cell types [41], which may provide the key for printing complex organs and tissues. However, the needs of using LBB to prepare the construct with high resolution (<50 μm) and cell density have to be considered, as LBB requires a highly intricate setup, making it the most expensive modality, and the long-term effect of laser exposure on the cells is still unknown [37,38].

Apart from laser, other light sources have been used as well, such as ultraviolet (UV) lamp and light-emitting diode (LED) sources. A common example would be digital light projector (DLP), with the use of selective UV radiation to create layerwise solid that builds from liquid photopolymer. However, the use of UV radiation induces the creation of free radicals that can cause cell damage and death [42]. Several studies have experimented on utilizing cell suspension in prepolymer solutions, and employed masks for inducing UV exposure only in the desired areas for the purpose of dimensional accuracy and formation of vasculature [43,44]. Several parameters and material combinations have to be controlled here for effective tissue printing and adequate cell viability. Despite the added complexities, porous hydrogel structure fabricated by this process shows narrow pore size distributions, good pore interconnectivity, and enhanced mechanical properties, with certain materials showcasing superior cell adhesion and proliferation [42].

Although there have been many bioprinting successes, including but not limited to skin [45,46], bone [47–50], cartilage [48,51–53], liver [32,54,55], and heart [56–59], many challenges must be overcome before human-scale organs become a reality. It is necessary to understand the advantages and limitations of each method of bioprinting in order to select the correct one for a given tissue and/or application. Table 1.1 summarizes the different aspects that should be considered for this purpose. A major issue at this stage is functionality, with printed organs only offering a fraction of the functionality of its natural counterpart [22]. Most printed tissues have only one dimension of functionality, but nativelike tissue should be bioprinted in a way that they will address most of the

Table 1.1: Differences between several parameters based on the printing methods: extrusion-, droplet-, and laser-based bioprinting.

Printer property	Extrusion-based	Droplet-based	Laser-based	References
Material	Large variety of biocompatible materials	Multicell printing is possible, critical for complex organs	High gelation speed	[60]
Viscosity	30 mPa s to $>6 \times 10^7$ mPa s	3.5–12 mPa s	1–300 mPa s	[22,61,62]
Gelation methods	Chemical, photo-cross-linking, shear thinning, temperature	Chemical, photo-cross-linking	Chemical, photo-cross-linking	[22,62]
Mechanical properties	High with good structure integrity	Low with poor structure integrity	Low	[63–65]
Preparation time	Medium	Low	High	[22]
Resolution	5 μm to a few millimeters	<1 pL to >300 pL droplets, 50 μm wide cell	Single cell manipulation possible	[21,22,37,61]
Accuracy	Low	High, with high throughput	High	[21,31]
Print speed	Slow (10–50 μm/s)	Fast (1–10,000 droplets per second)	Medium-fast (200–1600 mm/s)	[22,31,51,61]
Nozzle dynamics	Shear stress induced by nozzle wall and extrusion pressure	Noncontact nozzle, but nozzle can clog	Nozzle-free	[21,31]
Cell damage source	Damage due to shearing in the nozzle	Cell aggregation may occur	Damage due to generation of heat	[21]
Cell viability	40%–80%	>85%	>95%	[21,22,51,63,66]
Cell density	High, cell spheroids	Low, $<10^6$ cells/mL	Medium, 10^8 cells/mL	[22,61]
Printer cost	Low	Medium	High	[22,67]

dimensions at the same time. In this perspective, the functionality of the bioprinted tissue is categorized into seven dimensions including cell density, vascularization, innervation, heterogeneity, engraftment, mechanics, and tissue-specific function.

1.2 The organization of the book

As the field of bioprinting is developing rapidly in recent years, we intend to cover the state-of-the-art advance in applications of bioprinting in this book. First of all, this book contains a comprehensive discussion on bioprinting, covering the major considerations during prebioprinting, bioprinting, and postbioprinting stages. Next, as major contents of this book, detailed description about applications of bioprinting in different biomedical fields will be presented by several chapters, such as skin, cartilage, bone, vascularized tissue, etc. As a separate chapter, overview about intraoperative bioprinting will also be presented in this book, which has been used for some of the abovementioned biomedical applications and widely considered as one of the important future trends in this area. Lastly, ethical and regulation concerns about the clinical utilization of bioprinting will be also discussed. Overall, as compared to current books which largely focus on the bioprinting techniques, this book is more application-oriented, showing reader the great value of bioprinting. This book is more suitable for a reader who has already some basic background about bioprinting, and is seeking a deep and broad understanding about biomedical applications of bioprinting.

The book is organized into 9 chapters: Introduction, Considerations of Bioprinting, Bioprinting of Cartilage, Bioprinting of Bone, Bioprinting of Skin, Bioprinting of Vascularized Tissues, Bioprinting of Other Tissues and Organs, Intraoperative Bioprinting, and Ethical and Regulatory Concerns of Bioprinting.

This chapter covers the background introduction about bioprinting for reader who is not familiar with this field. Particularly, introduction of different bioprinting modalities (including extrusion-, laser-, and droplet-based bioprinting) is presented, in terms of their principles, setups, pros and cons, etc.

Chapter 2, “Considerations of Bioprinting” presents the systematical discussion about the considerations in the entire procedure of bioprinting. These stages can be divided into three broad categories: prebioprinting, bioprinting, and postbioprinting. Each stage can influence others and has a bearing on the performance of fabricated constructs. For example, considerations prior to bioprinting include selection of bioprinting technique, cell source, imaging, etc. Considerations during bioprinting include bioink, resolution, repeatability, etc. Considerations after bioprinting include tissue maturation, stimulation, etc. All these factors have to be recognized and optimized to obtain the desired outcomes.

Chapter 3, "Bioprinting of Cartilage" presents the application of bioprinting in cartilage tissue reconstruction. The capabilities of different techniques including scaffold-based and scaffold-free have allowed duplication of anatomical structure, biological function, and mechanical properties of the native cartilage, and particularly enabled the advances toward zonal differentiation. This chapter reviews the state-of-the-art researches on bioprinted cartilage and demonstrates that bioprinting has potential capacity for clinical cartilage reconstruction.

Chapter 4, "Bioprinting of Bone" provides the reader with recent advancements in bioprinting of bone. The large number of skeletal disorders induced by trauma or disease have resulted in a huge demand for bone treatments. Three-dimensional bioprinting offers clinically relevant and mechanically robust bone constructs. Recent studies have shown promise in the field of bone tissue engineering through rebuilding the 3D microenvironment of the native bone. However, it needs more exploration to maintain the viability and differentiation potential of bioprinted constructs, and enable their subsequent preclinical testing.

Chapter 5, "Bioprinting of Skin" reviews the aspects related to the 3D bioprinting of skin, such as medical imaging, 3D modeling, biomaterials, bioprinting technologies, along with the challenges and future prospects. Bioprinting of skin substitutes helps overcome the limitations of traditional skin treatment methods, in terms of technology, time, and cost. Three-dimensional bioprinting of skin is a promising technology that can achieve rapid and reliable production of biomimetic cellular skin substitutes, satisfying both clinical and industrial needs.

Chapter 6, "Bioprinting of Vascularized Tissues" presents the latest progress on bioprinting of vascularized and functional tissues to the reader. Although organ bioprinting is attractive, it remains elusive due to limitations associated with biology, bioprinting technology, bioink material, and the postbioprinting maturation process. The bioprinting of vascularized and functional tissues is an intermediate stage toward achieving organ-level complexity. In recent years, more and more attempts have been reported to create microcirculation and large-sized vascular channels.

Chapter 7, "Bioprinting of Other Tissues and Organs" discusses applications of bioprinting in regeneration of other tissues and organs such as cardiac tissue, kidney, liver, nerve tissue, pancreatic tissue, and lung. In terms of organ bioprinting, different miniorgans (organoids) have been developed and bioprinted in recent years, such as islets for pancreases, alveolar sacs for lung, cardiac organoids for heart, miniliver, etc. Since the number of existing studies on these applications are relatively less compared to those introduced in previous chapters, they are combined and reviewed in this chapter.

Chapter 8, "Intraoperative Bioprinting" highlights the intraoperative bioprinting techniques, in which the defect can be rapidly scanned to get its geomatical information and then repaired via bioprinting on a live subject in a surgical setting. This chapter provides the reader the current achievement and limitations of intraoperative bioprinting, from engineering and clinical points of view, as well as possibilities of future translation of bioprinting technologies from bench to bedside.

Chapter 9, "Ethical and Regulatory Concerns of Bioprinting" presents challenges of bioprinting in terms of ethics, policies, regulations, and social acceptance. While the research and commercialization associated with bioprinting are moving forward rapidly, the ethical and regulatory issues surrounding the technology are not yet well addressed. Recognizing these concerns is not only the social responsibility of researchers in this field, but also in the interest of the future of bioprinting.

1.3 Summary

In this chapter, an evaluation of 3D bioprinting and notable achievements in the past decade are illustrated. The principles, elements, and classification of bioprinting are discussed primarily including extrusion-, droplet-, and laser-based technologies. Bioprinting has shown great promise in fabrication of in vitro tissues/organs for applications such as transplantation, drug screening, and tumor model. With the application of bioprinting in tissue engineering, it has begun to build anatomically correct tissue structures by patterning of bioactive substances in the predetermined locations with better cell-cell or cell-matrix interaction. Although bioprinting is still facing a number of challenges, it appears poised to advance tissue engineering toward organ regeneration, ultimately alleviating organ shortages and saving lives.

References

[1] C.W. Hull, Apparatus for Production of Three Dimensional Objects by Stereolithography, US Patent, 4,575,330, 1986, pp. 1–16.
[2] J.P. Martins, M.P.A. Ferreira, N.Z. Ezazi, J.T. Hirvonen, H.A. Santos, G. Thrivikraman, C.M. França, A. Athirasala, A. Tahayeri, L.E. Bertassoni, 3D printing: prospects and challenges, in: V. Uskoković, D.P. Uskoković (Eds.), Nanotechnologies in Preventive and Regenerative Medicine, Elsevier, 2018, pp. 299–379.
[3] R.J. Klebe, Cytoscribing: a method for micropositioning cells and the construction of two- and three-dimensional synthetic tissues, Experimental Cell Research 179 (2) (1988) 362–373.
[4] I.T. Ozbolat, K.K. Moncal, H. Gudapati, Evaluation of bioprinter technologies, Additive Manufacturing 13 (2017) 179–200.
[5] T. Xu, J. Jin, C. Gregory, J.J. Hickman, T. Boland, Inkjet printing of viable mammalian cells, Biomaterials 26 (1) (2005) 93–99.

[6] R. Lanza, H. Chung, J. Yoo, P. Wettstein, C. Blackwell, N. Borson, E. Hofmeister, G. Schuch, S. Soker, C. Moraes, M. West, A. Atala, Generation of histocompatible tissues using nuclear transplantation, Nature Biotechnology 20 (2002) 689−696.
[7] T.R. Olsen, F. Alexis, Bioprocessing of tissues using cellular spheroids, Journal of Bioprocessing & Biotechniques 4 (2014) 1−4.
[8] T. Wohlers, T. Gornet, History of Additive Manufacturing, 2016, pp. 1−24.
[9] I.T. Ozbolat, 3D Bioprinting: Fundamentals, Principles and Applications.
[10] H.W. Kang, S.J. Lee, I.K. Ko, C. Kengla, J.J. Yoo, A. Atala, A 3D bioprinting system to produce human-scale tissue constructs with structural integrity, Nature Biotechnology 34 (2016) 312−319.
[11] I.T. Ozbolat, W. Peng, V. Ozbolat, Application areas of 3D bioprinting, Drug Discovery Today 21 (8) (2016) 1257−1271.
[12] A. Bigham, F. Foroughi, E. Rezvani Ghomi, M. Rafienia, R.E. Neisiany, S. Ramakrishna, The journey of multifunctional bone scaffolds fabricated from traditional toward modern techniques, Bio-Design and Manufacturing 3 (4) (2020) 281−306.
[13] H. Lee, D.-W. Cho, One-step fabrication of an organ-on-a-chip with spatial heterogeneity using a 3D bioprinting technology, Lab on a Chip 16 (14) (2016) 2618−2625.
[14] W. Hou, S. Hu, K.-t. Yong, J. Zhang, H. Ma, Cigarette smoke-induced malignant transformation via STAT3 signalling in pulmonary epithelial cells in a lung-on-a-chip model, Bio-Design and Manufacturing 3 (4) (2020) 383−395.
[15] F. Sharifi, O. Yesil-Celiktas, A. Kazan, S. Maharjan, S. Saghazadeh, K. Firoozbakhsh, B. Firoozabadi, Y.S. Zhang, A hepatocellular carcinoma−bone metastasis-on-a-chip model for studying thymoquinone-loaded anticancer nanoparticles, Bio-Design and Manufacturing 3 (3) (2020) 189−202.
[16] L.G. Zhang, J.P. Fisher, K.W. Leong, S.C. Sklare, T.B. Phamduy, J.L. Curly, Y. Huang, D.B. Chrisey, 3D Bioprinting and Nanotechnology in Tissue Engineering and Regenerative Medicine, 2015.
[17] J.W. Jung, J.-S. Lee, D.-W. Cho, Computer-aided multiple-head 3D printing system for printing of heterogeneous organ/tissue constructs, Scientific Reports 6 (1) (2016) 21685.
[18] S. Knowlton, A. Joshi, B. Yenilmez, I.T. Ozbolat, C.K. Chua, A. Khademhosseini, S. Tasoglu, Advancing cancer research using bioprinting for tumor-on-a-chip platforms, International Journal of Bioprinting 2 (2016) 3−8.
[19] I.T. Ozbolat, M. Hospodiuk, Current advances and future perspectives in extrusion-based bioprinting, Biomaterials 76 (2016) 321−343.
[20] W. Peng, D. Unutmaz, I.T. Ozbolat, Bioprinting towards physiologically relevant tissue models for pharmaceutics, Trends in Biotechnology 34 (2016) 722−732.
[21] H. Gudapati, M. Dey, I. Ozbolat, A comprehensive review on droplet-based bioprinting: past, present and future, Biomaterials 102 (2016) 20−42.
[22] S.V. Murphy, A. Atala, 3D bioprinting of tissues and organs, Nature Biotechnology 32 (8) (2014) 773−785.
[23] R. Chang, J. Nam, W. Sun, Effects of dispensing pressure and nozzle diameter on cell survival from solid freeform fabrication-based direct cell writing, Tissue Engineering A 14 (2008) 41−48.
[24] T. Billiet, E. Gevaert, T. De Schryver, M. Cornelissen, P. Dubruel, The 3D printing of gelatin methacrylamide cell-laden tissue-engineered constructs with high cell viability, Biomaterials 35 (1) (2014) 49−62.
[25] B. Duan, L.A. Hockaday, K.H. Kang, J.T. Butcher, 3D bioprinting of heterogeneous aortic valve conduits with alginate/gelatin hydrogels, Journal of Biomedical Materials Research A 101 (5) (2013) 1255−1264.
[26] A.B. Dababneh, I.T. Ozbolat, Bioprinting technology: a current state-of-the-art review, Journal of Manufacturing Science and Engineering 136 (6) (2014).
[27] C. Xu, W. Chai, Y. Huang, R.R. Markwald, Scaffold-free inkjet printing of three-dimensional zigzag cellular tubes, Biotechnology and Bioengineering 109 (12) (2012) 3152−3160.
[28] S.N. Jayasinghe, A.N. Qureshi, P.A.M. Eagles, Electrohydrodynamic jet processing: an advanced electric-field-driven jetting phenomenon for processing living cells, Small 2 (2006) 216−219.

[29] M.S. Onses, E. Sutanto, P.M. Ferreira, A.G. Alleyne, J.A. Rogers, Mechanisms, capabilities, and applications of high-resolution electrohydrodynamic jet printing, Small 11 (34) (2015) 4237−4266.
[30] L. Gasperini, D. Maniglio, C. Migliaresi, Microencapsulation of cells in alginate through an electrohydrodynamic process, Journal of Bioactive and Compatible Polymers 28 (2013) 413−425.
[31] S. Tasoglu, U. Demirci, Bioprinting for stem cell research, Trends in Biotechnology 31 (1) (2013) 10−19.
[32] A. Faulkner-Jones, C. Fyfe, D.-J. Cornelissen, J. Gardner, J. King, A. Courtney, W. Shu, Bioprinting of human pluripotent stem cells and their directed differentiation into hepatocyte-like cells for the generation of mini-livers in 3D, Biofabrication 7 (4) (2015) 044102.
[33] Y. Wu, B. Wu, V. Sanjairaj, Y. Wong, J. Fuh, Crimped fiber with controllable patterns fabricated via electrohydrodynamic jet printing, Materials & Design 131 (2017).
[34] A.D. Graham, S.N. Olof, M.J. Burke, J.P.K. Armstrong, E.A. Mikhailova, J.G. Nicholson, S.J. Box, F.G. Szele, A.W. Perriman, H. Bayley, High-resolution patterned cellular constructs by droplet-based 3D printing, Scientific Reports 7 (1) (2017) 7004.
[35] T. Xu, H. Kincaid, A. Atala, J. Yoo, High-throughput production of single-cell microparticles using an inkjet printing technology, Journal of Manufacturing Science and Engineering 130 (2008).
[36] L. Koch, M. Gruene, C. Unger, B. Chichkov, Laser assisted cell printing, Current Pharmaceutical Biotechnology 14 (2013) 91−97.
[37] B. Guillotin, M. Ali, A. Ducom, S. Catros, V. Keriquel, A. Souquet, M. Remy, J.-C. Fricain, F. Guillemot, Laser-assisted bioprinting for tissue engineering, in: G. Forgacs, W. Sun (Eds.), Biofabrication Micro-Nano-Fabrication Printing Patterning Assem, William Andrew Publishing, Boston, 2013, pp. 95−118.
[38] A.N. Leberfinger, D.J. Ravnic, A. Dhawan, I.T. Ozbolat, Concise review: bioprinting of stem cells for transplantable tissue fabrication, Stem Cells Translational Medicine 6 (2017) 1940−1948.
[39] E.S. Bishop, S. Mostafa, M. Pakvasa, H.H. Luu, M.J. Lee, J.M. Wolf, G.A. Ameer, T.-C. He, R.R. Reid, 3-D bioprinting technologies in tissue engineering and regenerative medicine: current and future trends, Genes & Diseases 4 (4) (2017) 185−195.
[40] B. Hopp, T. Smausz, N. Kresz, N. Barna, Z. Bor, L. Kolozsvári, D.B. Chrisey, A. Szabó, A. Nógrádi, Survival and proliferative ability of various living cell types after laser-induced forward transfer, Tissue Engineering 11 (11−12) (2005) 1817−1823.
[41] B. Guillotin, A. Souquet, S. Catros, M. Duocastella, B. Pippenger, S. Bellance, R. Bareille, M. Rémy, L. Bordenave, J. Amédée, F. Guillemot, Laser assisted bioprinting of engineered tissue with high cell density and microscale organization, Biomaterials 31 (28) (2010) 7250−7256.
[42] B.K. Gu, D.J. Choi, S.J. Park, M.S. Kim, C.M. Kang, C.-H. Kim, 3-dimensional bioprinting for tissue engineering applications, Biomaterials Research 20 (2016) 12.
[43] X. Ma, X. Qu, W. Zhu, Y.-S. Li, S. Yuan, H. Zhang, J. Liu, P. Wang, C.S.E. Lai, F. Zanella, G.-S. Feng, F. Sheikh, S. Chien, S. Chen, Deterministically patterned biomimetic human iPSC-derived hepatic model via rapid 3D bioprinting, Proceedings of the National Academy of Sciences 113 (2016) 2206−2211.
[44] W. Zhu, X. Qu, J. Zhu, X. Ma, S. Patel, J. Liu, P. Wang, C.S.E. Lai, M. Gou, Y. Xu, K. Zhang, S. Chen, Direct 3D bioprinting of prevascularized tissue constructs with complex microarchitecture, Biomaterials 124 (2017) 106−115.
[45] N. Cubo, M. Garcia, J.F. Del Cañizo, D. Velasco, J.L. Jorcano, 3D bioprinting of functional human skin: production and in vivo analysis, Biofabrication 9 (1) (2016) 015006.
[46] A. Skardal, D. Mack, E. Kapetanovic, A. Atala, J.D. Jackson, J. Yoo, S. Soker, Bioprinted amniotic fluid-derived stem cells accelerate healing of large skin wounds, Stem Cells Translational Medicine 1 (11) (2012) 792−802.
[47] L.J. Pourchet, A. Thepot, M. Albouy, E.J. Courtial, A. Boher, L.J. Blum, C.A. Marquette, Human skin 3D bioprinting using scaffold-free approach, Advanced Healthcare Materials 6 (2017) 1601101.
[48] G. Gao, T. Yonezawa, K. Hubbell, G. Dai, X. Cui, Inkjet-bioprinted acrylated peptides and PEG hydrogel with human mesenchymal stem cells promote robust bone and cartilage formation with minimal printhead clogging, Biotechnology Journal 10 (10) (2015) 1568−1577.

[49] A.E. Jakus, R.N. Shah, Multi and mixed 3D-printing of graphene-hydroxyapatite hybrid materials for complex tissue engineering, Journal of Biomedical Materials Research A 105 (1) (2017) 274−283.
[50] H. Zhang, X. Mao, Z. Du, W. Jiang, X. Han, D. Zhao, D. Han, Q. Li, Three dimensional printed macroporous polylactic acid/hydroxyapatite composite scaffolds for promoting bone formation in a critical-size rat calvarial defect model, Advanced Materials 17 (2016) 136−148.
[51] A.C. Daly, S.E. Critchley, E.M. Rencsok, D.J. Kelly, A comparison of different bioinks for 3D bioprinting of fibrocartilage and hyaline cartilage, Biofabrication 8 (4) (2016) 045002.
[52] N. Khoshnood, A. Zamanian, A comprehensive review on scaffold-free bioinks for bioprinting, Bioprinting 19 (2020) e00088.
[53] X. Cui, K. Breitenkamp, M.G. Finn, M. Lotz, D.D. D'Lima, Direct human cartilage repair using three-dimensional bioprinting technology, Tissue Engineering Part A 18 (2012) 1304−1312.
[54] S. Massa, M.A. Sakr, J. Seo, P. Bandaru, A. Arneri, S. Bersini, E. Zare-Eelanjegh, E. Jalilian, B.-H. Cha, S. Antona, A. Enrico, Y. Gao, S. Hassan, J.P. Acevedo, M.R. Dokmeci, Y.S. Zhang, A. Khademhosseini, S.R. Shin, Bioprinted 3D vascularized tissue model for drug toxicity analysis, Biomicrofluidics 11 (4) (2017) 044109.
[55] C. Zhong, H.-Y. Xie, L. Zhou, X. Xu, S.-S. Zheng, Human hepatocytes loaded in 3D bioprinting generate mini-liver, Hepatobiliary and Pancreatic Diseases International 15 (5) (2016) 512−518.
[56] R. Gaetani, P.A. Doevendans, C.H.G. Metz, J. Alblas, E. Messina, A. Giacomello, J.P.G. Sluijter, Cardiac tissue engineering using tissue printing technology and human cardiac progenitor cells, Biomaterials 33 (2012) 1782−1790.
[57] C.S. Ong, T. Fukunishi, A. Nashed, A. Blazeski, H. Zhang, S. Hardy, D. DiSilvestre, L. Vricella, J. Conte, L. Tung, G. Tomaselli, N. Hibin, Creation of cardiac tissue exhibiting mechanical integration of spheroids using 3D bioprinting, Journal of Visualized Experiments 125 (125) (2017) e55438.
[58] R. Gaebel, N. Ma, J. Liu, J. Guan, L. Koch, C. Klopsch, M. Gruene, A. Toelk, W. Wang, P. Mark, F. Wang, B. Chichkov, W. Li, G. Steinhoff, Patterning human stem cells and endothelial cells with laser printing for cardiac regeneration, Biomaterials 32 (2011) 9218−9230.
[59] M. Izadifar, D. Chapman, P. Babyn, X. Chen, M.E. Kelly, UV-assisted 3D bioprinting of nano-reinforced hybrid cardiac patch for myocardial tissue engineering, Tissue Engineering Part C Methods 24 (2) (2018) 74−88.
[60] M. Hospodiuk, M. Dey, D. Sosnoski, I.T. Ozbolat, The bioink: a comprehensive review on bioprintable materials, Biotechnology Advances 35 (2) (2017) 217−239.
[61] K. Hölzl, S. Lin, L. Tytgat, S. Van Vlierberghe, L. Gu, A. Ovsianikov, Bioink properties before, during and after 3D bioprinting, Biofabrication 8 (3) (2016) 032002.
[62] Y. He, F. Yang, H. Zhao, Q. Gao, B. Xia, J. Fu, Research on the printability of hydrogels in 3D bioprinting, Scientific Reports 6 (2016) 29977.
[63] J.H.Y. Chung, S. Naficy, Z. Yue, R. Kapsa, A. Quigley, S.E. Moulton, G.G. Wallace, Bio-ink properties and printability for extrusion printing living cells, Biomaterials Science 1 (7) (2013) 763−773.
[64] T. Boland, X. Tao, B.J. Damon, B. Manley, P. Kesari, S. Jalota, S. Bhaduri, Drop-on-demand printing of cells and materials for designer tissue constructs, Materials Science and Engineering: C 27 (3) (2007) 372−376.
[65] J.M. Courtney, Mechanical properties of biomaterials, Journal of Biomedical Engineering 3 (3) (1981) 260−261.
[66] H. Cui, M. Nowicki, J.P. Fisher, L.G. Zhang, 3D bioprinting for organ regeneration, Advanced Healthcare Materials 6 (1) (2017), https://doi.org/10.1002/adhm.201601118.
[67] A.N. Leberfinger, K.K. Moncal, D.J. Ravnic, I.T. Ozbolat, 3D printing for cell therapy applications, in: D. Emerich, G. Orive (Eds.), Cell Therapy. Molecular and Translational Medicine, Humana Press, Cham, 2017.

This page intentionally left blank

CHAPTER 2

Considerations of bioprinting

2.1 Introduction

In the past few years, the applications of tissue engineered constructs have expanded from clinical tissue regeneration to fabrication of tissue models for drug discovery [1,2], pathological understanding [3,4] and controlled drug delivery systems [5]. The key enablers for these applications are advanced fabrication techniques that allow generation of tissue constructs mimicking the complex native extracellular matrix (ECM) organization [6]. One of the most emerging techniques is bioprinting, which allows for precise deposition of cells and biomaterial components in predefined computer generated designs [7]. Indeed, experimental evidences on bioprinting have accrued at very rapid pace with increasing number of publications and involved research groups worldwide in recent times [8]. These concoctions of cells and biomaterials (in some cases only cell aggregates) are often referred to as bioinks [9]. The success of bioprinted tissue constructs is invariably determined by the properties of bioink. Usually, the process of generating bioprinted tissue constructs involves several steps. The first step is the creation of a computer-aided design model, suitable for bioprinting, whose resolution is determined by the applied image acquisition techniques, such as three-dimensional (3D) laser scanning, microcomputed tomography (μ-CT), and magnetic resonance imaging (MRI). In the design stage, it is also important to note if the methods used for generating a 3D model could be easily deployed in a surgical setting (e.g., short computational interval, and good compatibility between software and hardware). After the design is finalized, the fabrication process commences along with obtaining cells with sufficient quantity and robustness. Bioink can be characterized by different parameters prior to bioprinting. In addition, clinical application becomes more feasible if the cellular and biomaterial components are obtained by minimally invasive surgical procedures and if the protocols followed for expansion of cells are cost effective and achievable under general good laboratory practice (GLP) conditions. Thereafter, at the bioprinting stage, multiple factors influence the properties of engineered constructs. Cell densities that can be printed along with appropriate physicochemical properties become important determinants of dispensation through printheads. Such physicochemical properties include rheology, surface properties, and most importantly, the gelation kinetics of the bioink. One of the most important challenges is to figure out a balance between printability and immediate solidification after bioprinting, so that the desired structure is retained. Alternatively, bioprinting can be performed in a microgel

3D Bioprinting in Tissue and Organ Regeneration. https://doi.org/10.1016/B978-0-12-824291-9.00008-7

(e.g., carbopol) support bath or using nanoclays (e.g., laponite) to directly print structures in air without the need for instantaneous gelation [10–14]. Bioink formula must also be affordable and biocompatible. In particular, for fabrication of hollow organ structures, it is required to use sacrificial inks and hence, the difference in properties of two types of bioink becomes important. In turn, the use of sacrificial inks is determined by the physical properties of the functional inks and aspect ratio of the vascular network to be fabricated. Subsequently, the applied bioprinting technique makes an important contribution to the mechanical and structural properties of constructs.

As stated in Chapter 1, current bioprinting technologies are based on one among the following: extrusion-based bioprinting (EBB), droplet-based bioprinting (DBB), or laser-based bioprinting (LBB), as depicted in Fig. 2.1. EBB exploits automated three-axis robotic system for continuous extrusion of bioinks in filament forms. Herein, pneumatic or mechanical driven dispensing systems are mostly employed. In EBB, high extrusion pressure and resulting shear stress are the cause of concern for cell survival, but the modality usually produces most mechanically robust constructs amongst all bioprinting techniques. In DBB, the bioink made up of living cells and other biological materials (e.g., hydrogels) in culture media is deposited in droplets form with precise noncontact positioning. The droplets are generated by one of thermal-, piezoelectric- or electrostatic drop-on-demand technologies. DBB generally provides appreciable cell viability, though electrohydrodynamic jetting or microvalve bioprinting can facilitate 80%–90% viability [15,16]. DBB is a relatively rapid technique with a low cost and high resolution, but it can result in nonhomogenous droplet size and cause nozzle-clogging while printing high density bioinks [15]. LBB operates on the principle of a laser energy beam utilized for

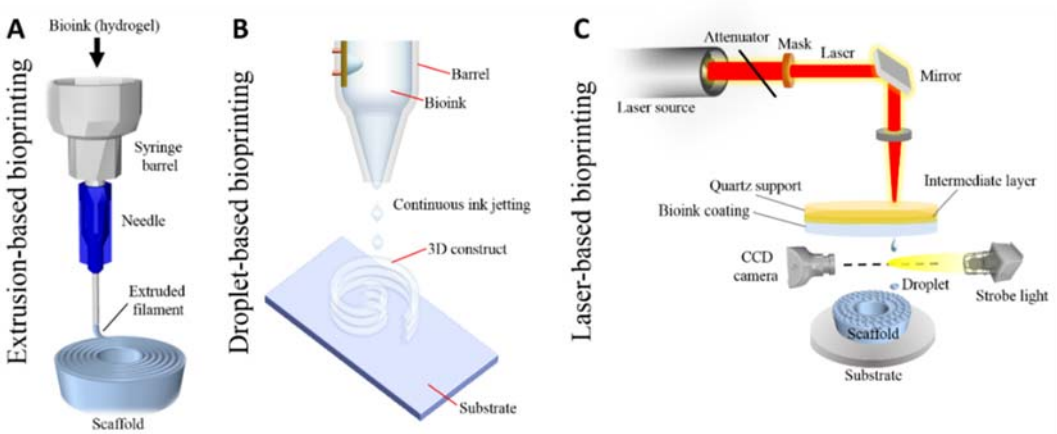

Figure 2.1
Mechanisms of bioprinting techniques: (A) extrusion-based bioprinting, (B) droplet-based bioprinting, (C) laser-based bioprinting.

precise patterning of cells. Laser energy can be used in two different modalities, one of which involves photopolymerization (e.g., stereolithography or two-photon polymerization), and the other modality is based on cell transfer (e.g., laser guided direct writing and laser induced forward transfer). LBB is advantageous over the other modalities as it causes minimal clogging and damage to cell survival. Several advances in digital projection stereolithography techniques have been applied for bioprinting applications [17,18]. Though LBB also provides high resolution, it is an expensive and time consuming modality [19,20]. Each bioprinting technique has advantages and disadvantages with respect to cell survival against the process. Apart from the basic processes associated with each bioprinting modality, several innovations like aerosol-assisted cross-linking, use of electric fields to reduce shear stresses, hybrid electrospinning-bioprinting, and core/shell bioprinting have been developed [21,22]. In all cases, it is important that cellular biomaterials are printed in a manner that allows intricate cell-material interactions, which are crucial for the tissue development. During this phase, it is essential that cells are printed with sufficient resolution to facilitate proper cell-cell interactions. Finally, bioprinted tissue constructs are required to become mature in suitable bioreactors before they can be implanted. Degradation of the biomaterial support, if present, also demonstrates significance during the post-bioprinting stage.

In this chapter, we critically present the current literature on abovementioned aspects of bioprinting technology from the design phase to postbioprinting steps. The complete bioprinting process, including prebioprinting, bioprinting and postbioprinting along with their components, is schematically illustrated in Fig. 2.2. As shown in Fig. 2.2, bioprinting is a multidisciplinary area, and the successful fabrication of tissue constructs requires

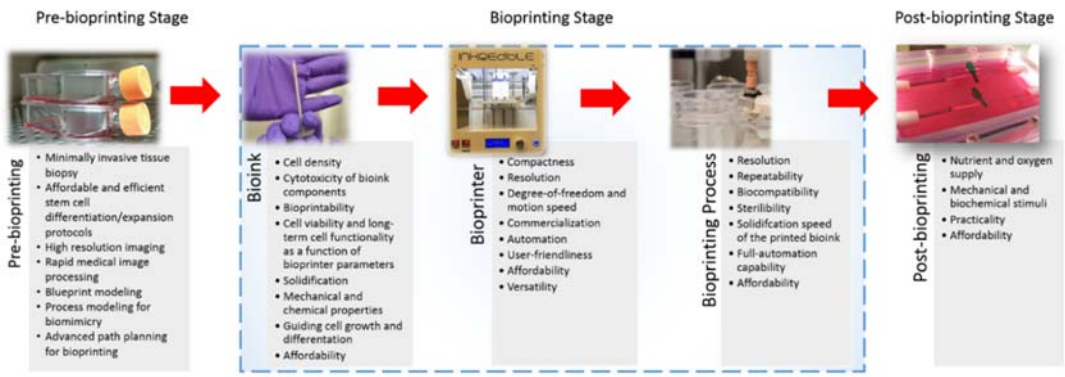

Figure 2.2

Stages in the entire 3D bioprinting process, including prebioprinting, bioprinting, and postbioprinting, and their major components. *Bioreactor image taken with permission from C. Norotte, F.S. Marga, L.E. Niklason, G. Forgacs, Scaffold-free vascular tissue engineering using bioprinting, Biomaterials 30 (30) (2009) 5910–5917.*

understanding the dynamic interaction between different disciplines. However, most reviews available till date only concentrate on single domain specific analysis of current literatures, and a comprehensive presentation on all aspects has not been demonstrated yet. Therefore, we provide all the stages involved in this process and thoroughly discuss these stages including prebioprinting, bioprinting, and postbioprinting with their essential components.

2.2 Prebioprinting stage

The pre-bioprinting stage plays an extremely crucial role in determining the properties of bioprinted constructs. To ensure that the adequate quality of cells is obtained along with anatomically correct tissue models and appropriate process planning for bioprinting, it becomes extremely important in pre-bioprinting stage that the correct procedures are adopted. Fig. 2.3 demonstrates the essential components of prebioprinting stages including minimally invasive tissue biopsy, affordable and efficient stem cell differentiation/expansion protocols, high resolution imaging, rapid medical image processing, blueprint modeling, process modeling for biomimicry, and advanced path planning for bioprinting, which are thoroughly discussed in the following subsections.

2.2.1 Minimally invasive tissue biopsy

In order to minimize the chance of immune-rejection of bioprinted tissues, patient's own cells are preferred as the cell source. Cell acquisition methods are important since most laboratories working on bioprinting primarily focus on material, process, and structure development, in which model/standard cell lines are employed. However, for bioprinting to overcome the barrier of clinical translation, primary cells obtained from the patients are essential and should be provided equal importance. A patient-lab-patient strategy is essential for the success of the process. Cells with different phenotypes and genotypes are bound to show different survival, proliferation, and maturation kinetics under the bioprinting conditions and hence topical overview is provided as the roadmap that should be followed to obtain functional constructs by bioprinting. Similarly, in situ tissue engineering using recruitment of host cells is a useful strategy but limited to younger patients or patients with good nutritional status. Additionally in vitro tissue engineering is advantageous for generating vascularized constructs. Therefore, the acquisition of cells is an important aspect for bioprinting. For collecting cells, minimally invasive biopsy is gaining importance for successful 3D bioprinting and other regenerative approaches. In medical diagnosis, biopsy has been the gold standard and sometimes the only choice of harvesting tissue for disease prognosis [29,30]; however, the need of routine screening has increased dramatically with increase in healthcare awareness. To meet up the requirement, surgical oncology has been evolving toward minimally invasive biopsy methods. For

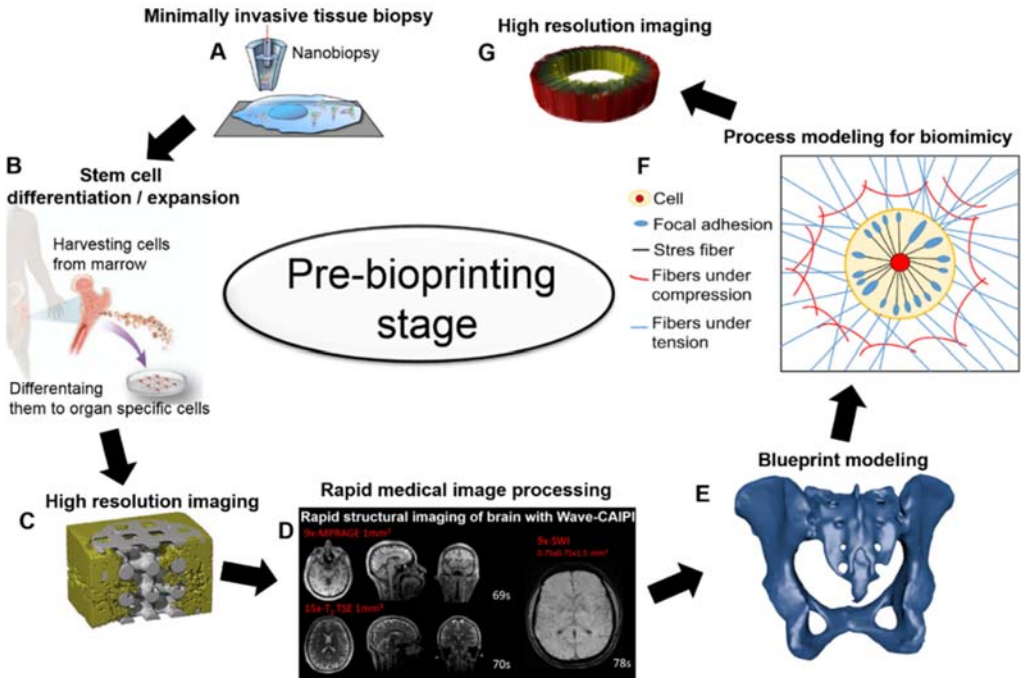

Figure 2.3

The major components of the prebioprinting stage: (A) A schematic of nanobiopsy; (B) A schematic of stem cell isolation; (C) 3D Reconstruction of scaffold (white) and bone ingrowth (yellow); only part of the cylindrical scaffold is displayed, as to be able to look inside the scaffold; (D) A high resolution whole brain imaging of MPRAGE, T2-TSE and SWI; (E) An STL file of a pelvis; (F) A schematic of a cell adhered to fibrous ECM; (G) Advanced path planning for multilayered structure printing. *Modified with permission from (A) P. Actis, M.M. Maalouf, H.J. Kim, A. Lohith, B. Vilozny, R.A. Seger, N. Pourmand, Compartmental genomics in living cells revealed by single-cell nanobiopsy, ACS Nano 8 (1) (2014) 546–553. (B) J. Vacanti, R.S. Langer, R. Lanza, Principles of Tissue Engineering, Academic Press, 2007. (C) G. Van Lenthe, H. Hagenmuller, M. Bohner, S. Hollister, L. Meinel, R. Muller, Nondestructive micro-computed tomography for biological imaging and quantification of scaffold–bone interaction in vivo, Biomaterials 28 (15) (2007) 2479–2490. (D) B.A. Poser, K. Setsompop, Pulse sequences and parallel imaging for high spatiotemporal resolution MRI at ultra-high field, NeuroImage (December 2016) (2017) 1–18. (G) I.T. Ozbolat, A.K.M.B. Khoda, Design of a new parametric path plan for additive manufacturing of hollow porous structures with functionally graded materials, Journal of Computing and Information Science in Engineering 14 (4) (2014) 41005–41013.*

example, through special vacuum assisted needle biopsy system [31], a tiny amount of skin sample can be collected which was not earlier possible with conventional systems. Another advantage of such system is to introduce a very little deformation or secondary wound at the biopsy site, which recovers within minimal time without any scar formation. Upon early diagnosis, the treatment of primary tumor site without surgical intervention can be performed through different emerging minimally invasive procedures such as

focused ultrasound, MRI or X-ray, CT-guided biopsy. Another approach called percutaneous stereotactic method has been recently applied for biopsy collection [32]. Among several minimally invasive approaches, the most extensive work has been done on radiofrequency ablation [33]. In this method, under imaging guidance, a radio frequency probe is inserted at the tumor site, and high frequency alternating current is applied through the probe that causes an irreversible destruction of tumor cells [34]. Another approach for such treatment is focused ultrasound ablation, in which ultrasound is focused on the target tumor and temperature is increased rapidly through converting the acoustic energy to heat [35]. For this method, high resolution imaging guide (e.g., MRI) is required for diagnostic accuracy [36,37].

In bioprinting, apart from harvesting of cells as source for in vitro tissue engineering, harvesting of a volumetric tissue sample (i.e., adipose) is gaining importance for preparation of decellularized ECM-based bioink [38]. In this regard, minimally invasive biopsy is becoming popular for obtaining live tissues. Although there are several ways for harvesting tissues [39], they require incisional process to collect the tissue and multilayered suturing to close the incision site, which sometimes give rise to different clinical complications such as stitch abscesses and formation of hematoma or seroma. Due to fast development of tissue engineering technology, minimally invasive technique will play the critical role in making the autologous tissue engineering a clinical reality [40].

Researchers have explored the possibility of microbiopsy or needle biopsy, in which a small amount of tissue of approximately 15−20 mg is collected through an automatic 14 gauge microbiopsy needle. In this method, a small skin puncture is sufficient for successful collection of a biopsy sample [41]. Though it is at present a challenge if adequate cell numbers can be generated from single cell biopsy and may require conjunction with cloning techniques in the future, some authors have started exploring their potential in tissue engineering [42]. Recently, a research team has reported robotic "nanobiopsy" method for collection of extremely tiny amount of samples (even isolation of single cell) [24]. A nanopipette (50 nm) is inserted through cell membrane by minimally invasive method without damaging the target cell (see Fig. 2.3A).

2.2.2 Affordable and efficient stem cell differentiation/expansion protocols

In the field of regenerative medicine, there is a growing interest to apply bioprinting methods [43]; however, there remain a plethora of biological challenges. One of the important hurdles is the viability of stem cells and their long-term functionality during sequential differentiation. Researchers are continuously trying to identify optimum source of stem cells and develop appropriate and efficient protocols for isolation and explosion of stem cells through affordable and rapid methods (see Fig. 2.3B). Several stem cell sources including embryonic stem cells (ESCs) and human mesenchymal stem cells (hMSC)

isolated from bone marrow and adipose tissue have already been explored for bioprinting [44–46]. ESCs are the ideal source of stem cells since they are able to differentiate into any cell type. Prior to differentiation into target lineage, ESCs aggregate into embryoid bodies (EBs) demonstrating early stage of embryogenesis [47]. Overall, the EBs establish the microenvironment for lineage-specific differentiation of stem cells [48,49]. However, the application of ESCs is limited in many countries due to ethical restriction. Other than ethical constraints, another disadvantage of ESCs is that the cellular differentiation process is not always readily controlled, and cells may exhibit immunogenicity. To overcome such limitations, induced pluripotent stem cells (iPSCs) offer an alternative approach that is subject to neither ethical nor immunogenic concerns [50]. The differentiation state of stem cells depicts its immunogenic potential. It has been observed that undifferentiated stem cells are more immune-tolerated in comparison to the differentiated stem cells. Such immune-modulatory behavior of undifferentiated stem cells allows successful implantation and reduces host rejection of grafts [51–54]. Despite the continuous effort for the development of robust and rapid protocols for differentiation of stem cells into target cell lineages, most of the available methods are time consuming and lack reproducibility [55]. A recent approach reported by some research groups [56,57] reveals that the forced expression of lineage-specific master regulators induces direct reprogramming of somatic cells, and it has potential to be an alternative to direct rapid cellular differentiation. In this process, the differentiation of human pluripotent stem cells (hPSCs) is modulated by forward programming that enables scalable and faster production of lineage-specific cell types [58]. The forward programming method presently used in regenerative biology is based on lentiviral transduction of hPSCs [59]; however, transgenes are inserted randomly into the genome in lentiviral method, probably resulting in unwanted interference with cellular endogenous transcription program. To overcome this limitation, researchers have been trying to develop an alternative forward programming system by identifying more specific dual genomic safe harbor targeting strategies, which are required to induce expressions of transcription factors [60,61]. For neurogenic differentiation of ESCs or iPSCs, the available protocols require the animal factors for EBs formation, which reduces yield and efficiency of differentiation process. A recent study by Lukovic et al. has demonstrated a method for neural conversion of ESCs/iPSCs without employing any animal factors [62]. They have fortified the culture media with insulin to promote direct differentiation of stem cells into functional neural cell lineage.

Monocytic cells are important cells for promoting immune response under pathological condition. These cells are generally differentiated from ESCs or iPSCs through embryonic body or feed coculture method. However, all these methods employ xenogeneic material, which subsequently compromises the reproducibility of the differentiation process. Recent studies have reported a highly efficient alternative for differentiation of monocytic cells without using serum and feeder layer [63]. Since the isolation of embryonic stem cells

from mouse embryo by Ref. [64], considerable progress has been made in stem cell research. However, till date several challenges still exist, such as definition of the culture conditions that are adequately compatible with the clinical applications. Although most of adult stem cells derived from tissues are able to maintain considerable self-renewal capacity and lineage specificity, challenges remain in expanding the lineage-specificity of the stem cells for generating more patient-specific cell types. The cellular reprogramming is one approach for fulfilling this need, although it is often proved that large-scale production is inefficient, and the number of fully reprogrammed cells are very limited (<0.01%) [65,66]. Application of small molecules (e.g., epigenetic-related compounds valproic acid (VPA), BIX-01294, parnate, pluripotin) may provide an alternative approach to overcome this situation [67]. Effect of small molecules on biological systems is rapid, reversible, and dose dependent. By modulating the synthesis process, shape and size of these molecules can be tailored, and functional optimization is also possible. Although handling of such molecules is relatively easier than genetic intervention, some researchers reported the disadvantages of these molecules in terms of their target specificity and toxic effects observed in vivo. Chen et al. proved that a small molecule such as pluripotin (also known as SC1) was able to maintain the long-term self-renewal of mouse embryonic stem cells (mESC), even in absence of any feeder layer or animal serum in culture media [68]. Identification of this small molecule revealed the possible strategy of maintaining self-renewal capacity of stem cells by effectively balancing the endogenous differentiation pathway of stem cells. In 2008, Buehr et al. applied combination of two inhibitors, PD0325901 and CHIR99021, for maintaining the self-renewal of mESCs without any feeder layer or exogenous cytokines [69]. In addition to maintaining the self-renewal capacity, these small molecules have also played a role in dictating lineage specificity of their differentiation [69]. One such compound, StemRegenin1 (SR1), in combination with growth cytokines was reported to promote the ex vivo expansion of hematopoietic stem cells (HSCs) and their differentiation toward the lineage of blood cells [70,71].

2.2.3 High resolution imaging

Designing of tissue constructs before bioprinting assumes great significance in the process workflow. Bioprinted constructs must not only conform to injury-specific geometrical dimensions but also match the tissue-specific ECM attributes. Thus, medical imaging, especially 3D imaging in tissue engineering, exhibits increased significance (see Fig. 2.3C) [72–74]. In addition, as cell viability inside a construct is a critical bottleneck for their clinical application, medical imaging techniques must also provide accurate information on geometry of vessel networks to ensure adequate nutrient transport. For optimal patient compliance, medical imaging techniques should be noninvasive and ensure minimum radiation exposure. Presently, X-ray, MRI, and CT are the most popular imaging techniques to design, preferably 3D, implants with anatomical geometries (e.g.,

cardiovascular, orthopedic, and nervous tissues), from among several other modalities including modality angiography, fluoroscopy, 3D photogrammetry, optical coherence tomography (OCT), or ultrasound [75,76]. MRI is the mostly recommended imaging method for soft tissue visualization, which produces contrast in images based on state of water molecules in the tissue. An underlying pathology alters the proton density and/or how water molecules of tissue are bound with tissue, thus altering the intensity of absorption of magnetic energy or relaxation time of constituent protons upon excitation in an external magnetic field change, which can be detected by magnetic resonance coils. Since its discovery, the resolution of MRI imaging has been constantly improving. The most common method of achieving a higher resolution is to increase the strength of external magnetic field. Presently, MRI machines with range of field strengths from 1.5 to 11.7 T are often employed. Typically, they can attain resolution up to $0.22 \times 0.22 \times 0.41\ mm^3$ in certain brain cancer tissues, though resolution of 250 μm and above are more common with 3T MRI scans, and spatial resolutions of ~100 μm can be achieved in 7–9 T machines. The use of contrast agents (e.g., super paramagnetic iron oxide nanoparticles) further enhances the resolutions achievable with MRI [77]. It must be noted that high resolution scanning increases scan time and distorts signals due to patient movements. On the other hand, though MRI does not use ionizing radiation and is considered safe to some extent, patients might feel discomfort due to high magnetic field exposures. MRI has been used in observation of tissue engineered constructs. For example, the technique can efficiently record cell distribution in polymeric scaffolds, vascularization in hydroxyapatite hydrogels or glycosaminoglycan secretion and production in tissue engineered scaffolds in vivo [72]. Generally, imaging techniques have been applied to investigate the scaffold behavior and visualization after implantation [73]. Recently, their utility for prosthetics or as templates for scaffold design is being realized. Khoda has designed scaffolds with interconnected pores with different spatial distributions by suitable processing of geometric and topology of target tissue, tessellating the 3D contours of tissue volume with triangles using a mesh or stereolithography (STL) model [78,79]. Researchers also have described scaffold fabrication from MRI images [80,81].

Typically, CT imaging renders higher resolution compared to MRI with less scan time, but requires contrast agents to image tissues, which results in significant radiation exposure. CT images are more convenient to be processed into 3D anatomical geometry. Microcomputed tomography (μ-CT) provides very high resolutions (1–200 μm), but cannot be used to image higher volumes [73]. On the contrary, ultrasound techniques do not cause exposure to ionizing radiation with a short scan time, and at the same time they can image a wide scope; however, the resolution of ultrasound is limited to $1 \times 1.5 \times 0.2\ mm^3$. Three-dimensional photogrammetry can provide images with resolution up to 150 μm with an extremely short scan time (<1 min), but it is only applicable for external tissues.

The selection of the most appropriate imaging method depends on the target tissue. For example, the approach to obtain medical imaging data from a patient to generate a femoral head articular surface and bony structure without contrast agents is very different from imaging the meniscus or heart leaflet valve. In the case of the femoral head, although CT would provide the highest resolution for the bony structure, cartilage or soft tissues could not be imaged readily. Also, the size of femoral head is highly large to fit into current CT devices. In the case of meniscus, the most medically effective choice is MRI. High-resolution images of the meniscus can be obtained via MRI by increasing the scan time. The alternative would be to extract the tissue from the joint, and soak it in a contrast agent to allow for CT scanning. It is important to note that MRI can acquire geometries under loaded condition, whereas CT may have altered geometry due to being soaked in a contrast agent. In the case of the heart valve, MRI and CT both require contrast agents to visualize the inner workings of the heart and have similar image resolutions. Due to the high radiation exposure needed to perform a CT scan of the heart and the high expense associated with MRI usage, echocardiography (cardiac ultrasound) is becoming a more widely used noninvasive method to obtain 3D geometric models of mitral valves [75]. However, to maximize resolution, the valve can still be extracted, soaked in a contrast agent, and scanned via CT.

Recently, Park et al. have shown fabrication of 3D scaffold using MRI imaging for bile duct regeneration [81], and another study on brain tissue engineering from MRI image processing has been also reported. Duan et al. have used the CT image to demonstrate the design of bioprinted heart valves [82]. Apart from the tomographic imaging, developments in molecular imaging also enable high resolution images with functional information about the target tissues. In the future, molecular imaging could be combined with tomographic imaging for target tissue design for bioprinting [83].

2.2.4 Rapid medical image processing

Three-dimensional printing is rapidly expanding in the field of healthcare and medical applications including fabrication of customized prosthetics, implants, or tissue and organ fabrications. The exact anatomical model of target organ can be acquired through various medical imaging modalities as discussed in the previous subsection. To generate the design of tissue constructs, it is necessary to perform suitable processing steps such as image segmentation and pattern recognition [84,85]. Presently, most image acquisition is performed in common digital formats such as Analyze, Nifti, Minc, VPX, Interfile, though sometimes specific formats like Digital Imaging and Communications in Medicine (DICOM) are necessary [86]. Image processing steps include image preprocessing, image segmentation, feature extraction, and data mining. In image preprocessing, image scaling is performed, followed by image enhancement through noise removal and brightness,

illumination, or contrast correction. After the image registration is conducted, image segmentation is a crucial step to seek to identify the region of interest, which is performed by thresholding, edge, region or cluster-based methods. Image segmentation can be further performed by supervised or unsupervised methods, and conform to deformable, parametric, or geometric models. Segmentation software is vital for convenient extraction of surface structures of interest from 3D images (see Fig. 2.3D). After image segmentation, extraction of morphological and textural features or identification of specific spatial patterns is performed. It must be noted that in many cases, image processing is necessary, not only to depict the architecture of construct to be bioprinted, but also to obtain optimal stress distribution and oxygen perfusion for incorporated cells through the optimization of the internal architecture [87–89]. Furthermore, design software is required for 3D modeling, such as MIMICS, TSIM, Solidworks, 3D slicer, MATLAB, and OsiriX. For example, the use of finite element analysis (FEA) for creating tissue engineering constructs by stereolithography has been reported [90]. In another work, Mahmoud et al. have shown the use of an automated scaffold design technique by use of k-means clustering algorithm and isosurface rendering technique for reconstruction and visualization of 3D volume of bone defects [91]. Moreover, a computer-aided system for tissue scaffolds (CASTS) has been reported, which could automatically design 3D porous constructs in accordance with a defined external geometry [92]. Such methods are required for rapid scaffold design in bioprinting for clinics. CAD models are also useful to design scaffolds with gradient porosity for bioprinting [93]. Recently, Bücking et al. have described an optimized workflow, in which CT images were taken as input, followed by segmentation by means of thresholding, connected-component-filter or fill-holes-filter [94]. Subsequently, mesh refinement was performed and CAD models were further converted to slices, which was fed into numerical control (NC) coding for bioprinting [95,96].

2.2.5 Blueprint modeling

For most bioprinters, it is essential that the CAD model of defect site is converted to an STL format (see Fig. 2.3E), or a 3D graphics or virtual reality modeling language (VRML) [97,98]. After the conversion, they can be further analyzed with FEA software to rapidly evaluate properties of bioprinted constructs in silico before performing the physical bioprinting. To generate models for bioprinting, different CAD systems have been developed, including constructive solid geometry (CSG), spatial occupancy enumeration and boundary-representation methods (B-rep) [99]. Among these methods, CSG and SOE utilize the joining of primitives and cubic unit cells to build a large model, which is computationally expensive. Sun et al. has reported an example of combining unit primitives to build spine models using Boolean operations [85]. On the other hand, B-rep uses the boundary elements (e.g., edges and vertices) to define closed objects. Alternately, models can be built by algorithm which can identify negative geometry in CT-scanned

models by image segmentation, and subsequently subtract the negative geometry to create the porous internal architectures. Moreover, an extension of B-rep methods using isogeometric analysis (IGA) with volumetric representation (V-rep) involving trimmed B-spline trivariates is also developed, which may have applications in more precise defining of interior architecture of heterogenous scaffolds [100]. However, the efficiency of CAD-based systems is inadequate for rapid model generation.

In a different approach, 3D images extracted from CT scan can be used to directly define the external contours of tissue constructs, which can be filled by unit cells to generate the bioprinting file rapidly. Moreover, the limitation of CSG, which is that the porosity of the generated construct is identical, can be overcome by using a freeform systems approach, in which the whole structure can be partitioned into different subregions and each one is further assigned different porosity and material properties. An example of using this method has been already reported for a wound device design. In this method, a 3D image was extrapolated from a 2D scan and processed in ImageJ software [101]. Further, the image was rationally partitioned into nonuniform B-spline surfaces, which were then filled with different material properties. Printing of bioink with different sodium alginate concentrations was then performed for each surface. Three-dimensional models of different organs have been shown using this method. Another major limitation of most CAD-based designs is the inability to model irregular and complex geometrical patterns. This can be addressed by the use of implicit functions with periodic minimal surfaces, which can divide the geometrical space into periodic interconnected domains. Using minimal surfaces, design of scaffolds with gyroid and diamond structures as well as structures with heterogeneous porosity has been illustrated [102–104]. Another important limitation of the traditional CAD design is their incompatibility with most common extrusion-based bioprinters. It can be stated that most of the abovementioned approaches are more suitable for LBB or DBB. The extrusion-based bioprinters rely on deposition in a 0/90° raster pattern. To address this challenge, toolpaths using space filling curves can be employed, which with lay-down angles of 0/45/90/135 have been reported [105]. In this respect, Hilbert curves, a continuous fractal plane-filling function that allows for precise mapping from 1D to 2D space to fill a square, are also very useful [106,107]. One important requirement for development of bioprinting is to make open source software available, which allows end-users to generate their own toolpath using G-codes [21,22,108].

2.2.6 Process modeling for biomimicry

In the realm of bioprinting for tissue engineering, biomimicry can be one of the most effective tools to optimize process parameters for enhanced cell growth and differentiation. In natural tissues, cells with the ECM are in dynamic interaction with each other, which

impacts cell fate at various levels [109,110]. In certain tissues, one primary cell type interacts with another cell type, which influences the overall tissue functionality [111,112]. The ECM forms the essential cell microenvironment and hence, it is necessary that all design should consider adequately the incorporation of proper ECM into the scaffolds (see Fig. 2.3F) [113]. For example, many tissues require a porosity gradient or a spatiotemporal gradient of certain matrix proteins, which exerts important influence on cell behavior [114]. Apart from the chemical and architectural factors, biophysical attributes of microenvironment (e.g., matrix stiffness) also impact on cell behavior [115].

In the literature, several studies have attempted to perform processing modeling for biomimicry. Fuzzy modeling approach is described as one of the powerful mathematical tools for biomimicry [116]. In general, modeling tissue growth can be performed by adopting a continuum viscoelastic tissue approach or discrete cell-based approach. Although the former considers tissue as a deformable substance conforming to principles of continuum mechanics, which is capable of generating small system using coupled partial differential equations with a few nonlinear parameters, it is insensitive to identify the morphology and properties at the cellular level. On the other hand, discrete cell-based models allow for analysis of cellular-level features but contain more free parameters [117–119]. In a comparative study, Gardiner et al. modeled cell behavior by considering various cell components including membrane, nucleus, cytoskeleton and ECM as groups of particles. Thereafter, particle-particle interaction laws were employed to understand phenomena such as cadherin mediated cell-cell adhesion and integrin-mediated cell-substrate adhesion. The advantage of discrete modeling was clearly evidenced by the results of simulation study [120]. Further, it is important that tissue growth models are adequately testified by experimental data. The experimental results of developmental biology and tissue self-assembly are often important data source for such modeling. Discrete cell-based modeling has demonstrated the effect of cell seeding on cell growth and dynamics for tissue engineering, which can become an important source for bioprinting modeling [121]. Recently, Cao et al. have developed a multiscale model showing the relationship between matrix stiffness and cell adhesion, which can be further extended for design of bioprinting tissue constructs [122]. In addition, the agent-based models involved biomaterial degradation kinetics and vascularization, and could substantially aid in the process modeling [123].

2.2.7 Advanced path planning for bioprinting

Path planning for bioprinting is sufficient for converting a digital CAD model into a physical tissue construct with desired accuracy. For bioprinting, there are two methods for generating path plan, namely Cartesian and parametric forms. In Cartesian form, path planning has been implemented for almost all types of bioprinting modalities. For

example, studies on EBB have shown that 0/90° lay-down pattern generated constructs with high mechanical integrity compared to 0/45° and 0/135° patterns [124]. However, the distortion of structure is mostly observed at the turning points, where the bioprinting speed decelerates or accelerates. This limitation might be addressed by a tangential continuity of the substrate. At the turning points, it also becomes difficult to incorporate functional gradients as bioink deposition does not follow the designed amount due to the speed variation of the substrate deposition. These limitations can be overcome to a certain extent by providing smaller raster sizes as input. Moreover, Cartesian path plan is also not suitable for hollow construct bioprinting. In the parametric form, path planning is performed using parametric coordinates for complex heterogeneous geometries. A method has been demonstrated by Ozbolat and coworker in which CAD file was sliced into different layers, and each layer was assigned a spline curve [125]. The path plan was generated for two consecutive layers, wherein the first layer was printed based on the parametric line, whereas the spiral toolpath was fed for the next layer (see Fig. 2.3G). This toolpath algorithm allowed tangential continuity, and enabled better printing for heterogeneous bioink compositions. Wang et al. has also shown a parametric path planning algorithm including mesh parameterization, distance transform, contouring, and smooth interpolation steps [126]. In the future, it is expected that path planning algorithms could be tailored according to the material properties of different bioink solutions [127]. One of the interesting works has demonstrated the use of predictive algorithms to generate the path plan that compensates for shape distortions due to differences in buoyancy of bioinks [128]. Such predictive compensatory algorithms are required not only for 2-dimensional (2D) but also for 3D bioprinting.

2.3 Bioprinting stage

The physical bioprinting stage is predominantly composed of three phases including bioink, bioprinter, and bioprinting process. Several parameters require strict optimization to obtain successful fabrication of tissue constructs, which may include physicochemical properties (rheological properties, gelation kinetics, etc.), biological properties (cell density, viability, and biocompatibility), and process parameters (bioprinting time, presence of radiation, etc.). The different quantitative aspects of the bioinks under the three different major bioprinting modalities are summarized in Table 2.1 and discussed below.

2.3.1 Bioink phase

Bioink is the bioprintable material consisting of various biologics including cells, media, serum, genes, proteins, etc. (see Fig. 2.4A). Bioinks can be composed of cells with biomaterials like hydrogel or only cell aggregates and spheroids (in scaffold-free bioprinting) [144]. The ideal bioink formulation is an optimization of material properties

Table 2.1: Quantitative comparison of bioink properties under different bioprinting modalities.

Parameters	Extrusion-based bioprinting (EBB)	Laser-based bioprinting (LBB)	Droplet-based bioprinting (DBB)	References
Rheological properties viscosity	$3-6 \times 10^7$ mPa s	1–300 mPa s	<10 mPa s	[129–133]
Cell density	Very high cell density such as cell aggregates	Medium cell density ($\sim 10^8$ cells/mL)	Lower cellular density ($<16 \times 10^6$ cells/mL)	[129–131,134]
Gelation speed	Fast gelation (i.e., ionic cross-linker)	Slow gelation	Medium gelation speed	[134]
Definition of bioprintability	Extrudability or the formation of continuous filaments	Formation of jets on the substrate	Formation of well-defined dotted patterns	
Surface tension	+	++	+++	
Factors affecting cell viability	Dispensing pressure, nozzle size, bioink viscosity, cell density	Laser radiation, bioink viscosity	Dispensing pressure, droplet generation mechanism, bioink viscosity, cell density	[135–137]
Cell viability	++	+++	++	
Mechanical strength	+++	+	++	
Resolution	+	++	+++	[138–143]
Application	Tissue engineering and regenerative medicine, disease modeling and research	Tissue models for toxicity testing, tissue engineering	Stem cell research, high-throughput screening, drug testing, tissue engineering	

(printability and degradation) and biocompatibility. Printability is influenced by rheological properties of bioinks including the viscosity, gelation kinetics, shear thinning properties, yield stress, and shear recovery (see Fig. 2.4B). Such properties are directly associated with print fidelity and mechanical strength. However, improvement in one such property often comes at the cost of other, thus making bioink formulation design and selection an extremely vital process in bioprinting workflow as detailed in the following subsections. Embedding cells in a bioink poses several challenges. To start with, in order to obtain effective bioprintability with hydrogel-based bioinks, concentrations of each ingredient must be precisely optimized [145]. An ideal bioink should not require any pre- or postprinting processes such as chemical-, physical-, or photo-crosslinking to make bioinks cell-friendly, homogenously mixed within other components, and reduce cell encapsulation time [146]. One of the major limitations in cell-laden bioink is that cells are required to be suspended in an aqueous precursor solution, along with other water-only soluble constituents [146]. Further, volume of suspension can affect stability and strength

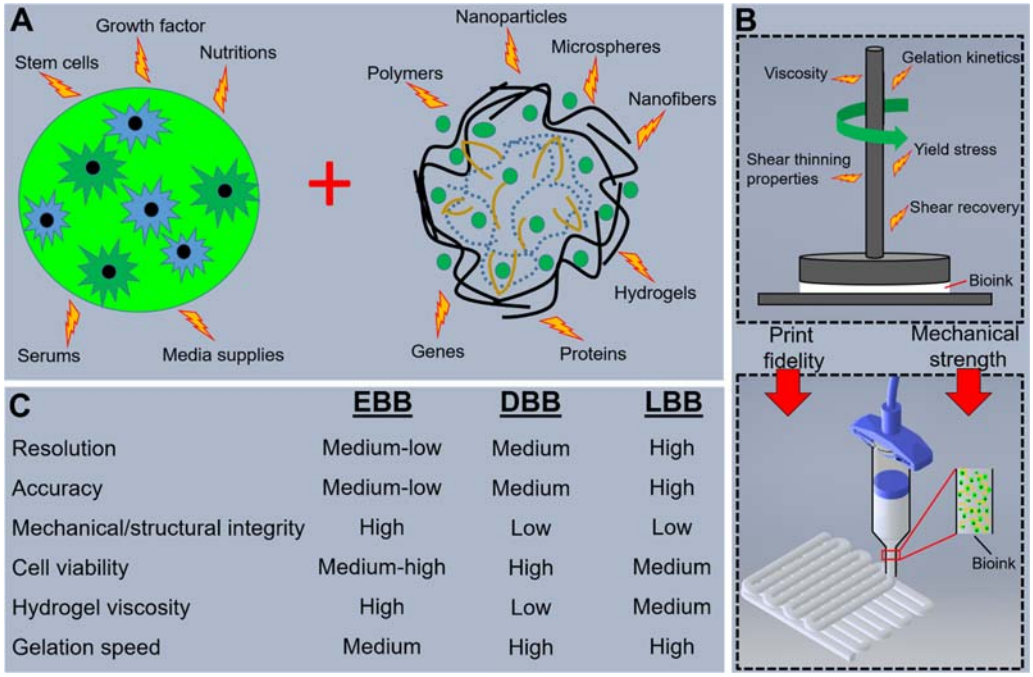

C	EBB	DBB	LBB
Resolution	Medium-low	Medium	High
Accuracy	Medium-low	Medium	High
Mechanical/structural integrity	High	Low	Low
Cell viability	Medium-high	High	Medium
Hydrogel viscosity	High	Low	Medium
Gelation speed	Medium	High	High

Figure 2.4
(A) Essential components of bioink; (B) Rheological properties affecting print fidelity and mechanical strength; (C) Comparison of bioink-induced properties among different bioprinting techniques (further details are presented in Table 2.1).

of the hydrogel-based bioink by changing the final concentrations of cells and hydrogels in bioink [147]. In addition, it can delay cross-linking time for the bioink and affect other major properties such as swelling, mechanical and gelation time [148].

In addition, cells can be bioprinted without encapsulating in any other support hydrogel or media requirement on substrate surfaces. This technique is known as scaffold-free cell bioprinting such as bioprinting spheroids or tissue strands as demonstrated by Yu et al. [149]. In such cases, if adequate liquid precursor is not available, cells delivered with scaffold-free bioprinting technique or within the bioink solution will not have enough oxygen and nutrients to sustain viability during the bioprinting process and undergo necrosis due to hypoxia and starvation. In order to avoid starvation, researchers have prepared bioink solutions using ingredients within the culture media. Another approach was to combine bioink with microspheres filled with oxygen to allow oxygen to permeate through the pores into microenvironment avoiding hypoxia and thus maintaining high cell viability during the bioprinting process [150].

Mixing cells uniformly within bioink solutions is another common issue especially when hydrogels are also a constituent, which affects the subsequent bioink extrusion in a

homogenous manner. If the bioink solution has substantial chain entanglements, it is difficult to break down the structure and suspend cells homogenously within the bioink. In many cases, even after breaking down the entanglements, cells do not attach on the surface of cross-linked network and are likely to accumulate in certain regions due to phase compartmentalization of polymers. Thus, mechanical mixing systems have been used to homogenously suspend cells in fibrous hydrogels such as collagen, methylcellulose, and fibrin [151,152]. Encapsulating cells uniformly in hydrogels should be carefully carried out in order to minimize any possible bubble formation within the solution, which otherwise may influence the bioprintability. Depending on ingredients of the bioink, cells can be suspended either initially or after addition of all other ingredients of the bioink to avoid nonhomogenous suspension. However, cell encapsulation within hydrogel-based bioink is not always desirable depending on the stability of the bioprinted constructs as well as pH, toxicity of the bioink reagents [146], biocompatibility of hydrogels, and/or their degradation products. For example, Pluronic F127 is a thermoreversible material, which behaves like a gel at 37°C [153] but dissolves rapidly in aqueous media affecting the stability of bioprinted constructs [154]. At the same time, high concentration of Pluronic could be detrimental for cells [155]. Thus in such cases, seeding cell on bioprinted constructs is much more desirable instead of encapsulating cells within bioink.

2.3.1.1 Cell density

In a bioprinting process, the bioink principally comprises of target/progenitor cells of target tissue and/or hydrogel biomaterial. Unlike traditional scaffold fabrication techniques, bioprinting skips the cell-seeding process, as the cells are dispersed into desired locations inside constructs during the fabrication process itself. In order to construct the desired tissue, it is essential to understand the relation among various parameters including bioink types, the required cell density, and the cross-linking mechanism [9]. Bioprinting can also be performed using scaffold-free bioinks, wherein cells at much higher densities can be bioprinted without the use of exogenous biomaterials. Scaffold-free bioprinting additionally avoids the biocompatibility-related limitations of common scaffold biomaterials. Though tissue development can be faster compared to scaffold-based approaches, mechanical strengths of the constructs may be compromised in the scaffold-free approach [156]. Initially, it was expected that high cell density may lead to faster tissue formation. Several reports are available regarding the selection of optimum cell density for 3D printing process. The selection of cell density will also depend upon target tissue to be bioprinted. For example, values are found in articular cartilage at 10 cells per unit area (0–22 mm^2), in costal cartilage at seven cells per unit area, and trabecular osteons at 2×10^6 per m^2 in healthy human adults [157,158]. Details about the total number of cells in different tissues can be found in Ref. [159].

Shear stress during bioprinting has a negative influence on cellular viability and damage to cell membrane [9,137], and hence it is desirable to select low viscous (<10 mPa s) bioink with low initial cell density (<10^6 cells/mL) [132,133]. In LBB (i.e., laser induced forward transfer (LIFT)), the viscosity range of a bioink should be selected between 1 and 300 mPa s, and medium cell density (~10^8 cells/mL) is suitable for the process [131]. EBB is extensively used for construction of cell-laden tissue constructs [160]. Such system is able to print viscous bioinks (3–6 × 10^7 mPa s) with a very high cell density without affecting cellular viability [129]. In contrast, inkjet bioprinting employs less viscous bioinks (<10 mPa s) with lower cellular density (<16 × 10^6 cells/mL) [134]. The MEMS-based printer head of inkjet bioprinter cannot squeeze viscous bioinks, as relatively small deformation take place by the thermal/piezoelectric actuation at the nozzle opening. Generally, higher cell densities increase the average viscosity of the bioink resulting in clogging of the printer head [161–163]. Billiet et al. have compared the printability of methacrylamide-modified gelatin (Gel-MOD) both in the presence and absence of hepatocytes [164]. Results demonstrated that above gelation temperature, the viscosity of bioink was reduced to half for cell density up to 1.5 × 10^6 cells/mL. With the increased cell density (2.5 × 10^6 cells/mL), further reduction was obtained. Skardal et al. reported that density of human intestinal epithelial cells above certain threshold (>25 × 10^6 cells/mL) interfere with the hyaluronan-based hydrogel formation [165]. Fig. 2.4C presents the comparison of bioink-induced properties, including cell density, among different bioprinting techniques.

The relationship between cell density and mechanical properties of the hydrogels was also studied [166], in which chondrocytes were cultured on agarose hydrogels over a period of 2 months in free-swelling and dynamic loading conditions. Initially, constructs containing low cell concentration (10 × 10^6 cells/mL) were stiffer in comparison to that with high cell concentration (60 × 10^6 cells/mL). As the culture time increased, the constructs with higher cell density exhibited similar Young's modulus to constructs prepared with lower cell density. For example, the initial cell density of 20 × 10^6 cells/mL is preferable for cartilage tissue engineering, and cell density below this concentration may reduce cartilage formation [151]. Chang and coworkers have demonstrated the effect of different cell densities on remodeling of hydrogels depending on external loading conditions [167]. Based on such studies, numerous models have been developed to understand the effect of cell density on the properties of bioprinted constructs [168].

2.3.1.2 Cytotoxicity of bioink components

While an ideal bioink must meet the requirement of printing process, its cytocompatibility is another crucial criterion for successful bioprinting [169,170]. As a bioink, hydrogels are preferred due to their higher water content and low cytotoxicity [171,172]. An overview on cytocompatibility of various hydrogels fabricated through different techniques is

available [173]. A study showed that 3D printing with methacrylamide-modified gelatin hydrogels resulted in >97% cellular survival. Hsieh et al. reported excellent compatibility and proliferation of neural stem cells embedded on 20%−30% polyurethane hydrogels [174]. A composite bioink of nanofibrillated cellulose and alginate was tested by Markstedt et al. and constructs exhibited 86% viability of chondrocytes several days after printing [175]. Construct bioprinted using silk fibroin-gelatin bioink showed multilineage differentiation of encapsulated stem cells for targeted tissue formation [176]. To enhance the cytocompatibility, researchers have also tried to prepare a bioink from biological samples. For example, decellularized liver matrix (dLM)-based bioink was prepared (containing the intrinsic proteins of dLM), which improved the compatibility of encapsulated cells [177]. Similarly, to improve cell-adhesiveness of alginate bioinks, enzymatic cross-linking schemes exploiting phenolic hydroxyl moieties and horseradish peroxidase have been attempted [178].

Among various bioprinting techniques, printing of live cells with DBB is relatively challenging as the increased viscosity of bioink and higher cell density requires excessive forces to eject the droplets, which can cause damage to cells [132]. Another limitation is the aggregation of cell suspension within the reservoir that causes clogging within narrow tubing of droplet-based bioprinters, which also increases the mechanical stress, and hence affects the cellular viability. Nonuniform droplet formation may also take place. Bioink additives may overcome this problem; however, surfactant materials affect the cellular membrane integrity [88,89,179]. The cytotoxic effects of various nanocellulose bioinks were studied against different cell lines [180,181]. Due to the absence of toxic effect, nanocellulose bioink is considered as suitable wound dressing material. Although the compatibility of natural materials (i.e., alginate, silk, fibrin, and collagen) is preferable, due to their weak structure and fast degradability in physiological condition, cross-linking is necessary to improve the mechanical strength. However, cross-linking agents may decrease the material homogeneity, cellular compatibility, and enhance the complexity of bioprinting [8].

2.3.1.3 Bioprintability

The printability of a bioink depends on certain factors. First, the bioink should be in liquid form without clogging the printer nozzle before/after printing. Secondly, the applicability of the bioink is determined by the "biofabrication window" [182]. The term has been recently proposed to define the compromises necessary to obtain bioinks with adequate print fidelity and cell viability [183]. Though depending upon the bioprinting modality, printability has different definitions. For example, printability of EBB refers to the extrudability or the formation of continuous filaments followed by formation of the integrated 3D structure. In DBB and LBB, printability is used to characterize formation of well-defined dotted patterns and jets on the substrate, respectively. This property of the

bioink determines its printability, cell viability, structural resolution, etc. For printability, several parameters such as rheological properties, gelation kinetics, and surface tension of the bioink are necessary to be characterized. Moreover, the viscosity of bioink should be tunable with temperature for certain biomaterials while shear thinning is necessary for EBB. Colosi et al. printed low viscous bioink of alginate and gelatin methacroyl (GelMA) blend through a coaxial nozzle [184]. Initial concentration of GelMA was kept low, which upregulated cellular viability; however, it was not printable. Blending with alginate produced mechanically stable cross-linked fibers [185]. The coaxial system is able to tune the gelation kinetics of bioink by modulating the ink composition. Two-step polymerization system was used by Skardal et al. for printing of bioink comprising methacrylated ethanol amide derivative of gelatin and methacrylated hyaluronic acid with high viscosity [186]. The construct was completely photopolymerized to obtain the final constructs. In addition, there is a relation between the concentration of cells and the printability of bioink. Higher cellular load increases the viscosity of bioink which may affect its printability. Hence, selection of optimum cell concentration is also important for successful bioprinting [9].

Other process parameters have also great influence on the fate of bioprinting, such as the fusion of hydrogels, deformation due to gravity, nonuniform droplet size, and nonuniform extrusion due to alteration in printing speed. The density of the cross-linker also influences the printing fidelity. In general, high cross-linker concentration limits the cellular migration but possesses better printability, whereas low cross-linker concentration reduces the bioprintability [182]. For most optimization studies, a "biofabrication window" thus becomes a useful tool to quantify the suitability for fabrication.

Apart from viscosity, other relevant rheological parameters are the shear thinning properties, gelation kinetics, and yield stress of the bioink. Shear thinning defines the shear-rate dependent viscosity of bioink, which essentially behaves as a non-Newtonian fluid. Shear induces a reorganization of macromolecules to a less entangled configuration decreasing the viscosity. The viscosity of the most commonly used bioink, sodium alginate, is several times less at shear rates of 100–500 s^{-1} (most commonly encountered for bioprinting), compared to plateau region at lower values of shear suggesting strong shear thinning behavior, which is more prominent at higher concentrations. Shear thinning is desirable for bioprinting, as it enables smooth flow avoiding clogging during extrusion but regaining of the viscosity after bioprinting contributing to improved bioprinting fidelities [173,187]. Thus along with shear thinning, shear recovery is also an essential rheological property in order to attain a better construct resolution [188]. During bioprinting, another rheological property of importance is the yield stress, which is the initial minimum stress that is required to be supplied to initiate flow. Yield stress can potentially improve the bioprinting fidelity and reduce cell sedimentation. An example of yield stress effect on bioprinting is

demonstrated by addition of the gellan gum to GelMA hydrogels [173]. Likewise, shear elastic modulus determines deformations and ease of printing hydrogel due to shear forces exerted during extrusion. The evolution of gel parameters is also important as the gelation kinetics will determine the cross-linking time. The major mechanisms of hydrogel gelation are physical (i.e., ionic), chemical, or covalent, and enzymatic cross-linking. Physical gelation is achieved at bioprinting duration and provides ignorable viscosity fluctuations during bioprinting, but results in formation of relatively weaker constructs. Physical cross-linking can be reversible. Chemical cross-linking requires appreciable gelation times, which are impediment to fabrication of multilayered constructs. Also, the toxic cross-linkers must be removed completely before implantation [183,189–191]. Cross-linking under light irradiation is another option for instantaneous cross-linking, but the effect of light wavelengths and duration of exposure on cells must be considered [192]. On the other hand, enzymatic cross-linking offers a more biologically acceptable process, but it increases the cost and decreases practicality of the process. Ionic cross-linking is also achieved at rapid rates and can be carried out at physiologically amenable conditions. For example, alginate forms an ionotropic bond with calcium ions, while chitosan with phosphate ions. However, ionic cross-linking is prone to undergo rapid dissociation in physiological fluids. Ideally, solidification should occur at fast enough rate so that bottom layers acquire sufficient mechanical characteristics to withstand loads of subsequent layer. In addition, faster solidification prevents flowability of bioink after bioprinting and improves the structure fidelity.

Another parameter of importance, especially for DBB, is the surface tension of bioink to determine high fidelity bioprinting. Surface tension is determined by the net balance of cohesive forces among all components of the bioink and influences if either a jet or droplet would be formed after ejection. Since cells tend to adsorb at the air-water interface, surface tension of a bioink is reduced as cell density increases. Surface tension influences printing resolution, quality, fidelity and dimensions of printed lines, and proper matching of the surface tension can be engineered by contact angle measurements. In fact, it has been proposed that hydrogels could be printed with smaller dimensions such that the desired dimensions are achieved after swelling post-bioprinting [193]. The physicochemical properties of a bioink including rheological behavior, surface tension, gelation kinetics, and swelling property are not only important for its printability, but also for maintenance of its postprinting integrity [9]. Tuning of these parameters is important for the reproducibility and fidelity of bioprinted constructs. Incorporation of physical/chemical cues can improve the printability of polymers. In EBB, it has been observed that incorporation of cues (e.g., metal ions and gluteraldehyde) can improve bioprintability [194]. For example, Na^{+} was incorporated in gelatin by replacing Ca^{2+} and Fe^{2+} present in gelatin. This significantly altered the molecular interactions and improved the cross-linking density and mechanical strength of gelatin gels [195].

2.3.1.4 Cell viability and long-term cell functionality as a function of bioprinting parameters

Bioprinting enables spatial manipulation of cells, where the viability of cells during pre- and postbioprinting is crucial. Researchers have been exploring different combinations of biomaterials and cell types in order to understand cell-biomaterial interactions. However, the optimal process parameters for certain cell type may not be suitable for another. Nair et al. have studied cell viability during EBB, and their study indicated that dispensing pressure affected the cell viability [135]. In another study, it was observed that nozzle insulation improved the viability of HEK 293FT cells when printed with a gelatin-based bioink [196]. Zhao et al. reported that bioink viscoelasticity was the key parameter for cellular viability and printability of polymers [197]. In microvalve-based DBB process, it has been observed that shear stress is the key factor to balance the printing resolution and cellular integrity [136]. Previous study achieved approximately 90% viability of fibroblasts by controlling the shear stress within 5 kPa [137]. DBB is suitable for handling with higher cellular densities. A study has reported that cellular homogeneity and viability could be enhanced by changing bioprinting parameters of polyvinyl pyrrolidone (PVP)-based bioink [198]. The effect of photo-cross-linking on cellular activity has been tested [199]. In a study, methacrylated hyaluronic acid (MA-HA) and GelMA were cross-linked with UV for fabrication of valvular interstitial cell laden constructs. Approximately 92% of cellular viability was observed up to 7 days after printing, which concluded that there was no noticeable toxic effect of photo-cross-linking on the encapsulated cells. They also optimized the compressive modulus of the bioink at about 13 kPa to obtain optimum polymer viscosity and effective photo-crosslinking. Printing of thermoresponsive polymers (i.e., poly (N-isopropylacrylamide)-grafted hyaluronan (HA-pNIPAAM) and MA-HA) has been investigated [200], in which printable constructs with high resolution and cell viability were produced. However, in another study on thermoresponsive hydrogel bioprinting, the blend of PU/PCL was bioprinted through a two-step chemical reaction, and a low cell viability of mesenchymal stem cells (~40%) was observed a day after bioprinting [201–203]. The effect of photoinitiators on cellular viability has been also intensively studied, and ~98% viability of hepatocarcinoma cells was observed using the VA-086 photoinitiator [164]. It has been reported that during temperature-based cross-linking process, the viability of cells is remarkably compromised, since cells can only survive in a narrow temperature range [204]. Gelation time is another factor; longer gelation period generally reduces the cellular viability. Viscosity of hydrogel is often modulated for increasing the printability of bioink and resolution of tissue constructs. Such alteration induces stress on cell population, and hence reduces the viability of cells [205]. Despite the capacity of bioprinter to deposit cells at high rates, the bioink composition (especially cell-laden bioink) also determines the practical speed that can be attained, since cell viability and cell division postbioprinting would be reduced, resulting from the

high stress induced by higher extrusion speeds. Additionally, long standing time inside a reservoir due to slow printing rate can reduce the cell viability.

2.3.1.5 Solidification

Most of the available natural and synthetic bioinks are solidified through physical, chemical, or enzymatic cross-linking methods. For example, alginate is ionotrophically cross-linked through calcium chloride ($CaCl_2$) or calcium sulfate ($CaSO_4$) solutions. Solidification of polymer occurs through transition of polymer solution to gel at a transition temperature. Hot solution (40−80°C) of polymers such as agarose, gelatin, and methycellulose are transformed into gel when printed on a cooled stage [206,207]. Hydrogels prepared through physical cross-linking is mechanically weak, and reinforcement of other materials is required to enhance the stability. Photocurable hydrogels can be printed on illuminated stage through the incorporation of an appropriate photoinitiator [186]. Three-dimensional printing of photocurable bioink with and without cell population was reported in several studies [164,208,209]. Printing of photocurable polymers has several advantages, one of which is that the printing process is very rapid, and has less detrimental effect on cells [210]. Moreover, no additional cross-linking bath is required, and the degree of cross-linking can be easily adjusted by changing the intensity of light. Gelation of the extruded ionotropic polymers also occurs in a reactive substance bath [207,211]. The advantage of reactive printing is the rapid solidification of polymers. Since gelation can occur at physiological temperature (i.e., 37°C), the impact on cell population is minimal. Printing of gellan gum solutions by this method along with the cell culture media has also been reported [212].

Material dispensing rate is impacted by the initial viscosity of bioink and the cross-linker density. Generally, bioinks with higher viscosity can be bioprinted at a faster rate requiring less amount of cross-linker, and bioprinted constructs are more stable under physiological conditions. In EBB, the extrusion force is exerted pneumatically or mechanically enabling bioprinting of highly viscous bioinks in comparison to DBB methods. Slower gelation kinetics can cause cell death and typically, the gelation time for alginate, and PEG-DA are shorter compared to that for collagen, and chitosan [213]. A highly viscous solution requires less time of cross-linking and hence, can be deposited at faster rates. Similarly, high cross-linker density can create fast solidification, and hence faster dispensing rate can be used. However, the toxicity of cross-linker with high concentration should be considered. In addition, EBB requires a fast gelation process for a desired fidelity, which can be adequately obtained by ionic cross-linking [134]. Bioprinting with supporting nanoclays is able to minimize the impact of gelation speed on print fidelity [14]. Another challenge in bioprinting is the selection of appropriate cross-linking density for achieving the structural integrity of construct without inducing any cytotoxic response [143]. For optimum solidification, optimization of cellular

density is also important, since high cell concentration might interfere with the cross-linking mechanism of hydrogels occasionally [165].

2.3.1.6 Mechanical and chemical properties

For fabrication of stable and transplantable 3D bioprinted constructs, it is necessary to investigate the rheological properties of a bioink to obtain sufficient printing accuracy and also provide an optimal environment for cellular migration and spreading [214]. In bioprinting, bioinks that are able to immediately solidify or regain structural integrity after extrusion are desired [138,215]. Mechanical properties of constructs can be further improved through photo-cross-linking using a photo-sensitive bioink as a precursor material. The mechanical stability of physically cross-linked constructs is relatively poor compared to that of chemically or photo-cross-linked constructs [216]. To improve the mechanical stability, some chemical functional groups can be incorporated, which form an irreversible cross-linked network through covalent cross-linking [217,218]. Mechanical properties of the constructs can be further improved by using nanoparticle/hydrogel composites such as Laponite/alginate and nanosilicate/collagen as evidenced from several studies [219,220].

Combination of physical and chemical cross-linking methods has also been employed for improving the stability [218,221]. Physical cross-linking process is preferable during bioprinting, whereas chemical process is usually followed to enhance the stability of post-cross-linked products [214,216]. Billiet et al. used photo-induced cross-linking after bioprinting of methacrylamide-modified gelatin bioink [164]. Along with mechanical properties of a bioink, the cellular compatibility is also a matter of concern. Mauck et al. have tested the impact of density of encapsulated chondrocytes on mechanical properties of the resultant agarose hydrogel [166]. It is challenging to maintain the structural integrity of the construct during cell growth. Along with a physical support, maintaining the mechanical strength, which is alike in in vivo conditions is also necessary for cellular proliferation and differentiation [138,139]. A recent study by Hölzl et al. showed a decrease in stiffness of hydrogels by 13% with the increase in cell density from 12 to 15 million cells/mL [9]. Elsewhere, compressive moduli of constructs using collagen were at the range of 25 kPa while those with alginate hydrogels were found from 15 to 20 kPa [222,223]. The selection of a particular bioprinting modality should be made depending upon the target tissue. The greatest advantage of EBB is its ability for scale-up biofabrication, user friendliness, and high mechanical strength of the constructs. Therefore, EBB should be explored for obtaining volumetric organs in clinical tissue engineering. On the other hand, in applications which require high bioprinting resolutions and closer cell-cell or cell-material interactions like tissue models for toxicity testing, DBB may be preferred. At present, LBB instruments are costlier but provide very high cell viability and resolutions, and thus for stem cell research, LBB may be generally recommended.

2.3.1.7 Guiding cell growth and differentiation

Stem cells are the attractive cell types for tissue biofabrication due to their ability of multipotent differentiation. The growth and differentiation of stem cells require a microenvironment with proper physical and chemical cues [204]. Hence, careful consideration of the bioink is essential for successful differentiation of stem cells [224,225]. Specific signaling molecules have been immobilized to control stem cell fate in bioprinting of stem cells through DBB. Bone morphogenic protein-2 (BMP-2) was used to control the differentiation of muscle-derived stem cells (MDSCs) blended with fibrin bioink [226]. An in vitro study reported that MDSCs differentiated into osteogenic lineage in the presence of BMP-2, whereas they differentiated into myogenic lineages in the absence of these signaling cues. Miller et al. used heparin-binding epidermal growth factor (EGF) as signaling molecules to control the differentiation of MSCs [227]. In a recent study, growth factors (i.e., Wnt protein) were immobilized on bioactive beads that facilitated the asymmetric division of embryonic stem cells (ESCs) [228]. After division, the daughter cells proximal to the beads showed more pluripotent characteristics, whereas daughter cells at the distal side showed increased expressions of differentiation markers [229].

In addition, stem cell fate could be also regulated by signaling molecules (e.g., transforming growth factor-β (TGF-β), fibroblast growth factor (FGF), Wnt signaling proteins, and hedgehog proteins) during postbioprinting incubation [230]. Bioprinting of iPSC and ESCs with RGD coupled-alginate hydrogels has been found to differentiate into hepatocyte-like cells [231]. In that study, the differentiation process was initiated prior to bioprinting, and allowed to continue for 11 days after bioprinting. This experiment indicated that bioprinting did not influence the cellular differentiation process. Hydrogels can instruct stem cell differentiation through mimicking the ECM network, in which they positioned cells in contact with tropic support, signaling cues and topographical information [232]. An interesting observation has been reported that differentiation of MSCs can be altered in the presence of different cross-linking agents for the same bioink. A study by Das et al. reported that cross-linking of bioprinted silk fibroin-gelatin hydrogels with tyrosinase showed the differentiation of MSCs toward chondrocytes [176], whereas physical cross-linking of the bioinks by sonication tended the differentiation into osteocyte lineage.

2.3.1.8 Affordability

The affordability of bioinks depends on their raw material. For example, cell-laden bioinks are relatively expensive, since the incorporation of cells needs precise control, sophisticated instrumentation, and skilled manpower. Maintenance of cell number in each batch also needs precise control. Moreover, the price of a bioink depends on the cell type, their doubling time, culture media, culture conditions, and the rate of ECM deposition.

Without considering cell incorporation, most of the printable hydrogels that are available commercially are affordable, except some natural hydrogels, such as collagen, laminin, and hyaluronin, due to the complex isolation protocol [233]. The abundance of biopolymer also influences the affordability of bio-printed constructs. For example, the synthetic polymers are more readily available, wherein the biomaterials from natural origin have limited resources. In addition, some polymers extracted from natural sources (e.g., alginate and chitosan) are comparatively affordable, due to more standardized convenient extraction procedures and abundance of their sources.

2.3.2 Bioprinter phase

Bioprinting technology had emerged as a cytoscribing technique by the pioneering work of Klebe in 1988, in which a Hewlett Packard (HP) modified printer was used. The evolution of bioprinters has been reviewed in detail elsewhere [234]. In the past decade, several enterprises have innovated bioprinter products with different capabilities like generating functional perfusable tissues, which are important to be compared for their ability to produce constructs with different characteristics. Persistent efforts in bioprinter technology development are expected to produce hybrid vascularized tissues with the ability to scale up to clinically relevant sizes and emergence of 4D bioprinting and hybrid bioprinters. Below subsections discuss the essential requirements of an ideal bioprinter in order to successfully bioprint living tissue and organ constructs for clinical use in the future. The different quantitative aspects of the bioprinters are summarized in Table 2.2 and discussed below.

2.3.2.1 Compactness

For the efficient clinical deployment, it is highly desirable that bioprinters are compact in size such that they can be directly placed inside a laminar flow unit for maintaining sterility, and easily fit inside an operation theater. Most bioprinters are designed to fabricate tissue constructs in centimeter scale, but the hardware usually takes a large space. Thus, from the beginning of bioprinter development, compactness has been one of the important goals which the manufacturers are striving to achieve. For example, the upgraded version of BioBots bioprinter occupies only 28,317 cm^3 totally, and is easily accommodated inside a laminar-flow hood, while the previous Biobot2 model consumes 64,327 cm^3. Similarly, the inkjet bioprinter Autodrop Compact, which is manufactured by Microdrop Technologies GmbH, has dimensions of 562 × 772 × 550 mm. Similarly, Microfab technologies have Jetlab 4 model with a footprint of 63 × 57 cm. Compactness results in small dimensions of the products that can be printed, so the manufacturers also supply models with larger size in most cases. For example, the substrate size for Jetlab 4 is 160 × 120 mm, and the advanced version has a working area of 200 × 200 mm. For example, Autodrop Compact model has a positional accuracy of 25 μm, maximum speed

Table 2.2: Quantitative comparison of bioprinter technologies under different bioprinting modalities.

Parameters	EBB	LBB	DBB	References
Compactness	++	+++	+	[234]
Dimensions of the products	+++	+	++	[234]
Bioprinter resolution	Resolutions with micrometer ranges (5–15 μm)	Lateral plane resolution from 30 to 100 μm	Single cell resolution (50 μm) and high lateral resolutions, their resolution in the z-direction is limited	[142,143,234]
Nozzle size/ejected volumes	In micrometers	Picoliter droplet sizes	Droplet size in 1–300 nano to picoliters	
Deposition rate	Slowest	Moderate	1–10,000 droplets per second	[141]
Printing speed	10 μm s^{-1} –700 mm s^{-1}	200–1600 mm s^{-1}	1–10,000 droplets s^{-1}	[141,234]
Multi-material configurations	Multiarm or multihead extrusion-based bioprinter	Multiarray laser-based stereolithography	Multinozzle droplet	[235–237]
Commercialization	Fastest	Slowest for commercial transformation	Medium	
User friendliness	+++	+	++	
Price/affordability	$5k–$250k	>$100k	$10k–$50k	[234]
Versatility	+++ (Biobot series are one example of versatile bioprinters, Fab@Home offers remarkable versatility)	+	++ (Nordson Pico series and MD series from Microdrop technologies, suitable for high-throughput applications, and provide significant versatility)	
Bioink	Various bioink materials with a wide range of viscosities	Only the bioink which can be irradiated by laser or photopolymerization	Bioinks with lower viscosities can be bioprinted as nozzle clogging is frequently observed for high viscosity bioinks	
Bioprinting resolution	100 μm	5 μm	50 μm	[15,234,238,239]
Repeatability	+	++	+++	
External stresses on cells	Mechanical	Optical or thermal	Mechanical, thermal, or electrical	[141]
Cell viabilities	40%–90%	95%	~85%	[141]

of 75 mm/s, and a payload of 5 kg for Y axis compared to 5 μm, 125 mm/s, and 10 kg values, respectively, for the larger model [234].

The clinical translation also raises the demand for a compact bioprinter with a high accuracy, deposition velocity, and resolution. Toward this end, miniaturized robotic arms with remote and wireless control possibilities [240,241] and light materials of construction with high specific strengths should be explored. Additionally, the type of tissue to be printed impacts the bioprinter selection. For example, a more compact bioprinter may be ideal for scaffold-free printing, as bioink volume would be small [242]. At the same time, scaffold-free bioprinting may also require higher resolutions to control cell-cell distances [243]. To achieve this objective, there is a need for developing robotics at mesoscale-level (1−4 mm) with a number of degrees of freedom, so that even nonplanar surface can be used as a substrate [244].

2.3.2.2 Bioprinter resolution

One of the important considerations for the bioprinter selection is its resolution, which allows the fabrication of constructs with high fidelity. In fact, the resolution of bioprinted constructs is generally inferior to the nominal resolution of the bioprinter used, which is because of the additional factors of bioink stability, solidification, and nozzle clogging observed in most bioprinting modalities. However, motion stages with micrometer scale resolution are vital to achieve bioprinted constructs in higher resolutions. In bioprinting, the size of nozzle is another consideration, which also determines the accuracy of final bioprinted constructs [234]. Droplet-based bioprinters can provide droplet size in 1−300 pL with single cell resolution (50 μm), and at the same time deposition rate of 1−10,000 droplets per second can be achieved [141]. There are many mechanisms on which DBB bioprinters base, and the droplet size has a bearing on the mechanism. With a similar orifice diameter, micro-valve print heads generate droplets of larger diameter (∼100 μm) in comparison to thermal or piezoelectric (∼50 μm) and acoustic droplet bioprinters (∼10 μm). Example of microvalve bioprinter is Biofactory, which produces droplets in range of 5−10 nL corresponding to >100 μm droplet diameter [15]. On the other hand, electrohydrodynamic jetting bioprinters can achieve resolutions which are not constrained by nozzle diameters, but they are not capable of generating one droplet at a time and thus reduce the precision of the system. Although DBB is capable of providing high lateral resolutions, their resolution in the z-direction is limited.

For extrusion-based bioprinters, positional resolutions with micrometer ranges are common (e.g., Allevi (previously Biobots): 5 μm, Fab@Home: 15 μm, Inkredible: 10 μm). Recently, Suntornnoud et al. have proposed a mathematical method to predict the bioprinter resolution of EBB based on a function of printing velocity, nozzle diameter, and applied pressure [140]. Most laser bioprinters can also achieve very high instrumental resolutions in lateral planes (30−100 μm) depending upon the wavelength of laser.

Generally, laser-based direct write methods have higher instrument resolution than LIFT [142,143]. Final resolution of LBB constructs is also determined by other factors such as fluence energy, surface properties, and air gap [245]. Improvement of the resolution of bioprinters is often associated with increased costs and printing times due to deposition of larger bioink loads and a greater number of dots per square inch specified in the design.

2.3.2.3 Degree of freedom and motion speed

Earlier bioprinting technologies were mostly developed from commercial paper printers. Groups of Boland and Nakamura initiated studies to transform Epson or HP printers into bioprinters [246,247]. Compared to the paper printers with a single movement direction, bioprinters need additional axes in order to build 3D constructs. Thus, several in-house modifications, such as providing integrated motorized table for a vertical axis movement, have been carried out with limited success. On the other hand, most commercial bioprinters are designed to only operate in three axes which is not adequate for intraoperative bioprinting of irregular-shaped defects in clinical settings. To bioprint nonplanar surfaces and concavities, more degrees of freedom are required [248,249]. The BioAssemblyBot with a 6-axes robotic arm, which is based on pneumatic microextrusion, is an improvement over the traditional extrusion bioprinters with three axes. In particular, the robotic arm is able to adjust the arm spacing (i.e., position level of the interconnected set of links and joints forming the robot manipulator in 2D Cartesian space location with respect to the taught location) to correspond with the porosity of designed constructs, along with additional options such as rotation about z-axis and allowing interchange of the lateral or dual rotation axis.

High printing speed is another important criterion for the bioprinter selection. The average speed of bioprinting in different modalities varies (e.g., LIFT: 200−1600 mm s^{-1}, acoustic DBB: 1−10,000 droplets s^{-1}, and EBB: 10 μm s^{-1}−700 mm s^{-1} [141,234]). The process may take several hours to complete, especially for multilayer constructs. In LBB, speed is limited as a single laser beam is used to irradiate each point of bioprinting. For example, the direct writing methods have high resolution but slow speed ($<10^2$ drops per second), while forward transfer methods have lower resolutions but can print up to 5×10^3 drops per second [142]. In commercially available extrusion-based bioprinters, typical speed is 25 mm/s. The printing speeds are specified by the stepper motor configuration and driver. Recently, the use of multiarray laser-based stereolithography [236,237], multinozzle droplet [235], or extrusion-based bioprinters and a multiarm robotic extrusion-based bioprinter have been proposed to reduce the bioprinting time [237].

Despite the capacity of bioprinter to deposit cells at high rates, the bioink composition especially cell-laden bioinks also determines the practical speeds that can be attained, since cell viability and cell division postprinting would be reduced, resulting from the

higher stresses induced by the higher deposition speed. Additionally, long standing time inside a reservoir due to slow printing rate can reduce the cell viability.

2.3.2.4 Commercialization

There has been great interest in 3D bioprinters and their potential to solve organ transplantation problems; however, commercialization of bioprinters has not kept as similar pace as the interest in exploring new applications of bioprinting. Overall, it can be concluded that extrusion-based bioprinters have achieved a more in-depth investigation compared to laser- or droplet-based bioprinters. Laser bioprinters have been the slowest for commercial transformation, due to their system complexities and tedious operations; though some commercial bioprinters based on stereolithography apparatus are available. In terms of extrusion-based bioprinters, there exists small difference between the working principles, and different manufacturers provide advanced functions such as automatic bioink cartridge filling and software control for robotic movement. Likewise, a wide range of droplet-based printers are available commercially, but most of them are not capable for printing mammalian cells, due to the small nozzle diameters compared to cell diameters (20–25 μm for cells and 150–500 μm for tissue spheroids [96,250,251]). Moreover, there exist many open-source 3D printers, which can be customized into bioprinters for early-stage researchers [88,89]. For example, a fused-deposition modeling (FDM)-based extruder can be modified into a pneumatically controlled extrusion-based bioprinter for deposition of Pluronic F-127 hydrogels [252].

Some commercial bioprinters are packed and delivered in the form of parts, in which case the end-users are expected to self-assemble. Hence, it may be necessitated for clinical deployment that skilled service engineers from the manufacturers could work together with other clinical personnel. In the future, it would also be expected that well-defined industrial norms for bioprinters are developed, which can be conformed to by the manufacturers to widen the acceptability of bioprinters in the medical community. Currently, software for many 3D printers is being standardized with respect to attributes such as error compensation, tolerance, temperature variations, and dimensional performance [253], and they can also be used as platforms for bioprinters. Standardization of software will facilitate the compatibility among different bioprinters, which enables cross-communications. Moreover, software should be able to not only communicate with the bioprinting hardware, but also enable the design of constructs. Such improvement will no doubt give a major fillip for fast commercialization of bioprinters, since it would be difficult for the end-user to integrate different software from different vendors for certain operation. A bioprinter with wide range of deposition speed, high resolution, multiplicity of dispensation, and compatibility with various types of bioinks will be the ultimate goal for bioprinting instrumentation, so that different users can benefit from the same platform.

2.3.2.5 Automation

A concern with current bioprinting modalities is the absence of a completely automated workflow [254], which has been already achieved by some other 3D printing technologies. So far, most of the suboperations of 3D printing ranging from extrusion of raw materials, fusion of metal powder, and photopolymerization have been automated [255–257]. A major hurdle for automation of bioprinting is the nature of bioinks, which should undergo sol-gel transition in physiological ambient conditions without use of high temperature. Due to the shape distortions, sol-gel form is not readily bioprinted with high resolution deposition. In practice, it is often observed that either the nozzle or printed material does not contact the previous layer due to inherent hydrogel swelling or dehydration processes, which causes significant structural deformation and requires manual intervention.

Moreover, in many bioprinting applications, multiple bioinks are coprinted, and each of them owns different swelling or shrinking kinetics which make the automation of bioprinting complicated. Such deficiencies are sought to be improved by implementation of real-time monitoring technologies, which use optical camera to observe construct height and provide feedback signal for subsequent dispensation [258]. It must be noted that automation of dispensing should be compatible with other liquid handling and cell culture protocols. Several automated protocols for cell culture are now reported, and they should be integrated with bioprinting modalities for in situ applications [259–261]. Recently, an automated process for creation of surface topographic cues with a robotic bioink dispensation system has been demonstrated for tissue engineering applications [262].

2.3.2.6 User-friendliness

Since a large number of end-users are expected to be in medical and biotechnological areas, it is desirable that the user interface of bioprinters is user-friendly. User-friendliness can be evaluated by the time and steps required to get functional outputs and the minimum time required to train a new user. The end-users should not be bothered much with the intricate instrumentation operation, and should be allowed to focus more on the clinical problems. Therefore, user-friendliness should be taken into account seriously for the bioprinter development. It may be seen that most of the extrusion- and some droplet-based bioprinters are quite user-friendly. In fact, some of the bioprinters are transshipped as separated parts, which can be assembled by end-users themselves. Besides ease of installation, they also allow ease of operation with interactive software. During operation, point to be noted is the change of bioink after dispensation of a unit quantity initially loaded. In this respect, bioprinters with attached peristaltic pumps are desirable. Apart from operation, troubleshooting is also important and a manual with clear descriptions should be provided. Since a bioprinter is made up of several small electronic and mechanical components, such as microchips, microcontrollers, stepper motors, gears, and belts, it is essential to use the components following international standard. Bioprinters

such as Inkredible and Biobots are quite user-friendly, whereas Envisiontec and Gesim Bioscaffolder are sophisticated, which required professional training for operation and troubleshooting [21,22]. Moreover, laser-based bioprinters are generally less user-friendly as they require more learning time and they are more intricate to operate.

2.3.2.7 Affordability

The high cost of bioprinters remains a bottleneck for mass deployment of the technology in regular clinical use. It is also emphasized that bioprinting processes are quite expensive as the essential sterility required. However, cost of any instrument is known to plummet as demand increases. Therefore, it may be predicted that with rising number of users and proof-of-concept demonstration of applications, bioprinters will start finding commercial demand and price will drop as seen in plastic 3D printers. At present, most of clinically relevant bioprinters are available at pricing of $150−200k. However, several start-up companies are trying to develop affordable bioprinters for customers across the country, though most of these bioprinters are based on extrusion principle and have inferior fabrication properties. Certain pneumatic extrusion bioprinters can also be very expensive (e.g., BioAssembly bots at $\sim$ $160k and nSrypt at $>$ $200k). The recently launched bioprinters in this category like BioBots and Inkredible are available in range of $10k. Laser-based bioprinters, which can be developed from scratch, are around $100k. On contrary, biaxial droplet-based bioinks without live-cell dispensing capabilities can be developed using commercial paper-jet printers at very low cost. For biological application, however, the cost may increase to $20−70k. Generally, the system automation, resolution, number of print heads are important determinants of the cost. For instance, dual-head bioprinter with photo-cross-linking capability costs $5−10k, while a basic one with bioink extruder only costs as little as $500. It is essential that a component cost analysis is performed to find out strategies for cost reduction. In a recent study, Reid et al. have developed an automated bioprinting system with the protocol of human-induced pluripotent cell differentiation. A low-cost Felix 3D printer was adapted and the resolution of conventional extrusion process were improved by the use of finite element modeling [263].

2.3.2.8 Versatility

Another important property of bioprinters is the necessity of versatility, which refers to the compatibility with various types of bioinks, bioinks with wide range of viscosities and different gelation processes and various bioprinting processes. Versatile bioprinters should also allow end-users to customize the instrument for specific applications. Among different bioprinters, the Biobot series is one example of versatile bioprinters. The open source Fab@Home also offers bioprinters with remarkable versatility. In the droplet-based category, different series of bioprinters such as Nordson Pico series and MD series from Microdrop Technologies, which are suitable for high-throughput applications, provide

significant versatility by allowing enhanced control on generation of droplets and their spatial deposition. It can be deduced that extrusion-based bioprinters are more versatile as bioinks with wide ranges of viscosities can be dispensed. Comparatively, laser-based bioprinters are limited by the bioink which can be irradiated by laser or photopolymerization. In droplet-based bioprinters, different bioinks can be printed, but clogging of nozzles is frequently observed for high viscosity bioinks, which limits their versatility. As an example, most bioprinters are developed for alginate or Pluronic bioinks, which have limited clinical utility for tissue regeneration. Therefore, a system automation based on these bioinks may not be exactly suitable for an end-user, who seeks functional bioinks.

2.3.3 Bioprinting phase

After the selection of bioink formulation and appropriate bioprinter technology, physical bioprinting assumes significance, as process parameters comprise a range of selection which should be optimized in case-to-case basis to obtain the desired constructs. There is a need for process automation in this stage to generate constructs rapidly for clinical applications. Bioprinting process should also be carried out under highly defined and controlled environments with proper controls to allow for repetitive results. Some of the salient requirements of this stage are described below:

2.3.3.1 Bioprinting resolution

The resolution of a bioprinting process, which can be evaluated in terms of the smallest pattern that can be achieved, differs from the instrumental resolution of a bioprinter due to the rheological properties and noninstantaneous nature of solidification of most hydrogels. In practice, process bioprinting resolution of around 5, 50, and 100 μm are typically obtained by LBB, DBB, and EBB, respectively [15,234,238]. Likewise, resolution deteriorates as bioink is changed from hydrogel to cell aggregates (i.e., tissue spheroids or strands). One of the effective ways to improve bioprinting resolution is to allow quick cross-linking, but this often results in nozzle clogging and adherence of nozzle to bioprinted layers. Moreover, reduction in nozzle diameter is also not an effective solution, as it would increase shear force on the cells, resulting in decreased viability.

In case of DBB, ejection of one droplet is often accompanied by several satellite droplets, reducing its bioprinting resolution [264]. Other factors that influence bioprinting process resolution are the mechanism of actuation, droplet-nozzle and droplet-substrate interactions. For example, hydrophilicity of inner walls of the nozzle and the surface tension of bioink affect the print quality. Decreasing hydrophilicity of nozzle inner walls and lowering the surface tension of the bioink result in delayed droplet disintegration time and reduce droplet ejection velocities. Similarly, contact

angle of substrate determines the spreading of bioink, and hence influences the resolution of the bioprinting process.

In LBB, process parameters that influence resolution include jet dynamics and impact of ejected bioink. These forces can be modulated by the bioink rheology and by adjusting the distance between the ribbon and collector. Based on the above process understanding, Ali et al. have successfully bioprinted MSCs with minimal shear stress and high process resolution [265]. Additionally, the study of Guillotin also showed the effect of bioink viscosity and laser parameters on the bioprinting resolution [131]. In many cases, improving the bioprinting resolution often results in decrease of cellular functionality parameters (e.g., stem cell integrity, high dehydration time), and hence process parameters like shear stress are required to be optimized [136]. LBB can result in generally high bioprinting resolution compared to DBB and EBB. For EBB, bioprinting resolution should be endeavored to be improved by using a tapered nozzle to reduce the exposure time of cells to high shear stress, hyphenation with electrohydrodynamic effects [266,267] or ultimately using a nozzle-free extrusion system.

2.3.3.2 Repeatability

Tissue engineered constructs are required to meet specific and quantitative standards of safety and performance for clinical use [268,269]. Bioprinted constructs are more complex and customized compared to traditional constructs, making the standardization more difficult. In this respect, it has been observed that the use of tissue strands as a bioink, without liquid medium or molds, allows for repeatable bioprinting [149]. The major criteria of estimation of the repeatability of bioprinted structures for standardization include bioprint fidelity, mechanical properties, and cell viability. It must be noted that some properties such as mechanical strength are dynamic in nature and would change with time as cells deposit their own ECM. Therefore, standardized protocols should also be dynamic (i.e., analysis at multiple time points). Several automated methods for cell viability and mechanical property measurements of tissue in situ have been developed [270]. One of the examples is to use microscope for label-free cell viability determination, which should be more widely applied [271–273]. Among the bioprinting modalities, process repeatability is higher in DBB compared to LBB or EBB. EBB often suffers from unpredictable process interruptions due to swelling or shrinkage of hydrogels [182]. Though LBB is nozzle-free bioprinting and hence, the repeatability is not affected by clogging problems, the limited range of viscosities that can be handled restricts the mechanical strengths of the printed construct. In LBB, the processes are highly complicated with nonlinear physical relationship of parameters resulting in poor repeatability of the process.

2.3.3.3 Biocompatibility

Process biocompatibility is unarguably one of the most important considerations for bioprinting. One of the principal aims of bioprinting is to maintain viability and function.

In addition, the process must not induce any phenotypic and genotypic changes. Depending upon the modality, cells may be exposed to different external stresses including mechanical in EBB; mechanical, acoustic, thermal, or electrical in DBB; and optical or thermal in LBB, all of which can result in cell morbidities. In general, typical viabilities of 40%−80% for EBB, 85% for DBB, and 95% for LBB are observed [141]. From these, it can be deduced that shear stress is most detrimental to cells [137]. For each modality, apart from bioink compatibility, certain common stressors also exist (e.g., flow rate and bioprinting time), which may result in lower cell viabilities. In case of LBB, additional parameters such as laser pulse time and air gap between receiver and collector plates also determine the biocompatibility of the process [274]. In many cases, solidification is achieved by UV, which may become another factor to impact viability. Application of stereolithography in bioprinting commenced with the experiments of Boland and coworkers in 2004. In this method, cells and a photocurable hydrogel was charged onto a vat, and positioned on a table in which movement could be controlled in vertical axis. UV radiation was then made incident on the bioink, triggering generation of radical from photoinitiators and subsequent polymerization of the bioink. UV light traced the toolpath according to the CAD file, thus curing the bioink at designated places inside the vat. The process was repeated for each layer to generate the 3D constructs, which can be of few hundred μm to few mm in size. Initially, Chinese hamster ovary cells were bioprinted in PEO and PEO-dimethacrylate (PEGDMA) hydrogels with over 90% viability. Subsequently, SLA-based bioprinting of cylindrical constructs were shown for 3T3 fibroblasts within PEGDMA hydrogels. Other commonly used hydrogel for SLA bioprinting has been acrylate polymers with urethane segments and trimethylolpropane triacrylate. Apart from photocurable polymers, photoinitiators, e.g., Irgacure, are also a major component of this modality in order to improve solidification. Thus, the optimization of photoinitiator concentration in a bioink composition becomes crucial. Further, care is to be taken to determine the ideal photoinitiator concentration due to its toxicity [208,275]. Recently, the use of visible light-induced cross-linking of poly(ethylene glycol diacrylate), gelatin methacrylate, and eosin Y photoinitiator has shown promise to maintain high cell viability [276].

2.4 Postbioprinting stage

After bioprinting of constructs, tissue maturation is a time-dependent process and postbioprinting should be performed under tightly controlled conditions, especially in bioreactors (see Fig. 2.5A). Cell-cell interactions are highly influenced by these conditions and kinetics of any differentiation process can be modulated with wide variations of stimuli that can be exerted during postbioprinting processes. Such conditions can be optimized to mimic in vivo environment, which can be further enhanced by providing in vivo like environment such as explant culture as can be seen in Fig. 2.5B.

2.4.1 Conditioning of bioprinted constructs

Lack of mass transfer of nutrients and metabolites is one of the prime reasons for failure of generating tissue constructs with clinically relevant thickness in vitro, since the absence of internal vascular network restricts oxygen supply from the peripheral regions of the construct to the deeper regions even after homogeneous seeding [279]. This is also an issue for bioprinted tissue constructs. Though bioprinted constructs have been designed with vasculature as shown in Fig. 2.5C, effective oxygen supply is not readily achieved in conventional static tissue culture methods. Therefore, perfusion of bioprinted constructs in bioreactors becomes a necessary and essential step.

A bioreactor is broadly defined to be a vessel, in which a biochemical process can be carried out under controlled conditions, and allows simultaneous monitoring. In bioprinted tissue constructs, bioreactors also allow to create various stimulating conditions to regulate the maturation of the tissues. Several types of bioreactors including spinner flask, rotating

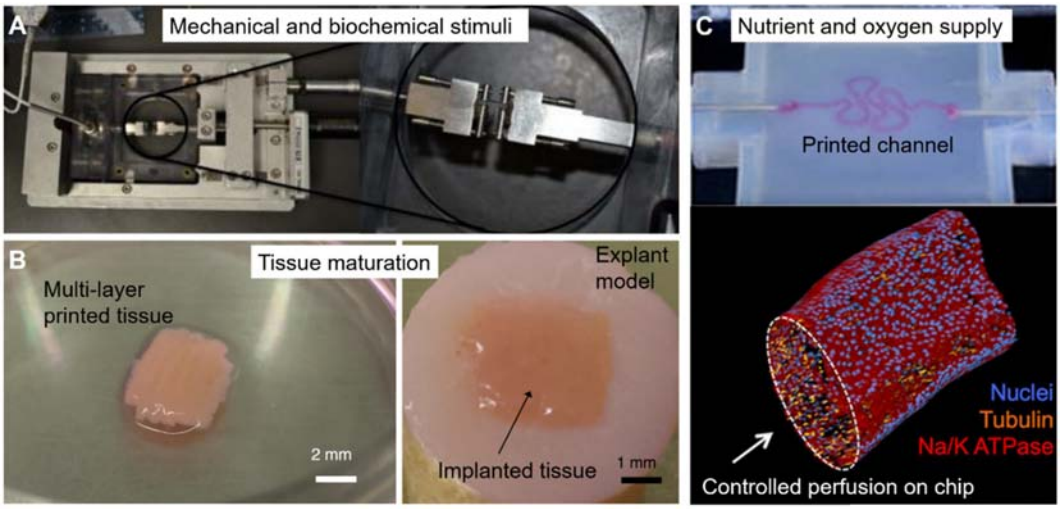

Figure 2.5
(A) A biotense perfusion bioreactor with a bioprinted vasculature; (B) Explant culture improved the maturation of bioprinted cartilage into a nativelike cartilage; (C) 3D Bioprinted convoluted renal proximal tubule where an open lumen circumscribed with an epithelial lining was perfused on chip. *Modified with permission from (A) F. Dolati, Y. Yu, Y. Zhang, D.A.M. Jesus, E.A. Sander, I.T. Ozbolat, In vitro evaluation of carbon-nanotube-reinforced bioprintable vascular conduits, Nanotechnology 25 (14) (2014) 145101. Modified from (B) Y. Yu, K.K. Moncal, J. Li, W. Peng, I. Rivero, J.A. Martin, I.T. Ozbolat, Three-dimensional bioprinting using self-assembling scalable scaffold-free "tissue strands" as a new bioink, Scientific Reports 6 (February) (2016) 28714. (C) K.A. Homan, D.B. Kolesky, M.A. Skylar-Scott, J. Herrmann, H. Obuobi, A. Moisan, J.A. Lewis, Bioprinting of 3D convoluted renal proximal tubules on perfusable chips, Scientific Reports 6 (2016) 34845.*

wall, compression, strain, hydrostatic pressure, flow perfusion, and some combined bioreactors have been used for engineering tissue constructs [280]. Among them, flow perfusion bioreactor is made up of a pump system and a chamber for tissue construct connected by tubes, such that media can flow through the tissue construct to enhance fluid transport.

Bioreactors have shown their utility in different types of tissues including bone, skin, cardiovascular, and cartilage. For example, in rotating wall vessel bioreactor, mature chondrocytes were observed after 6 weeks of culture from cartilage progenitor cells or 3 weeks from bone marrow stromal cells. In addition, cartilaginous tissues, approximately 1.25×0.60 cm in dimensions, have been obtained after 12 weeks of culture [281]. In spinner flask bioreactor, cartilage formation after 4 weeks is observed. Bone tissue type mineralization is obtained in spinner bioreactors after 3−5 weeks of culture. Several microfluidic perfusion bioreactors have also been developed, which allow bioprinted construct to differentiate at accelerated rate into desired tissues such as heart [202,203] and bone [282]. However, technological breakthrough of bioreactors should be performed for wider clinical translation through offering substantial user-friendliness. Further, process consistency and volume output are also necessary to be improved. This can be achieved by increasing the automation of bioreactors. For example, the perfusion bioreactor from Aastrom Bioscience Inc. allows for automated expansion of cells from bone marrow as raw material. Recent advances in bioreactors allow real-time monitoring and feedback control of several vital parameters including temperature, oxygen level, and pH, to allow optimal cell growth. In addition, novel oxygen-imaging sensor has been developed, which can be integrated with bioreactors to map oxygen distribution in 3D scaffolds [283]. The other physiological ambient conditions required to be maintained in bioreactor are oxygen partial pressure (pO_2), pH, CO_2, and temperature, as well as maintained concentrations of growth factor and nutrients.

In the classical paradigm of tissue engineering, cells, scaffold, and growth factors composed the triad which needs to be engineered to obtain functional tissues. However, it was realized that external stimuli can also induce differentiation of progenitor cells into specific cell types. Thus, apart from designing scaffold with architecture for cell infiltration and growth, it is necessary that physiologically mimetic mechanical and biochemical stimuli are exerted on tissue constructs in a bioreactor for cells to mature into relevant tissues [262]. Many bioreactors have been developed to exert such mechanical stimuli such as hydrostatic pressure, compression, shear, and tension [280].

Methods have also been developed to exert mechanical/biochemical or mechanical/electrical stimuli for accelerated maturation of some specific tissue types. For example, in cartilage tissue engineering, mechanical stimuli are applied to compress the cartilage to produce more ECM to improve mechanical strength. Mechanical stimulation can also aid

in better integration of cartilage construct with host tissue. For example, in cartilage tissue engineering, stimulation with 0.4 MPa pulsatile hydrostatic pressure or 1 Hz compression can lead enhanced chondrocytes differentiation, GAG production, and ECM synthesis [284]. Another study by Wernike et al. found that dynamic compression (10%–20% strain; 0.5 Hz; 1 h/day) and low oxygen tension (5%) were able to show a more stable phenotype of chondrocytes [285]. Similarly, for osteoblasts differentiation and alkaline phosphatase (ALP) activities were observed to be enhanced, when they were cultured with the shear stress of 0.16–32 N/m^2. For cardiac tissue engineering, electrical (e.g., 5 V for 2 ms, 1 Hz) or mechanical (e.g., 2 Hz) stimulation has been shown to improve tissue formation [286]. The extent and values of stimuli exerted in different studies for maturation of tissues in bioreactors have been mentioned and extensively detailed in other studies [287,288]. Recently, bioreactor systems for clinical heart valve tissue engineering have also been reported [289].

2.4.2 Practicality

One important parameter that is critical for success of bioprinting is the practicality with which mass-scale tissue production can be carried out. Prevalent technologies can result in production of proliferation/differentiation of cells into numbers, which are adequate only for laboratory scale studies. However, organ bioprinting for clinically relevant volumes and amounts require scale-up manufacturing of cells. Advanced, automated bioprocessing technologies conforming to good manufacturing practices and strict quality monitoring are thus needed to be implemented in clinical bioprinting establishments [290]. The source of cell in itself may have some constraints; for example, stem cells from relatively younger patients can be passed up to 40 generations and those from patients of higher age group can be limited to only 25 population cycles only [291]. For example, Organovo company has been successfully producing liver tissue lines for drug toxicity testing [292] and has also started making progress in kidney and skin tissue bioprinting. Apart from tissue constructs, bioprinting-assisted fabrication of tumor-on-chip platforms is emerging to provide practical solutions for cancer research [1].

2.4.3 Affordability

The bioreactor should not add significant costs to the whole system. Bioreactors are mostly composed of peristaltic pumps, filters, chamber vessel, tubings, and integrated sensors. Of these, filters have generally the highest cost contribution, apart from number of sensors that are integrated inside the system. Though addition of advanced monitoring and control systems for vital parameters as well as cellular phenotypes may contribute to cost of maturation bioreactors and hence tissue constructs, progresses and commercialization of systems like BioProfilew 400 (Nova Biomedical), Advanced Clinical Tissue Engineering

System ACTESe, or Stat Profilew Critical Care Xpress present an encouraging scenario [293]. Affordability of bioreactors is also determined by the tissue types and differentiation media to be used.

2.5 Conclusions and future remarks

It is widely speculated that future bioprinting will soon move toward fabrication of mechanically robust constructs with high resolutions as well as translation of bioprinters into operating rooms. Clinical translation of bioprinting demands scale-up to clinically relevant volume of tissues along with efficient vascularization for ready implantation. Rapid expansion in efforts for bioprinting of several tissues/organs like pancreas [294], osteochondral [295], and bone are visible [156,296]. To achieve this, bioprinting technological advancements are needed to be firmly supported by organic synchronization of all components of bioprinting. Since this is a multistep process, ultimate construct fabrication will be dependent on how each step is coordinated with others and appropriately optimized. Though one of the major milestones in bioprinter development may be considered to be started with the modification of desktop 3D printers for printing of live cells [133], bioprinting industry is still in its infancy with limited technological achievements in attaining a complete process chain for functional tissue biofabrication. The ExVive 3D bioprinted human tissues developed by the Organovo company is, however, an important milestone in bioprinting process chain. Similarly, in immediate past, a bioresorbable 3D-printed airway splint has been implanted in human infant. Approval of food and drug administration (FDA) was sought by the University of Michigan's Institutional Review Board, and the device was granted emergency-use exemption and has performed well in initial evaluations. It is expected that more of such milestones may be witnessed in the near future. On the other hand, inability to generate functional vascular network in bioprinted constructs is the weakest link in bioprinting process chain, and it would require specific solutions to overcome the limitations. Likewise, ample achievements have also been made in scale-up of bioprinted constructs, which had been thought to be a limitation initially [297]. Bioprinting of microvascular network is more challenging compared to bioprinting macro-level vasculature. Fugitive inks are often employed to fabricate the vascular networks [298]. Moreover, some recent achievements in intravascularization of tissue spheroids (such as pancreatic islets) indicate that it is possible to make significant inroads in overcoming this limitation for bioprinting [299]. Broadly, it is expected that major milestones in transplantation of organs not requiring vascularization for significant effects (like cartilage or skin) may be achieved sooner than organs with high metabolic activity (e.g., liver or heart) [19].

In the prebioprinting stage, minimally invasive cell harvesting followed by efficient expansion technologies of stem cell are essential to generate rapid and cost-effective

tissue-specific constructs from autologous cells. Different new cell types like pericytes are also attractive for functional bioprinting applications [300]. This apart, high-resolution images and more robust blueprint modeling should develop to ensure full potential of bioprinting is harnessed clinically. In the bioprinting stage, there is need for focused research on bioprintable biomaterials, which form the important component of bioinks since not all novel biomaterials are amenable to bioprinting. Instructive biomaterials that direct cells to a defined lineage apart from supporting adequate cell adhesion, proliferation, and appropriate host response are emerging but their bioprintability cannot be always guaranteed and hence needs special attention. Specifically, quick gelation in a physiologically acceptable environment (pH, temperature, radiation, etc.) is expected from these compatible biomaterials for successful bioprinting. In the bioprinting stage, another crucial area is the evolution of bioprinting technologies and the bioprinter themselves. Bioprinter should have high degree of freedom in multiaxis, multiple arms as well as design to reduce chances of bioink coagulation during long operating hours. Another important dimension would be full automation of the bioprinting process to maintain highest levels of aseptic conditions inside the operating rooms. Affordability and ease of operation would also require to be considered for use in clinical establishments. The advances in bioprinters and bioinks are needed to be complemented with process innovations to allow precise fabrication of constructs mimicking native tissue microenvironment causing minimal cell damages. Several in situ monitoring and sensing mechanisms are needed to be built in to enable detection of deviations and feedback control of the process. Subsequently, bioprinted constructs are transferred to bioreactors where tissue maturation is accelerated with aid of mechanical, electrical, and/or biochemical stimulation to obtain rigid and functional tissue construct, and monitored with the aid of biosensors.

Indeed, bioprinting technology is expected to provide constructs with improved functional quality, resolution, 3D design, and material complexities with spatial variations mimicking natural tissue, in the future. Deposition of various bioinks with different physicochemical properties simultaneously appears to be a realistic prospect. However, it can be concluded that a well-coordinated and multidisciplinary approach is necessary to ensure that tissue constructs with high quality and reproducibility are obtained for human transplantation.

References

[1] S. Knowlton, A. Joshi, B. Yenilmez, I.T. Ozbolat, C.K. Chua, A. Khademhosseini, S. Tasoglu, Advancing cancer research using bioprinting for tumor-on-a-chip platforms, International Journal of Bioprinting 2 (2016) 3–8.

[2] W. Peng, D. Unutmaz, I.T. Ozbolat, Bioprinting towards physiologically relevant tissue models for pharmaceutics, Trends in Biotechnology 34 (9) (2016) 722–732.

[3] E.L. Elson, G.M. Genin, Tissue constructs: platforms for basic research and drug discovery, Interface Focus 6 (1) (2016) 20150095.

[4] M.E. Gomes, M.T. Rodrigues, R.M.A. Domingues, R.L. Reis, Tissue engineering and regenerative medicine: new trends and directions—a year in review, Tissue Engineering Part B Reviews 23 (3) (2017) 211–224.
[5] A.-V. Do, A. Akkouch, B. Green, I. Ozbolat, A. Debabneh, S. Geary, A.K. Salem, Controlled and sequential delivery of fluorophores from 3D printed alginate-PLGA tubes, Annals of Biomedical Engineering 45 (1) (2017) 297–305.
[6] T. Guo, J. Lembong, L.G. Zhang, J.P. Fisher, Three-dimensional printing articular cartilage: recapitulating the complexity of native tissue, Tissue Engineering Part B Reviews 23 (3) (2016) 225–236.
[7] D.-J. Cornelissen, A. Faulkner-Jones, W. Shu, Current Developments in 3D Bioprinting for Tissue Engineering, Current Opinion in Biomedical Engineering in Press, 2017.
[8] M.J. Rodriguez, J. Brown, J. Giordano, S.J. Lin, F.G. Omenetto, D.L. Kaplan, Silk based bioinks for soft tissue reconstruction using 3-dimensional (3D) printing with in vitro and in vivo assessments, Biomaterials 117 (2017) 105–115.
[9] K. Hölzl, S. Lin, L. Tytgat, V.S. Vlierberghe, L. Gu, A. Ovsianikov, Bioink properties before, during and after 3D bioprinting, Biofabrication 8 (3) (2016) 32002.
[10] T. Bhattacharjee, S.M. Zehnder, K.G. Rowe, S. Jain, R.M. Nixon, W.G. Sawyer, T.E. Angelini, Writing in the granular gel medium, Science Advances 1 (8) (2015) e1500655–e1500655.
[11] T.J. Hinton, Q. Jallerat, R.N. Palchesko, J.H. Park, M.S. Grodzicki, H.J. Shue, M.H. Ramadan, A.R. Hudson, A.W. Feinberg, Three-dimensional printing of complex biological structures by freeform reversible embedding of suspended hydrogels, Science Advances 1 (9) (2015) e1500758.
[12] T.J. Hinton, A. Hudson, K. Pusch, A. Lee, A.W. Feinberg, 3D printing PDMS elastomer in a hydrophilic support bath via freeform reversible embedding, ACS Biomaterials Science & Engineering 2 (10) (2016) 1781–1786.
[13] Y. Jin, A. Compaan, T. Bhattacharjee, Y. Huang, Granular gel support-enabled extrusion of three-dimensional alginate and cellular structures, Biofabrication 8 (2016) 025016.
[14] Y. Jin, C. Liu, W. Chai, A. Compaan, Y. Huang, Self-supporting nanoclay as internal scaffold material for direct printing of soft hydrogel composite structures in air, ACS Applied Materials and Interfaces 9 (20) (2017) 17456–17465.
[15] H. Gudapati, M. Dey, I. Ozbolat, A comprehensive review on droplet-based bioprinting: past, present and future, Biomaterials 102 (2016) 20–42.
[16] W.L. Ng, J.M. Lee, W.Y. Yeong, M. Win Naing, Microvalve-based bioprinting - process, bio-inks and applications, Biomaterials Science 5 (4) (2017) 632–647.
[17] R. Gauvin, Y.-C. Chen, J.W. Lee, P. Soman, P. Zorlutuna, J.W. Nichol, H. Bae, S. Chen, A. Khademhosseini, Microfabrication of complex porous tissue engineering scaffolds using 3D projection stereolithography, Biomaterials 33 (15) (2012) 3824–3834.
[18] M. Gou, X. Qu, W. Zhu, M. Xiang, J. Yang, K. Zhang, Y. Wei, S. Chen, Bio-inspired detoxification using 3D-printed hydrogel nanocomposites, Nature Communications 5 (2014) 3774.
[19] P. Datta, B. Ayan, I.T. Ozbolat, Bioprinting for vascular and vascularized tissue biofabrication, Acta Biomaterialia 51 (2017) 1–20.
[20] W. Peng, P. Datta, B. Ayan, V. Ozbolat, D. Sosnoski, I.T. Ozbolat, 3D bioprinting for drug discovery and development in pharmaceutics, Acta Biomaterialia 57 (2017) 26–46.
[21] H. Lee, Y. Koo, M. Yeo, S. Kim, G.H. Kim, Recent cell printing systems for tissue engineering, International Journal of Bioprinting 3 (1) (2017).
[22] J. Lee, K.E. Kim, S. Bang, I. Noh, C. Lee, A desktop multi-material 3D bio-printing system with open-source hardware and software, International Journal of Precision Engineering and Manufacturing 18 (4) (2017) 605–612.
[23] C. Norotte, F.S. Marga, L.E. Niklason, G. Forgacs, Scaffold-free vascular tissue engineering using bioprinting, Biomaterials 30 (30) (2009) 5910–5917.

[24] P. Actis, M.M. Maalouf, H.J. Kim, A. Lohith, B. Vilozny, R.A. Seger, N. Pourmand, Compartmental genomics in living cells revealed by single-cell nanobiopsy, ACS Nano 8 (1) (2014) 546−553.
[25] J. Vacanti, R.S. Langer, R. Lanza, Principles of Tissue Engineering, Academic Press, 2007.
[26] G. Van Lenthe, H. Hagenmuller, M. Bohner, S. Hollister, L. Meinel, R. Muller, Nondestructive micro-computed tomography for biological imaging and quantification of scaffold−bone interaction in vivo, Biomaterials 28 (15) (2007) 2479−2490.
[27] B.A. Poser, K. Setsompop, Pulse sequences and parallel imaging for high spatiotemporal resolution MRI at ultra-high field, NeuroImage (2017) 1−18 (December 2016).
[28] I.T. Ozbolat, A.K.M.B. Khoda, Design of a new parametric path plan for additive manufacturing of hollow porous structures with functionally graded materials, Journal of Computing and Information Science in Engineering 14 (4) (2014) 41005−41013.
[29] S. Obeng-Gyasi, L.J. Grimm, E.S. Hwang, V.S. Klimberg, K.I. Bland, 28-Indications and Techniques for Biopsy BT - The Breast, fifth ed., 2018, pp. 377−385, e2.
[30] F. Pohlig, C. Kirchhoff, U. Lenze, J. Schauwecker, R. Burgkart, H. Rechl, R. von Eisenhart-Rothe, Percutaneous core needle biopsy versus open biopsy in diagnostics of bone and soft tissue sarcoma: a retrospective study, European Journal of Medical Research 17 (1) (2012) 29.
[31] H.-L. Park, L.S. Kim, The current role of vacuum assisted breast biopsy system in breast disease, Journal of Breast Cancer 14 (1) (2011) 1−7.
[32] R.E. Fine, P.W. Whitworth, J.A. Kim, J.K. Harness, B.A. Boyd, W.E. Burak, Low-risk palpable breast masses removed using a vacuum-assisted hand-held device, The American Journal of Surgery 186 (4) (2003) 362−367.
[33] G. Vlastos, H.M. Verkooijen, Minimally invasive approaches for diagnosis and treatment of early-stage breast cancer, The Oncologist 12 (1) (2007) 1−10.
[34] R. Hamazoe, M. Maeta, A. Murakami, H. Yamashiro, N. Kaibara, Heating efficiency of radiofrequency capacitive hyperthermia for treatment of deep-seated tumors in the peritoneal cavity, Journal of Surgical Oncology 48 (3) (1991) 176−179.
[35] L. Chen, D. Bouley, E. Yuh, H. D'Arceuil, K. Butts, Study of focused ultrasound tissue damage using MRI and histology, Journal of Magnetic Resonance Imaging 10 (2) (1999) 146−153.
[36] H.E. Cline, K. Hynynen, R.D. Watkins, W.J. Adams, J.F. Schenck, R.H. Ettinger, W.R. Freund, J.P. Vetro, F.A. Jolesz, Focused US system for MR imaging-guided tumor ablation, Radiology 194 (3) (1995) 731−737.
[37] N. McDannold, K. Hynynen, D. Wolf, G. Wolf, F. Jolesz, MRI evaluation of thermal ablation of tumors with focused ultrasound, Journal of Magnetic Resonance Imaging 8 (1) (1998) 91−100.
[38] F. Pati, D.-W. Cho, Bioprinting of 3D tissue models using decellularized extracellular matrix bioink, in: Z. Koledova, Z. Koledova (Eds.), 3D Cell Culture: Methods and Protocols, Humana Press, New York, NY, 2017, pp. 381−390.
[39] M.L. Levin, C. Lober, R.R. Levin, Harvesting auricular cartilage, Journal of Dermatologic Surgery & Oncology 15 (7) (1989) 712−713.
[40] C.A. Megerian, B.D. Weitzner, B. Dore, L.J. Bonassar, Minimally invasive technique of auricular cartilage harvest for tissue engineering, Tissue Engineering 6 (2000) 69−74.
[41] J. Ceusters, J.P. Lejeune, C. Sandersen, A. Niesten, L. Lagneaux, D. Serteyn, From skeletal muscle to stem cells: an innovative and minimally-invasive process for multiple species, Scientific Reports 7 (2017) 696.
[42] A. Tait, X. Charalambous, T. Proctor, K. Tsagovits, N. Hamilton, F. Veraitch, M.A. Birchall, M. Lowdell, Creating gmp epithelial and fibroblast cells from a single biopsy for the potential use in tissue engineering, Cytotherapy 19 (5) (2017) S194.
[43] S.F. Collins, Bioprinting is changing regenerative medicine forever, Stem Cells and Development 23 (S1) (2014) 79−82.

[44] M. Gruene, M. Pflaum, A. Deiwick, L. Koch, S. Schlie, C. Unger, M. Wilhelmi, A. Haverich, B. Chichkov, Adipogenic differentiation of laser-printed 3D tissue grafts consisting of human adipose-derived stem cells, Biofabrication 3 (1) (2011) 015005.
[45] M. Gruene, A. Deiwick, L. Koch, S. Schlie, C. Unger, N. Hofmann, I. Bernemann, B. Glasmacher, B. Chichkov, Laser printing of stem cells for biofabrication of scaffold-free autologous grafts, Tissue Engineering Part C Methods 17 (1) (2011) 79–87.
[46] F. Xu, B. Sridharan, S. Wang, U.A. Gurkan, B. Syverud, U. Demirci, Embryonic stem cell bioprinting for uniform and controlled size embryoid body formation, Biomicrofluidics 5 (2) (2011) 22207.
[47] J. Itskovitz-Eldor, M. Schuldiner, D. Karsenti, A. Eden, O. Yanuka, M. Amit, H. Soreq, N. Benvenisty, Differentiation of human embryonic stem cells into embryoid bodies compromising the three embryonic germ layers, Molecular Medicine 6 (2) (2000) 88–95.
[48] H. Kurosawa, Methods for inducing embryoid body formation: in vitro differentiation system of embryonic stem cells, Journal of Bioscience and Bioengineering 103 (5) (2007) 389–398.
[49] S. Tasoglu, U. Demirci, Bioprinting for stem cell research, Trends in Biotechnology 31 (1) (2013) 10–19.
[50] A.A. Youssef, E.G. Ross, R. Bolli, C.J. Pepine, N.J. Leeper, P.C. Yang, The promise and challenge of induced pluripotent stem cells for cardiovascular applications, Journal of the American College of Cardiology: Basic to Translational Science 1 (6) (2016) 510–523.
[51] B. Gao, Q. Yang, X. Zhao, G. Jin, Y. Ma, F. Xu, 4D bioprinting for biomedical applications, Trends in Biotechnology 34 (9) (2016) 746–756.
[52] F. Gao, S.M. Chiu, D.A.L. Motan, Z. Zhang, L. Chen, H.L. Ji, H.F. Tse, Q.L. Fu, Q. Lian, Mesenchymal stem cells and immunomodulation: current status and future prospects, Cell Death & Disease 7 (1) (2016) e2062.
[53] S.A. Irvine, S.S. Venkatraman, Bioprinting and differentiation of stem cells, Molecules 21 (2016).
[54] M. Madrigal, K.S. Rao, N.H. Riordan, A review of therapeutic effects of mesenchymal stem cell secretions and induction of secretory modification by different culture methods, Journal of Translational Medicine 12 (2014) 260.
[55] D.E. Cohen, D. Melton, Turning straw into gold: directing cell fate for regenerative medicine, Nature Review Genetics 12 (4) (2011) 243–252.
[56] P. Huang, L. Zhang, Y. Gao, Z. He, D. Yao, Z. Wu, J. Cen, X. Chen, C. Liu, Y. Hu, D. Lai, Z. Hu, L. Chen, Y. Zhang, X. Cheng, X. Ma, G. Pan, X. Wang, L. Hui, Direct reprogramming of human fibroblasts to functional and expandable hepatocytes, Cell Stem Cell 14 (3) (2014) 370–384.
[57] M. Ieda, J.-D. Fu, P. Delgado-Olguin, V. Vedantham, Y. Hayashi, B.G. Bruneau, D. Srivastava, Direct reprogramming of fibroblasts into functional cardiomyocytes by defined factors, Cell 142 (3) (2010) 375–386.
[58] Y. Zhang, C. Pak, Y. Han, H. Ahlenius, Z. Zhang, S. Chanda, S. Marro, C. Patzke, C. Acuna, J. Covy, W. Xu, N. Yang, T. Danko, L. Chen, M. Wernig, T.C. Südhof, Rapid single-step induction of functional neurons from human pluripotent stem cells, Neuron 78 (5) (2017) 785–798.
[59] R. Darabi, R.W. Arpke, S. Irion, J.T. Dimos, M. Grskovic, M. Kyba, R.C.R. Perlingeiro, Human ES- and iPS-derived myogenic progenitors restore DYSTROPHIN and improve contractility upon transplantation in dystrophic mice, Cell Stem Cell 10 (5) (2012) 610–619.
[60] M. Pawlowski, D. Ortmann, A. Bertero, J.M. Tavares, R.A. Pedersen, L. Vallier, M.R.N. Kotter, Inducible and deterministic forward programming of human pluripotent stem cells into neurons, skeletal myocytes, and oligodendrocytes, Stem Cell Reports 8 (4) (2017) 803–812.
[61] M. Sadelain, E.P. Papapetrou, F.D. Bushman, Safe harbours for the integration of new DNA in the human genome, Nature Reviews Cancer 12 (1) (2011) 51–58.
[62] D. Lukovic, A. Diez Lloret, P. Stojkovic, D. Rodríguez-Martínez, M.A. Perez Arago, F.J. Rodriguez-Jimenez, P. González-Rodríguez, J. López-Barneo, E. Sykova, P. Jendelova, J. Kostic, V. Moreno-Manzano, M. Stojkovic, S.S. Bhattacharya, S. Erceg, Highly efficient neural conversion of human

pluripotent stem cells in adherent and animal-free conditions, Stem Cells Translational Medicine 6 (4) (2017) 1217–1226.
[63] M.D. Yanagimachi, A. Niwa, T. Tanaka, F. Honda-Ozaki, S. Nishimoto, Y. Murata, T. Yasumi, J. Ito, S. Tomida, K. Oshima, I. Asaka, H. Goto, T. Heike, T. Nakahata, M.K. Saito, Robust and highly-efficient differentiation of functional monocytic cells from human pluripotent stem cells under serum- and feeder cell-free conditions, PLOS ONE 8 (4) (2013) e59243.
[64] G.R. Martin, Isolation of a pluripotent cell line from early mouse embryos cultured in medium conditioned by teratocarcinoma stem cells, Proceedings of the National Academy of Sciences of the United States of America 78 (12) (1981) 7634–7638.
[65] K. Hasegawa, P. Zhang, Z. Wei, J.E. Pomeroy, W. Lu, M.F. Pera, Comparison of reprogramming efficiency between transduction of reprogramming factors, cell–cell fusion, and cytoplast fusion, Stem Cells 28 (8) (2010) 1338–1348.
[66] K. Takahashi, S. Yamanaka, Induction of pluripotent stem cells from mouse embryonic and adult fibroblast cultures by defined factors, Cell 126 (4) (2006) 663–676.
[67] H. Zhou, W. Li, S. Zhu, J.Y. Joo, J.T. Do, W. Xiong, J.B. Kim, K. Zhang, H.R. Schöler, S. Ding, Conversion of mouse epiblast stem cells to an earlier pluripotency state by small molecules, Journal of Biological Chemistry 285 (39) (2010) 29676–29680.
[68] S. Chen, J.T. Do, Q. Zhang, S. Yao, F. Yan, E.C. Peters, H.R. Schöler, P.G. Schultz, S. Ding, Self-renewal of embryonic stem cells by a small molecule, Proceedings of the National Academy of Sciences 103 (46) (2006) 17266–17271.
[69] M. Buehr, S. Meek, K. Blair, J. Yang, J. Ure, J. Silva, R. McLay, J. Hall, Q.-L. Ying, A. Smith, Capture of authentic embryonic stem cells from rat blastocysts, Cell 135 (7) (2008) 1287–1298.
[70] A.E. Boitano, J. Wang, R. Romeo, L.C. Bouchez, A.E. Parker, S.E. Sutton, J.R. Walker, C.A. Flaveny, G.H. Perdew, M.S. Denison, P.G. Schultz, M.P. Cooke, Aryl hydrocarbon receptor antagonists promote the expansion of human hematopoietic stem cells, Science (New York, N.Y.) 329 (5997) (2010) 1345–1348.
[71] Y. Zhang, W. Li, T. Laurent, S. Ding, Small molecules, big roles–the chemical manipulation of stem cell fate and somatic cell reprogramming, Journal of Cell Science 125 (23) (2013) 5609–5620.
[72] A.A. Appel, M.A. Anastasio, J.C. Larson, E.M. Brey, Imaging challenges in biomaterials and tissue engineering, Biomaterials 34 (28) (2013) 6615–6630.
[73] S.Y. Nam, L.M. Ricles, L.J. Suggs, S.Y. Emelianov, Imaging strategies for tissue engineering applications, Tissue Engineering Part B Reviews 21 (1) (2014) 1–44.
[74] L. Teodori, A. Crupi, A. Costa, A. Diaspro, S. Melzer, A. Tarnok, Three-dimensional imaging technologies: a priority for the advancement of tissue engineering and a challenge for the imaging community, Journal of Biophotonics 10 (1) (2017) 24–45.
[75] J.J. Ballyns, L.J. Bonassar, Image-guided tissue engineering, Journal of Cellular and Molecular Medicine 13 (8a) (2009) 1428–1436.
[76] A.J. Reiffel, C. Kafka, K.A. Hernandez, S. Popa, J.L. Perez, S. Zhou, S. Pramanik, B.N. Brown, W.S. Ryu, L.J. Bonassar, J.A. Spector, High-fidelity tissue engineering of patient-specific auricles for reconstruction of pediatric microtia and other auricular deformities, PLOS ONE 8 (2) (2013) e56506.
[77] S.R. Iyer, S. Xu, J.P. Stains, C.H. Bennett, R.M. Lovering, Superparamagnetic iron oxide nanoparticles in musculoskeletal biology, Tissue Engineering Part B Reviews 23 (4) (2017) 373–385.
[78] A.M.M.N. Ahsan, R. Xie, B. Khoda, Direct bio-printing with heterogeneous topology design, Procedia Manufacturing 10 (2017) 945–956.
[79] B. Khoda, Build direction for improved process plan in multi-material additive manufacturing, in: International Design Engineering Technical Conferences and Computers and Information in Engineering Conference vol. 46353, 2014. V004T06A004.
[80] F. Fu, Z. Qin, C. Xu, X.Y. Chen, R.X. Li, L.N. Wang, D.W. Peng, H.T. Sun, Y. Tu, C. Chen, S. Zhang, M.L. Zhao, X.H. Li, Magnetic resonance imaging-three-dimensional printing technology fabricates customized scaffolds for brain tissue engineering, Neural Regeneration Research 12 (4) (2017) 614–622.

[81] S.H. Park, B.K. Kang, J.E. Lee, S.W. Chun, K. Jang, Y.H. Kim, M.A. Jeong, Y. Kim, K. Kang, N.K. Lee, D. Choi, H.J. Kim, Design and fabrication of a thin-walled free-form scaffold on the basis of medical image data and a 3D printed template: its potential use in bile duct regeneration, ACS Applied Materials and Interfaces 9 (14) (2017) 12290−12298.
[82] B. Duan, L.A. Hockaday, K.H. Kang, J.T. Butcher, 3D Bioprinting of heterogeneous aortic valve conduits with alginate/gelatin hydrogels, Journal of Biomedical Materials Research A 101A (5) (2013) 1255−1264.
[83] M.-A. Mycek, Clinical translation of optical molecular imaging to tissue engineering: opportunities & challenges, Optics in the Life Sciences (2015) OT1C-1. Vancouver.
[84] M. McCormick, X. Liu, J. Jomier, C. Marion, L. Ibanez, ITK: enabling reproducible research and open science, Frontiers in Neuroinformatics 8 (2014) 13.
[85] W. Sun, B. Starly, A. Darling, C. Gomez, Computer-aided tissue engineering: application to biomimetic modelling and design of tissue scaffolds, Biotechnology and Applied Biochemistry 39 (1) (2004) 49.
[86] M. Larobina, L. Murino, Medical image file formats, Journal of Digital Imaging 27 (2) (2014) 200−206.
[87] H. Shen, A.S. Goldstein, G. Wang, Biomedical imaging and image processing in tissue engineering, in: N. Pallua, V.C. Suscheck, N. Pallua, V.C. Suscheck (Eds.), Tissue Engineering: From Lab to Clinic, 2011, pp. 155−178. Berlin, Heidelberg.
[88] S. Xu, P.A. Mundra, H. Li, S. Zhu, R.E. Welsch, J.C. Rajapakse, Image analysis for cellular and tissue engineering, in: H. Yu, N.A.A. Rahim, H. Yu, N.A.A. Rahim (Eds.), Imaging in Cellular and Tissue Engineering, 2013, p. 223. Boca Raton.
[89] T. Xu, W. Zhao, J.-M. Zhu, M.Z. Albanna, J.J. Yoo, A. Atala, Complex heterogeneous tissue constructs containing multiple cell types prepared by inkjet printing technology, Biomaterials 34 (1) (2013) 130−139.
[90] L. Lin, H. Zhang, Y. Yao, A. Tong, Q. Hu, M. Fang, Application of image processing and finite element analysis in bionic scaffolds' design optimizing and fabrication, in: K. Li, X. Li, G.W. Irwin, G. He, K. Li, X. Li, G.W. Irwin, G. He (Eds.), Life System Modeling and Simulation: International Conference, LSMS 2007, Shanghai, China, September 14−17, 2007. Proceedings, 2007, pp. 136−145. Berlin, Heidelberg.
[91] S. Mahmoud, A. Eldeib, S. Samy, The design of 3D scaffold for tissue engineering using automated scaffold design algorithm, Australasian Physical & Engineering Sciences in Medicine 38 (2) (2015) 223−228.
[92] N. Sudarmadji, C.K. Chua, K.F. Leong, The development of computer-aided system for tissue scaffolds (CASTS) system for functionally graded tissue-engineering scaffolds, in: M.A.K. Liebschner, M.A.K. Liebschner (Eds.), Computer-Aided Tissue Engineering, 2012, pp. 111−123. Totowa, NJ.
[93] A.K.M. Khoda, I.T. Ozbolat, B. Koc, Designing heterogeneous porous tissue scaffolds for additive manufacturing processes, Computer-Aided Design 45 (12) (2013) 1507−1523.
[94] T.M. Bücking, E.R. Hill, J.L. Robertson, E. Maneas, A.A. Plumb, D.I. Nikitichev, From medical imaging data to 3D printed anatomical models, PLoS ONE 12 (5) (2017) 1−10.
[95] K. Arai, S. Iwanaga, H. Toda, C. Genci, Y. Nishiyama, M. Nakamura, Three-dimensional inkjet biofabrication based on designed images, Biofabrication 3 (3) (2011) 34113.
[96] J.M. Lee, W.Y. Yeong, Design and printing strategies in 3D bioprinting of cell-hydrogels: a review, Advanced Healthcare Materials 5 (22) (2016) 2856−2865.
[97] M.F. Coakley, D.E. Hurt, N. Weber, M. Mtingwa, E.C. Fincher, V. Alekseyev, D.T. Chen, A. Yun, M. Gizaw, J. Swan, T.S. Yoo, Y. Huyen, The NIH 3D print exchange: a public resource for bioscientific and biomedical 3D prints, 3D Printing and Additive Manufacturing 1 (3) (2014) 137−140.
[98] I.T. Ozbolat, 7−bioprinter technologies, in: I.T. Ozbolat, I.T. Ozbolat (Eds.), 3D Bioprinting: Fundamentals, Principles and Applications, London, United Kingdom, 2016, pp. 199−241.
[99] A.G. Requicha, Representations for rigid solids: theory, methods, and systems, ACM Computing Surveys 12 (4) (1980) 437−464.

[100] F. Massarwi, G. Elber, A B-spline based framework for volumetric object modeling, Computer Aided Design 78 (C) (2016) 36–47.
[101] I.T. Ozbolat, B. Koc, 3D hybrid wound devices for spatiotemporally controlled release kinetics, Computer Methods and Programs in Biomedicine 108 (3) (2012) 922–931.
[102] M. Afshar, A.P. Anaraki, H. Montazerian, J. Kadkhodapour, Additive manufacturing and mechanical characterization of graded porosity scaffolds designed based on triply periodic minimal surface architectures, Journal of the Mechanical Behavior of Biomedical Materials 62 (2016) 481–494.
[103] L. Elomaa, S. Teixeira, R. Hakala, H. Korhonen, D.W. Grijpma, V.J. Seppälä, Preparation of poly(ε-caprolactone)-based tissue engineering scaffolds by stereolithography, Acta Biomaterialia 7 (11) (2011) 3850–3856.
[104] F.P.W. Melchels, J. Feijen, D.W. Grijpma, A poly(d,l-lactide) resin for the preparation of tissue engineering scaffolds by stereolithography, Biomaterials 30 (23–24) (2009) 3801–3809.
[105] I.T. Ozbolat, W. Peng, V. Ozbolat, Application areas of 3D bioprinting, Drug Discovery Today 21 (8) (2016) 1257–1271.
[106] G. Ćwikła, C. Grabowik, K. Kalinowski, I. Paprocka, P. Ociepka, The influence of printing parameters on selected mechanical properties of FDM/FFF 3D-printed parts, IOP Conference Series: Materials Science and Engineering 227 (1) (2017).
[107] J.P. Li, J.R. de Wijn, C.A. van Blitterswijk, K. de Groot, The effect of scaffold architecture on properties of direct 3D fiber deposition of porous Ti6Al4V for orthopedic implants, Journal of Biomedical Materials Research Part A 92 (1) (2010) 33–42.
[108] T.J. Hinton, A. Feinberg, 3D printing hydrogel and elastomer scaffolds in a fugitive support, Frontiers in Bioengineering and Biotechnology 3031 (2016).
[109] W.P. Daley, K.M. Yamada, Cell–ECM interactions and the regulation of epithelial branching morphogenesis, in: D.W. DeSimone, R.P. Mecham, D.W. DeSimone, R.P. Mecham (Eds.), Extracellular Matrix in Development, Berlin, Heidelberg, 2013, pp. 75–104.
[110] M.F. Goody, C.A. Henry, Dynamic interactions between cells and their extracellular matrix mediate embryonic development, Molecular Reproduction and Development 77 (6) (2010) 475–488.
[111] S. Nagahara, T. Matsuda, Cell-substrate and cell-cell interactions differently regulate cytoskeletal and extracellular matrix protein gene expression, Journal of Biomedical Materials Research 32 (4) (1996) 677–686.
[112] R.P. Pirraco, A.P. Marques, R.L. Reis, Cell interactions in bone tissue engineering, Journal of Cellular and Molecular Medicine 14 (2010) 93–102.
[113] G. Cheng, B.B. Youssef, P. Markenscoff, K. Zygourakis, Cell population dynamics modulate the rates of tissue growth processes, Biophysical Journal 90 (3) (2006) 713–724.
[114] P. Smadbeck, M.P.H. Stumpf, Coalescent models for developmental biology and the spatio-temporal dynamics of growing tissues, Journal of The Royal Society Interface 13 (117) (2016) 20160112.
[115] M. Cavo, M. Fato, L. Peñuela, F. Beltrame, R. Raiteri, S. Scaglione, Microenvironment complexity and matrix stiffness regulate breast cancer cell activity in a 3D in vitro model, Scientific Reports 6 (1) (2016) 35367.
[116] M. Margaliot, Biomimicry and fuzzy modeling: a match made in heaven, IEEE Computational Intelligence Magazine 3 (3) (2008) 38–48.
[117] J.S. Kim, S.X. Sun, Continuum modeling of forces in growing viscoelastic cytoskeletal networks, Journal of Theoretical Biology 256 (4) (2009) 596–606.
[118] J. Lyu, J. Cao, P. Zhang, Y. Liu, H. Cheng, Coupled hybrid continuum-discrete model of tumor angiogenesis and growth, PLOS ONE 11 (10) (2016) e0163173.
[119] P.J. Murray, A. Walter, A.G. Fletcher, C.M. Edwards, M.J. Tindall, P.K. Maini, Comparing a discrete and continuum model of the intestinal crypt, Physical Biology 8 (2) (2011) 026011.
[120] B.S. Gardiner, K.K.L. Wong, G.R. Joldes, A.J. Rich, C.W. Tan, A.W. Burgess, D.W. Smith, Discrete element framework for modelling extracellular matrix, deformable cells and subcellular components, PLoS Computational Biology 11 (10) (2015) e1004544.

[121] G. Cheng, P. Markenscoff, K. Zygourakis, A 3D hybrid model for tissue growth: the interplay between cell population and mass transport dynamics, Biophysical Journal 97 (2) (2009) 401–414.
[122] X. Cao, E. Ban, B.M. Baker, Y. Lin, J.A. Burdick, C.S. Chen, V.B. Shenoy, Multiscale model predicts increasing focal adhesion size with decreasing stiffness in fibrous matrices, Proceedings of the National Academy of Sciences of the United States of America 114 (23) (2017) E4549–E4555.
[123] H. Mehdizadeh, E.S. Bayrak, C. Lu, S.I. Somo, B. Akar, E.M. Brey, A. Cinar, Agent-based modeling of porous scaffold degradation and vascularization: optimal scaffold design based on architecture and degradation dynamics, Acta Biomaterialia 27 (2015) 167–178.
[124] Y.-A. Jin, Y. He, G.-H. Xue, J.-Z. Fu, A parallel-based path generation method for fused deposition modeling, International Journal of Advanced Manufacturing Technology 77 (5) (2015) 927–937.
[125] I.T. Ozbolat, H. Chen, Y. Yu, Development of 'Multi-arm Bioprinter' for hybrid biofabrication of tissue engineering constructs, Robotics and Computer-Integrated Manufacturing 30 (3) (2014) 295–304.
[126] Z. Wang, J.K. Min, G. Xiong, Robotics-driven printing of curved 3D structures for manufacturing cardiac therapeutic devices, in: 2015 IEEE International Conference on Robotics and Biomimetics (ROBIO), 2015, pp. 2318–2323.
[127] M. Wojcik, L. Koszalka, I. Pozniak-koszalka, A. Kasprzak, MZZ-GA Algorithm for Solving Path Optimization in 3D Printing, ICONS 2015 : The Tenth International Conference on Systems MZZ-GA (C), 2015, pp. 30–35.
[128] K. Christensen, Z. Zhang, C. Xu, Y. Huang, Deformation compensation during buoyancy-enabled inkjet printing of three-dimensional soft tubular structures, Journal of Manufacturing Science and Engineering 140 (1) (2017) 011011.
[129] S.M. Peltola, F.P.W. Melchels, D.W. Grijpma, M. Kellomäki, A review of rapid prototyping techniques for tissue engineering purposes, Annals of Medicine 40 (4) (2008) 268–280.
[130] F. Guillemot, A. Souquet, S. Catros, B. Guillotin, J. Lopez, M. Faucon, B. Pippenger, R. Bareille, M. Rémy, S. Bellance, P. Chabassier, J.C. Fricain, J. Amédée, High-throughput laser printing of cells and biomaterials for tissue engineering, Acta Biomaterialia 6 (7) (2010) 2494–2500.
[131] B. Guillotin, A. Souquet, S. Catros, M. Duocastella, B. Pippenger, S. Bellance, R. Bareille, M. Rémy, L. Bordenave, J. Amédée, F. Guillemot, Laser assisted bioprinting of engineered tissue with high cell density and microscale organization, Biomaterials 31 (28) (2010) 7250–7256.
[132] J.D. Kim, J.S. Choi, B.S. Kim, Y. Chan Choi, Y.W. Cho, Piezoelectric inkjet printing of polymers: stem cell patterning on polymer substrates, Polymer 51 (10) (2010) 2147–2154.
[133] T. Xu, J. Jin, C. Gregory, J.J. Hickman, T. Boland, Inkjet printing of viable mammalian cells, Biomaterials 26 (1) (2005) 93–99.
[134] E. Axpe, M.L. Oyen, Applications of alginate-based bioinks in 3D bioprinting, International Journal of Molecular Sciences 17 (12) (2016) 1976.
[135] K. Nair, M. Gandhi, S. Khalil, K.C. Yan, M. Marcolongo, K. Barbee, W. Sun, Characterization of cell viability during bioprinting processes, Biotechnology Journal 4 (8) (2009) 1168–1177.
[136] A. Blaeser, D.F. Duarte Campos, U. Puster, W. Richtering, M.M. Stevens, H. Fischer, Controlling shear stress in 3D bioprinting is a key factor to balance printing resolution and stem cell integrity, Advanced Healthcare Materials 5 (3) (2016) 326–333.
[137] L. Ouyang, R. Yao, Y. Zhao, W. Sun, Effect of bioink properties on printability and cell viability for 3D bioplotting of embryonic stem cells, Biofabrication 8 (3) (2016) 035020.
[138] C.M. Murphy, A. Matsiko, M.G. Haugh, J.P. Gleeson, F.J. O'Brien, Mesenchymal stem cell fate is regulated by the composition and mechanical properties of collagen–glycosaminoglycan scaffolds, Journal of the Mechanical Behavior of Biomedical Materials 11 (2012) 53–62.
[139] S.K. Seidlits, Z.Z. Khaing, R.R. Petersen, J.D. Nickels, J.E. Vanscoy, J.B. Shear, C.E. Schmidt, The effects of hyaluronic acid hydrogels with tunable mechanical properties on neural progenitor cell differentiation, Biomaterials 31 (14) (2010) 3930–3940.
[140] R. Suntornnond, E.Y.S. Tan, J. An, C.K. Chua, A mathematical model on the resolution of extrusion bioprinting for the development of new bioinks, Materials 9 (9) (2016).

[141] V.S. Murphy, A. Atala, 3D bioprinting of tissues and organs, Nature Biotechnology 32 (8) (2014) 773–785.
[142] A. Bakhshinejad, R.M. D'souza, A brief comparison between available bio-printing methods, in: 2015 IEEE Great Lakes Biomedical Conference (GLBC), 2015, pp. 1–3.
[143] R.R. Jose, M.J. Rodriguez, T.A. Dixon, F. Omenetto, D.L. Kaplan, Evolution of bioinks and additive manufacturing technologies for 3D bioprinting, ACS Biomaterials Science & Engineering 2 (10) (2016) 1662–1678.
[144] A. Akkouch, Y. Yu, I.T. Ozbolat, Microfabrication of scaffold-free tissue strands for three-dimensional tissue engineering, Biofabrication 7 (3) (2015) 31002.
[145] J. Jia, D.J. Richards, S. Pollard, Y. Tan, J. Rodriguez, R.P. Visconti, T.C. Trusk, M.J. Yost, H. Yao, R.R. Markwald, Y. Mei, Engineering alginate as bioink for bioprinting, Acta Biomaterialia 10 (10) (2014) 4323–4331.
[146] G.D. Nicodemus, S.J. Bryant, Cell encapsulation in biodegradable hydrogels for tissue engineering applications, Tissue Engineering Part B Reviews 14 (2008).
[147] S. Ji, M. Guvendiren, Recent advances in bioink design for 3D bioprinting of tissues and organs, Frontiers in Bioengineering and Biotechnology 5 (April) (2017) 1–8.
[148] S. Derakhshanfar, R. Mbeleck, K. Xu, X. Zhang, W. Zhong, M. Xing, 3D bioprinting for biomedical devices and tissue engineering: a review of recent trends and advances, Bioactive Materials 3 (2) (2018) 144–156.
[149] Y. Yu, K.K. Moncal, J. Li, W. Peng, I. Rivero, J.A. Martin, I.T. Ozbolat, Three-dimensional bioprinting using self-assembling scalable scaffold-free "tissue strands" as a new bioink, Scientific Reports 6 (February) (2016) 28714.
[150] H.-Y. Lee, H.-W. Kim, J.H. Lee, S.H. Oh, Controlling oxygen release from hollow microparticles for prolonged cell survival under hypoxic environment, Biomaterials 53 (2015) 583–591.
[151] T. Möller, M. Amoroso, D. Hägg, C. Brantsing, N. Rotter, P. Apelgren, A. Lindahl, L. Kölby, P. Gatenholm, In vivo chondrogenesis in 3D bioprinted human cell-laden hydrogel constructs, Plastic and Reconstructive Surgery – Global Open 5 (2) (2017).
[152] J. Seidel, T. Ahlfeld, M. Adolph, S. Kümmritz, J. Steingroewer, F. Krujatz, T. Bley, M. Gelinsky, A. Lode, Green bioprinting: extrusion-based fabrication of plant cell-laden biopolymer hydrogel scaffolds, Biofabrication 9 (4) (2017) 45011.
[153] G.E. Newby, I.W. Hamley, S.M. King, C.M. Martin, N.J. Terrill, Structure, rheology and shear alignment of Pluronic block copolymer mixtures, Journal of Colloid and Interface Science 329 (1) (2009) 54–61.
[154] J.E. Matthew, Y.L. Nazario, S.C. Roberts, S.R. Bhatia, Effect of mammalian cell culture medium on the gelation properties of Pluronic F127, Biomaterials 23 (23) (2002) 4615–4619.
[155] S.F. Khattak, S.R. Bhatia, S.C. Roberts, Pluronic F127 as a cell encapsulation material: utilization of membrane-stabilizing agents, Tissue Engineering 11 (5–6) (2005) 974–983.
[156] A.N. Leberfinger, D.J. Ravnic, A. Dhawan, I.T. Ozbolat, Concise review: bioprinting of stem cells for transplantable tissue fabrication, Stem cells translational medicine 6 (10) (2017) 1940–1948.
[157] B. Clarke, Normal bone anatomy and physiology, Clinical Journal of the American Society of Nephrology: CJASN 3 (Suppl. 3) (2008) S131–S139.
[158] R.A. Stockwell, The cell density of human articular and costal cartilage, Journal of Anatomy 101 (Pt 4) (1967) 753–763.
[159] E. Bianconi, A. Piovesan, F. Facchin, A. Beraudi, R. Casadei, F. Frabetti, L. Vitale, M.C. Pelleri, S. Tassani, F. Piva, S. Perez-Amodio, P. Strippoli, S. Canaider, An estimation of the number of cells in the human body, Annals of Human Biology 40 (6) (2013) 463–471.
[160] J.H.Y. Chung, S. Naficy, Z. Yue, R. Kapsa, A. Quigley, S.E. Moulton, G.G. Wallace, Bio-ink properties and printability for extrusion printing living cells, Biomaterials Science 1 (7) (2013) 763.
[161] B.M. Gillette, J.A. Jensen, M. Wang, J. Tchao, S.K. Sia, Dynamic hydrogels: switching of 3D microenvironments using two-component naturally derived extracellular matrices, Advanced Materials 22 (6) (2010) 686–691.

[162] C. Mandrycky, Z. Wang, K. Kim, D.-H. Kim, 3D bioprinting for engineering complex tissues, Biotechnology Advances 34 (2016) 422–434.
[163] M.E. Pepper, V. Seshadri, T.C. Burg, K.J.L. Burg, R.E. Groff, Characterizing the effects of cell settling on bioprinter output, Biofabrication 4 (1) (2012) 11001.
[164] T. Billiet, E. Gevaert, T. De Schryver, M. Cornelissen, P. Dubruel, The 3D printing of gelatin methacrylamide cell-laden tissue-engineered constructs with high cell viability, Biomaterials 35 (1) (2014) 49–62.
[165] A. Skardal, J. Zhang, G.D. Prestwich, Bioprinting vessel-like constructs using hyaluronan hydrogels crosslinked with tetrahedral polyethylene glycol tetracrylates, Biomaterials 31 (24) (2010) 6173–6184.
[166] R.L. Mauck, C.C.B. Wang, E.S. Oswald, G.A. Ateshian, C.T. Hung, The role of cell seeding density and nutrient supply for articular cartilage tissue engineering with deformational loading, Osteoarthritis and Cartilage 11 (12) (2003) 879–890.
[167] S.C.N. Chang, J.A. Rowley, G. Tobias, N.G. Genes, A.K. Roy, D.J. Mooney, C.A. Vacanti, L.J. Bonassar, Injection molding of chondrocyte/alginate constructs in the shape of facial implants, Journal of Biomedical Materials Research 55 (4) (2001) 503–511.
[168] S. Eshraghi, S. Das, Micromechanical finite-element modeling and experimental characterization of the compressive mechanical properties of polycaprolactone–hydroxyapatite composite scaffolds prepared by selective laser sintering for bone tissue engineering, Acta Biomaterialia 8 (8) (2012) 3138–3143.
[169] R. Levato, J. Visser, J.A. Planell, E. Engel, J. Malda, M.A. Mateos-Timoneda, Biofabrication of tissue constructs by 3D bioprinting of cell-laden microcarriers, Biofabrication 6 (3) (2014) 35020.
[170] A. Skardal, M. Devarasetty, H.-W. Kang, I. Mead, C. Bishop, T. Shupe, S.J. Lee, J. Jackson, J. Yoo, S. Soker, A. Atala, A hydrogel bioink toolkit for mimicking native tissue biochemical and mechanical properties in bioprinted tissue constructs, Acta Biomaterialia 25 (2015) 24–34.
[171] J. Van Hoorick, H. Declercq, A. De Muynck, A. Houben, L. Van Hoorebeke, R. Cornelissen, J. Van Erps, H. Thienpont, P. Dubruel, S. Van Vlierberghe, Indirect additive manufacturing as an elegant tool for the production of self-supporting low density gelatin scaffolds, Journal of Materials Science: Materials in Medicine 26 (10) (2015) 247.
[172] S. Van Vlierberghe, P. Dubruel, E. Lippens, B. Masschaele, L. Van Hoorebeke, M. Cornelissen, R. Unger, C.J. Kirkpatrick, E. Schacht, Toward modulating the architecture of hydrogel scaffolds: curtains versus channels, Journal of Materials Science: Materials in Medicine 19 (4) (2008) 1459–1466.
[173] J. Malda, J. Visser, F.P. Melchels, T. Jüngst, W.E. Hennink, W.J.A. Dhert, J.R. Groll, D.W. Hutmacher, 25th anniversary article: engineering hydrogels for biofabrication, Advanced Materials 25 (36) (2013) 5011–5028.
[174] F.-Y. Hsieh, H.-H. Lin, S.-H. Hsu, 3D bioprinting of neural stem cell-laden thermoresponsive biodegradable polyurethane hydrogel and potential in central nervous system repair, Biomaterials 71 (2015) 48–57.
[175] K. Markstedt, A. Mantas, I. Tournier, H. Martínez Ávila, D. Hägg, P. Gatenholm, 3D bioprinting human chondrocytes with nanocellulose–alginate bioink for cartilage tissue engineering applications, Biomacromolecules 16 (5) (2015) 1489–1496.
[176] S. Das, F. Pati, Y.-J. Choi, G. Rijal, J.-H. Shim, S.W. Kim, A.R. Ray, D.-W. Cho, S. Ghosh, Bioprintable, cell-laden silk fibroin–gelatin hydrogel supporting multilineage differentiation of stem cells for fabrication of three-dimensional tissue constructs, Acta Biomaterialia 11 (2015) 233–246.
[177] V. Khati, Development of a Robust Decellularized Extracellular Matrix Bioink for 3D Bioprinting, 2016.
[178] K. Arai, Y. Tsukamoto, H. Yoshida, H. Sanae, T. Ahmad Mir, S. Sakai, T. Yoshida, M. Okabe, T. Nikaido, M. Taya, M. Nakamura, The development of cell-adhesive hydrogel for 3D printing, International Journal of Bioprinting 2 (2) (2016) (2016).
[179] T.A.E. Ahmed, V.E. Dare, M. Hincke, Fibrin: a versatile scaffold for tissue engineering applications, Tissue Engineering Part B Reviews 14 (2) (2008) 199–215.
[180] L. Alexandrescu, K. Syverud, A. Gatti, G. Chinga-Carrasco, Cytotoxicity tests of cellulose nanofibril-based structures, Cellulose 20 (4) (2013) 1765–1775.

[181] J. Vartiainen, T. Pöhler, K. Sirola, L. Pylkkänen, H. Alenius, J. Hokkinen, U. Tapper, P. Lahtinen, A. Kapanen, K. Putkisto, P. Hiekkataipale, P. Eronen, J. Ruokolainen, A. Laukkanen, Health and environmental safety aspects of friction grinding and spray drying of microfibrillated cellulose, Cellulose 18 (3) (2011) 775−786.
[182] Y. He, F. Yang, H. Zhao, Q. Gao, B. Xia, J. Fu, Research on the printability of hydrogels in 3D bioprinting, Scientific Reports 6 (2016) 29977.
[183] D. Chimene, K.K. Lennox, R.R. Kaunas, A.K. Gaharwar, Advanced bioinks for 3D printing: a materials science perspective, Annals of Biomedical Engineering 44 (6) (2016) 2090−2102.
[184] C. Colosi, S.R. Shin, V. Manoharan, S. Massa, M. Costantini, A. Barbetta, M.R. Dokmeci, M. Dentini, A. Khademhosseini, Microfluidic bioprinting of heterogeneous 3D tissue constructs using low-viscosity bioink, Advanced Materials 28 (4) (2016) 677−684.
[185] Y. Zhang, Y. Yu, A. Akkouch, A. Dababneh, F. Dolati, I.T. Ozbolat, In vitro study of directly bioprinted perfusable vasculature conduits, Biomaterials Science 3 (1) (2015) 134−143.
[186] A. Skardal, J. Zhang, L. McCoard, X. Xu, S. Oottamasathien, G.D. Prestwich, Photocrosslinkable hyaluronan-gelatin hydrogels for two-step bioprinting, Tissue Engineering Part A 16 (8) (2010) 2675−2685.
[187] R.A. Rezende, P.J. Bártolo, A. Mendes, R.M. Filho, Rheological behavior of alginate solutions for biomanufacturing, Journal of Applied Polymer Science 113 (6) (2009) 3866−3871.
[188] M. Kesti, P. Fisch, M. Pensalfini, E. Mazza, M. Zenobi-Wong, Guidelines for standardization of bioprinting: a systematic study of process parameters and their effect on bioprinted structures, BioNanoMaterials 17 (3−4) (2016) 193−204.
[189] M. Guvendiren, J. Molde, R.M.D. Soares, J. Kohn, Designing biomaterials for 3D printing, ACS Biomaterials Science & Engineering 2 (10) (2016) 1679−1693.
[190] M. Hospodiuk, M. Dey, D. Sosnoski, I.T. Ozbolat, The bioink: a comprehensive review on bioprintable materials, Biotechnology Advances 35 (2) (2017) 217−239.
[191] D.M. Kirchmajer, R. Gorkin Iii, An overview of the suitability of hydrogel-forming polymers for extrusion-based 3D-printing, Journal of Materials Chemistry B 3 (20) (2015) 4105−4117.
[192] Z. Wang, X. Jin, R. Dai, J.F. Holzman, K. Kim, An ultrafast hydrogel photocrosslinking method for direct laser bioprinting, RSC Advances 6 (25) (2016) 21099−21104.
[193] S. Kyle, Z.M. Jessop, A. Al-Sabah, I.S. Whitaker, 'Printability' of Candidate Biomaterials for Extrusion Based 3D Printing: State-of-the-Art, Advanced Healthcare Materials (May), 2017.
[194] I.T. Ozbolat, M. Hospodiuk, Current advances and future perspectives in extrusion-based bioprinting, Biomaterials 76 (2016) 321−343.
[195] Q. Xing, K. Yates, C. Vogt, Z. Qian, M.C. Frost, F. Zhao, Increasing Mechanical Strength of Gelatin Hydrogels by Divalent Metal Ion Removal, vol. 4, 2014, p. 4706.
[196] L. Ouyang, R. Yao, X. Chen, J. Na, W. Sun, 3D printing of HEK 293FT cell-laden hydrogel into macroporous constructs with high cell viability and normal biological functions, Biofabrication 7 (1) (2015) 015010.
[197] Y. Zhao, Y. Li, S. Mao, W. Sun, R. Yao, The influence of printing parameters on cell survival rate and printability in microextrusion-based 3D cell printing technology, Biofabrication 7 (4) (2015) 045002.
[198] W.L. Ng, W.Y. Yeong, M.W. Naing, Polyvinylpyrrolidone-based bio-ink improves cell viability and homogeneity during drop-on-demand printing, Materials 10 (2) (2017).
[199] B. Duan, E. Kapetanovic, L.A. Hockaday, J.T. Butcher, Three-dimensional printed trileaflet valve conduits using biological hydrogels and human valve interstitial cells, Acta Biomaterialia 10 (2014).
[200] M. Kesti, M. Müller, J. Becher, M. Schnabelrauch, M. D'Este, D. Eglin, M. Zenobi-Wong, A versatile bioink for three-dimensional printing of cellular scaffolds based on thermally and photo-triggered tandem gelation, Acta Biomaterialia 11 (2015) 162−172.
[201] Y.-C. Tsai, S. Li, S.-G. Hu, W.-C. Chang, U.S. Jeng, S.-h. Hsu, Synthesis of thermoresponsive amphiphilic polyurethane gel as a new cell printing material near body temperature, ACS Applied Materials and Interfaces 7 (50) (2015) 27613−27623.

[202] H.-B. Zhang, T.-L. Xing, R.-X. Yin, Y. Shi, S.-M. Yang, W.-J. Zhang, Three-dimensional bioprinting is not only about cell-laden structures, Chinese Journal of Traumatology 19 (4) (2016) 187–192.
[203] Y.S. Zhang, A. Arneri, S. Bersini, S.R. Shin, K. Zhu, Z. Goli-Malekabadi, J. Aleman, C. Colosi, F. Busignani, V. Dell'Erba, C. Bishop, T. Shupe, D. Demarchi, M. Moretti, M. Rasponi, M.R. Dokmeci, A. Atala, A. Khademhosseini, Bioprinting 3D microfibrous scaffolds for engineering endothelialized myocardium and heart-on-a-chip, Biomaterials 110 (2016) 45–59.
[204] P. Bianco, P.G. Robey, Stem cells in tissue engineering, Nature 414 (6859) (2001) 118–121.
[205] R. Chang, J. Nam, W. Sun, Effects of dispensing pressure and nozzle diameter on cell survival from solid freeform fabrication–based direct cell writing, Tissue Engineering Part A 14 (1) (2008) 41–48.
[206] R. Landers, U. Hübner, R. Schmelzeisen, R. Mülhaupt, Rapid prototyping of scaffolds derived from thermoreversible hydrogels and tailored for applications in tissue engineering, Biomaterials 23 (23) (2002) 4437–4447.
[207] R. Landers, A. Pfister, U. Hübner, H. John, R. Schmelzeisen, R. Mülhaupt, Fabrication of soft tissue engineering scaffolds by means of rapid prototyping techniques, Journal of Materials Science 37 (15) (2002) 3107–3116.
[208] B. Dhariwala, E. Hunt, T. Boland, Rapid prototyping of tissue-engineering constructs, using photopolymerizable hydrogels and stereolithography, Tissue Engineering 10 (9–10) (2004) 1316–1322.
[209] M. Di Biase, R.E. Saunders, N. Tirelli, B. Derby, Inkjet printing and cell seeding thermoreversible photocurable gel structures, Soft Matter 7 (6) (2011) 2639–2646.
[210] K.T. Nguyen, J.L. West, Photopolymerizable hydrogels for tissue engineering applications, Biomaterials 23 (22) (2002) 4307–4314.
[211] S. Khalil, J. Nam, W. Sun, Multi-nozzle deposition for construction of 3D biopolymer tissue scaffolds, Rapid Prototyping Journal 11 (1) (2005) 9–17.
[212] C.J. Ferris, K.J. Gilmore, S. Beirne, D. McCallum, G.G. Wallace, Bio-ink for on-demand printing of living cells, Biomaterials Science 1 (2) (2013) 224–230.
[213] S. Jana, A. Lerman, Bioprinting a cardiac valve, Biotechnology Advances 33 (2015).
[214] A. Khademhosseini, R. Langer, J. Borenstein, J.P. Vacanti, Microscale technologies for tissue engineering and biology, Proceedings of the National Academy of Sciences of the United States of America 103 (8) (2006) 2480–2487.
[215] J.-H. Shim, J.Y. Kim, M. Park, J. Park, D.-W. Cho, Development of a hybrid scaffold with synthetic biomaterials and hydrogel using solid freeform fabrication technology, Biofabrication 3 (3) (2011) 034102.
[216] H.J. Salacinski, N.R. Tai, R.J. Carson, A. Edwards, G. Hamilton, A.M. Seifalian, In vitro stability of a novel compliant poly(carbonate-urea)urethane to oxidative and hydrolytic stress, Journal of Biomedical Materials Research 59 (2) (2002) 207–218.
[217] C. Frantz, K.M. Stewart, V.M. Weaver, The extracellular matrix at a glance, Journal of Cell Science 123 (24) (2010) 4195–4200.
[218] H. Geckil, F. Xu, X. Zhang, S. Moon, U. Demirci, Engineering hydrogels as extracellular matrix mimics, Nanomedicine 5 (3) (2010) 469–484.
[219] M. Ghadiri, W. Chrzanowski, W.H. Lee, A. Fathi, F. Dehghani, R. Rohanizadeh, Physico-chemical, mechanical and cytotoxicity characterizations of Laponite/alginate nanocomposite, Applied Clay Science 85 (1) (2013) 64–73.
[220] J.R. Xavier, T. Thakur, P. Desai, M.K. Jaiswal, N. Sears, E. Cosgriff-Hernandez, R. Kaunas, A.K. Gaharwar, Bioactive nanoengineered hydrogels for bone tissue engineering: a growth-factor-free approach, ACS Nano 9 (3) (2015) 3109–3118.
[221] M.A. Traver, D.G. Assimos, New generation tissue sealants and hemostatic agents: innovative urologic applications, Reviews in Urology 8 (3) (2006) 104–111.
[222] A.G. Tabriz, M.A. Hermida, N.R. Leslie, W. Shu, Three-dimensional bioprinting of complex cell laden alginate hydrogel structures, Biofabrication 7 (2015) 045012.

[223] F. You, X. Wu, N. Zhu, M. Lei, B.F. Eames, X. Chen, 3D printing of porous cell-laden hydrogel constructs for potential applications in cartilage tissue engineering, ACS Biomaterials Science & Engineering 2 (2016) 1200–1210.
[224] R. Peerani, B.M. Rao, C. Bauwens, T. Yin, G.A. Wood, A. Nagy, E. Kumacheva, P.W. Zandstra, Niche-mediated control of human embryonic stem cell self-renewal and differentiation, The EMBO Journal 26 (22) (2007) 4744–4755.
[225] N.A. Raof, N.R. Schiele, Y. Xie, D.B. Chrisey, D.T. Corr, The maintenance of pluripotency following laser direct-write of mouse embryonic stem cells, Biomaterials 32 (7) (2011) 1802–1808.
[226] J.a. Phillippi, E. Miller, L. Weiss, J. Huard, A. Waggoner, P. Campbell, Microenvironments engineered by inkjet bioprinting spatially direct adult stem cells toward muscle- and bone-like subpopulations, Stem Cells 26 (1) (2008) 127–134.
[227] E.D. Miller, K. Li, T. Kanade, L.E. Weiss, L.M. Walker, P.G. Campbell, Spatially directed guidance of stem cell population migration by immobilized patterns of growth factors, Biomaterials 32 (11) (2011) 2775–2785.
[228] S.J. Habib, B.-C. Chen, F.-C. Tsai, K. Anastassiadis, T. Meyer, E. Betzig, R. Nusse, A localized Wnt signal orients asymmetric stem cell division in vitro, Science (New York, N.Y.) 339 (6126) (2013) 1445–1448.
[229] D.A. Brafman, Constructing stem cell microenvironments using bioengineering approaches, Physiological Genomics 45 (23) (2013) 1123–1135.
[230] G. Chen, C. Deng, Y.-P. Li, TGF-β and BMP signaling in osteoblast differentiation and bone formation, International Journal of Biological Sciences 8 (2) (2012) 272–288.
[231] A. Faulkner-Jones, C. Fyfe, D.-J. Cornelissen, J. Gardner, J. King, A. Courtney, W. Shu, Bioprinting of human pluripotent stem cells and their directed differentiation into hepatocyte-like cells for the generation of mini-livers in 3D, Biofabrication 7 (4) (2015) 044102.
[232] D.L. Jones, A.J. Wagers, No place like home: anatomy and function of the stem cell niche, Nature Reviews Molecular Cell Biology 9 (1) (2008) 11–21.
[233] J. Malda, C.G. Frondoza, Microcarriers in the engineering of cartilage and bone, Trends in Biotechnology 24 (7) (2006) 299–304.
[234] I.T. Ozbolat, K.K. Moncal, H. Gudapati, Evaluation of bioprinter technologies, Additive Manufacturing 13 (2017) 179–200.
[235] S. Park, S. Kim, J. Choi, Development of a multi-nozzle bioprinting system for 3D tissue structure fabrication, 2015 15th International Conference on Control, Automation and Systems (ICCAS) (2015) 1874–1877.
[236] S. Beke, F. Anjum, H. Tsushima, L. Ceseracciu, E. Chieregatti, A. Diaspro, A. Athanassiou, F. Brandi, Towards excimer-laser-based stereolithography: a rapid process to fabricate rigid biodegradable photopolymer scaffolds, Journal of The Royal Society Interface 9 (76) (2012) 3017–3026.
[237] A.P. Zhang, X. Qu, P. Soman, K.C. Hribar, J.W. Lee, S. Chen, S. He, Rapid fabrication of complex 3D extracellular microenvironments by dynamic optical projection stereolithography, Advanced Materials 24 (31) (2012) 4266–4270.
[238] J. Li, M. Chen, X. Fan, H. Zhou, Recent advances in bioprinting techniques: approaches, applications and future prospects, Journal of Translational Medicine 14 (2016) 271.
[239] A. Munaz, R.K. Vadivelu, J. St John, M. Barton, H. Kamble, N.-T. Nguyen, Three-dimensional printing of biological matters, Journal of Science: Advanced Materials and Devices 1 (1) (2016) 1–17.
[240] M.N. Huda, H. Yu, S. Cang, Robots for minimally invasive diagnosis and intervention, Robotics and Computer-Integrated Manufacturing 41 (C) (2016) 127–144.
[241] E. Susilo, P. Valdastri, A. Menciassi, P. Dario, A miniaturized wireless control platform for robotic capsular endoscopy using advanced pseudokernel approach, Sensors and Actuators, A: Physical 156 (1) (2009) 49–58.
[242] I.T. Ozbolat, 3D Bioprinting: Fundamentals, Principles and Applications, 2017.

[243] L. Moldovan, C. Babbey, M. Murphy, N.I. Moldovan, Comparison of biomaterial-dependent and -independent bioprinting methods for cardiovascular medicine, Current Opinion in Biomedical Engineering (2017) 120–127. Accepted M(June).
[244] C.L. Grames, B.D. Jensen, S.P. Magleby, L.L. Howell, A Compact 2 Degree of Freedom Wrist for Robot-Actuated Surgery and Other Applications, 2016, pp. 1–12.
[245] S.B. Ozler, C. Kucukgul, B. Koc, Bioprinting with live cells, in: K. Turksen, K. Turksen (Eds.), Bioprinting in Regenerative Medicine, Cham, 2015, pp. 67–88.
[246] Y. Nishiyama, M. Nakamura, C. Henmi, K. Yamaguchi, S. Mochizuki, H. Nakagawa, K. Takiura, Development of a three-dimensional bioprinter: construction of cell supporting structures using hydrogel and state-of-the-art inkjet technology, Journal of Biomechanical Engineering 131 (3) (2009) 35001.
[247] W.C. Wilson, T. Boland, Cell and organ printing 1: protein and cell printers, The Anatomical Record Part A: Discoveries in Molecular, Cellular, and Evolutionary Biology 272A (2) (2003) 491–496.
[248] J.-P. Gazeau, S. Zeghloul, Design and operation of two service robot arms: a wide surface printing robot and an artist robot, in: A. Information Resources Management, Robotics: Concepts, Methodologies, Tools, and Applications, USA, 2013, pp. 474–500.
[249] Y.S.E. Tan, W.Y. Yeong, Direct bioprinting of alginate-based tubular constructs using multi-nozzle extrusion-based technique, in: C.C. Kai, Y.W. Yee, T.M. Jen, L. Erjia, C.C. Kai, Y.W. Yee, T.M. Jen, L. Erjia (Eds.), 1st International Conference on Progress in Additive Manufacturing, Singapore, 2014, p. 93.
[250] D.J. Odde, M.J. Renn, Laser-guided direct writing of living cells, Biotechnology and Bioengineering 67 (3) (2000) 312–318.
[251] Y. Yu, H. Wen, J. Ma, S. Lykkemark, H. Xu, J. Qin, Flexible fabrication of biomimetic bamboo-like hybrid microfibers, Advanced Materials 26 (16) (2014) 2494–2499.
[252] H.-W. Kang, S.J. Lee, I.K. Ko, C. Kengla, J.J. Yoo, A. Atala, A 3D bioprinting system to produce human-scale tissue constructs with structural integrity, Nature Biotechnology 34 (3) (2016) 312–319.
[253] L.M. Galantucci, I. Bodi, J. Kacani, F. Lavecchia, Analysis of dimensional performance for a 3D open-source printer based on fused deposition modeling technique, Procedia CIRP 28 (2015) 82–87.
[254] M. Heller, H.-K. Bauer, E. Goetze, M. Gielisch, I.T. Ozbolat, K.K. Moncal, E. Rizk, H. Seitz, M. Gelinsky, H.C. Schroder, X.H. Wang, W.E.G. Muller, B. Al-Nawas, Materials and scaffolds in medical 3D printing and bioprinting in the context of bone regeneration, International Journal of Computerized Dentistry 19 (4) (2016) 301–321.
[255] P. Bidare, R.R.J. Maier, R.J. Beck, J.D. Shephard, A.J. Moore, An open-architecture metal powder bed fusion system for in-situ process measurements, Additive Manufacturing 16 (Suppl. C) (2017) 177–185.
[256] J. Frketic, T. Dickens, S. Ramakrishnan, Automated manufacturing and processing of fiber-reinforced polymer (FRP) composites: an additive review of contemporary and modern techniques for advanced materials manufacturing, Additive Manufacturing 14 (Suppl. C) (2017) 69–86.
[257] L. Ren, X. Zhou, Z. Song, C. Zhao, Q. Liu, J. Xue, X. Li, Process parameter optimization of extrusion-based 3D metal printing utilizing PW–LDPE–SA binder system, Materials 10 (3) (2017) 305.
[258] T. Wang, T.-H. Kwok, C. Zhou, In-situ droplet inspection and control system for liquid metal jet 3D printing process, Procedia Manufacturing 10 (2017) 968–981.
[259] R. Kato, D. Iejima, H. Agata, I. Asahina, K. Okada, M. Ueda, H. Honda, H. Kagami, A compact, automated cell culture system for clinical scale cell expansion from primary tissues, Tissue Engineering Part C Methods 16 (5) (2009) 947–956.
[260] R. Thomas, E. Ratcliffe, Automated adherent human cell culture (mesenchymal stem cells), in: R.R. Mitry, R.D. Hughes, R.R. Mitry, R.D. Hughes (Eds.), Human Cell Culture Protocols, Totowa, NJ, 2012, pp. 393–406.
[261] F. Triaud, D.-H. Clenet, Y. Cariou, T. Le Neel, D. Morin, A. Truchaud, Evaluation of automated cell culture incubators, JALA: Journal of the Association for Laboratory Automation 8 (6) (2003) 82–86.
[262] R. Bhuthalingam, P.Q. Lim, S.A. Irvine, S.S. Venkatraman, Automated robotic dispensing technique for surface guidance and bioprinting of cells, Journal of Visualized Experiments 117 (2016).

[263] J.A. Reid, P.A. Mollica, G.D. Johnson, R.C. Ogle, R.D. Bruno, P.C. Sachs, Accessible bioprinting: adaptation of a low-cost 3D-printer for precise cell placement and stem cell differentiation, Biofabrication 8 (2) (2016) 025017.
[264] J. Li, F. Rossignol, J. Macdonald, Inkjet printing for biosensor fabrication: combining chemistry and technology for advanced manufacturing, Lab on a Chip 15 (12) (2015) 2538–2558.
[265] M. Ali, E. Pages, A. Ducom, A. Fontaine, F. Guillemot, Controlling laser-induced jet formation for bioprinting mesenchymal stem cells with high viability and high resolution, Biofabrication 6 (2014) 045001.
[266] P.A.M. Eagles, A.N. Qureshi, S.N. Jayasinghe, Electrohydrodynamic jetting of mouse neuronal cells, Biochemical Journal 394 (2) (2006) 375–378.
[267] L. Gasperini, D. Maniglio, A. Motta, C. Migliaresi, An electrohydrodynamic bioprinter for alginate hydrogels containing living cells, Tissue Engineering Part C Methods 21 (2) (2014) 123–132.
[268] J.C. Nawroth, K.K. Parker, Design standards for engineered tissues, Biotechnology Advances 31 (5) (2013) 632–637.
[269] V. Salih, Introduction, Standardisation in Cell and Tissue Engineering' Woodhead Publishing Series in Biomaterials, 2013, pp. xxiii–xxvi.
[270] J. Dougherty, E. Schaefer, K. Nair, J. Kelly, A. Masi, Repeatability, Reproducibility, and Calibration of the MyotonPro on Tissue Mimicking Phantoms, vol. 55607, 2013. V01AT20A026.
[271] D. Cadena-Herrera, J.E. Esparza-De Lara, N.D. Ramírez-Ibañez, C.A. López-Morales, N.O. Pérez, L.F. Flores-Ortiz, E. Medina-Rivero, Validation of three viable-cell counting methods: manual, semi-automated, and automated, Biotechnology Reports 7 (2015) 9–16.
[272] N. Ke, X. Wang, X. Xu, Y.A. Abassi, The xCELLigence system for real-time and label-free monitoring of cell viability, in: M.J. Stoddart, M.J. Stoddart (Eds.), Mammalian Cell Viability: Methods and Protocols, 2011, pp. 33–43. Totowa, NJ.
[273] K.S. Louis, A.C. Siegel, Cell viability analysis using trypan blue: manual and automated methods, in: M.J. Stoddart, M.J. Stoddart (Eds.), Mammalian Cell Viability: Methods and Protocols, 2011, pp. 7–12. Totowa, NJ.
[274] S. Catros, B. Guillotin, M. Bacakova, J.-C. Fricain, F. Guillemot, Applied Surface Science Effect of laser energy, substrate film thickness and bioink viscosity on viability of endothelial cells printed by Laser-Assisted Bioprinting, Applied Surface Science 257 (2011) 5142–5147.
[275] N.E. Fedorovich, M.H. Oudshoorn, D. van Geemen, W.E. Hennink, J. Alblas, W.J. Dhert, The effect of photopolymerization on stem cells embedded in hydrogels, Biomaterials 30 (3) (2009) 344–353.
[276] Z. Wang, R. Abdulla, B. Parker, R. Samanipour, S. Ghosh, K. Kim, A simple and high-resolution stereolithography-based 3D bioprinting system using visible light crosslinkable bioinks, Biofabrication 7 (2015).
[277] F. Dolati, Y. Yu, Y. Zhang, D.A.M. Jesus, E.A. Sander, I.T. Ozbolat, In vitro evaluation of carbon-nanotube-reinforced bioprintable vascular conduits, Nanotechnology 25 (14) (2014) 145101.
[278] K.A. Homan, D.B. Kolesky, M.A. Skylar-Scott, J. Herrmann, H. Obuobi, A. Moisan, J.A. Lewis, Bioprinting of 3D convoluted renal proximal tubules on perfusable chips, Scientific Reports 6 (2016) 34845.
[279] W. Chan, C. Chong, Perfusion bioreactors improve oxygen transport and cell distribution in esophageal smooth muscle construct, in: 13th International Conference on Biomedical Engineering, Springer, 2009, pp. 1523–1526.
[280] N. Plunkett, F.J. O'Brien, Bioreactors in tissue engineering, Studies in Health Technology and Informatics 152 (1) (2010) 214–230.
[281] J. Zhao, M. Griffin, J. Cai, S. Li, P.E.M. Bulter, D.M. Kalaskar, Bioreactors for tissue engineering: an update, Biochemical Engineering Journal 109 (2016) 268.
[282] R. Detsch, A.R. Boccaccini, The role of osteoclasts in bone tissue engineering, Journal of Tissue Engineering and Regenerative Medicine 9 (10) (2015) 1133–1149.

[283] I. Westphal, C. Jedelhauser, G. Liebsch, A. Wilhelmi, A. Aszodi, M. Schieker, Oxygen mapping: probing a novel seeding strategy for bone tissue engineering, Biotechnology and Bioengineering 114 (4) (2017) 894–902.
[284] C. Correia, A.L. Pereira, A.R.C. Duarte, A.M. Frias, A.J. Pedro, J.T. Oliveira, R.A. Sousa, R.L. Reis, Dynamic culturing of cartilage tissue: the significance of hydrostatic pressure, Tissue Engineering Part A 18 (19–20) (2012) 1979–1991.
[285] E. Wernike, Z. Li, M. Alini, S. Grad, Effect of reduced oxygen tension and long-term mechanical stimulation on chondrocyte-polymer constructs, Cell and Tissue Research 331 (2008) 473–483.
[286] A. Trumbull, G. Subramanian, E. Yildirim-Ayan, Mechanoresponsive musculoskeletal tissue differentiation of adipose-derived stem cells, BioMedical Engineering Online 15 (1) (2016) 43.
[287] K. Li, C. Zhang, L. Qiu, L. Gao, X. Zhang, Advances in application of mechanical stimuli in bioreactors for cartilage tissue engineering, Tissue Engineering Part B Reviews 23 (4) (2017) 399–411.
[288] J. Rauh, F. Milan, K.-P. Günther, M. Stiehler, Bioreactor systems for bone tissue engineering, Tissue Engineering Part B Reviews 17 (4) (2011) 263–280.
[289] G.L. Converse, E.E. Buse, R.A. Hopkins, Bioreactors and operating room centric protocols for clinical heart valve tissue engineering, Progress in Pediatric Cardiology 35 (2) (2013) 95–100.
[290] M.R. Placzek, I.-M. Chung, H.M. Macedo, S. Ismail, T. Mortera Blanco, M. Lim, J. Min Cha, I. Fauzi, Y. Kang, D.C. Yeo, Stem cell bioprocessing: fundamentals and principles, Journal of The Royal Society Interface 6 (32) (2009) 209–232.
[291] K. Stenderup, J. Justesen, C. Clausen, M. Kassem, Aging is associated with decreased maximal life span and accelerated senescence of bone marrow stromal cells, Bone 33 (6) (2003) 919–926.
[292] D.G. Nguyen, J. Funk, J.B. Robbins, C. Crogan-Grundy, S.C. Presnell, T. Singer, A.B. Roth, Bioprinted 3D primary liver tissues allow assessment of organ-level response to clinical drug induced toxicity in vitro, PLOS ONE 11 (7) (2016) e0158674.
[293] I. Martin, D. Wendt, M. Heberer, The role of bioreactors in tissue engineering, Trends in Biotechnology 22 (2) (2004) 80–86.
[294] D.J. Ravnic, A.N. Leberfinger, I.T. Ozbolat, Bioprinting and cellular therapies for type 1 diabetes, Trends in Biotechnology 35 (11) (2017) 1025–1034.
[295] P. Datta, A. Dhawan, Y. Yu, D. Hayes, H. Gudapati, I.T. Ozbolat, Bioprinting of osteochondral tissues: a perspective on current gaps and future trends, International Journal of Bioprinting 3 (2) (2017), https://doi.org/10.18063/IJB.2017.02.007(2017).
[296] P. Datta, V. Ozbolat, B. Ayan, A. Dhawan, I.T. Ozbolat, Bone tissue bioprinting for craniofacial reconstruction, Biotechnology and Bioengineering 114 (11) (2017) 2424–2431.
[297] Y. Yu, Y. Zhang, I.T. Ozbolat, A hybrid bioprinting approach for scale-up tissue fabrication, Journal of Manufacturing Science and Engineering 136 (6) (2014) 61013.
[298] D.B. Kolesky, K.A. Homan, M.A. Skylar-Scott, J.A. Lewis, Three-dimensional bioprinting of thick vascularized tissues, Proceedings of the National Academy of Sciences 113 (12) (2016) 3179–3184.
[299] M. Hospodiuk, M. Dey, B. Ayan, D. Sosnoski, K.K. Moncal, Y. Wu, I.T. Ozbolat, Sprouting angiogenesis in engineered pseudo islets, Biofabrication 10 (3) (2018) 035003.
[300] G. Potjewyd, S. Moxon, T. Wang, M. Domingos, N.M. Hooper, Tissue engineering 3D neurovascular units: a biomaterials and bioprinting perspective, Trends in Biotechnology 36 (4) (2018) 457–472.

This page intentionally left blank

CHAPTER 3

Bioprinting of cartilage

3.1 Introduction

Clinical treatment of articular cartilage lesions remains a challenge. Several operative techniques exist for management of appropriate lesions including debridement, fixation, marrow stimulating techniques, cell-based techniques, and osteochondral auto and allografting [1,2]. Despite clinical success obtained with each of these procedures, only osteochondral autograft and allograft recreate the architecture and composition of the native, mature, and architecturally formed articular hyaline cartilage. Osteochondral grafts have limitations particularly with regard to graft availability, donor site morbidity for autograft, and biological risks with allograft. A seminal study has shown that injection of cultured autologous chondrocytes was able to repair articular cartilage defects indicated by the formation of hyalinelike cartilage [3], and a long-term follow-up study for more than 10 years has indicated that this method was effective and durable for the treatment of large cartilage and osteochondral lesions of the knee joint [4]. However, current clinical restorative technologies, as well as tissue engineering strategies, have been unable to recapitulate the structure of native hyaline cartilage, which is both heterogeneous and anisotropic, and composed of anatomic zones with specific mechanical and biologic properties.

The emergence of three-dimensional (3D) printing, and specifically 3D bioprinting, presents an opportunity to address numerous tissue engineering (TE) challenges from the ability to print complex tissues using additive manufacturing techniques. This technique has been used for the fabrication of blood vessels, heart, liver, neural tissue, and cartilage [5,6]. The self-assembly and self-organizing capabilities of cells have been delivered through applications of distinct bioprinting techniques (e.g., laser, droplet, and extrusion-based) [7–9]. Bioprinting may provide a means for implantation of stem cells into host tissue in a very organized and complex manner [10].

Given the emergence of 3D bioprinting and its possible applications in articular cartilage restoration, this chapter presents a systematic overview to assess (1) the status of research in this emerging field with regard to scaffold-based bioprinting, scaffold-free bioprinting, and in situ bioprinting and (2) how the existing bioprinted constructs address the current challenges in cartilage TE, specifically with regard to recapitulation of the zonal microarchitecture, mechanical enhancement, cell types and density, and mechanical

3D Bioprinting in Tissue and Organ Regeneration. https://doi.org/10.1016/B978-0-12-824291-9.00004-X

stimuli. We hypothesize that the collective literature demonstrates that the morphological, compositional and biomechanical mimicry of the bioprinted cartilage replicate the immunohistologic, microarchitectural, and biomechanical properties of the native hyaline cartilage.

3.2 Scaffold-based bioprinting

In the cases of scaffold-based bioprinting of cartilage, studies were further classified into extrusion-based bioprinting (EBB), droplet-based bioprinting (DBB), laser-based bioprinting (LBB), and bioprinting for zonally stratified arrangement.

3.2.1 Extrusion-based bioprinting

Among scaffold-based approaches, EBB has been the most popular one because of its high economic efficiency, ease of operation, and flexibility to a wide range of materials [11,12]. EBB takes advantages of automated robotic system for continuous extrusion of bioinks in a filament form, in which pneumatic- or mechanical-driven dispensing systems are mostly employed (Fig. 3.1A). Daly et al. [21] evaluated the effects of various bioinks (i.e., agarose, alginate, GelMA, and BioINK) to induce mesenchymal stem cell (MSC)-laden filaments, finding that alginate and agarose bioinks supported more hyalinelike cartilage tissues while gelatin-metacryloyl (GelMA)- and poly(ethylene glycol) methyl ether methacrylate (PEGMA)-based bioinks supported more fibrocartilaginous tissue. With the assistance of polycaprolactone (PCL) filaments, mechanically reinforced scaffold with cell-laden hydrogels was obtained with bulk compressive moduli comparable to articular cartilage (2−3 MPa).

Constantini et al. [13] assessed three different formulations of hydrogel for scaffold-based bioprinting of cartilage tissue, which were (1) GelMA, (2) GelMA and chondroitin sulfate amino ethyl methacrylate (CS-AEMA), and (3) GelMA, CS-AEMA, and HAMA. Each bioink also contained alginate to aid in stable fiber formation during bioprinting and was loaded with bone marrow−derived MSCs (BM-MSCs) (Fig. 3.1B). The bioink composed of alginate, GelMA, and CS-AEMA has been observed to be the best in chondrogenic formation with the highest COL-II versus COL-I and COL-X ratios. The deposition method also maintained shape fidelity with a layer thickness of 100 μm and interfiber distance of 300 μm.

Mouser et al. [22] investigated the effect of gellan gum (GG) on GelMA bioink systematically. Various concentrations (i.e., 3%−20% GelMA with 0%−1.5% GG) were evaluated to define a bioprinting window. They found a concentration of 10/0.5% GelMA/GG balanced the bioprintability and construct stiffness that impacted cell incorporation. From the same research group, Abbadessa et al. [14] designed a hydrogel system based on

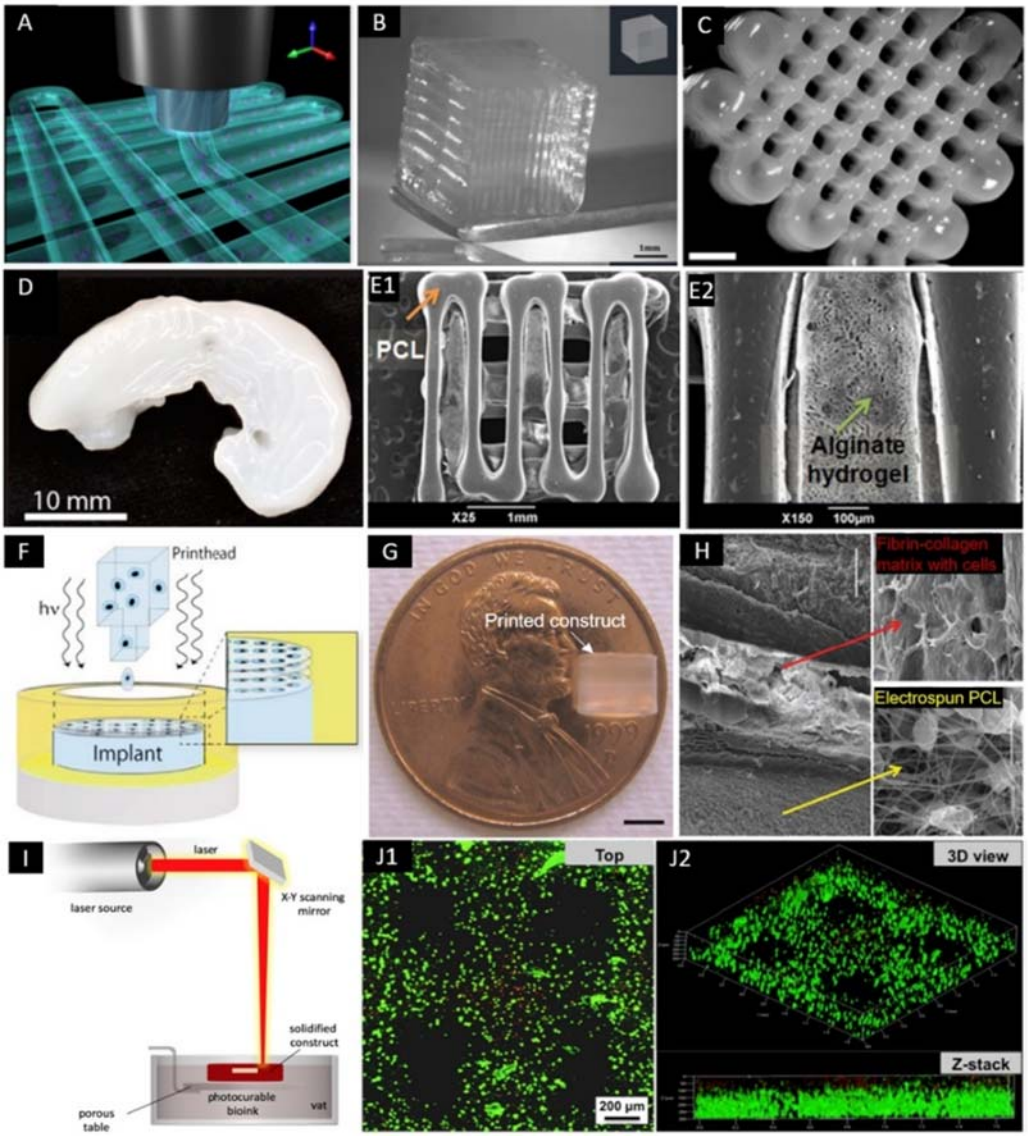

Figure 3.1

Bioprinted constructs using EBB, DBB, and LBB. (A) 3D illustration of hydrogel fibers deposition in EBB [13]. (B) 3D-printed construct using alginate with GelMA [13]. (C) 3D-printed porous constructs based on $M_{10}P_{10}$ blended with HAMA [14]. (D) 3D printed human sheep meniscus with bioink of nanofibrillated cellulose and alginate (scale bar = 2 mm) [15]. (E) 3D bioprinted hybrid constructs with PCL supporting structure and the cell-laden alginate hydrogel [16]. (F) Aschematic of DBB with simultaneous photo-polymerization process [17]. (G) A printed PEG hydrogel construct 4 mm in diameter and 4 mm in height (scale bar = 2 mm) [17]. (H) Multiple-layered printed construct which was comprised of layers of electro-spun PCL fibers and layers of cell-laden fibrin-collagen matrix printed by DBB (scale bar = 100 μm) [18]. (I) A schematic illustration of LBB for cartilage [19]. (J) Live-dead staining of MSCs within 5% PEGDA/GelMA bioprinted construct after culturing [20].

triblock copolymers of polyethylene glycol (PEG, 10 kDa in molecular weight) and poly(*N*-(2-hydroxypropyl) methacrylamide mono/dilactate) (i.e., polyHPMA-lac-PEG) with degree of methacrylation of 15%, as bioink (i.e., $M_{15}P_{10}$) for cartilage bioprinting. With the mixture of methacrylated chondroitin sulfate (CSMA), $M_{15}P_{10}$ exhibited superior mechanical and thermal properties compared to $M_{15}P_{10}$ alone, and was able to maintain cell viability of embedded chondrogenic ATDC5 cells for 6 days in a preliminary in vitro test. In a follow-up study, Abbadessa et al. [23] blended the $M_{10}P_{10}$ with methacrylated polysaccharides including chondroitin sulfate (CS) or hyaluronic acid (HAMA) (Fig. 3.1C). The bioink with incorporation of polysaccharides exhibited increased storage modulus and decreased degradation kinetics in cross-linked hydrogels, while the inclusion of HAMA improved printability versus $M_{10}P_{10}$ and yielded in 3D constructs with excellent cell viability (>90%) of equine chondrocytes at 42 days of culture. In another study, they further explored the printability of polyHPMA-lac-PEG with HAMA to optimize cartilagelike tissue formation by embedded chondrocytes [24]. On being seeded with equine chondrocytes, it has been found that intermediate HAMA concentrations (0.25%–0.5%) increased cartilagelike matrix production including collagen type II (COL-II), VI, and IV, and sulfated glycosaminoglycans (GAG) compared to HAMA-free hydrogels, while higher concentrations (~1%) resulted in undesirable fibrocartilage formation with the presence of collagen type I (COL-I). Similar to Daly's study, PCL was incorporated with the hydrogels in various construct designs in order to obtain mechanical reinforcement, with Young's moduli ranging from 3.5 to 4.6 MPa.

To exploit the cellulose in terms of mechanical strength and rheology, Markstedt et al. [15] evaluated the printability and cytotoxicity of nanofibrillated cellulose (NFC) and alginate bioink (Fig. 3.1D). The combination was utilized due to favorable shear thinning properties of the NFC with the fast cross-linking ability of alginate. Specifically, with regard to articular cartilage, human chondrocytes were bioprinted using this noncytotoxic bioink in gridded constructs. Viability was demonstrated at 86% after 7 days of culture. Successful mixing of the cells in the bioink was also shown via a homogenous cell distribution. Decrease in cell viability was observed, which was attributed to the shear stress in the mixing process. In another study, Nguyen et al. [25] compared NFC/alginate and NFC/hyaluronic acid (NFC/HA) composites for cartilage bioprinting. Human-derived induced pluripotent stem cells (iPSCs) were coprinted with irradiated human chondrocytes, and low proliferation and phenotypic changes away from pluripotency were seen in NFC/HA bioink. On the contrary, pluripotency in the bioprinted NFC/alginate constructs was maintained, and hyalinelike cartilaginous tissue with COL-II expression was observed without any presence of tumorigenic Oct4 expression. Moreover, a remarkable increase in cell number within the cartilaginous tissue was detected in cocultured constructs.

Kundu et al. [16] used a layer-by-layer deposition of PCL and chondrocyte-laden alginate hydrogel (Fig. 3.1E). The in vitro assessment indicated that the structure of 4% alginate

with the addition of transforming growth factor-β (TGF-β) produced more GAG, DNA, and cartilaginous extracellular matrix (ECM) than those of other groups. In a mouse model, scaffolds with the addition of TGF-β also resulted in more cartilage formation and COL-II fibril after 4 weeks of implantation, without any adverse tissue response.

Izadifar et al. [26] cultured two distinct cell populations from embryonic chick cartilage (i.e., rounded and fibroblastic), and have elucidated that printed hybrid constructs of melted PCL and cell-impregnated alginate with fibroblastic cells showed higher cell numbers than the rounded cells at 14 days. Rounded cells had a significantly higher expression of COL-II, while fibroblastic cells expressed significantly higher levels of COL-I and GAG matrix. A scale-up printing has also been performed using the ATDC5 chondrogenic cell line to create six-layer constructs which demonstrated good biofunctionality. In their in vivo study [27], bioprinted cartilage constructs with ATDC5 cells were implanted subcutaneously in mice over 21 days. The implants were characterized both noninvasively using a synchrotron radiation inline phase contrast imaging computed tomography (SR-inline-PCI-CT) approach and invasively to evaluate their cell viability (>70%) and secretion of cartilage-specific ECM. Secretion of GAG and COL-II increased progressively over time. Also, SR-inline-PCI-CT enabled visualization of the individual components of the 3D printed hybrid constructs (PCL and hydrogel), their time-dependent structural changes after implantation and their connection to surrounding host tissues in situ.

In another study, Yang et al. [28] mixed COL-I or agarose (AG) with sodium alginate (SA) as bioinks. The in vitro results using chondrocytes showed that the mechanical strength was improved in both SA/COL and SA/AG groups compared with SA alone. Among the three scaffolds, SA/COL could distinctly facilitate cell adhesion, accelerate cell proliferation, and enhance the expression of cartilage-specific genes such as aggrecan, COL-II, and Sox9 than the other two groups. Lower expression of COL-I was present in SA/COL group than that in both of SA and SA/AG groups. The results indicated that SA/COL effectively suppressed dedifferentiation of chondrocytes and preserved the phenotype.

3.2.2 Droplet-based bioprinting

In DBB, the bioink made up of living cells and other biological materials (e.g., hydrogels) is deposited in a droplet form with precise noncontact positioning (Fig. 3.1F) [11]. The droplets are generated by one of thermal, piezoelectric, or electrostatic drop-on-demand technologies. For cartilage TE applications, Cui et al. [29] have demonstrated the bioprinting with thermal inkjet-based technology utilizing a bioink composed of poly(ethylene glycol) dimethacrylate (PEGDMA) laden with human chondrocytes along with the addition of fibroblast growth factor-2 (FGF-2) and/or TGF-β1 (Fig. 3.1G), and

found that the cell proliferation and chondrocyte phenotype were optimized with a combination of the factors versus TGF-β1 only group. In another study, Cui et al. [17] used the same technique and materials to repair defects in osteochondral plugs. The printed construct exhibited the compressive modulus of 0.4 MPa, and bioprinted human chondrocytes were able to maintain the initial positions due to simultaneous photopolymerization of surrounded biomaterial. In an in vitro implantation using an osteochondral plug, the printed cartilage implant obtained a firm attachment with surrounding tissue, and greater proteoglycan deposition was observed at the interface of implant and native cartilage. In the follow-up studies from the same group, Gao et al. [30,31] extended the cell source to MSC and added other components (e.g., peptitede or GelMA) to optimize MSC differentiation. Their results showed successful printing of a layered structure that developed a higher modulus than PEG scaffolds after osteogenic and chondrogenic differentiation, which was also improved over PEG alone evidenced by gene and protein expression analysis.

In a mouse model, Gao et al. [32] implanted bioprinted constructs with nuclear receptor subfamily 2 group F member 2 (NR2F2) overexpressed MSCs for 21 days. Vascularized tissue membranes were found to grow around the implanted constructs in vivo. The compressive moduli of scaffolds with NR2F2 were significantly stiffer than controls with more proteoglycan growth. Observations among gene expression, biochemical analysis, histological assay, and biomechanical evaluation were consistent to indicate that NR2F2 overexpressed MSCs had enhanced chondrogenic potential for cartilage regeneration.

By combining inkjet printing and electrospinning techniques, Xu et al. [18] created 5-layered constructs that consisted of alternating layers of electrospun PCL/F-127 fibers (3 layers) and inkjet-printed chondrocytes/fibrin/collagen hydrogel (2 layers) (Fig. 3.1H). After culturing in vitro for 2 weeks, the hybrid constructs were implanted in mice subcutaneously for 8 weeks. The chondrocytes showed >80% viability 1 week after printing. The fabricated constructs formed cartilage-like tissues both in vitro and in vivo as evidenced by the deposition of type II collagen and GAG. Moreover, the bioprinted hybrid scaffolds demonstrated enhanced mechanical properties compared to printed alginate or fibrin/collagen gels alone.

3.2.3 Laser-based bioprinting

LBB was operated based on the principle of a laser energy beam used for precise patterning of biomaterials [11]. Laser energy can be used in two different modalities, one of which involves photopolymerization (e.g., stereolithography or 2-photon polymerization) (Fig. 3.1I), and the other modality is based on cell transfer (e.g., laser-guided direct writing and laser-induced forward transfer). As a rare example using LBB for cartilage TE, Zhu et al. [20] have reported the utilization of a tabletop

stereolithography-based bioprinter for cell-laden cartilage fabrication. The bioresin was composed of 10% GelMA base, various concentrations of polyethylene glycol diacrylate (PEGDA), a biocompatible photoinitiator, and TGF-β1 embedded nanospheres fabricated by the electrospraying technique, and MSCs were then mixed with the resin at density of 2×10^6 cells/mL. The addition of PEGDA into GelMA hydrogel greatly improved the printing resolution and modulus of the bioprinted scaffolds as compared with GelMA only. Importantly, cell viability and the bioactivity of growth factors were maintained after UV photopolymerization. TGF-β1 embedded in nanospheres kept a sustained release up to 21 days and improved the chondrogenic differentiation of encapsulated MSCs (Fig. 3.1J).

3.2.4 Bioprinting for zonally stratified arrangement

To generate a bilayered osteochondral model, Levato et al. [33] used microcarriers of polylactic acid (PLA) to load MSCs via static culture or spinner flask expansion, followed by encapsulating the cell-laden microcarriers in GelMA/GG. The cartilage region was printed with GelMA-GG and the bone region was represented by GelMA-GG with encapsulated microcarriers. The application of microcarriers allowed for extensive expansion of cells within the hydrogel, resulting in a higher compressive modulus of the construct and improved cell adhesion. In 2017, Levato et al. [34] reported another strategy for zonallike structure fabrication using articular cartilage-resident chondroprogenitor cells (ACPCs). GelMA-based hydrogels were used to culture ACPCs, MSCs, and chondrocytes as bioinks, in which ACPCs outperformed chondrocytes in terms of neocartilage production. Even though ACPC-laden hydrogels showed a lower production of ECM components compared with MSC-laden ones, ACPCs displayed a low expression of COL-X and a high expression of proteoglycan 4 (PRG4), suggesting a phenotype similar to superficial zone of cartilage. By bioprinting ACPC- and MSC-laden bioinks with a density of 2×10^7 and pluronic as a sacrificial ink, a bioprinted model of articular cartilage was generated, consisting of defined superficial and deep regions with distinct cellular and ECM composition (Fig. 3.2A).

Ren et al. [37] used bioprinted COL-II hydrogel scaffolds to create a biomimetic cell density gradient. A construct with 6-mm height and a 4-mm radius was bioprinted containing three layers (deep, middle, and superficial zones) with cell density gradient to imitate distribution of cell densities in native cartilage. The gradient in cell density resulted in a gradient of ECM, which further affected the biosynthetic ability of the chondrocytes.

Targeting at reconstruction of an osteochondral tissue in the knee joint, Shim et al. [38]. used PCL as supporting for multilayered hydrogel extrusion with human MSCs. The construct (5 mm in height) was divided into two distinct layers, which were subchondral bone layer printed using atelocollagen with MSCs and recombinant human bone

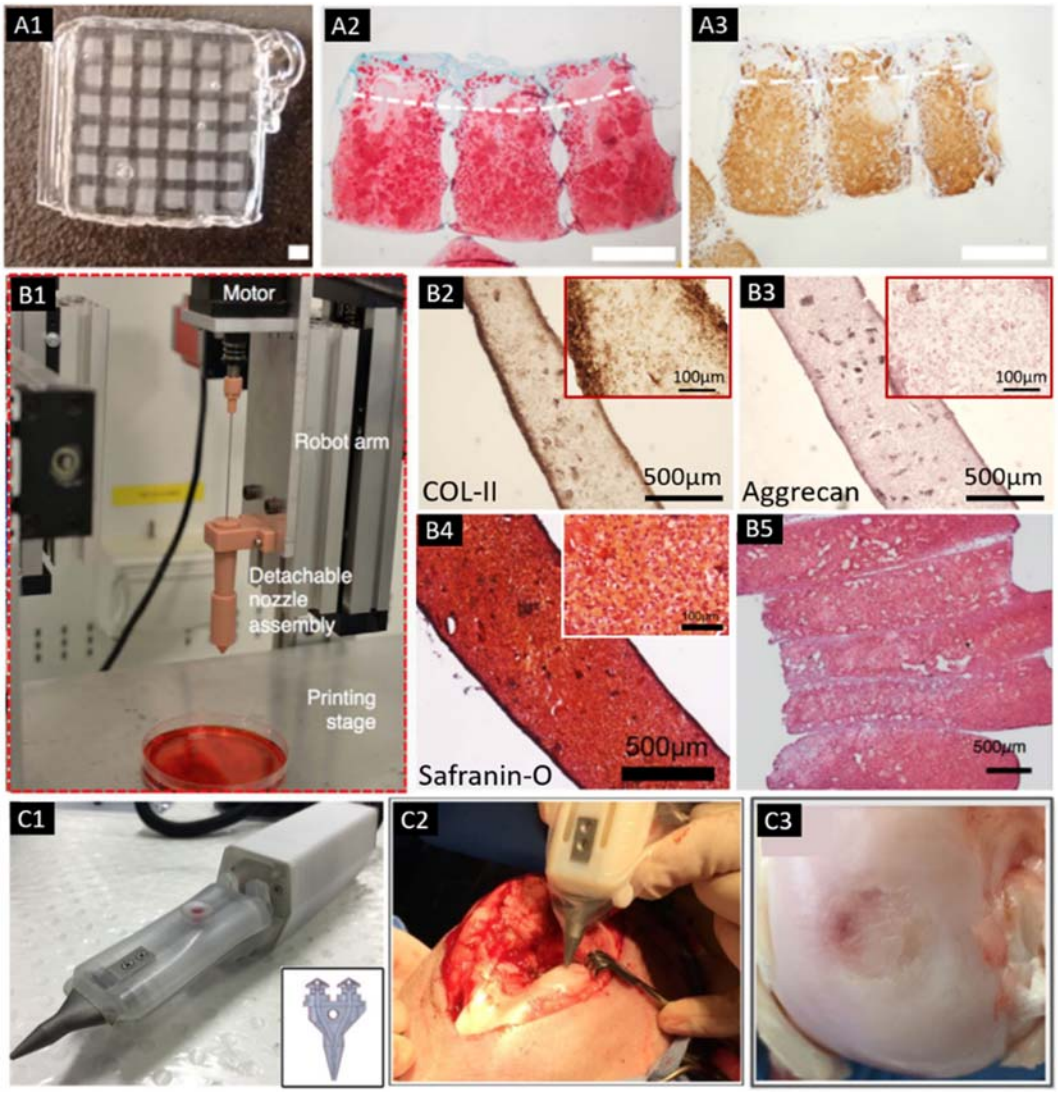

Figure 3.2

(A) Bioprinted cartilage constructs with the pluronic frame (A1), which was bioprinted with MSCs in the middle/deep layer and ACPCs in the superficial layer. Histological staining after 56 days of culture for (A2) sulfated GAGs and (A3) collagen type II (scale bar = 1 mm) [34]. (B) Bioprinting setup with detachable nozzle assembly for tissue strand bioprinting (B1). Positive COL II (B2), aggrecan (B3), and safranin-O staining (B4) were obtained in tissue strands. (B5) A bioprinted cartilage tissue patch showed sulfated GAG deposition throughout the entire construct [35]. (C) The biopen with two separate chambers. Insert showed that two chambers are connected to the printing nozzle (insert), which allows the coaxial printing of the two different bioinks in a core/shell distribution (C1). (C2) Intraoperative bioprinting using the biopen for treatment of a full-thickness chondral defect in sheep. (C3) Macroscopic appearance of the treated defect at 8 weeks after implantation [36].

morphogenic protein (rhBMP)-2, and superficial cartilage layer comprised of Cucurbit [6] uril-conjugated hyaluronic acid (CB [6]-HA), 1,6-diaminohexane-conjugated HA (DAH-HA), MSCs and TGF-β. Cell viability of ∼90% was observed in both layers with increased proliferation over time. The cells in the CB [6]/DAH-HA hydrogel exhibited upregulation in the expression of cartilage-related genes (aggrecan, COL-II, and SOX9) and deposition of GAG compared with those in the atelocollagen hydrogel layer, whereas atelocollagen hydrogels showed strong calcium deposition. Through implanting the bioprinted scaffold into New Zealand white rabbit knee joints, the newly regenerated cartilage tissues were smoothly integrated with ends of the host cartilage tissue at 8 weeks of implantation. They also found the lacuna structure to be similar to that of native cartilage. Immunochemical analysis also showed zonal cartilage regeneration, although COL-X was seen in the superficial layer which is abnormal in comparison to normal cartilage.

3.3 Scaffold-free bioprinting

One pioneer study in 2016 has evaluated scaffold-free bioprinting of articular cartilage. Yu et al. [35] fabricated tissue strands (TSs) of bovine chondrocytes by spinning the cells down into a cell mass, and then transferred them into an alginate capsule for incubation (Fig. 3.2B). Using an extrusion apparatus, the TSs were able to be directly bioprinted while maintaining the shape in culture. The printed construct maintained their fidelity for 10 days, with the observation of ECM deposition and cell-cell adhesion. Mechanical strength of the TSs also exhibited increase from 28 kPa at 1 week to 3.4 MPa at 3 weeks for ultimate strength, and from 1 to 5.3 MPa for the Young's modulus, which approached the native values. Chondrocyte phenotype maintained evidenced by expression of COL-II and aggrecan markers and the upregulated COL-II and aggrecan gene expression. Multilayer TSs were able to be 3D bioprinted into tight layers and ultimately fused into a single unit as early as 12 h after incubation. Implanted tissue into in vitro defects also demonstrated proteoglycan-rich ECM at 4 weeks.

Wu et al. presented a novel hybrid bioprinting strategy to generate zonally stratified cartilage [39]. TSs were made of human adipose-derived stem cells (ADSCs) or predifferentiated ADSCs. Cartilage TSs with predifferentiated ADSCs exhibited improved mechanical properties and upregulated expression of cartilage-specific markers at both transcription and protein levels as compared to TSs with ADSCs being differentiated in the form of strands and TSs of nondifferentiated ADSCs. Using the novel hybrid approach integrating aspiration-assisted and EBB techniques, the bioprinting of zonally stratified cartilage with vertically aligned TSs at the bottom zone and horizontally aligned TSs at the superficial zone was demonstrated, in which collagen fibers were aligned with designated orientation in each zone imitating the anatomical regions and matrix orientation

of native articular cartilage. In addition, mechanical testing study revealed a compression modulus of ~1.1 MPa, which was similar to that of human articular cartilage.

3.4 In situ bioprinting

A promising handheld device has been developed for in situ cartilage repair. O'Connell et al. [40] aimed to translate freeform biofabrication into the surgical field, and hence came up with a handheld biofabrication tool, named the "biopen," in which GelMA/HAMA hydrogel was manually extruded and ultraviolet (UV) cross-linked during the deposition process to generate surgically sculpted 3D structures (Fig. 3.2C). To progress toward translating this technique into clinical practice, Duchi et al. [41] further determined the ideal bioprinting conditions, which allowed the generation of core/shell GelMA/HAMA scaffolds with stiffness of 200 kPa, obtained after 10 s of exposure to 700 mW/cm^2 of 365 nm UV. The incorporated adipose-derived stem cells (ADSCs) retained >90% viability with proliferative capacity. In their in vivo work [36], full-thickness chondral defects were created in a large animal (i.e., sheep) model, which were treated with the hand-held in situ bioprinted scaffold. The regenerated cartilage at 8 weeks after surgery showed better overall macroscopic and microscopic scores, and higher amount of neocartilage evidenced by COL-II expression, when compared with control groups (preconstructed 3D bioscaffolds, microfractures, and untreated controls). Information of the abovementioned studies on cartilage bioprinting is summarized in Table 3.1.

3.5 Considerations for cartilage bioprinting and future perspectives

Cartilage is a tissue that exhibits great heterogeneity and complex microarchitecture. Articular cartilage is comprised of three anatomic zones, namely the superficial zone, the middle zone, and the deep zone [42]. The thin superficial zone occupies approximately 10%–20% of articular cartilage thickness. The middle zone lies deep to the superficial zone, composing 40%–60% of the total cartilage thickness, which contains proteoglycans and thicker collagen fibrils. The deep zone makes up approximately 30% of articular cartilage volume, in which collagen fibrils are arranged perpendicular to the articular surface. Separated by the tide mark, the deep zone is distinguished from the calcified cartilage, which plays an important role in transmitting from soft cartilage to bone [43]. Current clinical restorative technologies as well as TE strategies have been unable to recapitulate this complex microarchitecture and the resultant disorganized repair tissue is a major reason for failure of current basic science and clinical strategies [3]. Three-dimensional bioprinting has demonstrated the ability to reproduce chondral tissue with appropriate zonal structure owing to its capability of precise deposition of cells, biomaterials, growth factors, and other bioactive reagents to build cell-laden constructs [44]. This shows promise moving forward in clinical application of these 3D bioprinted

Table 3.1: Summaries of the technologies and properties of the bioprinted constructs for cartilage TE.

	Study	Materials	Cell source	Animal model	Mechanical reinforcement	Compressive modulus	Zonal structure	In vitro	In vivo
Scaffold-based bioprinting (EBB)	Daly et al. [21]	Agarose, alginate, GelMA and PEGMA	MSC	—	Extruded PCL fibers	W/o PCL: <40 kPa, w PCL: ~2–3 MPa	—	• MSC laden alginate hydrogels stained intensely for sulfated GAG and COL-II. GelMA and PEGMA stained stronger for COL-I. • High levels of cell viability were observed in all bioinks post-printing. • Alginate and agarose hydrogels best supported the development of hyalinelike. Cartilage, and GelMA and PEGMA supported the development of a more fibrocartilagelike tissue.	—
	Markstedt et al. [15]	Nanofibrillated cellulose (NFC) and alginate	Human nasoseptal chondrocytes (hNC)	—	—	~35 kPa	—	• Cell viability was 73% and 86% after 1 and 7 days of printing.	—
	Nguyen et al. [25]	NFC, alginate and HA	iPSCs and chondrocytes	—	—	—	—	• Low proliferation and phenotypic changes away from pluripotency were seen in NFC/HA. • In 3D-bioprinted NFC/A constructs, pluripotency was initially maintained, and hyalinelike cartilaginous tissue with COL-II expression and lacking tumorigenic Oct4 expression was observed after 5 weeks. • A marked increase in cell number within the cartilaginous tissue was detected.	—
	Mouser et al. [22]	GelMa-GG	Primary equine chondrocytes	—	—	~3–200 kPa	—	• The addition of GG supported chondrogenesis, evidenced by presence of GAGs. • High GG concentrations compromised cartilage matrix production and distribution, and even higher concentrations resulted in cell encapsulation.	—

Continued

Table 3.1: Summaries of the technologies and properties of the bioprinted constructs for cartilage TE.—cont'd

Study	Materials	Cell source	Animal model	Mechanical reinforcement	Compressive modulus	Zonal structure	In vitro	In vivo
Abbadessa et al. [14]	$M_{15}P_{10}$ and CSMA	ATDC5 cells	—	—	~8–60 kPa	—	• Embedded cells remained viable and proliferating over a culture period of 6 days.	—
Abbadessa et al. [14]	$M_{10}P_{10}$, CSMA and HAMA	Primary equine chondrocytes	—	—	~15 kPa	—	• The cell-laden hydrogel supported expression of proteoglycans, COL-II and VI for 42 days culture.	—
Mouser et al. [24]	polyHPMA-lac-PEG, HAMA and PCL	Primary equine chondrocytes	—	Extruded PCL fibers	w/o PCL: ~15–30 kPA, w PCL: ~4–8 MPa	—	• GAG and COL-II content increased with HAMA concentrations (0.25%–0.5%) compared to HAMA-free hydrogels. • A relatively high HAMA concentration (1%) resulted in increased fibro-cartilage formation. • The polyHPMA-lac-PEG hydrogels with 0.5% HAMA was optimal for cartilage-like tissue formation.	—
Constantini et al. [13]	GelMA, CS-AEMA and HAMA	BM-MSCs	—	—	~50–100 kPa	—	• Cell viability was ~90% for all the hydrogels. • Hydrogel with alginate, GelMA and CS-AEMA was the best candidate in neocartilage formation with the highest COL-II/COL-I and COL-II/COL-X ratios. • Addition of HAMA favored the differentiation toward hypertrophic cartilage.	—
Kundu et al. [16]	PCL and alginate	Human chondrocytes	Mouse	Extruded PCL fibers	—	—	• PCL-alginate gels with TGFβ showed higher ECM formation (GAG and total collagen content).	• Implants after 4 weeks revealed enhanced carti-lage tissue (GAG) and COL-II fibril formation in the PCL-alginate gel with TGFβ.

	Izadifar et al. [26]	PCL and alginate	Embryonic chick chondrocytes and ATDC5 cell line	—	Extruded PCL fibers	—	—	• Rounded cells had higher COL-II mRNA levels than the fibroblastic cells, while fibroblastic cells had higher COL-II mRNA levels than the rounded cells after biofabrication. • Rounded and fibroblastic cells demonstrated high viability in hybrid constructs. • Fibroblastic cells had higher proliferation than rounded cells in hybrid constructs. • Fibroblastic cells produced more Alcian blue-stained matrix than the rounded cells.	—
	Olubamiji et al. [27]	PCL and alginate	ATDC5 cell line	Mouse	Extruded PCL fibers	—	—	—	• Cells within the cartilage constructs remained viable over 21 days postimplantation. • Progressive secretion of cartilage matrix in implanted cartilage constructs (sulphated GAG and COLII) over 21 days • SR-inline-PCI-CT enabled noninvasive visualization of the individual components of cartilage constructs, surrounding host tissues and their structural changes postimplantation.

Continued

Table 3.1: Summaries of the technologies and properties of the bioprinted constructs for cartilage TE.—cont'd

	Study	Materials	Cell source	Animal model	Mechanical reinforcement	Compressive modulus	Zonal structure	In vitro	In vivo
	Yang et al. [28]	COL-I, agarose and alginate	Rat primary chondrocytes	—	—	~25–70 kPa	—	• SA/COL facilitated cell adhesion, accelerated cell proliferation, and enhanced the expression of cartilage specific genes (Aggeacan, COL-II and Sox9). • Lower expression of COL-I was present in SA/COL group than SA and SA/AG groups, indicating that SA/COL suppressed dedifferentiation of chondrocytes and preserved the phenotype.	—
Scaffold-based bioprinting (DBB)	Cui et al. [29]	PEGDMA	Human articular chondrocytes	—	—	~40–90 kPa	—	• The presence of TGFβ1 is essential for the induction or maintenance of the chondrocyte phenotype (COL-II and aggrecan). • Preculture or coculture with FGF-2 to stimulate cell proliferation does not interfere with the chondrogenic effect of TGF-β1. • FGF-2/TGF-β1 treated constructs showed overall higher amount of proteoglycan content. • ECM production per chondrocyte in low cell density was much higher than that in high cell seeding density.	—
	Cui et al. [17]	PEGDMA	Human articular chondrocytes	—	—	~300–500 kPa	—	• Viability of printed chondrocytes increased 26% in simultaneous polymerization than polymerized after printing. • Printed construct attached firmly with surrounding tissue and showed greater proteoglycan deposition at the interface of implant and native cartilage. • Printed cartilage in 3D OC plugs had elevated GAG content comparing to that without OC plugs.	—

	Gao et al. [31]	PEGDMA and GelMA	BM-MSCs	—	—	~40–60 kPa	—	• The procedure showed a good biocompatibility. • Gene expression analysis showed both osteogenic and chondrogenic differentiation was improved by PEG-GelMA in comparison to PEG alone.	—
	Gao et al. [30]	Peptide-conjugated PEG	BM-MSCs	—	—	~30–70 kPa	—	• Cell viability of >85% • The bioprinted bone and cartilage tissue demonstrated excellent mineral and cartilage matrix deposition with osteogenic and chondrogenic differentiation. • Bioprinted PEG-peptide scaffold inhibited hMSC hypertrophy during chondrogenic differentiation.	—
	Gao et al. [32]	PEGDA	BM-MSCs	Mouse	—	~75–100 kPa	—	• NR2F2 overexpressed MSCs showed significantly enhanced chondrogenesis in monolayer, 3D pellet and hypoxia cutures.	• Vascularized tissue membrane was formed surrounding the constructs. • More proteoglycan deposition was found in scaffold using NR2F2 overexpressed cells comparing to the control group.
	Xu et al. [18]	Collagen, fibrinogen and PCL	Rabbit articular chondrocytes	Mouse	Electrospun PCL fibers	~1.8 MPa	Alternant hydrogel and electrospun layers	• Cell viability >80% 1 week after printing • Constructs formed cartilagelike tissues as evidenced by the deposition of COL-II and GAG.	• Dense and well-organized collagen formation, GAG and COL-II production were observed after 8 weeks of implantation.
Scaffold-based bioprinting (LBB)	Zhu et al. [20]	GelMA, PEGDA and PLGA	BM-MSCs	—	—	~1–18 MPa	—	• Cells grown on 5%/10% (PEGDA/GelMA) hydrogel present the highest cell viability and proliferation rate. • The TGF-β1 embedded in nanospheres can keep a sustained release up to 21 days and improve chondrogenic differentiation.	—

Continued

Table 3.1: Summaries of the technologies and properties of the bioprinted constructs for cartilage TE.—cont'd

	Study	Materials	Cell source	Animal model	Mechanical reinforcement	Compressive modulus	Zonal structure	In vitro	In vivo
Scaffold-based bioprinting (zonally-stratified arrangement)	Levato et al. [33]	PLA and GelMA-GG	MSC	—	PLA microcarriers	~30—50 kPa	Cartilage region and bone region	• Microcarrier encapsulation facilitated cell adhesion and supported osteogenic differentiation and bone matrix deposition by MSCs. • Microcarrier-cell complexes displayed a high viability after the automated printing process.	—
	Levato et al. [34]	GelMA and pluronic F-127	Articular cartilage-resident chondroprogenitor cells (ACPCs), MSCs and chondrocytes	—	—	~100 —190 kPa	ACPC-laden and MSC-laden zones	• ACPCs outperformed chondrocytes in terms of sulfated GAG. • MSCs produced significantly more sulfated GAG and had higher gene expression of COL-II and aggrecan than both ACPCs and chondrocytes. • ACPCs had the lowest gene expression levels of COL-X, and the highest expression of PRG4. • MSC/ACPC cocultured matrices displayed the highest overall sulfated GAG concentration than MSC/chondrocytes and ACPC/chondrocytes. • In bioprinted zonallike constructs, different distributions of sulfated GAG, COL-I and II were observed in ACPC- and MSC-laden zones.	—
	Ren et al. [37]	Collagen type II	Chondrocytes from New Zealand white rabbits	—	—	—	Cell density gradient	• Gradient cell distribution patterns were established and maintained. • Cell viability was >90%. • GAG content was positively correlated with the total cell density. • Cellular biosynthetic ability was affected by both the total cell density and the cell distribution pattern.	—

	Shim et al. [38]	Atelocollagen, HA and PCL	Human mesenchymal stromal cells	Rabbits	Extruded PCL fibers	—	Subchondral bone layer and superficial cartilage layer	• Cell viability was ~90%. • Cells in the atelocollagen hydrogel layer exhibited increases in ALP, COL-I, and OSX genes. • The cells in the CB [6]/DAH-HA hydrogel exhibited increases in ACAN, COL-II, and SOX9 genes. • Cells in atelocollagen showed Runx2 expression and calcium deposition, and cells cultured in CB [6]/DAH-HA showed COL-II and GAG deposition.	• The defect treated by layered scaffold was covered with neotissue - without fiber exposure and exhibited a smooth surface. • Layered scaffold showed a remarkable capability for the osteochondral regeneration at week 8. The newly regenerated cartilage tissues were smoothly integrated with ends of the host cartilage tissue. • GAG, COL-II and X were strongly expressed in only layered scaffold.
Scaffold-free bioprinting	Yu et al. [35]	Cell ink	Primary cattle chondrocytes	—	—	~1–5 MPa	—	• Cell viability in strands was >85%. • TSs showed slightly higher proteoglycan production than native cartilage, and significant amount of COL II and aggrecan. • Printed tissue also had a significant amount of proteoglycan formation and the interface of each tissue strand was well integrated. • High sulfated GAG content and cell density, and chondrocytes with rounded morphology were observed in printed construct. • In a bovine osteochondral model, the explants tissue adhered to the defect, stayed intact and exhibited proteoglycan-rich ECM.	—

Continued

Table 3.1: Summaries of the technologies and properties of the bioprinted constructs for cartilage TE.—cont'd

	Study	Materials	Cell source	Animal model	Mechanical reinforcement	Compressive modulus	Zonal structure	In vitro	In vivo
	Wu et al. [39]	Cell ink	ADSCs	—	—		Bottom zone and superficial zone	• Water content of TSs was ~80%–95%. • Cartilage TSs with predifferentiated ADSCs exhibited improved mechanical properties and upregulated expression of cartilage-specific proteins and genes as compared to control groups. • Collagen fibers and cells were aligned with designated orientation in each zone. • The compression modulus was ~1.1 MPa, which was similar to that of human articular cartilage.	
In situ bioprinting	O'Connell et al. [40]	GelMA/HAMA	Human infrapatellar fat pad derived adipose stem cells	—	—	—	—	• Cell viability was >97%.	—
	Duchi et al. [41]	GelMA/HAMA	Sheep ADSCs	—	—	~9–380 kPa	—	• UV light exposure at 700 mW/cm^2 did not significantly affect cell viability compared to the untreated cells. • Cells printed by coaxial configuration were observed to retain viability and proliferative capability. • The monoaxial bioprinting configuration shows a viability decrease by 30% compared to coaxial printing.	—

	Di Bella et al. [36]	GelMA/HAMA	Sheep MSCs	Sheep	—	~0.5 MPa	—	—	• There was better overall macroscopic appearance in the handheld printed group compared with control groups. • Handheld printed construct showed a higher amount of newly regenerated cartilage with chondrocytes columnar alignment, and the absence of subchondral bone deformation or collapse. • Handheld printed construct showed positive safranin O and COL-II staining.

Note: ACAN = aggrecan; ACPCs = articular cartilage-resident chondroprogenitor cells; ADSCs = adipose-derived stem cells; AG = agarose; ALP = alkaline phosphatase; BMMSCs = bone marrow-derived mesenchymal stem cells; CB [6]-HA = cucurbit [6]uril-conjugated hyaluronic acid; COl-I, II, VI and X = collagen types; CS-AEMA = chondroitin sulfate amino ethyl methacrylate; CSMA = methacrylated chondroitin sulfate; ECM = extracellular matrix; FGF-2 = fibroblast growth factor-2; GAG = glycosaminoglycans; GelMA = gelatin-metacryloyl; GG = gellan gum; HA = hyaluronic acid; HAMA = methacrylated hyaluronic acid; hNC = human nasoseptal chondrocytes; iPSCs = induced pluripotent stem cells; MSC = mesenchymal stem cell; NFC = nanofibrillated cellulose; NFC/A = nanofibrillated cellulose/alginate; NR2F2 = nuclear receptor subfamily 2 group F member 2; OC = osteochondral; Osx = osterix; PAG = polyethylene glycol; PCL = polycaprolactone; PEGDA = polyethylene glycol diacrylate; PEGDMA = poly(ethylene glycol) dimethacrylate; PEGMA = poly(ethylene glycol) methyl ether methacrylate; PLA = polylactic acid; PLGA = poly(lactic-co-glycolic acid); PRG4 = proteoglycan 4; Runx2 = runt-related transcription factor 2; SA = sodium alginate; SR-inline-PCI-CT = synchrotron radiation inline phase contrast imaging computed tomography; TGF-β = transforming growth factor-β; TSs = tissue strands; UV = ultraviolet.

constructs for in vivo articular cartilage restoration. Several of the studies included in this chapter demonstrate the ability to recapitulate the complex zonal microarchitecture of native hyaline cartilage as discussed in the Section 3.2.4.

One of the principal functions of cartilage is to facilitate the transmission of loads. Engineered cartilage tissue ideally exhibits mechanical compressive strength which approaches to the value of native cartilage (e.g., compressive modulus: ~1.5 MPa [35]). Bioprinted cartilage tissue constructs have fallen short, demonstrating compressive moduli usually less than 100 kPa [13,15,23,30,33]. Researchers have strived to increase the mechanical properties by adjusting the concentration or chemical structure of the printed materials. Cui et al. [17] have doubled the concentration of PEGDMA (from 10% to 20%) to increase the compressive modulus nearly 10-fold (from ~40 to 400 kPa). Nevertheless, the enhanced mechanical properties remained insufficient for cartilage tissue engineering. In addition, there were concerns that the increased hydrogel concentration may hinder the cell proliferation and ECM formation.

Reinforcing the hydrogel carriers with synthetic polymers may serve as a method to reinforce their mechanical strength. PCL is one of the most popular biopolymers for engineering tissues due to its good elastomeric properties and high elasticity [45–47]. In addition to mechanical enhancement, it allows for the production of large constructs with high fidelity and fiber resolution [48,49]. Daly et al. [21] codeposited hydrogel bioinks with fused PCL fibers. As compared to the hydrogel constructs with insufficient mechanical strength (~5–35 kPa), the PCL-reinforced hydrogel generated scaffolds had compressive moduli (~2 MPa) similar to that seen with native articular cartilage. PCL has shown to be a successful substrate in various heat distributions and concentrations while also having increased mechanical stability in highly stacked hydrogels [16,26,38]. One major concern of printing fused PCL fibers concurrently with cell-loaded hydrogel was that high temperature (e.g., 65–80°C) was required to melt the PCL, which may decrease cell viability. Izadifar et al. [26] have monitored the surface temperature of the printed PCL fibers, and found that temperature dropped significantly once printed, and reached the values (e.g., 34–39°C) that were suitable for cell survival. Other strategies to reinforce the constructs have been also proposed, such as employing electrospun PCL layers [18] or imbedding PLA microcarriers [33] in conjunction with cell-laden hydrogel.

Hydrogels have traditionally been used as a scaffold in bioprinting for a number of reasons including a decrease in the toxicity to the bioprinted cells as well as the increase in the biocompatibility of the constructs [50]. Scaffold-free bioprinting is a novel technique that may eliminate that need, which has been highlighted here [35]. Scaffold-free bioprinting offers relatively high initial cell density without the inclusion of biomaterials. This results in more space for ECM deposition, facilitates better cell-to-cell interactions, generates

tissues with biomimicry, and preserves cell functionality with elimination of biodegradation issues [35,51].

Chondrocytes and MSCs were the most commonly used cell types. Chondrocytes are often difficult to obtain, whereas MSCs, which are more easily obtained, are capable of differentiating into both bone and cartilage cells [43]. It is well known that chondrocytes in different zones show distinct morphologies. The typical rounded shape of chondrocytes is found in the middle and deep zones, while the chondrocytes are more spread in the superficial zone [52]. Such morphological difference results in varied cellular activity in different zones of cartilage (e.g., ECM productions). Izadifar et al. [26] isolated chondrocytes with rounded and fibroblastic morphologies. A significantly higher expression of COL-II was observed within the rounded cells, while higher level of COL-I was found in the fibroblastic cells. Fibroblastic cells were similar to chondroprogenitors and acted functionally like stem cells where rounded cells expressed prototypical chondrocyte morphology. These findings provide promising strategies for future bioprinted cartilage TE, which could incorporate multiple cell types into a zonal/stratified construct or guide the cells to generate proper morphologies and ECM productions. Steadily decrease of chondrocytes' redifferentiation capacity after several passages constrains their efficacy for TE of larger defects [34]. To overcome this limitation, multipotent progenitor cells, such as MSC and ADSCs, have also been applied for various TE applications [53−55]. However, their tendency to undergo hypertrophic differentiation and trigger endochondral ossification remains a major concern [56]. Particularly, ACPCs were used in one of the abovementioned study [34], which are capable of in vitro self-renewal, and can be expanded to >60 passages while maintaining their potential in multilineage differentiation [57]. Moreover, different from MSCs, ACPCs showed resistance to formation of calcified tissue and hypertrophy, and maintained consistent production of hyalinelike cartilage [58,59].

In addition to the selection of cell type, cell seeding density must also be taken into account. Ren et al. [37] printed hydrogels with different total cell densities (i.e., 2, 1, and 0.5×10^7 cells/mL). The group with cell density of 1×10^7 cells/mL, which had a biomimetic cell density similar to native cartilage (10 million cells/mL [60]), demonstrated upregulated total GAG production and biosynthetic ability for single cell. Similarly, Cui et al. [29] used a low cell density of 0.8×10^7 cells/mL and a high cell density of 2×10^7 cells/mL. They found that ECM expression for single chondrocyte in low cell density was significantly greater than that in high cell density. Higher cell density demonstrated a more robust production of ECM. However, when evaluating the comparative ECM from individual chondrocytes, they produced more total ECM in lower density scenarios. This supports utilizing moderate cell density to balance cell number and

ECM production for an effectively engineered cartilage [16,17]. Constructs with elevated cell density may become metabolically quiescent due to limited nutrient supply while those with low cell density may have limitations in cell-cell interactions. Manipulation of the cell density and distribution does provide a potential outlet for the generation of the zonal distribution of cells seen in native articular cartilage [16,17].

During daily activity, articular cartilage is repeatedly subjected to forces generated by joint loading with varying frequencies between 0.1 and 10 Hz [61,62]. The transduction of mechanical signals stimulates changes in chondrocyte activity, such as metabolic events and structural adaptations [63,64]. The mechanical forces applied in the knee distribute stress within the articular zones in an asymmetrical pattern (e.g., high strain and shear stress in the superficial zone, small strain in lower and deep zones). Different ways of providing mechanical stresses have been reported, including unconfined uniaxial compression [65], direct shear stress [66], and hydrostatic pressure [67]. In development of bioprinted constructs, semiconfined compression, in which load was applied axially and rest of the construct is constrained is ideal, since it could closely mimic the native mechanical environment and resemble a gradient of the zones [68]. In future studies, this could be investigated with modulated mechanical environments into the culture, to give insights of how mechanical stimuli regulate the cell activities in the bioprinted constructs [69]. Since cartilage bioprinting is still a novel topic, innovative studies are being produced every few years with new advances. Finally, the clinical translation is not yet clear and significantly more research is warranted before the techniques can be applied in clinics.

To sum up, the unique abilities of the varied techniques including scaffold-based, scaffold-free and in situ bioprinting have allowed replication of anatomical structure, biological function, and mechanical properties of the native articular cartilage, and particularly enabled the advances toward zonal differentiation, which have been proved by relatively comprehensive in vitro and in vivo studies. This chapter demonstrates that bioprinting has potential capacity for clinical cartilage reconstruction and future in vivo implantation as techniques are advanced.

References

[1] A. Bedi, B.T. Feeley, R.J. Williams 3rd, Management of articular cartilage defects of the knee, Journal of Bone and Joint Surgery 92 (4) (2010) 994–1009.
[2] C.D. Murawski, J.G. Kennedy, Operative treatment of osteochondral lesions of the talus, Journal of Bone and Joint Surgery 95 (11) (2013) 1045–1054.
[3] M. Brittberg, A. Lindahl, A. Nilsson, C. Ohlsson, O. Isaksson, L. Peterson, Treatment of deep cartilage defects in the knee with autologous chondrocyte transplantation, New England Journal of Medicine 331 (14) (1994) 889–895.
[4] L. Peterson, H.S. Vasiliadis, M. Brittberg, A. Lindahl, Autologous chondrocyte implantation: a long-term follow-up, The American Journal of Sports Medicine 38 (6) (2010) 1117–1124.

[5] Y.S. Zhang, K. Yue, J. Aleman, K. Mollazadeh-Moghaddam, S.M. Bakht, J. Yang, W. Jia, V. Dell'Erba, P. Assawes, S.R. Shin, M.R. Dokmeci, R. Oklu, A. Khademhosseini, 3D bioprinting for tissue and organ fabrication, Annals of Biomedical Engineering 45 (1) (2017) 148–163.
[6] C. Mandrycky, Z. Wang, K. Kim, D.-H. Kim, 3D bioprinting for engineering complex tissues, Biotechnology Advances 34 (4) (2016) 422–434.
[7] A.B. Dababneh, I.T. Ozbolat, Bioprinting technology: a current state-of-the-art review, Journal of Manufacturing Science and Engineering 136 (6) (2014) 061016.
[8] H. Gudapati, M. Dey, I. Ozbolat, A comprehensive review on droplet-based bioprinting: past, present and future, Biomaterials 102 (2016) 20–42.
[9] I.T. Ozbolat, M. Hospodiuk, Current advances and future perspectives in extrusion-based bioprinting, Biomaterials 76 (2016) 321–343.
[10] C. Bauge, K. Boumediene, Use of adult stem cells for cartilage tissue engineering: current status and future developments, Stem Cells International 2015 (2015) 438026.
[11] P. Datta, A. Barui, Y. Wu, V. Ozbolat, K.K. Moncal, I.T. Ozbolat, Essential steps in bioprinting: from pre- to post-bioprinting, Biotechnology Advances 36 (5) (2018) 1481–1504.
[12] W. Peng, P. Datta, Y. Wu, M. Dey, B. Ayan, A. Dababneh, I.T. Ozbolat, Challenges in bio-fabrication of organoid cultures, Cell Biology and Translational Medicine 3 (2018) 53–71.
[13] M. Costantini, J. Idaszek, K. Szoke, J. Jaroszewicz, M. Dentini, A. Barbetta, J.E. Brinchmann, W. Swieszkowski, 3D bioprinting of BM-MSCs-loaded ECM biomimetic hydrogels for in vitro neocartilage formation, Biofabrication 8 (3) (2016) 035002.
[14] A. Abbadessa, V.H. Mouser, M.M. Blokzijl, D. Gawlitta, W.J. Dhert, W.E. Hennink, J. Malda, T. Vermonden, A synthetic thermosensitive hydrogel for cartilage bioprinting and its biofunctionalization with polysaccharides, Biomacromolecules 17 (6) (2016) 2137–2147.
[15] K. Markstedt, A. Mantas, I. Tournier, H. Martinez Avila, D. Hagg, P. Gatenholm, 3D bioprinting human chondrocytes with nanocellulose-alginate bioink for cartilage tissue engineering applications, Biomacromolecules 16 (5) (2015) 1489–1496.
[16] J. Kundu, J.H. Shim, J. Jang, S.W. Kim, D.W. Cho, An additive manufacturing-based PCL-alginate-chondrocyte bioprinted scaffold for cartilage tissue engineering, Journal of Tissue Engineering and Regenerative Medicine 9 (11) (2015) 1286–1297.
[17] X. Cui, K. Breitenkamp, M. Lotz, D. D'Lima, Synergistic action of fibroblast growth factor-2 and transforming growth factor-beta1 enhances bioprinted human neocartilage formation, Biotechnology and Bioengineering 109 (9) (2012) 2357–2368.
[18] T. Xu, K.W. Binder, M.Z. Albanna, D. Dice, W. Zhao, J.J. Yoo, A. Atala, Hybrid printing of mechanically and biologically improved constructs for cartilage tissue engineering applications, Biofabrication 5 (1) (2013) 015001.
[19] I.T. Ozbolat, 3D Bioprinting: Fundamentals, Principles and Applications, Academic Press, Cambridge, MA, 2016.
[20] W. Zhu, H. Cui, B. Boualam, F. Masood, E. Flynn, R.D. Rao, Z.-Y. Zhang, L.G. Zhang, 3D bioprinting mesenchymal stem cell-laden construct with core–shell nanospheres for cartilage tissue engineering, Nanotechnology 29 (18) (2018) 185101.
[21] A.C. Daly, S.E. Critchley, E.M. Rencsok, D.J. Kelly, A comparison of different bioinks for 3D bioprinting of fibrocartilage and hyaline cartilage, Biofabrication 8 (4) (2016) 045002.
[22] V.H. Mouser, F.P. Melchels, J. Visser, W.J. Dhert, D. Gawlitta, J. Malda, Yield stress determines bioprintability of hydrogels based on gelatin-methacryloyl and gellan gum for cartilage bioprinting, Biofabrication 8 (3) (2016) 035003.
[23] A. Abbadessa, M.M. Blokzijl, V.H. Mouser, P. Marica, J. Malda, W.E. Hennink, T. Vermonden, A thermo-responsive and photo-polymerizable chondroitin sulfate-based hydrogel for 3D printing applications, Carbohydrate Polymers 149 (2016) 163–174.
[24] V.H.M. Mouser, A. Abbadessa, R. Levato, W. Hennink, T. Vermonden, D. Gawlitta, J. Malda, Development of a thermosensitive HAMA-containing bio-ink for the fabrication of composite cartilage repair constructs, Biofabrication 9 (1) (2017) 015026.

[25] D. Nguyen, D.A. Hägg, A. Forsman, J. Ekholm, P. Nimkingratana, C. Brantsing, T. Kalogeropoulos, S. Zaunz, S. Concaro, M. Brittberg, Cartilage tissue engineering by the 3D bioprinting of iPS cells in a nanocellulose/alginate bioink, Scientific Reports 7 (1) (2017) 1–10.
[26] Z. Izadifar, T. Chang, W. Kulyk, X. Chen, B.F. Eames, Analyzing biological performance of 3D-printed, cell-impregnated hybrid constructs for cartilage tissue engineering, Tissue Engineering Part C Methods 22 (3) (2016) 173–188.
[27] A.D. Olubamiji, N. Zhu, T. Chang, C.K. Nwankwo, Z. Izadifar, A. Honaramooz, X. Chen, B.F. Eames, Traditional invasive and synchrotron-based noninvasive assessments of three-dimensional-printed hybrid cartilage constructs in situ, Tissue Engineering Part C Methods 23 (3) (2017) 156–168.
[28] X. Yang, Z. Lu, H. Wu, W. Li, L. Zheng, J. Zhao, Collagen-alginate as bioink for three-dimensional (3D) cell printing based cartilage tissue engineering, Materials Science and Engineering: C 83 (2018) 195–201.
[29] X. Cui, K. Breitenkamp, M.G. Finn, M. Lotz, D.D. D'Lima, Direct human cartilage repair using three-dimensional bioprinting technology, Tissue Engineering Part A 18 (11–12) (2012) 1304–1312.
[30] G. Gao, T. Yonezawa, K. Hubbell, G. Dai, X. Cui, Inkjet-bioprinted acrylated peptides and PEG hydrogel with human mesenchymal stem cells promote robust bone and cartilage formation with minimal printhead clogging, Biotechnology Journal 10 (10) (2015) 1568–1577.
[31] G. Gao, A.F. Schilling, K. Hubbell, T. Yonezawa, D. Truong, Y. Hong, G. Dai, X. Cui, Improved properties of bone and cartilage tissue from 3D inkjet-bioprinted human mesenchymal stem cells by simultaneous deposition and photocrosslinking in PEG-GelMA, Biotechnology Letters 37 (11) (2015) 2349–2355.
[32] G. Gao, X.F. Zhang, K. Hubbell, X. Cui, NR2F2 regulates chondrogenesis of human mesenchymal stem cells in bioprinted cartilage, Biotechnology and Bioengineering 114 (1) (2017) 208–216.
[33] R. Levato, J. Visser, J.A. Planell, E. Engel, J. Malda, M.A. Mateos-Timoneda, Biofabrication of tissue constructs by 3D bioprinting of cell-laden microcarriers, Biofabrication 6 (3) (2014) 035020.
[34] R. Levato, W.R. Webb, I.A. Otto, A. Mensinga, Y. Zhang, M. van Rijen, R. van Weeren, I.M. Khan, J. Malda, The bio in the ink: cartilage regeneration with bioprintable hydrogels and articular cartilage-derived progenitor cells, Acta Biomaterialia 61 (2017) 41–53.
[35] Y. Yu, K.K. Moncal, J. Li, W. Peng, I. Rivero, J.A. Martin, I.T. Ozbolat, Three-dimensional bioprinting using self-assembling scalable scaffold-free "tissue strands" as a new bioink, Scientific Reports 6 (2016) 28714.
[36] C. Di Bella, S. Duchi, C.D. O'Connell, R. Blanchard, C. Augustine, Z. Yue, F. Thompson, C. Richards, S. Beirne, C. Onofrillo, In situ handheld three-dimensional bioprinting for cartilage regeneration, Journal of Tissue Engineering and Regenerative Medicine 12 (3) (2018) 611–621.
[37] X. Ren, F. Wang, C. Chen, X. Gong, L. Yin, L. Yang, Engineering zonal cartilage through bioprinting collagen type II hydrogel constructs with biomimetic chondrocyte density gradient, BMC Musculoskeletal Disorders 17 (2016) 301.
[38] J.H. Shim, K.M. Jang, S.K. Hahn, J.Y. Park, H. Jung, K. Oh, K.M. Park, J. Yeom, S.H. Park, S.W. Kim, J.H. Wang, K. Kim, D.W. Cho, Three-dimensional bioprinting of multilayered constructs containing human mesenchymal stromal cells for osteochondral tissue regeneration in the rabbit knee joint, Biofabrication 8 (1) (2016) 014102.
[39] Y. Wu, B. Ayan, K.K. Moncal, Y. Kang, A. Dhawan, S.V. Koduru, D.J. Ravnic, F. Kamal, I.T. Ozbolat, Hybrid bioprinting of zonally stratified human articular cartilage using scaffold-free tissue strands as building blocks, Advanced Healthcare Materials 9 (22) (2020) 2001657.
[40] C.D. O'Connell, C. Di Bella, F. Thompson, C. Augustine, S. Beirne, R. Cornock, C.J. Richards, J. Chung, S. Gambhir, Z. Yue, Development of the Biopen: a handheld device for surgical printing of adipose stem cells at a chondral wound site, Biofabrication 8 (1) (2016) 015019.
[41] S. Duchi, C. Onofrillo, C.D. O'Connell, R. Blanchard, C. Augustine, A.F. Quigley, R.M. Kapsa, P. Pivonka, G. Wallace, C. Di Bella, Handheld co-axial bioprinting: application to in situ surgical cartilage repair, Scientific Reports 7 (1) (2017) 1–12.
[42] A.J. Sophia Fox, A. Bedi, S.A. Rodeo, The basic science of articular cartilage: structure, composition, and function, Sports Health 1 (6) (2009) 461–468.

[43] J.S. Temenoff, A.G. Mikos, Review: tissue engineering for regeneration of articular cartilage, Biomaterials 21 (5) (2000) 431–440.
[44] M. Hospodiuk, M. Dey, D. Sosnoski, I.T. Ozbolat, The bioink: a comprehensive review on bioprintable materials, Biotechnology Advances 35 (2) (2017) 217–239.
[45] M.A. Woodruff, D.W. Hutmacher, The return of a forgotten polymer-polycaprolactone in the 21st century, Progress in Polymer Science 35 (10) (2010) 1217–1256.
[46] Y. Wu, Z. Wang, J.Y.H. Fuh, Y. San Wong, W. Wang, E. San Thian, Mechanically-enhanced three-dimensional scaffold with anisotropic morphology for tendon regeneration, Journal of Materials Science: Materials in Medicine 27 (7) (2016) 115.
[47] Y. Wu, G. Sriram, A.S. Fawzy, J.Y. Fuh, V. Rosa, T. Cao, Y.S. Wong, Fabrication and evaluation of electrohydrodynamic jet 3D printed polycaprolactone/chitosan cell carriers using human embryonic stem cell-derived fibroblasts, Journal of Biomaterials Applications 31 (2) (2016) 181–192.
[48] C.H. Lee, S.A. Rodeo, L.A. Fortier, C. Lu, C. Erisken, J.J. Mao, Protein-releasing polymeric scaffolds induce fibrochondrocytic differentiation of endogenous cells for knee meniscus regeneration in sheep, Science Translational Medicine 6 (266) (2014) 266ra171.
[49] C. Ding, Z. Qiao, W. Jiang, H. Li, J. Wei, G. Zhou, K. Dai, Regeneration of a goat femoral head using a tissue-specific, biphasic scaffold fabricated with CAD/CAM technology, Biomaterials 34 (28) (2013) 6706.
[50] J.C. Reichert, A. Heymer, A. Berner, J. Eulert, U. Noth, Fabrication of polycaprolactone collagen hydrogel constructs seeded with mesenchymal stem cells for bone regeneration, Biomedical Materials 4 (6) (2009) 065001.
[51] I.T. Ozbolat, Scaffold-based or scaffold-free bioprinting: competing or complementing approaches? Journal of Nanotechnology in Engineering and Medicine 6 (2) (2015).
[52] J. Panadero, S. Lanceros-Mendez, J.G. Ribelles, Differentiation of mesenchymal stem cells for cartilage tissue engineering: individual and synergetic effects of three-dimensional environment and mechanical loading, Acta Biomaterialia 33 (2016) 1–12.
[53] X. Guo, H. Park, S. Young, J.D. Kretlow, J.J. Van den Beucken, L.S. Baggett, Y. Tabata, F.K. Kasper, A.G. Mikos, J.A. Jansen, Repair of osteochondral defects with biodegradable hydrogel composites encapsulating marrow mesenchymal stem cells in a rabbit model, Acta Biomaterialia 6 (1) (2010) 39–47.
[54] Y. Wu, Y. Han, Y.S. Wong, J.Y.H. Fuh, Fibre-based scaffolding techniques for tendon tissue engineering, Journal of Tissue Engineering and Regenerative Medicine 12 (7) (2018) 1798–1821.
[55] J.S. Park, M.-S. Shim, S.H. Shim, H.N. Yang, S.Y. Jeon, D.G. Woo, D.R. Lee, T.K. Yoon, K.-H. Park, Chondrogenic potential of stem cells derived from amniotic fluid, adipose tissue, or bone marrow encapsulated in fibrin gels containing TGF-β3, Biomaterials 32 (32) (2011) 8139–8149.
[56] J. Visser, D. Gawlitta, K.E. Benders, S.M. Toma, B. Pouran, P.R. van Weeren, W.J. Dhert, J. Malda, Endochondral bone formation in gelatin methacrylamide hydrogel with embedded cartilage-derived matrix particles, Biomaterials 37 (2015) 174–182.
[57] R. Williams, I.M. Khan, K. Richardson, L. Nelson, H.E. McCarthy, T. Analbelsi, S.K. Singhrao, G.P. Dowthwaite, R.E. Jones, D.M. Baird, Identification and clonal characterisation of a progenitor cell sub-population in normal human articular cartilage, PloS One 5 (10) (2010) e13246.
[58] H.E. McCarthy, J.J. Bara, K. Brakspear, S.K. Singhrao, C.W. Archer, The comparison of equine articular cartilage progenitor cells and bone marrow-derived stromal cells as potential cell sources for cartilage repair in the horse, The Veterinary Journal 192 (3) (2012) 345–351.
[59] A.J. Neumann, O.F. Gardner, R. Williams, M. Alini, C.W. Archer, M.J. Stoddart, Human articular cartilage progenitor cells are responsive to mechanical stimulation and adenoviral-mediated overexpression of bone-morphogenetic protein 2, PloS One 10 (8) (2015) e0136229.
[60] E. Hunziker, T. Quinn, H.-J. Häuselmann, Quantitative structural organization of normal adult human articular cartilage, Osteoarthritis and Cartilage 10 (7) (2002) 564–572.
[61] G. Van Kampen, J. Veldhuijzen, R. Kuijer, R. Van de Stadt, C. Schipper, Cartilage response to mechanical force in high-density chondrocyte cultures, Arthritis & Rheumatism 28 (4) (1985) 419–424.
[62] B.D. Elder, K.A. Athanasiou, Hydrostatic pressure in articular cartilage tissue engineering: from chondrocytes to tissue regeneration, Tissue Engineering Part B Reviews 15 (1) (2009) 43–53.

[63] L.Y. Sah, Y.J. Kim, J.Y.H. Doong, A.J. Grodzinsky, A.H.K. Plass, J.D. Sandy, Biosynthetic response of cartilage explants to dynamic compression, Journal of Orthopaedic Research Official Publication of the Orthopaedic Research Society 7 (5) (1989) 619.

[64] R.B. Salter, D.F. Simmonds, B.W. Malcolm, E.J. Rumble, D. Macmichael, N.D. Clements, The biological effect of continuous passive motion on the healing of full-thickness defects in articular cartilage. An experimental investigation in the rabbit, Journal of Bone & Joint Surgery American 68 (2) (1981) 1232−1251.

[65] A.H. Huang, M.J. Farrell, M. Kim, R.L. Mauck, Long-term dynamic loading improves the mechanical properties of chondrogenic mesenchymal stem cell-laden hydrogels, European Cells and Materials 19 (2010) 72.

[66] Z. Li, S.-J. Yao, M. Alini, M.J. Stoddart, Chondrogenesis of human bone marrow mesenchymal stem cells in fibrin−polyurethane composites is modulated by frequency and amplitude of dynamic compression and shear stress, Tissue Engineering Part A 16 (2) (2009) 575−584.

[67] K. Miyanishi, M.C. Trindade, D.P. Lindsey, G.S. Beaupré, D.R. Carter, S.B. Goodman, D.J. Schurman, R.L. Smith, Effects of hydrostatic pressure and transforming growth factor-β 3 on adult human mesenchymal stem cell chondrogenesis in vitro, Tissue Engineering 12 (6) (2006) 1419−1428.

[68] S.D. Thorpe, T. Nagel, S.F. Carroll, D.J. Kelly, Modulating gradients in regulatory signals within mesenchymal stem cell seeded hydrogels: a novel strategy to engineer zonal articular cartilage, PLoS One 8 (4) (2013) e60764.

[69] Z. Hao, S. Wang, J. Nie, D. Li, A. Fang, J. Kang, C. Liu, L. Wang, Effects of bionic mechanical stimulation on the properties of engineered cartilage tissue, Bio-Design and Manufacturing 4 (1) (2021) 33−43.

CHAPTER 4

Bioprinting of bone

4.1 Anatomy of native bone

Bone plays a crucial role in the musculoskeletal system, whose functions are to protect the various organs of the body, produce blood cells, store minerals, provide mechanical support for the body, and enable mobility [1]. Bone exhibits a hierarchical and functionally graded structure (Fig. 4.1), which can be categorized to be cancellous and cortical bone (macrostructure); Haversian canal, osteons, and lamellae (microstructure); fibrillar collagen (nanostructure); and molecular components such as mineral, collagen, and noncollagenous organic proteins (subnanostructure) [1].

From the viewpoint of the macrostructure, bones are classified as cortical (or compact) bone and cancellous (or trabecular) bone. In general, cortical bone occupies up to 80% of total bone mass which is dense with low porosity (e.g., ~6%), resulting in bone being mechanically strong [3,4]. In contrast, trabecular bone reveals a highly porous structure (e.g., ~80%), leading to this tissue demonstrating a low compressive strength (such as 10% of cortical bone) [3]. The trabecular bone offers an interconnected structure with a great surface-area-to-volume ratio, which allows for sufficient contact of bone cells with blood cells and subsequently controlling of hematopoiesis and homeostasis [5]. Taking long bone as an example, there are three main regions including a cylindrical dense shaft

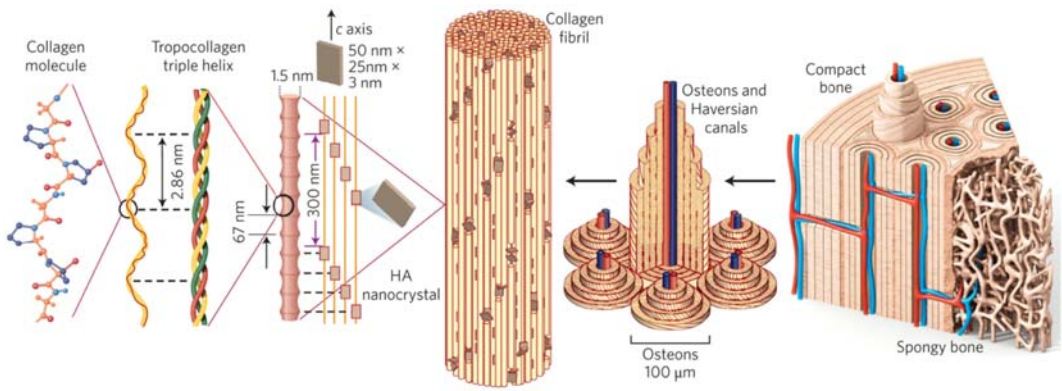

Figure 4.1
Hierarchical structure of bone from collagen molecules and nanohydroxyapatite crystals [2].

3D Bioprinting in Tissue and Organ Regeneration. https://doi.org/10.1016/B978-0-12-824291-9.00003-8

made of cortical bone (diaphysis) and two parts at the end made of trabecular bone (metaphysis). On the microscopic level of bone, lamella which consists of mineralized collagen fibers shows a planar arrangement with a width of 3–7 μm [6]. In some cortical bone, the lamellae wrap in the form of concentric layers (3–8 lamellae) around a central canal, which refers to as an osteon (or Haversian system). The trabecular bone arranges differently, in which the mineral platelets are organized along the direction of collagen fibers [3].

Furthermore, mineralized collagen fibrils (~100 nm in diameter) are present in the nanostructure of lamellae, which is considered the basic building block of bone. Collagen type I (COL-I) is the primary organic component of the matrix, which is secreted by osteoblasts followed by self-assembling. Apatite crystals are distributed discretely along the collagen fibrils. The organizations of both the lamellae and the collagen fibers contribute to the isotropic properties of bone, leading to the prevention of crack propagation and an increase in toughness [7].

As to substance composition in bone, the major contents are hydroxyapatite (~60%) and COL-I (~20%). In addition, bone contains several types of ion substitution impurities including Na^{+}, Mg^{2+}, and K^{+}, along with proteins including osteocalcin, osteonectin, and sialoprotein [8]. In terms of cellular components in bone, there are four main types of cells namely osteoblasts, osteocytes, osteoclasts, and bone lining cells, which are embedded in the extracellular matrix (ECM) of bone. Osteoblasts are bone-forming cells and comprise 4%–6% of the total number of bone cells. Osteoblasts synthesize ECM following a two-step mechanism which includes deposition of organic matrix and subsequent mineralization [9]. When osteoblasts get trapped within the calcified matrix, their structure and function change, and osteoblasts become known as osteocytes, which means osteocytes are the mature forms of osteoblasts. They distribute in the bone ECM and function as stress sensors. Some osteoblasts remain on the top of new bone and protect the underlying bone, which are hence known as lining cells. Osteoclasts are very large multinucleate cells that absorb bone matrix during growth and healing.

The utmost important role of bone is to provide mechanical support for the body. The bone acts as a composite material where calcium phosphate (CaP) is accountable for the mechanical durability and high resistance to compression, and in the meantime, collagen provides elasticity and resistance to tension. Native bones possess Young's modulus at an order of GPa and tensile/compressive strength of MPa, which vary depending on different locations in the body or different parts of the same bone. For an instant, cortical bone displays much higher Young's modulus (7–30 GPa vs. 50–500 MPa), tensile strength (50–150 MPa vs. 1.2–20 MPa), compressive strength (167–193 MPa vs. 1.9–10 MPa), and lower strain to failure (1%–3% vs. 5%–7%) in the longitudinal direction, as compared to cancellous bone [10,11].

4.2 Bioprinting of bone constructs

Currently, bioprinted bone constructs are primarily fabricated by extrusion-based bioprinting (EBB), since EBB is highly effective to print large-scale 3D constructs, and is flexible for a wide range of biomaterials (such as thermoplastics and cell-laden bioinks) to obtain sufficient mechanical strength for bone constructs. The state-of-the-art progress in bone bioprinting is introduced in detail in this section.

In an early study in 2008, Fedorovich et al. [12] compared the bioprinting of Lutrol F127, agarose, alginate, and methylcellulose hydrogels with an extrusion-based bioprinter. The applied extrusion conditions did not influence cell survival and differentiation potency of BMSCs. In particular, two fluorescently labeled cell populations were bioprinted within a single scaffold, indicating that this process was able to develop bone grafts containing multiple cell types. In their follow-up study, they bioprinted porous constructs encapsulating 2 cell types, which were endothelial progenitors (EPCs) and MSCs [13]. Rectangular 10-layer scaffolds, which consisted of two parts (i.e., EPC-laden Matrigel part and MSC-laden Matrigel part with the addition of biphasic calcium phosphate (BCP)), were bioprinted for in vitro study, demonstrating that cell distribution was retained after 2-week culture. Importantly, after 6 weeks of implantation in immune-deficient mice, the MSC/BCP-laden Matrigel part demonstrated apparent bone formation as verified by Goldner's trichrome and COL-I staining, whereas in the MSC/Matrigel part, cartilage formation was detected as evidenced by Safranin-O and COL-II stainings. In another study from the same group, they realized the variation of porosity (e.g., 35%–66%) and elastic modulus (4.5–7.6 kPa) through changing fiber spacing or angle of fiber deposition using a pneumatic extrusion process, to fabricate heterogeneous constructs as osteochondral grafts [14]. For bioprinting of osteochondral constructs, chondrocytes laden alginate and MSCs laden alginate that were supplemented with osteoinductive biphasic calcium phosphate particles (BCPs) were bioprinted to build heterogeneous scaffolds (1×2 cm) with cartilage and bone compartments. Cell viability of alginate constructs which were laden with human chondrocytes and osteogenic progenitors remained high during the printing process ($\sim$90%). Besides, distinct tissue formation in different parts of the construct was detected in vitro (3 weeks) and in vivo (6 weeks subcutaneously in immunodeficient mice), indicated by straining of osteogenic and chondrogenic makers.

In another study using a pneumatic extrusion system, Loozen et al. [15] developed constructs comprising alginate hydrogel supplemented with MSCs, BCP particles, and plasmid-DNA-encoding BMP-2 (pBMP-2), which were printed in a porous or a solid manner. Porous constructs consisted of 10 layers with a fiber distance of 3 mm and thickness of 1 mm, and solid ones were printed with a fiber distance of 1 mm. The cell viability of the printed porous constructs (80%–90%) was higher than that of solid constructs (70%–85%). With transfection of the plasmid DNA, osteogenic differentiation

of cells was demonstrated by the upregulated BMP-2 and ALP production. In addition, porous constructs performed superior concerning BMP-2 production as compared to solid constructs.

Lee et al. [16] reported a construct that consisted of polycaprolactone (PCL) and cell-embedded alginate fibers. Being a hybrid scaffold, cell (MC3T3-E1)-laden alginate fibers supported the biological functionality of the construct, and PCL fibers played the role in tailoring mechanical properties. Such design resulted in a remarkable increase in Young's modulus and ultimate tensile strength as compared to alginate-only scaffolds. Cells were observed evenly distributed all over the alginate fibers with a cell viability of 84%.

Based on the reversible thermal gelation of gelatin and irreversible chemical cross-linking of alginate, Wüst et al. [17] developed a two-step process. MSCs mixed into the hydrogel precursor presented high cell viability of 85% after the bioprinting process and 3-day culture in vitro. In addition, a geometry of two phases was produced with an HA-containing phase representing bone tissue along with an alginate-gelatin-filled tubular structure corresponding to a vascular structure. The inclusion of HA improved the suitability of the process for bone tissue engineering.

To modulate the biological outcomes of the bioprinted construct, Neufurth et al. [18] applied an overlay of agarose and calcium salt of polyphosphate (polyP$\cdot$Ca^{2+}-complex) onto the bioprinted alginate/gelatine/SaOS-2 cell scaffold. Strikingly, the addition of polyP$\cdot$Ca^{2+}-complex increased the capability of proliferation for the cells in the underlining hydrogel, with an average generation time of $\sim$50 h during a 6-day incubation period as compared to the invisible steady-state change of cells without this polymer. The hardness of alginate/gelatin hydrogel also noticeably increased when the overlaid polymer was present, while a significant increase in the mineralization of cells was detected. In their follow-up study, Wang et al. [19] explored the impact of bioglass (e.g., polyP$\cdot$Ca^{2+}-complex, silica, and biosilica) on the growth and mineralization of SaOS-2 cells, which were encapsulated and bioprinted with an alginate/gelatine hydrogel. The results revealed that the addition of bioglass particles significantly enhanced the potency of mineralization of the entrapped SaOS-2 cells proven by Alizarin Red S staining. In addition, element analysis of the mineral nodules formed by SaOS-2 indicated an accumulation of mineral contents (e.g., O, P, Ca, and C).

To obtain a mechanically strong construct, Sawkins et al. [20] bioprinted a microparticulate bioink comprised of poly(lactic-co-glycolic acid) (PLGA), polyethylene glycol (PEG), and carboxymethyl cellulose (CMC). The mechanical properties of these constructs (Young's modulus: 57.3 MPa) fitted the range of those of human cancellous bone. Meanwhile, the pore sizes for constructs with high viscosity CMC carriers were 65–77 μm. In addition, the release of the lysozyme from bioprinted constructs was able to sustain for 15 days and a high degree of protein activity was measured for 9 days.

As a unique study that used silk within bioprinted bone, Das et al. [21] bioprinted human nasal inferior turbinate tissue-derived mesenchymal progenitor cells encapsulated (hTMSCs) in silk fibroin-gelatin (SF-G) bioink, where gelation was induced via in situ cytocompatible gelation mechanisms (i.e., enzymatic cross-linking by mushroom tyrosinase and physical cross-linking via sonication, Fig. 4.2). The optimized dispensing parameters and the cross-linking process did not have any injurious effect on cells, highlighting the potential of SF-G bioink as a cell encapsulating material. Moreover, higher chondrogenic and adipogenic potentials were observed in the tyrosinase cross-linking group, while higher osteogenic differentiation was seen in the sonication cross-linking group, which was demonstrated by related ECM and gene expression.

As a rare example that utilized droplet-based bioprinting (DBB) for bone reconstruction, Campos et al. [22] inkjet-printed thermoresponsive agarose hydrogels (0.5−2.0 g/mL) with COL-I (0.21−0.05 g/mL) at different concentrations. The higher content of collagen in agarose-collagen led to the less precise contours of bioprinted tissue, since the viscosity and mechanical stiffness of the bioinks were improved via the addition of agarose, which

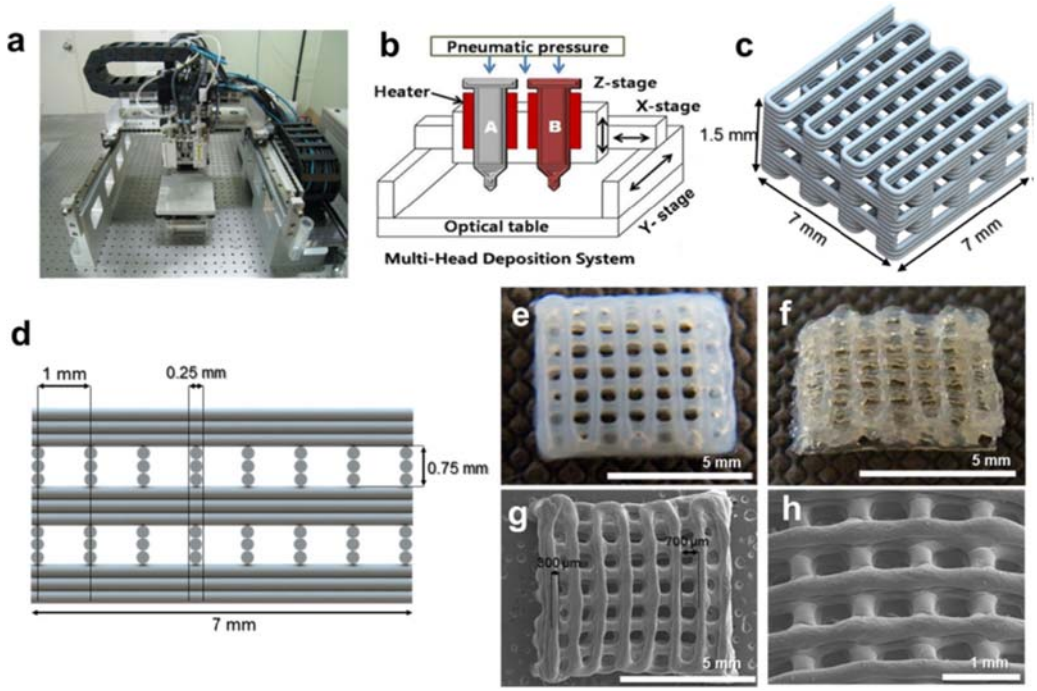

Figure 4.2

3D bioprinted silk-gelatin constructs. (A,B) Actual view and schematic diagram of the EBB bioprinter. (C,D) Dimensions and layer arrangement of the bioprinted structures. (E) Sonication-induced and (F) tyrosinase cross-linked SF-G constructs. (G) Top view and (H) inclined view of scanning electron microscope (SEM) images of the SF-G constructs [21].

facilitated their printability. MSCs in softer hydrogels showed the biggest elongation after osteogenic differentiation. MSCs survived during the 3D bioprinting process and also maintained the mesenchymal phenotype, as proved by high cell viability (>98%), immunocytochemistry (vimentin+ and CD34-), ALP activity, and bone-related gene expression.

Targeting building human-scale and mechanically stable tissues, Kang et al. [23] developed an integrated tissue-organ printer (ITOP) that can handle various hydrogels (i.e., gelatin, fibrinogen, hyaluronic acid (HA), and glycerol) as well as PCL and Pluronic F-127 as a sacrificial hydrogel. With the involvement of microchannels, the bioprinted constructs overcame the diffusion limit of 100–200 mm for cell survival, leading to ≥95% cell viability for at least 6 days of culture. In the mandible bone reconstruction, human amniotic fluid–derived stem cells (hAFSCs)-laden hydrogel, a mixture of PCL and tricalcium phosphate (TCP), and Pluronic F127 were printed. In addition, rat calvarial bone constructs in a circular shape were generated with hAFSCs, which showed regenerated vascularized bone tissue throughout the implants without necrosis (Fig. 4.3). On the contrary, the control group treated with scaffold only showed negligible bone tissue formation which was limited to the periphery of the implant. In the ear cartilage reconstruction, constructs with microchannels presented newly regenerated cartilaginous ECM internally, whereas those without microchannels showed merely restricted tissue formation in peripheral regions. In vivo study in the dorsal subcutaneous space of athymic mice showed that the shape of the bioprinted construct was well preserved for 2 months, with substantial cartilage formation indicated by glycosaminoglycan (GAG) content. Furthermore, in the skeletal muscle reconstruction in nude rats, the retrieved muscle constructs showed well-organized muscle fibers after 2 weeks of implantation, and the structural integrity of printed muscle constructs was able to be maintained with the observation of nerve integration and vascularization in vivo.

Inspired by replicating the vascularized Haversian system of bone, Cui et al. [24] designed a hierarchical structure using a hybrid bioprinting platform that combined FDM and SLA for deposition of polylactide (PLA) fibers and gelatin methacrylate (GelMA) hydrogel, respectively, to print a bone construct with internal vascularized networks. During the fabrication process, the morphogenetic protein 2 (BMP2) peptides were immobilized onto polydopamine (pDA)-coated PLA scaffolds without GelMA (bone region), followed by conjugating VEGF peptides onto the chains of GelMA (vascular region). The hMSCs were preseeded on PLA scaffolds, while hMSCs and human umbilical vein endothelial cells (HUVECs) were coencapsulated at a 1:1 ratio in the GelMA hydrogel. The pDA- and BMP2-modification promoted cell proliferation and spreading on the scaffold, whereas BMP2 improved osteogenic differentiation. With the assistance of perfusion culture, remarkable osteogenesis and generation of vascular networks were achieved, indicated by

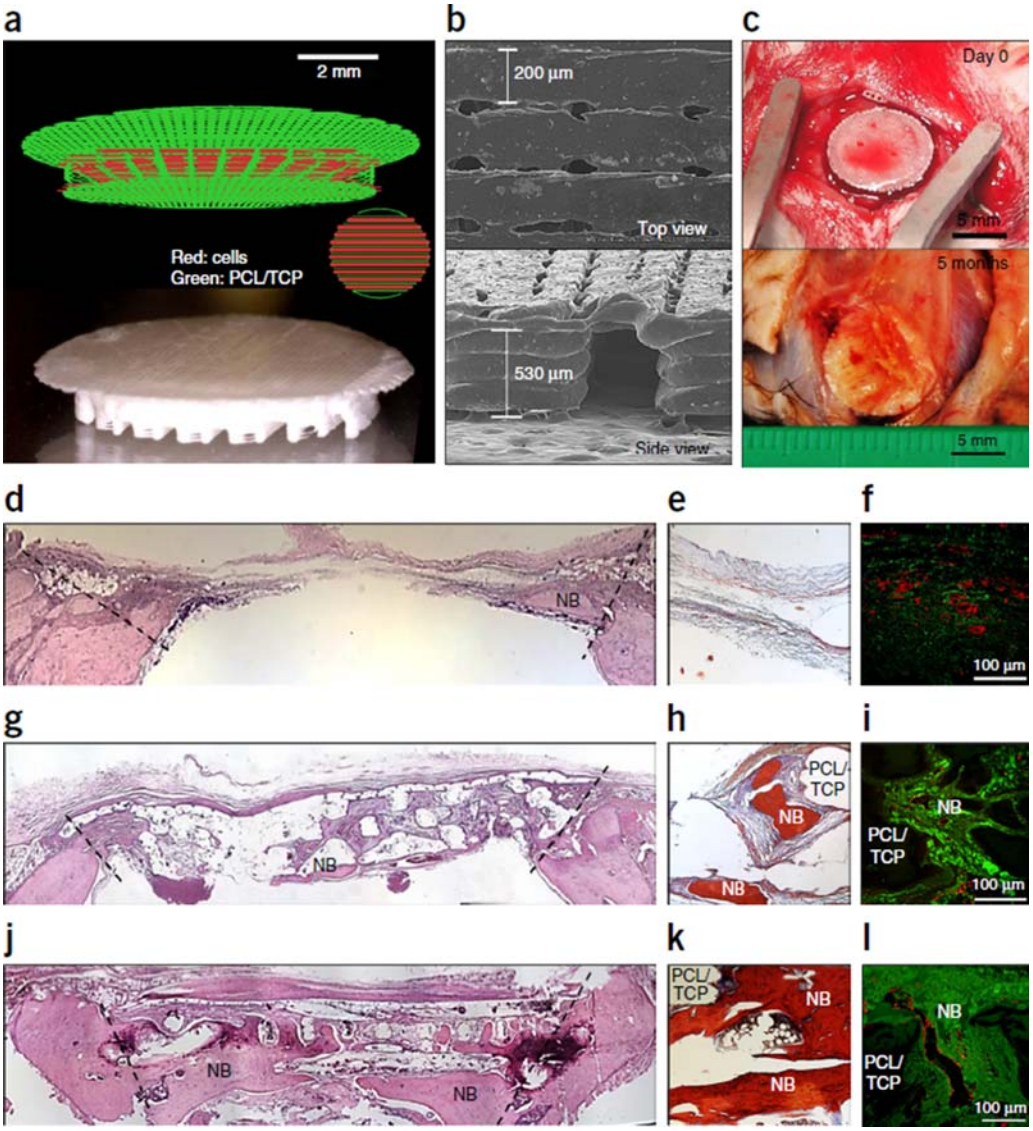

Figure 4.3

Calvarial bone reconstruction using ITOP bioprinted construct. (A) Visualized motion program (top) and image of the printed calvarial bone construct (bottom). (B) SEM images of the printed bone constructs. (C) Images of the printed bone constructs at day 0 (top) and 5 months (bottom) after implantation. (D–L) Histological and immunohistological images of nontreated (D–F), scaffold only without cells (G–I), and hAFSCs-printed construct at 5 months after implantation (J–L). H&E staining (D, G, J), modified tetrachrome staining (E, H,K) and vWF immunostaining (F, I, L). Tetrachrome staining: red, mature bone; blue, osteoid and lining of lacunae. vWF immunofluorescent image: red, blood vessel. NB: new bone; PCL/TCP: remaining scaffold [23].

the higher expression level of COL-I, calcium deposition, and VEGF in dynamic culture relative to static culture.

Utilizing the coaxial EBB, Raja et al. [25] fabricated 3D scaffolds with core/shell structures using bioinks of hydroxyapatite (HAp, core) and MC3T3-E1 cell-laden alginate (shell), in which the cement reaction of HAp took place of the conventional sintering process of ceramics after the simultaneous printing of the HAp and cell-laden hydrogel (Fig. 4.4). The compressive modulus of the core/shell scaffolds was significantly reinforced in comparison to alginate-only scaffolds (7 vs. 0.3 MPa), and the calcium-deficient HAp-only scaffolds disintegrated into pieces after the compression test, which depicted that the core/shell structure balanced the poor mechanical properties of hydrogel and the brittleness of ceramic.

Poldervaart et al. [26] investigated methacrylated hyaluronic acid (MeHA) bioink for bone bioprinting. UV light exposure led to increased storage modulus and elastic modulus of MeHA hydrogels, representing increased rigidity of hydrogels. Next, hBMSCs within MeHA hydrogels retained 64% cell viability after 21 days of culture. In absence of additional osteogenic stimuli, calcium deposition in hydrogels with higher concentrations of MeHA (e.g., 2.5%–3%) was greater as compared to that in a lower concentration (e.g., 1.5%). In addition, MeHA hydrogels showed compatibility with the bioprinting process and were printed into porous and vertebrae-shaped constructs.

Based on a systematic exploration of the effect of different materials with varying concentrations (alginate, phosphate, calcium, and alginate-polyvinyl alcohol (PVA)-HAp

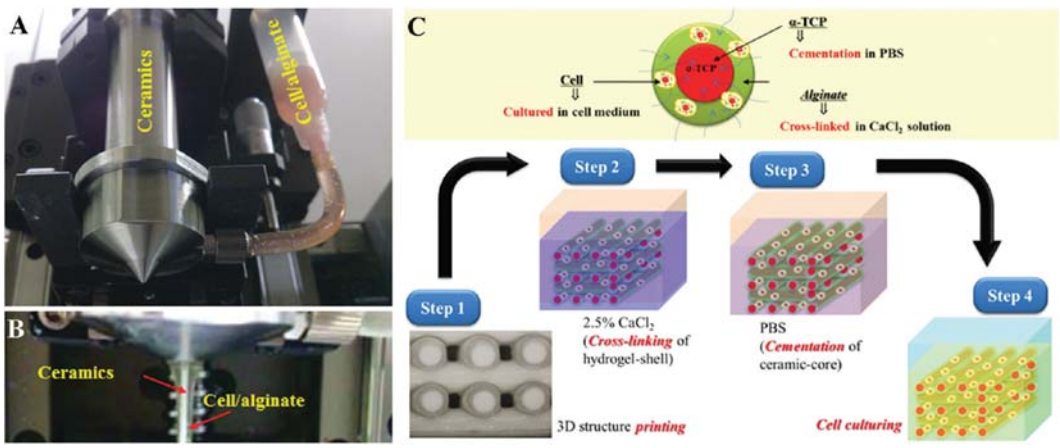

Figure 4.4

(A, B) Images of the coaxial EBB system and the extruding core/shell fiber. (C) Schematic of the postfabrication process, which included cross-linking in $CaCl_2$, cementation of the core in PBS, and cell culture [25].

suspension) on their resultant printability, Bendtsen et al. [27] bioprinted mouse calvaria 3T3-E1 (MC3T3) cells into alginate-PVA-HAp scaffolds. The bioprinted alginate-PVA-HAp scaffolds supported 96% cell viability, specifying that the incorporation of PVA-HAp suspension not only facilitated superior printability but also improved cellular activity after printing. In addition, scaffold degradation in α-MEM cell culture media exhibited that the bioprinted alginate-PVA-HAp scaffolds stayed intact for 14 days.

Using a two-step EBB process, Kim et al. [28] fabricated an alpha-tricalcium phosphate (α-TCP)/collagen cell-laden scaffold with MC3T3-E1 (Fig. 4.5). A porous layer of α-TCP/collagen fibers without cells was extruded to get a mechanically stable structure, followed by deposition of a cell-laden collagen bioink onto the α-TCP/collagen fibers. This two-step process was repeated until a 3D scaffold was obtained. A larger number of viable cells and more homogenous cell distribution were observed on the bioprinted scaffolds compared with that in control groups (i.e., cell-laden collagen-only scaffold and α-TCP/collagen scaffold with dipping-loaded cells). The results of in vitro study showed synergism between the homogeneity of printed cells and the release of calcium and phosphorus ions, where the bioprinted scaffolds exhibited greater osteogenic differentiation compared with the control groups (e.g., ALP activity, calcium deposition, and osteopontin).

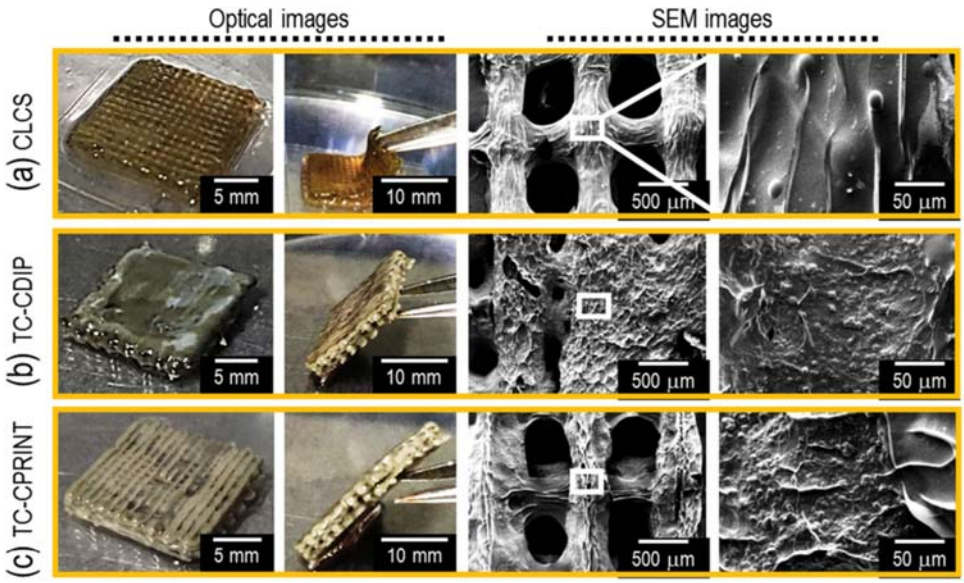

Figure 4.5
Optical and SEM images of (A) Cell-laden collagen scaffold (CLCS), (B) TC-CDIP scaffold fabricated by dipping the α-TCP/collagen scaffold into the cell/collagen mixture solution, and (C) TC-CPRINT fabricated using the two-step process, which was printing of α-TCP/collagen fibers and then bioprinting cell-laden collagen onto the α-TCP/collagen fibers [28].

Being another attempt to involve a perfusable vascular lumen, Byambaa et al. [29] extruded GelMA hydrogels containing different concentrations of chemically conjugated vascular endothelial growth factor (VEGF) to produce a gradient structure. A rod in the center of the construct was bioprinted using a rapidly degradable GelMA hydrogel, resulting in the formation of a perfusable lumen with an endothelial lining (Fig. 4.6). Cell viability in the coculture system (HUVECs and hMSCs) reached 93% by 7 days of culture. MSCs in the inner fibers were differentiated into smooth muscle cells (evidenced by active expression of α-SMA) that promoted the formation of vascular vessels, and meanwhile aided the proliferation of HUVECs. Three outer layers were printed with MSCs and bioactive silicate nanoplatelets encapsulated in GelMA-VEGF, which induced osteogenic differentiation in vitro. Moreover, perfusion of culture medium through the inner core vessel supported the survival of cells in the bone construct. The results of Alizarin Red S (ARS) staining, immunostaining (OCN, RUNX2, and CD31), and RT-qPCR (CD 31, COL-I, ALP, OCN, OPN, and RUNX2) confirmed that the encapsulated hMSCs formed a mature bone with angiogenesis after 21 days of culture.

Using stromal vascular fraction cells (SVFC) as a cell source that maintained the phenotypes of endothelial lineage, Kuss et al. [30] created bone constructs containing PCL/HAp and SVFC-laden hydrogel bioinks, which were methacrylated hyaluronic acid (MeHA) and methacrylated gelatin (GelMA). The osteogenic differentiation of SVFC was not impacted in a short-term (<21 days) hypoxic culture in vitro, which in reverse promoted vascular gene expression (e.g., VEGFA and HIF1A). In the in vivo study of athymic mice, short-term hypoxia (7-day hypoxia and 14-day normoxia) promoted the formation of microvessels in vivo as well as integration with the host vascular network at 4-week implantation, and meanwhile, osteogenic differentiation of SVFC was not affected. Furthermore, lumen sizes in the hypoxia group were significantly larger and vessel area distribution was broader than those cultured with 21 days of normoxia (e.g., normoxia group), demonstrating the benefit of short-term hypoxia in vascularization in bone regeneration.

Demirtaş et al. [31] reported the printing of chitosan and its composite with HAp, along with MC3T3-E1 cells using an EBB, in which alginate and alginate-HAp hydrogels were used as comparisons. The viscosity values of all solutions were in an applicable range for bioprinting. With the incorporation of HAp, the elastic modulus of both chitosan and alginate hydrogels increased ~3−6 folds. During in vitro study, the spherical morphology of cells in alginate and chitosan hydrogels was seen on day 7. On the contrary, well-spread cells were seen in alginate-HAp and chitosan-HAp hydrogels, indicating the positive impact of HAp on cellular morphology. Cells survived (>90%) in all groups after a 9-day culture, while a higher proliferation rate of cells within chitosan-HAp hydrogels was found as compared to alginate-HAp at day 21. Moreover, cells within chitosan-HAp hydrogel

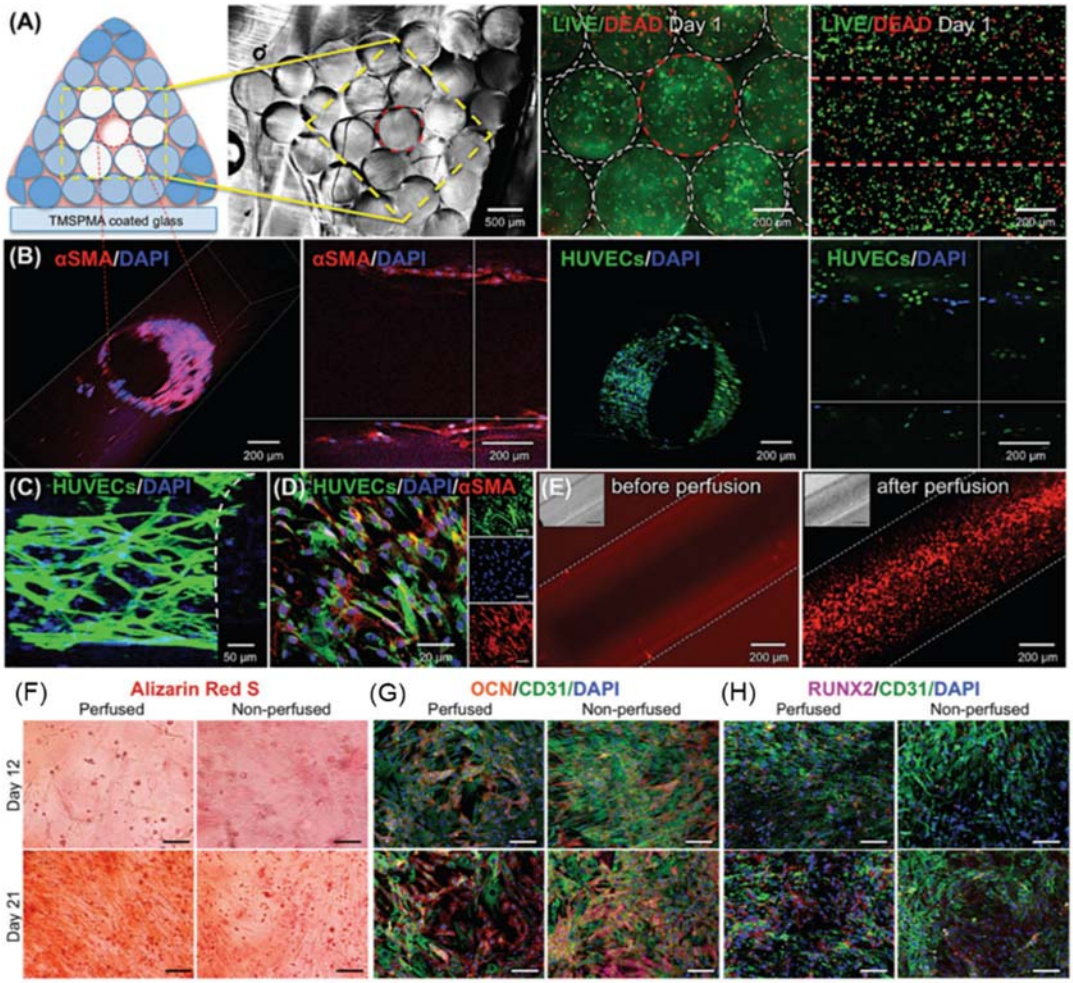

Figure 4.6

Formation of HUVEC/hMSC-lined perfusable lumen in the construct with media perfusion for 5 days. (A) The cross-sectional view of the entire bioprinted construct and Live/Dead staining of the encapsulated cells. (B) Cross- and top-sectioned confocal images of central vessel stained with α-SMA at day 12 post-culture showing the HUVEC-lined vessellike lumen structure. Encapsulated endothelial cells lined the vascular walls (green) and hMSC cells were differentiated into pericytes (red). (C) The lining of endothelial cells inside the central channel. (D) Immunostaining of endothelial cells and α-SMA-expressing hMSCs within the lumen. (E) Images of the construct before and after perfusion of fluorescent microbeads through the core hollow lumen. (F—H) Osteogenic and vasculogenic characterizations of vascularized bonelike tissue bioprinted construct demonstrated by ARS staining of mineralized extracellular matrix (F), immunostaining of OCN/CD31 (G), and RUNX2/CD31 (H) [29].

had the greatest expression levels for osteogenic markers (COL-I, RUNX2, OCN, and OPN) and calcium deposition than other groups, which revealed that chitosan-HAp hydrogels contributed to osteogenic differentiation of cells and tissue mineralization after 21 days of culture.

To facilitate the osseointegration of titanium implants that support cell attachment and trigger mineral deposition, McBeth et al. [32] presented a GelMA scaffold that could be directly printed onto the titanium surface. The scaffold was found to trigger the mineral deposition of both MG63 osteoblasts and primary normal human osteoblasts without the use of exogenous osteogenic factors, whereas films of the same formulation did not induce mineral deposition implying that the 3D structure contributed to the differentiation. Moreover, GelMA scaffolds were able to be directly grafted to titanium alloy and secured in vitro over 7 weeks (Fig. 4.7). Also, the GelMA hydrogel was protected from shearing forces in a marrow implantation model with grooves.

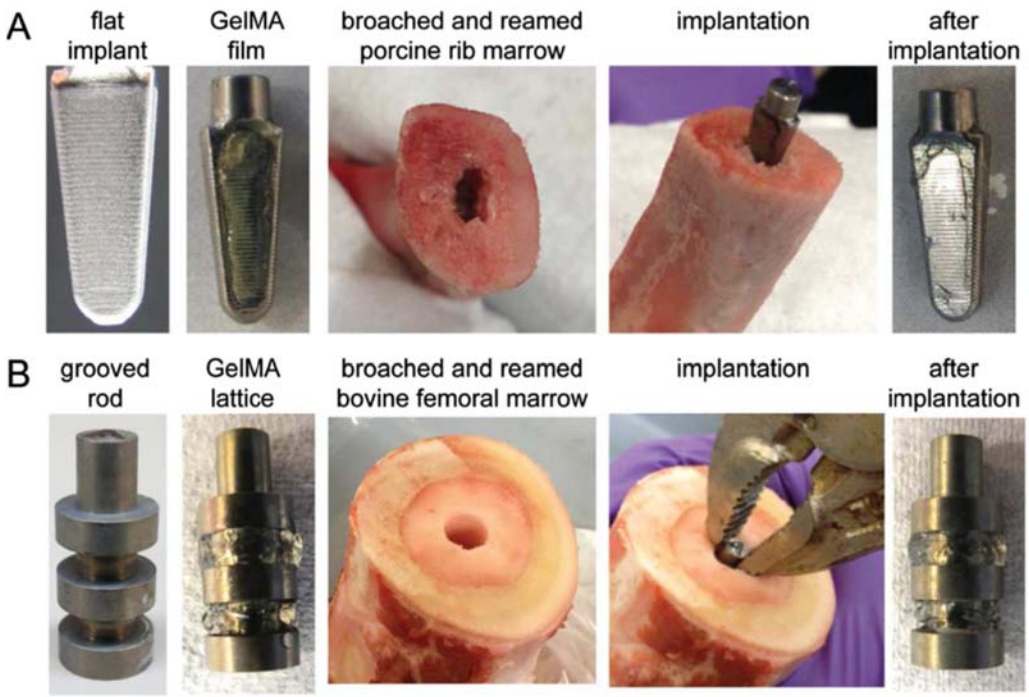

Figure 4.7
Durability test of grafted hydrogels using marrow implantation model. (A) TiAl6V4 substrates were grafted with GelMA films and pressed fit into porcine marrow, and the majority of the hydrogel was sheared from the flat implant surface. (B) TiAl6V4 substrates with protective grooves were grafted with GelMA lattices and pressed fit into bovine marrow, and the majority of the hydrogel was still attached after implantation [32].

4.3 Design of bioprinted bone construct

4.3.1 Biomaterials

So far, natural hydrogels used for bone bioprinting induce different cellular responses. Alginate has been a popular biomaterial for bone bioprinting, since it is biocompatible, low cost, and convenient for cross-linking by contact with Ca^{2+} ions [33]. However, alginate is limited by its low bioactivity. In comparison, collagen is an ideal choice for bone bioprinting due to its constituent similarity to native bone. However, the mechanical properties of collagen are weak, and it is challenging to generate collagen hydrogel with high viscosity which has fast gelation capability. As a result, collagen was only used in a few bone bioprinting studies and is usually incorporated with other biomaterials. Being derived from collagen, gelatin is a more cost-effective option and is combined with other biomaterials to be used as bioinks. In some cases, popular biomaterials, such as agarose, chitosan, and HA are also used to regulate the biological functions of the bioprinted bone constructs [34,35].

Besides mechanically blending multiple natural polymers with various concentrations to tailor the bioink properties, polymers can be modified to have new properties. A representative example for bioprinting is the wide use of methacrylate hydrogels, which are natural ECM components modified by methacrylation [36]. Among these hydrogels, GelMA is becoming one of the most attractive biomaterials in 3D bioprinting [37,38], since it is highly biocompatible and capable of being chemically cross-linked with UV light under physiological conditions to facilitate in situ cross-linking [39]. Methacrylated HA (MeHA) is another example of the family which is photo-cross-linkable [40] and has been combined with GelMA for bone bioprinting [30].

Although the abovementioned polymers can directly bioprint with cells, cell-laden hydrogels have been primarily limited by their low mechanical properties for applications in hard tissue regeneration [41,42]. Thus, biomaterials such as ceramics or thermoplastics, which were commonly used in the fabrication of conventional bone scaffolds, could be alleviated to promote the mechanical strength of the bioprinted bone tissue [41,43,44]. The prevalent options include HAp and TCP, which imitate the major inorganic component of bone, or PCL and PLA [45–49], which are famous for their superior mechanical properties. In addition, 45S5 bioglass, polyphosphate (polyP), and biosilica have been explored in bioprinted bone, which have been reported to enhance the potency of cells to synthesize mineral deposits and induce the expression of ALP and BMP-2 as well as of collagen type I [50,51].

4.3.2 Structure design of vascularized bone constructs

Since bone is a complex tissue with a well-organized hierarchical architecture, structure design becomes an important consideration before bioprinting. Bone cells are entrapped

within the mineral matrix which is encircled by vascular networks [52–55]. Hence, it is widely acknowledged that interconnected pores are crucial for the ingrowth of blood vessels and nutrient transportation. In the common viewpoints of tissue engineering, it has been suggested an optimal pore size of 5 μm for neovascularization, 5–15 μm for fibroblast ingrowth, 100–400 μm for bone regeneration, and 40–100 μm for osteoid ingrowth [16,56]. Besides the involvement of porous features, several strategies have been utilized to promote angiogenesis, such as the addition of angiogenic growth factors during tissue culture [57,58], dynamic culture [59], coculture of endothelial cells (EC) with MSC [60–62], and immunomodulation of adaptive immune cells [63].

Regarding the network level of vascularization, the effective restoration of the bone requires functional blood vessel structures within the implants. As to the vessel functionalization, the organization of endothelium and vessel wall in a networked manner is expected. Taking the advantage of bioprinting to construct highly precise and customized structures, remodeling of a hierarchically branched vascular network with anatomic similarity can be achieved.

For instance, a geometry with two phases was designed with a HAp-containing part (bone tissue) and an alginate-gelatin-filled tubular structure (vascular structure) [17]. In addition, Byambaa et al. [29] bioprinted a perfusable vascular lumen within a pyramidal construct, in which rods of GelMA bioinks functionalized with different concentrations of VEGF were organized in a functionally gradient fashion. With media perfusion for 5 days, the formation of a hollow perusable main vessel was targeted. As another example, Cui et al. [24] engineered a biphasic structure using a dual bioprinting process of FDM and SLA. Units with honeycombed pores in the hard portion of the scaffold resembled osteon or Haversian system of bone, while channels (central channel size: 1.5 mm and branched channel size: 200 μm) filled with GelMA hydrogel resembled the vascular network. The capillary network was expected to form via the cell growth and expansion within the hydrogel.

4.3.3 Cell source

Several cell types, those used in bone TE, have been continued to be used for bone bioprinting. MC3T3 is an osteoblast precursor cell line derived from mice, which has become one of the most convenient and physiologically relevant systems for bone bioprinting. However, caution should be used when extrapolating these results to normal cells. SaOS-2 is a cell line derived from primary osteosarcoma. SaOS-2 cells behave as osteoblastlike cells and are commonly used in bone-related research [64]. Advantages of the SaOS-2 cell line include the capability to get a large number of cells in a short time, and differentiation in a similar way as osteoblasts do [65].

Stem cells are alternative options and are more popular than cell lines or primary bone cells due to their multipotency. MSCs, such as marrow MSCs (BMSCs) and human turbinate MSCs (hTMSCs), have been the most commonly used in numerous studies for bone bioprinting [21]. Interestingly, MSCs can be obtained from induced pluripotent stem cells (iPSCs), which bypasses the issue of a limited number of autologous MSCs [66]. Adipose-derived stem cells (ADSCs) obtained from adipose tissue are abundant in the human body and surgical accessible, making ADSC an attractive cell source for bioprinting [67].

For angiogenesis in bioprinted bone constructs, endothelial cells (ECs) [24,29,40], endothelial progenitor cells (EPCs) [13], or endothelial colony-forming cells (ECFCs) [68] have been cocultured with abovementioned cell types to support therapeutic revascularization in bioprinted tissue constructs [68–70].

4.3.4 Differentiation factors

Ideally, bioprinted bones are supposed to support the osteogenesis of stem cells or osteoprogenitor cells, which is demonstrated by the expression of distinct cytokines such as transforming growth factor β (TGF-β), interferons, and interleukins [71,72]. Next, bioprinted bones should be capable of reaching osteoinduction by depositing bone-related proteins such as bone morphogenetic proteins (BMPs), insulinlike growth factors, and fibroblast growth factors [73–75]. Lastly, the constructs have to be osteoconductive and provide the porous 3D microenvironment for the differentiated bone cells and facilitate the synthesis of mineral and collagenous elements of bone [76].

In the abovementioned studies, many of them exhibited that the differentiation ability of stem cells could be preserved in bioprinted bone constructs, and in the meantime, their osteogenic differentiation could be modulated by using the proper printing process, biomaterials, construct design, and bioactive factors [77]. In general, the addition of BMP-2 and TGF-β leads to greater osteogenic differentiation [78,79]. In terms of bioink materials, an alginate-based hydrogel was reported to support the viability of MSCs, and the osteogenic potential of hMSCs was well maintained in bioprinted scaffolds [12]. Moreover, some bioinks benefit osteogenic differentiation. For example, MeHA has been reported to induce osteogenic differentiation of hBMSCs in bioprinted constructs in the absence of exogenous osteogenic factors [26]. Also, the GelMA scaffold triggered mineral deposition of MG63 osteoblasts and primary normal human osteoblasts (NHOst) without the need for any additional osteogenic factors [32]. Furthermore, HAp is another essential osteoconductive material for upregulated osteogenic differentiation of preosteoblast cells in vitro [31]. Moreover, by adding a layer of polyP·Ca^{2+}-complex to the bioprinted alginate/gelatin hydrogel, a significant increase in mineralization was observed on the SaOS-2 cell-embedded hydrogel [18]. The mechanical properties of biomaterial also affect

cellular activities, since it has been found that larger biomaterial stiffness triggered higher MSC osteogenic differentiation [26]. All these results demonstrated that stem cell activities, especially osteogenic induction, could be regulated and enhanced by using appropriate physical and chemical cues.

4.3.5 Mechanical properties and reinforcement

Three-dimensional bioprinted constructs engineered by using natural hydrogels have a low compression modulus (<10 kPa) [14,31]. In addition, hydrogels degrade fast and lose most of their structural integrity in a short period of culture. For instance, alginate lost ~40% of its strength after a 9-day culture [80]. Even though delicate gradient architecture was designed with different concentrations of GelMA hydrogel, mechanical stability was difficult to maintain for longer than 21 days in culture due to GelMA degradation [29]. Also, the alginate/gelatin construct overlaid with polyP·Ca^{2+} lost its mechanical stability after 5 days in culture [18]. Native bones possess Young's modulus at an order of GPa and tensile/compressive strength of MPa, which are several orders of magnitude larger than most hydrogel-based bioinks. Hence, it is very difficult to use hydrogel-only constructs in clinical applications, and there is a great need to develop constructs with high and retainable mechanical strength during culture or implantation.

The blending of mechanically strong particles could reinforce the bioprinted constructs to some extent (e.g., HAp blended within an alginate/gelatin hydrogel) [17,31]. Cell-laden constructs containing alginate, PVA, and HAp had a compression modulus of 10.3 kPa. However, it was reduced to 2.4 kPa over 14 days in culture [27]. The bioprinted TCP-collagen constructs had an elastic modulus of 0.55 ± 0.10 MPa [28], which is lower than that of the trabecular bone (20–52 MPa) [81].

To significantly reinforce the mechanical properties of bioprinted constructs, frames printed using thermoplastics or ceramics are usually utilized. In addition to mechanical enhancement, the incorporation of thermoplastic facilitates the creation of constructs with large-scale, superior fidelity, and high fiber resolution [82,83]. Cui et al. printed a PLA scaffold using FDM to imitate the Haversian system of bone and GelMA using SLA to imitate vascular channels. The entire construct revealed a similar mechanical strength as a native bone, demonstrated by the compressive modulus of ~0.38 GPa. In the vascular region, the elastic modulus was 10–30 kPa, which provided an appropriate microenvironment for cell encapsulation [24]. Kang et al. [23] printed PCL or PCL/TCP structures to support cell-laden hydrogels, and obtained compressive modulus of ~30–45 MPa with various PCL:TCP ratios. In another study, a TCP/collagen scaffold was printed along with cell-laden collagen [28]. As compared to the collagen-only constructs (0.04 MPa), the reinforced scaffolds had larger compressive moduli (~0.55 MPa). Instead of printing supporting scaffold and hydrogel separately, scaffolds

with core/shell structures were bioprinted, which were comprised of calcium-deficient HAp (core) and cell-laden alginate (shell) [25]. The incorporation of HAp core significantly upregulated the compressive modulus (7 MPa) as compared to alginate-only scaffolds, in which the structural preservation was obtained for 35 days in vitro.

4.3.6 Hypoxic environment

Hypoxia is another essential issue for the regulation of bone development via the hypoxia-inducible transcription (HIF) factors [84]. However, there is controversy about the impact of hypoxia and HIF on bone regeneration. It has been reported by some studies that hypoxia pretreatment enhanced the osteogenesis of BMSCs [85–87], whereas some studies reported that hypoxia inhibited the growth and bone-forming ability of osteoblasts, as well as osteogenic differentiation of MSCs [88,89]. Such paradoxical conclusions imply that hypoxia and HIF might have multiple functions for osteogenic induction.

On the other hand, It is well recognized that hypoxia will increase the expression of proangiogenic factors of MSCs such as vascular endothelial growth factor (VEGF) [85]. During the bone regeneration in the body, a short-term period of hypoxia exists at the early stage, which promotes vascularization in later stages by stimulating the deposition of various factors, including the VEGF and interleukin-6 (IL-6) [90]. Kuss et al. [30] reported that short-term (7 days) hypoxic conditioning did not downregulate the osteogenic differentiation of SVFC within 3D bioprinted constructs, but supported vascularization of SVFC verified by significantly upregulated VEGFA and HIF1A expression.

Considering hypoxia is helpful for capillary formation but might inhibit MSCs differentiating into osteoblasts [91–93], a practical strategy of bone bioprinting is to produce a hypoxic environment with a controllable diffusion of oxygen for the embedded HUVECs, in which design the oxygen supply is not expected to weaken for the bone region of the scaffold [24].

4.3.7 Dynamic culture

Bone continuously remodels under the stimulus of mechanical stresses in vivo, and it has been hypothesized that such stresses are mainly transferred to bone cells in the form of fluid shear stresses [94]. When a bone is subjected to the load, interstitial fluid flows through pores in the bone, and the shear stress is sensed by osteocytes. Subsequently, osteoblasts and osteoprogenitor cells communicate with these osteocytes via the neighboring matrix network. It is evaluated that bone cells experience shears from 8 to 30 dyn/cm^2 as they are subjected to loading in vivo [95,96]. Bioreactors are capable of building dynamic culture conditions to imitate the biological-relevant environments of bone, which enhance nutrient transport and expose cells to fluid shear stresses, and

subsequently promote cell seeding efficiency and functionalization [97,98]. In vitro mechanical stimulation induced by fluid shear stresses using bioreactors has been exhibited to benefit bone differentiation and mineralization [98–100].

Particularly in the studies of bone bioprinting, culture media at a flow rate of 5 mL/min induced significantly higher COL-I expression of hMSCs than the static culture [24]. In the meantime, the VEGF expression with media flow was up to 30% higher as compared to the static condition after a 4-week culture. Importantly, dynamic culture rendered superior calcium deposition which demonstrated that shear stress assisted osteogenesis and mineralization.

4.4 Conclusion and future prospects

Bone bioprinting has recently achieved remarkable progress with the use of varied hydrogels, cell types, and other osteoconductive and osteoinductive components. In addition, several examples of mineralized structures with the vascularized network have been presented. The bioprinted construct needs a long enough time (until healing and remodeling are complete) to generate a durable structure with proper mechanical properties and biological functions, which requests the balance between bioink degradation (in terms of the loss of mass and mechanical strength) and the growth of new tissue. Another challenge is to produce large-scale vascularized bone grafts that match clinical requirements and are the ease of integrating with host tissue in the body.

As reviewed in this chapter, researchers are striving to address limitations in current bone bioprinting. Further efforts to integrate an acellular 3D printed structure and cellular bioprinted hydrogels are recommended, to amend the mechanical properties of cellular bioprinted bone constructs. More advanced processes and bioprinters are expected, which are capable of depositing multiple biomaterials (cellular and acellular) with great efficiency, biocompatibility, and control over printing conditions (e.g., different temperature, oxygen tension, and humidity).

In terms of discovering new bioinks for bone bioprinting, the addition of electromagnetic materials to control the microenvironment of bioprinted bones could be an interesting direction for future research. Because of the piezoelectric nature of bone, electromechanical mechanisms participate to promote the adaptation and remodeling of bone tissue. Conductive polymers, such as carbon nanotube and graphene, can be combined into current bioink systems to provide structural stability, guide cell growth, and stimulate bone formation. In the future, more and more new biomaterials are expected to be developed to achieve functional bone 3D bioprinting. To gain ongoing and fruitful progress in this field of research, multidisciplinary knowledge and continuous financial support are required.

References

[1] N. Eliaz, N. Metoki, Calcium phosphate bioceramics: a review of their history, structure, properties, coating technologies and biomedical applications, Materials 10 (4) (2017) 334.

[2] U.G. Wegst, H. Bai, E. Saiz, A.P. Tomsia, R.O. Ritchie, Bioinspired structural materials, Nature Materials 14 (1) (2015) 23–36.

[3] P. Fratzl, R. Weinkamer, Nature's hierarchical materials, Progress in Materials Science 52 (8) (2007) 1263–1334.

[4] A. Bigham, F. Foroughi, E. Rezvani Ghomi, M. Rafienia, R.E. Neisiany, S. Ramakrishna, The journey of multifunctional bone scaffolds fabricated from traditional toward modern techniques, Bio-Design and Manufacturing 3 (4) (2020) 281–306.

[5] K.J. Koester, J. Ager, R. Ritchie, The true toughness of human cortical bone measured with realistically short cracks, Nature Materials 7 (8) (2008) 672–677.

[6] J.-Y. Rho, L. Kuhn-Spearing, P. Zioupos, Mechanical properties and the hierarchical structure of bone, Medical Engineering & Physics 20 (2) (1998) 92–102.

[7] P. Ke, X.-N. Jiao, X.-H. Ge, W.-M. Xiao, B. Yu, From macro to micro: structural biomimetic materials by electrospinning, RSC Advances 4 (75) (2014) 39704–39724.

[8] M. Vallet-Regí, D.A. Navarrete, D. Arcos, Biomimetic Nanoceramics in Clinical Use: From Materials to Applications, Royal Society of Chemistry, 2008.

[9] R. Florencio-Silva, G.R.d.S. Sasso, E. Sasso-Cerri, M.J. Simões, P.S. Cerri, Biology of bone tissue: structure, function, and factors that influence bone cells, BioMed Research International 2015 (2015).

[10] R. Murugan, S. Ramakrishna, Development of nanocomposites for bone grafting, Composites Science and Technology 65 (15–16) (2005) 2385–2406.

[11] W. Bonfield, M. Wang, K. Tanner, Interfaces in analogue biomaterials, Acta Materialia 46 (7) (1998) 2509–2518.

[12] N.E. Fedorovich, J.R. De Wijn, A.J. Verbout, J. Alblas, W.J. Dhert, Three-dimensional fiber deposition of cell-laden, viable, patterned constructs for bone tissue printing, Tissue Engineering A 14 (1) (2008) 127–133.

[13] N.E. Fedorovich, H.M. Wijnberg, W.J. Dhert, J. Alblas, Distinct tissue formation by heterogeneous printing of osteo-and endothelial progenitor cells, Tissue Engineering Part A 17 (15–16) (2011) 2113–2121.

[14] N.E. Fedorovich, W. Schuurman, H.M. Wijnberg, H.-J. Prins, P.R. Van Weeren, J. Malda, J. Alblas, W.J. Dhert, Biofabrication of osteochondral tissue equivalents by printing topologically defined, cell-laden hydrogel scaffolds, Tissue Engineering Part C Methods 18 (1) (2012) 33–44.

[15] L.D. Loozen, F. Wegman, F.C. Öner, W.J. Dhert, J. Alblas, Porous bioprinted constructs in BMP-2 non-viral gene therapy for bone tissue engineering, Journal of Materials Chemistry B 1 (48) (2013) 6619–6626.

[16] H. Lee, S. Ahn, L.J. Bonassar, G. Kim, Cell (MC3T3-E1)-Printed poly (ε-caprolactone)/Alginate hybrid scaffolds for tissue regeneration, Macromolecular Rapid Communications 34 (2) (2013) 142–149.

[17] S. Wüst, M.E. Godla, R. Müller, S. Hofmann, Tunable hydrogel composite with two-step processing in combination with innovative hardware upgrade for cell-based three-dimensional bioprinting, Acta Biomaterialia 10 (2) (2014) 630–640.

[18] M. Neufurth, X. Wang, H.C. Schröder, Q. Feng, B. Diehl-Seifert, T. Ziebart, R. Steffen, S. Wang, W.E. Müller, Engineering a morphogenetically active hydrogel for bioprinting of bioartificial tissue derived from human osteoblast-like SaOS-2 cells, Biomaterials 35 (31) (2014) 8810–8819.

[19] X. Wang, E. Tolba, H.C. Schröder, M. Neufurth, Q. Feng, B. Diehl-Seifert, W.E. Müller, Effect of bioglass on growth and biomineralization of SaOS-2 cells in hydrogel after 3D cell bioprinting, PLoS One 9 (11) (2014) e112497.

[20] M.J. Sawkins, P. Mistry, B.N. Brown, K.M. Shakesheff, L.J. Bonassar, J. Yang, Cell and protein compatible 3D bioprinting of mechanically strong constructs for bone repair, Biofabrication 7 (3) (2015) 035004.
[21] S. Das, F. Pati, Y.-J. Choi, G. Rijal, J.-H. Shim, S.W. Kim, A.R. Ray, D.-W. Cho, S. Ghosh, Bioprintable, cell-laden silk fibroin−gelatin hydrogel supporting multilineage differentiation of stem cells for fabrication of three-dimensional tissue constructs, Acta Biomaterialia 11 (2015) 233−246.
[22] D.F. Duarte Campos, A. Blaeser, K. Buellesbach, K.S. Sen, W. Xun, W. Tillmann, H. Fischer, Bioprinting organotypic hydrogels with improved mesenchymal stem cell remodeling and mineralization properties for bone tissue engineering, Advanced Healthcare Materials 5 (11) (2016) 1336−1345.
[23] H.-W. Kang, S.J. Lee, I.K. Ko, C. Kengla, J.J. Yoo, A. Atala, A 3D bioprinting system to produce human-scale tissue constructs with structural integrity, Nature Biotechnology 34 (3) (2016) 312−319.
[24] H. Cui, W. Zhu, M. Nowicki, X. Zhou, A. Khademhosseini, L.G. Zhang, Hierarchical fabrication of engineered vascularized bone biphasic constructs via dual 3D bioprinting: integrating regional bioactive factors into architectural design, Advanced healthcare materials 5 (17) (2016) 2174−2181.
[25] N. Raja, H.-S. Yun, A simultaneous 3D printing process for the fabrication of bioceramic and cell-laden hydrogel core/shell scaffolds with potential application in bone tissue regeneration, Journal of Materials Chemistry B 4 (27) (2016) 4707−4716.
[26] M.T. Poldervaart, B. Goversen, M. De Ruijter, A. Abbadessa, F.P. Melchels, F.C. Öner, W.J. Dhert, T. Vermonden, J. Alblas, 3D bioprinting of methacrylated hyaluronic acid (MeHA) hydrogel with intrinsic osteogenicity, PLoS One 12 (6) (2017) e0177628.
[27] S.T. Bendtsen, S.P. Quinnell, M. Wei, Development of a novel alginate-polyvinyl alcohol-hydroxyapatite hydrogel for 3D bioprinting bone tissue engineered scaffolds, Journal of Biomedical Materials Research A 105 (5) (2017) 1457−1468.
[28] W.J. Kim, H.-S. Yun, G.H. Kim, An innovative cell-laden α-TCP/collagen scaffold fabricated using a two-step printing process for potential application in regenerating hard tissues, Scientific Reports 7 (1) (2017) 1−12.
[29] B. Byambaa, N. Annabi, K. Yue, G. Trujillo-de Santiago, M.M. Alvarez, W. Jia, M. Kazemzadeh-Narbat, S.R. Shin, A. Tamayol, A. Khademhosseini, Bioprinted osteogenic and vasculogenic patterns for engineering 3D bone tissue, Advanced healthcare materials 6 (16) (2017) 1700015.
[30] M.A. Kuss, R. Harms, S. Wu, Y. Wang, J.B. Untrauer, M.A. Carlson, B. Duan, Short-term hypoxic preconditioning promotes prevascularization in 3D bioprinted bone constructs with stromal vascular fraction derived cells, RSC Advances 7 (47) (2017) 29312−29320.
[31] T.T. Demirtaş, G. Irmak, M. Gümüşderelioğlu, A bioprintable form of chitosan hydrogel for bone tissue engineering, Biofabrication 9 (3) (2017) 035003.
[32] C. McBeth, J. Lauer, M. Ottersbach, J. Campbell, A. Sharon, A.F. Sauer-Budge, 3D bioprinting of GelMA scaffolds triggers mineral deposition by primary human osteoblasts, Biofabrication 9 (1) (2017) 015009.
[33] K.Y. Lee, D.J. Mooney, Alginate: properties and biomedical applications, Progress in Polymer Science 37 (1) (2012) 106−126.
[34] T. Funakoshi, T. Majima, N. Iwasaki, N. Suenaga, N. Sawaguchi, K. Shimode, A. Minami, K. Harada, S. Nishimura, Application of tissue engineering techniques for rotator cuff regeneration using a chitosan-based hyaluronan hybrid fiber scaffold, The American Journal of Sports Medicine 33 (8) (2005) 1193−1201.
[35] M. Laranjeira, R.M.A. Domingues, R. Costa-Almeida, R.L. Reis, M.E. Gomes, 3D mimicry of native-tissue-fiber architecture guides tendon-derived cells and adipose stem cells into artificial tendon constructs, Small 13 (31) (2017) 1700689.
[36] J.W. Nichol, S.T. Koshy, H. Bae, C.M. Hwang, S. Yamanlar, A. Khademhosseini, Cell-laden microengineered gelatin methacrylate hydrogels, Biomaterials 31 (21) (2010) 5536−5544.

[37] K. Yue, G. Trujillo-de Santiago, M.M. Alvarez, A. Tamayol, N. Annabi, A. Khademhosseini, Synthesis, properties, and biomedical applications of gelatin methacryloyl (GelMA) hydrogels, Biomaterials 73 (2015) 254–271.
[38] B.J. Klotz, D. Gawlitta, A.J. Rosenberg, J. Malda, F.P. Melchels, Gelatin-methacryloyl hydrogels: towards biofabrication-based tissue repair, Trends in Biotechnology 34 (5) (2016) 394–407.
[39] C.D. O'Connell, C. Di Bella, F. Thompson, C. Augustine, S. Beirne, R. Cornock, C.J. Richards, J. Chung, S. Gambhir, Z. Yue, Development of the Biopen: a handheld device for surgical printing of adipose stem cells at a chondral wound site, Biofabrication 8 (1) (2016) 015019.
[40] A.J. Evinger, J.M. Jeyakumar, L.A. Hook, Y. Choo, B.R. Shepherd, S.C. Presnell, Osteogenic differentiation of mesenchymal stem/stromal cells within 3D bioprinted neotissues, Federation of American Societies for Experimental Biology 27 (2013) 193.
[41] W. Schuurman, V. Khristov, M.W. Pot, P.R. van Weeren, W.J. Dhert, J. Malda, Bioprinting of hybrid tissue constructs with tailorable mechanical properties, Biofabrication 3 (2) (2011) 021001.
[42] D.L. Cohen, E. Malone, H. Lipson, L.J. Bonassar, Direct freeform fabrication of seeded hydrogels in arbitrary geometries, Tissue Engineering 12 (5) (2006) 1325–1335.
[43] J. Schagemann, H. Chung, E. Mrosek, J. Stone, J. Fitzsimmons, S. O'driscoll, G. Reinholz, Poly-ε-caprolactone/gel hybrid scaffolds for cartilage tissue engineering, Journal of Biomedical Materials Research Part A 93 (2) (2010) 454–463.
[44] M. Endres, D. Hutmacher, A. Salgado, C. Kaps, J. Ringe, R. Reis, M. Sittinger, A. Brandwood, J.-T. Schantz, Osteogenic induction of human bone marrow-derived mesenchymal progenitor cells in novel synthetic polymer–hydrogel matrices, Tissue Engineering 9 (4) (2003) 689–702.
[45] Q. Pan, C. Gao, Y. Wang, Y. Wang, C. Mao, Q. Wang, S.N. Economidou, D. Douroumis, F. Wen, L.P. Tan, Investigation of bone reconstruction using an attenuated immunogenicity xenogenic composite scaffold fabricated by 3D printing, Bio-Design and Manufacturing 3 (4) (2020) 396–409.
[46] B.I. Oladapo, S.A. Zahedi, S.O. Ismail, F.T. Omigbodun, O.K. Bowoto, M.A. Olawumi, M.A. Muhammad, 3D printing of PEEK–cHAp scaffold for medical bone implant, Bio-Design and Manufacturing 4 (1) (2021) 44–59.
[47] C. Gao, M. Yao, C. Shuai, P. Feng, S. Peng, Advances in biocermets for bone implant applications, Bio-Design and Manufacturing 3 (4) (2020) 307–330.
[48] B. Huang, J.V. Helaehil, P.R. Nalesso, L. Bagne, M.A. de Oliveira, G.C. Albiazetti, A. Aldalbahi, M. El-Newehy, M. Santamaria Jr., F.A. Mendonça, In vivo study of conductive 3D printed PCL/MWCNTs scaffolds with electrical stimulation for bone tissue engineering, Bio-Design and Manufacturing 4 (2) (2021) 190–202.
[49] Y. Yang, Y. Cheng, F. Deng, L. Shen, Z. Zhao, S. Peng, C. Shuai, A bifunctional bone scaffold combines osteogenesis and antibacterial activity via in situ grown hydroxyapatite and silver nanoparticles, Bio-Design and Manufacturing 4 (3) (2021) 452–468.
[50] X. Wang, H.C. Schröder, K. Wang, J.A. Kaandorp, W.E. Mueller, Genetic, biological and structural hierarchies during sponge spicule formation: from soft sol–gels to solid 3D silica composite structures, Soft Matter 8 (37) (2012) 9501–9518.
[51] M. Wiens, X. Wang, H.C. Schröder, U. Kolb, U. Schloßmacher, H. Ushijima, W.E. Müller, The role of biosilica in the osteoprotegerin/RANKL ratio in human osteoblast-like cells, Biomaterials 31 (30) (2010) 7716–7725.
[52] L.H. Nguyen, N. Annabi, M. Nikkhah, H. Bae, L. Binan, S. Park, Y. Kang, Y. Yang, A. Khademhosseini, Vascularized bone tissue engineering: approaches for potential improvement, Tissue Engineering Part B Reviews 18 (5) (2012) 363–382.
[53] A. Oryan, S. Alidadi, A. Moshiri, N. Maffulli, Bone regenerative medicine: classic options, novel strategies, and future directions, Journal of Orthopaedic Surgery and Research 9 (1) (2014) 18.
[54] J. Wang, M. Yang, Y. Zhu, L. Wang, A.P. Tomsia, C. Mao, Phage nanofibers induce vascularized osteogenesis in 3D printed bone scaffolds, Advanced Materials 26 (29) (2014) 4961–4966.

[55] M.O. Wang, C.E. Vorwald, M.L. Dreher, E.J. Mott, M.H. Cheng, A. Cinar, H. Mehdizadeh, S. Somo, D. Dean, E.M. Brey, Evaluating 3D-Printed biomaterials as scaffolds for vascularized bone tissue engineering, Advanced Materials 27 (1) (2015) 138–144.
[56] K. Whang, K. Healy, D. Elenz, E. Nam, D. Tsai, C. Thomas, G. Nuber, F. Glorieux, R. Travers, S. Sprague, Engineering bone regeneration with bioabsorbable scaffolds with novel microarchitecture, Tissue Engineering 5 (1) (1999) 35–51.
[57] A.R. Amini, C.T. Laurencin, S.P. Nukavarapu, Differential analysis of peripheral blood-and bone marrow-derived endothelial progenitor cells for enhanced vascularization in bone tissue engineering, Journal of Orthopaedic Research 30 (9) (2012) 1507–1515.
[58] J.E. Samorezov, E. Alsberg, Spatial regulation of controlled bioactive factor delivery for bone tissue engineering, Advanced Drug Delivery Reviews 84 (2015) 45–67.
[59] M.I. Santos, R.L. Reis, Vascularization in bone tissue engineering: physiology, current strategies, major hurdles and future challenges, Macromolecular Bioscience 10 (1) (2010) 12–27.
[60] C.J. Kirkpatrick, S. Fuchs, R.E. Unger, Co-culture systems for vascularization-learning from nature, Advanced Drug Delivery Reviews 63 (4–5) (2011) 291–299.
[61] M.A. Brennan, J.-M. Davaine, P. Layrolle, Pre-vascularization of bone tissue-engineered constructs, Stem Cell Research & Therapy 4 (4) (2013) 1–3.
[62] R. Mishra, B.M. Roux, M. Posukonis, E. Bodamer, E.M. Brey, J.P. Fisher, D. Dean, Effect of prevascularization on in vivo vascularization of poly (propylene fumarate)/fibrin scaffolds, Biomaterials 77 (2016) 255–266.
[63] K.L. Spiller, S. Nassiri, C.E. Witherel, R.R. Anfang, J. Ng, K.R. Nakazawa, T. Yu, G. Vunjak-Novakovic, Sequential delivery of immunomodulatory cytokines to facilitate the M1-to-M2 transition of macrophages and enhance vascularization of bone scaffolds, Biomaterials 37 (2015) 194–207.
[64] S.B. Rodan, Y. Imai, M.A. Thiede, G. Wesolowski, D. Thompson, Z. Bar-Shavit, S. Shull, K. Mann, G.A. Rodan, Characterization of a human osteosarcoma cell line (Saos-2) with osteoblastic properties, Cancer Research 47 (18) (1987) 4961–4966.
[65] H.-J. Hausser, R.E. Brenner, Phenotypic instability of Saos-2 cells in long-term culture, Biochemical and Biophysical Research Communications 333 (1) (2005) 216–222.
[66] V. Sabapathy, S. Kumar, hiPSC-derived iMSCs: NextGen MSCs as an advanced therapeutically active cell resource for regenerative medicine, Journal of Cellular and Molecular Medicine 20 (8) (2016) 1571–1588.
[67] N. Ashammakhi, A. Hasan, O. Kaarela, B. Byambaa, A. Sheikhi, A.K. Gaharwar, A. Khademhosseini, Advancing frontiers in bone bioprinting, Advanced Healthcare Materials 8 (7) (2019) 1801048.
[68] M. Gruene, M. Pflaum, C. Hess, S. Diamantouros, S. Schlie, A. Deiwick, L. Koch, M. Wilhelmi, S. Jockenhoevel, A. Haverich, Laser printing of three-dimensional multicellular arrays for studies of cell-cell and cell-environment interactions, Tissue Engineering Part C Methods 17 (10) (2011) 973–982.
[69] S. Merfeld-Clauss, N. Gollahalli, K.L. March, D.O. Traktuev, Adipose tissue progenitor cells directly interact with endothelial cells to induce vascular network formation, Tissue Engineering Part A 16 (9) (2010) 2953–2966.
[70] Y. Wu, L. Chen, P.G. Scott, E.E. Tredget, Mesenchymal stem cells enhance wound healing through differentiation and angiogenesis, Stem Cells 25 (10) (2007) 2648–2659.
[71] L. Pederson, M. Ruan, J.J. Westendorf, S. Khosla, M.J. Oursler, Regulation of bone formation by osteoclasts involves Wnt/BMP signaling and the chemokine sphingosine-1-phosphate, Proceedings of the National Academy of Sciences 105 (52) (2008) 20764–20769.
[72] P. Guihard, Y. Danger, B. Brounais, E. David, R. Brion, J. Delecrin, C.D. Richards, S. Chevalier, F. Rédini, D. Heymann, Induction of osteogenesis in mesenchymal stem cells by activated monocytes/macrophages depends on oncostatin M signaling, Stem Cells 30 (4) (2012) 762–772.
[73] T. Albrektsson, C. Johansson, Osteoinduction, osteoconduction and osseointegration, European Spine Journal 10 (2) (2001) S96–S101.

[74] A. Brydone, D. Meek, S. Maclaine, Bone grafting, orthopaedic biomaterials, and the clinical need for bone engineering, Proceedings of the Institution of Mechanical Engineers, Part H: Journal of Engineering in Medicine 224 (12) (2010) 1329–1343.
[75] R. Dimitriou, E. Jones, D. McGonagle, P.V. Giannoudis, Bone regeneration: current concepts and future directions, BMC Medicine 9 (1) (2011) 1–10.
[76] P. Fratzl, H. Gupta, E. Paschalis, P. Roschger, Structure and mechanical quality of the collagen–mineral nano-composite in bone, Journal of Materials Chemistry 14 (14) (2004) 2115–2123.
[77] F. Kreimendahl, M. Köpf, A.L. Thiebes, D.F. Duarte Campos, A. Blaeser, T. Schmitz-Rode, C. Apel, S. Jockenhoevel, H. Fischer, Three-dimensional printing and angiogenesis: tailored agarose-type I collagen blends comprise three-dimensional printability and angiogenesis potential for tissue-engineered substitutes, Tissue Engineering Part C Methods 23 (10) (2017) 604–615.
[78] V. Karageorgiou, L. Meinel, S. Hofmann, A. Malhotra, V. Volloch, D. Kaplan, Bone morphogenetic protein-2 decorated silk fibroin films induce osteogenic differentiation of human bone marrow stromal cells, Journal of Biomedical Materials Research Part A: An Official Journal of The Society for Biomaterials, The Japanese Society for Biomaterials, and The Australian Society for Biomaterials and the Korean Society for Biomaterials 71 (3) (2004) 528–537.
[79] L. Zhao, S. Jiang, B.M. Hantash, Transforming growth factor β1 induces osteogenic differentiation of murine bone marrow stromal cells, Tissue Engineering Part A 16 (2) (2010) 725–733.
[80] M.S. Shoichet, R.H. Li, M.L. White, S.R. Winn, Stability of hydrogels used in cell encapsulation: an in vitro comparison of alginate and agarose, Biotechnology and Bioengineering 50 (4) (1996) 374–381.
[81] R. Mishra, B. Basu, A. Kumar, Physical and cytocompatibility properties of bioactive glass–polyvinyl alcohol–sodium alginate biocomposite foams prepared via sol–gel processing for trabecular bone regeneration, Journal of Materials Science: Materials in Medicine 20 (12) (2009) 2493.
[82] C.H. Lee, S.A. Rodeo, L.A. Fortier, C. Lu, C. Erisken, J.J. Mao, Protein-releasing polymeric scaffolds induce fibrochondrocytic differentiation of endogenous cells for knee meniscus regeneration in sheep, Science Translational Medicine 6 (266) (2014) 266ra171.
[83] C. Ding, Z. Qiao, W. Jiang, H. Li, J. Wei, G. Zhou, K. Dai, Regeneration of a goat femoral head using a tissue-specific, biphasic scaffold fabricated with CAD/CAM technology, Biomaterials 34 (28) (2013) 6706.
[84] E. Araldi, E. Schipani, Hypoxia, HIFs and bone development, Bone 47 (2) (2010) 190–196.
[85] W. Fan, R. Crawford, Y. Xiao, Enhancing in vivo vascularized bone formation by cobalt chloride-treated bone marrow stromal cells in a tissue engineered periosteum model, Biomaterials 31 (13) (2010) 3580–3589.
[86] A.A. Mamalis, D.L. Cochran, The therapeutic potential of oxygen tension manipulation via hypoxia inducible factors and mimicking agents in guided bone regeneration. A review, Archives of Oral Biology 56 (12) (2011) 1466–1475.
[87] L.B. Boyette, O.A. Creasey, L. Guzik, T. Lozito, R.S. Tuan, Human bone marrow-derived mesenchymal stem cells display enhanced clonogenicity but impaired differentiation with hypoxic preconditioning, Stem Cells Translational Medicine 3 (2) (2014) 241–254.
[88] C. Merceron, C. Vinatier, S. Portron, M. Masson, J. Amiaud, L. Guigand, Y. Chérel, P. Weiss, J. Guicheux, Differential effects of hypoxia on osteochondrogenic potential of human adipose-derived stem cells, American Journal of Physiology-Cell Physiology 298 (2) (2010) C355–C364.
[89] J. Utting, S. Robins, A. Brandao-Burch, I. Orriss, J. Behar, T. Arnett, Hypoxia inhibits the growth, differentiation and bone-forming capacity of rat osteoblasts, Experimental Cell Research 312 (10) (2006) 1693–1702.
[90] N. Haque, M.T. Rahman, N.H. Abu Kasim, A.M. Alabsi, Hypoxic culture conditions as a solution for mesenchymal stem cell based regenerative therapy, The Scientific World Journal 2013 (2013).
[91] J. Baldwin, M. Antille, U. Bonda, E.M. De-Juan-Pardo, K. Khosrotehrani, S. Ivanovski, E.B. Petcu, D.W. Hutmacher, In vitro pre-vascularisation of tissue-engineered constructs A co-culture perspective, Vascular Cell 6 (1) (2014) 1–16.

[92] A. Tufro-McReddie, V. Norwood, K. Aylor, S. Botkin, R. Carey, R. Gomez, Oxygen regulates vascular endothelial growth factor-mediated vasculogenesis and tubulogenesis, Developmental Biology 183 (2) (1997) 139–149.
[93] D. Shweiki, A. Itin, D. Soffer, E. Keshet, Vascular endothelial growth factor induced by hypoxia may mediate hypoxia-initiated angiogenesis, Nature 359 (6398) (1992) 843–845.
[94] V.I. Sikavitsas, J.S. Temenoff, A.G. Mikos, Biomaterials and bone mechanotransduction, Biomaterials 22 (19) (2001) 2581–2593.
[95] J. Rubin, C. Rubin, C.R. Jacobs, Molecular pathways mediating mechanical signaling in bone, Gene 367 (2006) 1–16.
[96] S. Weinbaum, S. Cowin, Y. Zeng, A model for the excitation of osteocytes by mechanical loading-induced bone fluid shear stresses, Journal of Biomechanics 27 (3) (1994) 339–360.
[97] A.B. Yeatts, J.P. Fisher, Bone tissue engineering bioreactors: dynamic culture and the influence of shear stress, Bone 48 (2) (2011) 171–181.
[98] K. Bilodeau, D. Mantovani, Bioreactors for tissue engineering: focus on mechanical constraints. A comparative review, Tissue Engineering 12 (8) (2006) 2367–2383.
[99] G.N. Bancroft, V.I. Sikavitsas, J. van den Dolder, T.L. Sheffield, C.G. Ambrose, J.A. Jansen, A.G. Mikos, Fluid flow increases mineralized matrix deposition in 3D perfusion culture of marrow stromal osteoblasts in a dose-dependent manner, Proceedings of the National Academy of Sciences 99 (20) (2002) 12600–12605.
[100] G.N. Bancroft, V.I. Sikavitsas, A.G. Mikos, Design of a flow perfusion bioreactor system for bone tissue-engineering applications, Tissue Engineering 9 (3) (2003) 549–554.

CHAPTER 5

Bioprinting of skin

5.1 Skin: anatomy and functions

The skin, also called as integument, is the largest organ of the body, accounting for about 15% of the total body weight in adults. Skin, along with its derivative structure, constitutes the integumentary system [1]. The skin has a very complex multilayered structure, which in turn consists of several other components such as cells, fibers, extracellular matrix (ECM), veins, capillaries, nerves, and the hair follicles. The skin predominantly consists of three layers namely epidermis, dermis, and hypodermis (also called as subcutaneous tissue). The epidermis is the outer most layer, consisting of keratinocytes (KCs), the middle layer is the dermis, consisting of collagen and fibroblasts (FCs), and the inner most layer is hypodermis, consisting of lipocytes and collagen (Fig. 5.1). The constituents of three layers [2], in detail, are summarized in Table 5.1. Malfunction of any one of these will cause undesirable skin conditions like rash, dermatitis, cellulitis, and even melanoma.

Skin, mostly seen just as a fleshy covering, does a lot more vital functions than we could possibly imagine, including (i) protective (barrier, UV light absorption, immune surveillance, mechanical), (ii) perceptive (touch, temperature, pain), and (iii) regulatory (thermal, hydration, excretory) functions. With all the above functions, skin thus aids in the maintenance of homeostasis [4].

Each and every component of the skin performs specialized functions, in addition to the general functions stated above. There are many reported works on the functions and mechanisms of keratinocytes [5–9], fibroblasts [10–13], melanocytes [14–19], merkel cells [20–24], Langerhans cells [25–30], mast cells [31–37], macrophages [27,38–41], and other components of skin as well.

5.2 Compelling needs for artificial biomimic skin

Artificial skins are biological or synthetic substitutes for human skin, produced in laboratories. There are two compelling reasons as to why the world is in need of artificial skins: (i) wound healing and skin regeneration—especially for burn victims, and (ii) drug and skin care products (cosmetics) testing.

Injury or illness that causes loss of skin integrity will lead to substantial physiological imbalance and ultimately to significant disability, sometimes even fatality. The 2016 global

3D Bioprinting in Tissue and Organ Regeneration. https://doi.org/10.1016/B978-0-12-824291-9.00006-3

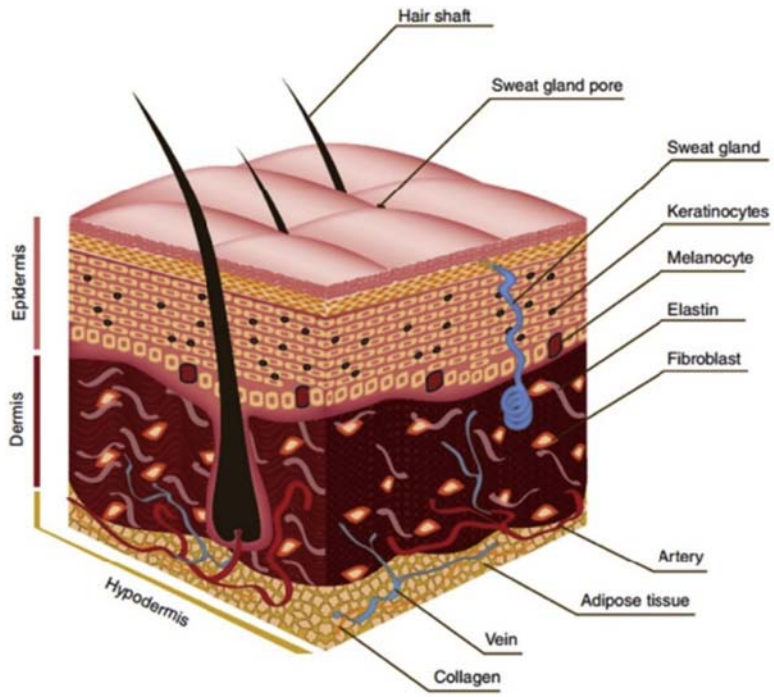

Figure 5.1
Anatomy of skin, showing the three layers (epidermis, dermis, hypodermis), the skin appendages (hair shaft, sweat gland), and the cellular constituents (keratinocytes and melanocytes in epidermis; fibroblasts in dermis; adipose tissue at the base of hypodermis; collagen in all three layers). *Reprinted by copyright permissions from R.F. Pereira, C.C. Barrias, P.L. Granja, P.J. Bartolo, Advanced biofabrication strategies for skin regeneration and repair, Nanomedicine 8 (4) (2013) 603–621.*

wound management market is expected to hit $15 billion and forecasted to be worth over $22 billion in 2024. The global tissue engineered skin substitutes market was valued at USD 958.8 million in 2014 and is projected to reach USD 3873.5 million by 2023, expanding at a Compound Annual Growth Rate (CAGR) of 17.2% from 2015 to 2023 [42]. American Burn Association recorded that, in the US, the number of burn injuries receiving medical treatment per year are 486,000 and the number of hospitalizations per year for acute burn injuries are 40,000, per the 2016 report [43]. Fire, flames, electricity, scald, and chemical products are the major causes of such acute burn injuries. The severity of the burn injury depends on the duration and intensity of exposure and can be classified accordingly [44,45].

Of the classification shown in Fig. 5.2, third degree and fourth degree burns are considered as full-thickness injuries and are the most difficult to treat. This requires the regeneration of the whole skin structure, multiple layers with each having specialized cells, appendages, and other components. Not only is the thickness or volume of skin to be regenerated, the

Table 5.1: Constituents and functions of the layers of skin.

Layer	Constituents	Function
Epidermis	Keratinocytes	Guards from environmental damage by pathogens, heat, UV radiation, and water loss
	Melanocytes	Responsible for the production of the pigment melanin, protection from UV-B light exposure
	Merkel cells	Associated with tactility (sense of touch)
	Langerhans cells	Antigen-presenting immune cells
Dermis	Collagen	Fibrous family of proteins responsible for stress-resistance and elasticity
	Fibroblasts	Synthesize ECM and collagen, play a critical role in wound healing
	Mast cells	Allergy response, anaphylaxis, wound healing, and angiogenesis
Hypodermis	Fibroblasts	Synthesize ECM and collagen, play a critical role in wound healing
	Lipocytes/Adipocytes	Energy storage in the form of fat
	Macrophages	Phagocytosis, adaptive immunity, wound healing

functionality of the original skin is to be restored. Understanding the wound healing mechanisms [45–49] will help achieve the objective of making functional skins by emerging advanced technologies.

The second important reason that accelerates the need for artificial skins is the drug and skincare products (cosmetics) testing. Not all drugs are mild enough to be tested directly on the humans. Researchers in pharmaceutical and skincare industries were and are using animals to test their products. However, testing the products on animals is not always predictive of responses in humans. In other words, the response to the same drug or product may be slightly or even drastically different from the response that is observed in animals, making the whole testing process unreliable, meaningless, and absurd. Also, these testing procedures may cause discomfort and pain to the animals [50–52]. Many organizations and associations were formed since long, like Alternatives to Animal Testing (SCAAT) Steering Committee formed by The European Cosmetics Association (COLIPA)

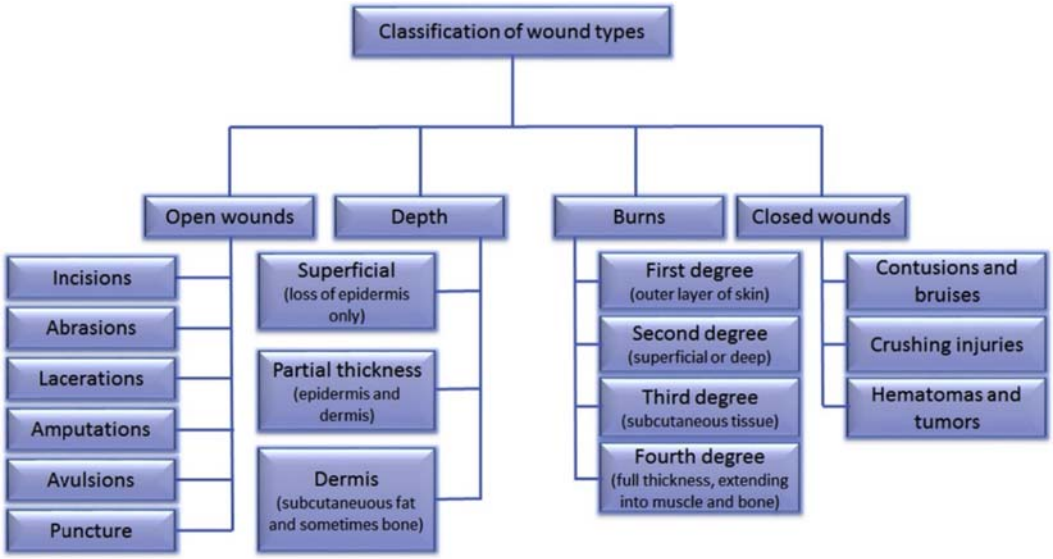

Figure 5.2
Classification of wounds based on four criteria namely open wounds, depth of the wound, burns, and closed wounds. Open wounds are those where the skin is broken and the underlying tissues are exposed to the external environment; depth refers to the depth of skin injury, where superficial wounds involve loss of epidermis only, partial thickness wounds involves loss of some part of dermis also along with epidermis and dermal wounds involve loss of both epidermis and dermis; burns, based on the extent of injury and severity can be classified into first up to fourth degree burns; closed wounds are those where the skin is intact and the underlying tissues are not exposed to the environment.

in 1992, the workshop on use of noninvasive methods in cosmetics testing organized by European Center for the Validation of Alternative Methods (ECVAM) in 1994 [52–56], pressing the need to regulate the policies and procedures of industrial animal testing and if possible, to ban them and find other alternatives. The voice is louder now than it was a decade ago. Due to increasing concerns on the animal welfare and constant pressure by newer and stronger organizations like PETA (People for the Ethical Treatment of Animals), urgency is created for alternative viable technologies. In summary, (i) people are concerned about using products which are tested on animals and many avoid such products; (ii) many countries (including EU, Israel, and India) have already banned industries from "testing their products" on animals; (iii) other countries also are considering deploying the ban (like the USA "The Humane Cosmetics Act (H.R.2858–114th Congress (2015–16))") [57]; and (iv) companies were classified as: brands that DO NOT test on animals, brands that DO test on Animals, brands whose animal testing status is unknown. People are encouraged not to buy the products of those companies that do product tests on animals [58,59]. These are the most important reasons

behind the need for artificial skins, not just an alternate, but biomimetic, fully functional human skin, which is a big challenge but not impossible.

5.3 Current skin substitutes

Skin substitutes are defined as a heterogeneous group of substances that help in either temporary or permanent closure of many types of wounds; wound coverage varies based on wound and product characteristics [60]. Skin substitutes help when standard surgical therapies like flap coverage or surgical debridement is not desirable, which is decided on a case-to-case basis, depending on the type and extent of burn, shallow or deep wounds, the degree of burn, and the area of the body that is injured. There is no perfect or ideal substitute for the original skin per se but something is better than nothing always. Not to mention, researchers around the world, in interdisciplinary teams, comprising of scientists in mechanical, chemical, biomedical engineering, biological, and medical sciences are progressing toward the greater goal of biomimicking the original skin, a fully functional skin substitute, with all its intricacies in it. We are not there yet, but good news is we are moving closer. There are a few important characteristics that a perfect skin substitute is expected to have [60,61] and they are summarized in Table 5.2.

Quantification of each of the properties listed in Table 5.2 is not straightforward and there is no catalog readily available to compare which is cceptable, which is not, and what is the best. It is up to the clinicians to decide how these tenets affect the product selection and availability, depending on the type of cases they are dealing with and the practice environment. There are many commercially available products, each having its own advantages and disadvantages, strengths and limitations, giving choices for the practitioners to choose. Comparison of some of these products is dealt with, in the later part of this section.

Table 5.2: Characteristics of an ideal skin substitute.

Able to resist infection
Able to prevent water loss or dehydration
Able to withstand the shear forces and wound hypoxia
Cost-efficient and affordable
Easy to prepare, store, and use
Wide availability and long shelf life
Lack of antigenicity
Flexible in thickness
Durable with long-term wound stability
Can be conformed to irregular wound surfaces
Provides permanent wound coverage
Recreates dermal and epidermal components

5.3.1 Classification of skin substitutes

Skin substitutes can be classified based on their durability, single or multilayer, the type of layer, and composite substitutes. Skin substitutes may be broadly classified as temporary or permanent and biological or synthetic, which is more practical. In response to the classification proposed by Balasubramani et al. [62], which is based on the plasticity and composition, Kumar et al. [63] had added upon to give a comprehensive framework for classification of skin substitutes, as given in Table 5.3.

There are other ways of classification too. Dorothy et al. [64] classifies the skin substitutes in to three classes namely acellular, cellular-allogenic, and cellular-autologous; Auger et al. [65] reports three classes namely epidermal substitutes, dermal substitutes, and bilayer substitutes. Some of the current skin substitutes available commercially are tabulated in Table 5.4. Many papers have reported the detailed information, application, clinical trial results of the listed skin substitutes [60,61,64–66].

5.3.2 Limitations of current skin substitutes

Skin substitutes help in the restoration and regeneration of skin to a greater extent but they are not without limitations. Mimicking the original skin in all aspects including functionality has not been done successfully to date, to the best of our knowledge. There

Table 5.3: Classification of skin substitutes.

Class	Subclasses	Examples
Class I: Temporary impervious dressing materials	(i) Single layer materials	– Biological dressing substitute (potato peel, amniotic membrane)
	(ii) Bilayered tissue engineered materials	– Synthetic dressing substitute (synthetic polymer sheet) (Tegaderm, Opsite), polymer foam or spray TransCyte
Class II: Single layer durable skin substitutes	(i) Epidermal substitutes	Cultured epithelial autograft (CEA), Apligraft
	(ii) Dermal substitutes	Bovine collagen sheet, e.g., Kollagen, porcine collagen sheet, bovine dermal matrix, e.g., Matriderm, human dermal matrix, e.g., Alloderm
Class III: Composite skin substitutes	(i) Skin graft	Allograft, xenograft
	(ii) Tissue engineered skin	Dermal regeneration template, e.g., Integra, Biobrane

Table 5.4: Engineered skin substitutes.

Product	Company	Description	Application
Alloderm	LifeCell Corporation, Branchburg, NJ	Acellular (freeze-dried) allogeneic dermis	Treat full- and partial-thickness wounds
Apligraf	Organogenesis Inc., Canton, MA	Allogeneic keratinocytes seeded over dermal scaffold (bovine collagen sponge) containing allogeneic fibroblasts	Treat venous and diabetic foot ulcers
Biobrane	UDL Laboratories Inc., Rockford, IL	Porcine collagen chemically bound to silicone/nylon membrane	Temporary covering of partial-thickness burns and wounds
CellSpray	Avita Medical. Perth, Australia	Preconfluent autologous keratinocytes delivered into a suspension for spray	Treat partial-thickness burns and chronic ulcers
Cymetra	LifeCell Corporation, Branchburg, NJ	Micronized particulate acellular cadaveric dermal matrix	Wound filler in plastic surgery
Dermagraft	Advanced Biohealing Inc., La Jolla, CA	Cryopreserved (viable cells) allogeneic fibroblast-derived dermal matrix	Treat full-thickness diabetic foot ulcers
Epicel	Genzyme Tissue Repair Corporation, Cambridge, MA	Confluent autologous keratinocytes from skin on petrolatum gauze backing	Treat full- and partial-thickness burns and chronic ulcers
Epidex	PharmaTec	Confluent autologous keratinocytes from hair follicles outer root sheath on silicone membrane	Treat full- and partial-thickness burns and chronic ulcers
EZ-Derm	Molnlycke Health Care, Sweden	Aldehyde-crosslinked porcine dermal collagen	Treat full- and partial-thickness wounds
FortaFlex	Organogenesis Inc., Canton, MA	Acellular porcine small intestine submucosa	Treat full- and partial-thickness burns, venous and diabetic ulcers
Hyalograft 3D	Fidia Advanced Biopolymers, Italy	Esterified hyaluronic acid matrix seeded with autologous fibroblasts	Treat full- and partial-thickness wounds
Hyalomatrix	Medline Industries Inc., Mundelien, IL	Bilayered, sterile and flexible layer made of a derivative of hyaluronic acid (HA) in fibrous form with an outer layer comprised of a semipermeable silicone membrane	Treat pressure ulcers, diabetic foot ulcers, and deep second-degree burns

Continued

Table 5.4: Engineered skin substitutes.—cont'd

Product	Company	Description	Application
ICX-RHY	Intercytex, Ltd, Manchester, UK	Suspension of human dermal fibroblasts (HDFs) in cell storage medium	Treat a variety of skin-related problems including epidermolysis bullosa and scar contractures
Integra	Integra Life Science Corporation, Plainsboro, NJ	Acellular temporary silicone epidermal substitute over dermal scaffold made of collagen and chondroitin-6 sulfate	Treat partial- or full-thickness burns
LaserSkin (Vivoderm)	Fidia Advanced Biopolymers, Italy	Subconfluent autologous keratinocytes seeded on esterified laser-perforated hyaluronic acid matrix	Treat full- and partial-thickness burns and chronic ulcers
MatriDerm	MedSkin Solutions Dr Suwelack AG, Germany	Acellular scaffold made with bovine collagen types I, III, V and elastin	Treat partial- or full-thickness burns
Myskin	CellTran Ltd, Sheffield, UK	Subconfluent autologous keratinocytes seeded on specially treated silicone sheet	Treat partial-thickness burns and chronic ulcers
OASIS	Smith & Nephew plc, London, UK	Acellular porcine small intestine submucosa	Treat full- and partial-thickness burns, venous and diabetic ulcers
OrCel	Ortec International, Inc., New York, NY	Allogeneic keratinocytes seeded over dermal scaffold (bovine collagen sponge) containing allogeneic fibroblasts	Treat skin graft donor sites and mitten-hand surgery for epidermolysis bullosa
Permacol	Tissue Science Laboratories, Andover, MA	Processed dermal xenograft	Temporary burn coverage and clean partial thickness wounds
Permaderm	Regenicin Inc., Little Falls, NJ	Autologous keratinocytes seeded onto dermal substitute made with autologous fibroblasts in bovine collagen matrix	Treat chronic wounds
Repliform		Acellular human dermal allograft	Urological plastic surgery applications
Suprathel	Institute of Textile and Process engineering, Denkendorf, Germany	Synthetic epidermal substitute made of DL-Lactide monolayer	Partial-thickness burns and skin graft donor sites
TissueTech	Fidia Advanced Biopolymers, Italy	Combination of Hyalograft 3D and LaserSkin	Treat partial- or full-thickness burns and chronic ulcers

Continued

Table 5.4: Engineered skin substitutes.—cont'd

Product	Company	Description	Application
VCT-01	Organogenesis Inc., Canton, MA	Keratinocytes seeded on top of dermal substitute made with fibroblasts secreting their own ECM	Treat partial thickness wounds

Data taken from J.T. Shores, A. Gabriel, S. Gupta, Skin substitutes and alternatives: a review, Advances in Skin & Wound Care 20 (9) (2007) 493–508; D.M. Supp, S.T. Boyce, Engineered skin substitutes: practices and potentials, Clinics in Dermatology 23 (4) (2005) 403–412; F.A. Auger, D. Lacroix, L. Germain, Skin substitutes and wound healing, Skin Pharmacology and Physiology 22 (2) (2009) 94–102.

are many reasons as to why we did not succeed, such as the technological limitations in creating a multilayered biomimicking structure, with each layer made of different cells and appendages. However, the most important challenges are vascularization and innervation. Boyce et al. [67] give an insightful discussion on the limitations of the skin grafts based on the wound healing physiology [68]. Lack of organogenesis is stated as one big shortcoming of the current models. Other disadvantages include mechanical fragility, susceptibility to microbial contamination, lesser rates of engraftment, time delay in healing, and of course the cost.

Most of the skin substitutes are predominantly acellular and even if they are cellular, they only use two types of cells, namely fibroblasts and keratinocytes, most of the cases, only either of them. This prevents the substitute from being fully functional like the native skin [64]. Another limitation was pigmentation [64], which can also be solved if the pigment secreting cells are made available in the substitutes. Vascularization and innervation are challenges, especially for drug and cosmetics testing, where fully functional skin is a requirement and not a choice. In wound healing applications, fully functional skin is not needed because the healthy skin can provide nourishment to the injured area where artificial skin is grafted.

5.4 Major approaches in tissue engineering of skin

Having said that about the limitations of the current skin substitutes, it is important to understand the approaches in using advanced skin regeneration strategies such as 3D bioprinting. There are two fundamental strategies for tissue engineering in general [69–74], namely (i) bottom-up approach and (ii) top-down approach.

The bottom-up approaches aim to fabricate a larger complex tissue by biological sintering of smaller building blocks, at micrometric scale, mimicking the natural tissue architecture. The building blocks may be cell aggregates, cell-laden hydrogel, polymer microbeads with a homogenous or heterogeneous composition. These smaller blocks are spatially arranged

in 3D to form a biomimetic complex architecture. Cell sheet technology, which aims at building up functional thick tissues without the use of biodegradable scaffolds and bioreactor by layering individual cell sheets of few microns thick and bottom-up assembly of cell-laden microgels are most common examples [75,76]. Some of the other technologies used in this approach are laser-assisted techniques like direct writing [77,78], laser-induced forward transfer [79,80], inkjet printers or drop-on-demand systems [81,82], and microdispensing techniques [83].

The top-down approaches aim at processing larger bulk materials into smaller complex structures. Top-down approaches generally involve the use of biodegradable scaffolds. The cells are seeded onto the scaffolds; growth factors are added to aid cell growth and proliferation; and scaffolds are usually preserved in a bioreactor that provides appropriate mechanical and hydrodynamic stimuli for maturation into a 3D tissue construct. Gel casting [84,85], sol-gel process, replication of polymer sponge [86,87], solvent casting and particulate leaching [88], phase separation technique [89], freeze drying, electrospinning [89–92], selective laser sintering (SLS), and stereolithography apparatus (SLA) [93–101] are some of the processes used in the fabrication of biodegradable scaffolds.

Both of the approaches have their own pros and cons. Bottom-up approach is said to have the potential to improve the vascularization in 3D constructs, by perfusing them with intraorgan vascular trees [3] and the feasibility of depositing multiple-cell types with desired spatial orientation in 3D. However, major drawbacks in this approach are the inability of certain cell types to secrete sufficient amounts of the extracellular matrix (ECM), migration of cells, and inability to form cell-cell junctions [72]. Top-down approach has many advantages such as the structural stability, ease of cell migration on the scaffold structure thus forming cell-cell junctions and better cell-cell interactions, and availability of a range of biodegradable, biocompatible materials for fabrication of scaffolding structure. The main disadvantage is the lack of understanding on the cell–scaffold interaction in detail. The mechanical and surface properties of the scaffold will affect the cell viability, growth, and proliferation of different types of cells. Also, if stem cells are seeded onto the scaffolds, it may differentiate into different types of cells based on the scaffold properties [102–106]. Though bottom-up approach is credited with the advantage of being scaffold-free, some of the approaches like extrusion bioprinting involve the fabrication of 3D structures with cell-laden hydrogels. For reasons like increasing the cell density, cells can be further added to the bioprinted constructs (printed from cell-laden hydrogels by extrusion bioprinting), where the properties of the bioprinted construct influence the behavior of cells that are added. Hence, understanding the cell-material interaction becomes critical in both the approaches. Fig. 5.3 diagrammatically explains both the approaches.

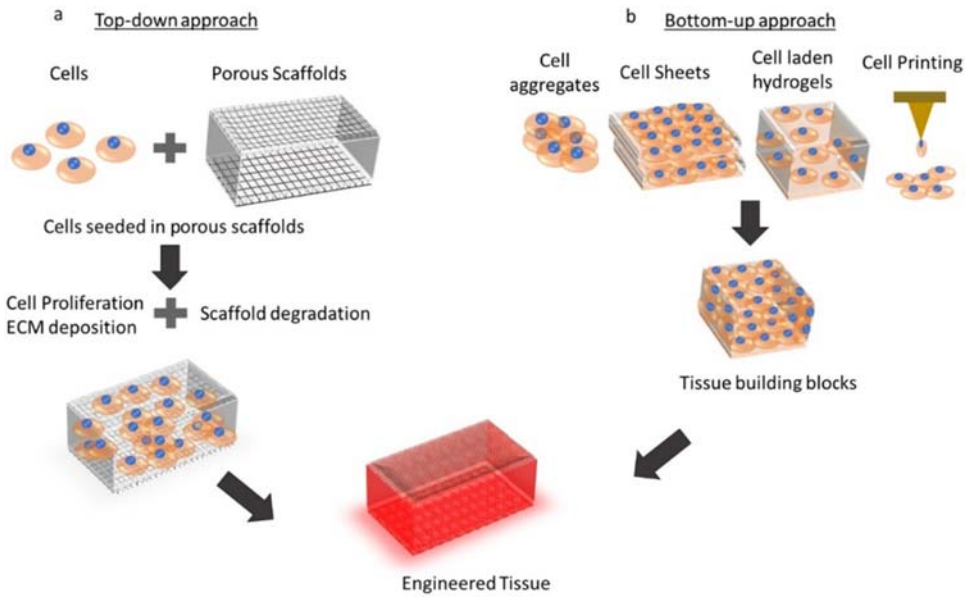

Figure 5.3

Top-down versus bottom-up approach in tissue engineering. (A) Top-down approach involves culturing of cells in a porous scaffold. Cells grow, proliferate, migrate on the scaffold structure, and create ECM, while the scaffolds undergo biodegradation and finally a matured tissue is obtained. (B) Bottom-up approach uses cell aggregates, cell sheets, or cell-laden hydrogels to produce modular blocks or tissue building blocks, which are then assembled together to form engineered tissues.

In order to successfully fabricate a biomimetic, fully functional skin substitute, it is important to have the advantages of both approaches, thus overcoming the limitations in using either of them separately. Integration of both the bottom-up and top-down approaches [107] is an excellent idea, yet to be experimented for skin tissue engineering. In bone tissue engineering, Ouyang et al. [108] used an integrated approach for engineering ligament analogs. They used bottom-up approach to fabricate a bone marrow stromal cells (bMSCs) sheet in the presence of ascorbic acid and top-down approach to fabricate a scaffold made of poly(L-lactide) (PLLA) and assembled them together using wrapping technique and it is reported to be a promising method for fabricating tissuelike and functional ligament analogs. Sargeant et al. [109] also reported an integrated approach for hybrid bone implants, where self-assembly of peptide amphiphile (PA) nanofibers (bottom-up approach) takes place within the pores of metallic Ti−6Al−4V foams (top-down approach). Though the integrated approach possesses many advantages, technical advancements are necessary to make the approach feasible for tissue engineering [107]. With 3D bioprinting, this integration is possible. As explained earlier, both bottom-up (inkjet printers/drop-on-demand systems) and top-down approaches (SLS, SLA) are

possible with 3D bioprinting technologies and hence, the integration is also not impossible. A hybrid system, consisting of various tenets of 3D bioprinting, can achieve this integration. Especially for 3D bioprinting of skin, bottom-up approach may be used for constructing each layer of the skin, the epidermis or dermis, and then these layers can be put together using top-down approaches.

5.5 3D bioprinting of skin

3D bioprinting of skin is a popular research area now and big players in the market are investing to further research in this area. L'Oreal USA, the largest subsidiary of the world's leading cosmetics company, signed a research collaboration agreement in May 2015 with a 3D bioprinting company, Organovo Holdings, Inc. to 3D bioprint skin models using the NoveGen Bioprinting platform of the latter, for testing their cosmetic products [110]. Procter & Gamble (P&G), another big player in consumer goods, launched a research project in Singapore (in May 2015), seeking research collaborations from academia on 3D bioprinting applications, especially for workable skin models [111]. Rokit, a market leader in 3D printing technology in Korea, announced in July 2015 that it is participating in a government funded project for the development of bioprinting technology and the first focus will be on bioprinting of human skin tissue [112]. Therefore, there is a huge demand for this technology and potential for immediate commercialization, if successfully developed. Broadly speaking, there are three important steps in 3D bioprinting process, namely, preprocessing (3D model generation, bioink preparation, etc.), 3D bioprinting, and postprocessing (using a bioreactor for tissue maturation). In general, the process flow given by Murphy et al. [113] holds good for most of the bioprinting processes (as given in Fig. 5.4).

5.5.1 Imaging, 3D modeling and design approach

The first and most important step in 3D bioprinting is the process of imaging. This involves scanning of the injured tissue or part of the body. Three scanning or medical imaging technologies X-ray, computed tomography, commonly called as CT scan, and magnetic resonance imaging or MRI are widely available and used in hospitals. Though the images from these scanning methods can be then converted to a 3D model using available software, in order to apply it for tissue or organ bioprinting, specialized techniques are required. For instance, a clinician requires to replace part of injured skin in the visible areas of a burn victim, may be on the face or hands. If the imaging system does not have the capability to scan and differentiate the color of the skin, then exact or at least a closer representation of the victim's skin color cannot be replicated in the printed skin and hence will not be aesthetically appealing. There are some technologies that are being developed to solve this problem.

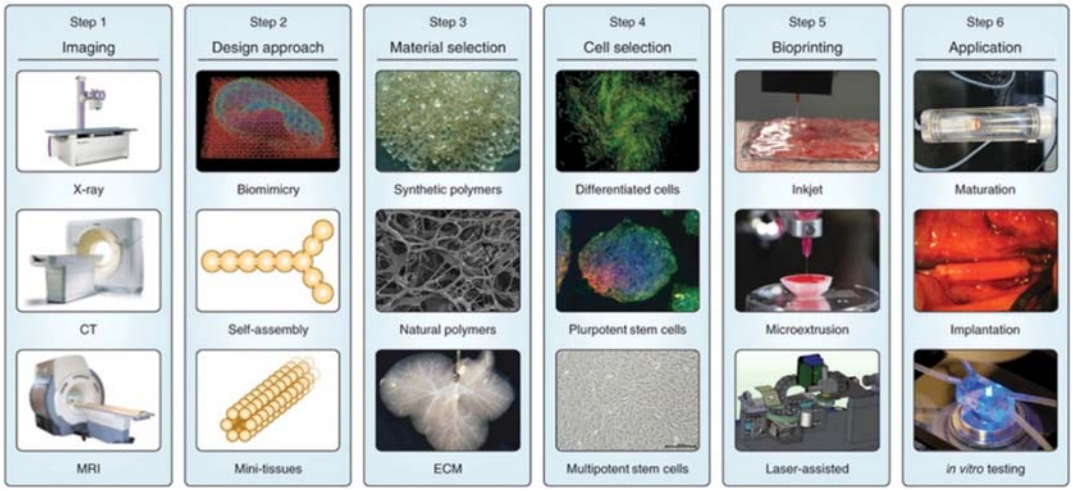

Figure 5.4

A typical process for bioprinting 3D tissues involving six steps namely imaging (imaging the injured site/tissue), design approach (image converted to 3D models; approach can be either printing the biomimetic structure along with cells, self-assembly of cells or constructing mini-tissues to be assembled later), material selection (based on the intended application, can be natural or synthetic polymers, ECM or combinations of them), cell selection (based on the intended application, can be stem cells or differentiated cells), bioprinting (using commercial or custom-made bioprinters) and application (postprocessing in a bioreactor for maturation, grafting, or implantation at the injury site). *Reprinted with permission from S.V. Murphy, A. Atala, 3D bioprinting of tissues and organs, Nature Biotechnology 32 (8) (2014) 773–785.*

Most clinicians, especially plastic surgeons, depend on either free-hand 2D sketches on picture printouts or computerized picture morphing for defining the goals of facial aesthetic procedures [114,115]. These sketches and morphs are then used for discussion with the patients to know their needs and wishes on the facial modification. Though creation of 3D facial shapes is possible with CT-scans [116,117], the radiation effect and the costs are impractical for aesthetic procedures. Other hardware-dependent techniques like laser or stereophotogrammetric scanners [118–120] are too expensive and much complex to handle. To overcome the complexity of hardware-dependent methods, many hardware-independent software techniques were proposed such as shape from shading [121], structure from motion [122,123], shape from silhouette [124,125], and statistical facial models [126], but all have limitations [127]. Oliveira-Santos et al. [127] proposed a hardware-independent web-based application, which used 2D-digital pictures to create 3D representation of a patient's face for planning the aesthetic procedures. The three important steps in this application are (i) 2D feature and contour points detection (from the 2D-digital image); (ii) 2D to 3D face reconstruction; and (iii) texture mapping. The greatest advantage of this application is that it is completely internet-based and no skilled

manpower is required to use, unlike the CT or MRI. The same method can be used for scanning the injured skin, to analyze the requirements for skin graft. Though the 3D reconstruction is not as precise as other advanced methods, its simplicity and ease of use gives this technique an edge over others and can be used in places where affordability is the main issue. Hani et al. [128] used various algorithms for useful wound data acquisition from laser scanned images. They used two methods for solid construction and volume computation namely mid-point projection and convex hull approximation, also called as Delaunay tetrahedralization. The main aim of this procedure is to determine critical wound data namely wound top area, true surface area, depth, and volume of the ulcer wounds in patients, in order to continuously monitor the healing progress throughout the treatment period. AutoCAD software is used to reconstruct the model, subject to the two methods earlier, from the input laser scan images; these reconstructed 3D models were then used to 3D print wax models of ulcer wounds; wound parameters were measured and compared against the surface scan measurements. This method can also be used to other wound causes like the burn injury, to assess the wound parameters, thus aiding the clinicians to get a customized skin graft for each injury site. Active dynamic thermography (ADT) or nondestructive thermography (NDT) is a noncontact imaging technique used widely in quality inspection of material defects in many industries including aerospace and automobile [129]. Recently, this technology has gained much attention in medical applications, for characterizing cutaneous lesions [130,131] and burns [132–135]. Nonhomogeneity of burn wounds, which refers to demarcation of different zones based on the severity of the injury, scaling from first to fourth degree can be done using ADT [132]. Many parameters including the healing time within 3 weeks are also assessed previously using this technique [133,135]. Pirindeze et al. [136] examined the optical resolution of ADT, to define the resolution limits of this system and to establish a set of parameters for thermal simulation using this system. In fact, they used human skin of varying thicknesses for this resolution study and have successfully demonstrated the ability of ADT's resolution to differentiate details of human skin as thin as 0.025″. ADT can be another potential technology for 3D imaging of burns or wounds in the preprocessing stage of 3D bioprinting. The imaging and 3D modeling systems are summarized in Table 5.5.

Color recognition is another important aspect, aiding to replicate the exact skin color of the patient in engineered skin grafts. Xiao et al. [137] developed a color reproduction system for processing of soft tissue prostheses accurately and automatically using advanced technologies like 3D bioprinting. A Minolta CM-2600d spectrophotometer was used for color measurement, along with SpectraMagic NX Color Data Software to decipher values in CIELAB values [138]. The study used Zcorp Z510 3D color printer. A protocol was developed using many mathematical models based on 240 training colors. Of all the mathematical models, the third-order polynomial regression based on least-square fitting provided the best model performance for color profile. Based on the color profile,

Table 5.5: Summary of imaging and 3D modeling systems.

Imaging/3D modeling methods	Pros	Cons	References
CT-scan	Accurate measurement of tissue depths	Radiation exposure, high cost	[117,118]
Stereophotogrammetric scanners	Fast capture speeds	Complex to handle, very expensive	[118–120]
Hardware-independent methods (shape from shading, structure from motion, shape from silhouette, statistical facial models)	Sophisticated hardware not required, relatively inexpensive	Used in research environments and not optimized for clinical use, limitations on speed and accuracy	[121–126]
Web-based application	Completely web-based, no hardware required	Less reproduction accuracy, suboptimal 3D reconstruction	[127]
Active dynamic thermography (ADT)	Accurate measurement of tissue/burn depths, high resolution	Necessity of using proper thermal models of living tissues, controlled experimental conditions required	[132–136]

the color reproduction system was established and parameters such as accuracy of color reproduction, performance of color repeatability and color gamut were evaluated using 14 known human skin shades. The printed prostheses demonstrated successful color reproduction of all these 14 skin shades. Simulation of color gamut for the proposed bioprinting system was done and except the extreme skin shades of dark and light, majority of skin colors are reproduced in the 3D bioprinted prostheses. The color gamut is shown in Fig. 5.5.

The 3D color image reproduction system developed by Xiao et al. [139] is represented in Fig. 5.6.

Jang et al. [140] proposed a spectrum-based color reproduction algorithm for makeup simulation of 3D facial avatar. All the color processing is based on RGB data as of now and its inability to represent a real make-up simulation on a 3D facial avatar encouraged them to work on a spectrum-based color reproduction process, which took into account the intrinsic characteristics of the objects and also the illuminant. The performance evaluation of the system was found acceptable. This method can be coupled along with other color reproduction techniques to recognize the skin color of the patient and also replicate the same color in 3D bioprinted skin grafts or prostheses. Wang et al. [141] developed a gradient-based multispectral method for face liveliness detection, which explored the reflectance of all the distinctive regions in a face and their spatial relationship, unlike the available methods, as a complement to the previous pixel-based methods. Application of

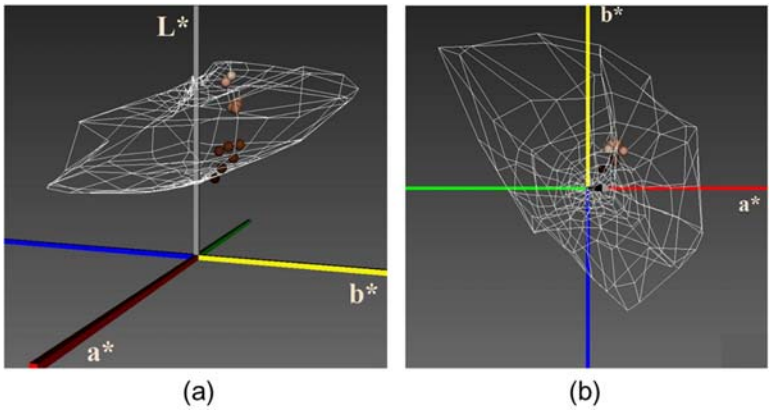

Figure 5.5
Color gamut of 3D printing system for 14 human skin colors: (A) top view and (B) side view. *Reprinted with permissions from K.D. Xiao, F. Zardawi, R. van Noort, J.M. Yates, Color reproduction for advanced manufacture of soft tissue prostheses, Journal of Dentistry 41 (2013) E15–E23.*

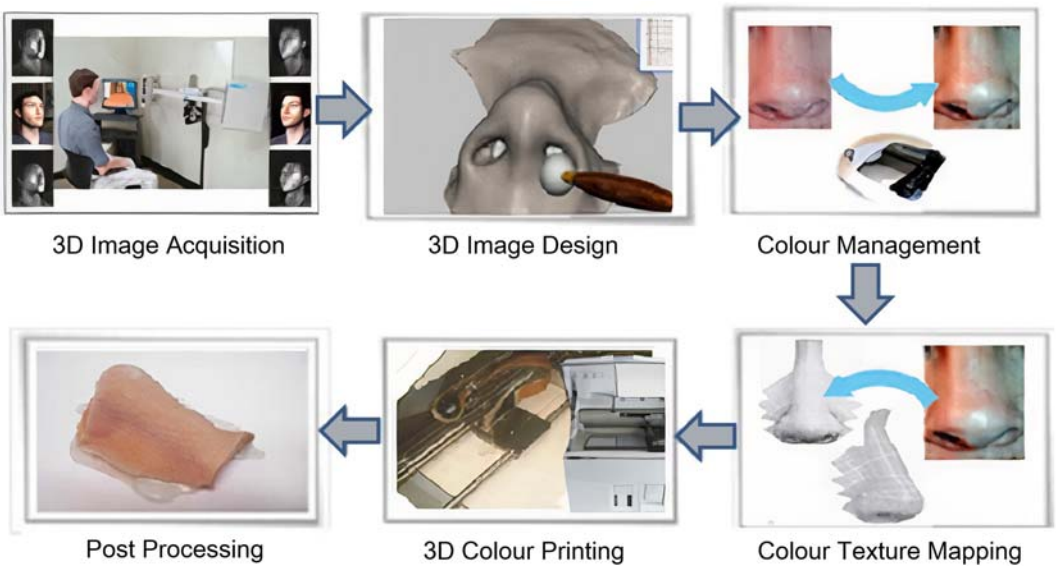

Figure 5.6
3D color image reproduction system for facial prostheses involving six steps namely 3D image acquisition (facial photos taken in different angles), 3D image design (processing of the acquired image and converting them to 3D models), color management (chosen based on the human skin shade), color texture mapping (texture matched to the original facial skin), 3D color printing, and postprocessing. *Reprinted with permission from K.D. Xiao, F. Zardawi, R. van Noort, J.M. Yates, Developing a 3D colour image reproduction system for additive manufacturing of facial prostheses, International Journal of Advanced Manufacturing Technology 70 (9–12) (2014) 2043–2049.*

this technology in 3D imaging, especially for medical applications like skin wound imaging, is yet to be explored.

The design approach should be based on the severity of the injury. If the wound or burn is a partial thickness injury, then epidermal layer skin graft should be fine. When the severity of the injury is of higher degree, multilayered structure is required. If the wound area to be treated is smaller, scaffold-free methods may be acceptable as against the larger wound area, where scaffold-based approach is necessary to facilitate easy cell migration, forming cell clusters and cell-cell junctions and finally tissue formation.

5.5.2 Materials

Material selection is one of the key steps in 3D bioprinting. Biomaterials are a group of materials which are biocompatible and biodegradable. Since the most common type of material used is polymer, they are also called as biopolymers. Based on their source of production, they can be broadly divided in to two, namely natural polymers and synthetic polymers.

Natural biopolymers are those that are naturally occurring, including (i) proteins (such as collagen, gelatin, albumin, thrombin, fibrinogen, etc.), and (ii) polysaccharides (such as chitosan, chitin, cellulose, etc.) [142]. Biocompatibility, biodegradability, hydrophilicity, biological characteristics, resemblance to the native ECM are strong reasons why natural polymers are preferred in tissue engineering applications.

Synthetic biopolymers are manmade polymers which include polylactic acid (PLA), polyglycolic acid (PGA), poly(ε-caprolactone) (PCL), poly(lactic-co-glycolic acid) (PLGA), poly(propylene fumarate), polyanhydrides, polycarbonates, polyorthoesters, polyurethanes, and polyphosphazenes. Synthetic biopolymers are known for their excellent mechanical properties, which are important for a scaffold material. Key advantage is the ability to tailor the mechanical properties and degradation kinetics, by altering the polymer structure, to suit various biomedical applications, for example, bone graft or skin graft [143].

Both of the above types suffer from certain limitations. Natural biopolymers, in spite of having the greatest advantage of mimicking the native tissue ECM, suffer from poor mechanical properties. On the other hand, synthetic biopolymers have the advantage of better mechanical properties but very different from the natural ECM. And hence, researchers use composite polymers, which has both natural and synthetic biopolymer constituents, thus combining the advantages of both and overcoming the limitations. This is extremely important with 3D bioprinting because, in addition to the basic requirements of a biopolymer, there is another important factor to be considered while preparing the bioink, which is “printability.” The requirements of an optimal biomaterial [142] are

biocompatibility with tissues; biodegradability at the ideal rate corresponding to the rate of new tissue formation; nontoxicity; nonimmunogenicity; optimal mechanical properties; adequate porosity and morphology for transporting of cells, gases, metabolites, nutrients, and signal molecules both within the biomaterial and between the biomaterial and the local environment; and printability.

The most common natural biopolymers used in skin tissue engineering are collagen, gelatin, chitosan, and silk fibroin; the synthetic biopolymers being PCL, PLA, PLGA, and PLLA. The composite biopolymers are formed by combining one from each group. Electrospinning is one of the most successful technologies to produce nanofibers of the above biopolymers, which serve as the scaffold material for skin tissue regeneration. A list of such electrospun nanofibrous scaffolds is tabulated in Table 5.6 (data taken from Ref. [144]). This information is included in this chapter as most of the biopolymers or composites that are electrospun can also be 3D bioprinted using inkjet and drop-on-demand systems. They are grouped into four main types, viz. natural, synthetic, natural composite (two or more natural biopolymers), and composites (at least one natural and one synthetic biopolymer).

As mentioned earlier, in addition to the satisfaction of basic requirements of a biomaterial, the bioink should be printable. Ideal properties of bioprinting hydrogels are tabulated in Table 5.7 [191]. Malda et al. [192] summarizes the properties of bioink or hydrogels, under two headings: (i) rheology, which includes viscosity, shear thinning, and yield stress and (ii) cross-linking mechanisms of hydrogels namely physical, ionic, chemical, stereocomplex, or thermal cross-linking. Nakamura et al. [193] discussed the roles of hydrogels for biofabrication, especially with inkjet and 3D bioprinting technologies. Murphy et al. [194] evaluated the properties of 12 different hydrogels, which are commercially available and commonly used in research. These evaluated properties are relevant to bioprinting of skin such as gelation time, swelling or contraction, stability, biocompatibility, and printability. The 12 hydrogels that are evaluated are collagen type I, collagen/fibrin, fibrin, Extracel Hydrogel, Extracel UV, tyramine substituted hyaluronic acid (TS-NaHy)-Corgel, methylcellulose-hyaluronan (MC-HA), chitosan, chitosan/collagen, alginate, alginate/gelatin, and polyethylene glycol diacrylate (PEGDA). The results revealed that Extracel-UV, the photocross-linkable HA-based hydrogel was the best candidate for bioprinting, possessing the desirable properties for bioprinting application. The regulatory, commercial, and financial aspects of each of the hydrogels were also discussed briefly. Wang et al. [191] reported a state-of-the-art review of smart hydrogels for 3D bioprinting; “smart” referring to the responsiveness of the hydrogel to various external stimuli such as pH, temperature, light, electric field, and magnetic field. The potential of combining smart hydrogels with 3D bioprinting, their challenges and future prospects were also reviewed.

Table 5.6: Electrospun nanofibrous scaffolds for skin tissue engineering.

Polymer	Type	Special feature	References
Collagen	Natural	Reduced wound contraction compared to freeze-dried scaffolds	[145]
		Higher cell proliferation in aligned fibers compared to random scaffold	[146]
Gelatin	Natural	Well-stratified dermal and epidermal layers including a continuous basal keratinocyte layer	[147]
		Cross-linking gelatin nanofibers with genipin improves cell proliferation but cell viability is reduced	[148]
		Promotes cell adhesion and spreading of type I collagen, suitable for wound dressing	[149,150]
Silk fibroin	Natural	Oxygen plasma-treated SF nanofibers showed higher cellular activities than the untreated ones	[151,152]
Chitosan	Natural	Sonication of chitosan nanofibers resulted in higher porosity and increased cell proliferation	[153]
Fibrinogen	Natural	Suitable for wound repair or hemostatic products	[154]
		Good mechanical properties, suitable for wound dressing	[155]
		Significantly increased peak stress and modulus values for the fibrinogen cross-linked with 1-ethyl-3-(3-dimethylaminopropyl) carbodiimide hydrochloride (EDC) and fibrinogen-genipin cross-linked scaffolds	[156]
Collagen/Silk fibroin	Natural composite	Better cellular responses in hybrid nanofibrous scaffolds than that of blend nanofibrous scaffolds	[157]
Chitosan/Silk fibroin	Natural composite	Addition of silk fibroin enhanced the mechanical properties of nanofibers	[158]

Continued

Table 5.6: Electrospun nanofibrous scaffolds for skin tissue engineering.—cont'd

Polymer	Type	Special feature	References
Chitosan/Collagen	Natural composite	Showed keratinocyte migration and wound reepithelization—a prerequisite for healing and regeneration	[159]
Chitosan/Chitin nanocrystals	Natural composite	Addition of chitin nanocrystals as well as cross-linking had a positive impact on the mechanical properties	[160]
PCL	Synthetic	Enhanced cell proliferation and wound healing due to the surface degradation of the polymer under physiological conditions and the formation of functional groups like hydroxyl and carboxyl groups that promoted cell proliferation	[161]
		A micromachined human skin pattern mold was used as a collector in an electrospinning setup to replicate the pattern onto the surface of the electrospun mat; exhibited guidance of cells along the skin pattern without significant deterioration of pattern geometry	[162]
PLLA	Synthetic	Nanofiber scaffolds enhanced epidermal skin cell migration across the wound when compared to a control group without scaffold. Aligned nanofibers promoted the infiltration of endothelial cells into the scaffolds	[163]
PDLLA-LL	Synthetic	Hybrid microfibers possessed a unique porous high surface area mimicking native extracellular matrix (ECM)	[164]
PLGA	Synthetic	Cells acquired a well-spread morphology, and collagen type III gene expression was significantly upregulated	[165]
		Good cellular penetration, with no adverse inflammatory response outside the scaffold	[166]

Continued

Table 5.6: Electrospun nanofibrous scaffolds for skin tissue engineering.—cont'd

Polymer	Type	Special feature	References
		margin and with no capsule formation around the periphery	
		The cell attachment and spreading were several times higher in the nano-/microfiber composite scaffolds than in the microfibrous scaffolds without nanofibers	[167]
		Highly porous scaffold provided mechanical support for cells to maintain uniform distribution; better cell migration and collagen secretion	[168]
PCL/Chitosan	Composite	The presence of chitosan aided a significant improvement in the hydrophilicity of the scaffold, bioactivity, and protein adsorption	[169]
		Amino-remained chitosan-graft-poly (ε-caprolactone) (2/8) mats with a moderate surface zeta-potential ($\zeta = 3$ mV) were the best in promoting the cell attachment and proliferation	[170]
		Novel polysaccharide-coated PCL fiber mats remarkably combine the mechanical resistance typical of PCL with the surface properties of chitosan	[171]
PCL/Collagen	Composite	Anisotropic nanofibers significantly triggered integrin β1 signaling pathway	[172]
		Collagen was immobilized on aminolysed PCL nanofibers using glutaraldehyde as cross-linker, enhancing cell proliferation	[173]
		PCL and collagen nanofiber matrices support the attachment and proliferation of human dermal fibroblasts; suitable for dermal substitutes	[174]

Continued

Table 5.6: Electrospun nanofibrous scaffolds for skin tissue engineering.—cont'd

Polymer	Type	Special feature	References
		Coaxial electrospinning of collagen-PCL showed superior cell proliferation than roughly collagen-coated PCL	[175]
		Acellular scaffold strength increased with increasing PCL content but the mechanical strength of the engineered skin was not enhanced by the use of collagen-PCL blended scaffolds, after a minimum amount of PCL (10%)	[176]
		Collagen gel coated PCL nanofibrous scaffolds showed better cell responses than PCL/collagen nanofibrous matrices	[177]
PCL/Gelatin	Composite	Coaxially electrospun PCL/gelatin scaffolds exhibited increased cellular adhesion and metabolism versus PCL alone or gelatin-PCL blended fiber scaffold	[178]
		Acetic acid-doped TFE solvent system was used to prevent phase separation during electrospinning	[179]
PCL/Gelatin/Collagen	Composite	Collagen type I-modified PCL/gelatin scaffold was successful in maintaining characteristic shape of fibroblasts, besides good cell proliferation than the PCL/gelatin scaffold	[180]
PLA/Chitosan	Composite	Core-shell structure nanofibers of PLA/chitosan were easier to fabricate than double-needle electrospinning	[181]
		Aligned PLA/chitosan fibrous scaffold was fabricated using a novel collector made of parallel blades; PLA/chitosan nanofiber had enhanced degradation than the pure PLA fibers	[182]
PLA/Gelatin	Composite	Modified PLA/gelatin (7/3) scaffold was more suitable for fibroblasts attachment and	[183]

Continued

Table 5.6: Electrospun nanofibrous scaffolds for skin tissue engineering.—cont'd

Polymer	Type	Special feature	References
		viability than the PLA or gelatin nanofiber alone	
PDLLA/Chitosan	Composite	Dual-layer chitosan/PDLLA structure resulted in aligned migration and directional penetration of skin fibroblasts into 3D domain	[184]
PLLACL/Collagen	Composite	PLLACL/collagen scaffolds showed better cell differentiation of MSCs than PLLACL scaffolds	[185]
PLLACL/Gelatin	Composite	Fibroblasts proliferation, morphology, CMFDA dye expression, and secretion of collagen were significantly increased in plasma-treated PLACL/gelatin scaffolds compared to PLACL nanofibrous scaffolds	[186]
PLGA/Chitosan	Composite	Hybrid PLGA/chitosan and core/shell structured PLGA/chitosan membranes showed better cytocompatibility than the PLGA membrane in adhesion, viability assays, as well as morphology observation	[187]
PLGA/Collagen	Composite	Highly porous fibrous mats of PLGA and type I collagen were produced by blend electrospinning; inoculation of collagen enhanced the cell attachment, proliferation, and extracellular matrix secretion, which were found to be dependent on the amount of collagen in the composite scaffold	[188]
		PLGA/collagen nanofibrous membranes were functionally active in responses in human fibroblasts, and were very effective as wound-healing accelerators in early stage wound healing	[189]

Continued

Table 5.6: Electrospun nanofibrous scaffolds for skin tissue engineering.—cont'd

Polymer	Type	Special feature	References
PCL/PLGA/Chitosan/Gelatin	Composite	The upper layer of PCL/PLGA nanofibers provided mechanical support and reduced degradation rate of the hydrogel layer. The lower layer of porous chitosan/gelatin hydrogel could retain moisture.	[190]

Data from M. Norouzi, S.M. Boroujeni, N. Omidvarkordshouli, M. Soleimani, Advances in skin regeneration: application of electrospun scaffolds, Advanced Healthcare Materials 4 (8) (2015) 1114–1133.

Table 5.7: Ideal bioprinting hydrogel properties [191].

Printability	Viscosity Shear-thinning property Response and transition time Sol-gel transition stimulus
Biocompatibility	Degradability Cell binding motifs Nontoxic Nonimmunogenic
Mechanical properties	Stiffness Elasticity Strength
Shape and structure	Pore size Micro/nano structure

Material selection is a key for any bioprinting process. For 3D bioprinting of skin, there is wide range of natural, synthetic, and composite biopolymers available, which can be selected based on the type of printing process used and bioink formulation can be done with or without cells, based on the tissue engineering approach that is aimed at. With the development of smart hydrogels, 3D bioprinting of functional skin will no more be just a dream, but a realistic goal that is achievable in the near future.

5.5.3 Cell selection

One of the most important factors that decide the success of tissue engineering is the choice of suitable cells, assuring persistence and function of the regenerated tissue for the patient's life time [195]. The most common type of cells used extensively in current skin substitutes is keratinocytes, which form the outer epidermal layer. There are many

advantages in using keratinocytes in skin tissue engineering; they can be cultured, maintained, and propagated in the laboratory with ease [196,197] and their resistance to senescence is so great that they can be passaged for many hundreds of generations [198]. However, there are overwhelming limitations that prevent the sole use of keratinocytes to engineer a fully functional skin substitute. The first major drawback is the time required to culture these cells. It takes about three weeks for a 2 cm^2 biopsy to expand on a surface, sufficient enough to cover the whole body (73 m^2), which may take even longer for elderly patients. Scarring is another problem, referred to as hypertrophic scarring. The presence and degree of scarring is directly proportional to the healing time, which is obviously longer when keratinocytes are used [199]. Fibroblasts come next to keratinocytes, present in the dermal layer of natural skin and obviously used in the dermal skin substitutes. They represent a diverse population of cells, with the ability to differentiate along a lineage from highly proliferative progenitor fibroblasts. They are ubiquitous, static in nature, and provide support and maintenance to the tissues. The inherent problem of long-term fragility of keratinocytes can be overcome by having a layer of dermal fibroblasts underneath it. It is reported that there are specialized subsets of fibroblasts and each respond to the different phases of wound healing and skin regeneration. And also, the fact that fibroblasts from different sites of the body possess different functional properties should be considered before selection for tissue engineering, as it may affect their suitability for dermal substitutes [12]. The bilayer or composite skin substitutes, normally referred to as full-thickness skin grafts, consist of both keratinocytes and fibroblasts, representing the epidermal and dermal layers, respectively. The production process of such a composite is complex, involving many phases [200,201] and there is no contention on the optimal product on long term [202,203]. Though the epidermal keratinocyte and dermal fibroblast composite is better than being individually used, there are so many other cells and appendages that are required to be present in order to make it fully functional per se. Irregular pigmentation, for example, is a limitation, which can be overcome by coculturing melanocytes along with keratinocytes, which ensures normal pigmentation by secreting melanin [204]. Vascularization is another problem, which can be managed to some extent by incorporating endothelial cells to facilitate angiogenesis. Genetically modified keratinocytes, which overexpress vascular endothelial growth factor (VEGF), were reported to promote vascularization [205]. Still, integration of pilosebaceous units, with hair follicles and sebaceous glands to the skin substitutes, remains an unsolved challenge [199].

Most of the current tissue engineering strategies depend on a sample of autologous cells from the damaged host tissue or organ. It becomes increasingly difficult to obtain the cells from the damaged host, especially when the injury or damage is extensive. Alternative cell sources become a necessity in such cases, which is debated in the field of regenerative medicine. In order for the tissues and organs to maintain a balance between cell loss and

replacement, the tissues must possess cells that are capable of self-renewal and differentiation and hence, stem cells are looked upon as a promising source for future skin regeneration and skin tissue engineering [206]. Many types of stem cells that inhabit the skin have been identified and located which includes epidermal stem cells (interfollicular stem cells and bulge stem cells), that are widely used recently, dermal stem cells [207], sebaceous stem cells, melanocyte stem cells, hair follicle stem cells [208,209], sweat gland stem cells, endothelial stem cells, mesenchymal stem cells (MSCs), hematopoietic stem cells (HSCs), and neural stem cells [210,211]. When using stem cells for bioprinting or tissue engineering in general, the relationship between regeneration and development should be understood well, where undifferentiated stem cells are used as the source from which differentiated cell types arise, to create or regenerate functional tissues [206]. Also, there are many ethical and technical problems, controversies surrounding stem cells to be overcome before we can attempt bioprinting stem cells, utilizing their full potential [212–214].

Having reviewed the types of cells that can be used for skin substitutes, 3D bioprinting has the luxury of using any kind of cells, or combination of cells, suspended in the same solution or bioink or different cells in different bioinks, that can be fed through different nozzles in a multinozzle bioprinting system. Based on the type of cells chosen, the bioink composition varies in order to satisfy the basic requirements of a printable bioink.

5.5.4 3D bioprinting processes

Bioprinting can be defined as a "computer-aided transfer processes for patterning and assembling living and nonliving materials with a prescribed layer-by-layer stacking organization in order to produce bio-engineered structures serving in regenerative medicine and other biological studies" [215]. The bioprinting techniques can be classified under three main topics namely, laser-based bioprinting or laser-induced forward transfer [77,216–221], inkjet bioprinting/droplet-based bioprinting [222–227], and robotic dispensing/extrusion/deposition bioprinting [228–235] (refer to Fig. 5.7).

Laser-induced forward transfer utilizes laser energy to deposit cell-encapsulated droplets of required volume, in any defined 3D spatial arrangement. The main components of such a system are the donor slide, the collector slide, and laser generation system. The donor slide has a conductive coating for laser energy absorption and a layer of the cell suspension or bioink that is to be bioprinted. The collector slide acts as the substrate, which can be biopaper or scaffolds or culture plates. When laser pulses are focused on the donor slide, the conducting layer absorbs the laser energy, creates a high gas pressure on absorption of laser energy and as a result, droplets of cell suspension are propelled toward the collector slide. Required spatial arrangement can be obtained by controlling the path of the laser beam. Inkjet printing is the second bioprinting technique. They are also called

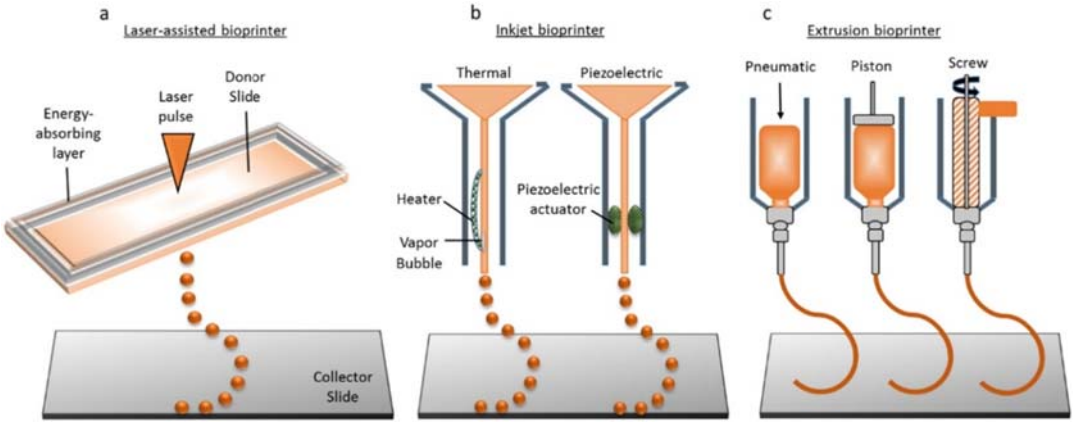

Figure 5.7

Three main bioprinting technologies (A) Laser-based bioprinting focuses laser pulses onto the donor slide, thus creating high pressure to propel droplets of cell-laden hydrogel onto the collector slide. (B) Inkjet printing ejects droplets of biopolymer or cell-laden hydrogels through a nozzle by either thermal energy application (electrically heating to produce vapor bubbles that forces droplets to come out through the nozzle) or piezoelectric actuator (actuation of piezoelectric crystals by applying electrical energy at high frequencies). (C) Extrusion or robotic dispensing bioprinters extrude biopolymers or cell-laden hydrogels through the nozzle by applying air pressure (pneumatic) or mechanical systems (piston or screw).

drop-on-demand systems as they propel drops of cell suspension or bioink on to the substrate. Based on the mechanism of how droplets are generated, they are classified as thermal and piezoelectric-based inkjet printing. In thermal inkjet printing, a heater or a heating filament produces a vapor bubble in the nozzle, which propels the droplet out of the nozzle onto the substrate. In piezoelectric-based systems, the changes in the volume of piezoelectric crystal, on application of electric pulses, expel the droplet through the nozzle. Third comes the robotic dispensing systems. In this type, the bioink is extruded out of the nozzle by application of mechanical force. The mechanical force can be pneumatic, piston-based, or screw type. An extensive review of these technologies has been done by Murphy et al. [113], Dababneh et al. [215], Malda et al. [192] and Ozbolat et al. [236]. Arslan-Yildiz et al. [237] had reviewed the recent advances in bioprinting technologies, current markets, approaches, and biomedical applications of bioprinting.

5.5.4.1 Laser-based bioprinting (LBB) of skin tissue

Current 2D cell culture and 2D tissue engineering do not well mimic the native tissue as the original natural tissue is in a 3D environment. Studies have already proved that cells behave differently in 2D and 3D environment and it is better with in 3D space as it mimics the complex 3D-microenvironment architecture in vivo [238–240]. Laser cell printing or laser-based bioprinting (LBB) or laser induced forward transfer is one

technology which can precisely place cells in 3D spatial arrangement. Advantages of LBB include capability of positioning small volumes of cell suspensions or bioink, down to a few hundred femtoliters, with high resolution [216,241] and ability to print high density cell suspensions [242] or hydrogel precursors or bioink with any desired viscosity, which is the main limitation with inkjet bioprinters, which can only handle lower viscosity ranges. Schiele et al. [243] comprehensively reviewed the laser-based direct write cell printing technologies, giving an overview of different realizations and denominations of this technique. Research group from Hannover Medical School, Germany, along with Laser Zentrum Hannover, had used this technique to print skin tissue [244,245].

Koch et al. [244] used LBB to arrange the vital cells of skin tissue, namely the keratinocytes and fibroblasts embedded in collagen, in a 3D arrangement, representing multicellular skin grafts that were analogous to the native archetype. The bioink used in this study was made of (a) murine cell line NIH-3T3 fibroblasts, representing the dermal layer, (b) keratinocytes cell line HaCaT from adult human skin, representing the epidermal layer, (c) suspended in a hydrogel, collagen, which is the main component of ECM in native skin, and (d) a sheet of Matriderm, which is a commercial dermal skin substitute, to serve as a scaffold or substrate. The main focus of this study was the arrangement of these skin cells under a set of different conditions or parameters, namely 3D cell pattern, cell density, and matrix material, in a way that the microenvironment was comparable to the native skin tissue and to study the tissue formation process. The experimental set-up [246] is shown in Fig. 5.8. It consists of two coplanar glass slides. The upper one is coated underneath with an energy absorbing layer or laser absorbing layer, to be specific; a 60-nm thin gold layer coating is used in this study and a layer of the cell suspension that is to be transferred or bioprinted, which is keratinocytes or fibroblasts suspended in collagen hydrogel. The lower glass slide acts as the substrate; scaffold or hydrogel layer can be positioned on this plate on which the cells will be printed. For better understanding, the upper glass slide is the “donor-slide” and the lower glass slide is the “collector-slide.” The cell suspension is printed onto the collector slide from the donor slide using laser induced forward transfer. Laser pulses are focused on the donor slide, which causes localized evaporation in the gold layer beneath, the absorption of laser energy generates a high gas pressure, thereby propelling the subjacent cell suspension toward the lower glass slide, which is the collector slide. The droplet size of the cell suspension transferred depends on a number of parameters namely the laser pulse energy, the gap between the upper and lower glass slide, the laser spot size, thickness of the laser absorbing layer, and the thickness of the cell suspension layer.

A bilayer skin construct, consisting of keratinocytes dominated outer epidermal layer and fibroblasts dominated the inner dermal layer, was printed; 20 cell-collagen sublayers of NIH-3T3 fibroblasts being printed first on a sheet of Matriderm, followed by 20 cell-collagen sublayers of HaCaT keratinocytes over it.

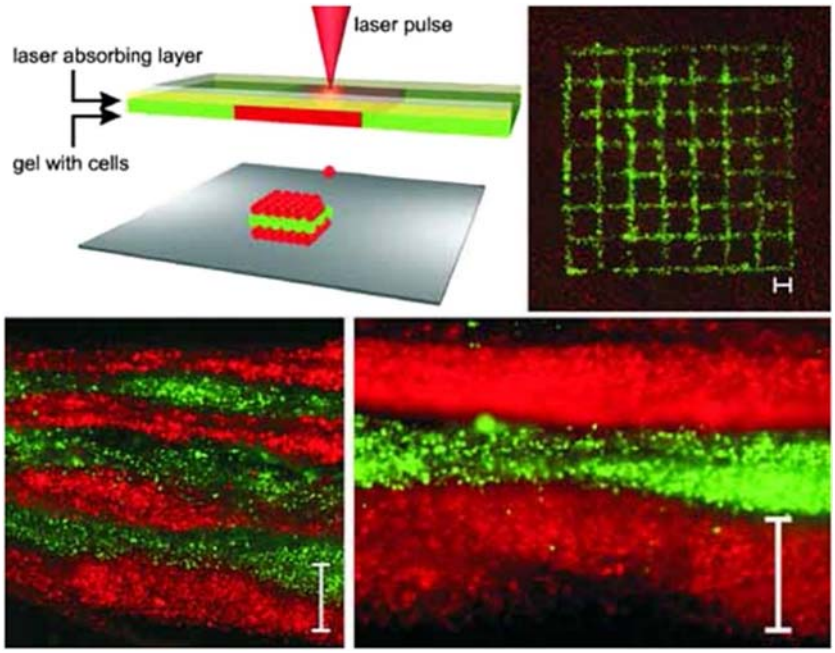

Figure 5.8

Top left: Sketch of the laser printing setup. The cell-hydrogel compound is propelled forward as a jet by the pressure of a laser-induced vapor bubble. Layer-by-layer, a 3D cell pattern is generated. Top right: A printed grid structure (top view) of fibroblasts (green) and keratinocytes (red) demonstrates micropatterning capabilities of the laser printing technique. Bottom: Seven alternating color-layers of red and green keratinocytes (left; detail right). Each color-layer consists of four printed sublayers. Scale bars are 500 μm. *Reprinted with permission from L. Koch, A. Deiwick, S. Schlie, S. Michael, M. Gruene, V. Coger, D. Zychlinski, A. Schambach, K. Reimers, P.M. Vogt, B. Chichkov, Skin tissue generation by laser cell printing, Biotechnology and Bioengineering 109 (7) (2012) 1855–1863.*

Important factors that indicate a successful skin tissue construct were studied on the printed bilayer construct including immunohistochemistry, analysis of gap junction coupling, postprinting cell proliferation, development of a basement membrane between epidermis and dermis like the natural skin, analysis of adherence and gap junctions (which is important for mechanical connection between cell-cell and cell-ECM). The cells remained in the printed pattern, i.e., as bilayer, and did not intermix even after 10 days in culture; proliferation post-printing was good; development of the basal lamina served as a sign of skin tissue formation; better adherence of the cells to neighboring cells and the ECM shown by the extensive formation of adherent junctions all went to say that this was a unique successful first demonstration of 3D arrangement of vital cells using LBB method as multicellular grafts analogous to the native skin.

Michael et al. [245], from the same group, used the same technique to print the bilayer skin construct and tested it in vivo in nude mice. In this work, same kind of cells used in

the previous study namely NIH3T3 fibroblasts and HaCaT keratinocytes suspended in collagen were used. A bilayer skin construct, having 20 layers of fibroblast-containing collagen and 20 layers of keratinocyte-containing collagen were printed onto a sheet of Matriderm (2.3 × 2.3 cm), followed by incubation under submerged conditions overnight in an incubator. The next day (defined as Day 0), nine round pieces (diameter 6.0 mm) were removed from the large construct with a biopsy punch, three of which were implanted into the skin fold chambers in vivo (one per mouse, four independent printing processes, tested in 12 animals in total). The remaining six pieces of each printing process served as in vitro controls. Two of them were directly fixed on Day 0 to depict the situation at the beginning of the experiments, whereas the remaining four pieces were raised to the air-liquid-interface. In vitro controls were then fixed on Days 5 and 11 (duplicates per time point) and in vivo specimen on Day 11.

The results were promising. The printed skin constructs placed into the full-thickness wounds in the dorsal skin chamber of nude mice, in vivo, were fully connected to the surrounding tissue when explanted after 11 days. Multilayered epidermis was formed by the printed keratinocytes, with initial differentiation and stratum corneum. Adherent junctions, which are the main indicators of tissue formation, detected by the E-cadherin, could be found in the epidermis, both in vivo and in vitro. The printed fibroblasts produced collagen, which is their main function, in both in vivo and in vitro conditions, staying partly on the top of the underlying matrix and partly migrated in to the matrix. Above all, some blood vessels were found growing from the wound bed and the wound edges toward the printed cells.

5.5.4.2 Robotic dispensing based 3D-bioprinter

Lee et al. [247] reported a novel method to construct stratified skin construct in 3D, layer by layer, using robotic cell dispensing technology. The schematic of the device is given in Fig. 5.9. The printer mainly consists of an array of four microvalves as dispensers and a three-axis Cartesian robotic stage. The dispensers, each with a pneumatically driven control mechanism, were mounted to the horizontal (x-y) robotic stage, which controlled the timing and location of dispensing of printable materials including hydrogel precursors and cell suspensions. The entire device was housed in a laminar flow hood. The MATLAB computing environment was used to generate the robot control codes dictating the dispensing spatial coordinates. Primary adult human dermal FBs and primary adult human epidermal KCs were used along with type I collagen as hydrogel precursor for a scaffold material. A total of 10 collagen layers were sequentially printed on a planar square in a 60 mm tissue culture dish. FB and KC layers were located in second and eighth layer of the collagen layers, counted from bottom, respectively. The five collagen layers sandwiched between the FB and KC layers demonstrate the ability to print spatially distinctive cell layers. Post-printing, the printed tissue construct was cultured in 37°C, 5%

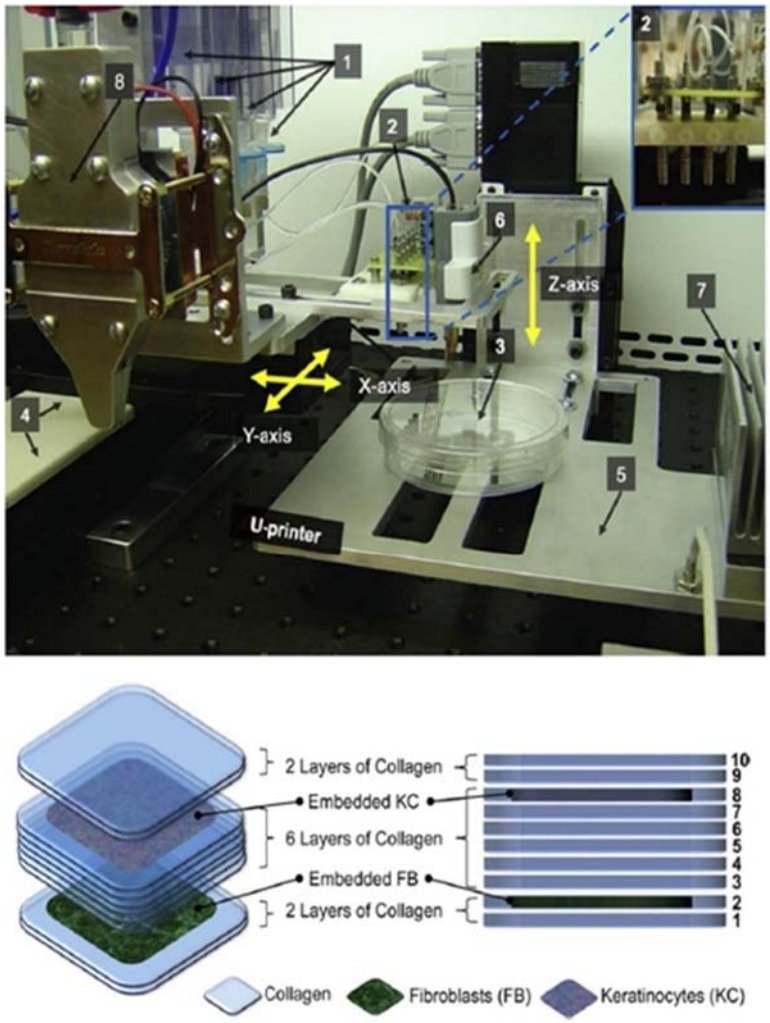

Figure 5.9

(Top) Picture of the modular tissue printing platform shown with: (1) four syringes as "cartridges" to load cell suspensions and hydrogel precursors; (2) an array of 4-channel dispensers; (3) target substrate; (4) horizontal stage; (5) vertical stage; (6) range finder; (7) vertical stage heater/cooler; (8) optional independent heating/cooling unit for the dispenser. Inset: close-up view of the 4-channel microdispensers. (Bottom) Schematic of layer-by-layer printing of the multilayered skin cells and collagen. *Reprinted with permission from W. Lee, J.C. Debasitis, V.K. Lee, J.H. Lee, K. Fischer, K. Edminster, J.K. Park, S.S. Yoo, Multi-layered culture of human skin fibroblasts and keratinocytes through three-dimensional freeform fabrication, Biomaterials 30 (8) (2009) 1587–1595.*

CO_2 in KC media. There are two important and unique advantages of this device. The first is the new cross-linking mechanism introduced and the second is printing on nonplanar surfaces. Instead of the traditional method of dipping the printed construct into the cross-

linking solution bath, here, the nebulized mists of cross-linking agents were coated on the surface before and after printing each layer. This new mechanism engenders the second advantage of printing on nonplanar surfaces, which was successfully demonstrated by printing on 3D nonplanar polydimethylsiloxane (PDMS) substrates. This characteristic of this method makes it possible to print the tissues directly on to the wound surfaces in vivo, even on the most complex, nonplanar, irregular wound area. One limitation of this system was reported to be the cap for thickness of printed tissues at 100 μm, as the resolution achieved was in the order of 700–1000 μm. Improvements in the dispensing system and printing mechanism should be made for increasing the resolution. With thicker tissues comes the problem of providing adequate perfusion, which can be overcome by introducing fluidic channels inside the hydrogel.

Lee et al. [248] utilized a similar system but with eight independently controlled cell-dispensing channels, instead of four, which can be utilized to place cells, ECM, scaffold materials, and other growth factors in any user-defined 3D arrangement. Each dispenser is independently operated by electromechanical valves, as in the previous system [247] and mounted on a three-axis, high precision, xyz robotic stage, with the option to precisely control the volume of dispensed droplets, with range as low as 15 nL, with high precision. FBs (HFF-1) and KCs (HaCaT) were used to construct the 3D skin tissue in this study. A total of six collagen layers for the dermis and two collagen layers for the epidermis were printed to obtain the desired dermal and epidermal thicknesses. FBs proliferated within the dermal layer and maintained a sparse distribution. KCs proliferated more rapidly on the top of the collagen matrix and fully covered the surface in 4–7 days. No cell invasion across the dermal and epidermal layers was observed, which is a notable advantage. A comparison of skin tissues fabricated via 3D bioprinting and manual deposition was made, which showed that printed skin samples retained their form, dimensions, and shape, whereas manually deposited structures shrank, buckled, and formed concave shapes under submerged culture condition after seven days. In vitro tests namely the viability tests and immunohistochemistry tests indicated the development of the printed construct into a skin tissue, mimicking the epidermal and dermal layers of native skin.

5.5.4.3 Cryogenic extrusion–based direct-plotting system

Kim et al. [249,250] studied an extrusion-based cryogenic direct-plotting system for skin tissue engineering. The device set-up is shown in Fig. 5.10 [249]. The cryogenic 3D plotting system is composed of a 3D robot system, a dispensing system, and a cryogenic manufacturing stage. The cryogenic refrigeration system consisted of two compressors, circulating silicone oil to cool the stage, and a circulation pump. A collagen scaffold of required thickness and pore size were processed by computer-driven direct deposition, layer by layer with a plotting needle under controlled pneumatic pressure on a cryogenic stage at −40°C and the ambient temperature being 10°C, to enable the printed collagen

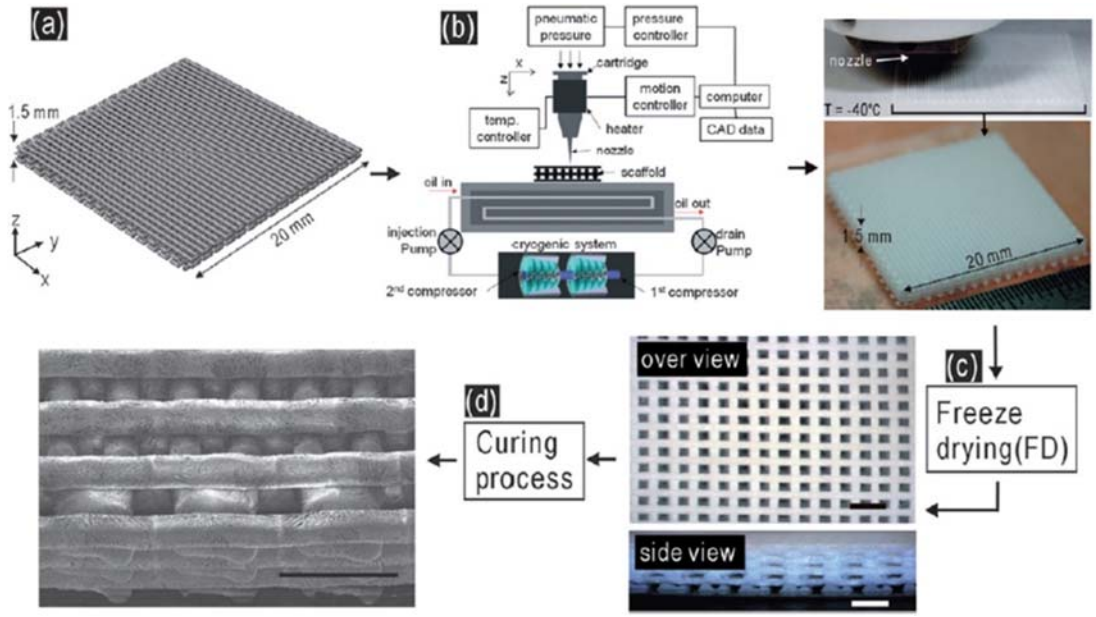

Figure 5.10

Fabrication procedure for 3D collagen scaffolds. (A) Schematic diagram of the desired scaffold ($20 \times 20 \times 1.5$ mm^3); (B) schematic diagram of the cryogenic plotting and processing system at $-40°$C (left) and images of the fabricated scaffold (right); (C) complete freezedrying of the fabricated 3D scaffold at $-76°$C over three days. (D) Electron micrograph of scaffold curing in 50 mM EDC in 95% ethanol for 24 h at room temperature. Scale bar = 1 mm. *Reprinted with permission from G. Kim, S. Ahn, H. Yoon, Y. Kim, W. Chun, A cryogenic direct-plotting system for fabrication of 3D collagen scaffolds for tissue engineering, Journal of Materials Chemistry 19 (46) (2009) 8817–8823.*

strands to freeze almost instantly as it touched the substrate. The nozzle was coated with silicone rubber to prevent clogging. The plotted scaffold was immediately placed in a freeze-dryer at $-76°$C for three days, followed by immersion in 50 mM 1-ethyl-(3-3-dimethylaminopropyl) hydrochloride (EDC) solution in 95% ethanol for 24 h at room temperature for cross-linking. Keratinocytes and fibroblasts are cocultured on the scaffolds then and in vitro studies performed. The well-designed pore structure of the scaffold enabled the cells to proliferate, readily migrate into, and differentiate in the scaffold. However, the structure suffered low shape stability due to highly porous structure and poor mechanical properties of collagen.

In order to overcome the limitation of poor mechanical properties, Kim et al. [250] plotted a core/shell structure scaffold using the same device set-up. Alginate and collagen were printed coaxially with alginate providing required mechanical strength to the scaffold. In vitro tests proved that the core/shell scaffold had completely similar cellular behavior to

that of the pure collagen scaffold, with the added advantage of enhanced mechanical stability. In addition to in vitro, in vivo studies had been conducted on adult male BALB/c/Bkl-nu/nu mice. The plotted scaffold with cocultured keratinocytes/fibroblasts, implanted as a dermal substitute on the wound area, provided good granulation tissue formation and rapid vascularization in the dermis and the scaffold. This technique can be used to coextrude other natural or synthetic biopolymers along with collagen or even cell-laden bioink and expanded further with other growth factors and peptides in the core area to make functional skin substitutes. However, one disadvantage of this system is that the whole process takes place in a cryogenic environment unlike the other systems where the processes take place at room temperature.

5.5.4.4 Microfluidic approach—based skin printer

Leng et al. [251], from University of Toronto, developed a skin printer based on a microfluidic approach, which is widely accepted as a technique that will aid in vascularization of tissue engineered constructs. The device [252] consisted of an annular gear pump, a microfluidic flow focusing device or a microfabricated cartridge and a collecting drum. The ECM used in this study was a mixture of alginate and collagen. The base layer carried to the device exit via a set of parallel microchannels, a time-varying content of the bioink. Additional layers located above can contain a different cell suspension, like keratinocytes (though not used in this study), or focusing streams containing the cross-linker can be printed. There was a rotating drum downstream that collected the printed sheets, which in addition to the shear stress exerted by the focusing fluid aids in continuous formation of hydrogel or bioink sheets, image-based inspection, and better collection. Human fibroblast cells were incorporated within a continuously extruded biopolymer sheet with precise spatiotemporal control over the cell location and cell seeding density (which was 1.94 million cells/mL in this study). Various shapes of biopolymer sheets like spots and parallel strips were printed, with fibroblasts seeded into the structure. The patterns can also be hollow to promote vascularization while providing relevant thickness. In vivo testing was carried out on immunodeficient mice by performing excisional skin biopsy and replacing the excised skin with printed biopolymer sheets patterned with fibroblasts. Trichrome and keratin 14 staining on the wounded site revealed that the printed skin construct led to keratinization and better wound healing. The greatest advantage of this device is the shortest lead time for printing skin, which is reported to be $10\ \mathrm{mm\,s^{-1}}$, i.e., it will take only 48 min to print a $1\ \mathrm{m^2}$ skin construct.

5.5.4.5 In situ bioprinting of skin

Binder et al. [253] from Wake Forest University developed a novel device for in situ bioprinting of skin. The criteria for developing this system included: (i) portability (the system must be capable of being quickly transported to patients with extensive burn wounds), (ii) accommodating a wide range of body types, (iii) being capable of tailoring

cell therapy to individual patient's specific needs, (iv) ease of sterilization, (v) allowing for repeated treatments, and (vi) inexpensive and easy maintenance. The first two criteria were accomplished using a movable lightweight frame on which an XYZ plotting system was mounted. The dimensions of the system were large enough to cover the torso of an average patient but small enough to easily pass through most doorframes. During the treatment, the system was positioned over the patient's wound area and locked at the optimal position. The powerful locks prevented the frame movement while bioprinting, thus preserving both the mobility of the system and its delivery precision. A belt-driven plotting system with 100 μm precise movements aided the XYZ axes in precise delivery of cell suspension onto the patient's body. The movement of Z axis could be independently controlled, thereby allowing the delivery system to track with the curvature of patient's body and thus being capable of accommodating many different body types. A laser-based wound scanning system was coupled with the cartridge-based delivery system, which helped in tailoring the cell therapy according to individual patient's need. The laser scanning system gathered length, width, and depth data about the wound; gathered data was processed to obtain a functional wound map and based on the wound map the software determined the exact cell composition and thickness of different areas of skin. The most important components of the device were cartridge-based delivery system, consisting of a number of nozzles, laser scanner for wound scanning, the mobile frame, and XYZ axes. In vivo experiments were performed on the porcine wound model, as porcine skin is similar to human skin. The bioprinting procedure was divided into two stages. In the first stage, skin from the shoulder area of the pig was removed using a dermatome for preparation of fibroblasts and keratinocytes for bioprinting. These cells isolated were then cultured and mixed with biopolymers namely fibrin and type I collagen to make the bioink. After expanding these cells in culture, four full-thickness 10×10 cm wounds were excised through the panniculus carnosus layer of the thoracic dorsa on the animals. Prior to surgery, the print head, cartridges, and tubing were sterilized. No part of the printer was in direct contact with the animal at any point during the printing procedure. The wound area was placed under a portable bioprinter and dermal cells and matrices were directly bioprinted onto the wound bed. One layer of 10 million fibroblasts (1.0×10^5 cells cm^{-2}) was bioprinted at 2 mm intervals between drops with thrombin being sprayed from the atomizing nozzles simultaneously to form a fibrin/type I collagen hydrogel, followed by a 15 min break to allow complete conversion of fibrinogen to fibrin and finally another layer of 10 million keratinocytes was bioprinted above the fibroblast layer. Results were very much promising. Complete reepithelialization could be witnessed at eight weeks. Keratinocytes proliferated over the course of 8 weeks to completely cover the wound and their epithelium was found connected to the advancing wound edge. Prelabeled autologous fibroblasts and keratinocytes as well as allogeneic fibroblasts were visible in the wound at eight weeks, demonstrating that bioprinted skin cells could survive, proliferate, and form skin tissue in an immunocompetent large wound model. One limiting

factor reported is that the performance of the laser imaging system is not up to the mark in vivo because of the breathing motion of the patient. This could be overcome by replacing the laser scanner with imaging system that can take instantaneous snapshots of the wound and create the wound map. Certain optimizations are also required to be made before using it for treating human wounds.

Sofokleous et al. [254] worked on developing a portable handheld electrohydrodynamic (EHD) multineedle spray gun for biomedical applications. The main component of the EHD spray gun is a multineedle device assembly with one to two brass needles, a Dremel glue gun used as the spray gun case, heat-shrinkable tubing with adhesive inner liner, high current wire, and silicone tubes. The number of brass needles can range from one up to four, based on the application. The working principle of an EHD spraying/spinning of liquids is application of an electric force to the surface of a conducting liquid to produce fibers and such a system consists of a high voltage supply, which creates the required electric field between a charged capillary filled with the material to be processed in liquid state and a ground collector. When the electrostatic force overcomes the surface tension of the liquid at the capillary tip, a fine jet emanates from the nozzle tip. PLGA and polymethysilsesquioxane (PMSQ) solutions were tested using the device. Simple, multicomponent and multifunctional products such as encapsulated fibers and particles having submicrometer to micrometee scale dimensions were successfully generated with the spray gun at different angles relative to a defined reference angle and deposited in a marked area of interest, proving its flexibility and portability. Though no cell-laden bioink has been printed and tested, the spray gun technology can evolve into a portable handheld in situ bioprinter in the future, facilitating ease of use by the clinicians.

The summary of all the skin bioprinting technologies is given in Table 5.8.

5.6 Challenges and future prospects

Having reviewed in detail the various processes of 3D bioprinting skin and their advantages, it is important to look at the realistic deployment potential of these technologies clinically. No technology is perfect and all of them suffer from certain limitations and pose challenges. Three-dimensional bioprinting is not an exception too. Current skin grafts suffer from the greatest limitations, in terms of long healing time and cost, which is reported to be over $50,000 to cover 40% burn area on an average male [64,66,255,256]. Though 3D bioprinting has the potential to reduce the healing time considerably, the cost factor should be taken into account. Affordability is the first challenge to be overcome. The next biggest challenge is to bioprint a fully functional skin substitute. Though most of the functions of the native skin can be mimicked in the bioprinted skin by using more types and number of cells in addition to keratinocytes and fibroblasts, like the melanocytes or Langerhans cells or even hair follicle cells, path to

Table 5.8: Summary of skin bioprinting technologies.

	Uniqueness	Cellular components	Size of the tissue construct	Cell viability	Resolution	Speed	In vivo animal model	In vivo results	Scalability	References
Laser-based bioprinting	First demonstration of 3D arrangement of vital cells by LBB as multicellular grafts analogous to native archetype; the individual layers of the skin construct do not intermix with each other.	FBs (murine cell line NIH-3T3) and KCs (cell line HaCaT from adult human skin) embedded in collagen	10 × 10 mm × 2 mm	Proved vitality of the printed cells 10 days after printing	Droplet volumes of 0.1–1 nL	—	—	—	Low	[244]
	Possibility to position different cell types in an exact three-dimensional (3D) spatial pattern.	NIH3T3 FBs and HaCaT KCs suspended in collagen	—	Normal cell viability	—	—	Male BALB/c-Nude mice	After 11 days, the borders of the skin constructs and the surrounding mouse skin were tightly grown together; neither inflammatory/ necrotic processes nor contraction of the wounds could be detected; small blood vessels could be found.	Low	[245]
	FBs and KCs, along with hMSCs were printed using laser bioprinting due	NIH3T3 FBs and HaCaT KCs, bone marrow-derived hMSC (Bm-hMSCs),	9.6 × 9.6 mm	FBs and KCs showed exponential growth starting on day 1 up to day 6;	Droplet sizes of 80–140 µm diameter	1200 printed cell droplets per minute	—	—	Low	[246]

Continued

Table 5.8: Summary of skin bioprinting technologies.—cont'd

	Uniqueness	Cellular components	Size of the tissue construct	Cell viability	Resolution	Speed	In vivo animal model	In vivo results	Scalability	References
	to their high potential in regeneration of human skin and new application possibilities of stem cell therapy.	adipose-derived hMSC		continuously increasing proliferation of Bm-hMSC until day 4 after printing						
Robotic dispensing	A method to create multilayered engineered tissue composites; direct, on-demand fabrication of the 3D tissue composites on nonplanar surfaces [246]; first study of printing both FB and KC in a single experiment with the formation of dermal/epidermallike distinctive layers in a 3D hydrogel scaffold [247].	Primary adult human dermal FBs and primary adult human epidermal KCs, type I collagen	—	There was no significant difference in cell viabilities between printed cells and manually plated cells as demonstrated in the viability assay	Droplet volumes of 7.6–10 nL	—		—	Medium	[247,248]
Cryogenic plotting	A novel system for the cryogenic plotting of 3D scaffolds developed to overcome the problems in fabricating highly hydrophilic natural polymers into a scaffold.	Normal human KCs and FBs; type I collagen for fabricating porous scaffolds	18.4 × 18.3 mm × 1.4 mm	Good cell migration and differentiation; stratum corneum was well expressed similar to the normal skin tissue	—	—	—	—	Low–medium	[249]

Cryogenic plotting	The hybrid core/shell (collagen/alginate) scaffolds fabricated by cryogenic plotting, exhibited good structural stability, increased Young's modulus about seven times compared to pure collagen scaffold, and good cell viability.	Normal human KCs and FBs; type I collagen and alginate for fabricating porous scaffolds	10 × 10 mm × 2 mm	Cell proliferation of core/shell (collagen/alginate) scaffold was completely similar to that of the pure collagen scaffold	—	—	Adult male BALB/c/Bkl-nu/nu mice	Provided good granulation dermal tissue formation and rapid vascularization; the epidermis was completely covered after 14 days.	Low —medium	[250]
Microfluidic skin printer	A scalable approach and uniquely addresses the need to provide skin substitutes at affordable prices that are easy to handle and apply, reduced wound recovery times; enables the continuous formation of cell-populated single-layer, bilayer, and vascularized sheets.	Human FBs	Up to 35 mm wide sheets	Normal cell viability	—	10 mm s^{-1} equivalent to 1 m^2 in 48 min	Immunodeficient mice	Better wound healing and keratinization, suggesting improved skin regeneration.	High	[251,252]

Continued

Table 5.8: Summary of skin bioprinting technologies.—cont'd

	Uniqueness	Cellular components	Size of the tissue construct	Cell viability	Resolution	Speed	In vivo animal model	In vivo results	Scalability	References
In situ skin printer	Fist demonstration of in situ skin printing on porcine wound model	FBs and KCs harvested from porcine model suspended in fibrin and type I collagen	10 × 10 cm	—	—	—	Porcine wound model	Complete reepithelialization could be witnessed at 8 weeks; KCs proliferated over the course of 8 weeks to completely cover the wound and their epithelium was found connected to the advancing wound edge.	Medium	[253]

vascularization and innervation in engineered tissues still remains murky. Use of stem cells is one option but the ethical issues, cost, and skill requirement hinder from utilizing them to their full potential. Genetically modified keratinocytes, which overexpress vascular endothelial growth factor (VEGF), were reported to promote vascularization [205] and it is worth trying to use them to see how well they can help the vascularization in bioprinted tissues, provided with all the other growth factors and tissue environment in a bioreactor. The neural crest stem cells are a multipotent cell population that can give rise to a diversity of neural and nonneural cell types in the adult, such as melanocytes, neurons, and glial cells of the sensory and autonomic ganglia of the peripheral nervous system, and some endocrine cells [211,257]. All these enhancements will benefit the wound healing application, where the bioprinted skin substitute will be implanted on a patient's body or printed in situ, either way, and the healthy part of the skin can provide nourishment to the grafted part. But, the drug testing and cosmetics testing remain a challenge as the skin substitutes will not be grafted onto humans but it requires a biomimetic skin substitute ex vivo, with all functionality of the native skin so that the drugs or cosmetics can be tested accurately. Application in personalized or precision medicine is another prospect which can be benefited much with 3D bioprinting of skin. As a matter of fact, all the steps in bioprinting skin explained in this chapter, right from imaging of wound site to the application, make bioprinting of skin a natural choice for personalized or precision medicine care. Another potential application is the study of melanoma and other types of skin cancer. In vitro 3D tumor models with engineered tumor microenvironment (TME) [258] are very helpful for studying the modus operandi of cancer cell proliferation, migration, and metastasis. Different melanoma cell types or numbers could be printed in designated skin areas or layers and cells are monitored for proliferation, motility, survival, and drug response [259]. Even before initiating the treatment process for a cancer patient, clinicians can bioprint cancer models to see how each patient's actual tumor responds to the drug and is there a possibility of metastasis. Such sophisticated 3D skin cancer models can be engineered with 3D bioprinting technology, for example, the "metastasis-on-a-chip" platform [260,261]. From a policy standpoint, standardization and government support for clinical implementation is the need of the hour. Three-dimensional bioprinting is thus far a promising technology but lacks coordinated efforts from multidisciplinary teams. A collaborative approach, including experts from various domains including engineering, medicine, biomedical, and biochemistry will further strengthen its prospects and bolster its potential to be available quickly in serving the people and saving their lives.

References

[1] J. Kanitakis, Anatomy, histology and immunohistochemistry of normal human skin, European Journal of Dermatology 12 (4) (2002) 390–400.
[2] P. Kolarsick, M.A. Kolarsick, C. Goodwin, Anatomy and physiology of the skin, Journal of the Dermatology Nurses' Association 3 (4) (2011) 203–213.

[3] R.F. Pereira, C.C. Barrias, P.L. Granja, P.J. Bartolo, Advanced biofabrication strategies for skin regeneration and repair, Nanomedicine 8 (4) (2013) 603–621.
[4] S.T. Boyce, Design principles for composition and performance of cultured skin substitutes, Burns 27 (5) (2001) 523–533.
[5] B.J. Nickoloff, R.S. Mitra, J. Green, X.G. Zheng, Y. Shimizu, C. Thompson, L.A. Turka, Accessory cell function of keratinocytes for superantigens. Dependence on lymphocyte function-associated antigen-1/ intercellular adhesion molecule-1 interaction, The Journal of Immunology 150 (6) (1993) 2148–2159.
[6] C. Albanesi, O. De Pita, G. Girolomoni, Resident skin cells in psoriasis: a special took at the pathogenetic functions of keratinocytes, Clinics in Dermatology 25 (6) (2007) 581–588.
[7] J.M. Schroder, The role of keratinocytes in defense against infection, Current Opinion in Infectious Diseases 23 (2) (2010) 106–110.
[8] D. Tsuruta, NF-kappa B links keratinocytes and lymphocytes in the pathogenesis of psoriasis, Recent Patents on Inflammation & Allergy Drug Discovery 3 (1) (2009) 40–48.
[9] E. Ranzato, Keratinocytes: Structure, Molecular Mechanisms and Role in Immunity, Nova Science, New York, 2013.
[10] M. Jordana, B. Sarnstrand, P.J. Sime, I. Ramis, Immune-inflammatory functions of fibroblasts, European Respiratory Journal 7 (12) (1994) 2212–2222.
[11] R. Millioni, L. Puricelli, E. Iori, R. Trevisan, P. Tessari, Skin fibroblasts as a tool for identifying the risk of nephropathy in the type 1 diabetic population, Diabetes-Metabolism Research and Reviews 28 (1) (2012) 62–70.
[12] S.V. Nolte, W. Xu, H.O. Rennekampff, H.P. Rodemann, Diversity of fibroblasts - a review on implications for skin tissue engineering, Cells Tissues Organs 187 (3) (2008) 165–176.
[13] R. Kalluri, M. Zeisberg, Fibroblasts in cancer, Nature Reviews Cancer 6 (5) (2006) 392–401.
[14] I.C. Lepoole, T. Mutis, R. Vandenwijngaard, W. Westerhof, T. Ottenhoff, R.R.P. Devries, P.K. Das, A novel, antigen-presenting function of melanocytes and its possible relationship to hypopigmentary disorders, The Journal of Immunology 151 (12) (1993) 7284–7292.
[15] K. Takeda, N.H. Takahashi, S. Shibahara, Neuroendocrine functions of melanocytes: beyond the skin-deep melanin maker, Tohoku Journal of Experimental Medicine 211 (3) (2007) 201–221.
[16] Y. Yamaguchi, M. Brenner, V.J. Hearing, The regulation of skin pigmentation, Journal of Biological Chemistry 282 (38) (2007) 27557–27561.
[17] J. Borovanskỳ, P.A. Riley, Physiological and Pathological Functions of Melanosomes, Melanins and Melanosomes: Biosynthesis, Biogenesis, Physiological, and Pathological Functions, 2011.
[18] Y. Lu, W.Y. Zhu, C. Tan, G.H. Yu, J.X. Gu, Melanocytes are potential immunocompetent cells: evidence from recognition of immunological characteristics of cultured human melanocytes, Pigment Cell Research 15 (6) (2002) 454–460.
[19] P.M. Plonka, T. Passeron, M. Brenner, D.J. Tobin, S. Shibahara, A. Thomas, A. Slominski, A.L. Kadekaro, D. Hershkovitz, E. Peters, J.J. Nordlund, Z. Abdel-Malek, K. Takeda, R. Paus, J.P. Ortonne, V.J. Hearing, K.U. Schallreuter, What are melanocytes really doing all day long...? Experimental Dermatology 18 (9) (2009) 799–819.
[20] N. Boulais, L. Misery, Merkel cells, Journal of the American Academy of Dermatology 57 (1) (2007) 147–165.
[21] K.M. Gottschaldt, C. Vahlehinz, Merkel cell receptors: structure and transducer function, Science 214 (4517) (1981) 183–186.
[22] A. Lucarz, G. Brand, Current considerations about Merkel cells, European Journal of Cell Biology 86 (5) (2007) 243–251.
[23] I. Moll, M. Roessler, J.M. Brandner, A.C. Eispert, P. Houdek, R. Moll, Human Merkel cells–aspects of cell biology, distribution and functions, European Journal of Cell Biology 84 (2–3) (2005) 259–271.
[24] H. Ogawa, The Merkel cell as a possible mechanoreceptor cell, Progress in Neurobiology 49 (4) (1996) 317–&.

[25] A. Kissenpfennig, S. Henri, B. Dubois, C. Laplace-Builhe, P. Perrin, N. Romani, C.H. Tripp, P. Douillard, L. Leserman, D. Kaiserlian, S. Saeland, J. Davoust, B. Malissen, Dynamics and function of langerhans cells in vivo: dermal dendritic cells colonize lymph node areas distinct from slower migrating langerhans cells, Immunity 22 (5) (2005) 643–654.
[26] G. Stingl, S.I. Katz, L. Clement, I. Green, E.M. Shevach, Immunologic functions of Ia-bearing epidermal Langerhans cells, The Journal of Immunology 121 (5) (1978) 2005–2013.
[27] G. Stingl, S.I. Katz, E.M. Shevach, A.S. Rosenthal, I. Green, Analogous functions of macrophages and langerhans cells in initiation of immune-response, Journal of Investigative Dermatology 71 (1) (1978) 59–64.
[28] G. Stingl, K. Tamaki, S.I. Katz, Origin and function of epidermal Langerhans cells, Immunological Reviews 53 (1980) 149–174.
[29] L.R. Braathen, E. Thorsby, Studies on human epidermal langerhans cells, Scandinavian Journal of Immunology 15 (1) (1982) 55–61.
[30] E. Klechevsky, R. Morita, M.C. Liu, Y.Y. Cao, S. Coquery, L. Thompson-Snipes, F. Briere, D. Chaussabel, G. Zurawski, A.K. Palucka, Y. Reiter, J. Banchereau, H. Ueno, Functional specializations of human epidermal langerhans cells and CD14(+) dermal dendritic cells, Immunity 29 (3) (2008) 497–510.
[31] R.C. Benyon, M.A. Lowman, M.K. Church, Human skin mast cells: their dispersion, purification, and secretory characterization, The Journal of Immunology 138 (3) (1987) 861–867.
[32] W. Dawicki, J.S. Marshall, New and emerging roles for mast cells in host defence, Current Opinion in Immunology 19 (1) (2007) 31–38.
[33] S.J. Galli, S. Nakae, M. Tsai, Mast cells in the development of adaptive immune responses, Nature Immunology 6 (2) (2005) 135–142.
[34] M. Metz, F. Siebenhaar, M. Maurer, Mast cell functions in the innate skin immune system, Immunobiology 213 (3–4) (2008) 251–260.
[35] J. Wedemeyer, M. Tsai, S.J. Galli, Roles of mast cells and basophils in innate and acquired immunity, Current Opinion in Immunology 12 (6) (2000) 624–631.
[36] K. Weller, K. Foitzik, R. Paus, W. Syska, M. Maurer, Mast cells are required for normal healing of skin wounds in mice, The FASEB Journal 20 (13) (2006) 2366–+.
[37] L.B. Schwartz, Mast cells: function and contents, Current Opinion in Immunology 6 (1) (1994) 91–97.
[38] S.K. Brancato, J.E. Albina, Wound macrophages as key regulators of repair origin, phenotype, and function, American Journal of Pathology 178 (1) (2011) 19–25.
[39] B.M. Delavary, W.M. van der Veer, M. van Egmond, F.B. Niessen, R.H.J. Beelen, Macrophages in skin injury and repair, Immunobiology 216 (7) (2011) 753–762.
[40] T. Lucas, A. Waisman, R. Ranjan, J. Roes, T. Krieg, W. Muller, A. Roers, S.A. Eming, Differential roles of macrophages in diverse phases of skin repair, The Journal of Immunology 184 (7) (2010) 3964–3977.
[41] B. Malissen, S. Tamoutounour, S. Henri, The origins and functions of dendritic cells and macrophages in the skin, Nature Reviews Immunology 14 (6) (2014) 417–428.
[42] Transparent Market Research Report 2015, Tissue Engineered Skin Substitutes Market - Global Industry Analysis, Size, Share, Growth, Trends, and Forecast 2015–2023.
[43] American Burn Association, Burn Incidence and Treatment in the United States 2016, Burn Incidence Fact Sheet.
[44] M. Blais, R. Parenteau-Bareil, S. Cadau, F. Berthod, Concise review: tissue-engineered skin and nerve regeneration in burn treatment, Stem Cells Translational Medicine 2 (7) (2013) 545–551.
[45] N. Mayet, Y.E. Choonara, P. Kumar, L.K. Tomar, C. Tyagi, L.C. Du Toit, V. Pillay, A comprehensive review of advanced biopolymeric wound healing systems, Journal of Pharmaceutical Sciences 103 (8) (2014) 2211–2230.
[46] J. Li, J. Chen, R. Kirsner, Pathophysiology of acute wound healing, Clinics in Dermatology 25 (1) (2007) 9–18.

[47] M.W.J. Ferguson, S. O'Kane, Scar-free healing: from embryonic mechanisms to adult therapeutic intervention, Philosophical Transactions of the Royal Society B: Biological Sciences 359 (1445) (2004) 839–850.
[48] R.F. Diegelmann, M.C. Evans, Wound healing: an overview of acute, fibrotic and delayed healing, Frontiers in Bioscience-Landmark 9 (2004) 283–289.
[49] T. Velnar, T. Bailey, V. Smrkoli, The wound healing process: an overview of the cellular and molecular mechanisms, Journal of International Medical Research 37 (5) (2009) 1528–1542.
[50] E. Boelsma, M.C.H. Verhoeven, M. Ponec, Reconstruction of a human skin equivalent using a spontaneously transformed keratinocyte cell line (HaCaT), Journal of Investigative Dermatology 112 (4) (1999) 489–498.
[51] M. Ponec, Skin constructs for replacement of skin tissues for in vitro testing, Advanced Drug Delivery Reviews 54 (2002) S19–S30.
[52] T. Welss, D.A. Basketter, K.R. Schroder, In vitro skin irritation: facts and future. State of the art review of mechanisms and models, Toxicology in Vitro 18 (3) (2004) 231–243.
[53] O. de Silva, C.S.C. Alternatives, The contributions of the European Cosmetics Industry to the development of alternatives to animal testing: dialogue with ECVAM and future challenges, Atla-Alternatives to Laboratory Animals 30 (2002) 189–193.
[54] E. Boelsma, S. Gibbs, C. Faller, M. Ponec, Characterization and comparison of reconstructed skin models: morphological and immunohistochemical evaluation, Acta Dermato-Venereologica 80 (2) (2000) 82–88.
[55] J.H. Fentem, P.A. Botham, ECVAM's activities in validating alternative tests for skin corrosion and irritation, Atla-Alternatives to Laboratory Animals 30 (2002) 61–67.
[56] J.H. Fentem, D. Briggs, C. Chesne, G.R. Elliott, J.W. Harbell, J.R. Heylings, P. Portes, R. Roguet, J.J.M. van de Sandt, P.A. Botham, A prevalidation study on in vitro tests for acute skin irritation: results and evaluation by the Management Team, Toxicology in Vitro 15 (1) (2001) 57–93.
[57] https://congress.gov/bill/114th-congress/house-bill/2858.
[58] http://mediapeta.com/peta/PDF/companiesdotest.pdf.
[59] http://peta.org/action/easy-ways-help-animals-used-killed-experiment.
[60] J.T. Shores, A. Gabriel, S. Gupta, Skin substitutes and alternatives: a review, Advances in Skin & Wound Care 20 (9) (2007) 493–508.
[61] A.S. Halim, T.L. Khoo, S.J.M. Yussof, Biologic and synthetic skin substitutes: an overview, Indian Journal of Plastic Surgery 43 (2010) S23–S28.
[62] M. Balasubramani, T.R. Kumar, M. Babu, Skin substitutes: a review, Burns 27 (5) (2001) 534–544.
[63] P. Kumar, Classification of skin substitutes, Burns 34 (1) (2008) 148–149.
[64] D.M. Supp, S.T. Boyce, Engineered skin substitutes: practices and potentials, Clinics in Dermatology 23 (4) (2005) 403–412.
[65] F.A. Auger, D. Lacroix, L. Germain, Skin substitutes and wound healing, Skin Pharmacology and Physiology 22 (2) (2009) 94–102.
[66] I. Jones, L. Currie, R. Martin, A guide to biological skin substitutes, British Journal of Plastic Surgery 55 (3) (2002) 185–193.
[67] S.T. Boyce, G.D. Warden, Principles and practices for treatment of cutaneous wounds with cultured skin substitutes, The American Journal of Surgery 183 (4) (2002) 445–456.
[68] N.S. Adzick, H.P. Lorenz, Cells, matrix, growth factors, and the surgeon. The biology of scarless fetal wound repair, Annals of Surgery 220 (1) (1994) 10–18.
[69] P.J. Bartolo, M. Domingos, T. Patricio, S. Cometa, V. Mironov, Biofabrication Strategies for Tissue Engineering, 1st International ECCOMAS Thematic Conference on Tissue Engineering, Polytechnic Institute Leiria, Leiria, PORTUGAL, 2009, pp. 137–176.
[70] P. Bartolo, J.P. Kruth, J. Silva, G. Levy, A. Malshe, K. Rajurkar, M. Mitsuishi, J. Ciurana, M. Leu, Biomedical production of implants by additive electro-chemical and physical processes, CIRP Annals - Manufacturing Technology 61 (2) (2012) 635–655.

[71] H.-T. Liao, K.-H. Chang, Y. Jiang, J.-P. Chen, M.-Y. Lee, Fabrication of tissue engineered PCL scaffold by selective laser-sintered machine for osteogeneisis of adipose-derived stem cells: the research has proven that a bone tissue-engineered scaffold can be made using the selective laser sintering method, Virtual and Physical Prototyping 6 (1) (2011) 57–60.
[72] J.W. Nichol, A. Khademhosseini, Modular tissue engineering: engineering biological tissues from the bottom up, Soft Matter 5 (7) (2009) 1312–1319.
[73] Y.A. Du, E. Lo, S. Ali, A. Khademhosseini, Directed assembly of cell-laden microgels for fabrication of 3D tissue constructs, Proceedings of the National Academy of Sciences of the United States of America 105 (28) (2008) 9522–9527.
[74] A. Khademhosseini, R. Langer, J. Borenstein, J.P. Vacanti, Microscale technologies for tissue engineering and biology, Proceedings of the National Academy of Sciences of the United States of America 103 (8) (2006) 2480–2487.
[75] F. Urciuolo, G. Imparato, A. Guaccio, B. Mele, P.A. Netti, Novel strategies to engineering biological tissue in vitro, Nanotechnology in Regenerative Medicine (2012) 223–244.
[76] J. Yang, M. Yamato, T. Shimizu, H. Sekine, K. Ohashi, M. Kanzaki, T. Ohki, K. Nishida, T. Okano, Reconstruction of functional tissues with cell sheet engineering, Biomaterials 28 (34) (2007) 5033–5043.
[77] Y. Nahmias, R.E. Schwartz, C.M. Verfaillie, D.J. Odde, Laser-guided direct writing for three-dimensional tissue engineering, Biotechnology and Bioengineering 92 (2) (2005) 129–136.
[78] N.A. Raof, N.R. Schiele, Y.B. Xie, D.B. Chrisey, D.T. Corr, The maintenance of pluripotency following laser direct-write of mouse embryonic stem cells, Biomaterials 32 (7) (2011) 1802–1808.
[79] Y.F. Lin, G.H. Huang, Y. Huang, T.R.J. Tzeng, D. Chrisey, Effect of laser fluence in laser-assisted direct writing of human colon cancer cell, Rapid Prototyping Journal 16 (3) (2010) 202–208.
[80] S. Catros, B. Guillotin, M. Bacakova, J.C. Fricain, F. Guillemot, Effect of laser energy, substrate film thickness and bioink viscosity on viability of endothelial cells printed by laser-assisted bioprinting, Applied Surface Science 257 (12) (2011) 5142–5147.
[81] R.E. Saunders, J.E. Gough, B. Derby, Delivery of human fibroblast cells by piezoelectric drop-on-demand inkjet printing, Biomaterials 29 (2) (2008) 193–203.
[82] A. Tirella, F. Vozzi, C. De Maria, G. Vozzi, T. Sandri, D. Sassano, L. Cognolato, A. Ahluwalia, Substrate stiffness influences high resolution printing of living cells with an ink-jet system, Journal of Bioscience and Bioengineering 112 (1) (2011) 79–85.
[83] S. Khalil, J. Nam, W. Sun, Multi-nozzle deposition for construction of 3D biopolymer tissue scaffolds, Rapid Prototyping Journal 11 (1) (2005) 9–17.
[84] P. Sepulveda, J.G.P. Binner, S.O. Rogero, O.Z. Higa, J.C. Bressiani, Production of porous hydroxyapatite by the gel-casting of foams and cytotoxic evaluation, Journal of Biomedical Materials Research 50 (1) (2000) 27–34.
[85] T.M.G. Chu, J.W. Halloran, S.J. Hollister, S.E. Feinberg, Hydroxyapatite implants with designed internal architecture, Journal of Materials Science: Materials in Medicine 12 (6) (2001) 471–478.
[86] Y. Zhang, M.Q. Zhang, Three-dimensional macroporous calcium phosphate bioceramics with nested chitosan sponges for load-bearing bone implants, Journal of Biomedical Materials Research 61 (1) (2002) 1–8.
[87] S.Y. Ni, J. Chang, L. Chou, A novel bioactive porous CaSiO3 scaffold for bone tissue engineering, Journal of Biomedical Materials Research Part A 76A (1) (2006) 196–205.
[88] C.M. Agrawal, J.E. Parr, S.T. Lin, Synthetic Bioabsorbable Polymers for Implants, 2000.
[89] F.J. Hua, G.E. Kim, J.D. Lee, Y.K. Son, D.S. Lee, Macroporous poly(L-lactide) scaffold 1. Preparation of a macroporous scaffold by liquid-liquid phase separation of a PLLA-dioxane-water system, Journal of Biomedical Materials Research 63 (2) (2002) 161–167.
[90] J. Lannutti, D. Reneker, T. Ma, D. Tomasko, D.F. Farson, Electrospinning for tissue engineering scaffolds, Materials Science & Engineering C-Biomimetic and Supramolecular Systems 27 (3) (2007) 504–509.

[91] S. Agarwal, J.H. Wendorff, A. Greiner, Progress in the field of electrospinning for tissue engineering applications, Advanced Materials 21 (32–33) (2009) 3343–3351.
[92] W.J. Li, C.T. Laurencin, E.J. Caterson, R.S. Tuan, F.K. Ko, Electrospun nanofibrous structure: a novel scaffold for tissue engineering, Journal of Biomedical Materials Research 60 (4) (2002) 613–621.
[93] C.X.F. Lam, X.M. Mo, S.H. Teoh, D.W. Hutmacher, Scaffold development using 3D printing with a starch-based polymer, Materials Science & Engineering C-Biomimetic and Supramolecular Systems 20 (1–2) (2002) 49–56.
[94] C. Bergmann, M. Lindner, W. Zhang, K. Koczur, A. Kirsten, R. Telle, H. Fischer, 3D printing of bone substitute implants using calcium phosphate and bioactive glasses, Journal of the European Ceramic Society 30 (12) (2010) 2563–2567.
[95] F.C. Fierz, F. Beckmann, M. Huser, S.H. Irsen, B. Leukers, F. Witte, O. Degistirici, A. Andronache, M. Thie, B. Muller, The morphology of anisotropic 3D-printed hydroxyapatite scaffolds, Biomaterials 29 (28) (2008) 3799–3806.
[96] S. Eshraghi, S. Das, Mechanical and microstructural properties of polycaprolactone scaffolds with one-dimensional, two-dimensional, and three-dimensional orthogonally oriented porous architectures produced by selective laser sintering, Acta Biomaterialia 6 (7) (2010) 2467–2476.
[97] W.Y. Yeong, N. Sudarmadji, H.Y. Yu, C.K. Chua, K.F. Leong, S.S. Venkatraman, Y.C.F. Boey, L.P. Tan, Porous polycaprolactone scaffold for cardiac tissue engineering fabricated by selective laser sintering, Acta Biomaterialia 6 (6) (2010) 2028–2034.
[98] K.H. Tan, C.K. Chua, K.F. Leong, C.M. Cheah, P. Cheang, M.S. Abu Bakar, S.W. Cha, Scaffold development using selective laser sintering of polyetheretherketone-hydroxyapatite biocomposite blends, Biomaterials 24 (18) (2003) 3115–3123.
[99] J.M. Williams, A. Adewunmi, R.M. Schek, C.L. Flanagan, P.H. Krebsbach, S.E. Feinberg, S.J. Hollister, S. Das, Bone tissue engineering using polycaprolactone scaffolds fabricated via selective laser sintering, Biomaterials 26 (23) (2005) 4817–4827.
[100] B. Dhariwala, E. Hunt, T. Boland, Rapid prototyping of tissue-engineering constructs, using photopolymerizable hydrogels and stereolithography, Tissue Engineering 10 (9–10) (2004) 1316–1322.
[101] T.M. Seck, F.P.W. Melchels, J. Feijen, D.W. Grijpma, Designed biodegradable hydrogel structures prepared by stereolithography using poly(ethylene glycol)/poly(D,L-lactide)-based resins, Journal of Controlled Release 148 (1) (2010) 34–41.
[102] A.J. Engler, S. Sen, H.L. Sweeney, D.E. Discher, Matrix elasticity directs stem cell lineage specification, Cell 126 (4) (2006) 677–689.
[103] E.K.F. Yim, M.P. Sheetz, Force-dependent cell signaling in stem cell differentiation, Stem Cell Research & Therapy 3 (2012).
[104] T. Iskratsch, H. Wolfenson, M.P. Sheetz, Appreciating force and shape—the rise of mechanotransduction in cell biology, Nature Reviews Molecular Cell Biology 15 (12) (2014) 825–833.
[105] S. Ghassemi, G. Meacci, S.M. Liu, A.A. Gondarenko, A. Mathur, P. Roca-Cusachs, M.P. Sheetz, J. Hone, Cells test substrate rigidity by local contractions on submicrometer pillars, Proceedings of the National Academy of Sciences of the United States of America 109 (14) (2012) 5328–5333.
[106] R. Tiruvannamalai-Annamalai, D.R. Armant, H.W.T. Matthew, A glycosaminoglycan based, modular tissue scaffold system for rapid assembly of perfusable, high cell density, engineered tissues, Plos One 9 (1) (2014).
[107] M. Ramalingam, E. Jabbari, S. Ramakrishna, A. Khademhosseini, Integrating Top-Down and Bottom-Up Scaffolding Tissue Engineering Approach for Bone Regeneration, 2013.
[108] H.W. Ouyang, S.L. Toh, J. Goh, T.E. Tay, K. Moe, Assembly of bone marrow stromal cell sheets with knitted poly (L-lactide) scaffold for engineering ligament analogs, Journal of Biomedical Materials Research Part B: Applied Biomaterials 75B (2) (2005) 264–271.
[109] T.D. Sargeant, M.O. Guler, S.M. Oppenheimer, A. Mata, R.L. Satcher, D.C. Dunand, S.I. Stupp, Hybrid bone implants: self-assembly of peptide amphiphile nanofibers within porous titanium, Biomaterials 29 (2) (2008) 161–171.

[110] http://ir.organovo.com/news/press-releases/press-releases-details/2015/LOreal-USA-Announces-Research-Partnership-with-Organovo-to-Develop-3D-Bioprinted-Skin-Tissue/.
[111] http://ft.com/intl/cms/s/0/02809474-ffe8-11e4-abd5-00144feabdc0.html#axzz3mMp5pa1N.
[112] http://3dprint.com/83334/rokit-bioprinting/.
[113] S.V. Murphy, A. Atala, 3D bioprinting of tissues and organs, Nature Biotechnology 32 (8) (2014) 773–785.
[114] T. Ozkul, M.H. Ozkul, Computer simulation tool for rhinoplasty planning, Computers in Biology and Medicine 34 (8) (2004) 697–718.
[115] S.A. Rabi, P. Aarabi, IEEE, Face fusion: an automatic method for virtual plastic surgery, in: 9th International Conference on Information Fusion, Florence, ITALY, 2006, pp. 131–137.
[116] H. Kim, P. Jurgens, S. Weber, L.P. Nolte, M. Reyes, A new soft-tissue simulation strategy for cranio-maxillofacial surgery using facial muscle template model, Progress in Biophysics and Molecular Biology 103 (2–3) (2010) 284–291.
[117] R.M. Koch, M.H. Gross, F.R. Carls, D.F. von Buren, G. Fankhauser, Y.I.H. Parish, Simulating Facial Surgery Using Finite Element Models, 1996.
[118] C.L. Heike, K. Upson, E. Stuhaug, S.M. Weinberg, 3D digital stereophotogrammetry: a practical guide to facial image acquisition, Head & Face Medicine 6 (2010).
[119] S.J. Lin, N. Patel, K. O'Shaughnessy, N. Fine, A new three-dimensional imaging device in facial aesthetic and reconstructive surgery, Otolaryngology-Head and Neck Surgery 139 (2) (2008) 313–315.
[120] M.S. See, M. Foxton, N. Miedzianowski-Sinclair, C. Roberts, C. Nduka, Stereophotogrammetric measurement of the nasolabial fold in repose: a study of age and posture-related changes, European Journal of Plastic Surgery 29 (8) (2007) 387–393.
[121] R. Zhang, P.S. Tsai, J.E. Cryer, M. Shah, Shape from shading: a survey, IEEE Transactions on Pattern Analysis and Machine Intelligence 21 (8) (1999) 690–706.
[122] T. Jebara, A. Azarbayejani, A. Pentland, 3D structure from 2D motion, IEEE Signal Processing Magazine 16 (3) (1999) 66–84.
[123] L. Torresani, A. Hertzmann, C. Bregler, Nonrigid structure-from-motion: estimating shape and motion with hierarchical priors, IEEE Transactions on Pattern Analysis and Machine Intelligence 30 (5) (2008) 878–892.
[124] B. Moghaddam, J. Lee, H. Pfister, R. Machiraju, Model-based 3D face capture with shape-from-silhouettes, in: IEEE International Workshop on Analysis and Modeling of Faces and Gestures (AMFG 2003), Nice, France, 2003, pp. 20–27.
[125] M. Salzmann, J. Pilet, S. Ilic, P. Fua, Surface deformation models for nonrigid 3D shape recovery, IEEE Transactions on Pattern Analysis and Machine Intelligence 29 (8) (2007) 1481–1487.
[126] V. Blanz, T. Vetter, A morphable model for the synthesis of 3D faces, in: Proceedings of the 26th Annual Conference on Computer Graphics and Interactive Techniques, 1999, pp. 187–194.
[127] T. Oliveira-Santos, C. Baumberger, M. Constantinescu, R. Olariu, L.-P. Nolte, S. Alaraibi, M. Reyes, 3D face reconstruction from 2D pictures: first results of a web-based computer aided system for aesthetic procedures, Annals of Biomedical Engineering 41 (5) (2013) 952–966.
[128] A.F.M. Hani, N.M. Eltegani, S.H. Hussein, A. Jamil, P. Gill, Assessment of Ulcer Wounds Size Using 3D Skin Surface Imaging, 1st International Visual Informatics Conference, Kuala Lumpur, Malaysia, 2009, pp. 243–+.
[129] Y.K. Zhu, G.Y. Tian, R.S. Lu, H. Zhang, A review of optical NDT technologies, Sensors 11 (8) (2011) 7773–7798.
[130] S.L. Lee, Y.H. Lu, Modeling of bioheat equation for skin and a preliminary study on a noninvasive diagnostic method for skin burn wounds, Burns 40 (5) (2014) 930–939.
[131] W.M. Liu, J. Maivelett, G.J. Kato, J.G. Taylor, W.C. Yang, Y.C. Liu, Y.G. Yang, A.M. Gorbach, Reconstruction of thermographic signals to map perforator vessels in humans, Quantitative Infrared Thermography Journal 9 (2) (2012) 123–133.

[132] N.J. Prindeze, P. Fathi, M.J. Mino, N.A. Mauskar, T.E. Travis, D.W. Paul, L.T. Moffatt, J.W. Shupp, Examination of the early diagnostic applicability of active dynamic thermography for burn wound depth assessment and concept analysis, Journal of Burn Care and Research 36 (6) (2015) 626–635.
[133] A. Renkielska, M. Kaczmarek, A. Nowakowski, J. Grudzinski, P. Czapiewski, A. Krajewski, I. Grobelny, Active dynamic infrared thermal imaging in burn depth evaluation, Journal of Burn Care and Research 35 (5) (2014) E294–E303.
[134] A. Renkielska, A. Nowakowski, M. Kaczmarek, J. Ruminski, Burn depths evaluation based on active dynamic IR thermal imaging—a preliminary study, Burns 32 (7) (2006) 867–875.
[135] J. Ruminski, M. Kaczmarek, A. Renkielska, A. Nowakowski, Thermal parametric imaging in the evaluation of skin burn depth, IEEE Transactions on Biomedical Engineering 54 (2) (2007) 303–312.
[136] N.J. Prindeze, H.A. Hoffman, B.C. Carney, L.T. Moffatt, M.H. Loew, J.W. Shupp, Evaluation of the Variable Depth Resolution of Active Dynamic Thermography on Human Skin, Biophotonics South America, International Society for Optics and Photonics, 2015, p. 95310P.
[137] K.D. Xiao, F. Zardawi, R. van Noort, J.M. Yates, Color reproduction for advanced manufacture of soft tissue prostheses, Journal of Dentistry 41 (2013) E15–E23.
[138] Technical C I E Report, Colorimetry, third ed., Publication 15, CIE Central Bureau, Vienna, 2004.
[139] K.D. Xiao, F. Zardawi, R. van Noort, J.M. Yates, Developing a 3D colour image reproduction system for additive manufacturing of facial prostheses, International Journal of Advanced Manufacturing Technology 70 (9–12) (2014) 2043–2049.
[140] I.S. Jang, J.W. Kim, J.Y. You, J.S. Kim, Spectrum-based color reproduction algorithm for makeup simulation of 3D facial avatar, ETRI Journal 35 (6) (2013) 969–979.
[141] Y.Y. Wang, X.L. Hao, Y.L. Hou, C.Q. Guo, IEEE, A new multispectral method for face liveness detection, in: 2nd IAPR Asian Conference on Pattern Recognition (ACPR), Naha, Japan, 2013, pp. 922–926.
[142] P. Agrawal, S. Soni, G. Mittal, A. Bhatnagar, Role of polymeric biomaterials as wound healing agents, The International Journal of Lower Extremity Wounds 13 (3) (2014) 180–190.
[143] P.A. Gunatillake, R. Adhikari, Biodegradable synthetic polymers for tissue engineering, European Cells and Materials 5 (2003) 1–16. January-June Cited May 23, 2003.
[144] M. Norouzi, S.M. Boroujeni, N. Omidvarkordshouli, M. Soleimani, Advances in skin regeneration: application of electrospun scaffolds, Advanced Healthcare Materials 4 (8) (2015) 1114–1133.
[145] H.M. Powell, D.M. Supp, S.T. Boyce, Influence of electrospun collagen on wound contraction of engineered skin substitutes, Biomaterials 29 (7) (2008) 834–843.
[146] S.P. Zhong, W.E. Teo, X. Zhu, R.W. Beuerman, S. Ramakrishna, L.Y.L. Yung, An aligned nanofibrous collagen scaffold by electrospinning and its effects on in vitro fibroblast culture, Journal of Biomedical Materials Research Part A 79A (3) (2006) 456–463.
[147] H. Powell, S. Boyce, Fiber density of electrospun gelatin scaffolds regulates morphogenesis of dermal–epidermal skin substitutes, Journal of Biomedical Materials Research Part A: An Official Journal of The Society for Biomaterials, The Japanese Society for Biomaterials, and The Australian Society for Biomaterials and the Korean Society for Biomaterials 84 (4) (2008) 1078–1086.
[148] J.H. Ko, H. Yin, J. An, D.J. Chung, J.H. Kim, S.B. Lee, D.G. Pyun, Characterization of cross-linked gelatin nanofibers through electrospinning, Macromolecular Research 18 (2) (2010) 137–143.
[149] B.M. Min, G. Lee, S.H. Kim, Y.S. Nam, T.S. Lee, W.H. Park, Electrospinning of silk fibroin nanofibers and its effect on the adhesion and spreading of normal human keratinocytes and fibroblasts in vitro, Biomaterials 25 (7–8) (2004) 1289–1297.
[150] B.M. Min, L. Jeong, Y.S. Nam, J.M. Kim, J.Y. Kim, W.H. Park, Formation of silk fibroin matrices with different texture and its cellular response to normal human keratinocytes, International Journal of Biological Macromolecules 34 (5) (2004) 281–288.
[151] L. Jeong, I.S. Yeo, H.N. Kim, Y.I. Yoon, D.H. Jang, S.Y. Jung, B.M. Min, W.H. Park, Plasma-treated silk fibroin nanofibers for skin regeneration, International Journal of Biological Macromolecules 44 (3) (2009) 222–228.

[152] B. Kundu, R. Rajkhowa, S.C. Kundu, X.G. Wang, Silk fibroin biomaterials for tissue regenerations, Advanced Drug Delivery Reviews 65 (4) (2013) 457–470.
[153] B.K. Gu, S.J. Park, M.S. Kim, C.M. Kang, J.I. Kim, C.H. Kim, Fabrication of sonicated chitosan nanofiber mat with enlarged porosity for use as hemostatic materials, Carbohydrate Polymers 97 (1) (2013) 65–73.
[154] G.E. Wnek, M.E. Carr, D.G. Simpson, G.L. Bowlin, Electrospinning of nanofiber fibrinogen structures, Nano Letters 3 (2) (2003) 213–216.
[155] M.C. McManus, E.D. Boland, H.P. Koo, C.P. Barnes, K.J. Pawlowski, G.E. Wnek, D.G. Simpson, G.L. Bowlin, Mechanical properties of electrospun fibrinogen structures, Acta Biomaterialia 2 (1) (2006) 19–28.
[156] S.A. Sell, M.P. Francis, K. Garg, M.J. McClure, D.G. Simpson, G.L. Bowlin, Cross-linking methods of electrospun fibrinogen scaffolds for tissue engineering applications, Biomedical Materials 3 (4) (2008).
[157] I.S. Yeo, J.E. Oh, L. Jeong, T.S. Lee, S.J. Lee, W.H. Park, B.M. Min, Collagen-based biomimetic nanofibrous scaffolds: preparation and characterization of collagen/silk fibroin bicomponent nanofibrous structures, Biomacromolecules 9 (4) (2008) 1106–1116.
[158] Z.X. Cai, X.M. Mo, K.H. Zhang, L.P. Fan, A.L. Yin, C.L. He, H.S. Wang, Fabrication of chitosan/silk fibroin composite nanofibers for wound-dressing applications, International Journal of Molecular Sciences 11 (9) (2010) 3529–3539.
[159] S.D. Sarkar, B.L. Farrugia, T.R. Dargaville, S. Dhara, Chitosan-collagen scaffolds with nano/microfibrous architecture for skin tissue engineering, Journal of Biomedical Materials Research Part A 101 (12) (2013) 3482–3492.
[160] N. Naseri, C. Algan, V. Jacobs, M. John, K. Oksman, A.P. Mathew, Electrospun chitosan-based nanocomposite mats reinforced with chitin nanocrystals for wound dressing, Carbohydrate Polymers 109 (2014) 7–15.
[161] R. Augustine, E.A. Dominic, I. Reju, B. Kaimal, N. Kalarikkal, S. Thomas, Electrospun poly(epsilon-caprolactone)-based skin substitutes: in vivo evaluation of wound healing and the mechanism of cell proliferation, Journal of Biomedical Materials Research Part B: Applied Biomaterials 103 (7) (2015) 1445–1454.
[162] J.H. Kim, J.H. Choi, J.Y. Sim, W.C. Jeong, S.M. Yang, S.H. Kim, Ordered packing of emulsion droplets toward the preparation of adjustable photomasks, Langmuir 30 (19) (2014) 5404–5411.
[163] K.T. Kurpinski, J.T. Stephenson, R.R.R. Janairo, H.M. Lee, S. Li, The effect of fiber alignment and heparin coating on cell infiltration into nanofibrous PLLA scaffolds, Biomaterials 31 (13) (2010) 3536–3542.
[164] P.J. Kluger, R. Wyrwa, J. Weisser, J. Maierle, M. Votteler, C. Rode, M. Schnabelrauch, H. Walles, K. Schenke-Layland, Electrospun poly(d/l-lactide-co-l-lactide) hybrid matrix: a novel scaffold material for soft tissue engineering, Journal of Materials Science: Materials in Medicine 21 (9) (2010) 2665–2671.
[165] S.G. Kumbar, S.P. Nukavarapu, R. James, L.S. Nair, C.T. Laurencin, Electrospun poly(lactic acid-co-glycolic acid) scaffolds for skin tissue engineering, Biomaterials 29 (30) (2008) 4100–4107.
[166] K.A. Blackwood, R. McKean, I. Canton, C.O. Freeman, K.L. Franklin, D. Cole, I. Brook, P. Farthing, S. Rimmer, J.W. Haycock, A.J. Ryan, S. MacNeil, Development of biodegradable electrospun scaffolds for dermal replacement, Biomaterials 29 (21) (2008) 3091–3104.
[167] S.J. Kim, D.H. Jang, W.H. Park, B.M. Min, Fabrication and characterization of 3-dimensional PLGA nanofiber/microfiber composite scaffolds, Polymer 51 (6) (2010) 1320–1327.
[168] X.L. Zhu, W.G. Cui, X.H. Li, Y. Jin, Electrospun fibrous mats with high porosity as potential scaffolds for skin tissue engineering, Biomacromolecules 9 (7) (2008) 1795–1801.
[169] K.T. Shalumon, K.H. Anulekha, K.P. Chennazhi, H. Tamura, S.V. Nair, R. Jayakumar, Fabrication of chitosan/poly(caprolactone) nanofibrous scaffold for bone and skin tissue engineering, International Journal of Biological Macromolecules 48 (4) (2011) 571–576.

[170] H.L. Chen, J. Huang, J.H. Yu, S.Y. Liu, P. Gu, Electrospun chitosan-graft-poly (epsilon-caprolactone)/poly (epsilon-caprolactone) cationic nanofibrous mats as potential scaffolds for skin tissue engineering, International Journal of Biological Macromolecules 48 (1) (2011) 13–19.
[171] F. Croisier, G. Atanasova, Y. Poumay, C. Jerome, Polysaccharide-coated PCL nanofibers for wound dressing applications, Advanced Healthcare Materials 3 (12) (2014) 2032–2039.
[172] C.Y. Huang, X.L. Fu, J. Liu, Y.M. Qi, S.H. Li, H.J. Wang, The involvement of integrin beta 1 signaling in the migration and myofibroblastic differentiation of skin fibroblasts on anisotropic collagen-containing nanofibers, Biomaterials 33 (6) (2012) 1791–1800.
[173] N. Krithica, V. Natarajan, B. Madhan, P.K. Sehgal, A.B. Mandal, Type I collagen immobilized poly(caprolactone) nanofibers: characterization of surface modification and growth of fibroblasts, Advanced Engineering Materials 14 (4) (2012) B149–B154.
[174] J. Venugopal, S. Ramakrishna, Biocompatible nanofiber matrices for the engineering of a dermal substitute for skin regeneration, Tissue Engineering 11 (5–6) (2005) 847–854.
[175] Y.Z. Zhang, J. Venugopal, Z.M. Huang, C.T. Lim, S. Ramakrishna, Characterization of the surface biocompatibility of the electrospun PCL-collagen nanofibers using fibroblasts, Biomacromolecules 6 (5) (2005) 2583–2589.
[176] H.M. Powell, S.T. Boyce, Engineered human skin fabricated using electrospun collagen-PCL blends: morphogenesis and mechanical properties, Tissue Engineering Part A 15 (8) (2009) 2177–2187.
[177] X.L. Fu, M. Xu, J. Liu, Y.M. Qi, S.H. Li, H.J. Wang, Regulation of migratory activity of human keratinocytes by topography of multiscale collagen-containing nanofibrous matrices, Biomaterials 35 (5) (2014) 1496–1506.
[178] B.N. Blackstone, J.W. Drexler, H.M. Powell, Tunable engineered skin mechanics via coaxial electrospun fiber core diameter, Tissue Engineering Part A 20 (19–20) (2014) 2746–2755.
[179] B. Feng, H.C. Duan, W. Fu, Y.L. Cao, W.J. Zhang, Y.Z. Zhang, Effect of inhomogeneity of the electrospun fibrous scaffolds of gelatin/polycaprolactone hybrid on cell proliferation, Journal of Biomedical Materials Research Part A 103 (2) (2015) 431–438.
[180] S. Gautam, C.F. Chou, A.K. Dinda, P.D. Potdar, N.C. Mishra, Surface modification of nanofibrous polycaprolactone/gelatin composite scaffold by collagen type I grafting for skin tissue engineering, Materials Science & Engineering C-Materials for Biological Applications 34 (2014) 402–409.
[181] Y.J. Li, F. Chen, J. Nie, D.Z. Yang, Electrospun poly(lactic acid)/chitosan core-shell structure nanofibers from homogeneous solution, Carbohydrate Polymers 90 (4) (2012) 1445–1451.
[182] K.T. Shalumon, D. Sathish, S.V. Nair, K.P. Chennazhi, H. Tamura, R. Jayakumar, Fabrication of aligned poly(lactic acid)-chitosan nanofibers by novel parallel blade collector method for skin tissue engineering, Journal of Biomedical Nanotechnology 8 (3) (2012) 405–416.
[183] E. Hoveizi, M. Nabiuni, K. Parivar, S. Rajabi-Zeleti, S. Tavakol, Functionalisation and surface modification of electrospun polylactic acid scaffold for tissue engineering, Cell Biology International 38 (1) (2014) 41–49.
[184] S.H. Chen, Y. Chang, K.R. Lee, J.Y. Lai, A three-dimensional dual-layer nano/microfibrous structure of electrospun chitosan/poly(D,L-lactide) membrane for the improvement of cytocompatibility, Journal of Membrane Science 450 (2014) 224–234.
[185] G.R. Jin, M.P. Prabhakaran, S. Ramakrishna, Stem cell differentiation to epidermal lineages on electrospun nanofibrous substrates for skin tissue engineering, Acta Biomaterialia 7 (8) (2011) 3113–3122.
[186] A.R. Chandrasekaran, J. Venugopal, S. Sundarrajan, S. Ramakrishna, Fabrication of a nanofibrous scaffold with improved bioactivity for culture of human dermal fibroblasts for skin regeneration, Biomedical Materials 6 (1) (2011).
[187] L.L. Wu, H. Li, S. Li, X.R. Li, X.Y. Yuan, X.L. Li, Y. Zhang, Composite fibrous membranes of PLGA and chitosan prepared by coelectrospinning and coaxial electrospinning, Journal of Biomedical Materials Research Part A 92A (2) (2010) 563–574.

[188] Y. Yang, X.L. Zhu, W.G. Cui, X.H. Li, Y. Jin, Electrospun composite mats of poly (D,L-lactide)-co-glycolide and collagen with high porosity as potential scaffolds for skin tissue engineering, Macromolecular Materials and Engineering 294 (9) (2009) 611–619.
[189] S.J. Liu, Y.C. Kau, C.Y. Chou, J.K. Chen, R.C. Wu, W.L. Yeh, Electrospun PLGA/collagen nanofibrous membrane as early-stage wound dressing, Journal of Membrane Science 355 (1–2) (2010) 53–59.
[190] R.A. Franco, T.H. Nguyen, B.T. Lee, Preparation and characterization of electrospun PCL/PLGA membranes and chitosan/gelatin hydrogels for skin bioengineering applications, Journal of Materials Science: Materials in Medicine 22 (10) (2011) 2207–2218.
[191] S. Wang, M.L. Jia, W.Y. Yeong, Smart Hydrogels for 3D Bioprinting, 2015.
[192] J. Malda, J. Visser, F.P. Melchels, T. Jungst, W.E. Hennink, W.J.A. Dhert, J. Groll, D.W. Hutmacher, 25th anniversary article: engineering hydrogels for biofabrication, Advanced Materials 25 (36) (2013) 5011–5028.
[193] M. Nakamura, S. Iwanaga, C. Henmi, K. Arai, Y. Nishiyama, Biomatrices and biomaterials for future developments of bioprinting and biofabrication, Biofabrication 2 (1) (2010).
[194] S.V. Murphy, A. Skardal, A. Atala, Evaluation of hydrogels for bio-printing applications, Journal of Biomedical Materials Research Part A 101 (1) (2013) 272–284.
[195] P. Bianco, P.G. Robey, Stem cells in tissue engineering, Nature 414 (6859) (2001) 118–121.
[196] J.G. Rheinwald, H. Green, Serial cultivation of strains of human epidermal keratinocytes: the formation of keratinizing colonies from single cells, Cell 6 (3) (1975) 331–343.
[197] J.G. Rheinwald, H. Green, Epidermal growth factor and the multiplication of cultured human epidermal keratinocytes, Nature 265 (5593) (1977) 421–424.
[198] L. Alonso, E. Fuchs, Stem cells in the skin: waste not, Wnt not, Genes & Development 17 (10) (2003) 1189–1200.
[199] L. Lootens, N. Brusselaers, H. Beele, S. Monstrey, Keratinocytes in the treatment of severe burn injury: an update, International Wound Journal 10 (1) (2013) 6–12.
[200] C.H. Fang, E.C. Robb, G.S. Yu, J.W. Alexander, G.D. Warden, Observations on stability and contraction of composite skin grafts: xenodermis or allodermis with an isograft overlay, Journal of Burn Care & Rehabilitation 11 (6) (1990) 538–542.
[201] E. Lineen, N. Namias, Biologic dressing in burns, Journal of Craniofacial Surgery 19 (4) (2008) 923–928.
[202] E. Middelkoop, A.J. van den Bogaerdt, E.N. Lamme, M.J. Hoekstra, K. Brandsma, M.M.W. Ulrich, Porcine wound models for skin substitution and burn treatment, Biomaterials 25 (9) (2004) 1559–1567.
[203] C.A. Harrison, S. MacNeil, The mechanism of skin graft contraction: an update on current research and potential future therapies, Burns 34 (2) (2008) 153–163.
[204] S.T. Boyce, E.E. Medrano, Z. Abdelmalek, A.P. Supp, J.M. Dodick, J.J. Nordlund, G.D. Warden, Pigmentation and inhibition of wound contraction by cultured skin substitutes with adult melanocytes after transplantation to athymic mice, Journal of Investigative Dermatology 100 (4) (1993) 360–365.
[205] C.O. Duncan, R.M. Shelton, H. Navsaria, D.S. Balderson, R.P.G. Papini, J.E. Barralet, In vitro transfer of keratinocytes: comparison of transfer fibrin membrane and delivery by aerosol spray, Journal of Biomedical Materials Research Part B: Applied Biomaterials 73B (2) (2005) 221–228.
[206] A.D. Metcalfe, M.W.J. Ferguson, Skin stem and progenitor cells: using regeneration as a tissue-engineering strategy, Cellular and Molecular Life Sciences 65 (1) (2008) 24–32.
[207] K.J.L. Fernandes, I.A. McKenzie, P. Mill, K.M. Smith, M. Akhavan, F. Barnabe-Heider, J. Biernaskie, A. Junek, N.R. Kobayashi, J.G. Toma, D.R. Kaplan, P.A. Labosky, V. Rafuse, C.C. Hui, F.D. Miller, A dermal niche for multipotent adult skin-derived precursor cells, Nature Cell Biology 6 (11) (2004) 1082–1093.
[208] S.B. Mahjour, F. Ghaffarpasand, H.J. Wang, Hair follicle regeneration in skin grafts: current concepts and future perspectives, Tissue Engineering Part B Reviews 18 (1) (2012) 15–23.
[209] P. Mistriotis, S.T. Andreadis, Hair follicle: a novel source of multipotent stem cells for tissue engineering and regenerative medicine, Tissue Engineering Part B Reviews 19 (4) (2013) 265–278.

[210] C.P. Zhang, X.B. Fu, Therapeutic potential of stem cells in skin repair and regeneration, Chinese Journal of Traumatology 11 (4) (2008) 209–221.
[211] A. Charruyer, R. Ghadially, Stem cells and tissue-engineered skin, Skin Pharmacology and Physiology 22 (2) (2009) 55–62.
[212] G. Ferrari, G. Cusella-De Angelis, M. Coletta, E. Paolucci, A. Stornaiuolo, G. Cossu, F. Mavilio, Muscle regeneration by bone marrow derived myogenic progenitors, Science 279 (5356) (1998) 1528–1530.
[213] E. Gussoni, Y. Soneoka, C.D. Strickland, E.A. Buzney, M.K. Khan, A.F. Flint, L.M. Kunkel, R.C. Mulligan, Dystrophin expression in the mdx mouse restored by stem cell transplantation, Nature 401 (6751) (1999) 390–394.
[214] D.A. Peterson, Stem cells in brain plasticity and repair, Current Opinion in Pharmacology 2 (1) (2002) 34–42.
[215] A.B. Dababneh, I.T. Ozbolat, Bioprinting technology: a current state-of-the-art review, Journal of Manufacturing Science and Engineering-Transactions of the ASME 136 (6) (2014).
[216] J.A. Barron, P. Wu, H.D. Ladouceur, B.R. Ringeisen, Biological laser printing: a novel technique for creating heterogeneous 3-dimensional cell patterns, Biomedical Microdevices 6 (2) (2004) 139–147.
[217] F. Guillemot, A. Souquet, S. Catros, B. Guillotin, J. Lopez, M. Faucon, B. Pippenger, R. Bareille, M. Remy, S. Bellance, P. Chabassier, J.C. Fricain, J. Amedee, High-throughput laser printing of cells and biomaterials for tissue engineering, Acta Biomaterialia 6 (7) (2010) 2494–2500.
[218] W. Wang, Y. Huang, M. Grujicic, D.B. Chrisey, Study of impact-induced mechanical effects in cell direct writing using smooth particle hydrodynamic method, Journal of Manufacturing Science and Engineering-Transactions of the ASME 130 (2) (2008).
[219] J.A. Barron, B.R. Ringeisen, H.S. Kim, B.J. Spargo, D.B. Chrisey, Application of laser printing to mammalian cells, Thin Solid Films 453 (2004) 383–387.
[220] B. Guillotin, A. Souquet, S. Catros, M. Duocastella, B. Pippenger, S. Bellance, R. Bareille, M. Remy, L. Bordenave, J. Amedee, F. Guillemot, Laser assisted bioprinting of engineered tissue with high cell density and microscale organization, Biomaterials 31 (28) (2010) 7250–7256.
[221] R. Gaebel, N. Ma, J. Liu, J.J. Guan, L. Koch, C. Klopsch, M. Gruene, A. Toelk, W.W. Wang, P. Mark, F. Wang, B. Chichkov, W.Z. Li, G. Steinhoff, Patterning human stem cells and endothelial cells with laser printing for cardiac regeneration, Biomaterials 32 (35) (2011) 9218–9230.
[222] M. Nakamura, A. Kobayashi, F. Takagi, A. Watanabe, Y. Hiruma, K. Ohuchi, Y. Iwasaki, M. Horie, I. Morita, S. Takatani, Biocompatible inkjet printing technique for designed seeding of individual living cells, Tissue Engineering 11 (11–12) (2005) 1658–1666.
[223] T. Xu, C.A. Gregory, P. Molnar, X. Cui, S. Jalota, S.B. Bhaduri, T. Boland, Viability and electrophysiology of neural cell structures generated by the inkjet printing method, Biomaterials 27 (19) (2006) 3580–3588.
[224] H. Geckil, F. Xu, X.H. Zhang, S. Moon, U. Demirci, Engineering hydrogels as extracellular matrix mimics, Nanomedicine 5 (3) (2010) 469–484.
[225] P.G. Campbell, L.E. Weiss, Tissue engineering with the aid of inkjet printers, Expert Opinion on Biological Therapy 7 (8) (2007) 1123–1127.
[226] T. Xu, J. Jin, C. Gregory, J.J. Hickman, T. Boland, Inkjet printing of viable mammalian cells, Biomaterials 26 (1) (2005) 93–99.
[227] H. Yamazoe, T. Tanabe, Cell micropatterning on an albumin-based substrate using an inkjet printing technique, Journal of Biomedical Materials Research Part A 91A (4) (2009) 1202–1209.
[228] C. Norotte, F.S. Marga, L.E. Niklason, G. Forgacs, Scaffold-free vascular tissue engineering using bioprinting, Biomaterials 30 (30) (2009) 5910–5917.
[229] C.M. Smith, A.L. Stone, R.L. Parkhill, R.L. Stewart, M.W. Simpkins, A.M. Kachurin, W.L. Warren, S.K. Williams, Three-dimensional bioassembly tool for generating viable tissue-engineered constructs, Tissue Engineering 10 (9–10) (2004) 1566–1576.

[230] A. Skardal, J.X. Zhang, L. McCoard, X.Y. Xu, S. Oottamasathien, G.D. Prestwich, Photocrosslinkable hyaluronan-gelatin hydrogels for two-step bioprinting, Tissue Engineering Part A 16 (8) (2010) 2675–2685.
[231] A. Skardal, J.X. Zhang, G.D. Prestwich, Bioprinting vessel-like constructs using hyaluronan hydrogels crosslinked with tetrahedral polyethylene glycol tetracrylates, Biomaterials 31 (24) (2010) 6173–6181.
[232] Y.B. Lee, S. Polio, W. Lee, G.H. Dai, L. Menon, R.S. Carroll, S.S. Yoo, Bio-printing of collagen and VEGF-releasing fibrin gel scaffolds for neural stem cell culture, Experimental Neurology 223 (2) (2010) 645–652.
[233] S. Moon, S.K. Hasan, Y.S. Song, F. Xu, H.O. Keles, F. Manzur, S. Mikkilineni, J.W. Hong, J. Nagatomi, E. Haeggstrom, A. Khademhosseini, U. Demirci, Layer by layer three-dimensional tissue epitaxy by cell-laden hydrogel droplets, Tissue Engineering Part C Methods 16 (1) (2010) 157–166.
[234] K. Jakab, C. Norotte, B. Damon, F. Marga, A. Neagu, C.L. Besch-Williford, A. Kachurin, K.H. Church, H. Park, V. Mironov, R. Markwald, G. Vunjak-Novakovic, G. Forgacs, Tissue engineering by self-assembly of cells printed into topologically defined structures, Tissue Engineering Part A 14 (3) (2008) 413–421.
[235] C.M. Smith, J.J. Christian, W.L. Warren, S.K. Williams, Characterizing environmental factors that impact the viability of tissue-engineered constructs fabricated by a direct-write bioassembly tool, Tissue Engineering 13 (2) (2007) 373–383.
[236] I.T. Ozbolat, Y. Yu, Bioprinting toward organ fabrication: challenges and future trends, IEEE Transactions on Biomedical Engineering 60 (3) (2013) 691–699.
[237] A. Arslan-Yildiz, R. El Assal, P. Chen, S. Guven, F. Inci, U. Demirci, Towards artificial tissue models: past, present, and future of 3D bioprinting, Biofabrication 8 (1) (2016).
[238] E. Cukierman, R. Pankov, D.R. Stevens, K.M. Yamada, Taking cell-matrix adhesions to the third dimension, Science 294 (5547) (2001) 1708–1712.
[239] E. Cukierman, R. Pankov, K.M. Yamada, Cell interactions with three-dimensional matrices, Current Opinion in Cell Biology 14 (5) (2002) 633–639.
[240] D.B. Edelman, E.W. Keefer, A cultural renaissance: in vitro cell biology embraces three-dimensional context, Experimental Neurology 192 (1) (2005) 1–6.
[241] M. Gruene, C. Unger, L. Koch, A. Deiwick, B. Chichkov, Dispensing pico to nanolitre of a natural hydrogel by laser-assisted bioprinting, BioMedical Engineering Online 10 (2011).
[242] B.R. Ringeisen, C.M. Othon, J.A. Barron, D. Young, B.J. Spargo, Jet-based methods to print living cells, Biotechnology Journal 1 (9) (2006) 930–948.
[243] N.R. Schiele, D.T. Corr, Y. Huang, N.A. Raof, Y.B. Xie, D.B. Chrisey, Laser-based direct-write techniques for cell printing, Biofabrication 2 (3) (2010).
[244] L. Koch, A. Deiwick, S. Schlie, S. Michael, M. Gruene, V. Coger, D. Zychlinski, A. Schambach, K. Reimers, P.M. Vogt, B. Chichkov, Skin tissue generation by laser cell printing, Biotechnology and Bioengineering 109 (7) (2012) 1855–1863.
[245] S. Michael, H. Sorg, C.T. Peck, L. Koch, A. Deiwick, B. Chichkov, P.M. Vogt, K. Reimers, Tissue engineered skin substitutes created by laser-assisted bioprinting form skin-like structures in the dorsal skin fold chamber in mice, Plos One 8 (3) (2013).
[246] L. Koch, S. Kuhn, H. Sorg, M. Gruene, S. Schlie, R. Gaebel, B. Polchow, K. Reimers, S. Stoelting, N. Ma, P.M. Vogt, G. Steinhoff, B. Chichkov, Laser printing of skin cells and human stem cells, Tissue Engineering Part C Methods 16 (5) (2010) 847–854.
[247] W. Lee, J.C. Debasitis, V.K. Lee, J.H. Lee, K. Fischer, K. Edminster, J.K. Park, S.S. Yoo, Multi-layered culture of human skin fibroblasts and keratinocytes through three-dimensional freeform fabrication, Biomaterials 30 (8) (2009) 1587–1595.
[248] V. Lee, G. Singh, J.P. Trasatti, C. Bjornsson, X.W. Xu, T.N. Tran, S.S. Yoo, G.H. Dai, P. Karande, Design and fabrication of human skin by three-dimensional bioprinting, Tissue Engineering Part C Methods 20 (6) (2014) 473–484.

[249] G. Kim, S. Ahn, H. Yoon, Y. Kim, W. Chun, A cryogenic direct-plotting system for fabrication of 3D collagen scaffolds for tissue engineering, Journal of Materials Chemistry 19 (46) (2009) 8817−8823.
[250] G. Kim, S. Ahn, Y. Kim, Y. Cho, W. Chun, Coaxial structured collagen-alginate scaffolds: fabrication, physical properties, and biomedical application for skin tissue regeneration, Journal of Materials Chemistry 21 (17) (2011) 6165−6172.
[251] L. Leng, S. Amini-Nik, Q. Ba, M. Jeschke, A. Günther, Skin Printer: Microfluidic Approach for Skin Regeneration and Wound Dressings, 2013.
[252] L. Leng, A. McAllister, B.Y. Zhang, M. Radisic, A. Gunther, Mosaic hydrogels: one-step formation of multiscale soft materials, Advanced Materials 24 (27) (2012) 3650−3658.
[253] K.W. Binder, J.J. Yoo, S.S. Soker, M. Lively, Walker, In Situ Bioprinting of the Skin by, Dissertations & Theses-Gradworks, 2011.
[254] P. Sofokleous, E. Stride, W. Bonfield, M. Edirisinghe, Design, construction and performance of a portable handheld electrohydrodynamic multi-needle spray gun for biomedical applications, Materials Science & Engineering C-Materials for Biological Applications 33 (1) (2013) 213−223.
[255] S. Amini-Nik, D. Glancy, C. Boimer, H. Whetstone, C. Keller, B.A. Alman, Pax7 expressing cells contribute to dermal wound repair, regulating scar size through a beta-catenin mediated process, Stem Cells 29 (9) (2011) 1371−1379.
[256] R.E. Horch, M.G. Jeschke, G. Spilker, D.N. Herndon, H. Kopp, Treatment of second degree facial burns with allografts - preliminary results, Burns 31 (5) (2005) 597−602.
[257] E. Dupin, G. Calloni, C. Real, A. Gongalves-Trentin, N.M. Le Douarin, Neural crest progenitors and stem cells, Comptes Rendus Biologies 330 (6−7) (2007) 521−529.
[258] W. Asghar, R. El Assal, H. Shafiee, S. Pitteri, R. Paulmurugan, U. Demirci, Engineering cancer microenvironments for in vitro 3-D tumor models, Materials Today 18 (10) (2015) 539−553.
[259] A. Vultur, T. Schanstra, M. Herlyn, The promise of 3D skin and melanoma cell bioprinting, Melanoma Research 26 (2) (2016) 205−206.
[260] A. Skardal, M. Devarasetty, S. Forsythe, A. Atala, S. Soker, A reductionist metastasis-on-a-chip platform for in vitro tumor progression modeling and drug screening, Biotechnology and Bioengineering 113 (9) (2016) 2020−2032.
[261] E. Lee, H.H.G. Song, C.S. Chen, Biomimetic on-a-chip platforms for studying cancer metastasis, Current Opinion in Chemical Engineering 11 (2016) 20−27.

CHAPTER 6

Bioprinting of vascularized tissues

6.1 Introduction

Three-dimensional (3D) printing technology has witnessed rapid strides from being considered a futuristic technology, as it promises to revolutionize clinical practice by making available customized equipment, organ models for surgical practices, organ replacement parts, and drugs, at a pace not witnessed before [1–5]. Though initially this technology was envisioned to provide surgical models and prototypes, scientists have quickly advanced the technology to produce tissue constructs for regenerative medicine; however, large-scale adaptation has still been limited due to the anatomical complexity and compositional (cellular and extracellular) diversity, and vascularization of native tissues [6]. In this respect, though significant advances have been made to recreate the geometric complexity, the concern of developing vascularization within tissue constructs still haunts scientists as the holy grail of tissue engineering [7,8]. In this context, bioprinting emerges as a promising method for fabrication of vascular constructs and vascularized tissues [9].

6.1.1 Anatomy of vascular tissue

The structure of blood vessels is characterized by a concentric layer arrangement; with cellular and noncellular composition of each layer showing distinct variations. The intima, or the innermost layer, contains a monolayer of endothelial cells (ECs) and forms a tight barrier between the vessel lumen and vessel wall. This layer provides nonthrombogenicity and resistance to infections. The basement membrane forms the next layer and is composed of Type IV collagen and laminin. This layer is followed by elastin layer, also known as internal elastic lamina [10]. After intimal layer, the medial layer is composed of Type I and III collagen, along with smooth muscle cells (SMCs). These cells possess coordinated contractile properties, which cause vessel contraction or dilation [11]. Herein, collagen fibers and SMCs are in spiral arrangement along the vessel axis. The medial layer is quite thickened in large arteries and may also contain nervous supply. Further, the medial layer is circumvented by external elastic lamina. The outermost layer is the adventitia, which is composed of fibroblasts rooted on a loose collagen matrix. These layers continually interact with each other in remodeling and perfusion of organs they supply [12]. It is worthwhile to note that while larger vasculature can be identified as

3D Bioprinting in Tissue and Organ Regeneration. https://doi.org/10.1016/B978-0-12-824291-9.00005-1

separate anatomical entities microvessels are structurally and functionally part of the tissue they supply. The microvasculature is composed of three types of vessels namely arterioles, capillaries, and venules, which form a network architecture. The arteries branch down to arterioles, which are typically 10–200 μm in diameter (average lumen diameter being 30 μm) composed of the three tunic layers as found in macrovessels, but with reduction in thickness of these layers. The endothelial lining of tunica intima is intact, while in tunica media, only one or two smooth muscle cell layers are found. The tunica externa also becomes thinner compared to arteries. The arterioles are richly innervated by sympathetic nerves, because of which they can control of blood volume or pressure. The arterioles continue into the capillaries, and the connecting arterioles are referred to as *meta*arterioles. Metarterioles act as precapillary sphincters and lack the true tunica media structures, wherein a single smooth muscle cell encircles the metarteriole-capillary. Capillaries are part of microscopic vessels with lumen diameter of approximately 5–10 μm. In the capillary walls, endothelial layer is surrounded by a basement membrane and generally does not contain any smooth muscle, though pericytes are present to stabilize the wall structure. This structural feature allows reduction in the distance of diffusion for solutes to reach the cells of the tissue. In addition, capillary structure of different tissues may allow different solute permeability, and accordingly capillaries are classified as continuous, fenestrated, or sinusoid capillaries. Found in muscle, skin, lung, central nervous system, basement membrane is continuous and intercellular clefts between adjacent endothelial cells have tight junctions. The fenestrated capillaries contain porous structures and are seen in exocrine glands, renal glomeruli, and intestinal mucosa, while capillaries with large intercellular gaps are observed in liver, spleen, and bone marrow. Sinusoidal capillaries are flattened with incomplete basement membranes and large gaps between cells. Capillaries arising out of a single metarteriole reunite and empty into a venule, which is generally 8–100 μm in diameter. Such multiple venules join to form veins. The venule walls contain an endothelium, a few muscle cells, and elastic fibers in the middle layer, and a thin tunica externa composed of connective tissue fibers [13,14].

6.1.2 Need for the vascular tissue toward fabrication of tissues and organs at the clinically relevant volumes

Since the past two decades, it has been agreed that it is essential to recreate the hierarchical vascular network which can ensure steady perfusion of implant-injury sites for successful engineering of most complex tissues [15]; however, this issue has persisted as a major limitation over years on generating engineered tissues of clinically relevant volumes and complexities [16,17]. Apart from providing diffusion and mass transport of nutrients, substantial evidence also suggest that integration of vascular network also plays a pivotal role in governing tissue formation [18,19]. Additionally, microvascularized tissue constructs would significantly improve clinical outcome with respect to innervations and

complete functional recovery, as indicated by revelation of several cross-talk mechanisms between vascular promoting factors, endothelial cells, and nerve cells [20–23]. Except for tissues, such as avascular cartilage or cornea, wherein vascularization may cause inflammatory reactions [24], engineered constructs with thickness of more than a millimeter do not remain viable without vascularization [25]. Currently, tissue constructs of greater than 200 μm in thickness (the diffusion limit of oxygen from nearest capillaries under in vivo conditions) have little chance of subsequent clinical success in most complex tissues [26]. In highly vascularized tissues, such as liver, kidney, lungs, spleen, heart, pancreas, or thyroid, formation of new blood vessels becomes essential for a tissue to grow beyond the diffusion limit [27,28]. Since most present tissue engineering strategies are evaluated in much smaller volumes than the requirements of larger clinical reconstruction, successful scaling is essential in order to ensure their clinical applicability. For example, in case of liver tissue, there exists a huge demand for tissue construct of clinically relevant volumes (i.e., about 500 cm^3) required of implantable liver with the cell density and functionality being close to native liver tissue [29–31].

Vascular tissue fabrication via the tissue engineering route comprises several approaches depending upon the function required. For one, vascular tissues are required for coronary vessel surgeries. Patients suffering from cardiovascular diseases, like cerebrovascular disease, coronary heart disease, deep vein thrombosis, and peripheral arterial disease, which are associated with vessel blockages and require long-term (life expectancy >2 years) revascularization are principally indicated for vascular replacements like coronary arterial bypass grafting. However, synthetic vascular grafts have satisfactory results documented only for large-diameter (>8 mm) such as aortoiliac or medium-diameter (6–8 mm) carotid or common femoral arteries replacements. Their performance in small-caliber vessels, (<6 mm) like coronary, infrainguinal, or infrageniculate arteries, reconstruction remains poorer compared to the gold standard autologous grafts harvested from internal thoracic or radial artery, and saphenous vein (SV). Thus, the Food and Drugs Administration (FDA) does not approve the synthetic biomaterial-based small-caliber vascular grafts (internal diameter <5 mm) due to poor patency rates though autologous grafting may not be suitable for a large number of patients due to poor quality of donor site. These failures are usually due to intimal hyperplasia, thrombosis, or infections of the graft. Absence of healthy endothelial cell layer, diameter mismatch, synthetic material surface properties, and compliance mismatch with the native tissue are contributory factors to all these mechanisms [32,33]. Bioprinting with suitable endothelial cell source into the diameters required is thus an attractive approach to engineer small diameter blood vessels and has been pursued.

Apart from fabrication of vascular grafts, vascularization is also endeavored to be improved for blood circulation by fabrication of a vascular microcirculatory network at affected regions of other tissues, to encourage vessel ingrowth into implanted constructs

from the host, or to generate new circulation system at the local site through stem cell therapy [34]. In human embryos as well as adult tissues, new vascular networks are formed by two distinct mechanisms known as vasculogenesis and angiogenesis. The former refers to de novo generation of blood vessel from vascular progenitor cells or the capillary plexus formation from circulating endothelial progenitor cells (EPCs), while angiogenesis is used to indicate sprouting of new blood vessels via extension or remodeling from preexisting capillaries. The process of angiogenesis can occur through elongation, inosculation, intussusception, or sprouting. Among them, intussusception involves bifurcation of existing lumen while sprouting is an outcome of multistep processes involving first the resorption of basement membrane, followed by infiltration and growth of ECs, lumen organization, and subsequent formation of vessel with the addition of pericytes. The process of inosculation is important for making connection between the transplanted vascular networks and host microcirculatory network. In the context of tissue engineering, it is observed that EPCs can be expanded ex vivo and transplanted to augment neovascularization for engineering of vascular structures. Further, EPC recruitment can be enhanced by stromal-derived factor-1, and granulocyte colony stimulating factor, among others [35–38]. Thus, vasculogenesis-driven mechanism of vascular tissue engineering can be adopted for bioprinting.

Angiogenesis promoting strategies have focused on either ingrowth of newly formed capillaries inside implanted constructs from the host or achieving a rapid blood supply within engineered constructs by stimulating inosculation with the help of prevascularized constructs [25,39]. After implantation, the prevascularized channels within the constructs develop interconnections with neighboring tissue vessel network to get perfused rapidly. In other approaches, angiogenesis promoting agents like vascular endothelial growth factor (VEGF), fibroblast growth factor (FGF), platelet-derived growth factor (PDGF), and transforming growth factor (TGF), either alone or in codelivery forms, are often employed [40,41]. The recruitment of circulating stem cells into ischemic sites by targeted activation of concerned pathways or by cell seeding into the constructs are other approaches for achieving vascularization. In this respect, Tasso et al. have reported that mesenchymal stem cells (MSCs) seeded into porous cubes resulted in homing of pericytelike cells or circulating endothelial progenitor cells (EPCs) inside engineered constructs after implantation. However, teratoma formation or tumorogenicity of various cell sources, including stem cells, remains unaddressed for standardization of tissue constructs [42]. Other potential sources for vascular cells are adult bone marrow, adipose tissue, hair follicle (HF), umbilical cord (UC), and muscles. Among them, the adipose-derived stem cells (ADSC) are shown to differentiate into multiple cell types of vascular tissue including smooth muscle cells on inducted by transforming growth factor-beta 1 (TGF-β1) or bone morphogenetic protein-4 (BMP-4) and found to be a rich source of endothelial cells. Provided the fact that adipose tissue is routinely harvested during liposuction

procedures, they constitute a promising source for vascular tissue engineering. On the other hand, hair follicles and umbilical cords can also be obtained without invasive procedures and the various stem cells isolated from these sources have shown promising differentiation potential into vascular tissue [43]. Further, newer biological understanding indicates that cellular cross-talk is involved in angiogenesis as well as organ remodeling process [44]. An example is the cross-interaction among ECs, osteoblasts, osteoclasts, and osteoprogenitors, which are mediated by secretion of soluble factors and gap junction proteins like connexin 43. Though it can be concluded that various cells types have been suitably engineered to form microcirculatory networks in vitro as well as implanted in vivo, further comparative assessment of more dynamic properties for extended time periods of intended application like extent of vascularization, remodeling, and regression, would be required [45].

For tissues at clinically relevant volumes, availability of cell sources becomes an important criterion along with current methods of cell expansion to obtain industrial scale cell numbers [46]. It may be noted here that many vascular network forming cell sources (e.g., human umbilical vein endothelial cells (HUVECs)), used in tissue engineering research, are not clinically available and hence more comparative studies are needed with EPCs or MSCs. These have turned the attention to explore alternative sources like autologous circulating EPCs, induced pluripotent stem cells (iPSCs), and postnatal stem cells, which are being continually experimented to produce stable and mature 3D capillary network [47,48]. It is further imperative to note that different tissue engineering techniques have been applied to fabricate blood vessels including traditional methods like solvent-casting [49], particulate leaching [50], gas foaming [51], fiber bonding [52,53], and phase separation [54,55], while electrospinning and self-assembly are also explored to obtain nanofibrous scaffolds [56,57]. These techniques offer sparse control over pore size and shape while also lacking in precision requirement of target architectures. To overcome these limitations, rapid prototyping techniques have been introduced such as vat photopolymerization [58,59], material extrusion [60,61], and sheet lamination [62]. Over conventional or any other techniques, they offer the advantage of high level of scaffold-to-scaffold consistency and the ability to cater to patient-specific geometries [63]. Among them, the principal advantage of bioprinting lies in the ability to directly fabricate heterocellular tissue constructs with ease of modulation of cell densities. This advantage is driving researchers to explore 3D bioprinting techniques at deeper scales to solve the vascularization problem in tissue engineering [64].

6.2 Bioprinting for vascular or vascularized tissue fabrication

In this chapter, we examine the use of bioprinting in blood vessel fabrication as well as for development of vascularized thick tissue constructs. Bioprinting of vascular constructs can

be performed using two main approaches: (i) scaffold-based or (ii) scaffold-free bioprinting. In scaffold-based bioprinting, cells are bioprinted in an exogenous biomaterial (i.e., hydrogel) resembling the target tissue structure, whereas in scaffold-free bioprinting, cells are coaxed to form neotissues and then bioprinted without any scaffold support [65]. In the former approach, living cells are encapsulated within hydrogels or decellularized matrix components. In the latter approach, postbioprinting cellular processes like cell sorting and tissue fusion, which in many ways resemble self-assembly phenomena observed in early embryonic development, are the driving mechanisms in tissue formation [66,67].

6.2.1 Scaffold-based approaches

In the past decade, scaffold-based bioprinting for vascular tissue fabrication has demonstrated significant advances, principally because several hydrogels can be conveniently bioprinted using the three major bioprinting modalities including extrusion-based bioprinting (EBB), droplet-based bioprinting (DBB), and laser-based bioprinting (LBB).

6.2.1.1 Extrusion-based bioprinting of vascular or vascularized constructs

The general principle of this bioprinting modality lies in continuous extrusion and writing as per a predetermined program [68,69]. During extrusion, the bioink, in form of cells encapsulated in cylindrical filaments, is deposited in a precise manner into targeted 3D custom-shaped structures. Tubular structures within core-shell morphologies like alginate shell and a poly(lactic-co-glycolic acid) (PLGA) core are conveniently fabricated for drug delivery applications using EBB [70]. For EBB, shear-thinning hydrogels, which can flow out of the nozzle at physiological temperatures, are preferred as the feeding material [71]. Ideally, the bioink should remain stable in the reservoir during the time of bioprinting and as it is extruded through the nozzle, the viscosity must decrease as a function of increased shear stresses in order to be extruded in the form of a filament. After extrusion, physical- or chemical-cross-linking takes place to facilitate rapid solidification to ensure geometrical fidelity of bioprinted constructs. These requirements put a demanding challenge on choice of bioinks [72]. Early attempts on bioprinting vascular tissue using EBB were reported by Smith et al., who utilized a commercial 3D printer containing two separate cold (2−10°C) cellular solutions of either bovine aortic endothelial cells (BAECs) suspended in Type I collagen and human fibroblasts in Pluronic-F127. Cell suspensions were bioprinted on a substrate allowing thermal gelation mechanism to take place [73]. Smith and colleagues further demonstrated five-layered arterial constructs using BAECs suspended in Type I collagen [74]. Other initial attempts described a bioink composed of magnetic nanoparticles, which were used to control creation of vessels within tissues by applying an

external magnetic field [75]. Gradually, EBB efforts for tissue engineering have evolved into direct and indirect extrusion.

6.2.1.1.1 Direct extrusion

In this method, cell-laden hydrogels are directly bioprinted as per desired vascular shapes and structures. After bioprinting, the bioink is solidified in a cell-friendly environment yielding rigid constructs followed by cellular proliferation and tissue remodeling. Bioink characteristics, including the cross-linking mechanism, shear-thinning properties, and biological and chemical properties of the bioink, are some of the important determinants of cell viability [76]. Early efforts on direct extrusion approach were reflected in a study reported by Li et al., who showed a method in which the vertical organization of hollow channels was feasible by use of different combinations of gelatin, alginate, chitosan, and fibrinogen hydrogels [77]. They extruded the composite bioink using a dual-nozzle assembly in a 6–8°C cooling chamber, allowing sol-gel transition of gelatin followed by cross-linking of other materials using cross-linking agents such as thrombin, calcium chloride ($CaCl_2$), and glutaraldehyde for fibrinogen, alginate, and chitosan, respectively. The authors first used a digital model to design a biomimetic liver construct, and bioprinted ADSCs in gelatin/alginate/fibrinogen composite gel to form vascular channels, while hepatocytes in gelatin/alginate/chitosan composite gel were bioprinted around the vascular constructs to form the liver channel. Bioartificial vessellike grafts employing the Fab@Home printing system were demonstrated by Skardal et al. using tetrahedral pentaerythritol derivatives of polyethylene glycol (PEG) with varying PEG chain lengths [78,79]. Multifunctionalized polymers were used to co-cross-link thiolated hyaluronic acid and gelatin, which were extruded as well. The authors showed bioprinting of NIH 3T3 cells into tubular structures maintaining viability up to 4 weeks and providing strong proof-of-concept for developing vascular constructs.

Some recent reports further demonstrated the potential of direct bioprinting for vascular tissue biofabrication. For example, Tan and Yeong demonstrated the fabrication of tubular alginate constructs in vertical configuration using multiple nozzles [81]. In their work, a circular structure with 6 mm radius was designed as the extrusion route for alginate followed by a secondary concentric loop of 4 mm radius for the dispensing of the cross-linking agent through a microvalve dispenser. Finally, they have constructed scaffolds up to 15 mm in length in the vertical configuration. The important advantage of this method is the feasibility of creating large diameter constructs with further potential to create a branching structure; however, this method still requires further optimization in design to accommodate loss in structural accuracy due to shrinkage after the cross-linking process. Recently, Hinton et al. customized a MakerBot Replicator for precise deposition of bioink solutions, where they termed their 3D bioprinting technique as freeform reversible embedding of suspended hydrogels (FRESH) [80] (Fig. 6.1). Essentially, the authors

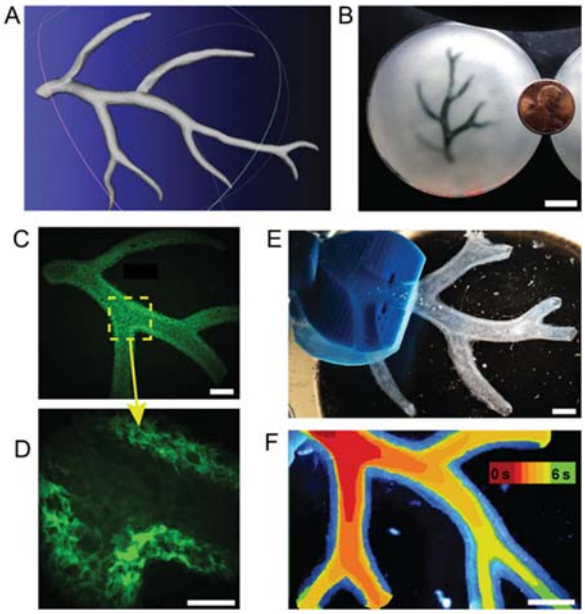

Figure 6.1

(A) A model of a section of a human right coronary arterial tree for bioprinting. (B) A photograph of bioprinted alginate (black) in a gelatin support bath. (C) A section of the arterial trees printed in fluorescent alginate (green) showing the hollow lumen and multiple bifurcations. (D) A zoomed-in view of (C) presenting the defined vessel wall and lumen. (E) An image of the arterial tree mounted in a perfusion fixture. (F) A time-lapsed image of arterial tree when a black dye was perfused through the system in 6 s time frame. *Reproduced/Adapted with permission from T.J. Hinton, Q. Jallerat, R.N. Palchesko, J.H. Park, M.S. Grodzicki, H.-J. Shue, M.H. Ramadan, A.R. Hudson, A.W. Feinberg, Three-dimensional printing of complex biological structures by freeform reversible embedding of suspended hydrogels, Science Advances 1 (9) (2015) e1500758.*

printed bioink solutions within a secondary hydrogel support bath to maintain their structural integrity. The support bath played the role of a Bingham plastic, such that it maintained its rigidity at conditions of low shear stress, but as the shear stress increased, the bath started acting as a viscous fluid. In the context of bioprinting, the support bath allowed unresisted movement of the needle due to high shear, whereas after the extrusion (where there was no shear on the hydrogel), the bioink extruded into the bath was kept from spreading out. The authors demonstrated the direct bioprinting of various bioink combinations comprising of Type I collagen, alginate, and fibrin hydrogels with embedded cells like myoblasts and fibroblasts to create constructs like vascular network.

Another commonly used category of direct extrusion is based on the use of a coaxial nozzle assembly as shown in Fig. 6.2A. Utilizing the concept of wet spinning in bioprinting [82–84], vessellike cellular microfluidic channels in form of hollow filaments

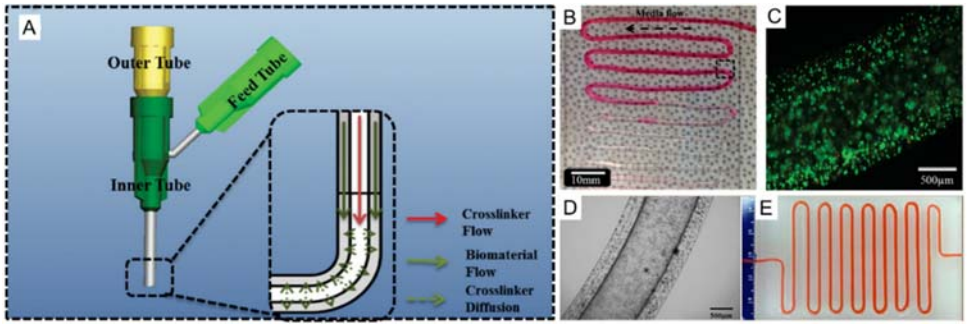

Figure 6.2

Coaxial bioprinting: (A) A schematic illustration of vascular like structures of the coaxial extrusion process, (B) An image of bioprinted alginate microfluidic channels, (C) where cell viability of 63% was achieved after 12 h of media perfusion, (D) An image showing the wall and lumen, and (E) cell media successfully perfused through a meter-long printed conduit. *Reproduced/Adapted with permission from (C) Y. Zhang, Y. Yu, I.T. Ozbolat, Direct bioprinting of vessel-like tubular microfluidic channels, Journal of Nanotechnology in Engineering and Medicine 4 (2) (2013) 020902. (E) F. Dolati, Y. Yu, Y. Zhang, A.M.D. Jesus, E.A. Sander, I.T. Ozbolat, In vitro evaluation of carbon-nanotube-reinforced bioprintable vascular conduits, Nanotechnology 25 (14) (2014) 145101.*

were directly bioprinted by Ozbolat group for the first time in the literature (Fig. 6.2B and C) [85]. In that work, the coaxial nozzle set up consisted of three tubes (feed tube on one hand, and an assembly of outer and inner tubes on other hand). The hydrogel solution flowed through the feed tube into the space between the outer and inner tubes and after contacting the cross-linking solution, gelation took place instantaneously resulting in tubular conduits [86]. The group further showed vascular tissue fabrication with human umbilical vein smooth muscle cells (HUVSMCs) loaded in alginate. The efficacy of conduits to support diffusion process was evaluated through perfusion and permeability experiments. Cell viability was 84% after 7 days of perfusion culture demonstrating the potential of this method [87,88]. To enhance the mechanical properties of vascular conduits, Dolati et al. demonstrated multiwalled carbon nanotube (MWCNT) reinforcement (see Fig. 6.2D and E), which enhanced the tensile strength of bioprinted conduits by about 1.5–2.1 times, depending upon the concentration [89]. Though the authors did not report any significant loss of cell viability due to the reinforcement with cell survival values recovering to 70% after 3 days of post-bioprinting culture, a limited ECM deposition was observed during prolonged in vitro culture. Though perfusable conduits up to submillimeter ranges (in diameter) were successfully demonstrated, further work to obtain typical capillary diameters would definitely make the process more versatile. The coaxial extrusion approach was further advanced by Gao et al., who demonstrated concurrent printing of scaffolds with microchannels [90]. In their work, the dispensing rates and concentrations of sodium alginate and $CaCl_2$ cross-linking solutions were varied to facilitate fusion of adjacent hollow filaments. Bioprinting was performed on

a stage that was lowered such that bioprinted constructs were immersed in a $CaCl_2$ pool and allowed for complete gelation. Hollow filament thus coalesced with previously bioprinted filaments, demonstrating the potential for perfusion in larger-scale tissue constructs. In another study, Selvaganapathy and Attala designed a modified microfluidic printhead, similar to the coaxial nozzle, for generation of complex vascular constructs by printing gel constructs with embedded hollow channels [91]. Their procedure exploited diffusion of calcium ions which allowed only inner alginate layer to be cross-linked instantaneously while peripheral layers were solidified slowly, only after some lateral spread of alginate solution in the space between two tubular channels had taken place, resulting in eventual amalgamation of one strand of tubular construct with other. This one-step strategy allowed the formation of solid gel consisting of hollow tubes embedded inside. The authors found that such unification would occur when adjacent strands were separated up to a distance of 3 mm [91]. The fabricated vascularlike structures were fabricated from extrudable gels such as GelMA with methacrylated hyaluronic acid (HAMA) [91–93]. Recently, using a Novogen MMX Bioprinter loaded with a coaxial nozzle device, GelMA/4-arm poly(ethylene glycol)-tetra-acrylate (PEGTA)/sodium alginate/MSC/HUVEC bioink was extruded into vascular constructs with outer diameter in the range of 500–1500 μm, the inner diameter in the range of 400–1000 μm, and the wall thickness in the range of 60–280 μm [94].

6.2.1.1.2 Indirect extrusion

In indirect extrusion approach, cell-laden hydrogels are first bioprinted as the base material to create tissue constructs; however, in contrast to direct extrusion, the bulk hydrogel additionally contains a sacrificial hydrogel (i.e., alginate, agarose, gelatin, or Pluronic) that can be removed post-printing either by thermal or chemical means [80] while the bulk hydrogel resin undergoes solidification leaving behind the vascular pattern. Indirect extrusion for vascularized tissue bioprinting was illustrated by work on bioprinting with agarose, which was used as a permissive template for the formation of perfusable channels [95]. In that work, fabrication of tissue constructs containing embedded channels inside the hydrogels was successfully demonstrated using GelMA, star poly(ethylene glycol-co-lactide) acrylate (SPELA), poly(ethylene glycol) dimethacrylate (PEGDMA), and poly(ethylene glycol) diacrylate (PEGDA) polymers. The tissue constructs embedded with microchannels exhibited significantly higher cell viability (>90%) compared to slab hydrogels (60%) while CD31 immunostaining was performed to show formation of endothelial cell monolayers within perfusable channels [95] pace (Fig. 6.3). Using the identical methodology, a thrombosis-on-chip model has been demonstrated in which Pluronic sacrificial microchannels were coated with HUVEC and/or fibroblasts, and embedded within GelMA hydrogels. It was demonstrated that fibroblasts coated in GelMA migrated into the clot and deposited collagen Type I when the endothelium was damaged [96].

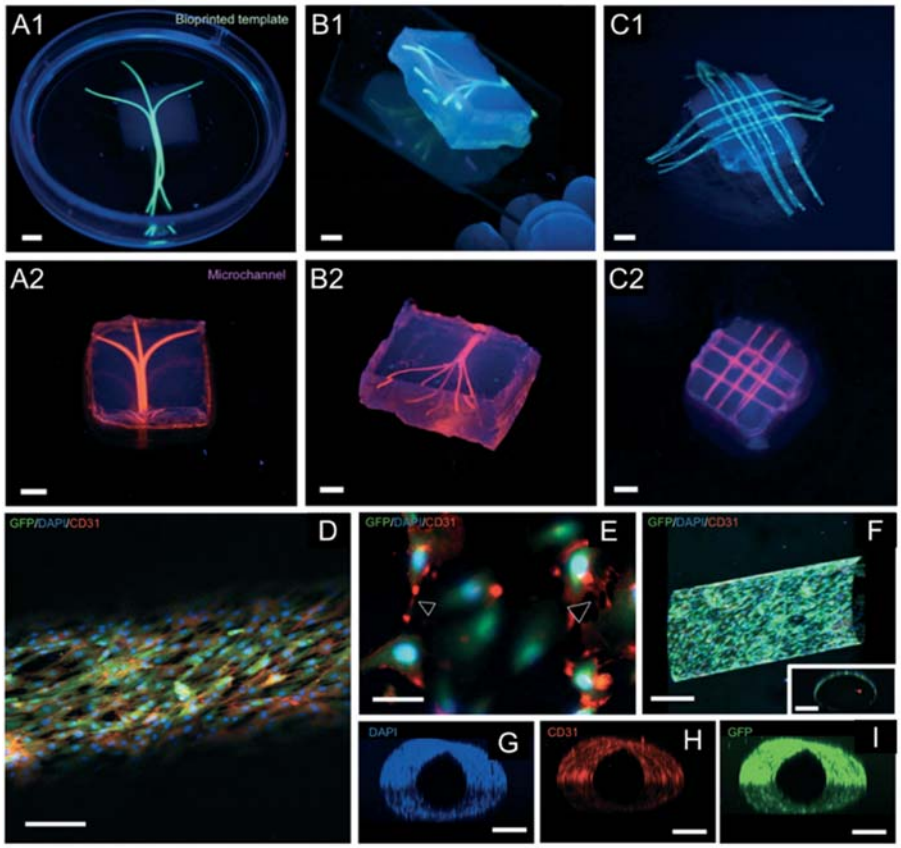

Figure 6.3

(A–C) Images of different bioprinted templates (green, A1, B1, and C1) enclosed in GelMA hydrogels and the respective microchannels perfused with a fluorescent microbead suspension (pink, A2, B2, and C2). (D) Confocal image of GFP/DAPI/CD31 markers from a HUVEC monolayer inside a channel. (E) Higher magnification fluorescence image of DAPI and CD31-stained GFP-expressing HUVECs illustrating the cell–cell interactions (arrowheads) along the endothelial monolayer. (F) Longitudinal view of z-stacked confocal images of a HUVEC-lined microchannel. (G–I) Perpendicular views of z-stacked DAPI, CD31, and GFP markers illustrating the complete lining of the microchannel lumen. *Reproduced/Adapted with permission from L.E. Bertassoni, M. Cecconi, V. Manoharan, M. Nikkhah, J. Hjortnaes, A.L. Cristino, G. Barabaschi, D. Demarchi, M.R. Dokmeci, Y. Yang, A. Khademhosseini, Hydrogel bioprinted microchannel networks for vascularization of tissue engineering constructs, Lab on a Chip 14 (13) (2014) 2202–2211.*

In a related procedure, but using filament printing technology using a dual-syringe extruder with a heated print-head, cell containing complex structures were bioprinted [97]. In their work, human MSC-loaded alginate-gelatin hydrogels were bioprinted by extruding the bioink at 40°C onto a glass substrate maintained at a lower (10°C) temperature. They created hollow channels through leaching of the support material (gelatin). Bioprinting

was performed in two orientations (horizontal and vertical) to find out the effect on the geometry of printed constructs. It was found that vertical alignment orientation produced a larger cross-sectional area than horizontal orientation. Indirect extrusion was demonstrated with Pluronic F127 as an aqueous fugitive ink which can be conveniently bioprinted as well as easily removed. The authors showed long-term perfusion of thick vascularized constructs, which were printed on a 3D perfusable chip [98].

6.2.1.2 Droplet-based bioprinting of vascular or vascularized constructs

In this bioprinting modality, the bioink, which is made up of living cells in culture media or hydrogels, is deposited in the form of droplets with precise position control by use of a noncontact bioprinting approach [99,100]. Typically, each droplet contains about a few cells. Thermal-, electrostatic- and piezoelectric-drop-on-demand technologies have been the most widely used approaches among different types of DBB techniques [101,102]. In thermal inkjet bioprinting, bioink droplets are generated by inducing small current to a heating element over a short time interval. The heating results in formation of a bubble, which collapses to provide pressure pulses required for ejection of the bioink from a chamber through a nozzle [103], where the droplet size is determined by the frequency of current pulses, temperature gradient, and viscosity of the bioink, and may vary from 10 to 150 pL [104,105]. In piezoelectric inkjet bioprinting, the current is rather applied to a piezoelectric actuator, which is typically made up of polycrystalline ceramic [106]. As the electric energy is converted to the mechanical energy, the piezocrystal vibrates and provides a transient pressure, which drives the ejection of the bioink through the nozzle orifice. In inkjet bioprinting, thermal or mechanical stresses are experienced at the nozzle tip during the droplet formation [107]. Thus, cell survival may be affected by the heat shock or membrane disruption [104,108,109]. The other principle of DBB is microvalve bioprinting, in which the bioink is contained in a pressurized fluid chamber whereas an electromechanical valve (consisting of a solenoid coil and a plunger) is turned on or off as per demand. In response to voltage pulses, the solenoid generates a magnetic field causing the plunger to be pulled, opening the nozzle orifice and generating droplets. In DBB techniques, the printhead can be positioned over the printing bed releasing bioink droplets in a desired pattern with high accuracy [99].

6.2.1.2.1 Direct bioprinting of vascular constructs using DBB

In this approach, tubular structures are bioprinted directly as per design. Initial work with this bioprinting technique was performed for vertical constructs, in which the direction of movement of the nozzle is circumferential to the axis of bioprinted tubular structures. Three-dimensional bioprinting of horizontal tubular structures with high shape fidelity has been made possible by accounting for the concavity distortions of the shape in a stepwise manner, as shown for alginate channels [110]. One of the pioneering studies using inkjet bioprinting to fabricate tubular hydrogel constructs was published by Kesari et al. [111]. In

their study, hematopoietic stem cells were entrapped in hydrogels, and cross-linked on demand to produce the patterns in liquid media using a modified Hewlett Packard (HP) printer. The authors were able to differentiate these cells into multiple lineages. In an extension of that work, Boland et al. showed that multiple layers of cells and alginic gel with uniform pore sizes could be obtained conforming to designed architectures [112]. A bioink solution composed of human microvascular endothelial cells (HMVECs) in fibrin was also utilized for fabrication of microvessel constructs using a modified thermal inkjet printer (HP Deskjet 500) by Cui and Boland [113]. Fifty firing nozzles were mounted on the printhead and simultaneously deposited HMVECs and fibrin at droplet volumes of 130 pL, and used fibrinogen, thrombin, and Ca^{2+} for rapid solidification of gel post-bioprinting. After a week culture, HMVECs showed proliferation along the printed patterns and established cell–cell adhesions. Confluent lining with good cell alignment and integrity of the printed structure was observed after 21 days giving rise to branched tubular structures mimicking capillaries. By modifying this method with electrostatic printhead, Nakamura et al. demonstrated fabrication of fibers and tubes by expulsion of alginate solutions into a $CaCl_2$ pool, which resulted in formation of well-defined tubes due to rapid diffusion of Ca^{+2} into alginate solution. This method allowed superior control over tubular conduits, which ranged from 35 to 40 μm in wall thickness and 30–200 μm in inner diameter [114–117].

Xu and coworkers have recently demonstrated fabrication of zigzag tubes using a piezo-inkjet head [118,119]. They fabricated alginate conduits using $CaCl_2$ as a complementary support material with hemibranching bifurcations, which is regarded as a milestone work in fabrication of complex anatomically correct vascular constructs [120,121]. Their method utilized $CaCl_2$ solution to provide a buoyancy force so that it can be utilized as both cross-linking agent and support material facilitating successful bioprinting of these constructs. In continuation of their initial results, Christensen et al. [122] have demonstrated both horizontal and vertical vessellike bifurcations, wherein 3T3 fibroblasts maintained more than 90% cell viability after an incubation period of 24 h. Valve-based bioprinting of hollow constructs within a liquid support material composed of high-density fluorocarbon has been reported by other groups as well [123–126]. Fluorocarbon solution enabled submerged bioprinting, wherein high buoyancy force allowed floating of soft hydrogels and overcame the concern of obtaining high aspect ratio constructs, due to the lack of mechanical integrity of hydrogels in conventional approaches. Using this technique, typically 30 mm-long constructs were generated with a cell viability ranging from 96% to 99%, immediately after bioprinting. The same group has extended their earlier work by utilizing contact angle properties of agarose gel to improve the precision of the bioprinting process [127,128].

6.2.1.2.2 Indirect bioprinting of vascular constructs using DBB

Similar to indirect extrusion, in indirect bioprinting of vascular construct using DBB, the sacrificial bioink (i.e., gelatin) is deposited in cylindrical form followed by bioprinting of cell-laden hydrogel layers. The sacrificial material is then liquefied through thermal decross-linking leaving behind tubular channels, while vascularization is obtained by lining endothelial cells within channels. Dai and his coworkers demonstrated this concept by creating perfusable vascular channels using a microvalve bioprinting [129]. The layer-by-layer approach consisted of first printing a block of collagen layer in a flow chamber, over which gelatin was printed in a strand shape and solidified. This step was followed by bioprinting a layer composed of 1:1 mixture of gelatin and HUVECs in a straight pattern and temperature was kept in room temperature to allow solidification of gelatin. More layers of collagen were then bioprinted over the structure followed by liquefaction of gelatin by incubating at 37°C in order to obtain the tubular channels. The flow chamber was then sealed and a gentle flow was started. The bioprinted construct formed a confluent endothelium (Fig. 6.4), while the channel was shown to support the viability of cells which lay up to 5 mm in distance from the channel under physiological flow conditions [129]. The same group also constructed two fluidic channels within fibrin gel and demonstrated angiogenic sprouting in between [17].

6.2.1.3 Laser-based bioprinting of vascular constructs

Laser-based bioprinting efforts can be classified under two main categories including the efforts undertaken using (i) processes based on cell transfer technologies and (ii) processes involving photopolymerization.

The former ones were developed from laser direct-write process [130] and laser-induced forward transfer (LIFT) technologies [131–133]. The important component of LIFT technologies is the laser energy absorbing material that is stimulated on laser irradiation. The energy-absorbing layer (e.g., titanium or gold) on top and the bioink material presenting below it comprise the donor layer and resemble a “ribbon” structure. During bioprinting, laser pulse is focused on a small area between absorbing layer and bioink resulting in subsequent vaporization of a portion of the donor layer, thus causing formation of a high-pressure bubble followed by jet formation [134,135]. The physical mechanism behind this phenomenon has been studied to certain details. Briefly, the absorption of the laser energy results in excitation of the receiving material to a higher vibrational energy state, which can relax to the ground state through mechanism of electron/phonon or phonon/phonon coupling producing localized heat. Localized heat generation then results in vaporization of the bioink and may cause partial or complete volatilization, which in turn causes the focused ejection. Some other mechanisms, like ablation, plasma generation or thermal-acoustic phenomenon may also take place and hence it is necessary to control the laser irradiation parameters precisely [136]. It has been shown that the jet size (around

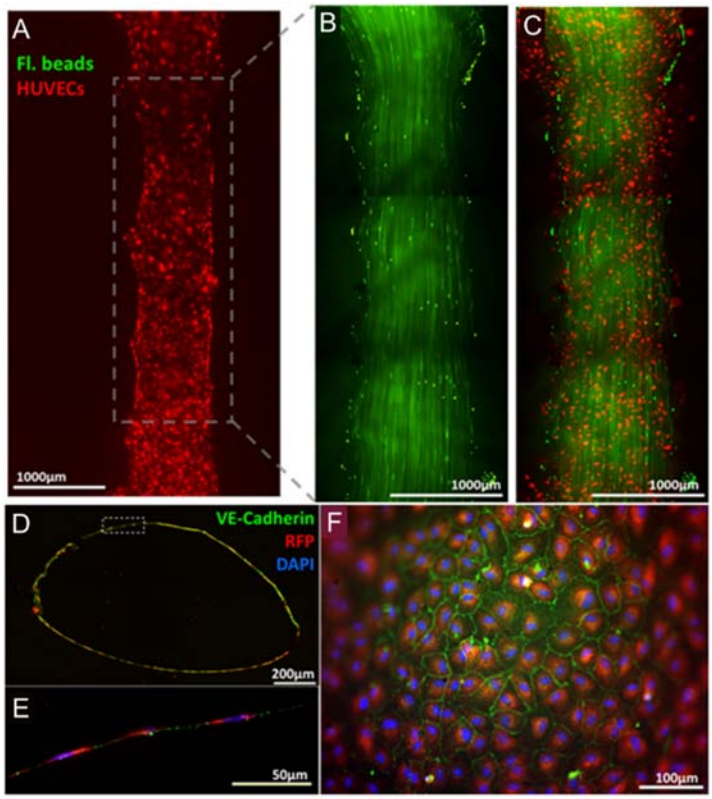

Figure 6.4

(A) A fluorescent image of HUVECs (red) seeded into a bioprinted channel, (B) laminar flow in the channel was represented by green fluorescent beads, and (C) a combined image of green fluorescent beads and seeded HUVECs. (D–E) Cross-section of vascular channel after 5 days of dynamic culture. (F) Fluorescent image of inner surface of vascular channel after 5 days of dynamic culture. blue: DAPI nuclei staining; red: RFP-transfected HUVEC; green: VE-cadherin. *Reproduced/Adapted with permission from V.K. Lee, D.Y. Kim, H. Ngo, Y. Lee, L. Seo, S.-S. Yoo, P.A. Vincent, G. Dai, Creating perfused functional vascular channels using 3D bio-printing technology, Biomaterials 35 (28) (2014) 8092–8102.*

few pL [137]) is governed by the laser pulse energy and the viscosity of the bioink [138], the distance between the collector and donor slide, cell density, bioink wettability, surface tension and the thickness of the bioink [139]. The ejected jets are collected on the receiving layer, which is precoated with gel materials, i.e., alginate and Matrigel, to absorb the energy of the impacting substances and subsequently cross-linked by thermal or ionic cross-linking.

In processes involving photopolymerization (such as traditional stereolithography and dynamic optical projection stereolithography), light-induced reactions (by using ultrafast

laser beams) are employed to polymerize and solidify the irradiated regions on the substrate. The beam path of the laser can be programmed according to a computer-aided design (CAD) model. These light-induced photopolymerization can be carried out in the presence of cells and bioactive molecules providing spatiotemporal control during the formation of tissue constructs [140,141]. After completion of each layer, the porous table moves down for bioprinting of subsequent layers.

In the literature, a limited number of work has been demonstrated in bioprinting of vascular or vascularized tissue, among whom, Wu and Ringeisen designed branch-stem vessel architectures using a laser-based bioprinter exploiting the single HUVEC encapsulation and deposition capabilities [143]. In their investigations, the authors could observe cells formed interconnections among each other within a day. However, these branches had limited stability, which was further improved with the printing of an upper layer of human umbilical vein smooth muscle cells (HUVSMCs) above the HUVEC layer [144]. Potential of LBB was also indicated by Xiong et al., who bioprinted both straight and bifurcated overhang structures using freeform bioprinting of mouse fibroblast-laden sodium alginate, shown in Fig. 6.5 [142]. They observed structurally stable 3D cellular Y-shaped tubes. Post-bioprinting cell survival rates were reported to be above 60% for both types of the tubes. Using biological laser printing (BioLP) platform, Barron et al. [145], Chichkov and coworkers [138], and Ovsianikov et al. [146] independently showed selective seeding of ovine vascular smooth muscle cells and endothelial cells in alginate

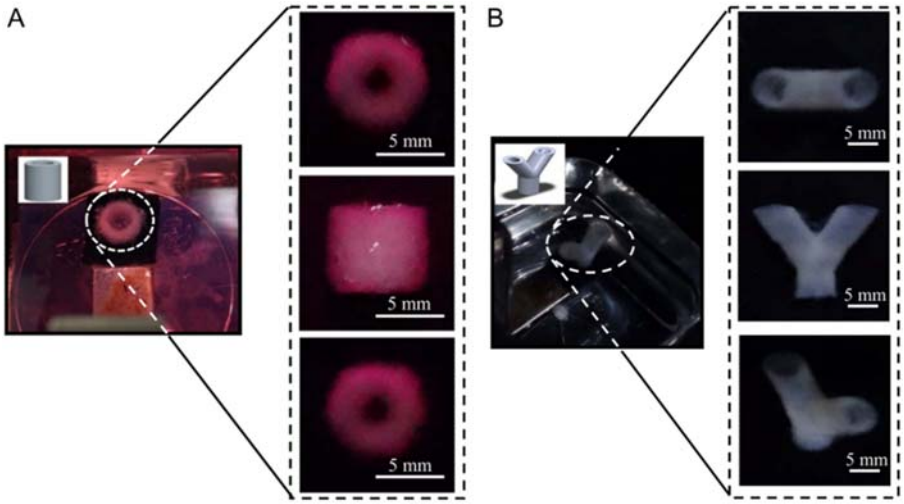

Figure 6.5

(A) Images of bioprinted fibroblast tubes made of 2% alginate loaded with 5×10^6 cells/mL and (B) different views of Y-shaped alginate tubes bioprinted using 8% sodium alginate solution. *Reproduced/Adapted with permission from R. Xiong, Z. Zhang, W. Chai, Y. Huang, D.B. Chrisey, Freeform drop-on-demand laser printing of 3D alginate and cellular constructs, Biofabrication 7 (4) (2015) 045011.*

bioink materials on acrylated PEG scaffolds. Similarly, HUVECs and human MSCs were also bioprinted on a polyester urethane urea (PEUU) patch for cardiac regeneration wherein it was evident that cell patterning through LIFT improved vessel formation [147]. In another work, vascularlike patterning of HUVECs was shown to be successful on collagen or Matrigel loaded porous poly-lactide-co-glycolide (PLGA) stackable biopaper substrates [144]. Hribar et al. have recently reported the use of gold nanorods within cell-encapsulating collagen hydrogels to in situ produce 3D cell patterns employing a near-infrared femtosecond laser. The nanorods absorbed the laser beam causing denaturation of adjoining collagen and resulting in formation of 3D channels. A high cell viability (>90%) was observed using higher writing speeds and lower laser intensities, and the channels supported endothelial tube formation demonstrating a suitable technique for vascular tissue engineering [148]. The use of gold nanorods within the cell-laden collagen bioink caused local denaturation of collagen due to highly focused absorption of near-infrared femtosecond laser energy, and resulted in formation of hollow channels. The endothelial cells, which migrated inside the channels, could subsequently proliferate, and attained a 3D alignment [149]. To reconstruct 3D vascular morphology, Huang et al. have employed a projection printing system called digital micromirror device-based projection printing (DMD-PP), which created an optical pattern according to the image acquired from a CAD model. After the pattern was projected, UV light was exposed onto a photosensitive bioink. The substrate was lowered after patterning for each layer using an automated stage. Using DMD-PP, they fabricated user-designed complex microstructures with channel widths of 25–120 μm in a very short time. Though authors proposed this system to study the behavior of different cell types on distinct geometric cues, the same can be adapted for creating vascularlike channels of different diameters for tissue engineering [150].

6.2.2 Scaffold-free bioprinting of vascular constructs

Since the seminal publication of tissue engineering paper in Science by Vacanti and Langer, most of strategies rely on the development of a scaffold support, in which cells are cultured, and expanded in vitro or in vivo [38,151]. Although designed to provide temporary support for cells to grow, scaffolds have evolved to play active role by providing biological, chemical, and mechanical cues to direct cell growth [152]. Certainly, scaffold-based approach has led to some successes into clinical translation [153], and especially for vascular tissue engineering [154,155]. However, even after extensive research, ideal biomaterial in terms of immunological reaction, inflammatory reactions in host, degradation rate that matches with neotissue formation rate, toxicity of degradation products, fibrosis after material degradation, and mechanical compatibility with the native tissue are yet elusive [65]. Specifically, the inadequate mechanical strength and residual polymer components, which hinder cell growth, have been identified as key bottlenecks

for development of engineered vascular grafts [156,157]. These deficiencies have led to interest in scaffold-free tissue engineering and thus scaffold-free bioprinting [158–160]. Almost a decade earlier, Kelm et al. have shown that when HUVEC-coated human myofibroblast microtissues (in μm^3 volumes) were assembled to form macrotissues (in mm^3 volumes), a vascular system was developed, which eventually integrated to the host vascular system after implantation in a chicken embryo [161]. The advantage of this method is to employ the cell-derived ECM, which is more biocompatible as well as reduces tissue maturation time and fabrication complexities arising out of the scaffold constraints.

Scaffold-free bioprinting of multilayered, small-diameter vascular tubes was reported by Norotte et al. [162] using HUVSMCs, human skin fibroblasts (HSFs), and porcine aortic smooth muscle cells (PASMCs), some results of which are represented in Fig. 6.6. In their study, cell pellets were incubated in capillary micropipettes (300–500 μm in diameters) and extruded to yield cylindrical bioink materials, which were then sliced into smaller rods and rounded into tissue spheroids. Tissue spheroids were dispensed using a mechanical ram-driven EBB system [65]. In parallel, an agarose mold structure was also 3D printed, where bioprinted spheroids were cast inside the mold. The spheroids then underwent fusion inside the mold, and matured toward vascular tissue, and the mold was then removed leaving behind the tissue. The authors also demonstrated fabrication of bifurcated blood vessels.

In another study, Tan et al. developed a 3D printing technology using alginate microdroplets and calcium-containing substrates to first produce alginate molds [160]. Tissue spheroids, consisting of endothelial and smooth muscle cells, were then robotically deposited into the molds, which underwent fusion to form vascular constructs. The study showed that cell-secreted collagen Type I played a vital role in tissue formation and maturation. Kucukgul et al. recently developed an algorithmic model for toolpath planning for scaffold-free macrovascular constructs based on patient-specific medical images [163]. Their proposed self-supported model was realized with cell pellets consisting of mouse embryonic fibroblast (MEF) aggregates and support structures (agarose) to fabricate aortic tissuelike constructs [164]. In above studies, agarose and alginate molds were chosen since they were inert to cell adhesion and served the purpose of facilitating tissue maturation. Despite these concentrated efforts to bioprint blood vessels, certain issues are still required to be addressed. These include optimization of mechanical properties that will provide adequate mechanical strength for structural integrity and at the same time allow flexibility for suturing. Moreover, scaffold-free bioprinted vascular tissues require long maturation time for the tissue to deposit sufficient collagen and elastin proteins and become mechanically robust. Another major limitation of this approach lies in the scale-up of constructs to make large tissues without involvement of a temporary molding structure.

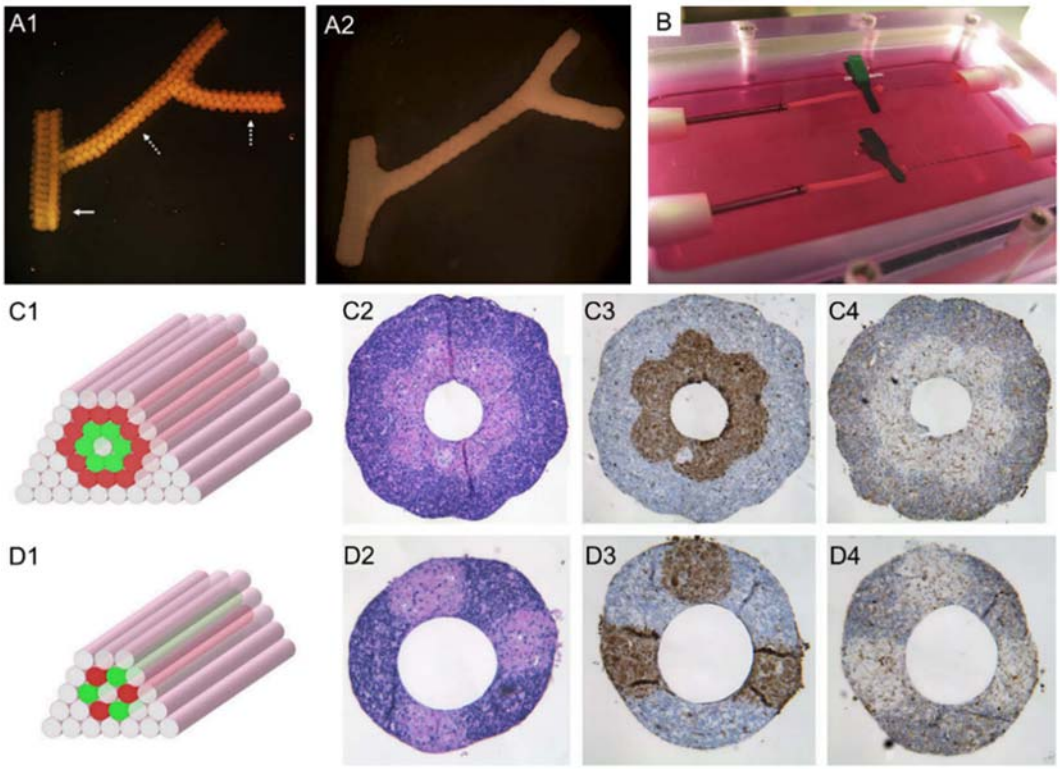

Figure 6.6
(A1) Scaffold-free bioprinting of a bifurcated vascular network using human skin fibroblast (HSF) spheroids, (A2) where spheroids fused and matured into tissue in 6 days. (B) Maturation of bioprinted tubes composed of porcine aortic smooth muscle cells (PASMCs). (C–D) Building a double-layered vascular wall. (C1 and D1) HUVSMC and HSF multicellular cylinders were assembled according to specific patterns (HUVSMC: green; HSF: red). Histological examination of the bioprinted structures including H&E (C2 and D2), smooth muscle α-actin (C3 and D3), and Caspase-3 (C4 and D4). *Reproduced/Adapted with permission from C. Norotte, F.S. Marga, L.E. Niklason, G. Forgacs, Scaffold-free vascular tissue engineering using bioprinting, Biomaterials 30 (2009) 5910–5917.*

6.3 Bioprinting for vascularized tissue fabrication

For the past few decades, fabrication of complex tissue and organ constructs have been impeded by the development of suitable technologies, which can ensure adequate cell density, viability, and functionality across the constructs (i.e., including the internal anatomy), a goal which necessitates the presence of vascularization. For replicating the complex pattern of branched vasculature in length scale assuring long-term tissue viability and functionality, 3D bioprinting provides the promising means to achieve the same [165,166]. Importantly, bioprinting can create a pattern of vascular network of desired

geometry or dimensional ranges directly utilizing bioactive factors that are responsible for prolonged vascularization. Additionally, bioprinting can be used in tandem to create the vasculature along with other tissue components. Therefore, it can be stated with conviction that bioprinting is one of the most promising engineering approaches to obtain a thick vascularized tissue construct of complex anatomy. Since a design can be created directly from patient-specific medical images, advancement in this technology may ultimately enable construction of anatomically correct solid organ substitutes. In previous sections, we have discussed the approaches which have been used for vascular tissue fabrication (>1 mm in diameter). Though, some of these approaches were demonstrated for coculture of vascular endothelial cells with some other cell types like fibroblasts, in the succeeding section, we emphasize the approaches which have been adopted to obtain necessarily heterogeneous, thick tissue constructs for generating clinically relevant volume of tissues or microvascular network (<100 μm), which is at the scales lower in dimensions than that of macrovascular channels.

6.3.1 Bioprinting macrovascular network

Bioprinting of macrovascularized tissue constructs has been attempted by several groups, principally exploring the bioprinting with fugitive ink onto a desired motif, the basic principle of which was described in Section 6.2. In this regard, Miller et al. have reported a method of using a sacrificial carbohydrate glass, which was printed at high temperatures followed by manual infiltration of cells in hydrogels (including PEGDA and acrylate-PEG-RGDS, fibrin-fibrinogen-thrombin, Matrigel, or alginate). The hydrogels were then allowed to solidify and the sacrificial material was then dissolved leaving behind vascularlike channels [167]. They developed a sacrificial material based on glucose, sucrose, and dextran to fabricate self-supporting perpendicular lattices, curved filaments, or even Y-junctions with fiber diameters in the range of 150–750 μm printed using an open source 3D printer. Additionally, the carbohydrate glass was coated with PLGA before infiltrating the hydrogels (fibrin, agarose, and Matrigel) so that PLGA can prevent carbohydrate solution to flow through the cell-laden polymer layer. After seeding endothelial cells, the authors have observed new capillary formation. Further, cellular viability was evident up to approximately 1 mm around the perfused channels. Such approach was further advanced by Kolesky et al., who coprinted multiple cell-laden vascular inks, interestingly, under ambient conditions. They demonstrated four-layer constructs by coprinting four inks namely poly(dimethyl siloxane) (PDMS), sacrificial Pluronic F127, human neonatal dermal fibroblast cells (HNDFs)/10T1/2s/mouse fibroblast-laden GelMA bioink, and a pure GelMA ink at 37°C. However, they found that since it was not possible to directly perfuse vascularized constructs, fabricated constructs were thus limited in thickness (1–2 mm) and culture times (<14 d), which were less than clinical requirements [168]. Therefore, to satisfy diverse requirements of biocompatibility,

processing ability, integration, and stability, the same group reported an advancement in their previous work, in which they used printable cell-laden bioink materials and castable gelatin-fibrinogen blend [98]. Specifically, they first bioprinted the cell-laden bioink (composed of gelatin, fibrinogen, and either of HUVECs, HNDFs, or hMSCs as cellular component) and a fugitive ink (composed of Pluronic and thrombin) on silicone perfusion chips specially fabricated on a glass substrate. A composite hydrogel containing gelatin, fibrinogen, thrombin, and transglutaminase was then printed. Pluronic containing ink was melted and removed upon cooling thus yielding a channel network, which was subsequently endothelialized and perfused. The authors could fabricate thick, vascularized tissue constructs recreating the geometry, complexity, heterogeneity, and longevity of human tissues, which was capable of being perfused for a long duration (>6 weeks) and showed differentiation of MSCs toward an osteogenic lineage. Using the same Pluronic as a sacrificial ink, Kang et al. showed the fabrication of large-scale bone (mandible), cartilage (ear), and skeletal muscle constructs by developing an integrated tissue-organ printing system [169]. Firstly, the team obtained the shape of desired constructs by processing radiological images. In this work, poly(caprolactone) (PCL) was used as a supporting structural frame which conferred mechanical stability to the construct. Authors printed different patterns of PCL around the composite hydrogel composed of cells to optimize the most stable structures. On the other hand, Pluronic was used as a fugitive ink, which was dissolved after cross-linking of the bioink yielding a porous structure. The work demonstrates successful fabrication of large-scale tissue constructs maintaining both mechanical strength and cell viability at the same time.

In order to develop 3D perfusable organ modules, Ozbolat group further introduced a microfabrication approach to generate tissue strands as a scalable scaffold-free bioink [170,171]. In that work, apart from cell-laden tubular alginate conduits, pellets of cells were injected into tubular conduits to fabricate tissue strands. When the tissue strands matured, they were used as a bioink for scale-up tissue bioprinting [172]. This group previously devised a hybrid bioprinting approach for assembling both vasculature network and tissue-specific strands on a single Multi-Arm BioPrinter platform [173]. While cells and their specific ECM formed the strands or building blocks for scale-up organ fabrication [170], macroscale single continuous luminal form was printed in parallel. The bioprinter used for this study allowed tissue self-assembly along a length of 1.5 cm of smooth muscle vasculature, where fibroblast tissue strands fused to each other after 1 day in culture while maturation was obtained in a week. Detailed histological observation also proved complete attachment of the tissue to the vasculature and tight adhesion to the smooth muscle matrix confirmed proof-of-concept for large-scale hybrid tissue bioprinting [174]. This work demonstrated an innovation on how both scaffold-based and scaffold-free bioprinting can be integrated into a single fabrication modality to obtain scalable constructs.

6.3.2 Bioprinting microvascular network

From the above discussion, it can be appreciated that vascularization is highly vital for cells to maintain their metabolic functions inside large-volume tissue constructs; however, the vascular system is characterized by a multiscale organization, which is not practical by most bioprinting technologies. To fulfill this, bifurcated vessels should ideally be fabricated with capillaries to mimic the natural vascular anatomy. In studies addressing capillary formation, heterogeneous constructs incorporating goat endothelial progenitor cells (EPCs) have been reported by Fedorovich et al., which were fabricated to obtain engineered bone grafts with vascularization [175]. In their work, composite Matrigel and alginate-based bioink containing both EPCs and multipotent stromal cells (MPSCs) were fabricated and also evaluated post-implantation. After 6 weeks, bone formation and prominent vascularization were observed. However, the mechanical integrity of these constructs was suboptimal for surgical implantation. Similarly, multihead tissue/organ building system was employed for capillarized tissue bioprinting [31]. The system was used to print 3D cell-laden construct for liver tissue engineering. While PCL was used as a frame material, the bioink was composed of three cell types—hepatocytes, HUVECs, and human normal lung fibroblasts with collagen. The bioink was infused into the PCL to induce the formation of capillarylike networks and hepatic tissue growth. The study highlighted that capillarization could accord several important advantages including improved survival of hepatocytes due to the presence of nonparenchymal cells (underlying the need for bioprinting heterocellular constructs), and an improvement in protein secretion and metabolism of hepatocytes, overall emphasizing the potential of this method for liver regeneration. A customized Bioassembly Tool (BAT) consisting of two controlled dispensing units, a servo-displacement and another pneumatic pump, has been used for extrusion of Pluronic-F127 sacrificial channels in a collagen microvascular construct with an aim to study mechanisms of postangiogenesis microcirculatory architecture formation. The results indicated the superior role of architectural cues in controlling the tissue environment over the role of vascular elements themselves [176].

Generating clinically relevant volumes of complex organs involves a much higher level of sophistication, which comprise various types of cells arranged in a specific hierarchy and a multiscale vasculature network consisting of stroma and parenchyma, apart from presence of lymphs and nerves to complete the functionality. Thus, researchers may explore bioprinting tissue-specific cells in a scaffold-free prevascularized spheroid form followed by coating with layer of angiogenic promoting material like fibrin. Formation of continuous vessellike channels within the spheroid assembly coupled with elongation of sprouts and their anastomosis between two spheroids can be observed [16]. Finally, sprouting of these capillaries from spheroids to the vessels makes it possible to bridge the gap and render a fully contiguous vascular network [68]. In light of the results of these

studies, it also becomes imperative that postbioprinting processes concerning cell assembly [177] and accelerated tissue maturation will govern the rate of vascularization in tissue constructs [178].

6.4 Comparison of different bioprinting modalities within the context of vascular or vascularized tissue bioprinting

Although various approaches can be used in fabrication of vascular or vascularized tissues, their performance in generating functional, anatomically correct, physiologically relevant, mechanically and structurally stable, and biologically appealing constructs vary considerably. Therefore, the appropriate approach should be selected and utilized depending on the target organ, including anatomical complexity, physiology, and biological function.

Extrusion-based bioprinting enables fabrication of vascular constructs that are volumetrically large as well as possess high aspect ratio. As EBB facilitates scale-up fabrication of tissue constructs compared to other bioprinting modalities including DBB and LBB [68], larger vascular constructs can be practical to build as demonstrated using all EBB approaches such as direct [170] and indirect [179] bioprinting. Coaxial extrusion of vascular network particularly generates high aspect ratio vascular constructs, which are virtually unlimited in length [88]. Despite its practicality and tight control on the dimensions, biofabrication of bifurcated channels using the coaxial extrusion approach is highly challenging as only a manual approach was demonstrated to generate branching points [88]. Fabrication of bifurcation is possible using direct or indirect bioprinting techniques, where the vasculature can be built layer by layer instead of extruding it directly. The other great benefit of EBB is the indirect bioprinting approach, where fugitive inks can be easily bioprinted in highly complex patterns generating open lumens for perfusion. Despite the great flexibility in complexity of channels, a native vascular network is oriented in 3D space rather than on a single plane and bioprinting of such vascular tree with 3D orientation in Cartesian space has yet to be performed. As 3D bioprinting is a layer-by-layer fabrication approach, there is a finite thickness of each layer and incrementing the position of the fugitive ink in each layer may induce stair-stepping effect [180], which in turn may generate occlusion or turbulence in the flow when the fugitive ink is removed.

Although a substantial progress has been made in indirect bioprinting approach for vascularized tissue bioprinting as it is highly convenient to build channels in bulky or slab gels as compared to free-standing channels, such tissue construct may exhibit challenges when they are utilized in regenerative medicine and transplantation areas. The major reason is that although lining endothelial cells within channels represents an endothelium

with tight junctions, native blood vessels have multiple layers as discussed in anatomical description of blood vessels (Section 6.1.1). Therefore, it is highly challenging to transplant such a construct as the vascular pedicle in the transplant site may not be easily sutured to the inlet and outlet of the construct. Besides, as the bulk hydrogel is prone to degrade, with different rates of degradation depending on the bioink type utilized, vascular channels can quickly lose their rigidity, and can enlarge and collapse resulting in failures in blood flow in vivo. Thus, vascular networks should be built with intimal, medial, and adventitia layers embedded within bulk hydrogels, which has not been demonstrated yet. One of the major limitations in EBB is its lack of high resolution and precision in printing cells. As bioprinting capillaries at the given cell level definitions is highly challenging using any of the bioprinting approaches demonstrated so far, current efforts in generating such microcapillaries using angiogenesis-driven mechanism is also highly attractive approach for persuasion [181]. Previous research work in DBB of endothelial cells demonstrated that when cells were deposited in patterns, which cannot be tightly controlled using manual approaches or even using EBB, they could generate tubular conduits [113]. Thus, generation of microcapillaries within EBB constructs has been a challenge so far.

Droplet-based bioprinting has the advantage of generating high-resolution constructs, which is of great value for microcapillary network development. Despite its greater benefits in bioprinting well-defined structures and high-resolution patterns with the ability to coculture multiple cell types in a high throughput manner, DBB suffers from enabling larger-scale constructs as bioprinting in 3D is a challenge [99]. By using the approach in bioprinting tubular construct into a cross-linker pool using the advantage of chemical cross-linking process, low aspect ratio vascular constructs have been demonstrated [121,123]. Despite these efforts, characterization of vascular constructs including mechanical testing (tensile, suture retention, and burst pressure) and long-term performance under perfusion culture has yet to be performed. In addition, as these vascular constructs are free-standing in the cross-linker pool, integration of the parenchymal tissue around the vascular construct is a critical barrier in order to translate the technology from basic research to functional vascularized tissue fabrication. A recent work demonstrated the indirect DBB for vascularized tissue construct fabrication using sacrificial biomaterials such as gelatin [17]; thus DBB has the potential to facilitate fabrication of tissue models for pharmaceutical testing and cancer research [182]. For inkjet bioprinting, the upper limit for the bioink viscosity is recommended to be in the order of 0.1 Pa s^{-1}, while highly viscous hydrogels are not ideal materials for processing by this technique as they can clog the nozzle tip [183,184]. Moreover, low reproducibility, extreme shear stress within the nozzle, undesired cell aggregation and settling in ink reservoir, formation of clogs at the nozzle tip, and the limited choice of compatible bioink materials are other disadvantages and challenges associated with this bioprinting technology [1,124,126,185]. This

technology, however, offers a great potential to overcome many of the inherent problems faced by the tissue engineering researchers, providing the ability to eject droplets of very small size composed of several bioink materials and pattern them spatially on demand [123–126].

Using processes involving photopolymerization, vascular tissue constructs have been built with well-defined architectures demonstrating native like branching configuration [149]; however, these approaches possess several limitations impeding the development of biologically superior constructs. First of all, bioprinting at the sufficient cell density that is close to native histological composition is not quite feasible. In addition, due to the limited number of photocurable bioink materials as well as the need for photoinitiators (that are toxic in general) [186], these processes do not support bioprinting vascular constructs that are mechanically and structurally stable and strong. The use of photoinitiators, such as Irgacure 2959 [187,188], limits the mechanical properties of the bioprinted constructs as the photoinitiators should be water-soluble. The LBB processes based on cell transfer (e.g., LIFT), on the other hand, have been recently utilized in fabrication of vascular constructs using a similar concept applied DBB, where the bioink is deposited into a cross-linker pool [142]. In general, processes based on cell transfer such as laser-guidance direct writing, matrix-assisted pulsed-laser evaporation-direct write, and LIFT are highly challenging to generate 3D larger tissue constructs due to the limited number of compatible bioink materials (i.e., Matrigel, alginate, gelatin) and lack of appropriate process setup facilitating rapid cross-linking of mechanically resilient constructs. Compared to EBB and DBB, LBB avoids shear stress–induced cell damage [189]. Laser-based bioprinting prevents cells from any shear stress–related damage due to nozzle-free nature, thus rendering high cell viabilities in general (95% and above) [190–192]. In addition, LBB can be used to print bioink materials with high viscosity and a wider range of bioink materials (i.e., fibrous proteins) [193]. Though the salient characteristics of LBB hold significant promise for tissue engineering, the complications and unfavorable effects of laser irradiation on different cell types are not yet comprehensively unraveled [189]. Moreover, high-intensity and high-resolution diode lasers are more expensive than equipment used in other bioprinting modalities, and the control of the laser printing process is highly difficult to manage. Thus, there is currently no laser-based bioprinters commercially available, as they are less user-friendly and more complicated and expensive in comparison to other types of bioprinters.

Scaffold-free bioprinting of vascular constructs has been a very exciting direction in building vascular grafts that are histologically close to native counterparts, where multiple layers can be easily incorporated with controlled cell type and population [162]. Further cultivation of these vascular constructs in perfusion bioreactors with pulsatile flow can improve their mechanical properties and induce the appropriate mechanical stimulation to deposit more collagen and elastin fibers in the desired orientation, which are essential for

long-term function after implantation. A recent work also demonstrated in vivo endothelialization of scaffold-free bioprinted vascular grafts in murine models, demonstrating further advantages of using this approach; however, long-term patency and performance of such grafts still need to be investigated [194].

Table 6.1 compares existing bioprinting methods used in vascular tissue biofabrication along with cell types, bioink, or bioprinters utilized in each method.

6.5 Future perspectives and conclusions

Vascularization is one of the most important factors that determine success of engineered constructs to remain viable as it ensures nutrients and oxygen supply for metabolizing cells; however, fabrication of vascular network has persisted as a challenge in tissue engineering. Meanwhile, 3D bioprinting has emerged as a promising tool to develop fully biomimetic tissue constructs and organs for clinical applications. In addition, high throughput methods to produce in vitro models for drug efficacy, metabolism, and toxicity screening assays would also be obtained with 3D bioprinting. This technique confers unparalled advantages to mimic anatomical features and functions of the native tissue. Though several initial successes on bioprinting vascularized tissue constructs have been reported, further developments are necessary for widespread implementation by practicing clinicians. For one, it would be expected that efforts toward direct in vivo bioprinting of biomimetic constructs to replace and accelerate regeneration of compromised organ parts would eventually be realized in clinics. Development of robotic instrumentation technologies for simplified, portable bioprinters at one hand and scalable automated biofabrication production lines at the other hand would hence be the focus of future works. Future bioprinters in clinics would be required to fabricate vascularized tissues with greater speed than that are used in laboratories to reliably manufacture constructs of clinically relevant volumes and meet patients' demands. While one approach would be to fabricate minitissue blocks and then scale up by joining of the minitissue blocks to clinically relevant volumes, the other approach may employ bioprinting of macroscale vascular network in tandem with microvascularized tissue strands [108,172,178]. The recent introduction of a novel scalable bioink, "tissue strands," for scaffold-free bioprinting is hence an important advancement toward obtaining vascularized tissues in the future [172].

In parallel, automated robotic-based methodology for generating multilayered small diameter tubular vessels with lumen diameters of 0.5–6 mm and individual layer thickness of <400 μm composed of GelMA, alginate, and chitosan are also expected to complement bioprinting methods [196]. It must be noted here that recent several reports showed how mechanical stiffness of matrices govern differentiation of progenitor or stem cells. Therefore, it needs future investigations to see if materials with tunable mechanical

Table 6.1: A comparison of different bioprinting methods for vascular tissue fabrication.

Method	Mechanism (bioprinted modalities)	Cell types	Bioink or substrate	Bioprinters	Remarks
Extrusion-based bioprinting	Direct bioprinting	Murine fibroblasts (NIH 3T3) [78,79], human hepatoma cells (HepG2 C3A) [78,79], human intestinal epithelial cells (Int 407) [78,79], C2C12 myoblasts [80], MC3T3 [80], adipose-derived stromal cells(ADSCs) and rat hepatocytes [76], cartilage progenitor cells (CPCs) [80,85], HCASMC [89], human umbilical vein endothelial cells (HUVECs) [88,168], human umbilical vein smooth muscle cells (HUVSMC) [171], escherichia coli K12 cells [86], L929 mouse fibroblasts [95]	Pentaerythritol derivatives of polyethylene glycol (PEG) [78,79], fibrinogen [80], alginate/chitosan [85], gelatin/alginate/fibrinogen (GAF) [77], gelatin/alginate/chitosan (GAC) [77], sodium alginate and calcium chloride [81,86,88–92,168,171]	Fab@Home printing system [78,79,97], MakerBot Replicator [80], REGENHU's Biofactory [81], EFD Nordson printer [85,86,88,89], Yinhua cell Assembler II [77], RepRapPro Mendel [91–93]	Larger tissue structures, save bioprinting time (faster), commercially available bioprinters, enabling multiple material in one time. Vascular constructs up to 15 mm in length has been bioprinted [81]. Using co-axial extrusion, >80 cm-long vascular conduits with an average conduit and lumen diameter of 1449 ± 27 μm and 990 ± 16 μm were obtained, respectively [88]
	Indirect bioprinting	MC3T3 [97], human umbilical vein endothelial cells (HUVECs)	Star poly(ethylene glycol-co-lactide) acrylate (SPELA) [95], poly(ethylene	A custom-built 3D printer [168], a custom-designed 3D bioprinter equipped	Micro-channels with diameter ranging from 150 μm to 1 mm were

Continued

Table 6.1: A comparison of different bioprinting methods for vascular tissue fabrication.—cont'd

Method	Mechanism (bioprinted modalities)	Cell types	Bioink or substrate	Bioprinters	Remarks
		[97,98,175], human neonatal dermal fibroblasts (HNDFs) [98], human bone marrow-derived mesenchymal stem cells (hMSCs) [98], human mesenchymal stem cells (hMSCs) [51]	glycol) dimethacrylate (PEGDMA) [95], poly(ethylene glycol) diacrylate (PEGDA) [95], silicone elastomer/Pluronic F127/methacrylated gelatin (GelMA) [98], Pluronic F127/ thrombin [98], methacrylated gelatin (GelMA) [31], alginate/gelatin [51]	with four independently addressable print heads [98], NovoGen MMX [173], Fab@Home printing system [51]	fabricated [95]. Heterogeneous tissue constructs (>1 cm thick and 10 cm^3 in volume) were demonstrated [168]
	Scaffold-free bioprinting	Chinese Hamster Ovary cells (CHOs)/ human umbilical vein smooth muscle cells (HUVMSCs)/human skin fibroblasts (HSFs)/porcine aortic smooth muscle cells (PASMCs) [173], mouse embryonic fibroblast (MEF) [170,174], human aortic smooth muscle cells (hSMCs)/human umbilical vein endothelial cells (HUVECs)	Agarose [173], Teflon [173], NovoGel [170,174], sodium alginate/ gelatin and calcium chloride [195]	Novogen Bioprinter [170,173,174], the Palmetto 3D Printer [160]	Multicellular spheroids or cylinders (300–500 μm diameter) were bioprinted and post-printing fusion resulted in single- and double-layered small diameter vascular tubes in 0.9–2.5 mm outer diameter range [162]
Droplet-based bioprinting	Piezo inkjet	Rat smooth muscle cells (SMCs) [112],	Sodium alginate/ gelatin and calcium	Modified-HP697c inkjet printer	Heterocellular tissue patterning with small

		NIH3T3 mouse fibroblasts [122]	chloride [112], sodium alginate and calcium chloride [120,123]	[111,112], MicroFab MJ-ABL piezoelectric inkjet printhead [120,122]	droplets (less than 100 μm)
	Valve-based inkjet	Human umbilical vein endothelial cells (HUVECs) [17,129]	Collagen/gelatin [17], fibrinogen/ thrombin [129]	Custom-built printer [17,129]	The smallest droplet size is 100 μm, but it enables printing constructs like fluidic channel with 0.7–1.5 mm width and 0.5–1.2 mm height) [129]
Laser-based bioprinting	Laser-assisted bioprinting	Murine fibroblasts (NIH 3T3) [143], bend3 endothelial cells [144]	Sodium alginate and calcium chloride [143], collagen [144]	ExciStarexcimer laser [143], NIR laser beam [144]	It is quite an expensive modality with high precision, and not able to get multiple material droplet. Micro-channel with widths of 25–120 μm were obtained [150]

properties are developed and if these specific mechanical properties are bioprinted at the clinical scale. Herein, another important consideration is not only creation of vascular network but also assuring stability of the same with the shape fidelity. Clinicians will expect that immediately after vascularization requirements are met in engineered constructs, nerve supply networks are also built to obtain innervated tissues.

Another dimension that requires extensive work in the domain of bioprinting of vascularized tissues is that the resolution of spatial and temporal control that can be attained over the positioning of cells, proteins, and even genetic materials should be proposed. In respect to the temporal control, 3D bioprinting approaches may eventually evolve into 4D bioprinting [197,198]. In 4D bioprinting, "time" factor is integrated as the fourth dimension and allows responsive cells and materials to alter their functionalities and shape in response to external stimuli. Thus, printed constructs can undergo appropriate reorganization to improve their functionality. However, it is also to be borne in mind that native vasculature is multiscalar in nature and future bioprinting technologies should be capable enough to produce vascularization at multiscale dimensions from arteries/veins down to capillaries. However, with current bioprinting technologies, it is difficult to bioprint submicron capillaries. Therefore, this should be the aim of future endeavors so that microvascular network can be printed in tandem with the rest of macrosized tissue. Moreover, blood vessels should not only contain endothelial cells but also smooth muscle cells, which are important to provide patency and mechanical strength; concentric bioprinting of endothelial and smooth muscle cells should therefore be an important area of investigation in the future. Finally, bioprinted constructs would be required to be sutured and remain integrated with the perfusion system of the host without collapsing or occlusion.

Apart from the scientific challenges, 3D bioprinting technology will also have to face the imminent regulatory and intellectual property concerns. Presently, bioprinting technology is not classified as such; however, proper classification under device/biological category would be required to be made for which standardization of bioprinted constructs will be required. Similarly, for commercial benefits to investors, proper intellectual protection is required. Bioprinting processes and products are discernibly different from natural tissues or tissue formation process, and importantly involve human intellectual intervention, and therefore could be considered for intellectual protection. These facts would be required for consideration for successful clinical translation.

Though the realm of 3D bioprinting has brought tremendous advances to obtain vessel structures with sound structural and functional integrity, it can still be observed that fabricating clinically relevant vascular and vascularized tissue constructs are still some milestones away. Specifically, newer insights in directions of enhancing resolution, obtaining more anatomically accurate constructs, and allowing scaling up of bioprinted

tissues are expected to provide potential solutions. Gradually, it may be expected that separate research on materials and cellular bioink materials for vascularization may cede place to more integrated and holistic approaches for developing bioprinters for vascularized tissue fabrication. Thus, the development of fully automated robust instrumentation, integrated with intricate modeling and design process software, would be critical to ensure that new vascular channels are assimilated with host vasculature. Further, bioprinting of complex pattern of vascular network at multiple scale ranges would be a challenge. Presently, prevalent technologies fall short of generating an intact capillary network at the single cell level. To achieve this goal, dispensing component of bioprinters will have to evolve to advance the spatial resolution. Ideally, tissue-specific bioink materials would be required to be formulated with vascularization-directing bioactives and operated under high throughput and by high resolution bioprinters to allow rapid fabrication of vascularized thick tissues at the clinically relevant volumes.

References

[1] C.L. Ventola, Medical applications for 3D printing: current and projected uses, Pharmacy and Therapeutics 39 (10) (2014) 704–711.
[2] J.A. Greene, Do-it-yourself medical devices—technology and empowerment in American health care, New England Journal of Medicine 374 (4) (2016) 305–308.
[3] A. Marro, T. Bandukwala, W. Mak, Three-dimensional printing and medical imaging: a review of the methods and applications, Current Problems in Diagnostic Radiology 45 (1) (2016) 2–9.
[4] H.H. Malik, A.R.J. Darwood, S. Shaunak, P. Kulatilake, A.A. El-Hilly, O. Mulki, A. Baskaradas, Three-dimensional printing in surgery: a review of current surgical applications, Journal of Surgical Research 199 (2) (2015) 512–522.
[5] N. Scoutaris, S. Ross, D. Douroumis, Current trends on medical and pharmaceutical applications of inkjet printing technology, Pharmaceutical Research 33 (8) (2016) 1799–1816.
[6] M. Nagata, H. Hoshina, M. Li, M. Arasawa, K. Uematsu, S. Ogawa, K. Yamada, T. Kawase, K. Suzuki, A. Ogose, I. Fuse, K. Okuda, K. Uoshima, K. Nakata, H. Yoshie, R. Takagi, A clinical study of alveolar bone tissue engineering with cultured autogenous periosteal cells: coordinated activation of bone formation and resorption, Bone 50 (5) (2012) 1123–1129.
[7] J. He, F. Xu, Y. Liu, Z. Jin, D. Li, Advanced tissue engineering strategies for vascularized parenchymal constructs, Journal of Mechanics in Medicine and Biology 14 (01) (2013) 1430001.
[8] J.G. Nemeno-Guanzon, S. Lee, J.R. Berg, Y.H. Jo, J.E. Yeo, B.M. Nam, Y.-G. Koh, J.I. Lee, Trends in tissue engineering for blood vessels, Journal of Biomedicine and Biotechnology 2012 (2012) 956345.
[9] P. Wang, Y. Sun, X. Shi, H. Shen, H. Ning, H. Liu, 3D printing of tissue engineering scaffolds: a focus on vascular regeneration, Bio-design and Manufacturing 4 (2) (2021) 344–378.
[10] J.P. Stegemann, S.N. Kaszuba, S.L. Rowe, Review: advances in vascular tissue engineering using protein-based biomaterials, Tissue Engineering 13 (11) (2007) 2601–2613.
[11] P. Berillis, The role of collagen in the aorta's structure, the open, Circulation & Vascular Journal 6 (1) (2013).
[12] H. Ardalani, A.H. Assadi, W.L. Murphy, Structure, function, and development of blood vessels: lessons for tissue engineering, in: W. Cai (Ed.), Engineering in Translational Medicine, Springer, London, 2014, pp. 155–182.
[13] S.Y. Yuan, R.R. Rigor, Regulation of Endothelial Barrier Function, Morgan & Claypool Life Sciences, San Rafael, CA, 2010.

[14] J.R. Levick, An Introduction to Cardiovascular Physiology, Butterworth-Heinemann, 1991, pp. 171–177.
[15] M.F. Leong, J.K.C. Toh, C. Du, K. Narayanan, H.F. Lu, T.C. Lim, A.C.A. Wan, J.Y. Ying, Patterned prevascularised tissue constructs by assembly of polyelectrolyte hydrogel fibres, Nature Communications 4 (1) (2013) 2353.
[16] I.T. Ozbolat, Bioprinting scale-up tissue and organ constructs for transplantation, Trends in Biotechnology 33 (7) (2015) 395–400.
[17] V.K. Lee, A.M. Lanzi, H. Ngo, S.-S. Yoo, P.A. Vincent, G. Dai, Generation of multi-scale vascular network system within 3D hydrogel using 3D bio-printing technology, Cellular and Molecular Bioengineering 7 (3) (2014) 460–472.
[18] H.C.H. Ko, B.K. Milthorpe, C.D. McFarland, Engineering thick tissues-the vascularisation problem, European Cells and Materials 14 (2007) 1–19.
[19] C. Maes, T. Kobayashi, M.K. Selig, S. Torrekens, S.I. Roth, S. Mackem, G. Carmeliet, H.M. Kronenberg, Osteoblast precursors, but not mature osteoblasts, move into developing and fractured bones along with invading blood vessels, Developmental Cell 19 (2) (2010) 329–344.
[20] J. Hatch, Y.-s. Mukouyama, Spatiotemporal mapping of vascularization and innervation in the fetal murine intestine, Developmental Dynamics 244 (1) (2015) 56–68.
[21] C. Gálvez-Montón, M.T. Fernandez-Figueras, M. Martí, C. Soler-Botija, S. Roura, I. Perea-Gil, C. Prat-Vidal, A. Llucià-Valldeperas, Á. Raya, A. Bayes-Genis, Neoinnervation and neovascularization of acellular pericardial-derived scaffolds in myocardial infarcts, Stem Cell Research & Therapy 6 (1) (2015) 108.
[22] T.L. Criswell, B.T. Corona, Z. Wang, Y. Zhou, G. Niu, Y. Xu, G.J. Christ, S. Soker, The role of endothelial cells in myofiber differentiation and the vascularization and innervation of bioengineered muscle tissue in vivo, Biomaterials 34 (1) (2013) 140–149.
[23] R.B. Reinert, Q. Cai, J.-Y. Hong, J.L. Plank, K. Aamodt, N. Prasad, R. Aramandla, C. Dai, S.E. Levy, A. Pozzi, P.A. Labosky, C.V.E. Wright, M. Brissova, A.C. Powers, Vascular endothelial growth factor coordinates islet innervation via vascular scaffolding, Development 141 (7) (2014) 1480–1491.
[24] H.Y. Wang, R.H. Wei, S.Z. Zhao, Evaluation of corneal cell growth on tissue engineering materials as artificial cornea scaffolds, International Journal of Ophthalmology 6 (6) (2013) 873–878.
[25] T. Kaully, K. Francis, A. Lesman, S. Levenberg, Vascularization—the conduit to viable engineered tissues, Tissue Engineering 15 (2) (2009) 159–169.
[26] J. Rouwkema, N.C. Rivron, C.A. van Blitterswijk, Vascularization in tissue engineering, Trends in Biotechnology 26 (8) (2008) 434–441.
[27] D. Richards, J. Jia, M. Yost, R. Markwald, Y. Mei, 3D bioprinting for vascularized tissue fabrication, Annals of Biomedical Engineering 45 (1) (2017) 132–147.
[28] M.I. Santos, R.L. Reis, Vascularization in bone tissue engineering: physiology, current strategies, major hurdles and future challenges, Macromolecular Bioscience 10 (1) (2010) 12–27.
[29] C.K. Griffith, C. Miller, R.C.A. Sainson, J.W. Calvert, N.L. Jeon, C.C.W. Hughes, S.C. George, Diffusion limits of an in vitro thick prevascularized tissue, Tissue Engineering 11 (1–2) (2005) 257–266.
[30] Y. Pang, K. Montagne, M. Shinohara, K. Komori, Y. Sakai, Liver tissue engineering based on aggregate assembly: efficient formation of endothelialized rat hepatocyte aggregates and their immobilization with biodegradable fibres, Biofabrication 4 (4) (2012) 045004.
[31] J.W. Lee, Y.-J. Choi, W.-J. Yong, F. Pati, J.-H. Shim, K.S. Kang, I.-H. Kang, J. Park, D.-W. Cho, Development of a 3D cell printed construct considering angiogenesis for liver tissue engineering, Biofabrication 8 (1) (2016) 015007.
[32] M. Neufurth, X. Wang, E. Tolba, B. Dorweiler, H.C. Schroder, T. Link, B. Diehl-Seifert, W.E. Muller, Modular small diameter vascular grafts with bioactive functionalities, PLoS One 10 (7) (2015) e0133632.
[33] S. Pashneh-Tala, S. MacNeil, F. Claeyssens, The tissue-engineered vascular graft—past, present, and future, Tissue Engineering Part B Reviews 22 (1) (2015) 68–100.

[34] M. Lovett, K. Lee, A. Edwards, D.L. Kaplan, Vascularization strategies for tissue engineering, Tissue Engineering Part B Reviews 15 (3) (2009) 353–370.
[35] J.C.Y. Chung, D. Shum-Tim, Neovascularization in tissue engineering, Cells 1 (4) (2012) 1246–1260.
[36] M.W. Laschke, M.D. Menger, Vascularization in tissue engineering: angiogenesis versus inosculation, European Surgical Research 48 (2) (2012) 85–92.
[37] Z. Lokmic, G.M. Mitchell, Engineering the microcirculation, Tissue Engineering Part B Reviews 14 (1) (2008) 87–103.
[38] J.V. Serbo, S. Gerecht, Vascular tissue engineering: biodegradable scaffold platforms to promote angiogenesis, Stem Cell Research & Therapy 4 (1) (2013) 8.
[39] S.B. Riemenschneider, D.J. Mattia, J.S. Wendel, J.A. Schaefer, L. Ye, P.A. Guzman, R.T. Tranquillo, Inosculation and perfusion of pre-vascularized tissue patches containing aligned human microvessels after myocardial infarction, Biomaterials 97 (2016) 51–61.
[40] J.E. Leslie-Barbick, J.E. Saik, D.J. Gould, M.E. Dickinson, J.L. West, The promotion of microvasculature formation in poly(ethylene glycol) diacrylate hydrogels by an immobilized VEGF-mimetic peptide, Biomaterials 32 (25) (2011) 5782–5789.
[41] R. Sooppan, S.J. Paulsen, J. Han, A.H. Ta, P. Dinh, A.C. Gaffey, C. Venkataraman, A. Trubelja, G. Hung, J.S. Miller, P. Atluri, In vivo anastomosis and perfusion of a three-dimensionally-printed construct containing microchannel networks, Tissue Engineering Part C Methods 22 (1) (2015) 1–7.
[42] J. Baldwin, M. Antille, U. Bonda, E.M. De-Juan-Pardo, K. Khosrotehrani, S. Ivanovski, E.B. Petcu, D.W. Hutmacher, In vitropre-vascularisation of tissue-engineered constructs A co-culture perspective, Vascular Cell 6 (2014) 13.
[43] V.K. Bajpai, S.T. Andreadis, Stem cell sources for vascular tissue engineering and regeneration, Tissue Engineering Part B Reviews 18 (5) (2012) 405–425.
[44] A. Geevarghese, I.M. Herman, Pericyte-endothelial crosstalk: implications and opportunities for advanced cellular therapies, Translational Research 163 (4) (2014) 296–306.
[45] J. Rouwkema, A. Khademhosseini, Vascularization and angiogenesis in tissue engineering: beyond creating static networks, Trends in Biotechnology 34 (9) (2016) 733–745.
[46] A. Kumar, B. Starly, Large scale industrialized cell expansion: producing the critical raw material for biofabrication processes, Biofabrication 7 (4) (2015) 044103.
[47] S. Yeasmin, J. Ceccarelli, M. Vigen, B. Carrion, A.J. Putnam, S.A. Tarle, D. Kaigler, Stem cells derived from tooth periodontal ligament enhance functional angiogenesis by endothelial cells, Tissue Engineering Part A 20 (7–8) (2013) 1188–1196.
[48] Y. Amano, A. Nishiguchi, M. Matsusaki, H. Iseoka, S. Miyagawa, Y. Sawa, M. Seo, T. Yamaguchi, M. Akashi, Development of vascularized iPSC derived 3D-cardiomyocyte tissues by filtration Layer-by-Layer technique and their application for pharmaceutical assays, Acta Biomaterialia 33 (2016) 110–121.
[49] D.G. Seifu, K. Mequanint, Fabrication of vascular tissue engineering scaffolds with enhanced oxygen diffusivity and cell infiltration, Journal of Biomaterials and Tissue Engineering 2 (4) (2012) 280–291.
[50] S.C. Baker, G. Rohman, J. Hinley, J. Stahlschmidt, N.R. Cameron, J. Southgate, Cellular integration and vascularisation promoted by a resorbable, particulate-leached, cross-linked poly(ε-caprolactone) scaffold, Macromolecular Bioscience 11 (5) (2011) 618–627.
[51] W. Thein-Han, H.H.K. Xu, Prevascularization of a gas-foaming macroporous calcium phosphate cement scaffold via coculture of human umbilical vein endothelial cells and osteoblasts, Tissue Engineering Part A 19 (15–16) (2013) 1675–1685.
[52] S. Singh, B.M. Wu, J.C.Y. Dunn, The enhancement of VEGF-mediated angiogenesis by polycaprolactone scaffolds with surface cross-linked heparin, Biomaterials 32 (8) (2011) 2059–2069.
[53] T. Simón-Yarza, F.R. Formiga, E. Tamayo, B. Pelacho, F. Prosper, M.J. Blanco-Prieto, Vascular endothelial growth factor-delivery systems for cardiac repair: an overview, Theranostics 2 (6) (2012) 541–552.

[54] I.S. Park, S.-H. Kim, Y.H. Kim, I.H. Kim, S.H. Kim, A collagen/smooth muscle cell-incorporated elastic scaffold for tissue-engineered vascular grafts, Journal of Biomaterials Science, Polymer Edition 20 (11) (2009) 1645–1660.
[55] H.-Y. Mi, X. Jing, J. McNulty, M.R. Salick, X.-F. Peng, L.-S. Turng, Approaches to fabricating multiple-layered vascular scaffolds using hybrid electrospinning and thermally induced phase separation methods, Industrial & Engineering Chemistry Research 55 (4) (2016) 882–892.
[56] R. Gauvin, T. Ahsan, D. Larouche, P. Lévesque, J. Dubé, F.A. Auger, R.M. Nerem, L. Germain, A novel single-step self-assembly approach for the fabrication of tissue-engineered vascular constructs, Tissue Engineering Part A 16 (5) (2009) 1737–1747.
[57] A. Hasan, A. Memic, N. Annabi, M. Hossain, A. Paul, M.R. Dokmeci, F. Dehghani, A. Khademhosseini, Electrospun scaffolds for tissue engineering of vascular grafts, Acta Biomaterialia 10 (1) (2014) 11–25.
[58] W. Meyer, S. Engelhardt, E. Novosel, B. Elling, M. Wegener, H. Krüger, Soft polymers for building up small and smallest blood supplying systems by stereolithography, Journal of Functional Biomaterials 3 (2) (2012) 257–268.
[59] B. Huber, S. Engelhardt, W. Meyer, H. Krüger, A. Wenz, V. Schönhaar, G.E.M. Tovar, P.J. Kluger, K. Borchers, Blood-vessel mimicking structures by stereolithographic fabrication of small porous tubes using cytocompatible polyacrylate elastomers, biofunctionalization and endothelialization, Journal of Functional Biomaterials 7 (2) (2016) 11.
[60] A. Owida, R. Chen, S. Patel, Y. Morsi, X. Mo, Artery vessel fabrication using the combined fused deposition modeling and electrospinning techniques, Rapid Prototyping Journal 17 (1) (2011) 37–44.
[61] M. Centola, A. Rainer, C. Spadaccio, S. De Porcellinis, J.A. Genovese, M. Trombetta, Combining electrospinning and fused deposition modeling for the fabrication of a hybrid vascular graft, Biofabrication 2 (1) (2010) 014102.
[62] S. Amensag, P.S. McFetridge, Rolling the human amnion to engineer laminated vascular tissues, Tissue Engineering Part C Methods 18 (11) (2012) 903–912.
[63] J. An, J.E.M. Teoh, R. Suntornnond, C.K. Chua, Design and 3D printing of scaffolds and tissues, Engineering 1 (2) (2015) 261–268.
[64] A.J. Melchiorri, J.P. Fisher, Chapter 20–bioprinting of blood vessels, in: A. Atala, J.J. Yoo (Eds.), Essentials of 3D Biofabrication and Translation, Academic Press, Boston, 2015, pp. 337–350.
[65] I.T. Ozbolat, Scaffold-based or scaffold-free bioprinting: competing or complementing approaches? Journal of Nanotechnology in Engineering and Medicine 6 (2) (2015) 024701.
[66] K. Jakab, C. Norotte, F. Marga, K. Murphy, G. Vunjak-Novakovic, G. Forgacs, Tissue engineering by self-assembly and bio-printing of living cells, Biofabrication 2 (2) (2010) 022001.
[67] P.A. Fleming, W.S. Argraves, C. Gentile, A. Neagu, G. Forgacs, C.J. Drake, Fusion of uniluminal vascular spheroids: a model for assembly of blood vessels, Developmental Dynamics 239 (2) (2010) 398–406.
[68] I.T. Ozbolat, M. Hospodiuk, Current advances and future perspectives in extrusion-based bioprinting, Biomaterials 76 (2016) 321–343.
[69] M. Hospodiuk, K.K. Moncal, M. Dey, I.T. Ozbolat, Extrusion-based biofabrication in tissue engineering and regenerative medicine, in: A. Ovsianikov, J. Yoo, V. Mironov (Eds.), 3D Printing and Biofabrication, Springer International Publishing, Cham, 2016, pp. 1–27.
[70] A.-V. Do, A. Akkouch, B. Green, I. Ozbolat, A. Debabneh, S. Geary, A.K. Salem, Controlled and sequential delivery of fluorophores from 3D printed alginate-PLGA tubes, Annals of Biomedical Engineering 45 (1) (2017) 297–305.
[71] N.E. Fedorovich, I. Swennen, J. Girones, L. Moroni, C.A. van Blitterswijk, E. Schacht, J. Alblas, W.J.A. Dhert, Evaluation of photocrosslinked lutrol hydrogel for tissue printing applications, Biomacromolecules 10 (7) (2009) 1689–1696.
[72] T. Jungst, W. Smolan, K. Schacht, T. Scheibel, J. Groll, Strategies and molecular design criteria for 3D printable hydrogels, Chemical Reviews 116 (3) (2016) 1496–1539.

[73] C.M. Smith, A.L. Stone, R.L. Parkhill, R.L. Stewart, M.W. Simpkins, A.M. Kachurin, W.L. Warren, S.K. Williams, Three-dimensional BioAssembly tool for generating viable tissue-engineered constructs, Tissue Engineering 10 (9–10) (2004) 1566–1576.
[74] C.M. Smith, J.J. Christian, W.L. Warren, S.K. Williams, Characterizing environmental factors that impact the viability of tissue-engineered constructs fabricated by a direct-write bioassembly tool, Tissue Engineering 13 (2) (2007) 373–383.
[75] V. Mironov, V. Kasyanov, R.R. Markwald, Nanotechnology in vascular tissue engineering: from nanoscaffolding towards rapid vessel biofabrication, Trends in Biotechnology 26 (6) (2008) 338–344.
[76] A. Panwar, L.P. Tan, Current status of bioinks for micro-extrusion-based 3D bioprinting, Molecules 21 (6) (2016) 685.
[77] L. Shengjie, X. Zhuo, W. Xiaohong, Y. Yongnian, L. Haixia, Z. Renji, Direct fabrication of a hybrid cell/hydrogel construct by a double-nozzle assembling technology, Journal of Bioactive and Compatible Polymers 24 (3) (2009) 249–265.
[78] A. Skardal, J. Zhang, G.D. Prestwich, Bioprinting vessel-like constructs using hyaluronan hydrogels crosslinked with tetrahedral polyethylene glycol tetracrylates, Biomaterials 31 (24) (2010) 6173–6181.
[79] A. Skardal, J. Zhang, L. McCoard, X. Xu, S. Oottamasathien, G.D. Prestwich, Photocrosslinkable hyaluronan-gelatin hydrogels for two-step bioprinting, Tissue Engineering Part A 16 (8) (2010) 2675–2685.
[80] T.J. Hinton, Q. Jallerat, R.N. Palchesko, J.H. Park, M.S. Grodzicki, H.-J. Shue, M.H. Ramadan, A.R. Hudson, A.W. Feinberg, Three-dimensional printing of complex biological structures by freeform reversible embedding of suspended hydrogels, Science Advances 1 (9) (2015) e1500758.
[81] E.Y.S. Tan, W.Y. Yeong, Concentric bioprinting of alginate-based tubular constructs using multi-nozzle extrusion-based technique, International Journal of Bioprinting 1 (2015), 49-45.
[82] H. Onoe, S. Takeuchi, Cell-laden microfibers for bottom-up tissue engineering, Drug Discovery Today 20 (2) (2015) 236–246.
[83] H. Onoe, T. Okitsu, A. Itou, M. Kato-Negishi, R. Gojo, D. Kiriya, K. Sato, S. Miura, S. Iwanaga, K. Kuribayashi-Shigetomi, Y.T. Matsunaga, Y. Shimoyama, S. Takeuchi, Metre-long cell-laden microfibres exhibit tissue morphologies and functions, Nature Materials 12 (6) (2013) 584–590.
[84] P. Sher, S.M. Oliveira, J. Borges, J.F. Mano, Assembly of cell-laden hydrogel fiber into non-liquefied and liquefied 3D spiral constructs by perfusion-based layer-by-layer technique, Biofabrication 7 (1) (2015) 011001.
[85] Y. Zhang, Y. Yu, I.T. Ozbolat, Direct bioprinting of vessel-like tubular microfluidic channels, Journal of Nanotechnology in Engineering and Medicine 4 (2) (2013) 020902.
[86] Y. Yu, Y. Zhang, J.A. Martin, I.T. Ozbolat, Evaluation of cell viability and functionality in vessel-like bioprintable cell-laden tubular channels, Journal of Biomechanical Engineering 135 (9) (2013) 091011.
[87] Y. Zhang, Y. Yu, H. Chen, I.T. Ozbolat, Characterization of printable cellular micro-fluidic channels for tissue engineering, Biofabrication 5 (2) (2013) 025004.
[88] Y. Zhang, Y. Yu, A. Akkouch, A. Dababneh, F. Dolati, I.T. Ozbolat, In vitro study of directly bioprinted perfusable vasculature conduits, Biomaterials Science 3 (1) (2015) 134–143.
[89] F. Dolati, Y. Yu, Y. Zhang, A.M.D. Jesus, E.A. Sander, I.T. Ozbolat, In vitro evaluation of carbon-nanotube-reinforced bioprintable vascular conduits, Nanotechnology 25 (14) (2014) 145101.
[90] Q. Gao, Y. He, J.-Z. Fu, A. Liu, L. Ma, Coaxial nozzle-assisted 3D bioprinting with built-in microchannels for nutrients delivery, Biomaterials 61 (2015) 203–215.
[91] R. Attalla, C. Ling, P. Selvaganapathy, Fabrication and characterization of gels with integrated channels using 3D printing with microfluidic nozzle for tissue engineering applications, Biomedical Microdevices 18 (2016) 1–12.
[92] R. Attalla, P.R. Selvaganapathy, 3D printing of gels with integrated vascular channels for cell culture using a microfluidic printhead, in: 18th International Conference on Miniaturized Systems for Chemistry and Life Sciences, Micro, 2014, pp. 479–481, 2014.

[93] P.R. Selvaganapathy, A. Rana, Microfluidic Vascular Channels in Gels Using Commercial 3D Printers, Proc, SPIE, 2016.
[94] W. Jia, P.S. Gungor-Ozkerim, Y.S. Zhang, K. Yue, K. Zhu, W. Liu, Q. Pi, B. Byambaa, M.R. Dokmeci, S.R. Shin, A. Khademhosseini, Direct 3D bioprinting of perfusable vascular constructs using a blend bioink, Biomaterials 106 (2016) 58–68.
[95] L.E. Bertassoni, M. Cecconi, V. Manoharan, M. Nikkhah, J. Hjortnaes, A.L. Cristino, G. Barabaschi, D. Demarchi, M.R. Dokmeci, Y. Yang, A. Khademhosseini, Hydrogel bioprinted microchannel networks for vascularization of tissue engineering constructs, Lab on a Chip 14 (13) (2014) 2202–2211.
[96] Y.S. Zhang, F. Davoudi, P. Walch, A. Manbachi, X. Luo, V. Dell'Erba, A.K. Miri, H. Albadawi, A. Arneri, X. Li, X. Wang, M.R. Dokmeci, A. Khademhosseini, R. Oklu, Bioprinted thrombosis-on-a-chip, Lab on a Chip 16 (21) (2016) 4097–4105.
[97] S. Wüst, R. Müller, S. Hofmann, 3D Bioprinting of complex channels—effects of material, orientation, geometry, and cell embedding, Journal of Biomedical Materials Research A 103 (8) (2015) 2558–2570.
[98] D.B. Kolesky, K.A. Homan, M.A. Skylar-Scott, J.A. Lewis, Three-dimensional bioprinting of thick vascularized tissues, Proceedings of the National Academy of Sciences 113 (12) (2016) 3179.
[99] H. Gudapati, M. Dey, I. Ozbolat, A comprehensive review on droplet-based bioprinting: past, present and future, Biomaterials 102 (2016) 20–42.
[100] J. Hendriks, C. Willem Visser, S. Henke, J. Leijten, D.B.F. Saris, C. Sun, D. Lohse, M. Karperien, Optimizing cell viability in droplet-based cell deposition, Scientific Reports 5 (1) (2015) 11304.
[101] A.B. Dababneh, I.T. Ozbolat, Bioprinting Technology: a current state-of-the-art review, Journal of Manufacturing Science and Engineering 136 (6) (2014) 061016.
[102] A. Munaz, R.K. Vadivelu, J.S. John, M. Barton, H. Kamble, N.-T. Nguyen, Three-dimensional printing of biological matters, Journal of Science: Advanced Materials and Devices 1 (1) (2016) 1–17.
[103] S.W. Hock, D.A. Johnson, M.A. Van Veen, Print Quality Optimization for a Color Ink-Jet Printer by Using a Larger Nozzle for the Black Ink Only, US Patent No. US5521622, 1996.
[104] X. Cui, T. Boland, D.D. apos, D. Lima, M.K. Lotz, Thermal inkjet printing in tissue engineering and regenerative medicine, Recent Patents on Drug Delivery and Formulation 6 (2) (2012) 149–155.
[105] P.B. Cowan, J.S. Gondek, K.R. Hudson, Ink Drop Volume Variance Compensation for Inkjet Printing, US Patent No. 6042211, 2000.
[106] J. de Jong, G. de Bruin, H. Reinten, M. van den Berg, H. Wijshoff, M. Versluis, D. Lohse, Air entrapment in piezo-driven inkjet printheads, Journal of the Acoustical Society of America 120 (3) (2006) 1257–1265.
[107] V. Tran, X. Wen, Rapid prototyping technologies for tissue regeneration, in: R. Narayan (Ed.), Rapid Prototyping of Biomaterials, Woodhead Publishing, 2014, pp. 97–155.
[108] I. Ozbolat, 3D Bioprinting: Fundamentals, Principles and Applications, 2016.
[109] F.T. Zohora, A. Yousuf, M. Anwarul, A.Y.M.A. Azim, Inkjet printing: an emerging technology for 3D tissue or organ printing, European Scientific Journal 10 (2014) 339–352.
[110] C. Xu, K. Christensen, Z. Zhang, Y. Huang, J. Fu, R.R. Markwald, Predictive compensation-enabled horizontal inkjet printing of alginate tubular constructs, Manufacturing Letters 1 (1) (2013) 28–32.
[111] P. Kesari, T. Xu, T. Boland, Layer-by-layer printing of cells and its application to tissue engineering, MRS Online Proceedings Library 845 (1) (2004) 5–11.
[112] T. Boland, X. Tao, B.J. Damon, B. Manley, P. Kesari, S. Jalota, S. Bhaduri, Drop-on-demand printing of cells and materials for designer tissue constructs, Materials Science and Engineering: C 27 (3) (2007) 372–376.
[113] X. Cui, T. Boland, Human microvasculature fabrication using thermal inkjet printing technology, Biomaterials 30 (31) (2009) 6221–6227.
[114] K. Arai, S. Iwanaga, H. Toda, C. Genci, Y. Nishiyama, M. Nakamura, Three-dimensional inkjet biofabrication based on designed images, Biofabrication 3 (3) (2011) 34113.

[115] M. Nakamura, A. Kobayashi, F. Takagi, A. Watanabe, Y. Hiruma, K. Ohuchi, Y. Iwasaki, M. Horie, I. Morita, S. Takatani, Biocompatible inkjet printing technique for designed seeding of individual living cells, Tissue Engineering 11 (2005) 1658–1666.
[116] M. Nakamura, T.A. Mir, K. Arai, S. Ito, T. Yoshida, S. Iwanaga, H. Kitano, C. Obara, T. Nikaido, Bioprinting with pre-cultured cellular constructs towards tissue engineering of hierarchical tissues, International Journal of Bioprinting 1 (2015) 39–48.
[117] M. Nakamura, Y. Nishiyama, C. Henmi, S. Iwanaga, H. Nakagawa, K. Yamaguchi, K. Akita, S. Mochizuki, K. Takiura, Ink jet three-dimensional digital fabrication for biological tissue manufacturing: analysis of alginate microgel beads produced by ink jet droplets for three dimensional tissue fabrication, Journal of Imaging Science and Technology 52 (2008) 060201.
[118] C. Xu, Inkjet Printing of Three-Dimensional Vascular-like Constructs from Cell Suspensions, Clemson University, 2014.
[119] C. Xu, Z. Zhang, K. Christensen, Y. Huang, J. Fu, R.R. Markwald, Freeform vertical and horizontal fabrication of alginate-based vascular-like tubular constructs using inkjetting, Journal of Manufacturing Science and Engineering 136 (6) (2014) 61020.
[120] C. Xu, M. Zhang, Y. Huang, A. Ogale, J. Fu, R.R. Markwald, Study of droplet formation process during drop-on-demand inkjetting of living cell-laden bioink, Langmuir 30 (2014) 9130–9138.
[121] C. Xu, W. Chai, Y. Huang, R.R. Markwald, Scaffold-free inkjet printing of three-dimensional zigzag cellular tubes, Biotechnology and Bioengineering 109 (12) (2012) 3152–3160.
[122] K. Christensen, C. Xu, W. Chai, Z. Zhang, J. Fu, Y. Huang, Freeform inkjet printing of cellular structures with bifurcations, Biotechnology and Bioengineering 112 (5) (2015) 1047–1055.
[123] A. Blaeser, D.F. Duarte Campos, M. Weber, S. Neuss, B. Theek, H. Fischer, W. Jahnen-Dechent, Biofabrication under fluorocarbon: a novel freeform fabrication technique to generate high aspect ratio tissue-engineered constructs, BioResearch Open Access 2 (5) (2013) 374–384.
[124] H.N. Chia, B.M. Wu, Recent advances in 3D printing of biomaterials, Journal of Biological Engineering 9 (2015) 1–4.
[125] D.F. Duarte Campos, A. Blaeser, M. Weber, J. Jäkel, S. Neuss, W. Jahnen-Dechent, H. Fischer, Three-dimensional printing of stem cell-laden hydrogels submerged in a hydrophobic high-density fluid, Biofabrication 5 (1) (2012) 015003.
[126] N.A. Sears, D.R. Seshadri, P.S. Dhavalikar, E. Cosgriff-Hernandez, A review of three-dimensional printing in tissue engineering, Tissue Engineering Part B Reviews 22 (4) (2016) 298–310.
[127] D.F. Duarte Campos, A. Blaeser, A. Korsten, S. Neuss, J. Jäkel, M. Vogt, H. Fischer, The stiffness and structure of three-dimensional printed hydrogels direct the differentiation of mesenchymal stromal cells toward adipogenic and osteogenic lineages, Tissue Engineering Part A 21 (3–4) (2014) 740–756.
[128] D.F. Duarte Campos, A. Blaeser, K. Buellesbach, K.S. Sen, W. Xun, W. Tillmann, H. Fischer, Bioprinting organotypic hydrogels with improved mesenchymal stem cell remodeling and mineralization properties for bone tissue engineering, Advanced Healthcare Materials 5 (11) (2016) 1336–1345.
[129] V.K. Lee, D.Y. Kim, H. Ngo, Y. Lee, L. Seo, S.-S. Yoo, P.A. Vincent, G. Dai, Creating perfused functional vascular channels using 3D bio-printing technology, Biomaterials 35 (28) (2014) 8092–8102.
[130] J. Bohandy, B.F. Kim, F.J. Adrian, Metal deposition from a supported metal film using an excimer laser, Journal of Applied Physics 60 (4) (1986) 1538–1539.
[131] N.T. Kattamis, P.E. Purnick, R. Weiss, C.B. Arnold, Thick film laser induced forward transfer for deposition of thermally and mechanically sensitive materials, Applied Physics Letters 91 (17) (2007) 171120.
[132] M. Duocastella, J.M. Fernández-Pradas, J. Domínguez, P. Serra, J.L. Morenza, Printing biological solutions through laser-induced forward transfer, Applied Physics A 93 (4) (2008) 941–945.
[133] M. Duocastella, J.M. Fernández-Pradas, P. Serra, J.L. Morenza, Laser-induced forward transfer of liquids for miniaturized biosensors preparation, Journal of Laser Micro/Nanoengineering 3 (1) (2008) 1–4.

[134] R. Devillard, E. Pagès, M.M. Correa, V. Kériquel, M. Rémy, J. Kalisky, M. Ali, B. Guillotin, F. Guillemot, Chapter 9 - cell patterning by laser-assisted bioprinting, in: M. Piel, M. Théry (Eds.), Methods in Cell Biology, Academic Press, 2014, pp. 159−174.
[135] H. Desrus, B. Chassagne, F. Moizan, R. Devillard, S. Petit, R. Kling, S. Catros, Effective parameters for film-free femtosecond laser assisted bioprinting, Applied Optics 55 (14) (2016) 3879−3886.
[136] B.R. Ringeisen, J.A. Barron, D. Young, C.M. Othon, D. Ladoucuer, P.K. Wu, B.J. Spargo, Laser printing cells, in: B. Bidanda, P. Bártolo (Eds.), Virtual Prototyping & Bio Manufacturing in Medical Applications, Springer US, Boston, MA, 2008, pp. 207−228.
[137] M. Gruene, C. Unger, L. Koch, A. Deiwick, B. Chichkov, Dispensing pico to nanolitre of a natural hydrogel by laser-assisted bioprinting, BioMedical Engineering Online 10 (1) (2011) 19.
[138] L. Koch, M. Gruene, C. Unger, B. Chichkov, Laser assisted cell printing, Current Pharmaceutical Biotechnology 14 (1) (2013) 91−97.
[139] N. Mehrban, G.Z. Teoh, M.A. Birchall, 3D bioprinting for tissue engineering: stem cells in hydrogels, International Journal of Bioprinting 2 (2016) 6−19.
[140] R.F. Pereira, P.J. Bártolo, 3D photo-fabrication for tissue engineering and drug delivery, Engineering 1 (2015) 090−112.
[141] A. Selimis, V. Mironov, M. Farsari, Direct laser writing: principles and materials for scaffold 3D printing, Microelectronic Engineering 132 (2015) 83−89.
[142] R. Xiong, Z. Zhang, W. Chai, Y. Huang, D.B. Chrisey, Freeform drop-on-demand laser printing of 3D alginate and cellular constructs, Biofabrication 7 (4) (2015) 045011.
[143] P.K. Wu, B.R. Ringeisen, Development of human umbilical vein endothelial cell (HUVEC) and human umbilical vein smooth muscle cell (HUVSMC) branch/stem structures on hydrogel layers via biological laser printing (BioLP), Biofabrication 2 (1) (2010) 014111.
[144] R.K. Pirlo, P. Wu, J. Liu, B. Ringeisen, PLGA/hydrogel biopapers as a stackable substrate for printing HUVEC networks via BioLP, Biotechnology and Bioengineering 109 (1) (2012) 262−273.
[145] J.A. Barron, P. Wu, H.D. Ladouceur, B.R. Ringeisen, Biological laser printing: a novel technique for creating heterogeneous 3-dimensional cell patterns, Biomedical Microdevices 6 (2) (2004) 139−147.
[146] A. Ovsianikov, M. Gruene, M. Pflaum, L. Koch, F. Maiorana, M. Wilhelmi, A. Haverich, B. Chichkov, Laser printing of cells into 3D scaffolds, Biofabrication 2 (1) (2010) 014104.
[147] R. Gaebel, N. Ma, J. Liu, J. Guan, L. Koch, C. Klopsch, M. Gruene, A. Toelk, W. Wang, P. Mark, F. Wang, B. Chichkov, W. Li, G. Steinhoff, Patterning human stem cells and endothelial cells with laser printing for cardiac regeneration, Biomaterials 32 (35) (2011) 9218−9230.
[148] K.C. Hribar, K. Meggs, J. Liu, W. Zhu, X. Qu, S. Chen, Three-dimensional direct cell patterning in collagen hydrogels with near-infrared femtosecond laser, Scientific Reports 5 (1) (2015) 17203.
[149] K.C. Hribar, P. Soman, J. Warner, P. Chung, S. Chen, Light-assisted direct-write of 3D functional biomaterials, Lab on a Chip 14 (2) (2014) 268−275.
[150] T.Q. Huang, X. Qu, J. Liu, S. Chen, 3D printing of biomimetic microstructures for cancer cell migration, Biomedical Microdevices 16 (1) (2014) 127−132.
[151] R. Langer, P. Vacanti Joseph, Tissue engineering, Science 260 (5110) (1993) 920−926.
[152] S. Shojaie, L. Ermini, C. Ackerley, J. Wang, S. Chin, B. Yeganeh, M. Bilodeau, M. Sambi, I. Rogers, J. Rossant, C.E. Bear, M. Post, Acellular lung scaffolds direct differentiation of endoderm to functional airway epithelial cells: requirement of matrix-bound HS proteoglycans, Stem Cell Reports 4 (3) (2015) 419−430.
[153] M.J. Webber, O.F. Khan, S.A. Sydlik, B.C. Tang, R. Langer, A perspective on the clinical translation of scaffolds for tissue engineering, Annals of Biomedical Engineering 43 (3) (2015) 641−656.
[154] V. Catto, S. Farè, G. Freddi, M.C. Tanzi, Vascular tissue engineering: recent advances in small diameter blood vessel regeneration, ISRN Vascular Medicine 2014 (2014) 923030.
[155] M. Deutsch, J. Meinhart, P. Zilla, N. Howanietz, M. Gorlitzer, A. Froeschl, A. Stuempflen, D. Bezuidenhout, M. Grabenwoeger, Long-term experience in autologous in vitro endothelialization of infrainguinal ePTFE grafts, Journal of Vascular Surgery 49 (2) (2009) 352−362.

[156] S.L.M. Dahl, C. Rhim, Y.C. Song, L.E. Niklason, Mechanical properties and compositions of tissue engineered and native arteries, Annals of Biomedical Engineering 35 (3) (2007) 348–355.
[157] N. Thottappillil, P.D. Nair, Scaffolds in vascular regeneration: current status, Vascular Health and Risk Management 11 (2015) 79–91.
[158] C.A. Czajka, A.N. Mehesz, T.C. Trusk, M.J. Yost, C.J. Drake, Scaffold-free tissue engineering: organization of the tissue cytoskeleton and its effects on tissue shape, Annals of Biomedical Engineering 42 (5) (2014) 1049–1061.
[159] Y. Jung, H. Ji, Z. Chen, H. Fai Chan, L. Atchison, B. Klitzman, G. Truskey, K.W. Leong, Scaffold-free, human mesenchymal stem cell-based tissue engineered blood vessels, Scientific Reports 5 (1) (2015) 15116.
[160] Y. Tan, D.J. Richards, T.C. Trusk, R.P. Visconti, M.J. Yost, M.S. Kindy, C.J. Drake, W.S. Argraves, R.R. Markwald, Y. Mei, 3D printing facilitated scaffold-free tissue unit fabrication, Biofabrication 6 (2) (2014) 024111.
[161] J.M. Kelm, V. Djonov, L.M. Ittner, D. Fluri, W. Born, S.P. Hoerstrup, M. Fussenegger, Design of custom-shaped vascularized tissues using microtissue spheroids as minimal building units, Tissue Engineering 12 (8) (2006) 2151–2160.
[162] C. Norotte, F.S. Marga, L.E. Niklason, G. Forgacs, Scaffold-free vascular tissue engineering using bioprinting, Biomaterials 30 (2009) 5910–5917.
[163] C. Kucukgul, B. Ozler, H.E. Karakas, D. Gozuacik, B. Koc, 3D hybrid bioprinting of macrovascular structures, Procedia Engineering 59 (2013) 183–192.
[164] C. Kucukgul, S.B. Ozler, I. Inci, E. Karakas, S. Irmak, D. Gozuacik, A. Taralp, B. Koc, 3D bioprinting of biomimetic aortic vascular constructs with self-supporting cells, Biotechnology and Bioengineering 112 (4) (2015) 811–821.
[165] R.P. Visconti, V. Kasyanov, C. Gentile, J. Zhang, R.R. Markwald, V. Mironov, Towards organ printing: engineering an intra-organ branched vascular tree, Expert Opinion on Biological Therapy 10 (3) (2010) 409–420.
[166] J. Visser, B. Peters, T.J. Burger, J. Boomstra, W.J.A. Dhert, F.P.W. Melchels, J. Malda, Biofabrication of multi-material anatomically shaped tissue constructs, Biofabrication 5 (3) (2013) 035007.
[167] J.S. Miller, K.R. Stevens, M.T. Yang, B.M. Baker, D.-H.T. Nguyen, D.M. Cohen, E. Toro, A.A. Chen, P.A. Galie, X. Yu, R. Chaturvedi, S.N. Bhatia, C.S. Chen, Rapid casting of patterned vascular networks for perfusable engineered three-dimensional tissues, Nature Materials 11 (9) (2012) 768–774.
[168] D.B. Kolesky, R.L. Truby, A.S. Gladman, T.A. Busbee, K.A. Homan, J.A. Lewis, 3D bioprinting of vascularized, heterogeneous cell-laden tissue constructs, Advanced Materials 26 (19) (2014) 3124–3130.
[169] H.-W. Kang, S.J. Lee, I.K. Ko, C. Kengla, J.J. Yoo, A. Atala, A 3D bioprinting system to produce human-scale tissue constructs with structural integrity, Nature Biotechnology 34 (3) (2016) 312–319.
[170] A. Akkouch, Y. Yu, I.T. Ozbolat, Microfabrication of scaffold-free tissue strands for three-dimensional tissue engineering, Biofabrication 7 (3) (2015) 31002.
[171] Y. Yu, I.T. Ozbolat, Tissue strands as "bioink" for scale-up organ printing, in: 2014 36th Annual International Conference of the IEEE Engineering in Medicine and Biology Society, 2014, pp. 1428–1431.
[172] Y. Yu, K.K. Moncal, J. Li, W. Peng, I. Rivero, J.A. Martin, I.T. Ozbolat, Three-dimensional bioprinting using self-assembling scalable scaffold-free "tissue strands" as a new bioink, Scientific Reports 6 (1) (2016) 28714.
[173] I.T. Ozbolat, H. Chen, Y. Yu, Development of 'Multi-arm Bioprinter' for hybrid biofabrication of tissue engineering constructs, Robotics and Computer-Integrated Manufacturing 30 (3) (2014) 295–304.
[174] Y. Yu, Y. Zhang, I.T. Ozbolat, A hybrid bioprinting approach for scale-up tissue fabrication, Journal of Manufacturing Science and Engineering 136 (6) (2014) 061013.
[175] N.E. Fedorovich, H.M. Wijnberg, W.J.A. Dhert, J. Alblas, Distinct tissue formation by heterogeneous printing of osteo- and endothelial progenitor cells, Tissue Engineering Part A 17 (15–16) (2011) 2113–2121.

[176] C.C. Chang, L. Krishnan, S.S. Nunes, K.H. Church, L.T. Edgar, E.D. Boland, J.A. Weiss, S.K. Williams, J.B. Hoying, Determinants of microvascular network topologies in implanted neovasculatures, Arteriosclerosis, Thrombosis, and Vascular Biology 32 (1) (2012) 5–14.
[177] K. Jakab, A. Neagu, V. Mironov, R.R. Markwald, G. Forgacs, Engineering biological structures of prescribed shape using self-assembling multicellular systems, Proceedings of the National Academy of Sciences of the United States of America 101 (9) (2004) 2864–2869.
[178] V. Mironov, V. Kasyanov, R.R. Markwald, Organ printing: from bioprinter to organ biofabrication line, Current Opinion in Biotechnology 22 (5) (2011) 667–673.
[179] L.E. Bertassoni, J.C. Cardoso, V. Manoharan, A.L. Cristino, N.S. Bhise, W.A. Araujo, P. Zorlutuna, N.E. Vrana, A.M. Ghaemmaghami, M.R. Dokmeci, A. Khademhosseini, Direct-write bioprinting of cell-laden methacrylated gelatin hydrogels, Biofabrication 6 (2) (2014) 024105.
[180] W. Wu, A. DeConinck, J.A. Lewis, Omnidirectional printing of 3D microvascular networks, Advanced Materials 23 (24) (2011) H178–H183.
[181] S. Bersini, J.S. Jeon, G. Dubini, C. Arrigoni, S. Chung, J.L. Charest, M. Moretti, R.D. Kamm, A microfluidic 3D in vitro model for specificity of breast cancer metastasis to bone, Biomaterials 35 (8) (2014) 2454–2461.
[182] I.T. Ozbolat, W. Peng, V. Ozbolat, Application areas of 3D bioprinting, Drug Discovery Today 21 (8) (2016) 1257–1271.
[183] J. Jang, H.-G. Yi, D.-W. Cho, 3D printed tissue models: present and future, ACS Biomaterials Science & Engineering 2 (10) (2016) 1722–1731.
[184] P. Calvert, Inkjet printing for materials and devices, Chemistry of Materials 13 (10) (2001) 3299–3305.
[185] S. Tasoglu, U. Demirci, Bioprinting for stem cell research, Trends in Biotechnology 31 (1) (2013) 10–19.
[186] C.G. Williams, A.N. Malik, T.K. Kim, P.N. Manson, J.H. Elisseeff, Variable cytocompatibility of six cell lines with photoinitiators used for polymerizing hydrogels and cell encapsulation, Biomaterials 26 (11) (2005) 1211–1218.
[187] Y. Lu, S. Chen, Projection printing of 3-dimensional tissue scaffolds, in: M.A.K. Liebschner (Ed.), Computer-Aided Tissue Engineering, Humana Press, Totowa, NJ, 2012, pp. 289–302.
[188] N.E. Fedorovich, M.H. Oudshoorn, D. van Geemen, W.E. Hennink, J. Alblas, W.J.A. Dhert, The effect of photopolymerization on stem cells embedded in hydrogels, Biomaterials 30 (3) (2009) 344–353.
[189] C. Mandrycky, Z. Wang, K. Kim, D.-H. Kim, 3D bioprinting for engineering complex tissues, Biotechnology Advances 34 (4) (2016) 422–434.
[190] S. Wüst, R. Müller, S. Hofmann, Controlled positioning of cells in biomaterials—approaches towards 3D tissue printing, Journal of Functional Biomaterials 2 (3) (2011) 119–154.
[191] F. Guillemot, A. Souquet, S. Catros, B. Guillotin, Laser-assisted cell printing: principle, physical parameters versus cell fate and perspectives in tissue engineering, Nanomedicine 5 (3) (2010) 507–515.
[192] M. Gruene, A. Deiwick, L. Koch, S. Schlie, C. Unger, N. Hofmann, I. Bernemann, B. Glasmacher, B. Chichkov, Laser printing of stem cells for biofabrication of scaffold-free autologous grafts, Tissue Engineering Part C Methods 17 (1) (2010) 79–87.
[193] V.K. Lee, A. Dias, M.S. Ozturk, K. Chen, B. Tricomi, D.T. Corr, X. Intes, G. Dai, 3D bioprinting and 3D imaging for stem cell engineering, in: K. Turksen (Ed.), Bioprinting in Regenerative Medicine, Springer International Publishing, Switzerland, 2015, pp. 33–43.
[194] M. Itoh, K. Nakayama, R. Noguchi, K. Kamohara, K. Furukawa, K. Uchihashi, S. Toda, J.-I. Oyama, K. Node, S. Morita, Scaffold-free tubular tissues created by a bio-3D printer undergo remodeling and endothelialization when implanted in rat aortae, PloS One (2015) e0136681.
[195] S.G. Dennis, T. Trusk, D. Richards, J. Jia, Y. Tan, Y. Mei, S. Fann, R. Markwald, M. Yost, Viability of bioprinted cellular constructs using a three dispenser cartesian printer, Journal of Visualized Experiments 103 (2015) e53156.
[196] C.A. Wilkens, C.J. Rivet, T.L. Akentjew, J. Alverio, M. Khoury, J.P. Acevedo, Layer-by-layer approach for a uniformed fabrication of a cell patterned vessel-like construct, Biofabrication 9 (1) (2016) 015001.

[197] B. Gao, Q. Yang, X. Zhao, G. Jin, Y. Ma, F. Xu, 4D bioprinting for biomedical applications, Trends in Biotechnology 34 (9) (2016) 746–756.
[198] J. An, C.K. Chua, V. Mironov, A perspective on 4D bioprinting, International Journal of Bioprinting 2 (2016) 3–5.

This page intentionally left blank

CHAPTER 7

Bioprinting of other tissues and organs

7.1 Introduction

Organ shortage has become more problematic despite an increase in willing donors. The solution to this problem requires long-term solutions by building or manufacturing living organs from a person's cells [1]. In the past decades, tissue engineering has emerged as a multidisciplinary field involving scientists, engineers, and physicians, to create biological substitutes mimicking native tissue to replace damaged tissues or restore malfunctioning organs [2]. The traditional tissue engineering strategy is to seed cells onto scaffolds, which can then direct cell proliferation and differentiation into three-dimensional (3D) functioning tissues and organs. Although significant success has been achieved in the past decades both in research and clinical applications [3], it is obvious that complex 3D organs require more precise multicellular structures, which cannot be fulfilled by traditional methods.

Bioprinting offers great precision in the spatial placement of the cells themselves, rather than providing scaffold support [4]. Although still in its infancy, this technology appears to be more promising for advancing tissue engineering toward organ fabrication, ultimately mitigating organ shortage and saving lives. Bioprinting offers a controllable fabrication process, which allows precise placement of various biomaterial and/or cell types simultaneously according to the natural compartments of the target tissue or organs. Multiple cell types, including organ-specific cells and blood vessel cells, i.e., smooth muscle cells and endothelial cells (ECs), constitute the entire organ.

Based on the depiction of previous chapters, this chapter further discusses the current state-of-the-art in bioprinting of other tissues and organs, including cardiac tissue, kidney, liver, nerve tissue, pancreatic tissue, and lung; challenges and future trends toward fabrication of living organs will also be expounded.

7.2 Bioprinting of cardiac tissue

Cardiovascular disease is one of the major causes of death worldwide. Alternative sources expect auto-/allographs for cardiac regenerative medicine are urgent due to the shortage of heart donors. Recently, great advances have been achieved in engineering cardiac tissues using bioprinting technologies, which have shown their potential as a promising strategy

3D Bioprinting in Tissue and Organ Regeneration. https://doi.org/10.1016/B978-0-12-824291-9.00001-4

for cardiovascular regeneration [5,6]. In this section, we emphasize the latest outcomes in cardiac 3D bioprinting.

To construct valve conduits with anatomical architecture, Duan et al. [7] implemented an extrusion-based technique to print alginate/gelatin hydrogel laden with aortic root sinus smooth muscle cells (SMCs) and aortic valve leaflet interstitial cells (VICs). Higher modulus and ultimate strength were obtained in cell-laden constructs than in the acellular group. Also, embedded SMCs and VICs expressed elevated α-smooth muscle actin and vimentin, respectively. In a follow-up study, heart valve conduits were bioprinted using methacrylated hyaluronic acid (HAMA) and methacrylated gelatin (GelMA), which were laden with human aortic valvular interstitial cells (HAVICs) [8]. Increased concentration of GelMA caused lower stiffness and higher viscosity, resulting in superior cell spreading, high viability, and maintenance of fibroblastic phenotype of HAVICs, indicated by deposition of collagen and glycosaminoglycans.

Zou et al. [9] used polyvinyl alcohol (PVA) as the sacrificial ink to print a frame, followed by extruding a hydrogel composite of sodium alginate, agarose, and platelet-rich plasma (PRP), which was loaded with H9c2 and human umbilical vein endothelial cells (HUVECs), into the internal pores of the sacrificial PVA scaffold. The PVA was then dissolved, leaving a complex structure with channel networks. The vascularlike structure was observed implied by the detection of CD31 around the fluid channels. Expression of the myocardial-specific protein (i.e., cardiac troponin-I, cTnI) by cardiac myocytes was also identified. Moreover, an aortic valve with multilevel fluid channels and an anatomic hollow heart with multilevel fluid channels have showcased the capability of this process.

Using an extrusion-based 3D bioprinter, Das et al. [10] deposited bioinks of heart tissue−derived extracellular matrix (hdECM) and collagen, which encapsulated primary rat cardiomyocytes (CMs), and cultured the bioprinted constructs with static and dynamic conditions. Maturation of CMs in hdECM bioink was enhanced qualitatively and quantitatively as compared to the collagen group. The α-sarcomeric actinin (α-SA) alignment and cTnT expression in hdECM groups with dynamic culture demonstrated the enhanced maturation of CMs compared to groups with static culture. In addition, the exposure of bioprinted tissues to fluid shear stress led to improved cell-cell contact, cell-matrix interaction, cellular alignment, and structural maturation of CMs. It was also observed that tissue with lower hdECM concentration (0.6%) under dynamic culture displayed both a beating motion and calcium sparks, while none of both were found in the group with higher hdECM concentration (1.2%) under the same culture condition.

Maiullari et al. [11] presented heterogeneous constructs containing HUVECs and iPSC-CMs with different spatial distributions. Cells were encapsulated within hydrogel strands of alginate and poly(ethylene glycol) (PEG)-fibrinogen, followed by being extruded. In vitro study indicated that bioprinted iPSC-CMs expressed cardiac genes and proteins,

showing the formation of cardiac tissues. In vivo subcutaneous implantation in mice exhibited that the bioprinted constructs amplified the cardiac differentiation, improved the overall alignment of CMs, and favored the formation of large vessels.

Bejleri et al. [12] bioprinted cardiac patch containing cardiac extracellular matrix (cECM) and GelMA for delivery of pediatric human cardiac progenitor cells (hCPCs). Integration of cECM resulted in a significant increase in cardiogenic gene expression of hCPCs, including connexin 43 (Cx43), β-myosin heavy chain (MYH7), and vascular endothelial cadherin (VE-Cad) compared to GelMA-only patches. GelMA-cECM patches showed increased angiogenic potential over GelMA-only patches, evidenced by the enriched formation of endothelial cell tubes. In addition, patch attached to the epicardium of rat heart revealed vascularization over a 14-day culture in vivo.

In a recent study, Kupfer et al. [13] used the technique of freeform reversible embedding of suspended hydrogels (FRESH) to print an inverted geometry of a scale-down human heart, followed by filling with optimized bioink composed of hiPSCs, GelMA, ColMA, fibronectin, and laminin-111 (LN). With further differentiation of hiPSCs to CMs, a human chambered muscle pump (hChaMP) with two chambers and a vessel inlet and outlet was obtained. CMs, smooth muscle cells, and ECs were found by positive staining of representative markers (i.e., cTnI, αSMA, and CD31), respectively. The thickness of the wall showed the thickest region exceeding 500 μm. The hChaMP also demonstrated contiguous electrical function and mechanical pump functions with responsiveness to drugs and electrical pacing frequency.

Lee et al. [14] presented a FRESH technique to bioprint collagen with 20 μm filament resolution. First, a small coronary artery-scale linear tube was bioprinted, and C2C12 cells within a collagen gel were cast around the printed collagen tube. To promote vascularization, collagen was then FRESH-printed with VEGF and displayed enhanced vascularization relative to cast controls. Next, a model of the left ventricle of the heart was bioprinted, with inner and outer walls of collagen and a central core region of hESC-CMs and cardiac fibroblasts. After seven days of culture, ventricles revealed a dense layer of interconnected hESC-CMs. The ventricles had a baseline spontaneous beat rate of $\sim$0.5 Hz and were paced at 1 and 2 Hz by field stimulation. To demonstrate the functionality of bioprinted constructs at an adult human scale, a tri-leaflet heart valve was bioprinted at 28 mm in diameter. By applying physiologic pressures, the valve leaflets could open and close cyclically, with the maximum transvalvular pressure $>$40 mmHg. Finally, to demonstrate organ-scale printing capabilities, a neonatal scale human heart was engineered, and μCT imaging confirmed the reproduction of all the anatomical structures, including the atrial and ventricular chambers, trabeculae, and pulmonary and aortic valves.

To replicate the three-layered structure of the aortic valve leaflets (i.e., fibrosa, spongiosa, and ventricularis), Valk et al. [15] engineered a bioprinted model of calcific aortic valve

disease. GelMA/HAMA hydrogels were tuned to duplicate layer-specific mechanical characteristics and bioprinted with human VICs. Bioprinted constructs were osteogenically differentiated, and VIC differentiation was assessed by near-infrared imaging and immunostaining. In terms of mechanical properties, Young's modulus of the cross-linked GelMa/HAMA hydrogels matched the native fibrosa and spongiosa.

Noor et al. [16] reprogrammed iPSCs from the stromal cells of human omental tissues and differentiated them into CMs and ECs. The decellularized omental tissue was processed into a personalized hydrogel, mixed with iPSC-CMs. The iPSC-ECs were mixed with gelatin, which served as a sacrificial bioink. Two bioinks were used to print the engineered cardiac tissue. In vivo implantation between two layers of rat omentum showed that cells in the bioprinted constructs were elongated and aligned, indicating the contractility potential. To print whole organs with high complexity, a FRESH process was developed using alginate microparticles in the xanthan gum-supplemented growth medium as a support material. In this way, perfusable patches with an actual triaxial lumen were printed. Next, a small-scale cellularized human heart with major blood vessels was fabricated to demonstrate the capability of this approach for constructing complex architectures with anatomical mimicry (Fig. 7.1). A 3D confocal image of the bioprinted heart revealed the spatial organization of CMs and ECs, and the cross-section of the bioprinted heart revealed the internal compartmental structure.

In another study, Izadifar et al. [17] biofabricated a cardiac patch using methacrylated collagen (MeCol) and carboxyl functionalized carbon nanotubes (CNTs), laden with human coronary artery endothelial cells (HCAECs). In the bioprinted constructs of CNT-incorporated alginate framework and cell-laden MeCol, the nanofibrous network within CNTs provided improved viscoelastic behavior and electrical conductivity of cross-linked MeCol. The nanofibrous network within alginate-coated CNTs promoted not only

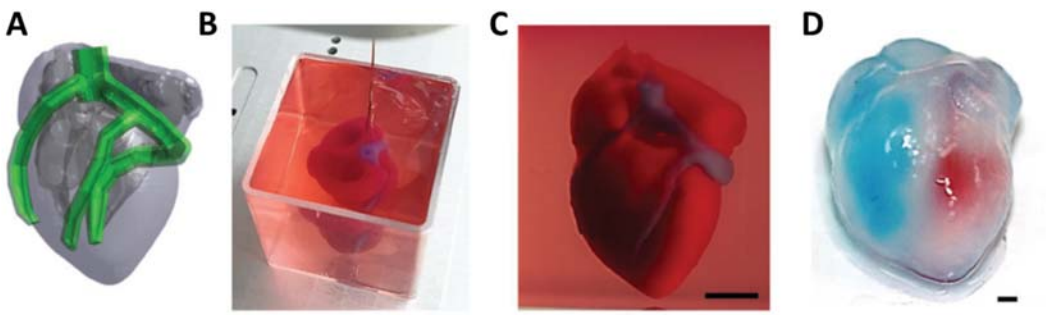

Figure 7.1
(A) CAD model of human heart, (B and C) Bioprinted heart within a support bath (scale bar = 0.5 cm), (D) After extraction, the left and right ventricles were injected with red and blue dyes, respectively, demonstrating hollow chambers (scale bars = 1 mm) [16].

electrical and mechanical properties but also HCAECs attachment and elongation compared to pristine alginate. Furthermore, CNT-reinforced bioprinted structure retained a higher swelling degree over a 20-day culture than CNT-free constructs. With the addition of CNTs, HCAECs presented significant cellular proliferation, migration, and differentiation (lumen formation) over a 10-day in vitro culture.

To bioprinted heart and liver tissues, Yu et al. [18] used a digital light processing (DLP)-based bioprinting technology to pattern GelMA bioinks, blended with dECM of porcine heart left ventricle (HdECM) and liver (LdECM), which provided a conducive environment for the maturation of hiPSC-CMs and hiPSC-hepatocytes. Both bioprinted tissues maintained a high level of cell viability and metabolic activity. For heart tissues, hiPSC-CMs in dECM bioink revealed larger staining areas of α-actinin and actin and significantly higher TnT gene expression in comparison to controls fabricated with collagen type I bioink. For liver tissues, hiPSC-hepatocytes presented more E-cadherin and albumin, and significantly higher gene expression of transthyretin and albumin relative to collagen type I control.

Liu et al. [19] adapted the light-based Micro-Continuous Optical Printing (μCOP) system for the direct printing of a humanized cardiac model using a mixture of human embryonic stem cell-derived cardiomyocytes (hESC-CMs) and GelMA. A cantilever structure was bioprinted using hyaluronic acid glycidyl methacrylate (HAGM) as a sacrificial ink and GelMA cantilevers for the hESC-CMs embedding. To constantly monitor calcium transients, green fluorescent protein/calmodulin/M13 Peptide (GCaMP3)-hESC-CMs were bioprinted. By treating with 500 nM and 1 μM of isoproterenol, the normalized fluorescence of GCaMP3-hESC-CMs increased by 18% and 40%, respectively.

Chikae et al. [20] used the layer-by-layer cell coating technique to cover human-induced pluripotent stem cell—derived cardiomyocytes (hiPSC-CMs) and normal human cardiac fibroblasts (NHCFs) with nanofilms consisting of fibronectin and gelatin. The coated cells were then mixed with thrombin and hyaluronic acid (HA), and printed using a droplet-based process, followed by being cross-linked with the second bioink of fibrinogen and HA. A 3D cardiac tissue was generated with a thickness of 60 μm, a diameter of 1.1 mm, and showed expression of the cardiac-specific protein (i.e., cardiac troponin T, cTnT), and synchronous beating (50—60 beats/min). From the same group, Tsukamoto et al. [21] fabricated a cardiac tissue with an oriented structure and vascular network. A gel frame of hydroxybutyl chitosan (HBC) was firstly deposited, followed by the deposition of fibronectin/gelatin-coated hiPSC-CMs and NHCFs into the HBC gel frame. Fluorescence staining of the cTnT and cytoskeleton revealed that both types of cells aligned within the construct. Results of the contractile behavior exhibited that orientation-controlled cardiac tissue contracted and relaxed twice as fast as uncontrolled counterparts. In addition, coculture with human cardiac microvascular endothelial cells (HMVECs) delivered a more

oriented vascular network in orientation-controlled tissue than the uncontrolled counterpart, which was indicated by the CD31 staining.

Yeung et al. [22] bioprinted cardiac patches using cellular spheroids aggregated from hiPSC-CMs, fibroblasts, and ECs. Cardiac patches were implanted into a rat myocardial infarction model in comparison to a control group without implantation. After 4-week implantation, the experimental and control groups revealed cell viability of 100% and 83%, respectively. In the cardiac patch group, the average vessel counts within the infarcted area were higher and the scar area was smaller, as compared to the control group. Besides, echocardiography showed improvement in cardiac function (ejection fraction and cardiac output) for the cardiac patch group. Table 7.1 summarizes some information from the abovementioned studies on bioprinting of cardiac tissue.

7.3 Bioprinting of kidney

The kidney is an important organ that plays a vital role in removing waste products from organisms [23]. Kidney diseases could be either acute or chronic, and may progressively develop into an end-stage renal disease, which is a stage when kidneys lose their function. In recent years, bioprinting of the kidney has shown great promise, which will be discussed in this section.

King et al. [24] used the Organovo NovoGen bioprinter to develop a scaffold-free model of the proximal tubule (PT) interstitial interface containing renal fibroblasts, HUVECs, and primary human renal proximal tubule epithelial cells (RPTECs). The formation of extensive microvascular networks was observed, which was supported by endogenous ECM deposition (e.g., collagen, CD31, cytokeratin 18, E-cadherin). RPTECs demonstrated tight junction formation and expression of renal uptake and efflux transporters. Treatment of the bioprinted tissues with the nephrotoxin cisplatin induced decreased cell viability in a dose-dependent fashion, whereas cimetidine mitigated such effect, confirming the role of the organic cation transporter 2 (OCT2) in cisplatin-induced nephrotoxicity. The tissue also demonstrated a fibrotic response to transforming growth factor-beta (TGF-β), as evidenced by an increased expression of genes related to human fibrosis (e.g., collagen type I, connective tissue growth factor, fibroblast-activating protein, and platelet-derived growth factor receptor β) and deposition of collagen.

Ali et al. [25] developed a photo-cross-linkable kidney ECM-derived bioink (KdECMMA), which was obtained from decellularized porcine whole kidneys followed by methacrylation. Such bioink was then mixed with human primary kidney cells and printed by an integrated tissue-organ printing (ITOP) system to generate renal tissue [25]. The KdECMMA-based bioinks showed improved cell proliferation and organization, sodium uptake capability, and hydrolase activity as compared with GelMA-based bioinks. In

Table 7.1: Summary of the studies on bioprinting of cardiac tissue.

Study	Technology	Materials	Cell source	Viability
Duan et al. [7]	Extrusion	Alginate, gelatin	Aortic root sinus SMC and aortic VIC	>80%
Duan et al. [8]	Extrusion	HAMA, GelMA	HAVIC	>90%
Zou et al. [9]	Extrusion	PVA, alginate, agarose, PRP	H9c2 rat myoblasts, HUVECs	96%
Das et al. [10]	Extrusion	hdECM, collagen	CMs	>97%
Maiullari et al. [11]	Extrusion	Alginate and PF	HUVECs and iPSC-CMs	80% −90%
Bejleri et al. [12]	Extrusion	GelMA	hCPC	>75%
Kupfer et al. [13]	Extrusion	GelMA, ColMA, FN and LN, gelatin	hiPSCs	94%
Lee et al. [14]	Extrusion	Collagen, alginate	C2C12 cells, hESC-CMs, and cardiac fibroblasts	96%
Valk et al. [15]	Extrusion	GelMA, HAMA, Pluronic F-127	Human VICs	—
Noor et al. [16]	Extrusion	Decellularized omentum, gelatin, alginate	iPSC-CMs and iPSC-ECs, rat neonatal CMs, HUVECs, and human neonatal dermal fibroblast	>98%
Izadifar et al. [17]	Laser	ColMA, alginate, CNTs	HCAECs	>90%
Yu et al. [18]	Laser-based	HdECM, LdECM, GelMA	hiPSC-CMs and hiPSC-hepatocytes	—
Liu et al. [19]	Laser-based	GelMA, GMHA	hESC-CMs	90%
Chikae et al. [20]	Droplet	Fibronectin, gelatin, thrombin and HA	hiPSC-CM and NHCFs	92%
Tsukamoto et al. [21]	Droplet	HBC, fibronectin, gelatin	hiPSC-CM, NHCF, HMVEC	—
Yeung et al. [22]	Scaffold-free	—	hiPSC-CMs, fibroblasts, and endothelial cells	100%

Note. *CMs* = cardiomyocytes; *CNTs* = carboxyl functionalized carbon nanotubes; *ColMA* = methacrylated collagen; *FN* = fibronectin; *GelMA* = methacrylated gelatin; *GMHA* = glycidal methacrylated hyaluronic acid; *HA* = hyaluronic acid; *HAMA* = methacrylated hyaluronic acid; *HAVIC* = human aortic valvular interstitial cells; *HBC* = hydroxybutyl chitosan; *HCAECs* = human coronary artery endothelial cells; *hCPC* = human cardiac progenitor cell; *hdECM* = heart tissue-derived extracellular matrix; *hESC-CMs* = human embryonic stem cell-derived cardiomyocyte; *hESC-CMs* = human embryonic stem cell-derived cardiomyocytes; *hiPSCs* = human induced pluripotent cells; *HMVEC* = human cardiac microvascular endothelial cells; *HUVECs* = human umbilical vein endothelial cells; *iPSC-CMs* = induced pluripotent cell-derived cardiomyocytes; *iPSC-ECs* = induced pluripotent cell-derived endothelial cells; *LN* = laminin-111; *NHCFs* = normal human cardiac fibroblasts; *PEG* = poly(ethylene glycol); *PF* = PEG-fibrinogen; *PRP* = platelet-rich plasma; *PVA* = polyvinyl alcohol; *SMC* = smooth muscle cells; *VIC* = valve interstitial cells.

addition, the bioprinted human kidney cells maintained kidney-specific phenotype and formed tubular and glomerularlike structures in the construct, which were indicated by the immunohistochemical analysis of tubular marker (AQP1) and glomerular marker (NPHS2).

Lawlor and Higgins et al. [26,27] presented rapid and high-throughput generation of kidney organoids using an extrusion-based bioprinting technique. Observations of bright field imaging and immunofluorescence revealed that bioprinted kidney organoids were morphologically equivalent to manually prepared ones. The response of kidney organoids to drugs was evaluated by treating organoids with several nephrotoxic aminoglycosides, which indicated that cell viability reduced in a concentration-dependent fashion. Furthermore, organoids consisting of the same total cell number in the form of a big single point or a line of cells were generated by the bioprinter. Superior nephron maturation and glomerular number were presented in bioprinted lines as compared with those in the construct of a single point. A kidney patch was further generated by printing a series of parallel lines. The patch demonstrated well-patterned nephrons indicated by the immunofluorescence of nephron relevant makers, and the live confocal imaging showed uptake of albumin into proximal tubules, confirming the functionality of nephron segments.

Homan et al. [28] reported a bioprinting method for creating a 3D model of human renal proximal tubules (PT), which were fully embedded within an ECM including fibrin and gelatin (Fig. 7.2). The tube was comprised of Pluronic F127, which was liquefied and removed from the final 3D construct. Proximal tubule epithelial cells (PTECs) adhered to the complex tubular architecture, which was actively perfused. As compared to the cells grown on 2D culture with or without perfusion, such 3D PT displayed enhanced epithelial morphology and functional properties, such as cell height, observation of primary cilia, expression of the epithelial markers, and microvilli density. With the application of Cyclosporine A, a nephrotoxin that damages proximal tubule cells, the epithelial barrier was disrupted in a dose-dependent fashion, indicating that the 3D PT model had the potential for qualitative and quantitative assessment of nephrotoxicity.

In another recent study, Addario et al. [29] successfully isolated primary murine tubular epithelial cells (pmTECs), which were then combined with HUVECs to load into polysaccharide bioink (e.g., alginate, gelatin, and a pectin solution). The bioinks were extruded, yielding high cell viability and metabolic activity. A core-shell structure was created to imitate the tubulointerstitium, in which the renal tubule was wrapped by the peritubular capillaries. Table 7.2 summarizes some information from the abovementioned studies on the bioprinting of the kidney.

7.4 Bioprinting of liver

Physiological functions of the liver include the metabolism of fat, carbohydrate, and protein; detoxification of xenobiotics; storage of glycogen; production of bile; synthesis of albumin; and so on [30]. Since the crucial role of the liver, failure of liver functions causes various liver dysfunction conditions and further affects other organs [31]. Acute liver

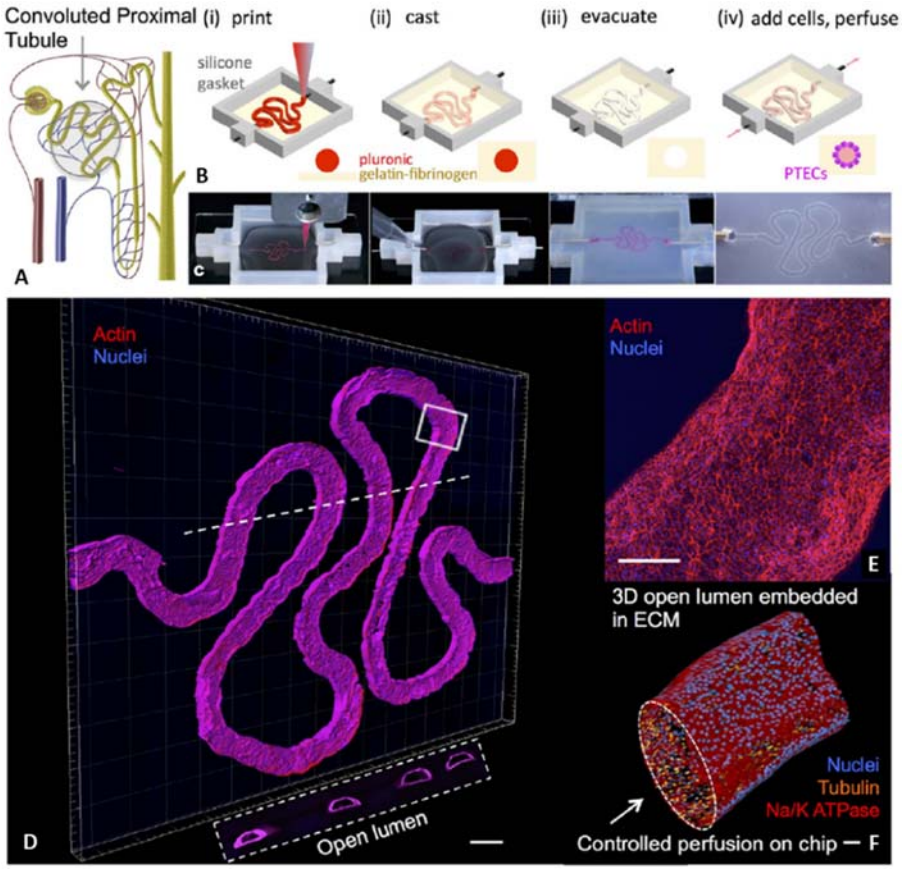

Figure 7.2
Bioprinting of the convoluted renal proximal tubule on a chip. (A) Schematic of a nephron with the convoluted proximal tubule, (B and C) schematics and images of different steps in the fabrication of 3D proximal tubules; (D) a confocal microscopic 3D image of the printed convoluted proximal tubule (scale bar = 500 μm); (E) higher magnification view of the region in (D) denoted by the white rectangle (scale bar = 200 μm), (F) 3D rendering of the convoluted renal proximal tubule where Na/K ATPase was stained in red, acetylated tubulin was orange highlighting the primary cilia, and nuclei were blue (scale bar = 50 μm) [28].

failure can cause complications such as infection, electrolyte deficiencies, and bleeding. Without proper treatment, both acute and chronic liver failure may eventually result in death [32,33]. Liver failure can affect many of the body's organs. In this section, the up-to-date advances in bioprinting of the liver are summarized and highlighted.

Goulart et al. [34] investigated the bioprinting of iPSC-derived hepatic spheroids within an alginate/pluronic F-127 bioink, which was compared with the cell dispersion of hepatocytes. The iPSC-derived nonparenchymal cells (i.e., endothelial and mesenchymal)

Table 7.2: Summary of the studies on bioprinting of kidney.

Study	Technology	Materials	Cell source	Viability
King et al. [24]	Extrusion	NovoGel BioInk	HUVECs, RPTECs, adult renal fibroblasts	—
Ali et al. [25]	Extrusion	KdECMMA, gelatin, hyaluronic acid (HA), glycerol, GelMA	Human primary kidney cells	95%
Lawlor and Higgins et al. [26,27]	Extrusion	NovoGen Bioink	iPSCs	93% −99%
Homan et al. [28]	Extrusion	Gelatin, fibrinogen, silicone, Pluronic F127	PTECs, RPTECs, A498 renal cancer cells, HNDF	—
Addario et al. [29]	Extrusion	Alginate, alginate andpectin	pmTECs, HUVECs	80% −90%

Note. *GelMA* = methacrylated gelatin; *HNDF* = human neonatal dermal fibroblasts; *HUVECs* = human umbilical vein endothelial cells; *iPSCs* = induced pluripotent cells; *KdECM* = kidney ECM-derived hydrogel; *KdECMMA* = KdECM methacrylate; *pmTEC* = primary murine tubular epithelial cells; *PTECs* = proximal tubule epithelial cells; *RPTECs* = renal proximal tubule epithelial cells.

were cocultured in both groups. Constructs with cell suspension exhibited lower cell viability, inferior hepatic function (e.g., albumin production, expression of hepatocyte proteins), and unbalanced protein/amino acid metabolism, relative to constructs with spheroids. Besides, the epithelial-mesenchymal transition was seen in constructs with cell suspension revealed, which resulted in rapid loss of hepatocyte phenotype as compared to the spheroid-based group.

Mazzocchi et al. [35] developed a simple bioink by combining methacrylated collagen type I with thiolated HA and UV cross-linker. A 3:1 collagen type I to HA ratio was found the best for printing and was blended with human hepatocytes to bioprint the liver microenvironments. To evaluate the functionality of hepatocytes, constructs were exposed to acetaminophen (APAP), a hepatic toxicant, followed by measuring the levels of albumin, urea, α-GST, and lactic acid dehydrogenase (LDH) in the media over time. Hepatocytes maintained the urea and albumin production, and responded appropriately to APAP, representing the bioink could support the physiologic response of hepatocytes to drugs.

To study the effect of scaffold geometries on the modulation of hepatocyte function, Lewis et al. [36] precisely controlled the pore geometry of 3D-printed gelatin scaffolds using the pneumatic extrusion process. An undifferentiated hepatocyte cell line (HUH7), which was seeded on 3D-printed scaffolds of two different geometries (interlayer angles of 60 degrees and 90 degrees), demonstrated high viability and proliferation. In addition, tests of hepatic functions, including albumin secretion, CYP activity, and bile transport, indicated the improved biological function of scaffolds with an interlayer angle of 60 degrees as compared to that with the angle of 90 degrees and 2D culture.

Bhise et al. [37] developed a liver-on-a-chip device for long-term culture of 3D human HepG2/C3A spheroids to test drug toxicity. A bioprinter was equipped with a bioreactor to produce 3D hepatic constructs of spheroids embedded in GelMA hydrogel. The bioprinted hepatic construct was evaluated by measurement of albumin secretion, alpha-1 antitrypsin, transferrin, and ceruloplasmin, which indicated that the construct kept hepatic functions during a culture period of 30 days. The functionality was also confirmed by the expression of hepatocyte markers (i.e., cytokeratin 18, MRP2 bile canalicular protein, and tight junction protein ZO-1). Furthermore, treatment with 15 mM acetaminophen triggered a toxic response in the hepatic construct which was comparable to those observed in other in vitro or in vivo models, demonstrating the efficacy of this device for toxicity assessment.

Nguyen et al. [38] bioprinted human liver tissues which were comprised of primary human hepatocytes, hepatic stellates, and HUVEC cells. After cell assembly, distinct intercellular hepatocyte junctions and CD31+ endothelial networks were detected. As compared to 2D hepatocyte culture, bioprinted tissues retained levels of adenosine triphosphate (ATP), albumin, and expression of Cytochrome P450s during a 28-day culture. To model the drug-induced liver injury (DILI), responses of the bioprinted tissue to Trovafloxacin were tested. After seven days of treatment, Trovafloxacin led to a significant reduction in both albumin and ATP in a dose-dependent manner. A decrease in tissue cohesion and an increase in hepatocyte necrosis were observed when a high dose of Trovafloxacin (100 μM) was applied, leading to the fragmentation of bioprinted constructs.

In a follow-up study, Norona et al. [39] used the same bioprinted construct to model methotrexate- and thioacetamide-induced liver injury, which led to fibrosis. The constructs were treated with fibrogenic agents, such as transforming growth factor-β1 (TGF-β1), prototype fibrogenic compounds methotrexate (MTX), and thioacetamide (TAA). Various modes of liver injury were detected, when exposing the bioprinted construct to low concentrations of these compounds, such as hepatocellular damage, and progressive fibrogenesis visualized by the deposition of fibrillar collagens. Transient cytokine production and upregulated expression of fibrosis-associated genes ACTA2 and COL1A1 replicated characteristics of a typical wound-healing response. In the early period of a 14-day culture, proinflammatory cytokines (e.g., IL-8, IL-1β) surged, which was followed by concentration- and drug-dependent alterations in immunomodulatory and chemotactic cytokines (e.g., IL-13, IL-6, and MCP-1).

Wu et al. [40] developed a hybrid bioink of alginate and cellulose nanocrystals (CNCs) laden with fibroblast and hepatoma cells and built a honeycomb 3D structure using an extrusion-based technique. The outer honeycomb frame was printed using fibroblast-containing bioinks, and the inner cavities were filled with a bioink loaded with hepatoma cells. Since the hydrogel lacked cell-binding sites, the cell viability of fibroblast and

hepatoma cells decreased to 59% and 50%, respectively, after culturing for three days. In another study, Jeon et al. [41] applied extrusion-based bioprinting to construct 3D hepatic constructs with alginate. HepG2 cells cultured in 3D structures proliferated faster and expressed more albumin, AFP, and also Ki-67 than those in 2D culture, indicating that the bioprinted structure benefited the HepG2 cells to proliferate without losing their hepatic phenotypes.

Ma et al. [42] presented a 3D hydrogel-based triculture model that contained hiPSC-derived hepatic progenitor cells (hiPSC-HPCs), HUVECs, and adipose-derived stem cells (ADSCs). In a two-step sequential manner, a DLP-based bioprinting technology was applied to create a hepatic construct, in which the first layer was GelMA laden with hiPSC-HPCs, and the second layer contained HUVECs and ADSCs embedded within GelMA and glycidal methacrylate-hyaluronic acid (GMHA). The model represented the native hepatic structure, comprising an array of liver lobules with physiological sizes. Compared to the 2D culture and 3D hiPSC-HPCs-only model, the 3D triculture model facilitated hiPSC-HPCs to improve not only anabolic and catabolic functions, which was proven by liver-specific genes (e.g., HNF4a, TTR, and ALB), but also the key CYP expression levels and the drug induction potential.

In a follow-up study, this group used the same process to pattern liver dECM with controllable mechanical properties, which targeted at being a platform to study the progression of hepatocellular carcinoma [43]. Viability of HepG2 cells improved with the addition of liver dECM and collagen into the GelMA scaffolds as compared to GelMA scaffolds alone. Using different exposure times, the dECM-based scaffolds possessed different stiffness. HepG2 cells exhibited a higher viability and growth rate in the less stiff scaffolds, while the expression of liver-specific markers (ALB and AFP) was significantly downregulated with a stiffness similar to a cirrhotic matrix. Furthermore, a cancer tissue model with tissue-scale organization and different regional stiffness allowed the visualization of HepG2 stromal invasion from the nodule with cirrhotic stiffness (Fig. 7.3).

Tsang et al. [44] engineered a hepatic tissue using a multilayered photopatterning process to embed cells in PEG hydrogels. Cell viability was higher in photopatterned hydrogels (structural feature: 500 μm in width) than in unpatterned hydrogels. The incorporation of RGDS (Arg-Gly-Asp-Ser peptide) increased the urea secretion and albumin production by fivefold over PEG controls. To imitate the branching architecture of the native liver, a multilayered hepatic construct was then created, which consisted of a three-layered hexagonal branching structure. After being cultured in a bioreactor with continuous flow for 12 days, the three-layered constructs induced higher levels of both albumin and urea than unpatterned constructs with identical cell numbers and external dimensions.

Grix et al. [45] bioprinted a liver organoid using a laser-based approach, which contained GelMA loaded with HepaRG and human stellate cells (SteCs). Within the hexagonal

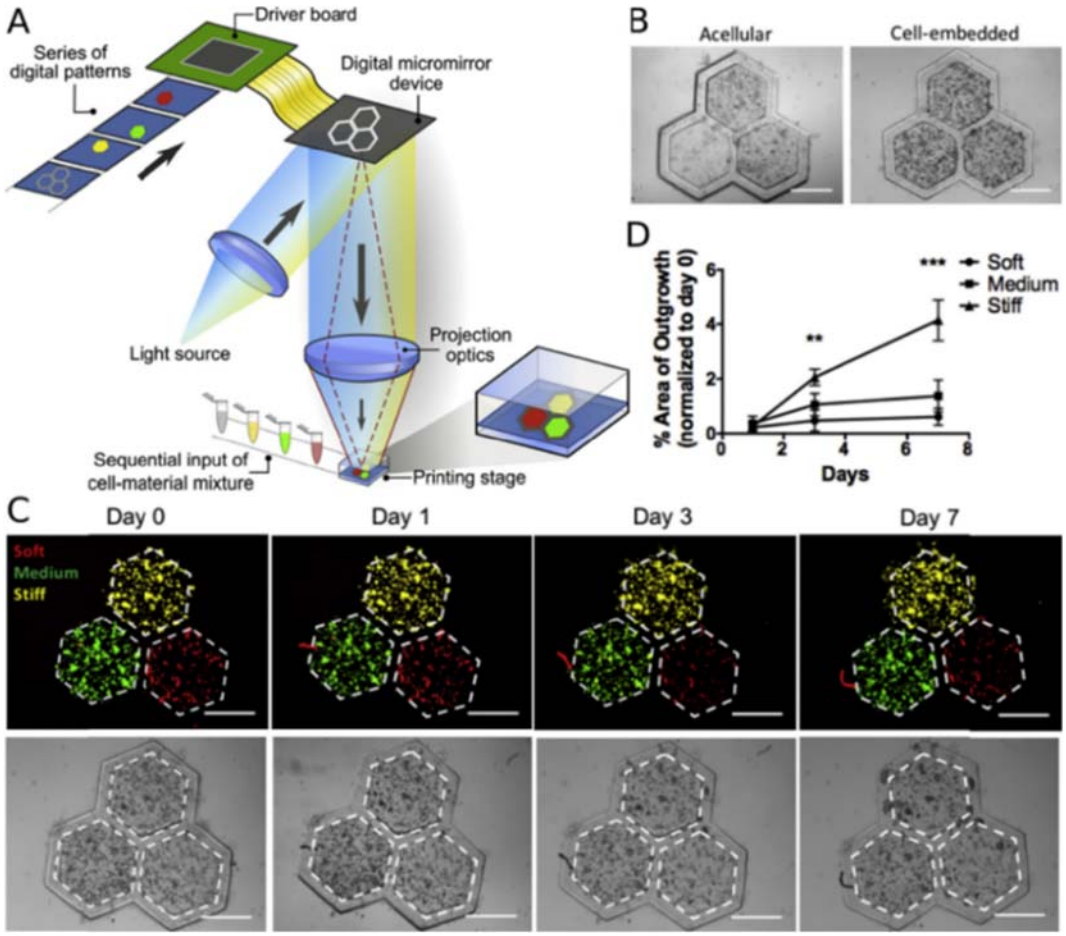

Figure 7.3

3D bioprinted liver cancer tissue platform with varied scaffold stiffness. (A) Schematic diagram showing the bioprinting setup of the dECM-based liver cancer tissue platform. (B) Images presenting bioprinted acellular and cell-embedded scaffolds (scale bar = 500 μm). (C) Merged fluorescence and bright-field images showing the tracked HepG2 cell locations relative to their assigned hexagonal regions (scale bar = 500 μm). (D) Quantitative plot showing the percent area of cell invasion originating from the three different scaffolds over time (n = 5, $^{**}P \leq .01$, $^{***}P \leq .001$) [43].

construct, hollow channels printed with PEG were integrated to facilitate perfusion. Higher albumin and cytochrome P4503A4 (CYP3A4) expressions were observed in bioprinted liver tissues than that in 2D culture over a 2-week duration. Moreover, the liver-specific bile transporter (multidrug resistance-associated protein 2 (MRP2)), glucose consumption, lactate, and lactate dehydrogenase (LDH) were quantified and found to be stable during a 2-week culture.

Faulkner–Jones et al. [46] reported the bioprinting of hiPSCs using a droplet-based technique. Hepatocytelike cells (HLCs) were differentiated from both hiPSCs and human embryonic stem cells (hESCs) and bioprinted. Both types of HLCs showed expression of nuclear factor 4 alpha, secretion of albumin, and morphology similar to that of hepatocytes. The hESC-derived HLCs were 3D printed using alginate hydrogel and were found to be hepatic which was indicated by albumin secretion. Bioprinted constructs with 40-layered HLC-containing alginate obtained peak albumin secretion on day 21 of culture. Table 7.3 summarizes some information from the abovementioned studies on bioprinting of the liver.

Table 7.3: Summary of the studies on bioprinting of liver.

Study	Technology	Materials	Cell source	Viability
Goulart et al. [34]	Extrusion	Alginate, pluronic F-127	iPSCs	80%
Mazzocchi et al. [35]	Extrusion	ColMA, thiolated HA	L×2 (human hepatic stellate cell line), HSCs, primary human hepatocytes	75% –85%
Lewis et al. [36]	Extrusion	Gelatin	HUH7 (human hepatocellular carcinoma cell line)	—
Bhise et al. [37]	Extrusion	GelMA	HepG2/C3A cells	—
Nguyen et al. [38]	Extrusion	NovoGel 2.0 Hydrogel	Primary human hepatocytes, hepatic stellates, HUVECs	—
Norona et al. [39]	Extrusion	NovoGel 2.0 Hydrogel	Human hepatocytes, HSCs, HUVECs	—
Wu et al. [40]	Extrusion	CNC, alginate	Fibroblasts, human hepatoma cells	50% –60%
Jeon et al. [41]	Extrusion	Alginate	HepG2 cells	—
Ma et al. [42]	Laser	GelMA, GMHA	hiPSC-HPCs, HUVECs and ADSCs	65%
Ma et al. [43]	Laser	GelMA	HepG2 cells	—
Tsang et al. [44]	Laser	PEG monoacrylate-peptide, PEGDA, acryloyl-PEG-RGDS	Hepatocytes, NIH 3T3-J2 cells	—
Grix et al. [45]	Laser	PEG, GelMA	HepaRG cells, SteCs	—
Faulkner-Jones et al. [46]	Droplet	RGD-coupled sodium alginate	hESCs, hiPSCs	70% –90%

Note. *ADSCs* = adipose-derived stem cells; *CNCs* = cellulose nanocrystals; *ColMA* = methacrylated collagen; *GelMA* = methacrylated gelatin; *GMHA* = glycidal methacrylated hyaluronic acid; *HA* = hyaluronic acid; *hESCs* = human embryonic stem cells; *hiPSC-HPCs* = hiPSC-derived hepatic progenitor cells; *hiPSCs* = human induced pluripotent cells; *HSCs* = hepatic stellate cells; *HUVECs* = human umbilical vein endothelial cells; *PEG* = poly(ethylene glycol); *PEGDA* = poly(ethylene glycol) diacrylate; *RGD* = arginylglycylaspartic acid; *RGDS* = Arg-Gly-Asp-Ser peptide; *SteCs* = human hepatic stellate cells.

7.5 Bioprinting of nerve tissue

Nerve tissue is easy to get damaged because of diseases and trauma and is also tough to be repaired due to limited intrinsic regenerative capability [47]. Bioprinting of nerve tissue involves the surgical implantation of cell-laden constructs to the injured nerve site, bridging the lesion and providing a direct guide for neural cells to eventually recover the neural function, which has become an encouraging field for nerve regeneration [48]. Here, the current achievements of bioprinting of nerve tissue are presented.

Lee et al. [49] used dispensing/printing technique to construct a nerve tissue, which contained murine neural stem cell (NSC) line C17.2, collagen, and VEGF-releasing fibrin gel. After bioprinting, cells remained highly active (e.g., 93% at 4 days) compared with the scaffold without the VEGF. Cells in scaffold with VEGF proliferated well and had an elongated shape. Moreover, cells, which were printed within 1 mm from the border of VEGF-containing fibrin, migrated toward the VEGF-containing fibrin and formed clusters, suggesting that the VEGF can support the function of nerve cells.

To overcome secondary disease and infection caused by the use of autografts to repair nerve rupture, Owens et al. [50] bioprinted scaffold-free constructs and implanted them into rats. The outer ring of the graft was made of mouse bone marrow stem cells (BMSCs). Cylinders with 90% BMSCs and 10% Schwann cells (SCs) were then alternated with agarose rods, which induced multiple lumina in the interior of the graft. Measurement of compound muscle action potential (CMAP) showed significantly different thresholds for scaffold-free constructs and collagen tubes which were used to treat injured legs of rats, compared to the control group (normal leg). This difference disappeared at 5× thresholds for scaffold-free constructs, but not for collagen tubes, implying that scaffold-free constructs may have a superior repair over the collagen tube. Besides, in the MAP measurement in response to afferent stimulation of the sciatic nerve (SPR), there were no differences between baseline blood pressure, maximum blood pressure, and the change in blood pressure among the autologous, collagen tube, and scaffold-free constructs. Finally, axon regrowth took place across the scaffold-free constructs.

Hsieh et al. [51] developed different polyurethane (PU) dispersions that cross-linked at 37°C, which can adjust the stiffness according to the solid content in the dispersion. NSCs in the culture medium were mixed with the preheated PU nanoparticle dispersions at different ratios. The expression level of related genes (e.g., nestin and β-tubulin) significantly increased in NSC-embedded PU hydrogel, as compared with TCP control. Moreover, bioprinted NSC-laden PU constructs were implanted into adult zebrafish with brain damage, with results showing a rescue rate of 81% in locomotion after six days and a mortality rate of 37% after eight days (control group: 85%).

A handheld printing process that enabled the printing of free-form 3D structures was developed by Lozano et al. [52] Neuronal cells were mixed into the arginylglycylaspartic acid-gellan gum (RGD-GG) gel, which was porous enough to maintain the cell activity of neuronal cells. After printing with $CaCl_2$ and Dulbecco's Modified Eagle's Medium (DMEM) as a cross-linking agent, cells still maintained high viability (73%). The diffusion experiment using bovine serum albumin (BSA) indicated that BSA uptake obtained equilibrium by 48 h. Layered printing showed that when the structure had up to five subsequent layers, the bottom section of the construct did not show deformation (Fig. 7.4). After five days of culture, cells generated a neuronal network with axons starting to enter into the acellular middle layer.

Gu et al. [53] developed a bioink that included polysaccharides alginate (AI), carboxymethyl-chitosan (CMC), agarose (Ag), and human NSCs. The bioink of 5% w/v Al, 5% w/v CMC, and 1.5% w/v Ag was found to have sufficient viscosities to obtain a well-defined scaffold. Also, this bioink was porous enough to efficiently uptake BSA and

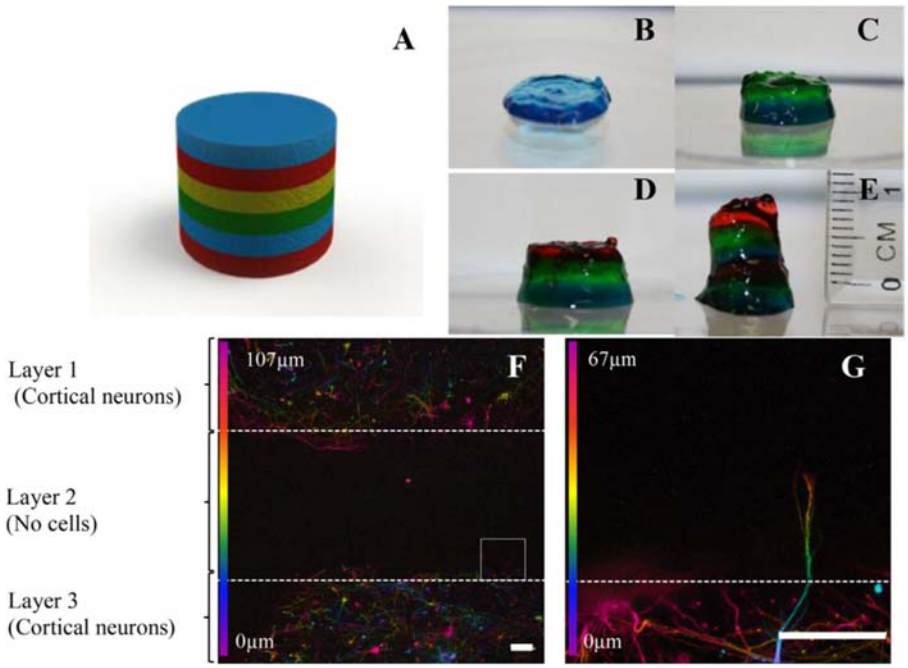

Figure 7.4
Printed brainlike layered structure. (A) CAD model representing the proposed brainlike layer structure. (B–E) The bioprinting process created a brainlike structure with each color representing a layer. (F) Confocal microscope images of neurons in different layers after five days of culture. (G) Expanded view of the area from the square of (F) showing an axon penetrating the adjacent layer (scale bars = 100 mm) [52].

maintain high cell viability (∼92%). After differentiation, upregulation of pan-neuronal and neuroglial markers was found. Cells with rounded soma and extensive neurite outgrowth were also observed.

Since GelMA has a porous structure and graphene can promote NSCs to produce neurons, Zhu et al. [54] added graphene nanoplatelets into GelMA, and blended it with NSCs. The 2D culture showed that the bioink was not cytotoxic. NSCs in bioprinted scaffolds expressed abundant β-tubulin III instead of glial fibrillary acidic protein (GFAP), indicating the tendency of neuronal differentiation. Moreover, NSCs in the scaffold processed neurites elongation.

To enhance the mechanical strength of collagen scaffolds, Chen et al. [55] added heparin sulfate (HS) to collagen solution to create a collagen/heparin sulfate scaffold. The internal structure of scaffolds was found to be regular, uniform, and highly porous. With the addition of HS, both the compression modulus and strengths of the scaffold were significantly enhanced as compared to scaffolds with collagen only. The release of basic fibroblast growth factor (bFGF) from scaffolds suggested that HS significantly enhanced bFGF immobilization and absorption into the collagen. The scaffold was also implanted into rats with spinal cord injury (SCI). It was found that scaffold could not only significantly shorten the latency but also enhance the amplitude of motor evoked potentials and somatosensory evoked potentials.

Huang et al. [56] mixed graphene oxide (GO) and pluronic-stabilized grapheme (G-P) with PU, respectively, to produce composite bioinks (PU/GO, PU/G-P). The mechanical test displayed that the storage moduli of PU, PU/GO, and PU/G-P were about 3 kPa, 1.5 kPa, and 1.3 kPa, respectively. NSCs encapsulated in all bioinks could survive and proliferate for 7 days. The oxygen consumption rate (OCR) of NSCs in PU/G-P was significantly greater than those in PU or PU/GO. In addition, NSCs-laden bioinks were bioprinted, and cells in PU/G-P exhibited higher gene expression levels of β-tubulin, glial fibrillary acidic protein (GFAP), and microtubule-associated protein 2 (MAP2).

Pateman et al. [57] used PEG as bioink to fabricate NGC (nerve guidance conduits) using a laser-based technique that could produce feature sizes of 50 μm. NG108-15 neuronal cell culture in vitro showed that the quality and quantity of cells growing on PEG were not significantly different from those on tissue culture plastic (TCP). Two structures were fabricated, which were channels for the in vitro culture of dorsal root ganglion (DRG) explants, and NGCs for in vivo implantation. In the culture of DRG explants, SCs and neurites were seen to migrate distally from the DRG body and adhere to the PEG channel. In the implantation of NGCs into mouse common fibular injury site, results showed that NGC supported reinnervation across a 3 mm injury gap after 21 days, with outcomes comparable to that of an autograft (Fig. 7.5). Table 7.4 summarizes some information from the abovementioned studies on bioprinting of nerve tissue.

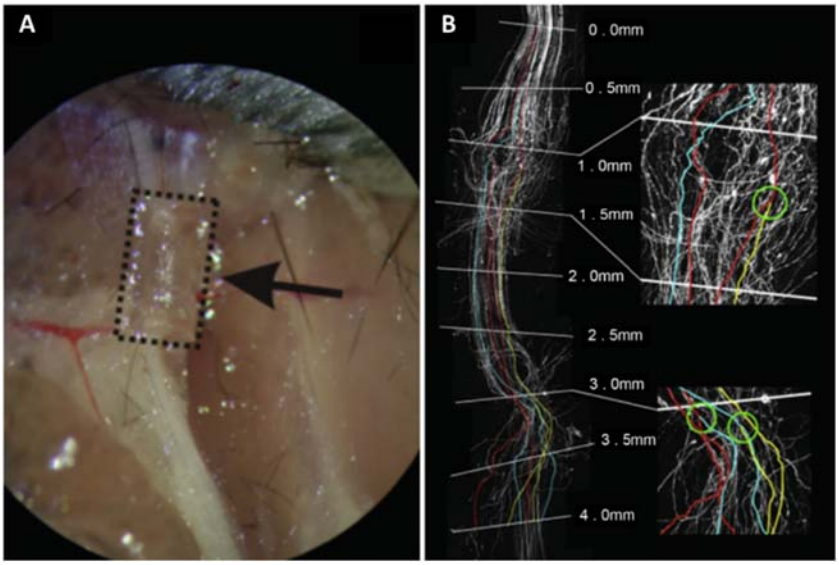

Figure 7.5
(A) Implantation of a PEG guide into a 3 mm injury model of a mouse. (B) Image of nerve graft repair showing intervals marked with sample axon tracing from 4 mm interval position back to 0 mm (start) interval [57].

Table 7.4: Summary of the studies on bioprinting of nerve tissue.

Study	Technology	Materials	Cell source	Viability
Lee et al. [49]	Extrusion	Collagen, VEGF-releasing fibrin	Murine NSC line C17.2	93%
Owens et al. [50]	Extrusion	Agarose	Mouse BMSCs, SCs	—
Hsieh et al. [51]	Extrusion	PU	NSCs	30% −100%
Lozano et al. [52]	Extrusion	RGD-GG	Primary neural cells	73%
Gu et al. [53]	Extrusion	Alginate, CMC, agarose	hNSCs	92%
Zhu et al. [54]	Extrusion	GelMA, graphene	Mouse NSCs	—
Chen et al. [55]	Extrusion	Collagen, HS	NSCs	—
Huang et al. [56]	Extrusion	PU, graphene, GO, G-P	NSCs	57%−67%
Pateman et al. [57]	Laser	PEG	NG108-15 neuronal cells	—

Note. BMSCs = bone marrow stem cells; *CMC* = carboxymethyl-chitosan; *GelMA* = methacrylated gelatin; *GG* = gellan gum; *GO* = graphene oxide; *G-P* = pluronic-stabilized graphene; *HS* = heparin sulfate; *LBLC* = layer-by-layer casting; *NSCs* = neural stem cells; *PEG* = poly(ethylene glycol); *PU* = polyurethane; *RGD* = arginylglycylaspartic acid; *SCs* = Schwann cells; *VEGF* = vascular endothelial growth factor.

7.6 Bioprinting of pancreatic tissue

Type 1 diabetes results from the destruction of β cells in the pancreatic islets, which causes the loss of insulin production and consequential hyperglycemia [58]. The β cells are one of the cell types in pancreatic islets, which make up 50%–70% of the cells in human islets, and secrete insulin and amylin. In this section, bioprinting technologies coupled with the utility of β cells are demonstrated to fabricate pancreatic tissues, which hold great potential for the treatment of type 1 diabetes.

To establish a 3D microenvironment proper for the long-term culture of human islet cells, Daoud et al. [59] inoculated human islets into gels with ECM (collagen type I, fibronectin, collagen type IV) and cultured them in a geometrically controlled poly(lactic-co-glycolic acid) (PLGA) scaffold. After 10-day culture in vitro, it was found that the insulin release profile was similar to that of freshly isolated islets, with the stimulus index of ~1.8. In addition, gene expression of insulin in ECM-supplemented PLGA scaffolds increased 50-fold, as compared to cell suspension culture. Distribution and the presence of pancreatic hormones (i.e., insulin, glucagon, and somatostatin) were also highly elevated in ECM-supplemented PLGA scaffolds compared to the cell suspension group.

Marchioli et al. [60] created a 3D alginate-based porous scaffold and used it for extrahepatic islet delivery. INS1Eβ cell viability was tested in several alginate mixtures, and 4% alginate/5% gelatin was determined. However, the use of highly viscous plotting materials resulted in dense mesh size, reducing the diffusion of glucose in the scaffold and limiting the function of the islets. Although the porous alginate scaffold has a higher surface-area-to-volume ratio as compared with bulk hydrogels, which effectively increased the diffusion of oxygen and nutrients, the nutrient diffusion in the hydrogel mixture was still insufficient. After being removed from the hydrogel, the islets recovered all their functions.

Duin et al. [61] used a plottable hydrogel mixture composed of ultra-pure sodium alginate and methylcellulose (Alg/MC) and used 3D extrusion bioprinting technology to embed the islets in a macroporous 3D hydrogel structure with specific geometric shapes while retaining their vitality, form, and functionality. The diffusion of glucose and insulin in Alg/MC hydrogel was equivalent to that in ordinary sodium alginate. During the entire observation process, the embedded islets continued to produce insulin and glucagon, and still responded to glucose stimulation, although the degree was lower than the control islets.

Song et al. [62] developed a retrievable macroporous device made of biocompatible polylactic acid (PLA). The clusters of stem cell–derived β cells (SC-β cells) were suspended in the fibrin gel, and distributed throughout the PLA device. Through the analysis of the finite element model, it was concluded that cell clusters with a

diameter <171 μm could avoid severe transient hypoxia. Using an in vitro setup with high oxygen permeability, it was verified that the resized clusters (143 μm in diameter) embedded in the device survived under physiological oxygen conditions. Three-dimensional-printed devices seeded with resized clusters were implanted subcutaneously into mice. After glucose injection, the cell clusters secreted insulin normally. The device functioned for up to 12 weeks, during which time the devices sustained their structural integrity and were retrievable.

Kim et al. [63] developed an ECM bioink derived from pancreatic tissue (pdECM), which was loaded with human pancreatic islets. The islet-laden pdECM bioink exhibited a higher capacity of insulin secretion than conventionally used bioencapsulation materials such as sodium alginate and collagen. In the 3D pdECM bioink environment, HUVECs and human islets were cocultured at an appropriate ratio, and the efficacy of islet transplantation can be significantly improved, which was proven by upregulated expression of insulin and pancreatic and duodenal homeobox 1 (Pdx1). Moreover, pdECM bioink was also used to improve the glycemic control of hiPSC-derived insulin-producing cells and promote physiological conditions. The printability of pdECM/islets/HUVECs bioink was also verified using extrusion-based bioprinting technology.

Liu et al. [64] proposed a method for fabricating 3D expandable islet delivery/implantation structures using alginate/GelMA bioinks. Mouse pancreatic endothelial cells and mouse primary islets were encapsulated in the bioink, which preserved high viability. The implantation in mice revealed that alginate/GelMA constructs preserved their dimensions and structural integrity in vivo for 21 days. Using coaxial bioprinting, islets were housed in the core and surrounded by endothelial progenitor cells (EPC) or T regulatory cells (Tregs). Unfortunately, measurement of insulin secretion showed that both the printed and free-standing islets did not work after 3 days of culture, demonstrating the compromised function.

Bernard et al. [65] used a laser-based process to fabricate a PEG-based microporous platform to produce mouse insulinoma 6 (MIN6) β-cell aggregates, which had uniform sizes ranging from 25 to 210 mm in diameter. By immunofluorescence staining, the formation of cell-cell junctions between aggregated MIN6 cells was validated. The aggregates were removed from the device and encapsulated in PEG hydrogel. Different from the encapsulated MIN6 single cells, aggregates showed higher vitality and metabolic activity and exhibited more than fourfold higher insulin secretion in response to glucose stimulation.

Hospodiuk et al. [66] reported the culture of murine pancreatic beta cell line (β-TC3 cells) and rat heart micro-vessel endothelial cells (RHMVECs) to produce engineered pseudoislets (EPI). During the culture process, EPI sprouted capillaries into the surrounding hydrogel matrix that sustainably maintained their vitality and function. The

existence of capillary vascularization was also found in EPI through ultramorphological analysis of tissue sections.

Akkouch et al. [67] proposed a scaffold-free approach in which sodium alginate conduits were coaxially extruded and used as a reservoir for cells to aggregate into tissue strands. Tubular alginate conduits possessed good permeability and mechanical properties, and

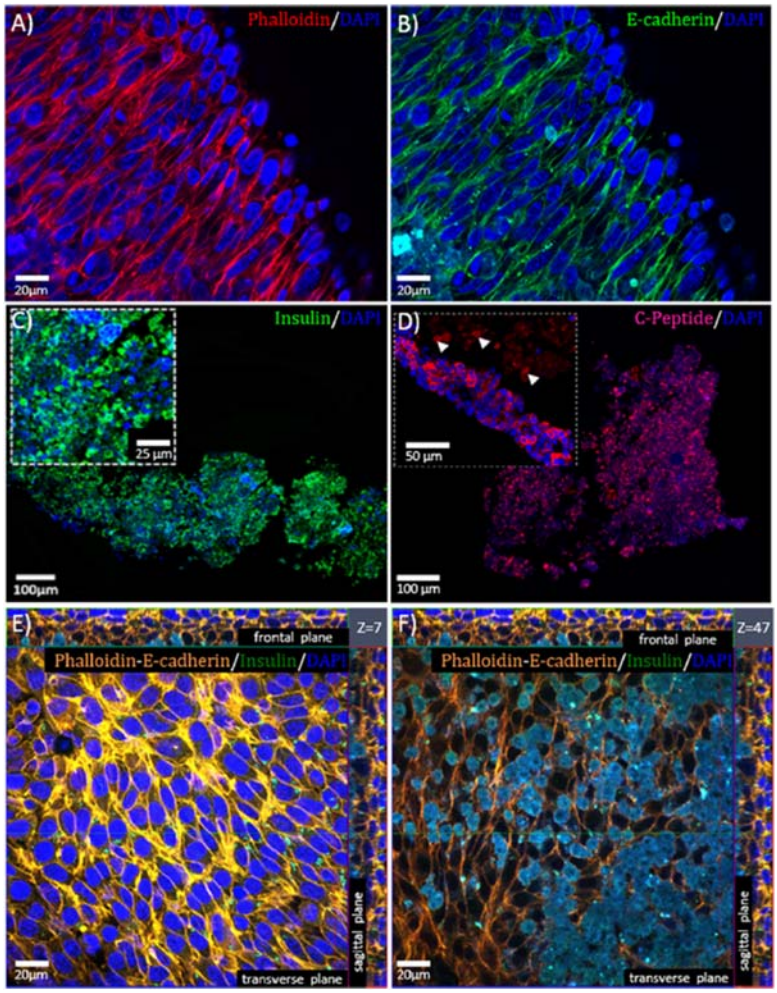

Figure 7.6

Confocal microscopy images of specific tissue proteins related to RDF and βTC-3. (A and B) Phalloidin and E-cadherin staining was performed on RDF tissue strands; (C and D) Insulin and C-peptide staining was performed on βTC-3 tissue strands. (E and F) Triple staining was performed on heterocellular tissue strands with phalloidin/E-cadherin and insulin markers; cross-sectional images represented the fibroblast core layer (E) and the outer layer made by βTC-3 cells (F) [67].

tissue strands could be obtained by ion de-cross-linking of the alginate conduits after cell aggregations. Single-cellular and heterocellular tissue strands were generated by rat dermal fibroblasts (RDFs) and mouse insulinoma βTC3 cells, which all presented high cell viability, self-assembly ability, and expression of cell-specific functional markers (Fig. 7.6). Furthermore, the fusion of tissue strands was guided successfully to create large tissue patches. Table 7.5 summarizes some information from the abovementioned studies on bioprinting of pancreatic tissue.

7.7 Bioprinting of lung

The lung plays a crucial role in the gas exchange of the body, which occurs in alveoli through a thin membrane termed the air–blood barrier [70]. Because of the complexity and small dimension of the alveoli [71] and air–blood barrier [72], bioprinting of the alveolilike structure is tough [73]. So far, studies about bioprinting of the lung are limited, and this section emphasizes two major pioneer studies.

Horvath et al. [68] engineered a human air–blood barrier using A549 human alveolar epithelial type II cell line and EA.hy926 endothelial cell line, which was separated by a thin basement membrane of Matrigel using droplet-based bioprinting. The manually deposited counterpart was created as control, which formed discrete cell clusters with a thickness of 20–30 μm that hindered cell–cell interactions. As compared, cells in thin

Table 7.5: Summary of the studies on bioprinting of pancreatic tissue.

Study	Technology	Materials	Cell source	Viability
Daoud et al. [59]	Extrusion	Collagen I, fibronectin, collagen IV, PLGA	Human islets	—
Marchioli et al. [60]	Extrusion	Alginate, gelatin	INS1E β-cells	95%
Duin et al. [61]	Extrusion	Alginate, methylcellulose	Rat islets	80%
Song et al. [62]	Extrusion	PLA	SC-β cells	—
Kim et al. [63]	Extrusion	pdECM bioink	Human and rat islets, HUVECs	75%
Liu et al. [64]	Extrusion	Alginate, gelatin	Mouse islets, EPC	95%
Bernard et al. [65]	Laser	PEG	MIN6 β-cells	>90%
Hospodiuk et al. [66]	Laser	Agarose	Mouse insulinoma βTC3 cells, RHMVECs	90%
Akkouch et al. [67]	Scaffold-free	Alginate	Rat dermal fibroblasts, mouse insulinoma βTC3 cells	>90%

Note. EPC = endothelial progenitor cells; *HUVEC* = human umbilical vein endothelial cells; *MIN6 β-cells* = mouse insulinoma 6 β-cells; *pdECM* = pancreatic tissue-derived extracellular matrix; *PEG* = poly(ethylene glycol); *PLA* = polylactic acid; *PLGA* = poly(lactic-co-glycolic acid); *RHMVECs* = rat heart microvascular endothelial cells; *SC-β cells* = stem cell-derived β cells.

layers of hydrogel (1−2 μm in thickness) exhibited uniform cellular distribution and close interaction, with outstretched morphology resembling that under physiological conditions. The barrier quality of A549 and EA.hy926 cells was examined, and results revealed that printed A549 epithelial cells were significantly less permeable than manually seeded cells, while there was no significant difference between printed and manually seeded EA.hy926 endothelial cells.

Grigoryan et al. [69] recognized photoinitiators whose absorbance spectra were in the range of wavelengths of visible light and generated biocompatible hydrogels that comprised poly(ethylene glycol) diacrylate (PEGDA). Using a customized stereolithography apparatus, multiple entangled vascular networks were printed, and the efficacy of intervascular interstitial transport was evaluated by measurement of the oxygen delivery. Oxygen and red blood cells (RBCs) were delivered to their respective vessels. RBCs alternated from dark red color at the inlet to bright red at the outlet during perfusion. In addition, a biomimetic alveolar model was developed with an ensheathing vasculature in the shape of 3D tessellations of the Weaire-Phelan foam. Such topology produced a surface containing both convex and concave regions, resembling native alveolar sacs with a shared airway atrium. The printed pattern using PEGDA hydrogel (20 wt%, 6 kDa) withstood >10,000 ventilation cycles (at 24 kPa, 0.5 Hz) over 6 h during RBC perfusion. Table 7.6 summarizes some information from the abovementioned studies on bioprinting of the lung.

7.8 Challenges and envisioned future of organ printing

7.8.1 Challenges of organ printing

Organ printing is a computer-aided process in which cells and/or cell-laden biomaterials are placed in the form of aggregates, which then serve as building blocks and are further assembled into a 3D functional organ. It is an automated approach that offers a pathway for scalable, reproducible mass production of engineered living organs where multiple cell types can be positioned precisely to mimic their natural counterparts. Developing a

Table 7.6: Summary of the studies on bioprinting of lung.

Study	Technology	Materials	Cell source	Viability
Horvath et al. [68]	Droplet	Matrigel	A549 human alveolar epithelial type II cell line, EA.hy926 hybrid human cell line	≥86%
Grigoryan et al. [69]	Laser	PEGDA, fibrin, GelMA	RBCs, hMSCs, HUVECs, rat hepatocytes	>85%

Note. GelMA = methacrylated gelatin; *hMSCs* = human mesenchymal stem cells; *HUVECs* = human umbilical vein endothelial cells; *PEGDA* = poly(ethylene glycol) diacrylate; *RBCs* = human red blood cells.

functional organ requires advances in and integration of three types of technology [74]: (1) cell technology, which addresses the procurement of functional cells at the level needed for clinical applications, (2) biomanufacturing technology, which involves combining the cells with biomaterials in a functional 3D configuration, and (3) technologies for in vivo integration, which addresses the issue of immune acceptance of biomanufactured construct, in vivo safety and efficacy, and monitoring of construct integrity and function postimplantation.

Success in the fabrication of functional organs highly depends on advancements in stem cell technology. A variety of cell types can be used for this application, such as embryonic stem cells (ESCs) [75], adult stem cells (ASCs) [76], induced pluripotent stem (iPS) cells [77], and tissue-specific cell lines [78,79]. Although a patient's stem cells can be differentiated into organ-specific cells for organ printing, there is still a risk of tissue rejection by the receiver [74]. Stem cell behaviors can even change during the bioprinting process. In addition, organ fabrication necessitates various types of organ-specific cells, which is not currently feasible considering the current isolation and differentiation technologies. Although stem cells offer great promise as an unlimited source of cells, a greater understanding of and control over the differentiation process is required to generate expandable organ-specific cells with consistent quality and desired phenotype. In this way, rejection by the recipient side will be minimized post-transplantation.

It should be ensured that the printed organ functions correctly. For example, a bioprinted pancreatic organ must be able to produce and secrete insulin just like its natural counterpart. Thus, multiple organ-specific cell types are required to be spatially organized to form the complex architecture of an organ. Advancements in bioprinting processes to precisely and selectively place cells are promising when it comes to achieving heterocellular architectures.

Despite the progress in tissue engineering, several challenges must be addressed for organ printing to become a reality. The most critical challenge in organ printing is the integration of a vascular network, which is also a problem that the majority of tissue engineering technologies are facing. Without vascularization, the engineered 3D thick tissue or organs cannot get enough nutrients, gas exchange, and waste removal, all of which are needed for maturation during perfusion. Low vascularization results in low cell viability and malfunction of artificial organs. Systems must be developed to transport nutrients, growth factors, and oxygen to cells while extracting metabolic waste products such as lactic acid, carbon dioxide, and hydrogen ions so the cells can grow and fuse, forming the organ. Cells in a large 3D organ structure cannot maintain their metabolic functions without vascularization, which is traditionally provided by blood vessels. Although several researchers have investigated developing vascular trees [80], successful maturation toward

functional and mechanically integrated bifurcated vessels and vascular networks is still challenging.

Another challenging site for organ printing technology is the rapid or accelerated tissue maturation process, where printed organ constructs should be rapidly fused, remodeled, and maturated toward a solid construct, ensuring mechanical rigidity for transplantation. Collagen and elastin are some of the proteins in the extracellular matrix of human organs, and they are abundant in the connective tissue stroma of parenchymal organs [81,82]. Thus, the production and deposition of these proteins during tissue maturation are essential to enhance the mechanical properties of the printed organs. After the organ printing process, the fabricated structure needs to be transferred to the bioreactor. Bioreactors such as an irrigation dripping perfusion bioreactor can be used to expedite the tissue maturation and organ formation process, providing an optimal environment. The transfer of a printed organ to the bioreactor should be performed gently without inducing any vibration that can degenerate the integrity of fragile gel-based structures. Thus, future bioprinters can be enclosed in a bioreactor system that will allow direct and rapid connection of printed structures to perfusion channels.

7.8.2 Envisioned future of organ printing

Considering the pathway from the isolation of stem cells to transplantation into a human, seamlessly automated protocols and systems are essential for customized functional organ fabrication. This pathway includes (1) blueprint modeling of an organ with its vascular architecture, (2) generation of a process plan for bioprinting, (3) isolation of stem cells, (4) differentiation of stem cells into organ-specific cells, (5) preparation and loading of organ-specific cells and blood vessel cells as well as a support medium, and (6) bioprinting process followed by organogenesis in a bioreactor for transplantation. To accelerate the entire process, one can envision a bioreactor enclosing a bioprinter that will immediately facilitate the fusion of tissues and keep the printed organ until desired maturation is achieved. In this way, a customized and automated system will facilitate delivering artificial organs to patients in a reasonable amount of time, preferably at earlier stages of their diseases when patients are healthier so that they are better able to withstand surgical interventions.

Miniature organs can be considered a future trend in organ printing and might be a transition toward fully functioning organs. Miniature organs, which can also be called a "factory in the human body," can be built on a smaller scale than their natural counterparts and closely perform the most vital function of the associated organ, such as a pancreatic organ that can produce and secrete insulin in substantial amounts to regulate the glucose level to normoglycemia in the human body. The miniature organ can be transplanted and placed in less immune-responsive sites in the human body as an extravascular device or

attached to blood vessels as an intravascular device to secrete insulin into the bloodstream. Although the pancreas serves two functions, which are carried out by two different cell groups within the organ, a patient with diabetes will be interested in correcting hyperglycemia through the fabrication and transplantation of a pancreatic organ that can restore the function of the endocrine portions of the pancreas, which makes only about 2% of pancreas cells. The endocrine portion is made of approximately a million cell clusters called islets of Langerhans [83]. Four main cell types exist in the islets. The α, β, delta, and gamma cells secrete glucagon, insulin, somatostatin (regulates/stops α and β cells), and pancreatic polypeptide, respectively. Miniature organs can also be designed and fabricated to bring new functionalities and superiorities to the human body rather than restoring the functionality of their natural counterparts, such as living organs that can continuously generate electricity to eliminate the use of batteries for internal devices such as pacemakers.

Another future trend in organ printing is in situ printing, where living organs can be printed in the human body during operations. Currently, in situ bioprinting has already been tested for repairing external organs such as skin [84]. A transitional approach seems to be logical to advance the state-of-the-art through printing and repairing partially damaged, diseased, or malfunctioning internal organs that do not have self-repair characteristics, such as the liver. With the recent advancements in robot-assisted surgery, computer-controlled robotic bioprinters will lead the evolution of this technology in the very near future.

References

[1] I.T. Ozbolat, Y. Yu, Bioprinting toward organ fabrication: challenges and future trends, IEEE Transactions on Biomedical Engineering 60 (3) (2013) 691–699.
[2] R. Langer, J.P. Vacanti, Tissue engineering, Science 260 (5110) (1993) 920–926.
[3] A. Atala, Tissue engineering for bladder substitution, World Journal of Urology 18 (5) (2000) 364.
[4] F. Melchels, M. Domingos, T.J. Klein, J. Malda, P.J. Bartolo, D.W. Hutmacher, Additive manufacturing of tissues and organ, Progress in Polymer Science 37 (2012) 1079–1104.
[5] N. Liu, X. Ye, B. Yao, M. Zhao, P. Wu, G. Liu, D. Zhuang, H. Jiang, X. Chen, Y. He, Advances in 3D bioprinting technology for cardiac tissue engineering and regeneration, Bioactive Materials 6 (5) (2021) 1388–1401.
[6] Y. Ma, P. Ding, L. Li, Y. Liu, P. Jin, J. Tang, J. Yang, Three-dimensional printing for heart diseases: clinical application review, Bio-design and Manufacturing 4 (3) (2021) 675–687.
[7] B. Duan, L.A. Hockaday, K.H. Kang, J.T. Butcher, 3D bioprinting of heterogeneous aortic valve conduits with alginate/gelatin hydrogels, Journal of Biomedical Materials Research Part A 101 (5) (2013) 1255–1264.
[8] B. Duan, E. Kapetanovic, L.A. Hockaday, J.T. Butcher, Three-dimensional printed trileaflet valve conduits using biological hydrogels and human valve interstitial cells, Acta Biomaterialia 10 (5) (2014) 1836–1846.

[9] Q. Zou, B.E. Grottkau, Z. He, L. Shu, L. Yang, M. Ma, C. Ye, Biofabrication of valentine-shaped heart with a composite hydrogel and sacrificial material, Materials Science and Engineering C 108 (2020) 110205.
[10] S. Das, S.-W. Kim, Y.-J. Choi, S. Lee, S.-H. Lee, J.-S. Kong, H.-J. Park, D.-W. Cho, J. Jang, Decellularized extracellular matrix bioinks and the external stimuli to enhance cardiac tissue development in vitro, Acta Biomaterialia 95 (2019) 188–200.
[11] F. Maiullari, M. Costantini, M. Milan, V. Pace, M. Chirivì, S. Maiullari, A. Rainer, D. Baci, H.E.-S. Marei, D. Seliktar, A multi-cellular 3D bioprinting approach for vascularized heart tissue engineering based on HUVECs and iPSC-derived cardiomyocytes, Scientific Reports 8 (1) (2018) 1–15.
[12] D. Bejleri, B.W. Streeter, A.L. Nachlas, M.E. Brown, R. Gaetani, K.L. Christman, M.E. Davis, A bioprinted cardiac patch composed of cardiac-specific extracellular matrix and progenitor cells for heart repair, Advanced Healthcare Materials 7 (23) (2018) 1800672.
[13] M.E. Kupfer, W.-H. Lin, V. Ravikumar, K. Qiu, L. Wang, L. Gao, D.B. Bhuiyan, M. Lenz, J. Ai, R.R. Mahutga, In situ expansion, differentiation, and electromechanical coupling of human cardiac muscle in a 3D bioprinted, chambered organoid, Circulation Research 127 (2) (2020) 207–224.
[14] A. Lee, A. Hudson, D. Shiwarski, J. Tashman, T. Hinton, S. Yerneni, J. Bliley, P. Campbell, A. Feinberg, 3D bioprinting of collagen to rebuild components of the human heart, Science 365 (6452) (2019) 482–487.
[15] D.C. Van der Valk, C.F. Van der Ven, M.C. Blaser, J.M. Grolman, P.-J. Wu, O.S. Fenton, L.H. Lee, M.W. Tibbitt, J.L. Andresen, J.R. Wen, Engineering a 3D-bioprinted model of human heart valve disease using nanoindentation-based biomechanics, Nanomaterials 8 (5) (2018) 296.
[16] N. Noor, A. Shapira, R. Edri, I. Gal, L. Wertheim, T. Dvir, 3D printing of personalized thick and perfusable cardiac patches and hearts, Advanced Science 6 (11) (2019) 1900344.
[17] M. Izadifar, D. Chapman, P. Babyn, X. Chen, M.E. Kelly, UV-assisted 3D bioprinting of nanoreinforced hybrid cardiac patch for myocardial tissue engineering, Tissue Engineering Part C Methods 24 (2) (2018) 74–88.
[18] C. Yu, X. Ma, W. Zhu, P. Wang, K.L. Miller, J. Stupin, A. Koroleva-Maharajh, A. Hairabedian, S. Chen, Scanningless and continuous 3D bioprinting of human tissues with decellularized extracellular matrix, Biomaterials 194 (2019) 1–13.
[19] J. Liu, J. He, J. Liu, X. Ma, Q. Chen, N. Lawrence, W. Zhu, Y. Xu, S. Chen, Rapid 3D bioprinting of in vitro cardiac tissue models using human embryonic stem cell-derived cardiomyocytes, Bioprinting 13 (2019) e00040.
[20] S. Chikae, A. Kubota, H. Nakamura, A. Oda, A. Yamanaka, T. Akagi, M. Akashi, Three-dimensional bioprinting human cardiac tissue chips of using a painting needle method, Biotechnology and Bioengineering 116 (11) (2019) 3136–3142.
[21] Y. Tsukamoto, T. Akagi, M. Akashi, Vascularized cardiac tissue construction with orientation by layer-by-layer method and 3D printer, Scientific Reports 10 (1) (2020) 1–11.
[22] E. Yeung, T. Fukunishi, Y. Bai, D. Bedja, I. Pitaktong, G. Mattson, A. Jeyaram, C. Lui, C.S. Ong, T. Inoue, Cardiac regeneration using human-induced pluripotent stem cell-derived biomaterial-free 3D-bioprinted cardiac patch in vivo, Journal of Tissue Engineering and Regenerative Medicine 13 (11) (2019) 2031–2039.
[23] S. Turunen, S. Kaisto, I. Skovorodkin, V. Mironov, A. Rak-Raszewska, 3D bioprinting of the kidney—hype or hope? AIMS Cell and Tissue Engineering 2 (3) (2018) 119–162.
[24] S.M. King, H.J. William, C.R. Nino, T.R. Smith, E.H. Paffenroth, C.E. Fairbairn, D. Abigail, V.D. Shah, A.E. Chen, S.C. Presnell, 3D proximal tubule tissues recapitulate key aspects of renal physiology to enable nephrotoxicity testing, Frontiers in Physiology 8 (123) (2017) 123.
[25] M. Ali, P.A. Kumar, J.J. Yoo, F. Zahran, A. Atala, J.L. Sang, A photo-crosslinkable kidney ECM-derived bioink accelerates renal tissue formation, Advanced Healthcare Materials 8 (7) (2019).

[26] K.T. Lawlor, J.M. Vanslambrouck, J.W. Higgins, A. Chambon, K. Bishard, D. Arndt, X.E. Pei, S.B. Wilson, S.E. Howden, K.S. Tan, Cellular extrusion bioprinting improves kidney organoid reproducibility and conformation, Nature Materials.
[27] J.W. Higgins, A. Chambon, K. Bishard, A. Hartung, D. Arndt, Bioprinted Pluripotent Stem Cell-Derived Kidney Organoids Provide Opportunities for High Content Screening, 2018.
[28] K.A. Homan, D.B. Kolesky, M.A. Skylar-Scott, J. Herrmann, H. Obuobi, A. Moisan, J.A. Lewis, Bioprinting of 3D convoluted renal proximal tubules on perfusable chips, Scientific Reports 6 (2016) 34845.
[29] G. Addario, B.S. Djudjaj, S. Fare, P. Bore, L. Moroni, C. Mota, Microfluidic bioprinting towards a renal in vitro model, Bioprinting 20 (2020).
[30] P. Godoy, N.J. Hewitt, U. Albrecht, M.E. Andersen, N. Ansari, S. Bhattacharya, J.G. Bode, J. Bolleyn, C. Borner, J. Boettger, Recent advances in 2D and 3D in vitro systems using primary hepatocytes, alternative hepatocyte sources and non-parenchymal liver cells and their use in investigating mechanisms of hepatotoxicity, cell signaling and ADME, Archives of Toxicology 87 (8) (2013) 1315–1530.
[31] Z. Heydari, M. Najimi, H. Mirzaei, A. Shpichka, M. Ruoss, Z. Farzaneh, L. Montazeri, A. Piryaei, P. Timashev, R. Gramignoli, Tissue engineering in liver regenerative medicine: insights into novel translational technologies, Cells 9 (2) (2020) 304.
[32] R. Bataller, D.A. Brenner, Liver fibrosis, The Journal of Clinical Investigation 115 (2) (2005) 209–218.
[33] S. Lu, J. Zhang, S. Lin, D. Zheng, Y. Shen, J. Qin, Y. Li, S. Wang, Recent advances in the development of in vitro liver models for hepatotoxicity testing, Bio-Design and Manufacturing 4 (4) (2021) 717–734.
[34] E. Goulart, L.C. de Caires-Junior, K.A. Telles-Silva, B.H.S. Araujo, S.A. Rocco, M. Sforca, I.L. de Sousa, G.S. Kobayashi, C.M. Musso, A.F. Assoni, 3D bioprinting of liver spheroids derived from human induced pluripotent stem cells sustain liver function and viability in vitro, Biofabrication 12 (1) (2019) 015010.
[35] A. Mazzocchi, M. Devarasetty, R. Huntwork, S. Soker, A. Skardal, Optimization of collagen type I-hyaluronan hybrid bioink for 3D bioprinted liver microenvironments, Biofabrication 11 (1) (2018) 015003.
[36] P.L. Lewis, R.M. Green, R.N. Shah, 3D-printed gelatin scaffolds of differing pore geometry modulate hepatocyte function and gene expression, Acta Biomaterialia 69 (2018) 63–70.
[37] N.S. Bhise, V. Manoharan, S. Massa, A. Tamayol, M. Ghaderi, M. Miscuglio, Q. Lang, Y.S. Zhang, S.R. Shin, G. Calzone, A liver-on-a-chip platform with bioprinted hepatic spheroids, Biofabrication 8 (1) (2016) 014101.
[38] D.G. Nguyen, J. Funk, J.B. Robbins, C. Crogan-Grundy, S.C. Presnell, T. Singer, A.B. Roth, Bioprinted 3D primary liver tissues allow assessment of organ-level response to clinical drug induced toxicity in vitro, PloS One 11 (7) (2016) e0158674.
[39] L.M. Norona, D.G. Nguyen, D.A. Gerber, S.C. Presnell, E.L. LeCluyse, Modeling compound-induced fibrogenesis in vitro using three-dimensional bioprinted human liver tissues, Toxicological Sciences 154 (2) (2016) 354–367.
[40] Y. Wu, Z.Y.W. Lin, A.C. Wenger, K.C. Tam, X.S. Tang, 3D bioprinting of liver-mimetic construct with alginate/cellulose nanocrystal hybrid bioink, Bioprinting 9 (2018) 1–6.
[41] H. Jeon, K. Kang, S.A. Park, W.D. Kim, S.S. Paik, S.-H. Lee, J. Jeong, D. Choi, Generation of multilayered 3D structures of HepG2 cells using a bio-printing technique, Gut and Liver 11 (1) (2017) 121.
[42] X. Ma, X. Qu, W. Zhu, Y.-S. Li, S. Yuan, H. Zhang, J. Liu, P. Wang, C.S.E. Lai, F. Zanella, Deterministically patterned biomimetic human iPSC-derived hepatic model via rapid 3D bioprinting, Proceedings of the National Academy of Sciences 113 (8) (2016) 2206–2211.
[43] X. Ma, C. Yu, P. Wang, W. Xu, X. Wan, C.S.E. Lai, J. Liu, A. Koroleva-Maharajh, S. Chen, Rapid 3D bioprinting of decellularized extracellular matrix with regionally varied mechanical properties and biomimetic microarchitecture, Biomaterials 185 (2018) 310–321.

[44] V.L. Tsang, A.A. Chen, L.M. Cho, K.D. Jadin, R.L. Sah, S. DeLong, J.L. West, S.N. Bhatia, Fabrication of 3D hepatic tissues by additive photopatterning of cellular hydrogels, The FASEB Journal 21 (3) (2007) 790–801.
[45] T. Grix, A. Ruppelt, A. Thomas, A.-K. Amler, B.P. Noichl, R. Lauster, L. Kloke, Bioprinting perfusion-enabled liver equivalents for advanced organ-on-a-chip applications, Genes 9 (4) (2018) 176.
[46] A. Faulkner-Jones, C. Fyfe, D.-J. Cornelissen, J. Gardner, J. King, A. Courtney, W. Shu, Bioprinting of human pluripotent stem cells and their directed differentiation into hepatocyte-like cells for the generation of mini-livers in 3D, Biofabrication 7 (4) (2015) 044102.
[47] C.E. Schmidt, J.B. Leach, Neural tissue engineering: strategies for repair and regeneration, Annual Review of Biomedical Engineering 5 (1) (2003) 293–347.
[48] Y. Han, J. Yin, Industry News: The Additive Manufacturing of Nerve Conduits for the Treatment of Peripheral Nerve Injury, Springer, 2021, pp. 1–3.
[49] Y.-B. Lee, S. Polio, W. Lee, G. Dai, L. Menon, R.S. Carroll, S.-S. Yoo, Bio-printing of collagen and VEGF-releasing fibrin gel scaffolds for neural stem cell culture, Experimental Neurology 223 (2) (2010) 645–652.
[50] C.M. Owens, F. Marga, G. Forgacs, C.M. Heesch, Biofabrication and testing of a fully cellular nerve graft, Biofabrication 5 (4) (2013) 045007.
[51] F.-Y. Hsieh, H.-H. Lin, S.-H. Hsu, 3D bioprinting of neural stem cell-laden thermoresponsive biodegradable polyurethane hydrogel and potential in central nervous system repair, Biomaterials 71 (2015) 48–57.
[52] R. Lozano, L. Stevens, B.C. Thompson, K.J. Gilmore, R. Gorkin III, E.M. Stewart, M. in het Panhuis, M. Romero-Ortega, G.G. Wallace, 3D printing of layered brain-like structures using peptide modified gellan gum substrates, Biomaterials 67 (2015) 264–273.
[53] Q. Gu, E. Tomaskovic-Crook, R. Lozano, Y. Chen, R.M. Kapsa, Q. Zhou, G.G. Wallace, J.M. Crook, Functional 3D neural mini-tissues from printed gel-based bioink and human neural stem cells, Advanced Healthcare Materials 5 (12) (2016) 1429–1438.
[54] W. Zhu, B.T. Harris, L.G. Zhang, Gelatin methacrylamide hydrogel with graphene nanoplatelets for neural cell-laden 3D bioprinting, in: 2016 38th Annual International Conference of the IEEE Engineering in Medicine and Biology Society (EMBC), IEEE, 2016, pp. 4185–4188.
[55] C. Chen, M.L. Zhao, R.K. Zhang, G. Lu, C.Y. Zhao, F. Fu, H.T. Sun, S. Zhang, Y. Tu, X.H. Li, Collagen/heparin sulfate scaffolds fabricated by a 3D bioprinter improved mechanical properties and neurological function after spinal cord injury in rats, Journal of Biomedical Materials Research A 105 (5) (2017) 1324–1332.
[56] C.-T. Huang, L.K. Shrestha, K. Ariga, S.-H. Hsu, A graphene–polyurethane composite hydrogel as a potential bioink for 3D bioprinting and differentiation of neural stem cells, Journal of Materials Chemistry B 5 (44) (2017) 8854–8864.
[57] C.J. Pateman, A.J. Harding, A. Glen, C.S. Taylor, C.R. Christmas, P.P. Robinson, S. Rimmer, F.M. Boissonade, F. Claeyssens, J.W. Haycock, Nerve guides manufactured from photocurable polymers to aid peripheral nerve repair, Biomaterials 49 (2015) 77–89.
[58] D.J. Ravnic, A.N. Leberfinger, I.T. Ozbolat, Bioprinting and cellular therapies for type 1 diabetes, Trends in Biotechnology 35 (11) (2017) 1025–1034.
[59] J.T. Daoud, M.S. Petropavlovskaia, J.M. Patapas, C.E. Degrandpré, R.W. DiRaddo, L. Rosenberg, M. Tabrizian, Long-term in vitro human pancreatic islet culture using three-dimensional microfabricated scaffolds, Biomaterials 32 (6) (2011) 1536–1542.
[60] G. Marchioli, L. van Gurp, P. Van Krieken, D. Stamatialis, M. Engelse, C. Van Blitterswijk, M. Karperien, E. de Koning, J. Alblas, L. Moroni, Fabrication of three-dimensional bioplotted hydrogel scaffolds for islets of Langerhans transplantation, Biofabrication 7 (2) (2015) 025009.
[61] S. Duin, K. Schütz, T. Ahlfeld, S. Lehmann, A. Lode, B. Ludwig, M. Gelinsky, 3D Bioprinting of functional islets of langerhans in an alginate/methylcellulose hydrogel blend, Advanced healthcare materials 8 (7) (2019) 1801631.

[62] J. Song, J.R. Millman, Economic 3D-printing approach for transplantation of human stem cell-derived β-like cells, Biofabrication 9 (1) (2016) 015002.
[63] J. Kim, I.K. Shim, D.G. Hwang, Y.N. Lee, M. Kim, H. Kim, S.-W. Kim, S. Lee, S.C. Kim, D.-W. Cho, 3D cell printing of islet-laden pancreatic tissue-derived extracellular matrix bioink constructs for enhancing pancreatic functions, Journal of Materials Chemistry B 7 (10) (2019) 1773−1781.
[64] X. Liu, S.S.D. Carter, M.J. Renes, J. Kim, D.M. Rojas-Canales, D. Penko, C. Angus, S. Beirne, C.J. Drogemuller, Z. Yue, Development of a coaxial 3D printing platform for biofabrication of implantable islet-containing constructs, Advanced healthcare materials 8 (7) (2019) 1801181.
[65] A.B. Bernard, C.-C. Lin, K.S. Anseth, A microwell cell culture platform for the aggregation of pancreatic β-cells, Tissue Engineering Part C Methods 18 (8) (2012) 583−592.
[66] M. Hospodiuk, M. Dey, B. Ayan, D. Sosnoski, K.K. Moncal, Y. Wu, I.T. Ozbolat, Sprouting angiogenesis in engineered pseudo islets, Biofabrication 10 (3) (2018) 035003.
[67] A. Akkouch, Y. Yu, I.T. Ozbolat, Microfabrication of scaffold-free tissue strands for three-dimensional tissue engineering, Biofabrication 7 (3) (2015) 031002.
[68] L. Horváth, Y. Umehara, C. Jud, F. Blank, A. Petri-Fink, B. Rothen-Rutishauser, Engineering an in vitro air-blood barrier by 3D bioprinting, Scientific Reports 5 (1) (2015) 1−8.
[69] B. Grigoryan, S.J. Paulsen, D.C. Corbett, D.W. Sazer, C.L. Fortin, A.J. Zaita, P.T. Greenfield, N.J. Calafat, J.P. Gounley, A.H. Ta, Multivascular networks and functional intravascular topologies within biocompatible hydrogels, Science 364 (6439) (2019) 458−464.
[70] E.R. Weibel, Morphological basis of alveolar-capillary gas exchange, Physiological Reviews 53 (2) (1973) 419−495.
[71] M. Ochs, J.R. Nyengaard, A. Jung, L. Knudsen, M. Voigt, T. Wahlers, J. Richter, H.J.G. Gundersen, The number of alveoli in the human lung, American Journal of Respiratory and Critical Care Medicine 169 (1) (2004) 120−124.
[72] C.G. Plopper, J.R. Harkema, The Respiratory System and its Use in Research, The Laboratory Primate, 2005, pp. 503−526.
[73] S.H. Mahfouzi, S.H.S. Tali, G. Amoabediny, 3D bioprinting for lung and tracheal tissue engineering: criteria, advances, challenges, and future directions, Bioprinting 21 (2021) e00124.
[74] R. Lanza, R. Langer, J.P. Vacanti, A. Atala, Principles of Tissue Engineering, Academic Press, 2020.
[75] W.W. Thein-Han, Y. Kitiyanant, Chitosan scaffolds for in vitro buffalo embryonic stem-like cell culture: an approach to tissue engineering, Journal of Biomedical Materials Research B: Applied Biomaterials 80 (1) (2007) 92−101.
[76] R.S. Tuan, G. Boland, R. Tuli, Adult mesenchymal stem cells and cell-based tissue engineering, Arthritis Research & Therapy 5 (1) (2002) 1−14.
[77] M.T. Lam, M.T. Longaker, Comparison of several attachment methods for human iPS, embryonic and adipose-derived stem cells for tissue engineering, Journal of Tissue Engineering and Regenerative Medicine 6 (S3) (2012) s80−s86.
[78] D. Seol, D.J. McCabe, H. Choe, H. Zheng, Y. Yu, K. Jang, M.W. Walter, A.D. Lehman, L. Ding, J.A. Buckwalter, Chondrogenic progenitor cells respond to cartilage injury, Arthritis & Rheumatism 64 (11) (2012) 3626−3637.
[79] Y. Yu, Identification and Characterization of Cartilage Progenitor Cells by Single Cell Sorting and Cloning, The University of Iowa, 2012.
[80] W.L. Mondy, D. Cameron, J.-P. Timmermans, N. De Clerck, A. Sasov, C. Casteleyn, L.A. Piegl, Computer-aided design of microvasculature systems for use in vascular scaffold production, Biofabrication 1 (3) (2009) 035002.
[81] B.D. McLees, G. Schleiter, S.R. Pinnell, Isolation of type III collagen from human adult parenchymal lung tissue, Biochemistry 16 (2) (1977) 185−190.
[82] V. Richmond, Lung parenchymal elastin isolated by non-degradative means, Biochimica et Biophysica Acta (BBA)-Protein Structure 351 (2) (1974) 173−177.

[83] B. Hellman, E. Gylfe, E. Grapengiesser, H. Dansk, A. Salehi, Insulin oscillations—clinically important rhythm. Antidiabetics should increase the pulsative component of the insulin release, Lakartidningen 104 (32–33) (2007) 2236–2239.

[84] N. Hakimi, R. Cheng, L. Leng, M. Sotoudehfar, P.Q. Ba, N. Bakhtyar, S. Amini-Nik, M.G. Jeschke, A. Günther, Handheld skin printer: in situ formation of planar biomaterials and tissues, Lab on a Chip 18 (10) (2018) 1440–1451.

This page intentionally left blank

CHAPTER 8

Intraoperative bioprinting

8.1 Advances from in vitro bioprinting to intraoperative bioprinting

In the past decade, bioprinting has considerably advanced and a large number of studies have shown attractive outcomes in different applications, such as engineering of various organs for regenerative medicine (i.e., skin [1], cartilage [2], and bone [3]), tissue vascularization [4], drug discovery [5], and disease modeling [6–8]. Despite this fact, the majority of bioprinting endeavors have been conducted in vitro, and in some cases, further validated in vivo [9]. Although bioprinting of solid organs directly into human body remains elusive, some attempts have been practiced in the realm of intraoperative bioprinting (IOB), also known as in situ or in vivo bioprinting [10–12], which refers to the bioprinting process performed on a live subject in a surgical setting, in which defect imaging, data processing, process planning, and bioprinting are performed consecutively in a single process. IOB of tissue substitutes directly into injury sites is greatly beneficial as it can facilitate the complex tissue heterogeneity in an anatomically accurate manner. Although IOB has not been performed in clinics yet, the field is steadily moving forward owing to the rapid developments in bioprinting technologies with contributions from interdisciplinary teams of researchers from different domains spanning from engineering and materials to medical sciences and surgery.

The realization of IOB will activate several benefits. First, bioprinted tissue substitutes, especially hydrogel- or cell aggregate–based constructs, usually have weak initial mechanical strengths due to the fluid-rich nature, which makes them difficult to handle with surgical tools, and further increases the likelihood of construct disintegration while being transferred to the surgical site and suturing. In contrast, with the assistance of a reverse engineering methodology enabling the real-time design of the graft, IOB is an effective process, where the defect can be repaired with minimum risk of contamination, graft disintegration, and manual interventions such as stacking multiple layers, in vitro culturing bioprinted scaffolds, transportation during surgery, or modifying prefabricated scaffolds conforming the defect shape [13]. More importantly, IOB is able to tackle natural defects with irregular topographies, which is common in clinical cases due to trauma and surgical excision. Comparatively, in vitro bioprinting usually assumes a flat working surface, which is inconsistent with clinical scenarios. Moreover, since intraoperatively repaired defects are surrounded by native tissue, endogenous cells could

3D Bioprinting in Tissue and Organ Regeneration. https://doi.org/10.1016/B978-0-12-824291-9.00010-5

be directed by proper biochemical and biophysical cues to migrate into the bioprinted constructs and differentiate into target tissue-specific lineages [13,14]. In addition, compared to manual injection of biomaterials into defect sites, IOB enables the precise deposition of cells, genes, or cytokines with localized control and anatomical biomimicry. For tissues that are heterocellular and formed of zonally stratified arrangement of extracellular matrix (ECM), IOB is a powerful technology to precisely reconstitute multiple layers that is quite challenging using manual approaches. Lastly, shape distortion of hydrogels (e.g., high degree of shrinkage of collagen during skin regeneration [15]) can be an issue during in vitro maturation of bioprinted constructs. In addition, during in vitro culture, cells remodel the matrix and eventually change the shape of the bioprinted constructs, which may pose a significant disruption of predesigned shapes. Therefore, IOB is also advantageous due to the concurrence of in vivo integration, where the regenerated tissue may occupy the void space due to shrinkage and regulate the remodeling of matrix.

8.2 Current developments in IOB

Although the concept of intraoperative bioprinting was first proposed in 2010 [16,17], very few studies have been reported on this topic. This is because intraoperative bioprinting is a multidisciplinary field, which needs researchers with background of mechanical and electrical engineering, imaging and processing, biomaterial science, biology, surgical techniques, and automation. More importantly, bioprinting into living body with a physiological ambient condition is more demanding with respect to bioink preparation, printing setup, sterilization, and surgical operation as compared to in vitro bioprinting. Since it is challenging to be proficient in all subjects, fundamental studies regarding individual aspects of IOB has been reported by different groups.

Toolpath planning targeted at IOB is an important concern. For example, an arbitrary two-dimensional (2D) mold with uniform depth was created to imitate the skin burn wound, followed by digital imaging, contour calibration, and toolpath planning, in order to bioprint cell-laden gelatin-alginate hydrogel [18]. A small-scale robotic arm was also invented to inkjet print poly(ethylene glycol) diacrylate (PEGDA) within a three-dimensional (3D) printed defect model, in order to estimate the potential of the entire system in IOB [19]. As an early study in this field, Cohen et al. [16] scanned the defects on a calf femur which was mounted on the bioprinting system, followed by imaging processing, creating path, and depositing alginate hydrogel on chondral and osteochondral defects.

Different from abovementioned studies that focused more on the automation of IOB technologies, studies on in vivo investigation have also showed promising outcomes. A handheld device has been developed for in situ cartilage repair [20] (Fig. 8.1A). Gelatin methacrylamide (GelMa)/hyaluronic acid methacrylate (HAMA) hydrogel was manually

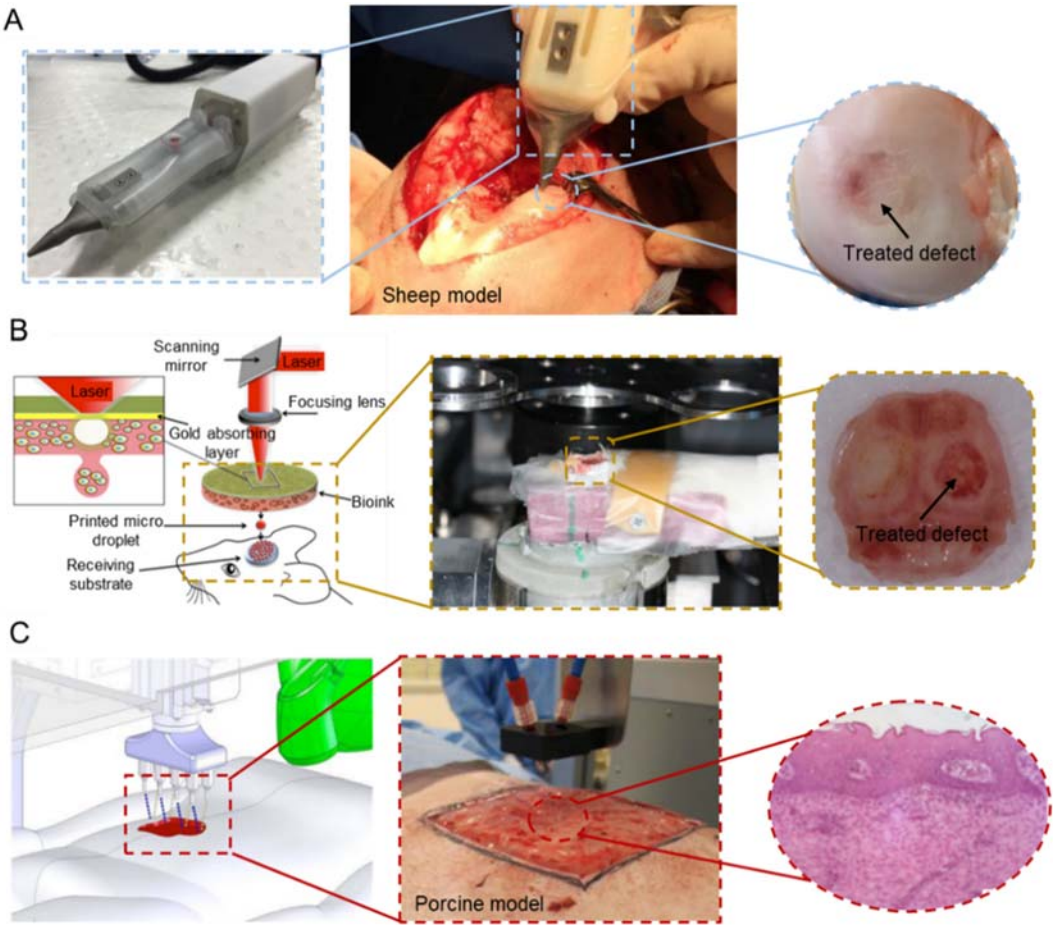

Figure 8.1

(A) Intraoperative bioprinting using the biopen for treatment of a full-thickness chondral defect in a sheep. (B) Laser-based intraoperative bioprinting for skull repair in a mouse calvaria defect. (C) Droplet-based intraoperative bioprinting for skin repair in a porcine model. *Adapted with permission from (A) C. Di Bella, S. Duchi, C.D. O'Connell, R. Blanchard, C. Augustine, Z. Yue, F. Thompson, C. Richards, S. Beirne, C. Onofrillo, In situ handheld three-dimensional bioprinting for cartilage regeneration, Journal of Tissue Engineering and Regenerative Medicine 12 (3) (2018) 611–621. (B) V. Keriquel, F. Guillemot, I. Arnault, B. Guillotin, S. Miraux, J. Amédée, J.-C. Fricain, S. Catros, In vivo bioprinting for computer-and robotic-assisted medical intervention: preliminary study in mice, Biofabrication 2 (1) (2010) 014101; V. Keriquel, H. Oliveira, M. Rémy, S. Ziane, S. Delmond, B. Rousseau, S. Rey, S. Catros, J. Amédée, F. Guillemot, In situ printing of mesenchymal stromal cells, by laser-assisted bioprinting, for in vivo bone regeneration applications, Scientific Reports 7 (1) (2017) 1778; O. Kérourédan, D. Hakobyan, M. Rémy, S. Ziane, N. Dusserre, J.-C. Fricain, S. Delmond, N.B. Thébaud, R. Devillard, In situ prevascularization designed by laser-assisted bioprinting: effect on bone regeneration, Biofabrication 11 (2019) 045002. (C) M. Albanna, K.W. Binder, S.V. Murphy, J. Kim, S.A. Qasem, W. Zhao, J. Tan, I.B. El-Amin, D.D. Dice, J. Marco, In situ bioprinting of autologous skin cells accelerates wound healing of extensive excisional full-thickness wounds, Scientific Reports 9 (1) (2019) 1856.*

extruded and ultraviolet (UV) cross-linked in chondral defects in a sheep model [21]. Upon 8-week treatment, the regenerated cartilage presented satisfactory macroscopic and microscopic scores. Although the bioprinting was performed manually, it has come up with a well-developed strategy to miniaturize the number of external equipment for cross-linking of cell-laden hydrogel, which could be flexible for system integration of an intraoperative bioprinter.

In terms of bone repair, Keriquel et al. [17] have performed IOB of nano-hydroxyapatite in the mouse calvaria defect model with a critical size using in-house developed biological laser printing (BioLP), which is equipped with a five-axes positioning system and charge-coupled device (CCD) camera for positioning control (Fig. 8.1B). Although heterogeneity has been observed in the regenerated bone, it was the first study to prove the possibility of IOB. In their follow-up study, mesenchymal stem cells (MSCs) were printed with different geometries, showing formation of the mature bone [22]. Most recently, the same team bioprinted human umbilical vein endothelial cells (HUVECs) intraoperatively, and gave rise to organized microvascular networks and bone regeneration rate into bone defects [23].

Currently, the most successful cases on IOB are mostly associated with skin repair, due to its ease of access and generative potential. Skardal et al. [24] used a droplet-based bioprinting technology to treat large-scale skin wounds in a mice model, in which amniotic fluid—derived stem cells (AFSCs) and bone marrow—derived mesenchymal stem cells (MSCs) were resuspended in fibrin-collagen gel as a bioink. More recently, they demonstrated the use of a fast photocross-linkable heparin-conjugated hyaluronic acid (HA-HP) hydrogel as a cell delivery carrier for sustained growth factor release [25]. The HA-HP hydrogel with AFS cells increased speed of wound closure in mice as compared to HA-only hydrogels and treatment-free controls, resulting in upregulated vascularization. In their latest work, Albanna et al. presented a mobile skin bioprinting system with integrated imaging technology for on-site management of extensive wounds [26] (Fig. 8.1C). Excisional wounds bioprinted with dual-layer dermal fibroblasts and epidermal keratinocytes in a fibrin/collagen hydrogel displayed rapid wound closure, reduced contraction, and accelerated reepithelialization in both murine and porcine full-thickness wound models. The reader is referred to Table 8.1 for a summary of the past work performed on IOB and their significant outcomes. A few excellent review articles provided more detailed information on the current status of in situ bioprinting [10—12]. Beyond the prior reviews, we here focus on the current major limitations of IOB from engineering and clinical points of view, highlight the potential of future translation of IOB technologies, and also expound the possibilities of using such a technology in reconstruction of composite and vascularized tissues.

Table 8.1: The summary of studies performed in the context of IOB.

Bioprinting modality	Study	Materials	Cell source	Animal type	Defect model	Target tissue	3D Scanning	Results
EXTRUSION-BASED BIOPRINTING	Di Bella et al. [21]	Gelatin methacrylamide (GelMA)/ Hyaluronic acid methacrylate (HAMA)	Mesenchymal stem cells (MSCs)	Sheep	Chondral defect	Cartilage	No	• Better overall macroscopic appearance in the handheld printed group compared to control groups; • Handheld printed constructs showed a higher amount of newly regenerated cartilage and the absence of subchondral bone deformation or collapse; • Handheld printed constructs showed positive Safranin O and collagen type II staining.
	Hakimi et al. [27]	Alginate/Fibrin/ Collagen/ Hyaluronic acid (HA)	Fibroblasts/ Keratinocytes	Mice/ Pig	Skin defect on dorsa	Skin	No	**Murine model:** • In situ deposition of an architected sheet was performed in the form of a fiber array onto a small and compliant wound surface; **Porcine model:** • The porcine model demonstrated successful in situ bioprinting to cover full thickness wounds with a hemostatic barrier where it did not impede normal reepithelialization or wound contraction;

Continued

Table 8.1: The summary of studies performed in the context of IOB.—cont'd

Bioprinting modality	Study	Materials	Cell source	Animal type	Defect model	Target tissue	3D Scanning	Results
LASER-BASED BIOPRINTING	Keriquel et al. [17]	Nano-hydroxyapatite	—	Mice	Calvaria defect	Bone	No	• Microscopic analysis of healed wounds on Day 20 revealed that both treated and control wounds formed complete granulation tissue and exhibited comparable levels of collagen deposition and cellularity. • Material was present in close contact with dura mater on the test sites after one week; • After one month, newly formed mature and immature bones and n-HA aggregates inside macrophages were observed; • Three months after printing, mature bone tissue was observed; • From one week to three months, the number of n-HA particles observed in situ decreased.
	Keriquel et al. [22]	Collagen/Nano-hydroxyapatite	MSCs	Mice	Calvaria defect	Bone	No	• Both nHA-collagen and nHA-collagen+ cells, printed in a ring geometry, showed only a marginal tissue reconstruction at two months post printing, particularly from the periphery of the defect;

	Kérourédan et al. [23]	Collagen/ Vascular endothelial growth factor (VEGF)	Stem cells from the apical papilla (SCAPs)/ Human umbilical vein endothelial cells (HUVECs)	Mice	Calvaria defect	Bone	No	• The nHA-collagen + cells, printed in disk geometry, showed a substantial new bone formation, well distributed throughout the defect, even in the center of the defect. • Randomly seeded cells were poorly organized within the region of interest in the defect at two months; • For the "ring" condition, the geometry of vascularized area was consistent with the initial printed pattern. For the "disc" and "crossed circle" patterns, the initial pattern was distorted; • Vascularization rate and bone regeneration rate significantly increased in the "disc" or "crossed circle" patterns of HUVECs; • HUVECs were not the only cells involved in the network formation, and host murine cells seemed to have a role in this process.
DROPLET-BASED BIOPRINTING	Skardal et al. [24]	Fibrin/Collagen	Amniotic fluid-derived stem cells (AFSCs)/ MSCs/ HUVECs	Mice	Skin wound on dorsa	Skin	No	• AFS cell- and MSC-driven wound closure and reepithelialization were significantly greater than wounds treated by fibrin-collagen only; • Microvessel density and capillary diameters in AFS cell-treated wounds increased compared with

Continued

Table 8.1: The summary of studies performed in the context of IOB.—cont'd

Bioprinting modality	Study	Materials	Cell source	Animal type	Defect model	Target tissue	3D Scanning	Results
								MSC-treated wounds, whereas the skin treated only with gel showed the least microvessels; • AFS cells secreted growth factors at higher concentrations than MSCs, resulting in increased wound closure rates and angiogenesis.
	Skardal et al. [25]	HA/Heparin-conjugated hyaluronic acid (HA-HP)	AFSCs	Mice	Skin wound on dorsa	Skin	No	• Deposition of the HA-HP + AFS cells accelerated closure of wounds faster than HA-only hydrogels and treatment-free controls, and induced increased vascularization; • The increased levels of elastin, GAGs, and proteoglycans, and decreased relative expression of collagen type I suggested the regenerated skin using HA-HP + AFS cells was more pliable and elastic compared to control groups.
	Albanna et al. [26]	Fibrin/Collagen	Fibroblasts/ Keratinocytes	Mice/ Pig	Skin defect on dorsa	Skin	Yes	**Murine Model:** • Printed skin cells closed the wound by three weeks postsurgery compared to five weeks for untreated and matrix-only groups;

								• Epithelialization of bio-printed wounds was observed, forming an immature epidermal barrier. **Porcine model:** • Bioprinting of autologous cells resulted in ~3-week acceleration in wound closure compared to other treatments (i.e., untreated, matrix and allogenic cell-treated); • Bioprinting autologous cells resulted in ~50% reduction in wound contraction compared to other treatments; • Bioprinting autologous cells resulted in a 4—5 week acceleration in wound reepithelialization compared to other treatments; • Collagen fibers present in the autologous cell-treated wounds appeared larger and more organized than other groups. **Comparison with cell spraying:** • Bioprinted wounds showed accelerated formation of epidermis and more mature dermis tissue; • Staining of collagen fibers were more prominent in the bioprinted wounds at week 4 compared to wounds treated with the sprayed cells.

8.3 Considerations and future outlook for IOB

8.3.1 Limitations of current bioprinting modalities

Bioprinting modalities can be categorized as extrusion-, droplet-, and laser-based [28–30]. For IOB, more challenges appear when adapting knowledge gained through in vitro systems. Extrusion-based bioprinting (EBB) can be considered an appropriate modality for IOB since manual injection (extrusion) of biomaterials has already been clinically applied for decades [31,32], and current surgical robots, used in some clinical applications such as urology and gynecology [33], can be easily reconfigured to hold EBB tips. However, the print tip might interfere with defect periphery since it is a contact-based technology. In terms of droplet-based bioprinting (DBB), although its resolution is superior than that of EBB, bioink deposition through a small orifice results in higher risk of nozzle clogging, which may increase the duration of surgery and may bring other complications. Limited by poor structural and mechanical integrity of bioprinted constructs, DBB is more suitable for bioprinting thin tissues such as skin. For LBB, it shares similar advantages (e.g., high resolution) and disadvantages (e.g., low integrity of bioprinted constructs) with respect to DBB. The miniaturization of LBB is a major challenge due to its complex setup (such as a laser source and optical components), which constrains its accessibility to internal tissues. Other challenges, such as the immobilization of light sources and the necessity of precise focusing of light, may limit its clinical translation.

8.3.2 Compatibility of bioinks to surgical settings

Since the deposition is performed directly into a defect in physiological conditions, an ideal bioink should not only meet the general bioink requirements [34] but also possess some features specific to IOB. In particular, such bioinks are expected to be (1) compatible with and intraoperatively bioprintable by the targeted modality to shorten the surgery duration, (2) rapidly cross-linkable in situ to retain the integrity and resolution of bioprinted constructs in physiological temperature and moist environment, and (3) commercially available and affordable to minimize the surgery cost. Therefore, most of the popular biomaterials (e.g., polycaprolactone, polylactic acid, etc.), which rely on volatile organic solvent and high melting temperature, become inappropriate. Among hydrogels, although collagen transitions to gel state at 37°C, its slow gelation hinders its use in IOB; however, nano-hydroxyapatite-reinforced collagen has shown promising results in bone regeneration [22]. Fibrinogen is also popular due to its rapid cross-linking when it is interchangeably bioprinted with thrombin into a defect. Photo-cross-linkable bioinks, such as gelatin methacrylamide (GelMA), hyaluronic acid methacrylate (HAMA), and poly(ethylene glycol), have been commonly used in bioprinting [34]. Since exposing UV light directly to a live subject can be dangerous [35], one practical example is to

expose UV light toward the side of a transparent nozzle during bioink extrusion [36]. Recently, visible light photo-initiating systems have become popular, which avoided the use of UV light favoring cell viability in photo-cross-linkable bioinks [37–39]. In addition to existing bioinks, more alternatives are expected to be developed to broaden the options for IOB. Newer materials may facilitate retention of the bioprinted constructs at the desired site without the utilization of a support dressing/scaffold, such as a vacuum assisted closure (VAC) device. The manufacture of rapidly integrable bioinks would expand the feasibility of bioprinting into enclosed cavities (e.g., abdomen, thorax), which are not conducive to graft immobilization techniques when compared to more superficial sites, such as the skin.

8.3.3 Automation of IOB processes

Imaging of defects during IOB should be performed in a minute timescale immediately after a surgical excision since the prolonged exposure of the defect can increase surgical complications [40]. To match this requirement, scanners based on 3D photogrammetry provide a supreme solution to obtain raw data of the defect topography during IOB. Several models of portable photogrammetric scanners (e.g., Artec Space Spider and CREAFORM HandySCAN) are able to reach a resolution up to $\sim$30 μm with an extremely short scan time (<5 min), and the portability offers the possibility to get the defect scanned easily. To create a model of tissue constructs, image processing is necessary including image pre-processing, segmentation, feature extraction, and data mining [41]. During IOB, all these processes should be completed in a few minutes after obtaining the scanned data. Hence, segmentation software is vital for convenient extraction of region of interest from 3D images [42,43]. Since defects have unique textural features case by case, improper post-processing of images might generate pointless 3D models, which needs to be carefully evaluated. Artificial intelligence (AI) and robotics can be incorporated to reduce the process time and variation caused by operators. So far, researchers have strived to optimize path planning targeted at IOB [18,19], including printing on a free-moving hand anatomy using motion tracking [44,45]. In the future, machine learning can be used to automatically generate optimal bioprinting strategies [46–49]. The integration of 3D scanner with a fixed relative coordinate to the robotic arm is also required to eliminate the need of prebioprinting calibration to minimize total processing time.

Due to shape distortions caused by the sol-gel transition of hydrogels and movement of the live subject during surgery (such as breathing), automation of IOB with tight control on high resolution is also challenging. This issue might be addressed by real-time monitoring technologies to observe construct deformation and provide feedback signal for subsequent deposition [45]. Commercially-available bioprinters with 3-axis coordinates are

usually not sufficient for IOB of irregular-shaped defects that necessitates the use of bioprinters with higher degrees of freedom (DOF), where robotic arms (such as surgical robots) can be the ideal solution. Although BioAssemblyBot with a 6-axis robotic arm from Advanced Solutions Inc. (Fig. 8.2A) is currently the only commercially-available bioprinter with higher DOF capability, there are many companies specialized in robotic surgeries (e.g., Intuitive Surgical, MAKO Surgical Corp, etc.) with potential of integrating bioprinting capabilities into surgical robots in the future.

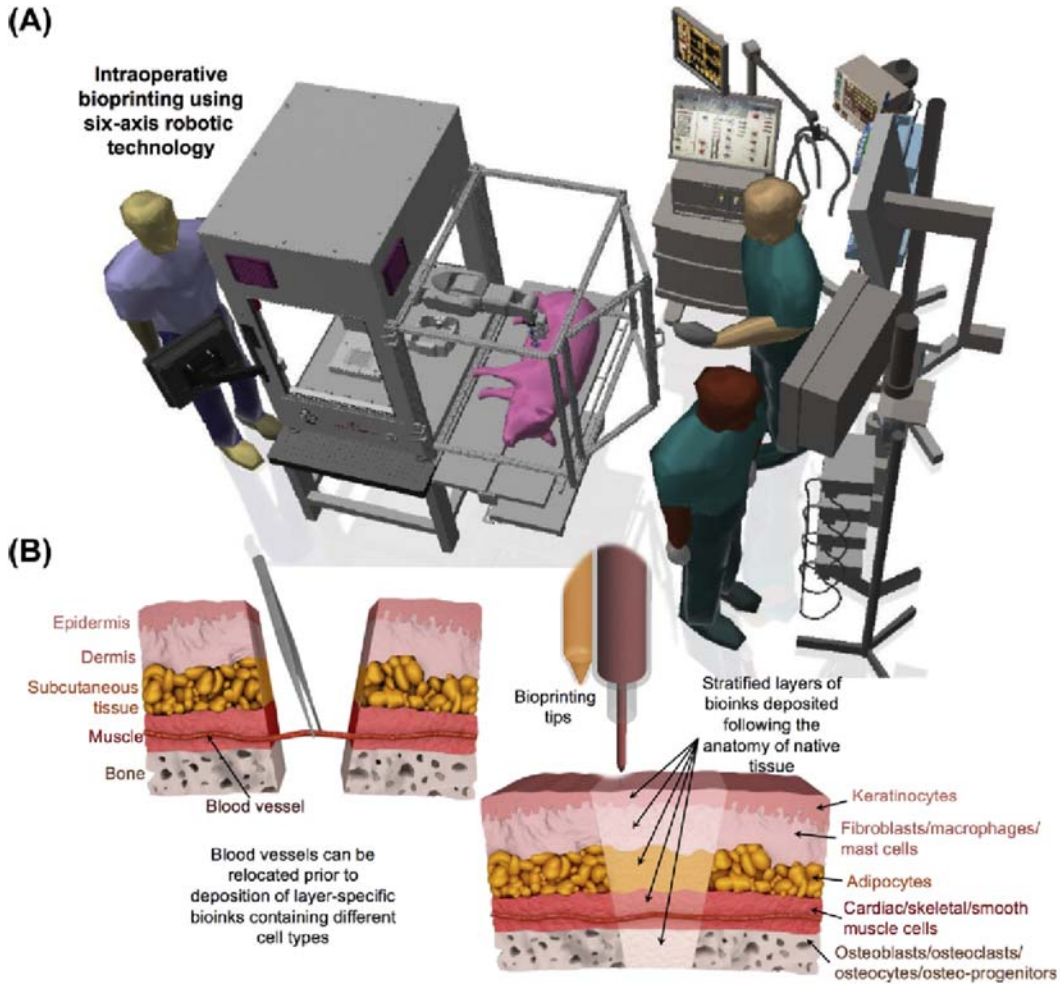

Figure 8.2

IOB in a surgical setting and its application for repair of composite tissues. Conceptual schematic diagram of (A) IOB in a surgical setting, and (B) the regeneration of composite tissues in a stratified manner. In the case of blood vessels retained in host tissue, they can be relocated (left) prior to the deposition of layer-specified bioinks containing different cell types (right).

8.3.4 Vascularization in intraoperatively bioprinted tissues

Vascularization is crucial for maturation of bioprinted constructs, especially in segmental defects. Although bioprinted constructs with an embedded microvasculature have been described [4], it is still not feasible to directly anastomose them to the recipient vasculature. Therefore, engineered grafts still rely on inosculation from the recipient bed for perfusion. In order to drive microvascularization within intraoperatively bioprinted tissues, there are multiple ways, such as bioprinting of endothelial progenitor cells, hypoxia-inducible factor (HIF), or vascular endothelial growth factor (VEGF). Since it usually takes more than 10 days for angiogenesis to take place [50], temporary strategies can be followed to extend the oxygen supply prior to inosculative angiogenesis. For example, oxygen (O_2)-filled microparticles or oxygen-generating biomaterials (OGBs) can be included within the bioink, which are expected to feed the cells until capillaries can actively transfer the blood [51,52]. Oxygenation rate of OGBs (e.g., peroxides) is the key parameter for viable outcome of organs, which can be controlled by factors such as pH, temperature, and solubility of peroxides [53]. Involvement of porous internal structures is an advantage of bioprinting and another option to facilitate infiltration of blood from host tissue, which offers the possibility for IOB of porous constructs. Introduction of macropores in IOB can be realized by bioprinting filaments in cross-hatched patterns similar to what has been achieved in conventional in vitro bioprinting [54].

However, the ultimate goal is to create a bioprinted construct that includes an embedded microvasculature with a continuous anastomosable artery and vein. With the development of supermicrosurgical techniques, it is now feasible to perform a direct anastomosis on vessels with an internal diameter <150 μm [55]. This advancement may provide a mechanism for the rapid establishment of blood flow in the graft without requisite exposure to main vascular tree. This is significant as the vascular pedicle of the graft can be kept quite short, simplifying the bioprinting process. To facilitate graft anastomosis and vascularization, the implanting surgeon can also utilize a variety of autologous conduits, including the creation of arteriovenous loops.

8.3.5 IOB of composite tissues and their translational potential

Currently, seamless reconstruction of tissues with multiple components such as craniomaxillofacial (CMF) defects (skin, bone, and muscle), osteochondral defects (cartilage and bone), and musculoskeletal defects (bone, muscle, tendon, and skin) possesses several limitations. Different tissue types exhibit local variations in terms of physiological, anatomical, and histological aspects, and precise layer-by-layer stacking of multiple tissue compartments is not trivial. Such compartmentalization necessitates the precision and effective use of stem cells and differentiation factors, since differentiating

stem cells into multiple lineages is crucial in order to recapitulate the native tissue anatomy. Taking a major musculoskeletal defect as an example, it comprises layers of bone, blood vessel, muscle, subcutaneous fat, and skin tissues from inside out, which contains more than 10 cell types (Fig. 8.2B), and has traditionally required an autologous composite fibula free-flap for correction.

IOB of composite tissue should allow rapid acquirement of the defect information with minimum manual interventions, enabling personalized reconstructions in an anatomically accurate and cosmetically appealing manner immediately after characterization of the defect. Although bioprinted constructs are usually designed based on the compartmentalization of native tissues, the maturation of bioprinted tissues may alter its anatomy and phenotype, leading to differences from the native tissue. Since composite tissues are usually thick, vascularization is particularly vital to enhance the proper tissue regeneration, such as bone formation in CMF defects, as necrotic scar tissue would take over if vascularization is not sufficient [56]. Currently, free-flap surgery is the standard of care for the repair of composite segmental defects. A free-flap is an autologous tissue transplant where expendable donor tissue along with its feeding vascular pedicle (artery and vein) is transferred to a remote recipient site [57]. This approach has revolutionized the treatment of large traumatic and oncologic defects. However, free-flap surgery can be restricted by limited donor site supply and donor site morbidity. Additionally, although the goal is to replace like tissue with like tissue, this is often impossible. For example, a fibula free-flap can be used for intraoral bone and soft tissue replacement in mandible reconstruction, but the amount of bone stock is reduced, sensation is lost, and skin is not equivalent to native mucosa. Therefore, it may be better to combine the principles of reconstructive microsurgery and IOB. The surgeon could configure the recipient vasculature to perfuse an adjacent bioprinted construct either via direct anastomosis or angiogenic induction (refer to Section 8.3.4). This would eliminate the concerns of donor supply and morbidity while providing an exact match of the desired replacement tissue. In the future, it is anticipated that bioprinted or tissue engineered grafts will be available instead of harvesting autologous flaps.

Another concern about IOB of composite tissues is the integration of bioprinted tissues to native tissue, especially for avascular tissues, such as cartilage due to its low metabolism and antiadhesive ECM [58]. Vertical integration of cartilage to underlying bone occurs due to the innate repair capability of bone [58]. In order to enhance the healing capability, intraoperatively bioprinted composite tissues with a histologically similar osteochondral interface will be a promising solution [2], which can be integrated into full-thickness bone-cartilage defects. However, lateral integration of the bioprinted cartilage to the adjacent cartilage is a major roadblock to achieve permanent cartilage replacement [58]. Strategies to enhance lateral integration may include bioink functionalization to enable direct bonding to the adjacent cartilage [59].

So far, animal models for IOB are almost nonload-bearing, such as skin and calvarial defects (Table 8.1). IOB for repairing load-bearing defect models, such as segmental bone defects in long bones and joint defects, will gain more attention in the future. Mechanical stiffness of intraoperatively bioprinted constructs depends on their inherent properties determined by the bioink, which can be resolved by developing new materials such as tough hydrogels [60] or integrating mechanically strong thermoplastics. In this regard, bioprinting of soft bioinks can be coupled with thermoplastics (e.g., PCL or PLGA), where one can envision a technology that can facilitate rapid cooling of deposited thermoplastics into a defect in a safe manner (such as laser-based cooling systems [61]). In addition, postoperative care and rehabilitation are still necessary (as in conventional surgeries) until intraoperatively bioprinted tissue restores sufficient mechanical strength.

8.4 Conclusions

IOB has already showed promise for regeneration of tissues, including cartilage, skin, and bone, in animals. However, regeneration of composite tissues, which are comprised of hard and soft tissues, and the interface layers in between, have hardly been explored, which require the development of new bioinks with rapid and stable cross-linking, and the integration of advanced bioprinting modalities.

In addition, seeking a practical way to facilitate and enhance vascularization is vital for long-term functionality of intraoperatively bioprinted tissues. Especially, IOB is appealing to combine with vascular anastomosis to repair composite segmental defects, which is currently treated by free-flap surgeries. In long term, automation of IOB does not only rely on the integration of sequential processes, but also requires a large number of clinical cases to optimize the bioprinting strategies. Beyond scientific considerations, clinical studies will be impeded by ethical and regulatory issues, and sharing of patient-specific information for database development will be related to the protection of private information and intellectual properties. Although it is predicted to be a long way to address all these issues, there is no doubt that IOB will be a game changer in regenerative surgical care.

References

[1] S. Vijayavenkataraman, W. Lu, J. Fuh, 3D bioprinting of skin: a state-of-the-art review on modelling, materials, and processes, Biofabrication 8 (3) (2016) 032001.
[2] Y. Wu, P. Kennedy, N. Bonazza, Y. Yu, A. Dhawan, I. Ozbolat, Three-Dimensional Bioprinting of Articular Cartilage: A Systematic Review, Cartilage, 2018, 1947603518809410.
[3] N. Ashammakhi, A. Hasan, O. Kaarela, B. Byambaa, A. Sheikhi, A.K. Gaharwar, A. Khademhosseini, Advancing frontiers in bone bioprinting, Advanced Healthcare Materials 8 (7) (2019) 1801048.
[4] P. Datta, B. Ayan, I.T. Ozbolat, Bioprinting for vascular and vascularized tissue biofabrication, Acta Biomaterilia 51 (2017) 1–20.

[5] W. Peng, P. Datta, B. Ayan, V. Ozbolat, D. Sosnoski, I.T. Ozbolat, 3D bioprinting for drug discovery and development in pharmaceutics, Acta Biomaterialia 57 (2017) 26–46.
[6] S. Vijayavenkataraman, W.-C. Yan, W.F. Lu, C.-H. Wang, J.Y.H. Fuh, 3D bioprinting of tissues and organs for regenerative medicine, Advanced Drug Delivery Reviews 132 (2018) 296–332.
[7] Y. Ma, P. Ding, L. Li, Y. Liu, P. Jin, J. Tang, J. Yang, Three-dimensional printing for heart diseases: clinical application review, Bio-design and Manufacturing 4 (3) (2021) 675–687.
[8] Z. Heydari, F. Moeinvaziri, T. Agarwal, P. Pooyan, A. Shpichka, T.K. Maiti, P. Timashev, H. Baharvand, M. Vosough, Organoids: a novel modality in disease modeling, Bio-design and Manufacturing 4 (4) (2021) 689–716.
[9] N. Hong, G.H. Yang, J. Lee, G. Kim, 3D bioprinting and its in vivo applications, Journal of Biomedical Materials Research B: Applied Biomaterials 106 (1) (2018) 444–459.
[10] N. Ashammakhi, S. Ahadian, I. Pountos, S.-K. Hu, N. Tellisi, P. Bandaru, S. Ostrovidov, M.R. Dokmeci, A. Khademhosseini, In situ three-dimensional printing for reparative and regenerative therapy, Biomedical Microdevices 21 (2) (2019) 42.
[11] S. Singh, D. Choudhury, F. Yu, V. Mironov, M.W. Naing, In situ bioprinting–Bioprinting from benchside to bedside? Acta Biomaterialia 101 (2019) 14–25.
[12] M. Wang, J. He, Y. Liu, M. Li, D. Li, Z. Jin, The trend towards in vivo bioprinting, International Journal of Bioprinting 1 (1) (2015) 15–26.
[13] I.T. Ozbolat, Bioprinting scale-up tissue and organ constructs for transplantation, Trends in Biotechnology 33 (7) (2015) 395–400.
[14] F. Qu, F. Guilak, R.L. Mauck, Cell migration: implications for repair and regeneration in joint disease, Nature Reviews Rheumatology (2019) 1.
[15] W.-C. Yan, P. Davoodi, S. Vijayavenkataraman, Y. Tian, W.C. Ng, J.Y. Fuh, K.S. Robinson, C.-H. Wang, 3D bioprinting of skin tissue: from pre-processing to final product evaluation, Advanced Drug Delivery Reviews 132 (2018) 270–295.
[16] D.L. Cohen, J.I. Lipton, L.J. Bonassar, H. Lipson, Additive manufacturing for in situ repair of osteochondral defects, Biofabrication 2 (3) (2010) 035004.
[17] V. Keriquel, F. Guillemot, I. Arnault, B. Guillotin, S. Miraux, J. Amédée, J.-C. Fricain, S. Catros, In vivo bioprinting for computer-and robotic-assisted medical intervention: preliminary study in mice, Biofabrication 2 (1) (2010) 014101.
[18] H. Ding, R.C. Chang, Simulating image-guided in situ bioprinting of a skin graft onto a phantom burn wound bed, Additive Manufacturing 22 (2018) 708–719.
[19] X. Li, Q. Lian, D. Li, H. Xin, S. Jia, Development of a robotic arm based hydrogel additive manufacturing system for in-situ printing, Applied Sciences 7 (1) (2017) 73.
[20] C. D O'Connell, C. Di Bella, F. Thompson, C. Augustine, S. Beirne, R. Cornock, C.J. Richards, J. Chung, S. Gambhir, Z. Yue, Development of the Biopen: a handheld device for surgical printing of adipose stem cells at a chondral wound site, Biofabrication 8 (1) (2016) 015019.
[21] C. Di Bella, S. Duchi, C.D. O'Connell, R. Blanchard, C. Augustine, Z. Yue, F. Thompson, C. Richards, S. Beirne, C. Onofrillo, In situ handheld three-dimensional bioprinting for cartilage regeneration, Journal of Tissue Engineering and Regenerative Medicine 12 (3) (2018) 611–621.
[22] V. Keriquel, H. Oliveira, M. Rémy, S. Ziane, S. Delmond, B. Rousseau, S. Rey, S. Catros, J. Amédée, F. Guillemot, In situ printing of mesenchymal stromal cells, by laser-assisted bioprinting, for in vivo bone regeneration applications, Scientific Reports 7 (1) (2017) 1778.
[23] O. Kérourédan, D. Hakobyan, M. Rémy, S. Ziane, N. Dusserre, J.-C. Fricain, S. Delmond, N.B. Thébaud, R. Devillard, In situ prevascularization designed by laser-assisted bioprinting: effect on bone regeneration, Biofabrication 11 (2019) 045002.
[24] A. Skardal, D. Mack, E. Kapetanovic, A. Atala, J.D. Jackson, J. Yoo, S. Soker, Bioprinted amniotic fluid-derived stem cells accelerate healing of large skin wounds, Stem Cells Translational Medicine 1 (11) (2012) 792–802.

[25] A. Skardal, S.V. Murphy, K. Crowell, D. Mack, A. Atala, S. Soker, A tunable hydrogel system for long-term release of cell-secreted cytokines and bioprinted in situ wound cell delivery, Journal of Biomedical Materials Research Part B: Applied Biomaterials 105 (7) (2017) 1986−2000.
[26] M. Albanna, K.W. Binder, S.V. Murphy, J. Kim, S.A. Qasem, W. Zhao, J. Tan, I.B. El-Amin, D.D. Dice, J. Marco, In situ bioprinting of autologous skin cells accelerates wound healing of extensive excisional full-thickness wounds, Scientific Reports 9 (1) (2019) 1856.
[27] N. Hakimi, R. Cheng, L. Leng, M. Sotoudehfar, P.Q. Ba, N. Bakhtyar, S. Amini-Nik, M.G. Jeschke, A. Günther, Handheld Skin Printer: in situ formation of planar biomaterials and tissues, Lab Chip 18 (10) (2018) 1440−1451.
[28] I.T. Ozbolat, M. Hospodiuk, Current advances and future perspectives in extrusion-based bioprinting, Biomaterials 76 (2016) 321−343.
[29] H. Gudapati, M. Dey, I. Ozbolat, A comprehensive review on droplet-based bioprinting: past, present and future, Biomaterials 102 (2016) 20−42.
[30] C. Mandrycky, Z. Wang, K. Kim, D.-H. Kim, 3D bioprinting for engineering complex tissues, Biotechnology Advances 34 (4) (2016) 422−434.
[31] J.M. Clark, T.A. Cook, Immediate reconstruction of extruded alloplastic nasal implants with irradiated homograft costal cartilage, The Laryngoscope 112 (6) (2002) 968−974.
[32] O. Besalti, A. Ozak, Z. Pekcan, S. Tong, S. Eminaga, T. Tacal, The role of extruded disk material in thoracolumbar intervertebral disk disease: a retrospective study in 40 dogs, Canadian Veterinary Journal 46 (9) (2005) 814.
[33] A. Hussain, A. Malik, M. Halim, A. Ali, The use of robotics in surgery: a review, International Journal of Clinical Practice 68 (11) (2014) 1376−1382.
[34] T. Jungst, W. Smolan, K. Schacht, T. Scheibel, J.r. Groll, Strategies and molecular design criteria for 3D printable hydrogels, Chemical Reviews 116 (3) (2015) 1496−1539.
[35] S. Duchi, C. Onofrillo, C.D. O'Connell, R. Blanchard, C. Augustine, A.F. Quigley, R.M. Kapsa, P. Pivonka, G. Wallace, C. Di Bella, Handheld co-axial bioprinting: application to in situ surgical cartilage repair, Scientific Reports 7 (1) (2017) 5837.
[36] L. Ouyang, C.B. Highley, W. Sun, J.A. Burdick, A generalizable strategy for the 3D bioprinting of hydrogels from nonviscous photo-crosslinkable inks, Advanced Materials 29 (8) (2017) 1604983.
[37] Z. Wang, R. Abdulla, B. Parker, R. Samanipour, S. Ghosh, K. Kim, A simple and high-resolution stereolithography-based 3D bioprinting system using visible light crosslinkable bioinks, Biofabrication 7 (4) (2015) 045009.
[38] K.S. Lim, B.S. Schon, N.V. Mekhileri, G.C. Brown, C.M. Chia, S. Prabakar, G.J. Hooper, T.B. Woodfield, New visible-light photoinitiating system for improved print fidelity in gelatin-based bioinks, ACS Biomaterials Science & Engineering 2 (10) (2016) 1752−1762.
[39] Z. Wang, H. Kumar, Z. Tian, X. Jin, J.F. Holzman, F. Menard, K. Kim, Visible light photoinitiation of cell-adhesive gelatin methacryloyl hydrogels for stereolithography 3D bioprinting, ACS Applied Materials & Interfaces 10 (32) (2018) 26859−26869.
[40] H. Cheng, B.P.-H. Chen, I.M. Soleas, N.C. Ferko, C.G. Cameron, P. Hinoul, Prolonged operative duration increases risk of surgical site infections: a systematic review, Surgical Infections 18 (6) (2017) 722−735.
[41] W. Sun, B. Starly, A. Darling, C. Gomez, Computer-aided tissue engineering: application to biomimetic modelling and design of tissue scaffolds, Biotechnology and Applied Biochemistry 39 (1) (2004) 49−58.
[42] I. Ozbolat, H. Gudapati, A review on design for bioprinting, Bioprinting 3 (2016) 1−14.
[43] S. Xu, P.A. Mundra, H. Li, S. Zhu, R.E. Welsch, J.C. Rajapakse, Image analysis for cellular and tissue engineering, in: H. Yu, N.A.A. Rahim (Eds.), Imaging in Cellular and Tissue Engineering, CRC Press, Boca Raton, 2013, p. 223.
[44] J.J. O'Neill, R.A. Johnson, R.L. Dockter, T.M. Kowalewski, 3D Bioprinting Directly onto Moving Human Anatomy, 2017 IEEE/RSJ International Conference on Intelligent Robots and Systems (IROS), IEEE, 2017, pp. 934−940.

[45] Z. Zhu, S.Z. Guo, T. Hirdler, C. Eide, X. Fan, J. Tolar, M.C. McAlpine, 3D printed functional and biological materials on moving freeform surfaces, Advanced Materials 30 (23) (2018) 1707495.
[46] J. Shi, J. Song, B. Song, W.F. Lu, Multi-objective optimization design through machine learning for drop-on-demand bioprinting, Engineering 5 (2019) 586–593.
[47] G.X. Gu, C.-T. Chen, D.J. Richmond, M.J. Buehler, Bioinspired hierarchical composite design using machine learning: simulation, additive manufacturing, and experiment, Materials Horizons 5 (5) (2018) 939–945.
[48] A. Menon, B. Póczos, A.W. Feinberg, N.R. Washburn, Optimization of silicone 3D printing with hierarchical machine learning, 3D Printing and Additive Manufacturing (2019).
[49] J. Dernowsek, R. Rezende, J. da Silva, BioCAE: a new strategy of complex biological systems for biofabrication of tissues and organs, Journal of Tissue Science & Engineering 8 (200) (2017) 2.
[50] C.A. Staton, S.M. Stribbling, S. Tazzyman, R. Hughes, N.J. Brown, C.E. Lewis, Current methods for assaying angiogenesis in vitro and in vivo, International Journal of Experimental Pathology 85 (5) (2004) 233–248.
[51] J.N. Kheir, L.A. Scharp, M.A. Borden, E.J. Swanson, A. Loxley, J.H. Reese, K.J. Black, L.A. Velazquez, L.M. Thomson, B.K. Walsh, Oxygen gas–filled microparticles provide intravenous oxygen delivery, Science Translational Medicine 4 (140) (2012), 140ra88-140ra88.
[52] E. Pedraza, M.M. Coronel, C.A. Fraker, C. Ricordi, C.L. Stabler, Preventing hypoxia-induced cell death in beta cells and islets via hydrolytically activated, oxygen-generating biomaterials, Proceedings of the National Academy of Sciences 109 (11) (2012) 4245–4250.
[53] C.L. Ward, B.T. Corona, J.J. Yoo, B.S. Harrison, G.J. Christ, Oxygen generating biomaterials preserve skeletal muscle homeostasis under hypoxic and ischemic conditions, PloS One 8 (8) (2013) e72485.
[54] J.M. Lee, W.Y. Yeong, Design and printing strategies in 3D bioprinting of cell-hydrogels: a review, Advanced Healthcare Materials 5 (22) (2016) 2856–2865.
[55] L. Walløe, Arterio-venous anastomoses in the human skin and their role in temperature control, Temperature 3 (1) (2016) 92–103.
[56] K.D. Hankenson, M. Dishowitz, C. Gray, M. Schenker, Angiogenesis in bone regeneration, Injury 42 (6) (2011) 556–561.
[57] Y. Shandalov, D. Egozi, J. Koffler, D. Dado-Rosenfeld, D. Ben-Shimol, A. Freiman, E. Shor, A. Kabala, S. Levenberg, An engineered muscle flap for reconstruction of large soft tissue defects, Proceedings of the National Academy of Sciences 111 (16) (2014) 6010–6015.
[58] D.J. Huey, J.C. Hu, K.A. Athanasiou, Unlike bone, cartilage regeneration remains elusive, Science 338 (6109) (2012) 917–921.
[59] D.-A. Wang, S. Varghese, B. Sharma, I. Strehin, S. Fermanian, J. Gorham, D.H. Fairbrother, B. Cascio, J.H. Elisseeff, Multifunctional chondroitin sulphate for cartilage tissue–biomaterial integration, Nature Materials 6 (5) (2007) 385.
[60] S. Hong, D. Sycks, H.F. Chan, S. Lin, G.P. Lopez, F. Guilak, K.W. Leong, X. Zhao, 3D printing of highly stretchable and tough hydrogels into complex, cellularized structures, Advanced Materials 27 (27) (2015) 4035–4040.
[61] G. Nemova, R. Kashyap, Laser cooling of solids, Reports on Progress in Physics 73 (8) (2010) 086501.

CHAPTER 9

Ethical and regulatory concerns of bioprinting

9.1 Introduction

"Bioprinting is defined as the use of 3D printing technology with materials that incorporate viable living cells to produce tissue for reconstructive surgery" (OED Online. Oxford University Press, March 2016). Accompanying this definition by Oxford dictionary is a clever example sentence, "Welcome to the age of bioprinting, where the machines we've built are building bits and pieces of us." It paints the real picture of this burgeoning technology in today's world. Researchers and scientists have already published quite a number of scientific articles on bioprinted tissues, with success stories of in vitro and in vivo testing and many of them are working hard to realize the greater goal of organ printing. This is substantiated by the fact that the number of scientific papers referencing bioprinting have quadrupled from 2012 to 2015 (A search in Scopus database with the keyword "bioprint*" gives 50 publications in 2012 and 202 publications in 2015). Companies are increasingly interested in providing novel hardware, supporting the research in this field. Market analysis report published by a research firm TechNavio (http://www.inside3dp.com/just-global-bioprinting-market-headed/) forecasts the global 3D bioprinting market to grow at a CAGR (Computed Annual Growth Rate) of 14.52% over the period 2013−18. Some companies have even started selling bioprinted tissue constructs commercially for drug testing. For example, Organovo Inc., a leader in the bioprinting arena, offers contract testing services utilizing exVive3D Liver, bioprinted human tissue models. The rapid development of this technology is the result of various factors including the advances in genomics, proteomics, and stem cell biology; introduction of novel biocompatible and biodegradable biomaterials; enhanced design of bioreactors for tissue maturation; and the increased knowledge and understanding of wound healing. The growth pace is alarming, considering the lag in policy making and regulatory concerns, which is foreseen as a snag in clinical deployment of this technology in the foreseeable future.

Three-dimensional bioprinting involves several different approaches including biomimicry, autonomous self-assembly, and mini-tissue building blocks, with the aim of fabricating functional 3D living tissues and organs, with biological and mechanical properties

3D Bioprinting in Tissue and Organ Regeneration. https://doi.org/10.1016/B978-0-12-824291-9.00002-6

qualified for clinical deployment [1]. The progress so far in bioprinting is very visible, which can be verified with the increasing number of perspectives, reviews and papers; incipient books on the subject [2–5]; new journals and societies; and the development of commercially available bioprinters, all serving as important progress milestones [6]. Three-dimensional bioprinting not only enables large-scale manufacturing of tissues or the establishment of organ factories, but it also comes with the inherent advantage of patient-specific customization [7–10]. Starting from the hardware (bioprinter) to the scaffold material, cell type, and software like the imaging and modeling system, there are critical properties that are required to be satisfied in each of these constituents. The specific system requirements of an ideal bioprinter includes high throughput, high resolution, simultaneous multimaterial dispensation, ease of use, nontoxicity, sterile environment, postprinting cell viability and affordability [11]. The requirements of an optimal biomaterial [12–14] are biocompatibility with tissues, biodegradability at the ideal rate corresponding to the rate of new tissue formation, nontoxicity, nonimmunogenicity, optimal mechanical properties, adequate porosity and morphology for transporting cells, gases, metabolites, nutrients, and signal molecules both within the biomaterial and between the biomaterial and the local environment, and printability. Cell selection also has strict requirements, which are to be satisfied to assure persistence and functionality of the regenerated tissue for the patient's life time [15]. Chosen cells should closely mimic the physiological state of cells in vivo and are expected to maintain their in vivo functions under optimized conditions [1,16]. Imaging and modeling systems require advanced capabilities to scan on complex irregular body contours, with intriguing morphological and structural details, sufficiently modeled in 3D, and in required file format for printing.

While all the above technical requirements are rapidly being fulfilled by the increased research and commercial industries, the road to clinical deployment still looks murky, bearing in mind the sulking ambience in ethical and regulatory circles. While there are certain guidelines in piecemeal, for separate parts of this technology say the license for a particular biomaterial to be used in vivo or transplanted like artificial skin grafts, the regulatory authorities still lack in assessing this technology in whole, in totality, given its potential to revolutionize the medical world. As Hockaday [17] puts it suitably, structural complexity, functional integration and completeness are all required in bioprinted organs; so they are in the bioprinting industry too, which is still emerging, much the way fabricated biomaterials emerge from the bioprinting process layer by layer. This chapter reviews and analyses the 3D bioprinting technology in three important tenets, namely ethical, legal, and social aspects, shortly referred to as ELSA (Fig. 9.1). The significance of this chapter will be to address a broad audience, associated with this technology, from scientists to businessmen, engineers to clinicians, laymen to lawmakers. The chapter will provide a guideline for policy makers to understand the potential of this technology and take appropriate measures aiding in its success as well as induce the researchers and

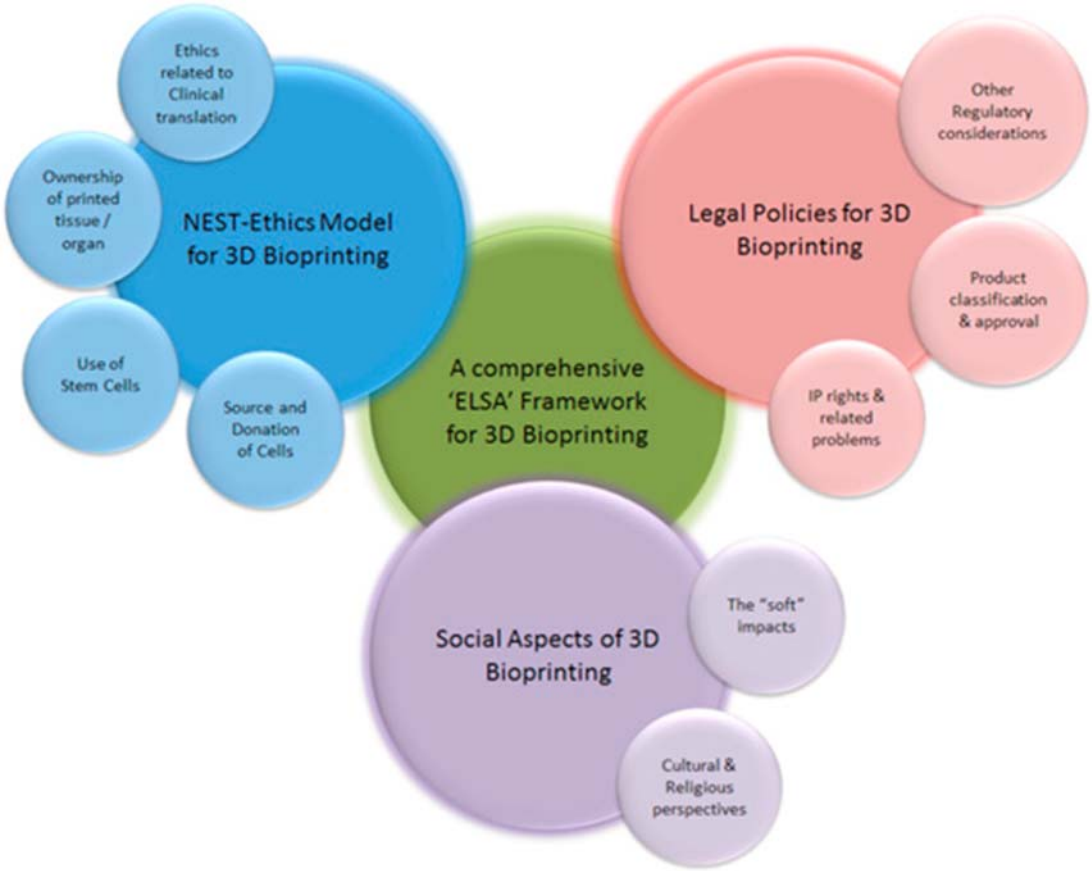

Figure 9.1
ELSA Framework for 3D bioprinting.

scientists working in this area to look at the practicality of this technology and the possibility of clinical translation so that the necessary changes that have to be imbibed in the course of the current research can be made at a much earlier stage.

9.2 Ethical aspects

Ethics is a broad term, considered to be a discipline of philosophy, and applied ethics is one branch of ethics. It is important that we distinguish the field of applied ethics from other tenets of ethics namely normative ethics, descriptive ethics, and metaethics [18]. Applied ethics deals with moral questions concerning specific contested practices, say the engineering ethics, medical ethics, bioethics and environmental ethics. Given the growth of 3D bioprinting, it is high time to think of "Bioprinting Ethics." People may argue that there are already active discussions on bioethical principles including the use of cells, stem

cells, and animals for research. But, that does not cover in full the field of bioprinting. A complete approach is needed rather than a piecemeal approach. This is particularly important for bioprinting because it is an umbrella term covering a host of heterogeneous technologies, from manufacturing to materials and onto the use of cells.

9.2.1 NEST-Ethics model

A perfect ethical model that can be applied to bioprinting is the Ethics of New and Emerging Science and Technology model, also called as NEST-Ethics. Swierstra et al. [19] had studied NEST-Ethics in detail. Existence of NEST-Ethics is by a set of recurring tropes and argumentative patterns. "Trope" means a recurring motif or argument that is supposed to have a particular force or impact. Argumentative "pattern" means two or more ethical arguments that hang together in the sense that they provoke each other into existence. Before we delve into the techno-ethical controversies, it is important to understand and differentiate between "morality" and "ethics." While morality is characterized by unproblematic acceptance, ethics is marked by explicitness and controversy. The relationship is intertwined and the underlying complexities should be understood in depth. Though it sounds more philosophical rather than being technological, this is highlighted briefly as it is important for any panel that discusses and makes decisions on bioprinting ethics, and they strongly understand these terms and the underlying implications.

NEST-Ethics are discussed at two levels. The first level, called as metaethical issues, includes (i) collective utility or the consequentialist arguments, also called utilitarianism or consequentialism, (ii) deontology which are the fundamental principles, rights, and duties, (iii) theories of justice, which is about the just distribution of costs and benefits, and (iv) conceptions of the good life, which are virtue ethics. The second level focuses on the relationship between technological and moral change, which includes the arguments between technological determinists and voluntarists, between optimists and pessimists, and most importantly the moral change induced by the technology [19,20]. Taking the metaethical issues first, there are two different views to look at, the technological determinism and social determination. For bioprinting, there are strong views on technological determinism, i.e., the "benefits" of this technology to the human kind. Bioprinting can replace tissues and even organs in the future, thereby saving hundreds and thousands of lives. On the other hand, the social determination deals with the perspectives of the people on the technology. Technological determinists argue that the newly emerging technologies will materialize anyhow, independent of what the public or common man thinks, deliberates, or decides. Social view holds that this argument is not true and involvement of human agency is necessary in the process of materialization of any emerging technology; if not, it will lead to misuse of these technologies causing societal

destruction. The topic at hand is trickier, in the sense that it should not be confused with the resistance to change. For instance, Louise Brown, the first baby from the then revolutionary technology, IVF (In Vitro Fertilization), was seen by some as a miracle and others as a monster, depending on their personal views. That was at the incipient state of the technology. But now, IVF is widely accepted by the public and is no more a jargon. With bioprinting, it is not different. A man with a bioprinted heart may be seen differently compared to the one with a heart transplant, at the beginning. This is normal for any new change. But, the real issues to be addressed are more than the resistance to change. It involves cultural perspectives and moral beliefs, which are discussed in detail under the section "Social Aspects."

Leaving the consequentialist and deontological arguments to the ethical experts, let us touch upon the justice arguments and "good life" ethics. Distributive justice is an important point for discussion in bioprinting, which is delineated by the way benefits and risks are distributed. Equality, need, merit, effort, and combinations of two or more of these are considered to be the constituents of distributive justice [21]. The widely accepted theory in distributive justice is the "maximin rule," which warrants that the new technology will only advance justice when it will benefit those who are now the worst off, poor people and poor countries. Can bioprinting be considered to be compliant with the "maximin rule" or the broader theory of distributive justice? Consider the costs of the hardware equipment and skill level of the operators currently working on bioprinting. The costs of bioprinters may come down in the future as market grows and competition increases, but what about the handling of cells and tissues, the postprinting maturation of tissues in a bioreactor, and the further application into the patients? Arguments on "Good Life" ethics revolve around one major question as to what sort of good life can be achieved with the new technology. One framing of this topic involves culturally shaped identities and aspirations, including the discourses of limits. With bioprinting, the immediate question will be "Can humans play God?," just like when IVF or cloning or other biotechnology developments occurred. Though bioprinting is not seen as a technology to "create" whole humans, the question of "playing God" is still valid when it comes to organ printing. While people may see a tissue construct as just another treatment method or an implant, the perspective might be different when it comes to organs.

The discussion on ethical aspects of tissue engineering, based on the NEST-Ethics, was given by Oerlemans et al. [22]. The study revealed that, from the NEST-Ethics perspectives of tissue engineering, the second level of arguments, those referring to the techno-moral change, receive much less attention. The terms "hard impacts" and "soft impacts" come in handy for better understanding of these second-level arguments. Hard impacts are quantifiable consequences of the new technology on the well-being of lives and soft impacts cover the category of effects that are not easy to quantify, such as changes to experience, habits, and perceptions [23–25]. Some probing questions may be:

"Does a kidney made from my cells and stored in a laboratory belong to me?" Will people's attitude change like "I can smoke any number of cigars now that I can buy a new pair of lungs and drink to my heart full and buy a liver from the organ shop"? How will the public perceive bioprinting? Will it be accepted without any questions or concerns? What are people resistant to, and can this be changed during the development process, either by refining the bioprinting aspects or informing people differently? After a detailed analysis of tissue engineering within the NEST-Ethics framework, Oerlemans et al. [22] reported a threefold conclusion. Firstly, the perception of "naturalness," where the process of bringing ultimately a foreign artifact into the human body, introducing a dynamic product into a dynamic structure, and the dynamic interaction between the two are highlighted as facts to ponder, given that the exact behavior of the engineered tissue in in vivo conditions is not completely known and once introduced and the process started, it cannot be completely reversed. Secondly, the lack of consideration of soft impacts in the ethical framework discussed earlier, including the discussion of distributive justice. Thirdly and finally, the lack of completeness is taken into account for the values and concerns of envisioned users, the general public. All these three conclusions are applicable directly to bioprinting as well. In addition, there is another factor to be considered, the "moral degradation." Will the easy availability of organs lead to degrading moral standards? Will this advanced technology change the perception of unhealthy practices (smoking, alcohol consumption) from "bad" to "good"? In most countries, there are warning labels on the cover of cigarette packets, "Smoking is injurious to health" and some even with petrifying pictures to increase awareness among the smokers. With the advent of bioprinting, the organ shops may advertise, "Why quit smoking, when you can have new set of lungs?" This is a clear example (prediction) of the possible change in the moral landscape when the technology matures.

9.2.2 Ethics related to source and donation of cells

Cells are the most important component of bioprinting. The type of cells that are used to formulate the bioink determines the characteristics of the bioprinted tissue or organ. Stem cells will play a crucial role in the development of this technology, though differentiated cells or cell lines are used currently. Hence, it is important to also consider the ethical aspects of use of cells, including stem cells, even when the technology is at the incipient state. De Vries [26] reviewed the ethical aspects of tissue engineering and listed 10 ethical issues that are most frequently discussed and debated in the scientific literature. After studying the journal articles extensively, it was reported that 70% of those selected articles refer to the use of human embryonic stem cells (hESCs) and the moral problems raised by these cells, making it the most dominant ethical question. Next comes the moral problems involving therapeutic or research cloning, with 20% of the selected articles talking about it. With bioprinting, the problem becomes even more complex, where both of these

dominant questions should be considered together. Based on their study [26], four clusters of ethical issues were identified, namely (1) the source of cells, (2) the donation of cells, (3) the use of animals in laboratory, and (4) morally problematic techniques, of which the first two will be briefly reviewed in this section.

Bioprinting will not be complete without the use of stem cells at some point. It is wise to consider the problems associated with the use of stem cells, right from an early stage. Source of cells is an important point to be debated. There were several contentious arguments on the use of fetal cells [27–31], embryonic germ cells [32–34], the primary source of which is induced abortion, which in a way, legitimizes the practice of abortion, encouraging hospitals to increase the number and even thought to the extent of women conceiving specifically just to get fetal cells via abortion [27,34]. Since the main question arises from the use of hESCs, many works had suggested alternate sources of stem cells including bone marrow–derived stem cells [35–39], stem cells derived from amniotic fluid [33,40,41], placenta [33,42–44], umbilical cord blood stem cells [45–51], collectively or commonly referred to as mesenchymal stem cells (MSCs). Other important alternative sources suggested are the stem cells that are derived by reprograming differentiated somatic cells [52–55] and finally novel techniques to acquire hESCs without destroying viable embryos [56–61].

Not only there are controversies raised about the stem cells and human cells, but also for the use of xenogeneic cells, cells derived from other species or animals. Cons of using xenogeneic cells include risk of introducing pathogens like virus, bacteria, and other infectious agents into the human body and the associated serious immunological problems [31,62–69] and the patient's acceptability of introducing animal cells or tissues into the body [68–70], especially those with strong religious beliefs. The reservations of Jews and Muslims for the use of cells or tissues from porcine [71] is one such example. Though use of allogeneic cells or tissues is less risky than xenogeneic, the problem of disease transmission and immunological issues still exists [69,72,73].

The second important concern regarding the use of cells is about the donor [26,74]. Four important issues related with the donation of cells are: (1) privacy of the donor, (2) informed consent of the donor, (3) possible invasiveness of the cell/tissue obtaining procedure, and (4) ownership of the donated cell/tissue. Preserving the donor's identity is the first and foremost concern. This can be achieved by anonymization of samples used in the research [75–80]. Informed consent of the donor comes next. Donors should be clearly informed on how the donated cells or tissues will be used in research or for transplantation. This is important because some of the donors may have reservations for certain research practices, say if their cells are going to be used for research cloning or for constructing a tissue that will be tested in vivo in a porcine model, based on their religious and cultural beliefs and moral perspectives. It would be highly unethical if the

donated cells or tissues are used for other purposes which are not briefed to the donor beforehand and consent obtained. Thirdly, the issues pertaining to the method of obtaining cells or tissues from donors should be addressed. Care should be taken not to induce pain or postdonation problems. Previous discussion about the hESCs, like acquiring cells from the umbilical cord or aborted embryo or IVF, may not be comfortable to all donors. Lastly, obscurity about the ownership of donated cells and organs poses a great challenge, which is discussed under the "Legal Aspects" section. The sense of ownership may vary with respect to the organ domain. For example, people may feel a stronger association with a heart or brain or kidney made out of their cells than a piece of bone or orthopedic graft or any other engineered tissue for that matter.

One issue that is widely debated in the field of organ transplantation is about the altruistic donation, whether it should be directed or kept anonymous [34]. The central argument is whether the donor should be given the right to choose the recipient, who may be the dear ones whose life one wishes to save by donation or it should follow the "first come first serve" basis, based on the waiting list. The ethical problem with the directed approach is that it favors some of the potential recipients, jumping to the top of the waiting list. Bioprinting solves this problem, in the sense that the organs are bioprinted and not directly donated. Though the source of cells for bioprinting the organ itself is under debate, it is justified in the contention that bioprinting still has a better edge than the problems associated with altruistic donation.

9.2.3 Ethics related to clinical translation

The first and foremost understanding required even before we talk about the clinical translation of bioprinted tissues and organs is that it is entirely different and more complicated than the therapeutic drugs and hence ethically more complex than the drugs or biologics [81]. Since bioprinting is an umbrella term with a deluge of other fields contained within, the medical devices, drugs, cells, and biomaterials, given the fact that each of these are governed by a different organization in many countries, the clinical translation becomes more complicated. The legal complications and possible solutions are discussed in the "Legal Aspects" section. However, it is worth mentioning the ethical questions that arise on clinical implementation in this section. Broadly speaking, this subject can be discussed under two headings, namely the preclinical and clinical testing.

Preclinical testing is required not only for the final bioprinted product, tissue construct, or organ, but also testing of individual elements of the product separately, say the effect of biomaterial or the type of cell on the body. Why is this required? Firstly, the irreversible impacts and consequences of implanting the artificial construct or organ into the body, partially if not completely irreversible, puts pressure on knowing the exact reaction of human body to these artificial artifacts. Once the procedure is complete, the patient has to

live with the consequences of it throughout one's life, which warrants for a detailed preclinical study, not only of the construct or organ but also the individual elements. Secondly, it is highly difficult to assess and deliberately decide which element of the bioprinted product provokes a particular bodily response, if some abnormality or uneasiness is detected after transplantation. For instance, Lalu et al. [82] carried out a metaanalysis of clinical trials which involved the use of intravascularly delivered MSCs to determine whether MSCs have any undesirable effects in the treatment of pulmonary diseases and this study included the data from more than a 1000 patients. In vitro and in vivo studies usually constitute the preclinical study and give significant information. In vivo studies are usually performed on small animals like a rat or nude mice or rabbit and sometimes porcine models. However, the results obtained do not fully elucidate the biochemical and physiological interactions that occur in humans and hence clinically relevant large animal studies, even in nonhuman primates become essential [81]. Animals and humans have the same organ systems performing the same tasks, and suffer from similar diseases including cancers, flu, and asthma. Also, it is easier to study the effect of a drug or medical procedure throughout the whole lifespan of animals, as they have a shorter life cycle than humans and the experimental conditions like diet, temperature, or lighting can be easily controlled, both of which would be difficult to do with humans. Though nonanimal methods like in vitro studies or computer models can be used to a certain extent, the complexity of the living system cannot be represented by these methods. However, even when such strong points in favor of animal testing are put forth, use of animals for testing, even small animals like mice or rabbit, becomes increasingly difficult these days, with many animal welfare organizations pressing the governments to ban the practice. Many had reported that the testing procedures cause discomfort and pain to the animals [83–85] and this cruelty meted out to the living beings must not be allowed. Testing with primates becomes even more stringent, taking into account these challenges.

Clinical testing should follow the preclinical testing procedures. It is necessary because there is always a difference in response between the animals and humans. When coming to clinical testing, the biggest ethical issue arises with the selection of patients for such a testing. Two components in patient selection are reported to be most important [81], namely (1) Inclusion of patients with least comorbidities (healthiest individuals) or those with highest number of comorbidities (sickest individuals), as each of these group will respond differently and give different data, and (2) Obtaining competent and informed consent from the selected individuals, bearing in mind the adequacy of social support, appropriate mental health and willingness to lose some degree of personal privacy, as the results mandate publication. In the first step of patient inclusion, the poorest sections of the society should not be taken for granted. Selecting those healthy individuals, who give their consent for clinical testing for money or trading their health for money, without

understanding in detail the effects that the whole procedure will have on their bodies, should not be encouraged. Even the decision of including patients with tertiary illness should not be made because they have only a limited period to die. Proper information has to be given to the patients and their dear ones, and consent should be obtained before they are included in clinical testing. On getting the informed consent, it is imperative to disclose the complete risk-benefit analysis [86] and make sure that the patient has actually understood what had been explained, rather than focusing on just getting the signature. This is important because most of the consent forms contain complicated medical jargons, which the general public cannot fully understand and appreciate. It is the duty of the medical professionals to explain clearly all these terms in laymen language before obtaining the signature officially, which serves as the legal document. Next in line is the problem of growing cost of conducting clinical trials, especially in highly regulated countries and who sponsors the testing. It is a common notion that the clinicians doubt the validity of the results from industry-sponsored clinical trials [87]. Here comes the role of governments to make decisions on funding the clinical trials, with the procedures and policies clearly delineated.

Patient specificity is another social aspect to be focused upon. The specificity of any clinical trial is the ability of the trial to correctly identify those patients without the disease, i.e., the true negative rate. Though 100% specificity should be the goal of any clinical trial, it is highly unlikely and unrealistic. A common method to improve the true negative rate is to subject patients who are initially positive to a test with high sensitivity/low specificity to a subsequent test with low sensitivity/high specificity. Here, sensitivity refers to the true positive rate or the ability of the clinical trial to correctly identify those patients with the disease. The feasibility of implementing such multiple tests should be evaluated for clinical trials of bioprinted tissues or organs. Finally, a global registry of all the preclinical and clinical testing results should be maintained, for the medical professionals and researchers all over the world to have a common and better acumen. Ethics comes into play here too, as the recorded results should not be over hyped. It is important that every minute detail of the testing and small observations are published without any concealment.

9.3 Legal aspects

Legal aspects of bioprinting command a wider and more focused attention. This includes patenting and related problems, regulatory policies, government interventions and decisions. Lack of understanding of this technology by the regulating authorities is the first problem to be addressed. While discussing about the field of tissue engineering as a new paradigm in medicine (which holds good for bioprinting also), Trommelmans et al. [88] rightly pointed out that addressing one or two major tenets/issues legally will not solve all

the legal problems that the technology faces in totality. To give an analogy, the very idea that addressing legally the bioethics related to use of stem cells and donation of cells will solve all the legal problems facing the whole technology should be dismissed. The deficiency of a special legal framework for bioprinting will lead to complications later. Bioprinting deserves a more organized and complete legal attention, given its huge potential in coming years.

9.3.1 Intellectual property (IP) rights and related problems

Patenting and IP rights dominate any new technology with a very high potential for commercialization and no wonder, bioprinting is one such technology. Yoo [89] identified five areas of potential IP in 3D bioprinting, namely (1) hydrogel/extracellular matrix (ECM) materials, (2) isolation and growth/differentiation of cells in the context of bioprinting, (3) bioreactor/method to grow printed organ precursors, (4) methods of dispensing/printing techniques, and (5) methods of novel 3D fabrication techniques, mostly hybrid approaches. Even before we go into possible areas of patenting in bioprinting and associated problems, the very question of "whether bioprinting is patentable?" should be answered. Tran [90] in his perspectives on patenting of bioprinting, differentiates between bioprinting process and bioprinting product. While there were patents on the bioprinting process filed already and some even approved, the problem of patentability of bioprinting products still remains unsolved. It depends on whether a bioprinted product is a product of human ingenuity and nonnaturally occurring, which is a two-prong test to pass the patent-eligible subject matters. While technically the first criterion of human ingenuity is clearly satisfied, the second test of nonnatural occurrence is debatable. Tran [90] concluded his article proposing a compromise that patents can be granted for only bioprinting process claims and not product claims. But this may not be a perfect solution. Critics may try proving the nonnatural occurrence of the bioprinted product, since it is extremely difficult to fabricate artificially a tissue or organ to exactly mimic the natural tissue or organ, in micro- and nanoscale and hence argue that the bioprinted products must also be permitted for patenting. Addressing this argument is extremely important to provide clarity with regard to another related issue of ownership of the bioprinted tissue or organ [29,73,91–95]. Does the donor of cells have the authority over the final bioprinted product, which may be a tissue or organ? Or does the ownership lie with the clinician/technologist who bioprinted the product using these cells? Or shared ownership? If no, why? If yes, in what way?

The next big concern is the intellectual property theft. Forecasts suggest that by 2018, 3D printing will result in a loss of at least 100 billion USD per year in intellectual property globally [96]. Open source is said to be a solution to prevent IP theft. But, significant concerns about piracy, quality control, and unauthorized products are raised by the

inventors of novel bioprinted materials and devices, and it becomes critical in such cases to actively pursue patent protection. If anybody can bioprint a brain, heart, or a kidney, the questions on safety and quality of the product arises and has to be addressed appropriately. On the other hand, if patents are filed and granted for individual elements of bioprinting technology, will it hinder the maturation of technology to address the most important problem of organ printing and transplantation? This is a valid point to mull over. Provided all technologies have the potential to be abused, a careful consideration of all the consequences should be made prior to embarking on major patenting decisions.

9.3.2 Policies and regulations

Government intervention in research and novel technologies is imperative as it will determine the very future of the technology itself. Policy decisions and appropriate regulatory concerns have to be made and addressed, even at an earlier stage of technology development. With bioprinting, the technology which has the potential to save lives and revolutionize the medical field deserves special attention in having a legal framework. Smith [97] had studied in detail the government's role in advancing regenerative medicine and tissue engineering, taking the United States as an example. The first regulatory issue comes with the current classification of medical products into a medical device, drug, or biologic and as a "combination product," which may be device/drug or device/biologic. The classification is important because it determines the further processes of review and approval by Food and Drug Administration (FDA). For information, FDA has been vested with the authority of control and distribution of medical products in the United States, under two statutes namely the Food, Drug & Cosmetics Act (or FD&C Act) and the Public Health Service Act (or the PHS Act). Each product classification has a different set of regulatory reviews with different agencies reviewing the product and different approval pathways. Namely there are three principal agencies under FDA, (1) Center for Biologics Evaluation and Research, (2) Center for Devices and Radiological Health and (3) Center for Drug Evaluation and Research, with each responsible for review and approval of biologics, devices, and drugs, respectively. With bioprinting, which is an umbrella term of various elements, the review process and approval pathways are not clearly delineated. Also, the classification itself becomes complicated as bioprinted products are not readily classifiable as a device, drug, or biologic. To overcome this challenge, steps were taken to recognize "combination products" and they are assigned to a particular center, which then decides on the classification of the product as a drug, device, or biologic, based on its primary mode of action, as determined by FDA. However, there are always disputes between various interested parties on the classification and it is not a perfect solution. The classification also influences the marketing review and approval processes, which come later and directly affect the marketability and business scenario of the product. For marketing devices, the sponsor has to submit a device premarket application (PMA) or

product development protocol (PDP), whereas a New Drug Application (NDA) is required for marketing a drug. Biologics are covered under the PHS Act and submission of a biologics license application (BLA) is required; sometimes a special designation is carried out for some biologics as "orphan drugs" under the Orphan Drug Act (ODA). For clinical approval, devices follow investigational device exemption (IDE) approval by FDA and drugs and biologics should have got the approval of investigational new drug (IND) application. This complex review and approval pathway based on the product classification is given in Fig. 9.2 [97]. With such complex and convoluted regulatory pathways, we can be sure of a deluge of arguments and debates when bioprinted products hit the market. This is just the case of the United States and other countries having their own regulatory mechanisms for medical products, which makes it even more complex on a global scale. Heinonen et al. [98] studied the issues in the regulation of tissue-engineered products in the European Union. Gheisari et al. [99] reviewed the progress made in stem cell and tissue engineering research in the Islamic Republic of Iran and stress the importance of government policies and decisions, keeping in mind the stringent religious norms in prevalence. Hence, an international agency is required, with representatives from different countries, to look at the regulatory issues of bioprinting and to decide on a common framework of policies, with due consideration to the differences in cultural, social, and religious perspectives of different groups of people. This initiative will help clear the snags en route in the development of this technology and prevent delays in the clinical translation of this life saving invention. A good point to start will be to set up regulatory panels at national level to look into the various aspects of bioprinting namely the acceptance of the technology (given the cultural and religious views of its population), the benefits that this technology can offer, the associated risks of misuse and economic opportunities that come with its implementation.

9.3.3 Other regulatory considerations

In addition to the regulatory issues related to classification of bioprinted products, its review and approval pathways, there are other aspects related to it like Good Manufacturing Practices (GMP), that aid in assuring best product quality and consistency. Some constituents of GMP are: maintaining a clean and hygienic bioprinting area, controlled environmental conditions thus preventing cross-contamination or infection, clearly defined processes, documentation and effective control, good documentation practices, recording deviations and retention and maintaining records of manufacture including distribution (that enable the complete history of a batch to be traced) in a comprehensible and accessible form. GMPs are enforced by different countries under different titles, current GMP or "cGMP" in the United States by FDA, "EU-GMP" in the European Union, the Medicines Act or "The Orange Guide" in the UK and so on. Care should be taken to include GMP when acting upon the legal framework for bioprinting.

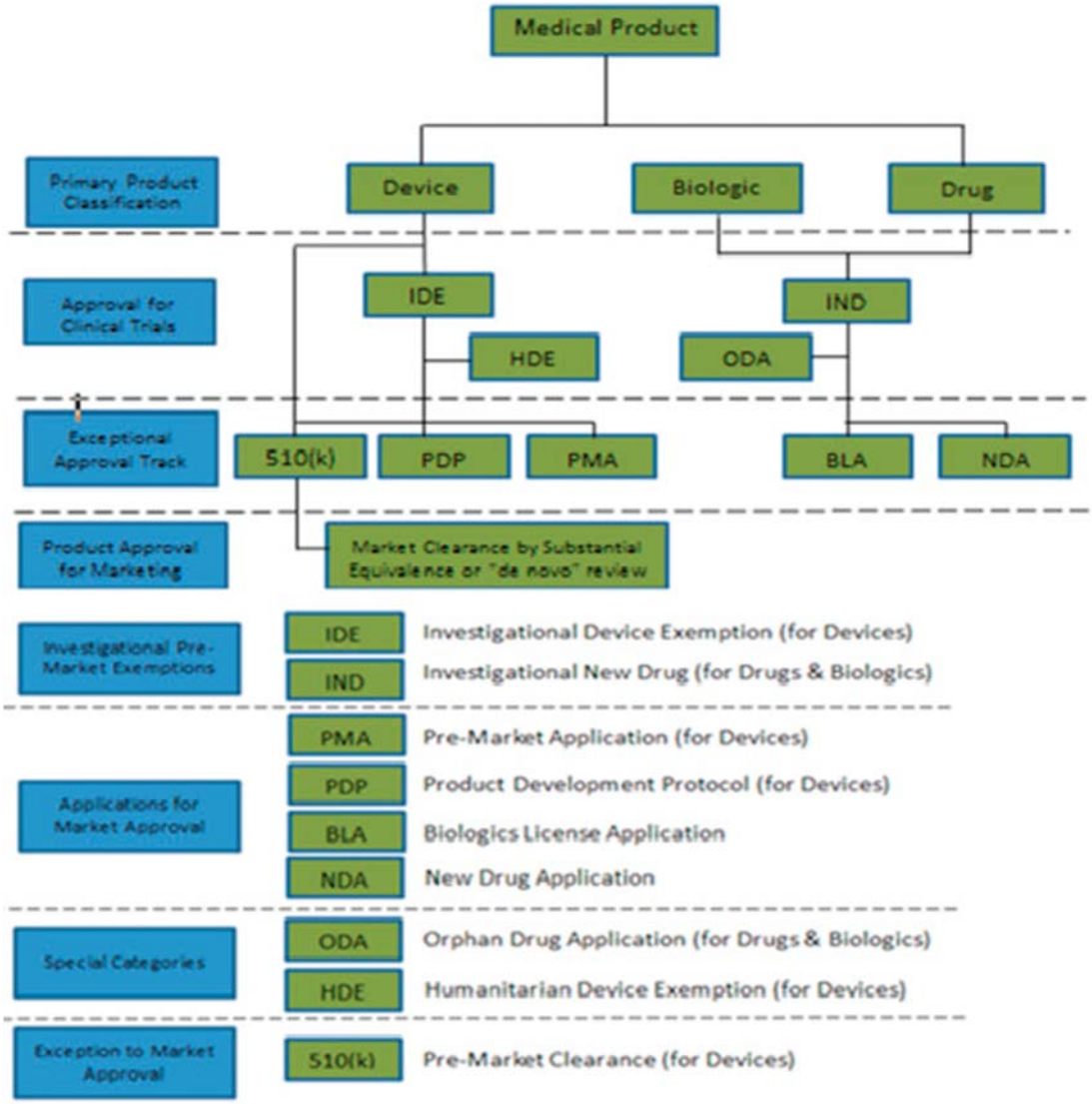

Figure 9.2
Review and approval pathways by the US FDA product classification [97].

Since bioprinting is a very promising technology, it poses a greater risk of falling into wrong hands. To prevent this from happening, discussion is needed if licensing would help. Rather than having a scenario where anybody who can afford to buy a bioprinter, can print any organ that they wish to (though basic skills of cell culturing and other bio experience is a prerequisite, assuming easily learnt) and may be a complete human body sometime, is it not better to license it to certain medical clinics or trained and certified

professionals? Many can have alternating views on the topic but it is worth including in the discussions about the future regulations of bioprinting technology.

9.4 Social aspects

A new technology can succeed only if it is accepted by the general public. Reproductive cloning, for example, is an exciting technology for researchers and scientists, but is dismissed by the majority of public, due to their notion of "playing God." Bioprinting may face a similar fate too, if the social aspects are not taken in to consideration. The soft impacts, which are the impacts on human psyche, the cultural and religious perspectives of the people, play a significant role in successful translation of any emerging technology.

9.4.1 The "soft impacts"

Any new technology should be assessed not only based on the direct impacts of it but also the indirect influences. This is referred to as the "societal relevance" or "broader impacts" or more appealingly "soft impacts" of the technology [24]. To further define the term "soft impacts," it reflects the effects of the technology on the quality of human life, which are difficult to quantify and more related to the psychological capacities such as experience, motivation, emotion, perception, habit, and deliberation about action. Any new technology has a tremendous impact on these terms, which determine the success of the technology in the society. For example, microwave technology has said to have curbed the habit of family dinners in a large part of the world [100]. The drastic change in the way that people relate to each other after mobile phones penetrated the market and internet altering experiences of friendship and love [101,102] are other examples. These subjective, partisan, emotional, value-laden impacts are not dismissible in the larger social framework of the technology and if these impacts are overlooked, the framework is deemed to be short-sighted. Morris [103], taking the example of Genetically Modified Organisms (GMOs), went to explain that the overlooking of these soft impacts on any technology may lead to public discontent and controversy, jeopardizing the technology itself, at a later stage. The technology of bioprinting is not an exception to it. Though bioprinted products mimic the native tissue or organ, it is still considered a foreign artifact and how people perceive and react to it is important. One of the major determinants of positive soft impact is the "naturalness" of the product. Though the bioprinted product is definitely more natural than the mechanical substitutes, translating the "naturalness" into numbers is very difficult. In fact, the three dimensions which differentiate hard and soft impacts are valuation, quantifiability, and causality (causal link between technology and impact) [25]. It is not a right approach to neglect the impacts that score on one or more of these three dimensions, which may thwart the intended aim of the technology, called as revenge-effects [104]. Some of the questions regarding the soft impacts of bioprinted products that

are to be addressed are: What is the perception of people about the bioprinted product? Do they consider it on par with the organ transplantation from a donor? Given a choice, will people prefer bioprinted organ over an altruistic organ donation? If yes, why? If no, what are the changes required to make bioprinted products more promising and acceptable? Addressing these questions will help alleviate the doubts of common man and easy adoption of this technology into the society.

9.4.2 Cultural and religious perspectives

People are inseparable from their cultural and religious values and any technology will not be spared if it is against the interests of the people, in terms of these values. People are different and so are their perspectives on different technologies. Henon [105] discussed in detail the perceptions of various religions and cultures on the use of hESCs in tissue engineering and the reasons for their reservations. Excerpts from the study are explained here. Catholic and Orthodox views completely prohibit the research on hESCs, therapeutic and reproductive cell cloning because they believe that life begins at conception. Protestant Christians accept hESCs research and therapeutic cloning, if conducted reasonably and ethically but do not accept reproductive cell cloning. Muslims too accept hESCs research and therapeutic cell cloning because of their belief that the fetus has moral existence only at the end of the fourth month but they too prohibit reproductive cloning. Jewish view accepts all three, hESCs research and therapeutic cloning based on the belief that an embryo has no moral status until 40 days and reproductive cell cloning, in case of sterility only. Buddhists, on the other hand prohibit hESCs research and therapeutic cell cloning, as they also believe that life begins at conception but accept reproductive cell cloning, provided there is no genomic modification. It has to be noted that reproductive cloning is still not matured to perfection and current scientific experience indicates that between 95% and 98% of mammalian cloning experiments have resulted in miscarriages, still births, and life-threatening abnormalities. There is increasing evidence that mammalian clones are likely to have subtle abnormalities of complex and poorly understood genetic control mechanisms. Similarly, though bioprinting is not mature yet, it is desirable to have a similar debate to evaluate the perspectives of various religions on bioprinting. What is acceptable and what is not, according to their faiths. Some religions may accept bioprinted tissues, constructed from animal cells, and other may not (for example, Jews and Muslims, if porcine cells are used). Some may accept bioprinted tissues but not bioprinted organs, as they see tissues as just biological substances but organs as procreation or “playing God”.

The views and perceptions change with countries too [105,106]. For instance, therapeutic cell cloning is prohibited in France, Germany, Spain, Italy, Austria, Ireland, Israel, Sweden, Belgium, India, Canada, and Australia but authorized in the UK, Denmark,

Japan, the Netherlands, and Korea. It is important to note that, despite their geographical proximity, say the UK and Ireland, the sentiments are very different, while it is authorized in the UK, and it is prohibited in Ireland, authorized in Denmark but prohibited in Sweden. The perception also varies with each technology, despite how closely related they are. Though use of stem cell lines and therapeutic cell cloning are very much related, the former is authorized in many countries like Israel, Sweden, Belgium, and India but the latter is prohibited in the same countries. The same might be the case with bioprinting too. Determining these complex perceptions, which are greatly influenced by the cultural, political, and national sentiments, is very important.

Keeping in mind that the perspectives of people are dynamic, the evaluation of any technology should not be restricted to just once but should be made from time to time. What may not be acceptable now may be accepted after a decade from now. This effect is partly due to the lack of understanding and the resulting fear and partly due to the inherent human tendency of resistance to change. Bioprinting is a technology, which is not free from controversies. A critical analysis of the social aspects of this technology should be made (including the cultural, political, and religious perspectives), included in the larger ELSA framework and reviewed at regular intervals, catching up the changing societal views from time to time.

9.5 Tissue engineering and bioprinting

While reviewing the ELSA framework for bioprinting, an important question may come to our minds. Are not these aspects common to the broad field of tissue engineering as well? What is unique to bioprinting? Though bioprinting is a subset of tissue engineering and seen as a sophisticated tool for engineering complex tissues, there are certain aspects that are unique to bioprinting. First and foremost is the ability of bioprinting technology to fabricate complex biomimetic structures that gives the hope to print whole functional organs, which was never thought of before the advent of bioprinting. The moment we talk about organ printing, there are a bunch of ethical, legal, and social questions arising. For example, the problem of ownership of the printed organ is, in a way, unique to bioprinting. Though issues pertaining to source and donation of cells/stem cells are common for the overall field of tissue engineering, the question of ownership is amplified when it comes to bioprinted organs than the engineered tissue grafts. Secondly, with affordable bioprinters being introduced into the market, the chances of technology misuse are high. Very soon, the bioinks for printing different kinds of tissues and organs may also become commercially available. Then, any person who can read the manual and follow the steps effectively can have their tissues or organs printed at home. Though this may be a very ideal situation and can be expected only after a decade or two, the chances cannot be completely ruled out. Classification of the bioprinted product for regulatory approval

process is the third concern. Given the potential of this technology, there are many interdisciplinary fields that can be integrated into a single bioprinted product. For example, say an artificial organ is printed with an additional feature of controlled and targeted release of growth factors or drugs. What classification type will suit such a multifunctional product? And are the available protocols good enough to test and approve such a product or are new set of requirements and rules to be put in place? Though there are combination products in tissue engineering too, the subfield of bioprinting takes the complexity to another level. Fourth comes the ethical question of moral degradation. Imagine the technology is mature and you have organ factories and shops that come up. Will people drink more because they can buy a pair of liver? Will people smoke more because they can have their lungs replaced? These are some of the unique aspects of bioprinting and more questions may come as the technology is getting matured. Many of these unique aspects of bioprinting are discussed throughout this paper. This section is included to highlight the most important of them and to give the readers a clear distinction between the general tissue engineering field and more specialized subfield of bioprinting.

9.6 Recommendations and conclusions

The first and foremost need of the hour is to appreciate the potential of bioprinting and its impact in the society as well as to recognize the needs for a special focus on this technology, in establishing the framework, encompassing all the aspects, facilitating this life-saving technology to move into clinical translation, in the near future. Having reviewed in detail all the aspects of bioprinting, in terms of the ethical, legal and social tenets, the following recommendations are made.

1. Recognition of the need to have a focused ELSA framework for bioprinting by the policy makers and global organizations, which to start with, can be in the form of discussions and debate organized at regional and global level with experts in various fields airing their views to hit a common ground;
2. Setting up regulatory panels at national level to look into the various aspects of bioprinting, namely the acceptance of the technology (given the cultural and religious views of its population), the benefits that this technology can offer, the associated risks of misuse, and economic opportunities that come with its implementation;
3. Setting up an international multidisciplinary agency, including engineers, scientists, clinicians, industrialists, venture capitalists, funding agency representatives, philosophers, and religious leaders to discuss, debate, argue, and establish ELSA framework for bioprinting and review it regularly, addressing the concerns raised;
4. Charting NEST-Ethics framework for bioprinting, with all aspects including the arguments of justice and good life ethics; ensuring ethical guidelines are in place for every step and protecting rights from the source and donation of cells to the ownership of

the printed organ; preventing the unfairness of benefiting only the rich and making it affordable to the underprivileged;

5. An international team of experts on IP rights and patenting to bring clarity and provide guidelines on what is patentable and what is not, in bioprinting;
6. A clear legal framework for classification of bioprinting processes and products and the related review and approval pathways for clinical translation, marketing, and commercialization;
7. Appreciation and acknowledgment of effective controls in technology usage to prevent the technology to be in wrong hands, by licensing; prescribing strict guidelines for usage including approval hierarchies to obtain prior approvals and provisions for verification and surprise audits to ensure compliance;
8. Appreciation and acknowledgment of the importance of "soft impacts" in the success of bioprinting and inclusion of the same in policy decisions and ELSA framework;
9. Cultural and religious perception play the greatest role, especially with technologies like bioprinting, where the notion of "playing God" should be countered with to the satisfaction of the opponents;
10. Last but not least, a time frame for the above recommendations should be arrived at with clear action plans for significant milestones.

The technology of 3D bioprinting is a life-saving innovation and its huge potential is much felt by the scientists and clinicians. The ethical, legal, and social aspects play a crucial role in successful market translation of any technology. An ELSA framework for 3D bioprinting technology was reviewed in this chapter, highlighting the intriguing questions that are to be appreciated and addressed. The most important point stressed is to take a "complete" approach of these aspects pertaining to this technology under "Bioprinting ethics" rather than trivializing or settling down with a "piecemeal" approach of individual tenets of this technology, be it the use of stem cells or animals for research. The ethical framework (NEST-Ethics) must take into consideration the "hard" and "soft" impacts of this technology, source and donation of cells, and clinical translation including the preclinical studies and posttreatment follow-up. IP rights and related challenges should be the immediate focus in the legal framework, given the fact that the number of patent filing on 3D bioprinting is on the rise. The long-term objective is to look at the policies and regulations where government's role is significant, which includes the bioprinted product classification, approval authority, and the guidelines and proper licensing rules to prevent the technology from falling into wrong hands. No matter how innovative a technology is, people's perception and acceptance decide its final success. Social aspects of 3D bioprinting, encompassing the psychological, cultural, and religious perspectives have to be considered when making the framework. Recommendations were made on these tenets, the most important being the formation of an international multidisciplinary agency to work on the ELSA framework.

References

[1] S.V. Murphy, A. Atala, 3D bioprinting of tissues and organs, Nature Biotechnology 32 (8) (2014) 773–785.
[2] B.R. Ringeisen, B.J. Spargo, P.K. Wu, Cell and Organ Printing, Springer Science & Business Media, 2010.
[3] W.Y. Yeong, C.K. Chua, Bioprinting: Principles and Applications, World Scientific Publishing Co Inc, 2014.
[4] L.G. Zhang, J.P. Fisher, K. Leong, 3D Bioprinting and Nanotechnology in Tissue Engineering and Regenerative Medicine, academic press, 2015.
[5] K. Turksen, Bioprinting in Regenerative Medicine, Springer, 2015.
[6] V. Mironov, V. Kasyanov, R.R. Markwald, Organ printing: from bioprinter to organ biofabrication line, Current Opinion in Biotechnology 22 (5) (2011) 667–673.
[7] K. Jakab, C. Norotte, F. Marga, K. Murphy, G. Vunjak-Novakovic, G. Forgacs, Tissue engineering by self-assembly and bio-printing of living cells, Biofabrication 2 (2) (2010) 022001.
[8] V. Mironov, R.P. Visconti, V. Kasyanov, G. Forgacs, C.J. Drake, R.R. Markwald, Organ printing: tissue spheroids as building blocks, Biomaterials 30 (12) (2009) 2164–2174.
[9] D.L. Cohen, E. Malone, H. Lipson, L.J. Bonassar, Direct freeform fabrication of seeded hydrogels in arbitrary geometries, Tissue Engineering 12 (5) (2006) 1325–1335.
[10] P.G. Campbell, L.E. Weiss, Tissue engineering with the aid of inkjet printers, Expert Opinion on Biological Therapy 7 (8) (2007) 1123–1127.
[11] X. Tao, J. Rodriguez-Devora, D. Reyna-Sariano, M. Bhuyan, L. Zhu, K. Wang, Y. Yuan, Principles of Bioprinting Technology, Regenerative Medicine Applications in Organ Transplantation, Elsevier, San Diego, CA, 2013, pp. 67–79.
[12] P. Agrawal, S. Soni, G. Mittal, A. Bhatnagar, Role of polymeric biomaterials as wound healing agents, The International Journal of Lower Extremity Wounds 13 (3) (2014) 180–190.
[13] S. Wang, J.M. Lee, W.Y. Yeong, Smart hydrogels for 3D bioprinting, International Journal of Bioprinting 1 (1) (2015).
[14] J. Malda, J. Visser, F.P. Melchels, T. Jüngst, W.E. Hennink, W.J. Dhert, J. Groll, D.W. Hutmacher, 25th anniversary article: engineering hydrogels for biofabrication, Advanced Materials 25 (36) (2013) 5011–5028.
[15] P. Bianco, P.G. Robey, Stem cells in tissue engineering, Nature 414 (6859) (2001) 118–121.
[16] F. Ambesi-Impiombato, L. Parks, H. Coon, Culture of hormone-dependent functional epithelial cells from rat thyroids, Proceedings of the National Academy of Sciences 77 (6) (1980) 3455–3459.
[17] L. Hockaday, 3D bioprinting: a deliberate business, Genetic Engineering & Biotechnology News 35 (1) (2015) 14–17.
[18] N. Nijsingh, M. Düwell, Interdisciplinarity, applied ethics and social science, Evaluating New Technologies (2009) 79–92.
[19] T. Swierstra, A. Rip, Nano-ethics as NEST-ethics: patterns of moral argumentation about new and emerging science and technology, Nanoethics 1 (1) (2007) 3–20.
[20] T. Swierstra, D. Stemerding, M. Boenink, Exploring techno-moral change: the case of the obesitypill, Evaluating New Technologies (2009) 119–138.
[21] J. Rawls, Theory of Justice, Harvard University Press, Belknap, 1971.
[22] A. Oerlemans, M. van Hoek, E. van Leeuwen, S. van der Burg, W. Dekkers, Towards a richer debate on tissue engineering: a consideration on the basis of NEST-ethics, Science and Engineering Ethics 19 (3) (2013) 963–981.
[23] M. Boenink, T. Swierstra, D. Stemerding, Anticipating the interaction between technology and morality: a scenario study of experimenting with humans in bionanotechnology, Studies in Ethics, Law, and Technology 4 (2) (2010).

[24] S. van der Burg, Taking the "soft impacts" of technology into account: broadening the discourse in research practice, Social Epistemology 23 (3–4) (2009) 301–316.
[25] T. Swierstra, H. Te Molder, Risk and soft impacts. Handbook of Risk Theory: Epistemology, Decision Theory, Ethics, and Social Implications of Risk, Springer Netherlands, 2012, pp. 1049–1066.
[26] R.B. de Vries, A. Oerlemans, L. Trommelmans, K. Dierickx, B. Gordijn, Ethical aspects of tissue engineering: a review, Tissue Engineering Part B Reviews 14 (4) (2008) 367–375.
[27] A. Daar, A. Bhatt, E. Court, P. Singer, Stem cell research and transplantation: science leading ethics, Transplantation Proceedings (2004) 2504–2506. Elsevier.
[28] Y. Yoshimura, Bioethical aspects of regenerative and reproductive medicine, Human Cell 19 (2) (2006) 83–86.
[29] T. Awaya, Chapitre 5. Common ethical issues in regenerative medicine, Journal International de Bioethique 16 (1) (2005) 69–75.
[30] H. Fiegel, C. Lange, U. Kneser, W. Lambrecht, A. Zander, X. Rogiers, D. Kluth, Fetal and adult liver stem cells for liver regeneration and tissue engineering, Journal of Cellular and Molecular Medicine 10 (3) (2006) 577–587.
[31] H. Löwenheim, S. Dazert, M. Bücheler, O. Guntinas-Lichius, Regenerative Medicine/cellular Engineering for Diseases of the Head and Neck, Mary Ann Liebert, Inc, 2003.
[32] T.S. Sadiq, D.A. Gerber, Stem cells in modern medicine: reality or myth? Journal of Surgical Research 122 (2) (2004) 280–291.
[33] D. Fauza, Amniotic fluid and placental stem cells, Best Practice and Research Clinical Obstetrics and Gynaecology 18 (6) (2004) 877–891.
[34] G.M. Abouna, Ethical issues in organ transplantation, Medical Principles and Practice 12 (1) (2003) 54–69.
[35] C.B. Ballas, S.P. Zielske, S.L. Gerson, Adult bone marrow stem cells for cell and gene therapies: implications for greater use, Journal of Cellular Biochemistry 85 (S38) (2002) 20–28.
[36] M. Körbling, Z. Estrov, Adult stem cells for tissue repair—a new therapeutic concept? New England Journal of Medicine 349 (6) (2003) 570–582.
[37] M. Krampera, G. Pizzolo, G. Aprili, M. Franchini, Mesenchymal stem cells for bone, cartilage, tendon and skeletal muscle repair, Bone 39 (4) (2006) 678–683.
[38] M. Markowicz, A. Heitland, G. Steffens, S. Neuss, N. Pallua, Human mesenchymal stem cell implantation and collagen modification as a tool for tissue engineering, European Journal of Plastic Surgery 28 (4) (2005) 284–289.
[39] F. Tögel, C. Westenfelder, Adult bone marrow–derived stem cells for organ regeneration and repair, Developmental Dynamics: An Official Publication of the American Association of Anatomists 236 (12) (2007) 3321–3331.
[40] L. Perin, S. Giuliani, D. Jin, S. Sedrakyan, G. Carraro, R. Habibian, D. Warburton, A. Atala, R. De Filippo, Renal differentiation of amniotic fluid stem cells, Cell Proliferation 40 (6) (2007) 936–948.
[41] A.R. Prusa, E. Marton, M. Rosner, G. Bernaschek, M. Hengstschläger, Oct-4-expressing cells in human amniotic fluid: a new source for stem cell research? Human Reproduction 18 (7) (2003) 1489–1493.
[42] K. Igura, X. Zhang, K. Takahashi, A. Mitsuru, S. Yamaguchi, T. Takahashi, Isolation and characterization of mesenchymal progenitor cells from chorionic villi of human placenta, Cytotherapy 6 (6) (2004) 543–553.
[43] O. Parolini, F. Alviano, G.P. Bagnara, G. Bilic, H.J. Bühring, M. Evangelista, S. Hennerbichler, B. Liu, M. Magatti, N. Mao, Concise review: isolation and characterization of cells from human term placenta: outcome of the first international Workshop on Placenta Derived Stem Cells, Stem Cells 26 (2) (2008) 300–311.
[44] B.L. Yen, C.-C. Chien, Y.-C. Chen, J.-T. Chen, J.-S. Huang, F.-K. Lee, H.-I. Huang, Placenta-derived multipotent cells differentiate into neuronal and glial cells in vitro, Tissue Engineering A 14 (2) (2008) 9–17.

[45] G. Katz-Benichou, Umbilical cord blood banking: economic and therapeutic challenges, International Journal of Healthcare Technology and Management 8 (5) (2007) 464–477.
[46] J.L. Goldberg, M.J. Laughlin, V.J. Pompili, Umbilical cord blood stem cells: implications for cardiovascular regenerative medicine, Journal of Molecular and Cellular Cardiology 42 (5) (2007) 912–920.
[47] D.T. Harris, M. Badowski, N. Ahmad, M.A. Gaballa, The potential of cord blood stem cells for use in regenerative medicine, Expert Opinion on Biological Therapy 7 (9) (2007) 1311–1322.
[48] M.W. Lee, M.S. Yang, J.S. Park, H.C. Kim, Y.J. Kim, J. Choi, Isolation of mesenchymal stem cells from cryopreserved human umbilical cord blood, International Journal of Hematology 81 (2) (2005) 126–130.
[49] C.P. McGuckin, N. Forraz, M.O. Baradez, S. Navran, J. Zhao, R. Urban, R. Tilton, L. Denner, Production of stem cells with embryonic characteristics from human umbilical cord blood, Cell Proliferation 38 (4) (2005) 245–255.
[50] H.S. Wang, S.C. Hung, S.T. Peng, C.C. Huang, H.M. Wei, Y.J. Guo, Y.S. Fu, M.C. Lai, C.C. Chen, Mesenchymal stem cells in the Wharton's jelly of the human umbilical cord, Stem Cells 22 (7) (2004) 1330–1337.
[51] M.L. Weiss, D.L. Troyer, Stem cells in the umbilical cord, Stem Cell Reviews 2 (2) (2006) 155–162.
[52] R. Alberio, K.H. Campbell, A.D. Johnson, Reprogramming somatic cells into stem cells, Reproduction 132 (5) (2006) 709–720.
[53] S. Cai, X. Fu, Z. Sheng, Dedifferentiation: a new approach in stem cell research, BioScience 57 (8) (2007) 655–662.
[54] P. Collas, R. Gammelsæter, Novel approaches to epigenetic reprogramming of somatic cells, Cloning and Stem Cells 9 (1) (2007) 26–32.
[55] M. Wernig, A. Meissner, R. Foreman, T. Brambrink, M. Ku, K. Hochedlinger, B.E. Bernstein, R. Jaenisch, In vitro reprogramming of fibroblasts into a pluripotent ES-cell-like state, Nature 448 (7151) (2007) 318–324.
[56] Y. Chung, I. Klimanskaya, S. Becker, J. Marh, S.-J. Lu, J. Johnson, L. Meisner, R. Lanza, Embryonic and extraembryonic stem cell lines derived from single mouse blastomeres, Nature 439 (7073) (2006) 216–219.
[57] H. Fangerau, Can artificial parthenogenesis sidestep ethical pitfalls in human therapeutic cloning? An historical perspective, Journal of Medical Ethics 31 (12) (2005) 733–735.
[58] J. Hipp, A. Atala, Tissue engineering, stem cells, cloning, and parthenogenesis: new paradigms for therapy, Journal of Experimental & Clinical Assisted Reproduction 1 (1) (2004) 1–10.
[59] D.W. Landry, H.A. Zucker, M.V. Sauer, M. Reznik, L. Wiebe, Hypocellularity and Absence of Compaction as Criteria for Embryonic Death, 2006.
[60] I.L. Weissman, Politic stem cells, Nature 439 (7073) (2006) 145–147.
[61] X. Zhang, P. Stojkovic, S. Przyborski, M. Cooke, L. Armstrong, M. Lako, M. Stojkovic, Derivation of human embryonic stem cells from developing and arrested embryos, Stem Cells 24 (12) (2006) 2669–2676.
[62] J. Garner, Tissue engineering in surgery, The Surgeon 2 (2) (2004) 70–78.
[63] A. Faulkner, J. Kent, I. Geesink, D. FitzPatrick, Purity and the dangers of regenerative medicine: regulatory innovation of human tissue-engineered technology, Social Science & Medicine 63 (9) (2006) 2277–2288.
[64] K. Iijima, Y. Igawa, T. Imamura, T. Moriizumi, T. Nikaido, I. Konishi, O. Nishizawa, Transplantation of preserved human amniotic membrane for bladder augmentation in rats, Tissue Engineering 13 (3) (2007) 513–524.
[65] O. Nieminen, P. Kurki, Risk management for biological products, International Journal of Pharmaceutical Medicine 18 (3) (2004) 149–157.
[66] I.R. Schwab, N.T. Johnson, D.G. Harkin, Inherent risks associated with manufacture of bioengineered ocular surface tissue, Archives of Ophthalmology 124 (12) (2006) 1734–1740.
[67] E.S. Tzanakakis, D.J. Hess, T.D. Sielaff, W.-S. Hu, Extracorporeal tissue engineered liver-assist devices, Annual Review of Biomedical Engineering 2 (1) (2000) 607–632.

[68] M.R. Hammerman, R. Cortesini, Organogenesis and tissue engineering, Transplant Immunology 12 (3–4) (2004) 191–192.
[69] D. Longley, P. Lawford, Engineering human tissue and regulation: confronting biology and law to bridge the gaps, Medical Law International 5 (2) (2001) 101–115.
[70] J. Garner, Tissue engineering and the trauma surgeon, Trauma 4 (3) (2002) 177–183.
[71] S. Enoch, H. Shaaban, K. Dunn, Informed consent should be obtained from patients to use products (skin substitutes) and dressings containing biological material, Journal of Medical Ethics 31 (1) (2005) 2–6.
[72] J. Kent, A. Faulkner, I. Geesink, D. Fitzpatrick, Culturing cells, reproducing and regulating the self, Body & Society 12 (2) (2006) 1–23.
[73] J. Black, Thinking twice about "tissue engineering" [ethical issues], IEEE Engineering in Medicine and Biology Magazine 16 (4) (1997) 102–104.
[74] A.J. Oerlemans, P.P. van den Berg, E. van Leeuwen, W.J. Dekkers, Ethical issues regarding the donation and source of cells for tissue engineering: a European focus group study, Tissue Engineering Part B Reviews 17 (4) (2011) 229–234.
[75] L. Tsang, Legal and ethical status of stem cells as medicinal products, Advanced Drug Delivery Reviews 57 (13) (2005) 1970–1980.
[76] T. Bredehorn, B. Rudolph, Legal problems in tissue transplantation, Transplantation Proceedings (2002) 2345–2346.
[77] S. Orr, E. Alexandre, B. Clark, R. Combes, L.M. Fels, N. Gray, A.-C. Jönsson-Rylander, H. Helin, J. Koistinen, T. Oinonen, The establishment of a network of European human research tissue banks, Cell and Tissue Banking 3 (2) (2002) 133–137.
[78] P. Pascal, O. Damour, J.-J. Colpart, F. Braye, French legal framework relating to human tissues and cells, Medical, & Biological Engineering & Computing 38 (2) (2000) 241–247.
[79] C. Trouet, New European guidelines for the use of stored human biological materials in biomedical research, Journal of Medical Ethics 30 (1) (2004) 99–103.
[80] J. Gunning, Umbilical cord cell banking—implications for the future, Toxicology and Applied Pharmacology 207 (2) (2005) 538–543.
[81] D.A. Taylor, A.L. Caplan, P. Macchiarini, Ethics of bioengineering organs and tissues, Expert Opinion on Biological Therapy 14 (7) (2014) 879–882.
[82] M.M. Lalu, L. McIntyre, C. Pugliese, D. Fergusson, B.W. Winston, J.C. Marshall, J. Granton, D.J. Stewart, C.C.C.T. Group, Safe ty of cell therapy with mesenchymal stromal cells (safecell): a systematic review and meta-analysis of clinical trials, PloS One 7 (10) (2012) e47559.
[83] E. Boelsma, M.C. Verhoeven, M. Ponec, Reconstruction of a human skin equivalent using a spontaneously transformed keratinocyte cell line (HaCaT), Journal of Investigative Dermatology 112 (4) (1999) 489–498.
[84] M. Ponec, Skin constructs for replacement of skin tissues for in vitro testing, Advanced Drug Delivery Reviews 54 (2002) S19–S30.
[85] T. Welss, D.A. Basketter, K.R. Schröder, In vitro skin irritation: facts and future. State of the art review of mechanisms and models, Toxicology in Vitro 18 (3) (2004) 231–243.
[86] A. Caplan, Is it Sound Public Policy to Let the Terminally Ill Access Experimental Medical Innovations? Taylor & Francis, 2007.
[87] A.S. Kesselheim, C.T. Robertson, J.A. Myers, S.L. Rose, V. Gillet, K.M. Ross, R.J. Glynn, S. Joffe, J. Avorn, A randomized study of how physicians interpret research funding disclosures, New England Journal of Medicine 367 (12) (2012) 1119–1127.
[88] L. Trommelmans, J. Selling, K. Dierickx, Is tissue engineering a new paradigm in medicine? Consequences for the ethical evaluation of tissue engineering research, Medicine, Healthcare & Philosophy 12 (4) (2009) 459–467.
[89] S.-S. Yoo, 3D-printed biological organs: medical potential and patenting opportunity, Expert Opinion on Therapeutic Patents 25 (5) (2015) 507–511.

[90] J.L. Tran, Patenting bioprinting, Harvard Journal of Law and Technology Digest 29 (2015).
[91] D.B. Resnik, The commercialization of human stem cells: ethical and policy issues, Health Care Analysis 10 (2) (2002) 127–154.
[92] A. Dhai, J. Moodley, D. McQuoid-Mason, C. Rodeck, Ethical and legal controversies in cloning for biomedical research-a South African perspective, South African Medical Journal 94 (11) (2004).
[93] E. Salvaterra, L. Lecchi, S. Gobbi, P. Rebulla, The ethics of cord blood banking in light of ownership, informed consent, and solidarity, Cell Preservation Technology 4 (2) (2006) 91–96.
[94] A. Samanta, J. Samanta, D. Price, Who owns my body–thee or me? The human tissue story continues, Clinical Medicine 4 (4) (2004) 327.
[95] W.E. Thasler, T.S. Weiss, K. Schillhorn, P.-T. Stoll, B. Irrgang, K.-W. Jauch, Charitable state-controlled foundation human tissue and cell research: ethic and legal aspects in the supply of surgically removed human tissue for research in the academic and commercial sector in Germany, Cell and Tissue Banking 4 (1) (2003) 49–56.
[96] H. Wolinsky, Printing organs cell-by-cell: 3-D printing is growing in popularity, but how should we regulate the application of this new technology to health care? EMBO Reports 15 (8) (2014) 836–838.
[97] D.S. Smith, The Government's role in advancing regenerative medicine and tissue engineering–science, safety, and ethics, Periodontology 2000 41 (1) (2006) 16–29.
[98] M. Heinonen, O. Oila, K. Nordström, Current issues in the regulation of human tissue-engineering products in the European Union, Tissue Engineering 11 (11–12) (2005) 1905–1911.
[99] Y. Gheisari, H. Baharvand, K. Nayernia, M. Vasei, Stem cell and tissue engineering research in the Islamic Republic of Iran, Stem Cell Reviews and Reports 8 (3) (2012) 629–639.
[100] P.-P. Verbeek, Accompanying technology: philosophy of technology after the ethical turn, Techné: Research in Philosophy and Technology 14 (1) (2010) 49–54.
[101] A. Briggle, Love on the Internet: a framework for understanding eros online, Journal of Information, Communication and Ethics in Society 6 (2008) 216–232.
[102] A. Briggle, Real friends: how the Internet can foster friendship, Ethics and Information Technology 10 (1) (2008) 71–79.
[103] C. Marris, Public views on GMOs: deconstructing the myths: stakeholders in the GMO debate often describe public opinion as irrational. But do they really understand the public? EMBO Reports 2 (7) (2001) 545–548.
[104] E. Tenner, Why Things Bite Back: Technology and the Revenge of Unintended Consequences, Vintage, 1997.
[105] P.R. Henon, Human embryonic or adult stem cells: an overview on ethics and perspectives for tissue engineering, Tissue Engineering, Stem Cells, and Gene Therapies (2003) 27–45.
[106] R.M. Isasi, B.M. Knoppers, Beyond the permissibility of embryonic and stem cell research: substantive requirements and procedural safeguards, Human Reproduction 21 (10) (2006) 2474–2481.

Index

Note: 'Page numbers followed by "f" indicate figures, and "t" indicate tables.'

C

D

E

F

G

H

I

K

L

M

N

O

P

R

S

3D BIOPRINTING IN TISSUE AND ORGAN REGENERATION

Yang Wu, PhD, Assistant Professor, School of Mechanical Engineering and Automation, Harbin Institute of Technology, Shenzhen, China

Jerry Fuh, PhD, Professor, Department of Mechanical Engineering, National University of Singapore, Singapore

Ibrahim Tarik Ozbolat, PhD, Professor, Engineering Science and Mechanics Department, Department of Biomedical Engineering, and Department of Neurosurgery, Penn State University, State College, PA, USA

3D Bioprinting in Tissue and Organ Regeneration covers the state-of-the-art advances in applications of bioprinting. Beginning with an introduction of considerations of bioprinting, the authors then move into a detailed review of applications of bioprinting in different biomedical fields (skin, cartilage, bone, vascularized tissue, etc.), followed by a chapter overview of intraoperative bioprinting, which is widely considered one of the important future trends in this area. Finally, the authors tackle ethical and regulatory concerns regarding the utilization of bioprinting.

Written by three global experts in the field, for students and professionals with some basic knowledge of bioprinting, but who are seeking a deeper understanding of the biomedical applications involved in bioprinting.

Key Features

- Introduces readers to the bioprinting modalities, as well as pre-bioprinting, bioprinting, and post-bioprinting procedures
- Focuses on the biomedical applications used in bioprinting in chapters specific to skin, cartilage, bone, vascularized tissue, and organs
- Provides the readers with original ideas from engineering and clinical points of view based on the authors' extensive experience in this field, as well as possibilities of future translation of bioprinting technologies from bench to bedside

ELSEVIER

ACADEMIC PRESS
An imprint of Elsevier
elsevier.com/books-and-journals

ISBN 978-0-12-824291-9
9 780128 242919